june 1960
the
institute
of
radio
engineers

Proceedings of the IRE

PART II

INDEX
TO
ABSTRACTS
AND
REFERENCES
1959

VOLUME 48, NUMBER 6, PART II

June, 1960

published monthly by The Institute of Radio Engineers, Inc.

Proceedings of the IRE®

contents

INDEX TO ABSTRACTS AND REFERENCES 1959

This index is reprinted from the April, 1960 issue of *Electronics & Radio Engineer* (Incorporating *Wireless Engineer*), London, England and covers Abstracts and References published monthly in PROCEEDINGS OF THE IRE from February, 1959 through January, 1960.

PROCEEDINGS OF THE IRE, published monthly by The Institute of Radio Engineers, Inc. at 1 East 79 Street, New York 21, N. Y. Manuscripts should be submitted in triplicate to the Editorial Department. Responsibility for contents of papers published rests upon the authors, and not the IRE or its members. All republication rights, including translations, are reserved by the IRE and granted only on request. Abstracting is permitted with mention of source.

Thirty days advance notice is required for change of address. Price per copy: members of the Institute of Radio Engineers, one additional copy $1.25; non-members $3.00. Yearly subscription price: to members $9.00, one additional subscription $13.50; to non-members in United States, Canada, and U. S. Possessions $18.00; to non-members in foreign countries $19.00. Second-class postage paid at Menasha, Wisconsin under the act of March 3, 1879. Acceptance for mailing at a special rate of postage is provided for in the act of February 28, 1925, embodied in Paragraph 4, Section 412, P. L. and R., authorized October 26, 1927. Printed in U.S.A.

Cross References to Abstracts Published in PROCEEDINGS

Abstract Numbers	*Issue of* PROCEEDINGS	*Pages*
1– 327	February, 1959	356– 368
328– 660	March	500– 512
661–1038	April	614– 628
1039–1421	May	1030–1044
1422–1750	June	1176–1188
1751–2077	July	1288–1300
2078–2443	August	1398–1412
2444–2807	September	1686–1700
2808–3176	October	1799–1812
3177–3535	November	2040–2053
3536–3899	December	2134–2148
3900–4256	January, 1960	131– 144

Symbols used in the Index

(A) Abstract, (B) Book Review, (C) Note of Correction, (D) Discussion

Abbreviations used in the Index

a.c.	= alternating current
d.c.	= direct current
h.v.	= high voltage
l.v.	= low voltage
a.f.	= audio frequency
i.f.	= intermediate frequency
r.f.	= radio frequency, including:—
v.l.f.	= very low frequency, <30 kc/s
l.f.	= low frequency, 30–300 kc/s
m.f.	= medium frequency, 300–3000 kc/s
h.f.	= high frequency, 3–30 Mc/s
v.h.f.	= very high frequency, 30–300 Mc/s
u.h.f.	= ultra high frequency, >300 Mc/s
a.m.	= amplitude modulation
f.m.	= frequency modulation
p.m.	= pulse modulation, including:—
p.a.m.	= pulse amplitude modulation
p.c.m.	= pulse code modulation
p.f.m.	= pulse frequency modulation
p.ph.m.	= pulse phase modulation
p.p.m.	= pulse position modulation
p.w.m.	= pulse width modulation
ph.m.	= phase modulation
v.m.	= velocity modulation

c.w.	= continuous wave
i.c.w. m.c.w	= modulated c.w.
s.w.*	= short wave
u.s.w.*	= ultra short wave
λ	= wavelength
c.r.	= cathode ray
c.r.o.	= cathode ray oscilloscope
d.f.	= direction finding
e.m.	= electromagnetic, *but*
e.m.f.	= electromotive force
a.f.c.	= automatic frequency control
a.g.c.	= automatic gain control
a.ph.c.	= automatic phase control
a.v.c.	= automatic volume control
m.u.f.	= maximum usable frequency
p.p.i.	= plan position indicator
s.s.b.	= single sideband
d.s.b.	= double sideband
s.w.r.	= standing wave ratio
v.f.o.	= variable frequency oscillator
R/T	= radiotelephony
W/T	= wireless telegraphy
TV	= television

* No clearly defined limits

AUTHOR INDEX

A name followed by "and" is that of the first author of a jointly written paper, while the word "with" indicates that the name indexed is that of the second author.

A

B

C

D

G

H

I

J

K

L

N

O

P

Q

R

S

T

Y

Z

SUBJECT INDEX

A

D

E

F

G

H

I

Q

R

S

T

U

V

W

ERRATA

IN ABSTRACTS AND REFERENCES 1959

Abstract No.	
515	Change U.D.C. number to 537.311.33 : 535.215
1052	For 'F. A. Vaniar' read 'F. A. Veniar'
1529	In line 5, for 'auroral' read 'annual'
1824	In line 7, for 'frequency band' read 'energy band'
1958	For 'J. F. Ditton, Jr' read 'J. F. Dillon, Jr'
1986	Change U.D.C. number to 621.384.8 : 537.54
2113	In line 4, for 'three-part' read 'three-port'
2159	In line 7, for 'joints' read 'points'
2278	In title, for 'Electric' read 'Elastic'
2408	In line 7, for '605-line' read '625-line'
2669	For 'S. Asanabo' read 'S. Asanabe'
2720	Change U.D.C. number to 621.384.8 : 537.54
2831	In title, for '$TE°_{10}$–$TE°_{01}$' read 'TE°_{10}–TE°_{01}'
2857	In title, for '$m\sqrt{N}$' read '$N^{1/m}$'
2958	In line 4, for 'change-exchange' read 'charge-exchange'
3030	In line 5, for 'function' read 'junction'
3136	In line 5, for '3136' read '3138
3171	For 'W. R. Aitken' read 'W. R. Aiken'
3256	Change U.D.C. number to 538.566 : 535.42
3350	Change U.D.C. number to 537.311.3 : 539.23
3836	For 'J. L. Veshaeghe' read 'J. L. Verhaeghe'

IN PAPERS ABSTRACTED

The practice of allocating individual abstract numbers to corrections has been largely discontinued; a list of published corrections noted during 1959 is given below. The journal in which the correction appeared was in each case the same as that in which the original paper was published.

Abstract No.	
3235 of 1955	Jan. 1959, Vol. 14, No. 1, pp. 115–116
1405 of 1957	July 1957, Vol. AP-5, No. 3, p. 313
2959 of 1957	Dec. 1958, Vol. 5, No. 6, pp. 510–513
84 of 1958	Jan. 1959, Vol. 6, No. 1, p. 80
295 of 1958	Sept. 1959, Vol. 36, No. 9, p. 352
971 of 1958	Sept. 1958, Vol. 29, No. 9, p. 1383
1228 of 1958	Dec. 1959, Vol. 47, No. 12, p. 2105
1858 of 1958	April 1958, Vol. 3, No. 30, p. 312
1892 of 1958	April 1958, Vol. 3, No. 30, p. 312
3028 of 1958	Sept. 1958, Vol. 29, No. 9, p. 1383
3271 of 1958	Dec. 1959, Vol. 47, No. 12, p. 2084
3472 of 1958	Dec. 1958, Vol. 18, No. 12, p. 714
3544 of 1958	15th Dec. 1958, Vol. 112, No. 6, p. 2139
3890 of 1958	15th Sept. 1959, Vol. 115, No. 6, p. 1778
3902 of 1958	15th March 1959, Vol. 113, No. 6, p. 1697
3962 of 1958	Dec. 1958, Vol. 46, No. 12, p. 1913
173 of 1959	15th March 1959, Vol. 113, No. 6, p. 1696
239 of 1959	July 1957, Vol. AP-5, No. 3, p. 313
337 of 1959	Dec. 1957, Vol. CP-4, No. 4, pp. 135–137
379 of 1959	Feb. 1959, Vol. 4, No. 37, p. 220
385 of 1959	May 1959, Vol. 4, No. 39, p. 272
501 of 1959	1st June 1959, Vol. 73, No. 474, p. 976
635 of 1959	Oct. 1958, Vol. 17, No. 10, p. 117
745 of 1959	Feb. 1959, Vol. 4, No. 37, p. 220
855 of 1959	March 1959, Vol. 36, No. 3, p. 95
890 of 1959	March 1959, Vol. 9, Nos. 3/4, p. 340
1233 of 1959	15th June 1959, Vol. 114, No. 6, p. 1652
1368 of 1959	Sept. 1959, Vol. 47, No. 9, pp. 1653–1654
1372 of 1959	June 1958, Vol. 2, No. 3, p. 144
1493 of 1959	Dec. 1958, Vol. 17, No. 12, p. 36
1498 of 1959	Feb. 1959, Vol. 4, No. 37, p. 220
1559 of 1959	April 1959, Vol. 47, No. 4, p. 567
1615 of 1959	1st Sept. 1959, Vol. 3, No. 5, p. 244
1693 of 1959	Feb. 1959, Vol. 4, No. 37, p. 220
1795 of 1959	May 1959, Vol. 65, No. 5, p. 232
1952 of 1959	1st June 1959, Vol. 73, No. 474, p. 976
2024 of 1959	Oct. 1958, Vol. 2, No. 5, p. 252
2202 of 1959	15th June 1959, Vol. 114, No. 6, p. 1652
2408 of 1959	Aug. 1959, Vol. 36, No. 8, p. 314
2410 of 1959	July 1959, Vol. 47, No. 7, p. 1252
2503 of 1959	July 1959, Vol. 31, No. 377, p. 427
2750 of 1959	Aug. 1959, Vol. 47, No. 8, p. 1324
2841 of 1959	Jan. 1959, Vol. AP-7, No. 1, p. 104
3076 of 1959	Jan. 1959, Vol. 16, No. 1, p. 56
3077 of 1959	Jan. 1959, Vol. 16, No. 1, p. 56
3078 of 1959	April 1959, Vol. 14, No. 4, p. 547
3081 of 1959	Dec. 1958, Vol. 10, No. 12, p. 576
3419 of 1959	Oct. 1958, Vol. 2, No. 5, p. 252
3588 of 1959	Nov. 1959, Vol. 47, No. 11, p. 1840
3965 of 1959	July 1959, Vol. AP-7, No. 3, p. 251

LISTS OF JOURNALS

A selection of the journals which are regularly scanned is given below, together with the addresses of their publishers or editorial offices and the abbreviations of their titles as used in the Abstracts and References. Applications for copies of any journal should be made to the addresses given.

The full title of each journal is given in bold type and is followed by the address, the abbreviated title being shown within brackets. In a few cases the nature of a journal is indicated, where neither the title nor the address shows it clearly.

A

Acta Polytechnica Scandinavica, Publishing Office, Box 5073, Stockholm 5, Sweden. (*Acta polyt. scand.*)

Acustica, S. Hirzel Verlag, Stuttgart-N, Germany. (*Acustica*)

Advances in Physics, Taylor & Francis Ltd, Red Lion Court, Fleet Street, London, E.C.4, England. (*Advances Phys.*)

Akusticheskii Zhurnal, Moskva, B-64, Podsosenskii per., 21, U.S.S.R. (*Akust. Zh.*)

Akustische Beihefte, as for Acustica. (*Akust. Beihefte*)

Alta Frequenza, Associazione Elettrotecnica Italiana, Milano (202), Via S. Paolo 10, Italy. (*Alta Frequenza*)

Annalen der Physik, J. A. Barth, Leipzig C1, Salomonstrasse 18B, East Germany. (*Ann. Phys., Lpz.*)

Annales de Géophysique, Service des Publications du C.N.R.S., 13 Quai Anatole France, Paris 7ᵉ, France. (*Ann. Géophys.*)

Annales de Physique, Masson & Cie, 120 Boulevard Saint-Germain, Paris 6ᵉ, France. (*Ann. Phys., Paris*)

Annales de Radioélectricité, 10 rue Carducci, Paris 19ᵉ, France. (*Ann. Radioélect.*)

Annales des Télécommunications, 3 & 5 Boulevard Pasteur, Paris 15ᵉ, France. (*Ann. Télécommun.*)

Applied Scientific Research, Martinus Nijhoff, The Hague, Netherlands. (*Appl. sci. Res.*)

Archiv der elektrischen Übertragung, S. Hirzel Verlag, Stuttgart, Germany. (*Arch. elekt. Übertragung*)

Archiv für Elektrotechnik, Springer Verlag, Berlin-Wilmersdorf, Heidelberger Platz 3, Germany. (*Arch. Elektrotech.*)

Archiv für technisches Messen, R. Oldenbourg KG, München 8, Rosenheimer Str. 145, Germany. (*Arch. tech. Messen*)

Arkiv för Fysik, published for Royal Swedish Academy of Sciences by Almqvist & Wiksell, Stockholm, Sweden. (*Ark. Fys.*)

A.T.E. Journal, Automatic Telephone & Electric Co. Ltd, Strowger Works, Liverpool 7, England. (*A.T.E. J.*)

Audio, Radio Magazines, Inc., P.O. Box 629, Mineola, N.Y., U.S.A. (*Audio*)

Australian Journal of Physics, Commonwealth Scientific and Industrial Research Organization, 314 Albert Street, East Melbourne C.2, Victoria, Australia. (*Aust. J. Phys.*)

Avtomatika i Telemekhanika, Moskva, I-53, Kalanchevskaya ul., 15a, U.S.S.R. (*Avtomatika i Telemekhanika*)

A.W.A. Technical Review, Amalgamated Wireless (Australasia) Ltd, Sydney, Australia. (*A.W.A. tech. Rev.*)

B

B.B.C. Engineering Division Monographs, British Broadcasting Corporation, 35 Marylebone High Street, London, W.1, England. (*B.B.C. Engng Div. Monographs*)

Beama Journal, British Electrical and Allied Manufacturers' Association, 36 Kingsway, London, W.C.2, England. (*Beama J.*)

Bell Laboratories Record, 463 West Street, New York 14, N.Y., U.S.A. (*Bell Lab. Rec.*)

Bell System Technical Journal, American Telephone and Telegraph Company, 195 Broadway, New York 7, N.Y., U.S.A. (*Bell Syst. tech. J.*)

British Communications & Electronics, Heywood & Co. Ltd, Drury House, Russell Street, Drury Lane, London, W.C.2, England. (*Brit. Commun. Electronics*)

British Journal of Applied Physics, 47 Belgrave Square, London, S.W.1, England. (*Brit. J. appl. Phys.*)

Brown Boveri Review, Baden, Switzerland. (*Brown Boveri Rev.*)

Bulletin de l'Association Suisse des Électriciens, Seefeldstrasse 301, Zurich 8, Switzerland. (*Bull. schweiz. elektrotech. Ver.*)

Bulletin of the Technical University Istanbul, Istanbul Teknik Universitesi, Gumussuyu, Istanbul, Turkey. (*Bull. tech. Univ. Istanbul*)

C

Câbles & Transmission, Sotelec, 16 rue de la Baume, Paris 8e, France. (*Câbles & Transm.*)

Cahiers de Physique, 165 rue de Sèvres, Paris 15e, France. (*Cah. Phys.*)

Canadian Electronics Engineering, Maclean-Hunter Publishing Co. Ltd, P.O. Box 100, Toronto, Canada. (*Canad. Electronics Engng*)

Canadian Journal of Physics, National Research Council, Ottawa 2, Ont., Canada. (*Canad. J. Phys.*)

Chalmers tekniska Högskolas Handlingar, Gumperts Forlag, Goteborg, Sweden. (*Chalmers tek. Hoegsk. Handl.*)

Communication and Electronics, American Institute of Electrical Engineers, 20th and Northampton Streets, Easton, Pa, U.S.A. (*Commun. & Electronics*)

Communications on Pure and Applied Mathematics, Interscience Publishers Inc., 250 Fifth Avenue, New York 1, N.Y., U.S.A. (*Commun. pure appl. Math.*)

Comptes Rendus Hebdomadaires des Séances de l'Académie des Sciences, Gauthier-Villars, 55 Quai des Grands Augustins, Paris 6e, France. (*C. R. Acad. Sci., Paris*)

D

Doklady Akademii Nauk S.S.S.R., Moskva, B-64, Podsosenskii per., 21, U.S.S.R. (*Dokl. Ak. Nauk S.S.S.R.*)

E

E.B.U. Review, 32 Avenue Albert Lancaster, Bruxelles 18, Belgium. (*E.B.U. Rev.*)

Electrical Communication, International Telephone and Telegraph Corporation, 67 Broad Street, New York 4, N.Y., U.S.A. (*Elect. Commun.*)

Electrical Engineering, American Institute of Electrical Engineers, 33 West 39th Street, New York 18, N.Y., U.S.A. (*Elect. Engng, N.Y.*)

Electrical Journal, Bouverie House, 154 Fleet Street, London, E.C.4, England. (*Elect. J.*)

Electrical Manufacturing, 205 East 42nd Street, New York 17, N.Y., U.S.A. (*Elect. Mfg*)

Electrical Review, Dorset House, Stamford Street, London, S.E.1, England. (*Elect. Rev., Lond.*)

Electronic Applications, N. V. Philips' Gloeilampenfabrieken, Technical and Scientific Literature Department, Eindhoven, Netherlands. (*Electronic Applic.*)

Electronic Engineering, 28 Essex Street, London, W.C.2, England. (*Electronic Engng*)

Electronic Equipment Engineering, Sutton Publishing Company Inc., 172 South Broadway, White Plains, N.Y., U.S.A. (*Electronic Equipm. Engng*)

Electronic Industries, Chestnut and 56th Sts, Philadelphia 39, Pa, U.S.A. (*Electronic Ind.*)

Electronic & Radio Engineer, Iliffe & Sons Ltd, Dorset House, Stamford Street, London, S.E.1, England. (*Electronic Radio Engr*)

Electronics, 330 West 42nd Street, New York 36, N.Y., U.S.A. (*Electronics*)

Elektronische Rundschau, Verlag fur Radio-Foto-Kinotechnik G.m.b.H., Berlin Borsigwalde, Eichborndamm 141–167, Germany. (*Elektronische Rundschau*)

Elektrosvyaz', Moskva, K-9, ul. Gor'kogo, 7, 8-I pod"ezd, 3-I etazh, U.S.S.R. (*Elektrosvyaz'*)

Elektrotechnik und Maschinenbau, Journal of the Elektrotechnischer Verein Österreichs, Springer Verlag, Wien 1, Molkerbastei 5, Austria. (*Elektrotech. u. Maschinenb.*)

Elektrotechnische Zeitschrift, Edition A & B, VDE-Verlag G.m.b.H., Berlin Charlottenburg 2, Bismarckstrasse 33, Germany. (*Elektrotech. Z.*)

Endeavour, Imperial Chemical Industries Ltd, North Block, Thames House, Millbank, London, S.W.1, England. (*Endeavour*)

Engineer, 28 Essex Street, London, W.C.2, England. (*Engineer, Lond.*)

Engineering, 36 Bedford Street, London, W.C.2, England. (*Engineering, Lond.*)

Ericsson Review, Telefonaktiebolaget L. M. Ericsson, Stockholm 32, Sweden. (*Ericsson Rev.*)

Ericsson Technics, as for Ericsson Review. (*Ericsson Tech.*)

F

Fizika Tverdogo Tela, Leningrad, V-164, Mendeleevskaya lin., 1, U.S.S.R. (*Fiz. Tverdogo Tela*)

Frequenz, Fachverlag Schiele & Schon G.m.b.H., Berlin S.W.61, Markgrafenstrasse 11, Germany. (*Frequenz*)

Funk-Technik, Verlag fur Radio-Foto-Kinotechnik G.m.b.H., Berlin-Borsigwalde, Eichborndamm 141–167, Germany. (*Funk Technik, Berlin*)

G

G.E.C. Journal, General Electric Company Ltd, Magnet House, Kingsway, London, W.C.2, England. (*G.E.C. J.*)

G.E.C. Telecommunications, General Electric Company Ltd, Coventry, England. (*G.E.C. Telecommun.*)

Geofisica Pura e Applicata, Istituto Geofisico Italiano, Milano, Piazza Leonardo da Vinci 12, Italy. (*Geofis. pura appl.*)

Geophysical Journal of the Royal Astronomical Society, Burlington House, London, W.1, England. (*Geophys. J. R. astr. Soc.*)

H

Helvetica Physica Acta, Journal of the Schweizerische Physikalische Gesellschaft, Birkhauser Verlag, Basel, Switzerland. (*Helv. phys. Acta*)

Hochfrequenztechnik und Elektroakustik, Akademische Verlagsgesellschaft Geest & Portig K. G., Leipzig C1, Sternwartenstr. 8, East Germany. (*Hochfrequenztech. u. Elektroakust.*)

I

IBM Journal of Research and Development, International Business Machines Corporation, 590 Madison Avenue, New York 22, N.Y., U.S.A. (*IBM J. Res. Developm.*)

Indian Journal of Physics (and Proceedings of the Indian Association for the Cultivation of Science), Jadavpur, Calcutta 32, India. (*Indian J. Phys.*)

Izvestiya Akademii Nauk S.S.S.R. (a) seriya fizicheskaya, Moskva, B-64, Podsosenskii per., 21, U.S.S.R., (b) seriya geofizicheskaya, Moskva, B. Gruzinskaya, 10, U.S.S.R., (c) otdelenie tekhnicheskikh nauk, Moskva, M. Khariton'evskii per., 4, U.S.S.R. (*Izv. Ak. Nauk S.S.S.R.*, (a) *ser. fiz.*, (b) *ser. geofiz.*, (c) *otd. tekh. nauk*)

J

Journal of the Acoustical Society of America, American Institute of Physics, 335 East 45th Street, New York 17, N.Y., U.S.A. (*J. acoust. Soc. Amer.*)

Journal of the American Ceramic Society, 20th and Northampton Streets, Easton, Pa, U.S.A. (*J. Amer. ceram. Soc.*)

Journal of Applied Physics, American Institute of Physics, 335 East 45th Street, New York 17, N.Y., U.S.A. (*J. appl. Phys.*)

Journal of Atmospheric and Terrestrial Physics, Pergamon Press Ltd, 4 & 5 Fitzroy Square, London, W.1, England. (*J. atmos. terr. Phys.*)

Journal of the Audio Engineering Society, P.O. Box 12, Old Chelsea Station, New York 11, N.Y., U.S.A. (*J. audio Engng Soc.*)

Journal of the British Institution of Radio Engineers, 9 Bedford Square, London, W.C.1, England. (*J. Brit. Instn Radio Engrs*)

Journal of the British Interplanetary Society, 12 Bessborough Gardens, London, S.W.1, England. (*J. Brit. interplan. Soc.*)

Journal of the Electrochemical Society, 1860 Broadway, New York 23, N.Y., U.S.A. (*J. electrochem. Soc.*)

Journal of Electronics and Control, Taylor & Francis Ltd, Red Lion Court, Fleet Street, London, E.C.4, England. (*J. Electronics Control*)

Journal of the Franklin Institute, Benjamin Franklin Parkway at Twentieth Street, Philadelphia 3, Pa, U.S.A. (*J. Franklin Inst.*)

Journal of Geomagnetism and Geoelectricity, Society of Terrestrial Magnetism and Electricity of Japan, Geophysical Institute, Kyoto University, Kyoto, Japan. (*J. Geomag. Geoelect.*)

Journal of Geophysical Research, 1515 Massachusetts Avenue, N.W., Washington 5, D.C., U.S.A. (*J. geophys. Res.*)

Journal of the Indian Institute of Science, Indian Institute of Science, Bangalore 12, India. (*J. Indian Inst. Sci.*)

Journal of the Institute of Navigation, John Murray Ltd, 50 Albemarle Street, London, W.1, England. (*J. Inst. Nav.*)

Journal of the Institution of Telecommunication Engineers, Post Box 481, New Delhi, India. (*J. Instn Telecommun. Engrs, India*)

Journal of Mathematics and Physics, Massachusetts Institute of Technology, Cambridge 39, Mass., U.S.A. (*J. Math. Phys.*)

Journal of Meteorology, Prince and Lemon Streets, Lancaster, Pennsylvania, U.S.A. (*J. Met.*)

Journal of the Optical Society of America, American Institute of Physics, 335 East 45th Street, New York 17, N.Y., U.S.A. (*J. opt. Soc. Amer.*)

Journal of the Physical Society of Japan, Maruzen Publishing Co., P.O. Box 605 Central, Tokyo, Japan. (*J. phys. Soc. Japan*)

The Journal of the Physics and Chemistry of Solids, Pergamon Press Ltd, 4 & 5 Fitzroy Square, London, W.1, England. (*J. Phys. Chem. Solids*)

Journal de Physique et le Radium, 12 place Henri Bergson, Paris 8e, France. (*J. Phys. Radium*)

Journal of the Radio Research Laboratories, Ministry of Posts and Telecommunications, Koganei-shi, Tokyo, Japan. (*J. Radio Res. Labs, Japan*)

Journal of Research of the National Bureau of Standards, U.S. Government Printing Office, Washington 25, D.C., U.S.A. (*J. Res. nat. Bur. Stand.*)

Journal of Scientific Instruments, 47 Belgrave Square, London, S.W.1, England. (*J. sci. Instrum.*)

Journal of the Society of Motion Picture and Television Engineers, 55 West 42nd Street, New York 36, N.Y., U.S.A. (*J. Soc. Mot. Pict. Telev. Engrs*)

Journal of the Television Society, 166 Shaftesbury Avenue, London, W.C.2, England. (*J. Telev. Soc.*)

M

Marconi Review, Marconi House, Chelmsford, England. (*Marconi Rev.*)

Metal Industry, Iliffe & Sons Ltd, Dorset House, Stamford Street, London, S.E.1, England. (*Metal Ind., Lond.*)

Metallurgia, 31 King Street West, Manchester 3, England. (*Metallurgia, Manchr*)

Meteorological Magazine, Her Majesty's Stationery Office, York House, Kingsway, London, W.C.2, England. (*Met. Mag., Lond.*)

Microtecnic, 23 Avenue de la Gare, Lausanne, Switzerland. (*Microtecnic*)

Modern Plastics, 575 Madison Avenue, New York 22, N.Y., U.S.A. (*Mod. Plast.*)

Monthly Notices of the Royal Astronomical Society, Burlington House, London, W.1, England. (*Mon. Not. R. astr. Soc.*)

Mullard Technical Communications, Mullard House, Torrington Place, London, W.C.1, England. (*Mullard tech. Commun.*)

N

Nachrichtentechnik, V.E.B. Verlag Technik, Berlin C2, Oranienburger Str. 13/14, East Germany. (*Nachr Tech.*)

Nachrichtentechnische Zeitschrift, F. Vieweg & Sohn, (20b) Braunschweig, Burgplatz 1, Germany. (*Nachrichtentech. Z.*)

Nature, Macmillan & Co. Ltd, St. Martin's Street, London, W.C.2, England. (*Nature, Lond.*)

Naturwissenschaften, Springer Verlag, Berlin-Wilmersdorf, Heidelberger Platz 3, Germany. (*Naturwissenschaften*)

Note Recensioni e Notizie, Istituto Superiore delle Poste e delle Telecomunicazioni, Viale Trastevere 189, Roma, Italy. (*Note Recensioni Notiz.*)

Nucleonics, 330 West 42nd Street, New York 36, N.Y., U.S.A. (*Nucleonics*)

Nuovo Cimento, Editore Nicola Zanichelli, Bologna, Via Irnerio 34, Italy. (*Nuovo Cim.*)

O

Observatory, Royal Greenwich Observatory, Herstmonceux Castle, Hailsham, Sussex, England. (*Observatory*)

l'Onde Électrique, Éditions Chiron, 40, rue de Seine, Paris 6e, France. (*Onde élect.*)

Optik, Wissenschaftliche Verlagsgesellschaft m.b.H., Stuttgart 1, Postfach 40, Germany. (*Optik, Stuttgart*)

P

Philips Research Reports, N.V. Philips' Gloeilampenfabrieken, Eindhoven, Netherlands. (*Philips Res. Rep.*)

Philips Technical Review, as for Philips Research Reports. (*Philips tech. Rev.*)

Philips Telecommunication Review, Philips Telecommunication Division, P.O. Box 32, Hilversum, Netherlands. (*Philips Telecommun. Rev.*)

Philosophical Magazine, Taylor & Francis Ltd, Red Lion Court, Fleet Street, London, E.C.4, England. (*Phil. Mag.*)

Philosophical Transactions of the Royal Society, Burlington House, Piccadilly, London, W.1, England. (*Phil. Trans.*)

Physica, Physica Foundation, Lucas Bolwerk 4, Utrecht, Netherlands. (*Physica*)

Physical Review, American Institute of Physics, 335 East 45th Street, New York 17, N.Y., U.S.A. (*Phys. Rev.*)

Physical Review Letters, American Institute of Physics, 335, East 45th Street, New York 17, N.Y., U.S.A. (*Phys. Rev. Lett.*)

Physics and Chemistry of Solids. See Journal of the Physics and Chemistry of Solids.

Point to Point Telecommunications, Communications Division, Marconi's Wireless Telegraph Co. Ltd, Chelmsford, England. (*Point to Point Telecommun.*)

Post Office Electrical Engineers' Journal, Engineer in Chief's Office, Alder House, Aldersgate Street, London, E.C.1, England. (*P.O. elect. Engrs' J.*)

Poste e Telecomunicazioni, Roma, Via della Vite 107, Italy. (*Poste e Telecomunicazioni*)

Priroda, Moskva, Tsentr, Malyi Khariton'evskii per., 4, U.S.S.R. (*Priroda, Mosk.*)

Proceedings of the Cambridge Philosophical Society (Mathematical and Physical Sciences), Cambridge University Press, Bentley House, 200 Euston Road, London, N.W.1, England. (*Proc. Camb. phil. Soc.*)

Proceedings of the Institute of Radio Engineers, 1 East 79th Street, New York 21, N.Y., U.S.A. (*Proc. Inst. Radio Engrs*)

Proceedings of the Institution of Electrical Engineers, Parts A, B and C, Savoy Place, London, W.C.2, England. (*Proc. Instn elect. Engrs*)

Proceedings of the Institution of Radio Engineers, Australia, Science House, 157 Gloucester Street, Sydney, N.S.W., Australia. (*Proc. Instn Radio Engrs Aust.*)

Proceedings of the Physical Society, 1 Lowther Gardens, Prince Consort Road, London, S.W.7, England. (*Proc. phys. Soc.*)

Proceedings of the Royal Society, Burlington House, Piccadilly, London, W.1, England. (*Proc. roy. Soc.*)

Progress of Theoretical Physics, The Publication Office, Yukawa Hall, Kyoto University, Kyoto, Japan. (*Progr. theor. Phys.*)

Q

QST, American Radio Relay League Inc., 38 La Salle Road, West Hartford 7, Conn., U.S.A. (*QST*)

Quarterly of Applied Mathematics, Brown University, Providence 12, R.I., U.S.A. (*Quart. appl. Math.*)

Quarterly Journal of Mathematics, Oxford University Press, Amen House, London, E.C.4, England. (*Quart. J. Math.*)

Quarterly Journal of Mechanics and Applied Mathematics, Oxford University Press, Amen House, London, E.C.4, England. (*Quart. J. Mech. appl. Math.*)

Quarterly Journal of the Royal Meteorological Society, 49 Cromwell Road, London, S.W.7, England. (*Quart. J. R. met. Soc.*)

R

Radio, Moskva, B-66, Novo-Ryazanskaya ul., 26, U.S.S.R. (*Radio, Mosk.*)

Radio & TV News, Ziff Davis Publishing Company, 434 South Wabash Avenue, Chicago 5, Ill., U.S.A. (*Radio TV News*)

Radio-Electronics, 154 West 14th St., New York 11, N.Y., U.S.A. (*Radio-Electronics*)

Radioschau, Technischer Verlag Erb, Wien VI, Mariahilferstrasse 71, Austria. (*Radioschau*)

Radiotekhnika, Moskva, K-9, ul. Gor'kogo, 7, 3-I pod"ezd, U.S.S.R. (*Radiotekhnika, Mosk.*)

Radiotekhnika i Elektronika, Moskva, K-9, Mokhovaya, 11, U.S.S.R. (*Radiotekhnika i Elektronika*)

RCA Review, RCA Laboratories, Princeton, N.J., U.S.A. (*RCA Rev.*)

Referativnyi Zhurnal, Fizika, Moskva, D-129, Baltiiskaya ul., 14, U.S.S.R. (*Referativnyi Zh. Fiz.*)

Report of Ionosphere Research in Japan, Ionosphere Research Committee, Science Council of Japan, Ueno Park, Tokyo, Japan. (*Rep. Ionosphere Res. Japan*)

Reports of the Electrical Communication Laboratory, Nippon Telegraph and Telephone Public Corporation, 1551 Kichijoji, Musashino-shi, Tokyo, Japan. (*Rep. elect. Commun. Lab., Japan*)

Research, Butterworth's Scientific Publications Ltd, 88 Kingsway, London, W.C.2, England. (*Research, Lond.*)

Review of Scientific Instruments, American Institute of Physics, 335 East 45th Street, New York 17, N.Y., U.S.A. (*Rev. sci. Instrum.*)

Reviews of Modern Physics, American Institute of Physics, 335 East 45th Street, New York 17, N.Y., U.S.A. (*Rev. mod. Phys.*)

Revista Española de Electrónica, Apartado 5252, Barcelona, Spain. (*Rev. española Electrónica*)

Revista de Telecomunicación, Palacio de Comunicaciones, Madrid, Spain. (*Rev. Telecomunicación, Madrid*)

Revista Telegrafica Electrónica, Arbó Editores, Buenos Aires, Argentina. (*Rev. telegr. Electronica, Buenos Aires*)

Revue générale de l'Électricité, 12 place Henri-Bergson, Paris 8e, France. (*Rev. gén. Élect.*)

Revue HF, 55 rue Defacqz, Bruxelles, Belgium. (*Rev. HF, Brussels*)

Revue d'Optique, 3 & 5 Boulevard Pasteur, Paris 15e, France. (*Rev. d'Optique*)

Ricerca scientifica, Consiglio Nazionale delle Ricerche, Piazzale delle Scienze, 7, Roma, Italy. (*Ricerca sci.*)

R.S.G.B. Bulletin, New Ruskin House, Little Russell Street, London, W.C.1, England. (*R.S.G.B. Bull.*)

Rundfunktechnische Mitteilungen, H. H. Nolke G.m.b.H., Hamburg 20, Hegestrasse 40, Germany. (*Rundfunktech. Mitt.*)

S

Science, 1515 Massachusetts Avenue, N.W., Washington 5, D.C., U.S.A. (*Science*)

Science Reports of the Research Institutes Tohoku University, Series A and B, Tohoku University, Sendai, Japan. (*Sci. Rep. Res. Inst. Tohoku Univ.*)

Short Wave Magazine, 55 Victoria Street, London, S.W.1, England. (*Short Wave Mag.*)

Sylvania Technologist, Sylvania Electric Products Inc., Bayside, N.Y., U.S.A. (*Sylvania Technologist*)

T

Technical News Bulletin of the National Bureau of Standards, U.S. Government Printing Office, Washington 25, D.C., U.S.A. (*Tech. News Bull. nat. Bur. Stand.*)

Technische Mitteilungen aus dem Betriebslaboratorium für Rundfunk und Fernsehen, Agastrasse, Berlin-Adlershof, East Germany. (*Tech. Mitt. BRF, Berlin*)

Technische Mitteilungen PTT, Journal of the Swiss Post Office, Bern, Speichergasse 6, Switzerland. (*Tech. Mitt. PTT*)

Telefunken Zeitung, Telefunken G.m.b.H., Berlin-Charlottenburg 1, Ernst-Reuter Platz, Haus der Elektrizitat, Germany. (*Telefunken Ztg*)

Télévision, 42 rue Jacob, Paris 6e, France. (*Télévision*)

Tellus, Linnhagensgatan 124, Stockholm, Sweden. (*Tellus*)

Tijdschrift van het Nederlands Radiogenootschap, Jagtlustlaan 3, Santpoort-Zuid, Netherlands. (*Tijdschr. ned. Radiogenoot.*)

Toute la Radio, 9 rue Jacob, Paris 6e, France. (*Toute la Radio*)

Transactions of the Institute of Radio Engineers, 1 East 79th Street, New York 21, N.Y., U.S.A. (*Trans. Inst. Radio Engrs*)

Transactions of the South African Institute of Electrical Engineers, The Associated Scientific and Technical Societies of South Africa, P.O. Box 5907, Johannesburg, South Africa. (*Trans. S. Afr. Inst. elect. Engrs*)

TSF et TV, Éditions Chiron, 40 rue de Seine, Paris 6e, France. (*TSF et TV*)

U

Uspekhi Fizicheskikh Nauk, Moskva, V-71, Leninskii Prospekt, 15, U.S.S.R. (*Usp. fiz. Nauk*)

V

Le Vide, Journal of the Societe française des Ingenieurs et Techniciens du Vide, 44 rue de Rennes, Paris 6e, France. (*Le Vide*)

W

Weather, 49 Cromwell Road, London, S.W.7, England. (*Weather*)

Wireless World, Iliffe & Sons Ltd, Dorset House, Stamford Street, London, S.E.1, England. (*Wireless World*)

Z

Zeitschrift für angewandte Mathematik und Physik, Birkhauser Verlag, Basel, Switzerland. (*Z. angew. Math. Phys.*)

Zeitschrift für angewandte Physik, Springer-Verlag, Berlin-Wilmersdorf, Heidelberger Platz 3, Germany. (*Z. angew. Phys.*)

Zeitschrift fur Metallkunde, Dr. Riederer Verlag G.m.b.H., Stuttgart, Marienstrasse 52, Germany. (*Z. Metallkde*)

Zeitschrift fur Meteorologie, Akademie Verlag G.m.b.H., Berlin W.1, Leipziger Strasse 3–4, East Germany. (*Z. Met.*)

Zeitschrift für Naturforschung, (14b) Tubingen, Postfach 61, Germany. (*Z. Naturf.*)

Zeitschrift für Physik, Springer-Verlag, Berlin, Wilmersdorf, Heidelberger Platz 3, Germany. (*Z. Phys.*)

Zhurnal eksperimental'noi i teoreticheskoi Fiziki, Moskva, V-133, Vorob'evskoe shosse, 2, U.S.S.R. (*Zh. eksp. teor. Fiz.*)

Zhurnal tekhnicheskoi Fiziki, Leningrad V-164, Mendeleevskaya lin., 1, U.S.S.R. (*Zh. tekh. Fiz.*)

june 1960
the
institute
of
radio
engineers

Proceedings of the IRE

report of the
Television Allocations Study Organization

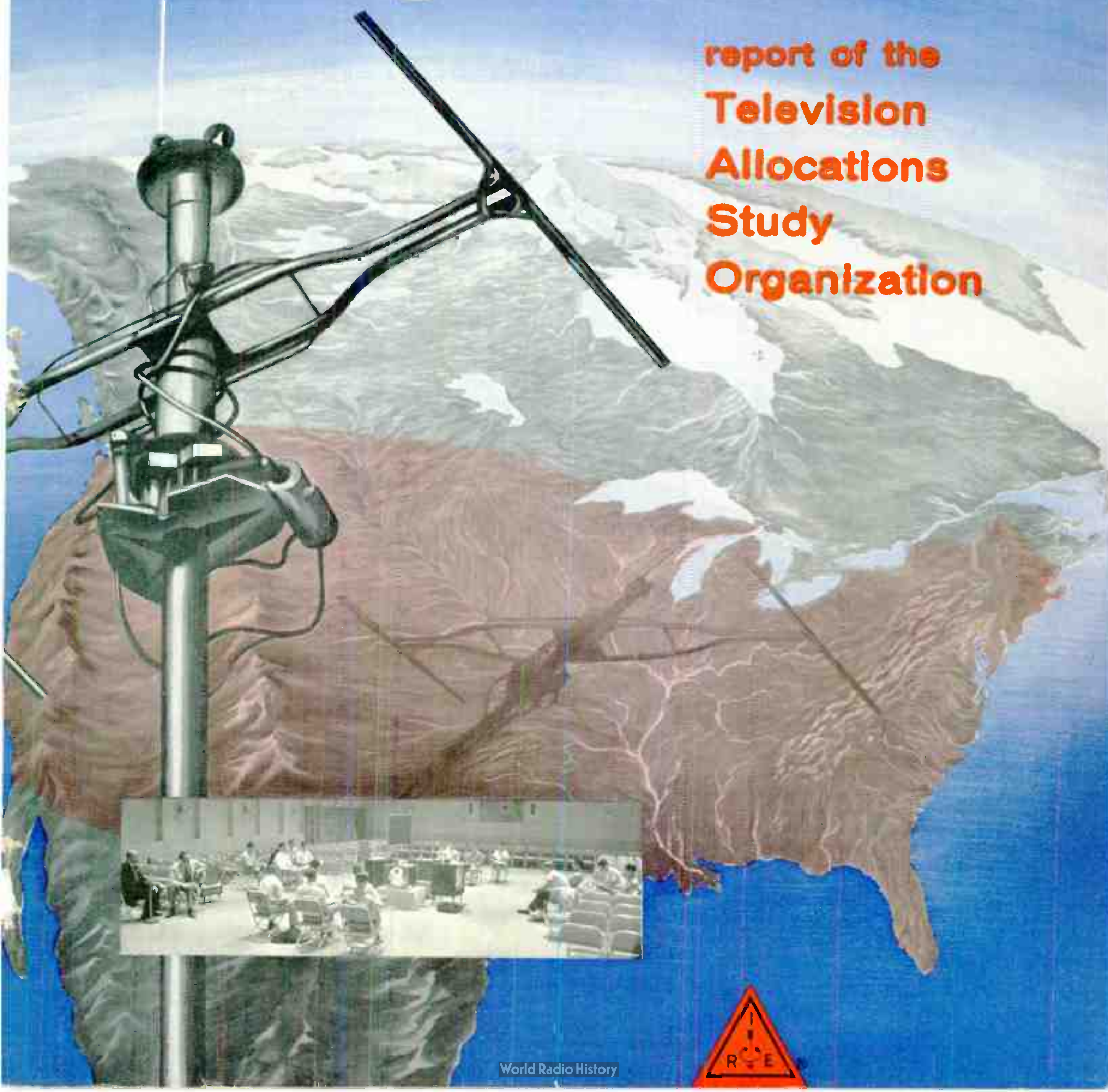

I R E

NEW*

Revolutionary† DO-T and DI-T TRANSISTOR TRANSFORMERS

FROM STOCK—Hermetically Sealed to MIL-T-27A Specs.

TRANSFORMERS PICTURED ACTUAL SIZE

DO-T: 5/16 Dia. x 13/32", 1/10 Oz.; DI-T: 5/16 Dia. x 1/4", 1/20 Oz.

There is no transformer even twice the size of the DO-T and DI-T series which has as much as 1/10th the power handling ability . . . which can equal the efficiency . . . or equal the response range. And none to approach the reliability of the DO-T and DI-T units (proved to, but exceeding MIL-T-27A grade 4).

High Power Rating	up to 10 times greater.
Excellent Response	twice as good at low end.
Low Distortion	reduced 80%.
High Efficiency	up to 30% better . . . compare DCR.
Moisture Proof	hermetically sealed to MIL-T-27A.
Rugged	completely metal cased.
Anchored Leads	will withstand 10 pound pull test.
Printed Circuit Use	(solder melting) plastic insulated leads.
Suited to Clip Mounting	use Augat #6009-8A clip.

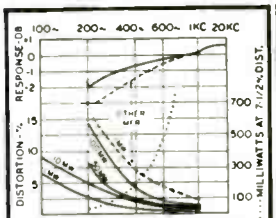

TYPICAL DO-T PERFORMANCE
SOURCE: RATED PRI. IMP. AND D.C.
LOAD: RATED SEC. IMP.

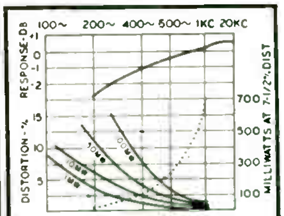

TYPICAL DI-T PERFORMANCE
SOURCE: RATED PRI. IMP. AND D.C.
LOAD: RATED SEC. IMP.

DO-T No.	Pri. Imp.	D.C. Ma.‡ in Pri.	Sec. Imp.	Pri. Res. DO-T	Pri. Res. DI-T	Mw. Level	DI-T No.
DO-T1	20,000 30,000	.5 .5	800 1200	850	815	50	DI-T1
DO-T2	500 600	3 3	50 60	60	65	100	DI-T2
DO-T3	1000 1200	3 3	50 60	115	110	100	DI-T3
DO-T4	600	3	3.2	60		100	
DO-T5	1200	2	3.2	115	110	100	DI-T5
DO-T6	10,000	1	3.2	790		100	
DO-T7	200,000 500	0 0	1000 100,000	8500 —		25	
	Reactor 2.5 Hys./2 Ma., .9 Hy./4 Ma				630		DI-T8
DO-T8	" 3.5 Hys./2 Ma., 1 Hy./5 Ma.			630			
DO-T9	10,000 12,000	1 1	500 CT 600 CT	800	870	100	DI-T9
DO-T10	10,000 12,500	1 1	1200 CT 1500 CT	800	870	100	DI-T10
DO-T11	10,000 12,500	1 1	2000 CT 2500 CT	800	870	100	DI-T11
DO-T12	150 CT 200 CT	10 10	12 16	11		500	
DO-T13	300 CT 400 CT	7 7	12 16	20		500	
DO-T14	600 CT 800 CT	5 5	12 16	43		500	
DO-T15	800 CT 1070 CT	4 4	12 16	51		500	
DO-T16	1000 CT 1330 CT	3.5 3.5	12 16	71		500	
DO-T17	1500 CT 2000 CT	3 3	12 16	108		500	
DO-T18	7500 CT 10,000 CT	1 1	12 16	505		500	
DO-T19	300 CT	7	600	19	20	500	DI-T19
DO-T20	500 CT	5.5	600	31	32	500	DI-T20
DO-T21	900 CT	4	600	53	53	500	DI-T21
DO-T22	1500 CT 600	3 5	600 1500 CT	86 —	87	500	DI-T22
DO-T23	20,000 CT 30,000 CT	.5 .5	800 CT 1200 CT	850	815	100	DI-T23
DO-T24	200,000 CT 500 CT	0 0	1000 CT 100,000 CT	8500 —		25	
DO-T25	10,000 CT 12,000 CT	1 1	1500 CT 1800 CT	800	870	100	DI-T25
	Reactor 4.5 Hys./2 Ma., 1.2 Hys./4 Ma.				2300		DI-T26
DO-T26	" 6 Hys./2 Ma., 1.5 Hys./5 Ma.			2100			
	Reactor .9 Hy./2 Ma., .5 Hy./6 Ma.				105		DI-T27
DO-T27	" 1.25 Hys./2 Ma., .5 Hy./11 Ma.			100			
	Reactor .1 Hy./4 Ma., .08 Hy./10 Ma.				25		DI-T28
DO-T28	" .3 Hy./4 Ma., .15 Hys./20 Ma.			25			
DO-T29	120 CT 150 CT	10 10	3.2 4	10		500	
DO-T30	320 CT 400 CT	7 7	3.2 4	20		500	
DO-T31	640 CT 800 CT	5 5	3.2 4	43		500	
DO-T32	800 CT 1000 CT	4 4	3.2 4	51		500	
DO-T33	1060 CT 1330 CT	3.5 3.5	3.2 4	71		500	
DO-T34	1600 CT 2000 CT	3 3	3.2 4	109		500	
DO-T35	8000 CT 10,000 CT	1 1	3.2 4	505		100	
DO-T36	10,000 CT 12,000 CT	1 1	10,000 CT 12,000 CT	950	970	100	DI-T36
*DO-T37	2000 CT 2500 CT	3 3	8000 Split 10,000 Split	195		100	
*DO-T38	10,000 CT 12,000 CT	1 1	2000 Split 2400 Split	560		100	
*DO-T39	20,000 CT 30,000 CT	.5 .5	1000 Split 1500 Split	800		100	
*DO-T40	40,000 CT 50,000 CT	.25 .25	400 Split 500 Split	1700		50	
*DO-T41	400 CT 500 CT	8 6	400 Split 500 Split	46		500	
*DO-T42	400 CT 500 CT	8 6	120 Split 150 Split	46		500	
*DOT-43	400 CT 500 CT	8 6	40 Split 50 Split	46		500	
*DO-T44	80 CT 100 CT	12 10	32 Split 40 Split	9.8		500	
DO-TSH	Drawn Hipermalloy shield and cover 20/30 db						DI-TSH

‡ DCMA shown is for single ended useage (under 5% distortion—100MW—1KC) . . . for push pull, DCMA can be any balanced value taken by .5W transistors (under 5% distortion—500MW—1KC)

† DO-T & DI-T units designed for transistor application only. Pats. Pend.

* DO-T37 thru DO-T44 newly added to series.

And Special Units to Your Specifications

UNITED TRANSFORMER CORPORATION

150 Varick Street, New York 13, N. Y.

PACIFIC MFG. DIVISION: 4008 W. JEFFERSON BLVD., LOS ANGELES 16, CALIF.

EXPORT DIVISION: 13 EAST 40th STREET, NEW YORK 16, N. Y. CABLES: "ARLAB"

VOLUME 48, NUMBER 6, PART I

June, 1960

published monthly by The Institute of Radio Engineers, Inc.

Proceedings of the IRE®

contents

COVER

The shadow of a television transmitting antenna falling across the United States is suggestive of the special nature of this issue, which presents the results of a 2½ year study by the Television Allocations Study Organization of technical factors related to television channel allocation.

published monthly by The Institute of Radio Engineers, Inc.

Proceedings of the IRE®

continued

PROCEEDINGS OF THE IRE, published monthly by The Institute of Radio Engineers, Inc. at 1 East 79 Street, New York 21, N. Y. Manuscripts should be submitted in triplicate to the Editorial Department. Responsibility for contents of papers published rests upon the authors, and not the IRE or its members. All republication rights, including translations, are reserved by the IRE and granted only on request. Abstracting is permitted with mention of source.
Thirty days advance notice is required for change of address. Price per copy: members of the Institute of Radio Engineers, one additional copy $1.25; non-members $3.00. Yearly subscription price: to members $9.00, one additional subscription $13.50; to non-members in United States, Canada, and U. S. Possessions $18.00; to non-members in foreign countries $19.00. Second-class postage paid at Menasha, Wisconsin under the act of March 3, 1879. Acceptance for mailing at a special rate of postage is provided for in the act of February 28, 1925, embodied in Paragraph 4, Section 412, P. L. and R., authorized October 26, 1927. Printed in U.S.A.

June, 1960
Vol. 48 No. 6

Proceedings of the IRE

Poles and Zeros

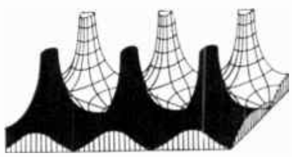

TASO: This Special Issue of the PROCEEDINGS publishes results of a study carried out by the Television Allocations Study Organization. At the request of the Federal Communications Commission the Study Organization was formed, in 1956, by the television industry. The object of the study was "to develop full, detailed and reliable technical information, and engineering principles based thereon, concerning present and potential VHF and UHF television service."

The Professional Group on Broadcasting, through the intense interest and cooperation of its members, has assembled this Special Issue. The Editorial Board expresses its appreciation to the many PGBC members who helped by reviewing the papers; to the Administrative Committee of the PGBC for providing the underlying support; to Raymond F. Guy, former IRE President, for encouragement and help; and, in particular, special thanks to the PGBC Chairman, George F. Hagerty, and to George R. Town, formerly Executive Director of TASO.

The findings of the two and one-half year study comprise an assembly of vital new information which is of inestimable value nationally and internationally. A perusal of the issue will demonstrate how effectively and thoroughly TASO consummated its assigned task. The PROCEEDINGS is pleased to be the vehicle to publish this work for the profession.

Research Goals: A Conference on Research Goals, sponsored by the National Science Foundation in cooperation with fifteen professional societies (of which IRE was one), was held last December at Worcester Polytechnic Institute under the chairmanship of Arthur Bronwell, President of Worcester Polytechnic Institute. Through President Bronwell's cooperation, Poles and Zeros is making a brief report on this Conference to the IRE membership.

The specific question posed to the Conference was: "How can young research scientists and engineers be brought more stimulatively, imaginatively, and creatively into contact with the frontiers of science and technology in such a way as to accelerate significant discovery, both in the advancement of science and in translation of science into new technology?" Fifty-one of the nation's leading educators, research scientists, and engineers examined the basic issues in a two-day session. Out of this examination emerged the general conclusion that "Our nation's scientific and technological progress could be greatly accelerated if conditions more favorable to achieving bold, imaginative pioneering in basic research and in technological innovation could be realized."

The detailed report of the Conference includes specific recommendations to colleges and universities and to scientific and engineering societies. The seven recommendations to scientific and engineering societies follow:

"1. Establish more effective practices which will increase the attendance and participation of talented, young members at meetings of scientific and engineering societies. Develop programs which will bring these young people into stimulative personal association with leading scientists and engineers.

"2. Encourage the presentation and publication of papers of a philosophical nature which look to the future of science and technology. Invited speakers, who are pioneers in research thought, could do much to lift the visions and ambitions of talented young people to more promising research goals.

"3. Develop comprehensive programs for digesting the state of the art. Young people are confused by the disorganized state of research knowledge. A comprehensive study, now completed as a project of the National Science Foundation, which outlines the state of the art and future research possibilities in the various fields of astronomy is the sort of compilation which could be exceedingly helpful in many fields.

"4. Establish society meetings for the purpose of developing a more effective interchange of ideas between scientists and engineers in research areas of broad mutual interest This cross-fertilization of ideas among scientists and engineers is becoming increasingly important and is not nearly as effective as it should be.

"5. Establish free forums at engineering society conventions where any member can make a short presentation of his creative work, allowing the widest latitude of subject matter, with no publication requirement, except in abstract form. These presentations should be handled without critical review by society committees, which occasionally emasculate original work. Such sessions are regular practice in some scientific societies but as yet have not been adopted by the engineering societies. They provide rapid interchange of experiences and a highly effective means of bringing current research to the attention of the society membership without cluttering up the publications.

"6. Actively promote and encourage financial support for research. Consider the possibility of the Society itself sponsoring research using funds contributed by industry. Some trade associations have been highly effective in this kind of operation.

"7. Recognizing that creativity begins in the individual at an early age, foster among the Society members a recognition of the contribution which they can make individually by stimulating the creative development of youth. This can be accomplished by undertaking youth projects in their own homes, by youth programs developed in their business establishments, or by other means which will encourage young people to develop ideas and which will give them the means of implementation."

The IRE should consider the extent to which it is already achieving the intent of these recommendations and the steps that it might institute to further achieve these desirable goals.

—F.H., Jr.

P. E. Haggerty

Director, 1960

Patrick E. Haggerty (A'45–SM'53–F'58) was born March 17, 1914 in Harvey, N. D. He received the B.S.E.E. degree in 1936 from Marquette University, Milwaukee, Wis. From 1949 to 1951 he did part-time graduate work at Southern Methodist University, Dallas, Texas. In 1959 he received an honorary LL.D. degree from St. Mary's University, San Antonio, Texas.

From 1935 to 1942 he was employed by the Badger Carton Company, Milwaukee, Wis. While still a student, he worked at the company as a cooperative student engineer. Following graduation he became production manager of the company. He later became Assistant General Manager with responsibility for all engineering, manufacturing and administrative functions except sales.

During World War II he served as a lieutenant, U. S. Naval Reserve, in the Bureau of Aeronautics, Department of the Navy, Washington, D. C. In 1945 he joined Geophysical Service Inc. as General Manager of the Laboratory and Manufacturing Division. This organization eventually became the company that is now known as Texas Instruments Inc. In 1950 Mr. Haggerty became Executive Vice President and Director of Texas Instruments, and in 1959 he was elected President. He also serves as Director or officer in major wholly-owned subsidiaries.

Mr. Haggerty is Section Advisor for the Dallas Section of the IRE. He is a member of the General Management Division Planning Council of the American Manufacturers Association; a member of the Board of Directors of Texas Manufacturers Association; and a former vice chairman of the Board of Trustees of the National Security Industrial Association. He is also a member of the American Association for the Advancement of Science, the Society for Exploration Geophysicists, the American Ordnance Association, and the Navy League of the United States, Sigma Phi Delta, Tau Beta Pi and Alpha Sigma Nu.

The Television Allocations Study Organization—A Summary of Its Objectives, Organization and Accomplishments*

GEORGE R. TOWN†, FELLOW, IRE

Summary—**During the past three years, a comprehensive study has been made of the engineering factors underlying the allocation of frequencies for television broadcasting. This work has been carried on by an industry-wide group known as the Television Allocations Study Organization (TASO). This paper outlines the objectives and organization of TASO, and summarizes the more significant findings relating to field strength measurement and analysis, field tests of television reception, laboratory studies of television picture quality, tropospheric wave propagation, and performance of receiving and transmitting equipment. The performance capabilities of UHF and VHF television broadcasting systems are compared.**

Objectives and Organization of TASO

The Television Allocations Study Organization was established late in 1956 by the television industry, in response to a request by the Federal Communications Commission (FCC) that a study be conducted of "the technical principles which should be applied in television channel allocation." Five organizations representing both television broadcasters and manufacturers of television equipment joined to sponsor TASO. These were the Association of Maximum Service Telecasters, representing high-power, principally-VHF broadcasters; the Committee for Competitive Television, representing UHF broadcasters; the Electronic Industries Association, representing manufacturers; the Joint Council on Educational Television, representing those interested in educational uses of television; and the National Association of Broadcasters, representing broadcasters in general. Representatives of these five organizations formed the TASO Board of Directors, the policy making group. These five organizations also paid the administrative expenses of TASO, while the operating expenses were borne by these same groups and by contributions from many broadcasters and manufacturers.

The objectives of TASO were stated as follows in the "Charter" which was drawn up by the Board of Directors. "The objectives of the organization shall be to develop full, detailed and reliable technical information, and engineering principles based thereon, concerning present and potential UHF and VHF television service. . . . TASO's functions shall be limited solely to technical study, fact finding and investigation, and interpretation of technical data." This statement was approved by the FCC.

* Original manuscript received by the IRE, January 22, 1960.
† College of Engineering, Iowa State University, Ames; formerly Executive Director, Television Allocations Study Organization.

After considering various alternatives, the Board of Directors concluded that the necessary studies should be carried on by groups, or panels, of engineers representing all phases of the television industry, in much the same manner that the standards for monochrome and for color television had been developed by the first and second National Television System Committees. The Board also concluded that a full-time executive director should administer the affairs of TASO during the most active part of its existence.

An analysis of the task facing TASO indicated that the engineering factors affecting television allocations could be divided into several classes. The first of these related to the characteristics of equipment, both transmitting and receiving. The second concerned wave propagation phenomena in both the service and interfering areas of a transmitter, and included the development of specifications for measuring field strength, the collection of propagation data, and the analysis of these data. The third factor was a determination of the limiting amounts of interference of various types which could be tolerated, still retaining a television picture which was satisfactory to the average observer. The fourth necessary task was a field study of television reception. Finally, there was the problem of the over-all analysis of the technical performance of the television system.

Six panels were established to carry out assignments roughly in accord with this outline of the tasks. The names of these panels and of their chairmen follow.

- Panel 1—Transmitting Equipment, William J. Morlock;
- Panel 2—Receiving Equipment, William O. Swinyard;
- Panel 3—Field Tests, Knox McIlwain;
- Panel 4—Propagation Data, Frank G. Kear;
- Panel 5—Analysis and Theory, Robert M. Bowie;
- Panel 6—Levels of Picture Quality, Charles E. Dean.

A total of over 40 committees, subcommittees, and task forces carried out studies of particular topics within the framework of the panel structure. The chairmen and vice chairmen of the panels, together with the executive director, formed the Panel Coordinating Committee, which had over-all responsibility for the engineering program. The organizational structure of TASO can best be visualized by study of Fig. 1.

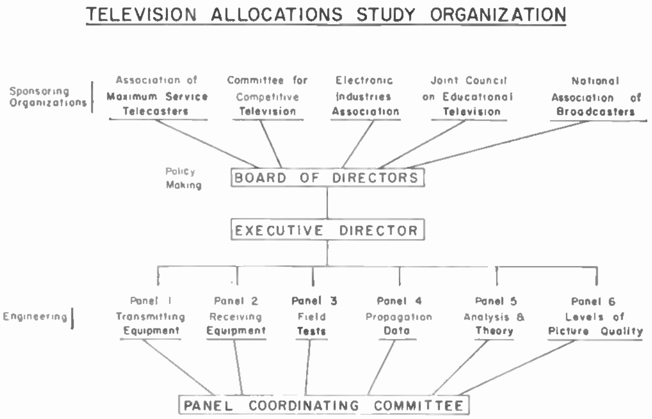

Fig. 1—TASO organization chart.

A few statistics regarding the operation of TASO indicate the extent of its activities. A total of 271 leading engineers from 139 companies composed the membership of the six panels and their subsidiary committees. These men came from literally all branches of the television industry—from manufacturers of television transmitting, receiving, and measuring equipment, from television networks, from individual high- and low-power, UHF and VHF broadcasting stations, from consulting engineering firms, from educational institutions, from governmental agencies, from community television distribution groups, from technical publishing houses, and from the television service industry. Among them were 43 Fellows of the IRE. There were over 150 formal meetings of the Board of Directors, the Panel Coordinating Committee and the six panels, plus many meetings of committees, subcommittees, and task forces. A total of over 750 formal documents were issued by the TASO office. These ranged from single page agendas of meetings to reports hundreds of pages in length. The greatest activity in TASO extended over a period of 27 months, though some important activities were not completed for another nine months. The major product of TASO was a series of detailed engineering reports covering the work, the findings, and the conclusions of the panels and task forces. These reports, and other significant work of TASO, were summarized in a 731-page book, the over-all TASO report, entitled "Engineering Aspects of Television Allocations." The first copy of this report was presented to Chairman Doerfer of the FCC on March 16, 1959, and printed copies became generally available on June 12, 1959.

Summary of General Accomplishments of TASO

The following papers in this group of TASO papers give details of major engineering accomplishments of the organization. The remainder of this paper will be devoted to a summary of the more significant results of a general nature. First, however, the boundaries of the activities of TASO will be noted.

TASO did not undertake any cooperative equipment development or research. Prior to the establishment of TASO, the FCC stated its wish for a crash, all-industry, joint development program of UHF equipment. The television industry rejected this proposal as impracticable, in part because of patent considerations and antitrust laws. TASO's equipment studies were confined to equipment presently available commercially. Predictions of the nature of future equipment were not undertaken nor, in fact, even considered by the panels. This limitation in the scope of activity was made necessary by interpretations of the antitrust laws which prohibit joint activities by competing companies which might be considered to constitute lack of individual freedom in future designs or prices. It was, in fact, necessary for TASO to obtain assurance from the Department of Justice that its activities, within the scope of its charter, were not illegal before the work of the panels could proceed.

TASO did not undertake the preparation of an allocations plan. Such a plan is obviously dependent upon other considerations, in addition to engineering factors. TASO limited its activities to a consideration of engineering factors only. These should be basic to any allocations plan; but the preparation of such a plan is the responsibility of the FCC. It might be noted parenthetically that the decision to concentrate on engineering problems only, and to determine authoritatively the engineering facts, was probably the principal reason that the organizations sponsoring TASO, with their diverse and sometimes conflicting interests, could join in such an industry-wide endeavor.

Field Strength Measurements and Analysis

Turning now to technical accomplishments, one of the most significant was the collection and analysis of a large body of reliable data on the propagation of UHF and VHF signals within the service range of television stations. TASO was, of course, far from the first to collect this type of information. Prior to the TASO operations, however, relatively little data had been taken in the UHF television band; and at both UHF and VHF, measurements had been made in such a wide variety of manners that the results of different studies could not properly be compared. One of TASO's first tasks, therefore, was to draw up acceptable specifications whereby measurements of field strength would be made in a standard manner. These specifications were followed in all of the TASO studies of signal propagation within the service area.

Extensive field strength surveys were conducted at Baton Rouge, La., Buffalo, N. Y., Columbia, S. C., Fresno, Calif., Madison, Wis., New Orleans, La., Philadelphia, Pa., and Wilkes-Barre, Pa. Additional data taken at Albany, N. Y., Boston, Mass., Charlotte, N. C., Dallas, Tex., and Indianapolis, Ind., were made available to TASO. The areas chosen for the TASO surveys were selected because both UHF and VHF stations of comparable power output and quite closely adjacent transmitting antennas of comparable heights were available as signal sources. In addition, a wide variety of topographic and climatic conditions were represented. This field strength measurement program provided an excellent set of reliable data.

The analysis of the field strength data resulted in the development of improved means for predicting field strength. These included the preparation of propagation curves, essentially relating median field strength and distance from the transmitter, and the development of means for estimating with reasonable accuracy local deviations from these median curves. Pertinent factors involved in these latter calculations include meteorological conditions, path topography, and forestation in the vicinity of the receiving antenna. The development of the prediction means was based on both theoretical analysis and empirical studies of field-strength data. The recommended curves of median field strength as a function of distance are the theoretical smooth earth curves, using an effective radius of the earth appropriate to existing meteorological conditions, and with empirically determined correction factors of −1 db in the low VHF band, −4 db in the upper VHF band, and −22 db in the UHF band.

Frequency is obviously a most significant parameter in propagation studies, and is of major interest in allocation studies. Many measurements were made in such a manner as to permit a direct comparison between UHF and VHF fields. Generalizations drawn from such comparisons are fraught with danger, since such pertinent factors as transmitting-antenna height and location, exact path profile, and exact time of measurement are never entirely the same. Nevertheless, the results of some such comparisons will be given as an indication of trends.

The quantities compared are median values of UHF and VHF field strength taken from continuous runs at least 100 feet in length, at a receiving antenna height of 30 feet. Comparisons are also made between the variation in UHF and VHF field strengths along such runs. The results obtained from 1232 pairs of such runs (one at UHF, the other at VHF) along 60 radials in eight geographical areas across the country are shown in Figs. 2 and 3, in which the data from all comparisons in any one area are averaged and represented by one point. In Fig. 2, the ratio of the VHF to the UHF field strength per kilowatt of effective radiated power is shown as a function of carrier frequency f and transmitting-antenna height h, these two quantities being combined as the ratio $h_v f_u^{1/2}/h_u f_v^{1/2}$, the subscripts u and v designating UHF and VHF respectively. Except for Wilkes-Barre, where the terrain is exceptionally rugged, and New Orleans, where there was some question as to whether the power of the UHF transmitter was actually as high as reported, the data can be represented reasonably well by a straight line. In Fig. 3, the average ratio D of the maximum to the minimum field strengths, measured along the single continuous runs in the same eight geographical areas, is plotted as a function of the square root of the carrier frequency. Again, a straight line represents most of the data reasonably well. The points taken at Wilkes-Barre are again high. Here, runs of 500 feet were taken, thus making it more probable that deep nulls would be encountered than in the 100-foot runs taken elsewhere. The values of D obtained from the Wilkes-Barre data would thus be expected to be high. Part of the area around

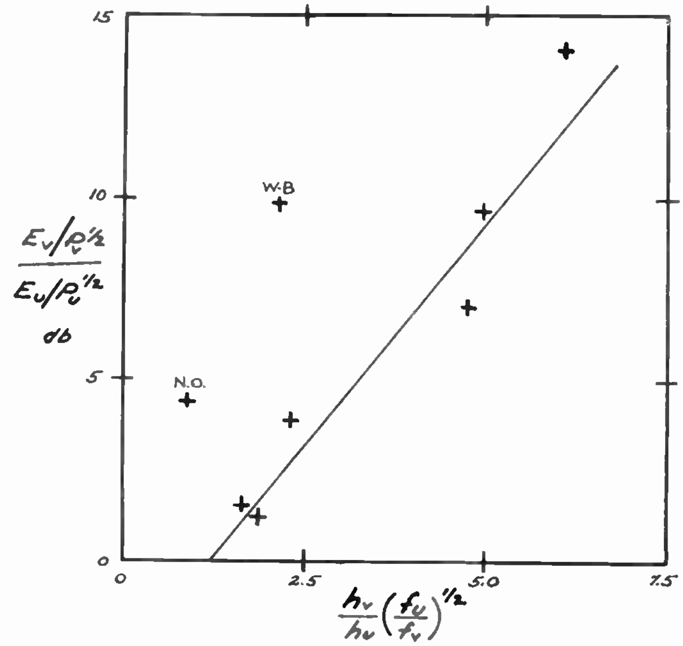

Fig. 2—Average ratio of VHF to UHF field strength per kilowatt of effective radiated power as a function of carrier frequency and transmitting antenna height.

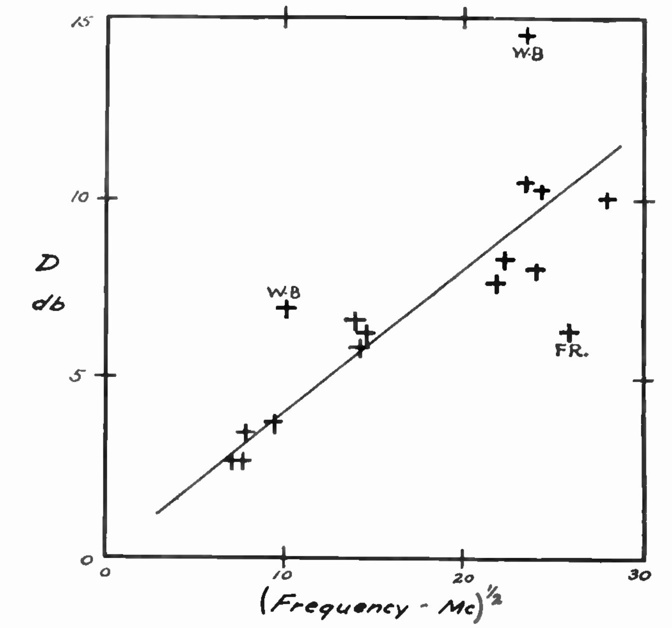

Fig. 3—Average ratio of maximum to minimum field strength along short paths as a function of carrier frequency.

Fresno was exceedingly flat and quite treeless, resulting in a low value of D. It is not suggested that Figs. 2 and 3 would give valid results if applied to other specific locations. The plotted points do, however, represent accurately the data which were taken, and the curves indicate the trends shown by the data which were taken in areas of average terrain and vegetation. In rough areas, the advantage of VHF over UHF is greater than indicated by the curve of Fig. 2. In flat, unvegetated areas, UHF shows to a greater advantage. In fact, in such areas and within line-of-sight distances, UHF field strength is frequently higher than VHF field strength for equal effective radiated powers and transmitting-antenna heights.

The significance of local conditions on received field strength is so important that it is worthwhile to give a few illustrations. A most striking case was that of a radial at New Orleans which ran northward across the 22-mile long Lake Pontchartrain bridge. Along the flat unobstructed path across the bridge, the UHF (507.25 mc) field strength averaged 8.1 db higher than the VHF (205.25 mc) field strength. Immediately to the north of the bridge, however, the UHF field strength dropped suddenly, and over the next 20 miles to the north it averaged 11.6 db lower than the VHF field strength. Another striking case occurred on a radial running southward from the Fresno transmitters, which are located on mountain tops overlooking Fresno and the San Joaquin Valley. In the foothills and rolling country near the stations, the VHF (209.75 mc) field strength averaged 5.2 db higher than the UHF (669.25 mc) field strength. Along the next 80 miles across the flat, almost treeless valley, the UHF field strength averaged higher by 9.2 db. As soon as the rolling country approaching the foothills on the far side of the valley was reached, the UHF field strength dropped to an average of 6.2 db below the VHF field strength. Because of the extremely high location of the transmitting antennas, essentially the entire length of this radial was within line-of-sight from both transmitters. With terrain which approached ideal, line-of-sight, flat, unobstructed conditions, the fields varied with frequency in accord with the smooth-earth theory of wave propagation, but under less ideal conditions, UHF performance deteriorated rapidly. Over-all, throughout the eight geographical regions covered by the TASO measurements, UHF field strength averaged 7.5 db lower than low-band VHF field strength and 4.5 db lower than high-band VHF field strength, all on the basis of equal effective radiated power. All but one set of UHF measurements were made in the lower half of the UHF television band.

It should be noted that these comparisons of field strength are valid only for limited distances, specifically for the distance at which UHF field strength could be measured. Beyond these distances, no quantitative comparisons could be made. If such comparisons could have been made, the average difference between VHF and UHF fields would have been much greater.

Field Tests of Television Reception

A second major technical accomplishment was the extensive program of field observations in which picture quality, as judged in typical homes by both technical observers and householders, was compared with field strength measurements made concurrently in the same areas. These field observations were made at varying distances from television transmitters out to the fringes of service areas. Thus, they took into account the fact that television receiving installations are not all the same, but increase in quality with distance from the transmitter, to compensate, more or less, for the decreasing field strength out to a distance where satisfactory reception becomes economically impractical. This "negative feedback" factor had been partially recognized before, but had not been evaluated quantitatively through consistently conducted observations under a variety of conditions.

The TASO field tests were made at Albany, N. Y., Bakersfield, Calif., Baton Rouge, La., Buffalo, N. Y., Columbia, S. C., Fresno, Calif., Harrisburg, Pa., Madison, Wis., and New Orleans, La., in the Connecticut Valley, and in Northern Minnesota. In all but two areas, which were chosen because of the availability of other necessary facilities, both UHF and VHF service existed. A wide variety of topography was represented in the eleven areas. In each geographical area, an average of nine measurement locations were chosen. In each of these, an average of eleven receivers were observed, and twelve field strength measurements of each principal television station were made. The homes in which observations were made were chosen in an unbiased, random manner. The television receiver was operated by the householder. The picture quality was rated independently by the householder and the two TASO observers, using a six-point rating scale. The field strength measurements were made in a manner consistent with that used in the propagation measurements.

The data taken in these field studies were classified and plotted in a variety of ways. The most fruitful methods of representing the data are shown in Figs. 4 and 5, which are typical of the many plots that were made. In Fig. 4, the ordinate is the median of the judgments of picture quality in the eleven or so homes in a single measurement location, while the abscissa is the median field strength at a height of 30 feet in the same measurement location. In Fig. 5, the ordinate is the same, but the abscissa is the distance from the transmitter to the measurement location. The final results of the analysis of these, and similar figures, are shown in Table I. The listed values of field strength which result in pictures of specified qualities are those chosen by Panel 3 after a thorough study by one of its committees of all of the data plotted in the manner of Fig. 4. The values of critical distance were obtained after a study of data plotted as in Fig. 5. The term critical distance requires some clarification. It is not a distance up to which excellent service exists and beyond which service

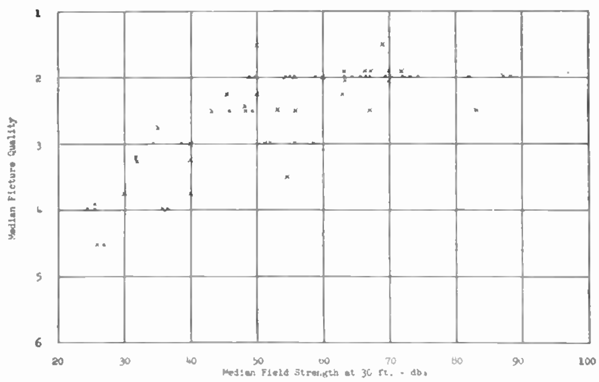

Fig. 4—Plot of median picture quality in a small area vs median field strength in that area for low VHF channels.

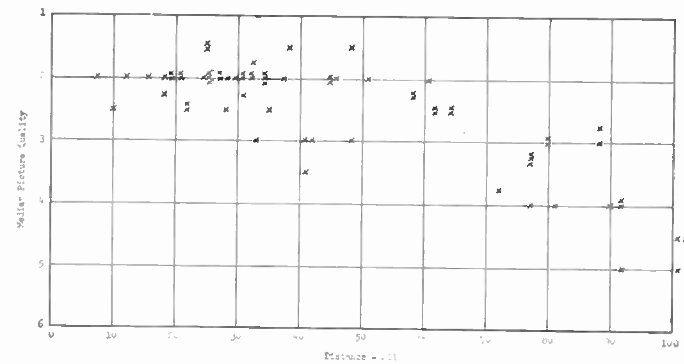

Fig. 5—Plot of median picture quality in a small area vs distance from transmitter for low VHF channels.

TABLE I

Frequency Range	Channel Range	Median Field Strength in DBU Resulting in Median Picture Quality of		Critical Distance (Miles)	Average ERP (kw)	Average Transmitting-Antenna Height* (Feet)
		Grade 2—Good	Grade 3—Passable			
Low VHF	2–6	50 and above	40–45	65	99	820
High VHF	7–13	60 and above	50–55	55	265	1010
Low UHF	14–40	65 and above	55–60	40	365	770
Middle and High UHF	41–83	72 and above	62–67	30		

* Above average terrain.

suddenly ceases. Rather, it is a distance up to which most residents can obtain reasonably adequate pictures [between passable (grade 3) and good (grade 2), and probably closer to passable than good] with economically practicable receiving installations. Beyond the critical distance, the percentage of viewers receiving adequate picture service decreases rather rapidly, while the percentage receiving poorer service increases correspondingly. Some persons beyond the critical distance will, of course, receive good service, while some within the critical distance will not. Moreover, in exceptionally favorable or unfavorable terrain, the critical distance will be appreciably greater or appreciably less than the values given. Speaking in broad, general terms, however, the TASO field surveys showed that, under average conditions, with currently used effective radiated powers and transmitting antenna heights, service fell off rapidly beyond the listed values of critical distances. The data in Table I show the average powers and antenna heights of the stations used in the surveys, and it should be noted that these values are quite typical of existing, well-operated stations.

The significance of the results given in Table I is that they were obtained by carefully designed and conducted field tests, using receiving installations as found in typical homes. No assumptions were made regarding such diverse factors as receiving antenna gain and height, condition of receiver lead-in, receiver sensitivity, receiver adjustment, transmission-path topography, obstructions in the vicinity of the receiving antenna, etc. Detailed analyses, which compare the results obtained in the field tests of television reception with those derived from the analysis of propagation data and from the laboratory studies of the performance of receiving equipment, are given in the TASO report. The results are not inconsistent, and in most cases, they are amazingly similar.

From Table I, the decrease in critical distance with increasing frequency is plainly evident. It is interesting to plot critical distance as a function of the mean carrier frequency of the stations observed. The results are shown in Fig. 6. The studies also showed that beyond the critical distance, UHF service fell off more rapidly and more completely than did VHF service. Within the critical distance, service was more variable at UHF than at VHF and was, on the average, poorer.

Laboratory Studies of Television Picture Quality

A third major project was a study of the relationship between subjective picture quality, as judged by representative groups of observers drawn from the general public, and technical picture impairment due to controlled additions of interferences of different types and amounts. A comprehensive series of laboratory tests was conducted by TASO to determine the statistical relationship between picture quality, as rated on the six-point scale, and desired-to-undesired signal ratio, using for the undesired signal thermal noise, cochannel interference (with normal, precise and very precise carrier frequency offset), and adjacent-channel interference (upper and lower), as well as certain combinations

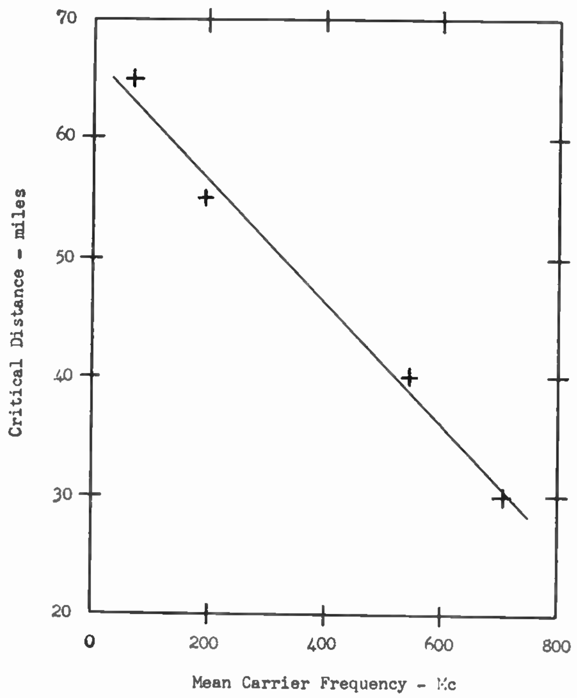

Fig. 6—Plot of critical distance, beyond which average service deteriorates rather rapidly, vs carrier frequency.

of these types of interference. Observations were made using both color and monochrome receivers judged to be of type and quality representative of upper middle grade receivers. These tests were conducted by TASO panel members skilled in the design, conduct, and interpretation of psychological tests, as well as by those skilled in television engineering. A variety of still pictures were used for the desired and interfering television signals. Tests were made to determine the effects of different pictures and groups of observers, and to check the self-consistency of observations. These checks showed a satisfactory degree of reliability of the results which were obtained.

It is difficult to summarize briefly the large amount of data which were taken. Representative values of interference resulting in a passable (grade 3) picture are given in Table II. The tests of combined thermal noise and cochannel interference showed that the greater interference predominated until the two levels of interference were within a few decibels of each other. In some cases, the presence of thermal noise appeared to lessen the disturbing effects of cochannel interference.

TABLE II

Type of Interference	Average Ratio of Desired-to-Undesired Signal (DB) Required for a Passable Picture
Thermal noise	27
Co-channel, 360-cycle carrier offset	22
Co-channel, 604-cycle carrier offset	41
Co-channel, 9985-cycle carrier offset	22
Co-channel, 10,010-cycle carrier offset	18
Co-channel, 19,995-cycle carrier offset	26
Co-channel, 20,020-cycle carrier offset	18
Lower adjacent channel	−26*
Upper adjacent channel	−27

* This value must be used with caution, as it depends upon the lower adjacent channel trapping in the receiver and upon the signal level. The trapping in the average receiver now in use in the home will not permit as high a level of lower adjacent channel interference as indicated here. A value of perhaps −10 db to 15 db rather than −26 db might be more representative of results obtained with average receivers currently in the hands of the public.

Tropospheric Propagation Curves

Allocation studies require not only a knowledge of the propagation of desired signals within the service range of a television station, but also information regarding the propagation of interfering signals from stations located at distances much greater than their service ranges. The results of more than a million hours of measurements of distant signals made by the Central Radio Propagation Laboratory of the National Bureau of Standards were made available to TASO, and curves representing the best current information on tropospheric propagation of UHF and VHF signals over distances of between 100 and 300 miles were prepared from these and other data. Generally speaking, for comparable conditions, UHF interfering fields were shown to be lower than VHF interfering fields, but the difference is not as great as in the case of service fields.

Equipment Performance

A final major accomplishment of TASO was the critical evaluation of the performance of modern UHF and VHF television transmitting and receiving equipment. Of the two, receiving equipment is of greater significance as a limiting factor in the operation of a television system.

The work on receiving equipment included the collection of data on the gain (and other characteristics) of receiving antennas, the loss in transmission lines, the noise factor and sensitivity (and other characteristics) of receivers, and the performance of vacuum tubes and other electron devices used in television tuners. Incidentally, before data on the performance of receivers could be gathered, it was necessary to draw up specifications for standard methods of measuring the characteristics of modern television receivers, as existing standards were seriously out of date. A consideration of the various factors as combined in a receiving system led to conclusions regarding the basic limitations of receiving equipment at the various frequencies employed in television broadcasting. The general conclusions were that, with presently available equipment of average quality, a high-band VHF signal must be 8.1 db higher than a low-band VHF signal to produce the same signal-to-noise ratio, and that a UHF signal must be 23.2 db higher than the low-band VHF signal. These figures were based on the use of new, dry transmission line. If old, wet line is used, the corresponding figures are 9.3 and 26.9 db, respectively. In the field and within the service range of a transmitter, these differences may be partially (but only partially) compensated in any given area by a factor previously noted, that the viewer will purchase as good a receiving installation as is necessary to receive adequate pictures out to the limit of service. The limiting differences in receiver performance quoted above do, of course, enter very directly into the determination of the limit of the service area.

The studies of transmitting equipment included a consideration of economic as well as technical factors. The TASO activities were directed toward studies of the characteristics, performance, reliability, and cost of currently available transmitters; the characteristics and cost of antennas, towers, and transmission lines; the performance of translators; and the applicability of new techniques in the operation of transmitting equipment. In very brief summary, the cost of a complete, maximum-power (316 kw) high-band VHF transmitting installation was found to average about 25 per cent higher than that of a complete, maximum power (100 kw) low-band VHF installation. UHF installations operating at powers up through 300-kw effective radiated power were shown to cost, on the average, about 10 per cent less than maximum-power low-band VHF stations. Little information was obtained regarding 500- and 1000-kw UHF stations, but it appeared that their cost was comparable to that of maximum-power low-band VHF stations. UHF translators appeared to be effective in providing television service in areas remote from regular broadcasting stations and in "filling in" areas of low signal strength within the "normal" service range of television transmitters.

A major task of special significance was the thorough testing of high-power, directional television transmitting antennas under field conditions at WBZ-TV, Boston, Mass., and WKY-TV, Oklahoma City, Okla. The WBZ-TV installation involved the modification of an existing antenna, while at WKY-TV a specially designed antenna was installed and tested. The WKY-TV installation included means for rotating the complete transmitting antenna, as well as the provision of an auxiliary, rotatable, reference antenna. These tests not only gave reliable information regarding two specific directional antenna installations under field conditions, but also served to demonstrate the validity of procedures developed by TASO for conducting reliable performance tests of directional transmitting antennas. These tests indicate that satisfactory performance could be obtained with supression ratios as great as 15 db.

Interference

A factor which favors UHF operation is that of greater freedom from interference. Although TASO did not make quantitative measurements of interference, the observations made in the field surveys of television reception, the results of a questionnaire survey of television servicemen, and the results of inquiries directed to service managers of leading television receiver manufacturers showed clearly that UHF television is substantially free from atmospheric interference, from such man-made interference as ignition and other impulsive electrical noise, and from airplane flutter. Multipath difficulties were not found to be a really serious factor except in large cities. In most locations where it existed, multipath was more objectionable at VHF than at UHF. Galactic, or cosmic, noise, which may be a bothersome source of interference in fringe areas in the low VHF band, is of no consequence at UHF. Finally, although there were frequent reports of co-channel and adjacent-channel interference at VHF, there were practically no such reports at UHF. This, however, may well be due at least in part to the relatively small number of UHF stations on the air to cause such interference, since the curves of interfering (or tropospherically propagated) field strength developed by TASO indicate that, at equal distances and for comparable effective radiated powers and transmitting-antenna heights, interfering field strengths at UHF are only some 6 db lower than at VHF.

UHF vs VHF Operation

The preceding discussion indicates several significant factors affecting the difference in performance of a television system at UHF and VHF. Some of these factors are truly basic in their nature, and are not susceptible to complete compensation by the application of known techniques. Others stem from equipment limitations which may or may not change as the art progresses. The most significant differences between UHF and VHF performance are due to propagation effects, receiving-antenna characteristics, receiver noise factor, and external noise. The first three factors favor VHF, while the fourth favors UHF. Propagation effects depend upon laws of nature, and the differences between UHF and VHF propagation are likely always to exist. Differences between UHF and VHF receiving antennas are due to both basic and equipment limitations. Future inventions may reduce, but not erase, these differences. Improvement in the noise factor of UHF receivers is to a considerable extent a matter of economics, and is almost certain to occur. The present limitation is the lack of a good economical radio-frequency amplifier tube or other electron device. The noise factor of VHF receivers will probably also be improved; but in the long run the advantage of VHF receivers over UHF receivers with respect to noise factor will probably be reduced. The lower external noise at UHF is largely a basic factor, and probably will not change greatly. Over-all, it appears that while future developments will probably reduce the difference between UHF and VHF television performance, VHF television will continue to enjoy a substantial advantage.

Significance of the Work of TASO

The significance of the work of TASO is difficult to evaluate at this time. TASO has presented to the FCC a very large amount of reliable information regarding engineering factors which should be taken into consideration in arriving at decisions regarding television allocations. It seems that such decisions should be better because of the work of TASO.

The Measurement of Television Field Strengths in the VHF and UHF Bands*

H. T. HEAD† AND O. L. PRESTHOLDT‡

Summary—**The effective and intelligent administration of television broadcast channel allocations requires acceptably accurate estimates of field strengths which will be produced by television broadcast stations. Propagation curves and prediction methods in use at the time of the founding of TASO were in many respects inadequate. Insufficient data were available for the preparation of new propagation curves; a new standard measuring specification was prepared, and an extensive program of field strength measurements was undertaken.**

This paper discusses the details of the TASO field strength measuring specification and describes the program of field strength measurements. A summary of the results of the measurements is presented.

INTRODUCTION

ONE of the principal engineering requirements in formulating plans for the allocation of television channels is that of estimating the service ranges of television stations. This requires a determination of the field strengths of both desired and undesired signals within the service areas. Previous methods of predicting field strengths have taken into account the effects of frequency, power, and antenna height, but have not provided means for assessing the influence of topographic and other conditions.

Historically, field strength prediction was first dealt with by employing classical curves of field strength vs distance derived on the assumptions of a smooth spherical earth and a homogeneous standard atmosphere.[1] Increasing experience, however, indicated that deviations from these classical propagation path assumptions all too frequently resulted in field strengths markedly different from those predicted.

The field strength measurement data available at the time of the formation of TASO were inadequate to provide the needed improvement in the tools and techniques for estimating field strengths within the service ranges. There was a particular paucity of measured field strength data at the ultrahigh frequencies, and much of the information available at both the ultrahigh and the very high frequencies had been accumulated by such a wide variety of means as to greatly reduce its value for this purpose.

The Ad Hoc Committee of 1948 had reviewed the field strength measurement data available at that time (principally at VHF) and prepared new empirical curves of VHF field strength vs distance as a function of antenna height.[2] Separate families of curves were prepared for 63 mc and 195 mc, but the available data did not permit taking into account many important influences, such as terrain roughness, and the curves were applied uniformly on an average basis throughout the entire United States. The UHF measurements available at that time were extremely meager, but indicated generally that the average UHF field strengths out to a distance of about 20 miles from the antenna were approximately the same as those found at 63 mc.

The Federal Communications Commission adopted the curves prepared by the Ad Hoc Committee at 63 mc and 195 mc and, for the lack of any better data, applied the 63-mc curves throughout the UHF band (470–890 mc).[3] Subsequent experience indicated that the UHF service curves were seriously in error in many situations,[4] but little additional measurement data became available at the UHF. A need for substantial additional information at both VHF and UHF was apparent.

Faced with this need for additional field strength data within the service ranges of television stations, TASO assigned to Panel 4 the task of collecting the data needed to provide more adequate information on VHF and UHF propagation characteristics and to support a sound approach to the propagation problems involved. It was apparent that an extensive field strength measuring program was essential to fill important gaps in existing knowledge. Data were needed to permit the derivation of improved average curves of field strength vs distance, and to assist in the evaluation of the effect of terrain roughness on these curves. It was hoped that the results would lead to the development of methods for improved predictions of field strengths in small areas.

TECHNICAL PROBLEM

The measurement of field strengths in the frequency bands employed for television broadcasting is not a simple problem. The fields may vary widely from one location to another, even within small areas, and at

* Original manuscript received by the IRE, February 18, 1960.
† A. D. Ring & Associates, Washington, D. C.
‡ CBS Television Network, 485 Madison Ave., New York 22, N. Y.

[1] K. A. Norton, "The calculation of ground-wave field intensity over a finitely conducting spherical earth," PROC. IRE, vol. 29, pp. 623–639; December, 1941.

[2] Ad Hoc Committee for the Evaluation of the Radio Propagation Factors Concerning the Television and Frequency Modulation Broadcast Service in the Frequency Range Between 50 and 250 mc, FCC Rept. No. 36830, vol. I; May 31, 1949.

[3] "Sixth Report and Order," FCC Rept. No. 52-294, 74219, docket nos. 8736, 8975, 9175, 8976, Paragraph 89; April 14, 1952.

[4] E. W. Chapin, "UHF field intensity measurement experience," IRE TRANS. ON BROADCAST TRANSMISSION SYSTEMS, no. PGBTS-3, pp. 32–38; January, 1956.

greater distances may also vary appreciably with the passage of time. The classical prediction of a linear increase in field with receiving antenna height is rarely realized in practice.[5] Many other influences, often largely unknown, may affect the strength of the received signals.

As a consequence of these variable influences, field strength measurement surveys made by different methods have often been found to yield substantially different data. Frequently, surveys made on the same transmitter are not directly comparable because of differences in the measuring techniques. A method of making field strength measurements in these frequency bands is detailed in the Federal Communications Commission's Technical Standards,[6] but experience has shown that this method is not necessarily the most suitable for the collection of data for propagation analysis purposes. In addition, this method suffers from various shortcomings, even when applied for its originally intended purpose of establishing the coverage areas of operating television and FM stations.

Measuring Standards

The Commission's Radio Propagation Advisory Committee (RPAC) has established the following requirements for field strength measurements on television stations.

1) They should indicate whether or not the transmitter and antenna system are performing in the manner predicted in the application for the facility.

2) They should determine the extent and quality of service rendered by the operation, showing the areas not getting satisfactory service as well as those getting good service.

3) At least some of the measurements should be suitable for technical studies and should add to the general knowledge of propagation conditions in the frequency bands involved.

4) The measurements should be reasonably reproducible, so that they may be checked at a future date if desired.

5) The techniques for making these measurements should not be too impractical or expensive.

Prior to the formation of TASO, however, no definite measuring specifications meeting these requirements had been drawn up, and many workers employing various techniques had accumulated data which were difficult or impossible to correlate. Under these circumstances, TASO Panel 4 was, therefore, faced with the initial problem of standardizing on a measuring technique. This required the establishment of measuring specifications which would provide uniform data suitable for analysis by various methods,[7] and measurements so taken as to provide an insight into propagation mechanisms.

[5] H. T. Head, "Measurement of television field strength," *Elec. Engrg.*, vol. 77, pp. 289–302; April, 1958.

[6] Rules and Regulations of the FCC, Television Technical Standards, Part 3, §3,686.

[7] A. H. LaGrone, "Forecasting television service fields," this issue, p. 1009.

TASO Committee 4.1 divided the measuring specification problem into two parts—techniques for collecting data for analysis purposes, and methods of measuring the service areas of operating stations. Agreement was reached on techniques for making measurements to be used primarily for propagation analysis. The establishment of techniques to measure service areas of television stations is a controversial problem and TASO did not reach unanimous agreement for the adoption of any technique.

TASO Measuring Specification for Propagation Analysis

The process of establishing the measuring specifications required a substantial amount of exploratory measurement work in the field. This initial work included several series of continuous mobile measurements in varying types of terrain at both 10- and 30-foot receiving antenna heights over complete radial routes. These data indicated that the antenna height-gain relationship was extremely variable and depended on factors which could not be accurately evaluated. An analysis of these data also demonstrated that suitable sampling techniques would provide adequate data.

Because of the variability of the height-gain function, it was felt desirable to make the field strength measurements at a receiving antenna height of 30 feet above ground, which is the standard for allocation purposes. Continuous mobile measurements at this receiving antenna height would involve prohibitive labor, but the results of the sampling analysis had established the acceptability of a sampling technique, such as a short mobile run or a "cluster" of spot measurements.

Since the received fields are a function of the characteristics of the propagation path, it is desirable to make measurements in a radial pattern from the transmitting antenna. However, a random selection of measuring locations is desirable to provide a representative selection of receiving sites; also, successive measurements should be sufficiently separated to minimize the effects of serial correlation.

A consideration of the problems presented led to the ultimate preparation of a specification for the "Measurement of Television Field Strengths in the VHF and UHF Bands," which is included in the final report of TASO to the Commission. Copies of the final specification, which describes the recommended measuring process in detail, are available from Dr. George R. Town, Dean of Engineering, Iowa State University, Ames, Iowa. The principal features of this specification will be briefly described.

The specification provides for measurements along eight or more approximately equally spaced radial routes from the transmitter to be laid out on large scale topographic maps. The routes should be chosen so as to encounter representative samples of the terrain. Starting at ten miles from the transmitter, exact two-mile intervals are laid out along each radial. The measuring location is specified as the intersection of the radial and an accessible road nearest to each of the two-mile markers. If such a measuring location is not available, a substitute location suitably identified should be selected along the road nearest the appropriate mileage marker and as nearly as possible at the same elevation as the mileage marker.

Ordinarily, the radial lines are laid out on the topographic maps using ordinary drafting methods, exercising care to produce a great circle track as accurately as possible. For certain types of analysis, some workers in the propagation analysis field require that the radial lines be more precisely established. A method of laying out the radials by calculation is appended to the measuring specification and was used in laying out the measuring routes for some of the later surveys.

The measurements made at each location consist of continuous recordings for a distance of approximately 100 feet along the road with the receiving antenna at a height of 30 feet above ground. The detailed procedure consists of the following routine at each measuring location. First, check the calibration of the instruments; second, elevate the receiving antenna to a height of 30 feed above ground; third, rotate the receiving antenna and determine whether the maximum signal is arriving from the direction of the transmitter. Next, with the chart recorder operating and the receiving antenna oriented toward the transmitter, record the field strength on the chart while making a run of 100 feet along the road, centered on the intersection of the radial route with the road. Mark the exact position of the measuring location on the topographic map, and in the notebook characterize in detail the topography, height and type of vegetation, habitation, obstacles, weather, and any other local features believed to have an influence on the received field. Identify the data by suitable numbering.

If overhead obstacles will not permit a run of 100 feet, a cluster of five spot measurements should be substituted. If at the beginning of a 100-foot mobile run the maximum signal appears to come from a direction other than that of the transmitter, the mobile run should be made with the antenna oriented toward the transmitter and a five point cluster should also be measured, making two observations at each point, one with the antenna oriented for maximum response and the other with the antenna oriented toward the transmitter.

Either visual or aural carrier may be measured; if the visual carrier is measured, a peak reading voltmeter must be employed to assure that the field strength observed corresponds to the synchronizing peak.

The TASO field strength measuring specification recognizes the considerable hazard involved in operating a moving vehicle with an erected 30-foot mast. An appendix to the specifications details suitable safety precautions to be observed in the operation of the measuring vehicle.

Measuring Methods for Determining Station Coverage

Field strength measurements to determine the coverage of an operating station present a different problem from that of collecting data for propagation analysis. Techniques best suited to the latter purpose may not provide adequate results for the preparation of coverage maps or may involve unnecessary labor.

TASO did not establish measuring specifications to determine station coverage. Recommendations were agreed upon for changes in the method now prescribed by the FCC Technical Standards, and a radically new method of measuring station coverage was recommended for field trials.

A. Recommended Modification of FCC Method

The method now prescribed by the FCC Technical Standards requires continuous mobile recordings along roads extending generally radially outward from the transmitting antenna. The routes are required to follow the cardinal and subcardinal points of the compass. The received fields (at a receiving antenna height on the order of 10 feet) are converted to those expected at the 30-foot antenna height by undefined means.

TASO recommended changes in the selection of measuring routes and the application of height-gain factors. It was recommended that the measuring routes be selected with engineering judgment, so as to encounter terrain representative of the sectors being sampled. The number and direction of the measuring routes should be chosen so that an interpolation between adjoining routes may be reasonably expected to represent propagation conditions actually obtaining. Height-gain factors as shown in Table I were recommended for the 10-foot to 30-foot conversion.

TABLE I

Recommended 10-Foot to 30-Foot Height-Gain Functions

Channel	Smooth Unobstructed Terrain	Rolling Hilly Terrain	Rough Terrain
2–6	9.5 db	8 db	7 db
7–13	9.5 db	7 db	5 db
14–83	9.5 db	5 db	2 db

B. Proposed Circular Arc Technique

The newly proposed technique is a radical departure from past practice and is based on a proposal by Kirby.[8] The following background information will be helpful in establishing a proper perspective for this technique.

Current knowledge of wave propagation indicates that statistical methods may be appropriately used in reporting VHF and UHF field strength behavior. A group of measurements taken by a uniform sampling

[8] R. S. Kirby, "Measurement of service area for television broadcasting," IRE Trans. on Broadcast Transmission Systems, no. PGBTS-7; pp. 23–30; February, 1957.

technique, in a small area at a fixed distance from a transmitter, will in most types of terrain exhibit an appreciable variation from one location to another. TASO has referred to such small areas as "cells." A series of such groups of data at different distances from the transmitter over typical terrain will show a variation of the mean field strength with distance.

If such measurements are taken in groups along two different radials but over the same general kind of terrain, it will usually be found that the variation of mean field strength with distance is similar for the two radials and that the scatter of the data in individual groups is also similar. The distribution of field strengths in these groups, when measured in dbu,[9] is found to closely approximate a normal distribution. The range between the field strength exceeded at 50 per cent of the locations and that exceeded at 84 per cent of the locations (the standard deviation) is comparable to the variation of the mean itself with distance over a range of 5 to 15 miles, depending on frequency and terrain.

The mean field strengths vary with distance generally as shown by standard propagation curves such as those contained in the FCC Technical Standards. It has also been found that the terrain influences the mean widely, that the curve may be lowered or raised from the reference curve, and, equally important, that its slope or its shape may be altered materially. Experience has also shown that the standard deviation varies with frequency and terrain roughness. It is not known whether there is an important variation of this parameter with distance.

In the general case, neither of these field strength parameters can be deduced from the other. Thus both are important in determining the service from a broadcast station. To summarize, the field strength in a "cell" may be described in terms of a mean field strength and a standard deviation describing a normal statistical distribution.

The proposed new technique specifies that measurements be taken along a pattern of circular arcs rather than radial lines. The samples would be selected along a series of three to five uniformly spaced concentric circles about the transmitter. The radii of the circles would range from a distance approximating the principal city contour to that approximating the service limit of the station. A total sample of about 400 spot measurements would be used, with the division of measurements among circles approximately proportional to the square root of the circle radius. The measuring locations should be uniformly distributed over each circle. The measurements are to be single spot measurements taken at a receiving antenna height of 30 feet.

For a typical high-power VHF station, a pattern of five circles might be used with radii of approximately 20, 35, 50, 65 and 80 miles. The number of points per circle would be 52, 69, 82, 94 and 104, respectively. This suggested layout is shown in Fig. 1, and cells at distances of 20 and 65 miles are indicated.

In analyzing the data, the area around the station should be divided into eight or more sectors not exceeding 45° in width of reasonably homogeneous terrain. In smooth or gently rolling terrain, which is more or less uniform in all directions, these sectors could be at exact 45° intervals (starting, for example, with true north).

The spot measurements on each circle within each sector (each cell) would be considered an individual group of data for analysis purposes. The mean and standard deviation for each individual data group should be determined. From these data, curves of mean field strength vs distance for each of the sectors may be drawn. For percentages of locations other than 50 per cent, similar field strength vs distance curves may be drawn for each sector by reference to the specific data for each cell.

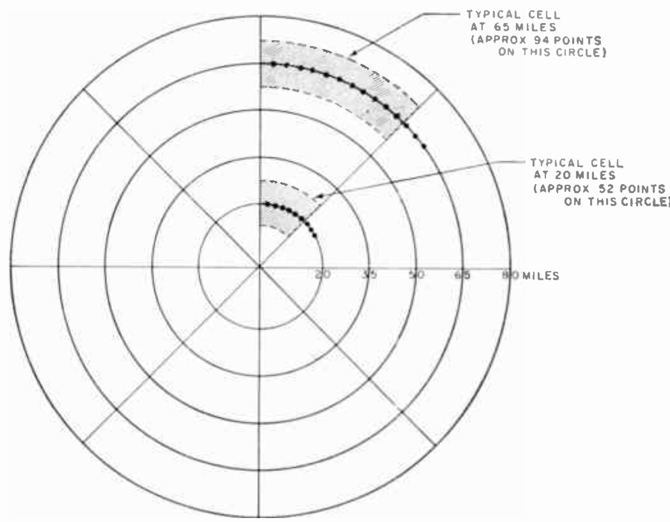

Fig. 1—Partial layout of measurement program for a typical maximum service VHF station.

C. Coverage Measurements in Cities

TASO considered that the usual application of the two techniques just described would not provide adequate data for determining coverage of cities. A separate specification for a measuring technique for this purpose was recommended by TASO without qualification.

Measurements to determine the coverage of cities should consist of single spot measurements at a receiving antenna height of 30 feet. The measuring pattern provided by the TASO specifications is a rectangular grid laid down on a map of the city. The measurements are to be taken at the intersections of the lines of the grid or as close to the intersections as is practical. The dimensions of the grid should be such that the total number of measurements is at least three times the square root of the population of the city taken in thousands.

[9] DBU: a term coined by the FCC, signifying the field strength in decibels above 1 μv/meter.

These spot measurements are to be analyzed as a single group. The mean and the standard deviation should be determined either by computation or by ordering and plotting the data on probability graph paper, expressing the field strength in dbu. From this analysis, a determination may be made as to the percentage of locations in the city which receive a field strength equal to or greater than any specified value.

Measurement Program

Concurrently with the drafting of the field strength measuring specifications, a program of actual field strength measurements was begun. The objective of the measuring program was the collection of field strength measurement data in substantial accord with the measuring specifications, representing propagation over as wide a range of frequencies, antenna heights, terrain and other conditions as practical. Obviously, it was not feasible to investigate and measure transmitters operating under all combinations of conditions. However, the selection of areas under the guidance of TASO Panel 4 was such as to provide a reasonably representative sampling of many important combinations of the various influences.

In selecting the areas where the measurement surveys were to be conducted, an attempt was made wherever possible to choose situations where both VHF and UHF signals could be measured simultaneously and, where possible, from transmitting antennas in close proximity to each other. Table II lists the areas in which complete

TABLE II
TASO Field Strength Surveys

Location	Frequency in mc	Average Effective Antenna Height in feet
Wilkes-Barre, Pa.	98.5	1160
	559.75	1220
Philadelphia, Pa.	90.9	463
	601.74	503
Madison, Wis.	61.25	795
	585.26	690
Fresno, Calif.	209.75	2000
	669.25	1787
Columbia, S. C.	193.24	640
	789.26	624
Springfield, Mass.	93.1	968
	631.75	1000
Baton Rouge, La.	59.75	890
	559.75	490
Buffalo, N. Y.	59.75	380
	493.75	686

surveys were made in accordance with the field strength measuring specification, giving the frequencies of the transmissions and the average effective antenna heights above the terrain between 2 and 10 miles from the transmitting antenna.

In addition to the complete surveys listed in the table, a limited number of measurements were made on VHF transmissions in the Boston, Mass., area and UHF transmissions in the Albany, N. Y., area. However, the measurements tabulated constituted the bulk of the data taken specifically for TASO purposes.

1) *Equipment:* The TASO equipment specification requires the use of a field strength meter of professional quality and prescribes that the measurements be made at a receiving antenna height of 30 feet above ground. These requirements dictate the use of an automobile or light truck for transporting the equipment.[10] This vehicle is additionally equipped with a chart recorder so arranged as to provide chart motion approximately proportional to vehicle motion.

Fig. 2 is a photograph of one of the mobile units equipped for these measuring surveys, showing the hydraulic mast in the retracted position for traveling. The same unit is shown with the mast extended in Fig. 3,

Fig. 2—Mobile field strength survey unit equipped for TASO surveys (photographs courtesy Association of Maximum Service Telecasters, Inc.).

Fig. 3—Mobile unit with hydraulic mast extended to 30-foot height.

[10] "NAB Engineering Handbook," 5th Ed., Sect. 2, Pt. 8, McGraw-Hill Book Co., Inc., New York, N. Y.; 1960.

which also shows a UHF receiving antenna mounted on top of the mast. The mast supports the receiving antennas at the 30-foot height while the vehicle is in motion and is rotatable.

Fig. 4 is an interior view of the mobile unit, showing the mounting of the UHF and VHF field strength meters. Two Esterline-Angus chart recorders, one for each field strength meter, were mounted on a platform in the front seat of the vehicle and were driven by means of a connection to the speedometer cable. Fig. 5 shows the mounting of the chart recorders.

The TASO field strength measuring specification prescribes the antennas to be employed for making the surveys. For UHF measurements, the antenna employed should have directivity in the horizontal plane and exhibit a single main lobe over the appropriate frequency range. The antenna should have a gain of 6 to 10 db with respect to a half-wave dipole. For VHF, a half-wave or shorter dipole should be employed. In areas where VHF signals may be contaminated by interfering fields, directional antennas may be employed.

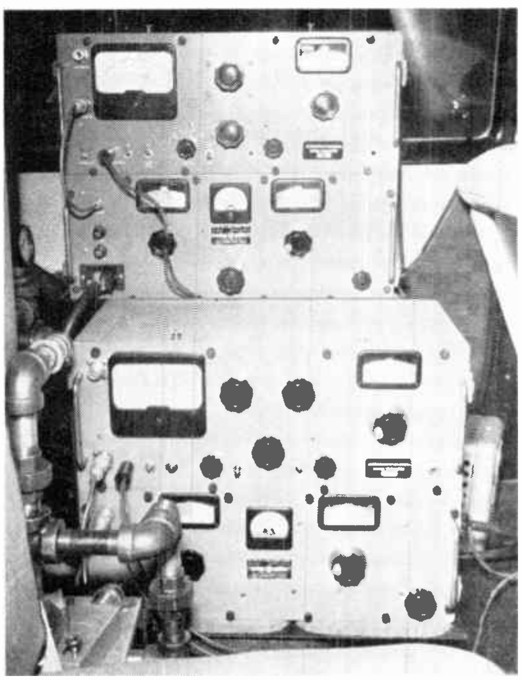

Fig. 4—UHF and VHF field strength meters in operation in mobile unit.

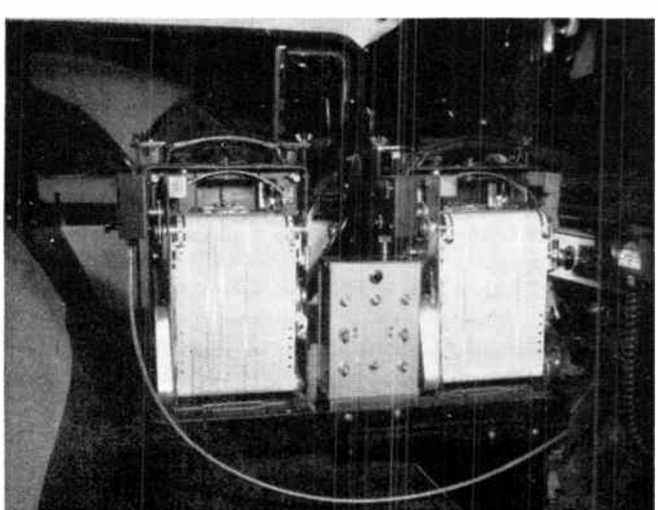

Fig. 5—Chart recorders for mobile unit.

In establishing the specifications for the receiving antennas, it was recognized that high-gain UHF antennas may not develop their free space gain in some areas, especially in rugged terrain. In situations where this is true and field strength data are gathered with a dipole receiving antenna, estimates of service available to installations using high-gain antennas in such areas will be optimistic. By gathering field strength data with a receiving antenna having characteristics approximating those of a typical home antenna, the errors in estimating the voltage delivered to the receiver input terminals are largely self-canceling. Additionally, available UHF field strength meters are not sufficiently sensitive to measure very weak signals without the use of receiving antenna gains. These considerations established the basis for the UHF antenna specifications. For measurements in the VHF range, the arguments are different. VHF field strength meters will measure to a sufficiently low signal level without antenna gain, experience has shown that the loss of antenna gain is less likely to occur on VHF, and the physical size of a high-gain antenna becomes excessive on the lowest VHF channels. It was, therefore, decided that the VHF standard antenna would be a half wavelength or shorter dipole, with the proviso that in areas subject to interfering fields, directional antennas might be employed.

The TASO equipment specification provides for the use of a shielded transmission line between the antenna and field strength meter. The antenna impedance should be matched to the transmission line and, if an unbalanced line is used, a suitable balun is to be employed to join the balanced antenna to the transmission line.

The use of a receiving antenna other than the standard dipole requires the determination of the gain of the measuring antenna relative to the dipole. This calibration should be made in a clear level area at least 10 miles from the transmitter and in an area where the signal is quite uniform, a variation of 1 db or less being considered adequate. The area must permit a mobile run of 100 to 500 feet with the mast erected. At least three runs should be made over the calibration route with each antenna. In addition to establishing the antenna gain, the horizontal pattern of the antenna should be measured by rotating the antenna through a full 360° and observing relative field strength at 10° intervals.

The measuring equipment employed in making the field strength surveys listed in Table II was calibrated against laboratory standards at periodic intervals. In addition, a calibration program of all the equipment employed was undertaken by the Electrical Engineering Department of Iowa State University, Ames, Iowa. This calibration program assured that any instrumental errors which might be introduced into the data were on the order of something less than 1 db.

2) *Reporting of Results:* The TASO measuring specification recommends the data to be included in reporting the field strength measurements. Tables should be included of the measured field strengths in each direction from the transmitting antenna, giving the distance from the antenna, the ground elevation at the measuring location, the median, minimum and maximum field strengths for each 100-foot mobile run reduced to dbu for 1 kw radiated, and any pertinent notes. Fig. 6 is a sample of a portion of one of these tables listing this information and, in addition, giving additional data for continuous mobile measurements at a 10-foot receiving antenna height.

The report of the measurements should also include large scale topographic maps showing the exact locations at which the measurements were made. In addition, a detailed description of each transmitting installation, a list of the calibrated measuring equipment used, and a detailed description of the calibration should be supplied. It is also recommended that terrain profile graphs be prepared for each direction in which measurements are made, drawn on "curved earth" graph paper for an equivalent four-thirds earth's radius. The reports which were supplied to TASO included these terrain profile graphs for each radial route and, in addition, included graphs of measured field strength vs distance plotted directly above the terrain profile graphs. Figs. 7 through 10 are sample graphs showing the terrain profiles and plots of field strength vs distance for several representative measuring runs. Fig. 7 shows measurements of a VHF signal over smooth terrain. Fig. 8 shows measurements on a UHF transmitter over essentially the same path. Figs. 9 and 10 are similar measurements over a path in very rugged terrain.

The dashed lines on Figs. 7 through 10 show the predicted fields based on smooth earth theory taking into account the expected atmospheric refractivity gradient. The individual measurements are plotted with the cross representing the median field for each 100-foot mobile run, and the excursions of the vertical line representing the minimum and maximum ranges of field strength as recorded at each individual measuring location. Similar graphs were prepared for each radial path which was measured, and were included in the reports of the field strength measurement surveys.

3) *Summary of Results:* Table III has been prepared as a brief summary of the results of the field strength measurements. Each line in Table III summarizes the results of the measurements over one complete measuring route, giving the frequency of the transmission, the average height of the transmitting antenna above the best fit curve to the measuring points along the radial route,[11] estimates of the roughness of the terrain (R/λ), and the per cent of forest cover (P_f)[12] for each radial. The last column gives the average difference between the measurements along each radial and the fields predicted by the classical smooth earth curves corrected

[11] R. M. Bowie, "The television system from the allocation engineering point of view," this issue, p. 1112.

[12] H. T. Head, "The influence of trees on television field strengths at ultrahigh frequencies," this issue, p. 1016.

FIELD STRENGTH MEASUREMENTS
WBRZ—Baton Rouge, Louisiana
59.75 mc 890 feet
(All fields in dbu for 1 kw radiated)
Direction 317° True

Distance, Miles	Ground Elevations Above M.S.L.	Standard Time	30-foot antenna 100-foot Mobile Run			10-foot antenna Cont. Mobile			Standard Time	Note
			Minimum	Median	Maximum	Minimum	Median	Maximum		
42	45.0		42.5	43.5	43.5	18.0	25.0	30.0		18
44	40.0		41.0	42.0	42.5	14.5	28.0	36.0		19
46	50.0		40.0	40.5	40.5	9.0	23.0	31.0		20
48	44.0		38.0	39.0	39.0	21.0	29.0	33.0		21
50	40.1		37.5	38.5	39.0	5.0	27.5	34.0		22
52	45.0		35.0	35.5	37.0	6.0	20.0	25.0		23
54	45.0		34.0	35.0	35.5	14.5	21.0	25.0		24
56	55.0		37.0	38.0	38.5	7.0	21.0	23.0		25
58	50.0		34.0	35.5	36.0	5.0	17.5	19.0		26
60	60.0		28.0	29.5	31.0	6.0	16.5	22.5		27
62	45.0		27.0	28.5	29.0	9.0	16.0	23.5		28
64	50.0		21.5	22.0	26.0	6.0	14.5	24.0		30
66	50.0		27.0	29.0	32.0	5.0	11.0	16.0		31
68	75.0		25.0	27.0	28.0	5.0	14.0	21.0		32
70	75.0		26.0	28.5	29.5	7.0	12.5	21.0		33
72	50.0		23.5	25.0	28.0	5.5	12.5	17.0		34
74	50.0		21.0	22.0	24.0					35

Fig. 6—Sample of tabulated data from field strength survey.

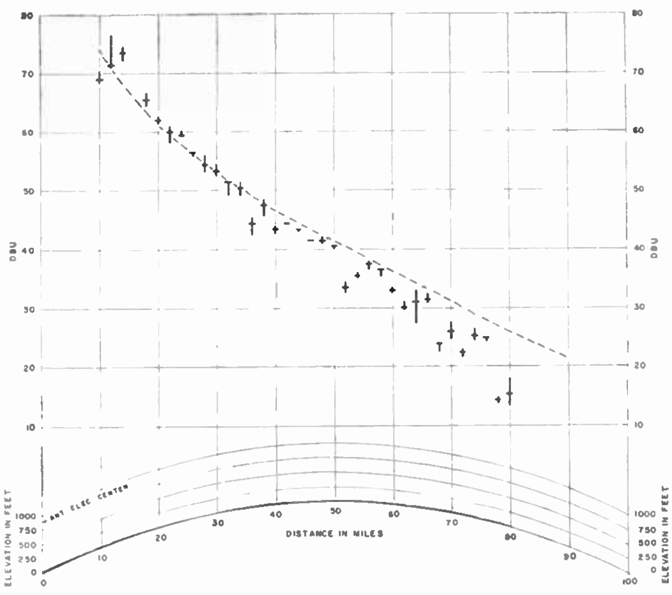

Fig. 7—Measured VHF field strengths vs distance in smooth terrain. The dashed curve is the refractivity corrected smooth earth prediction.

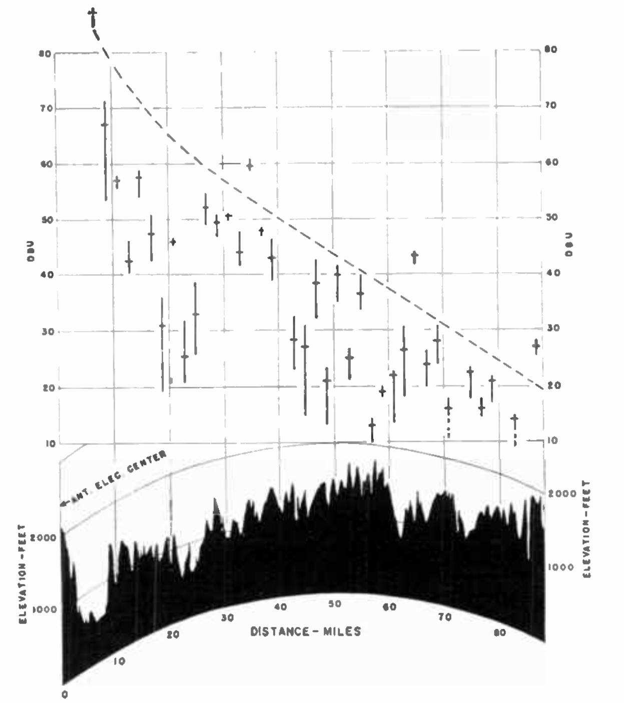

Fig. 9—Measured VHF field strengths vs distance in very rugged terrain. The dashed curve is the refractivity corrected smooth earth prediction.

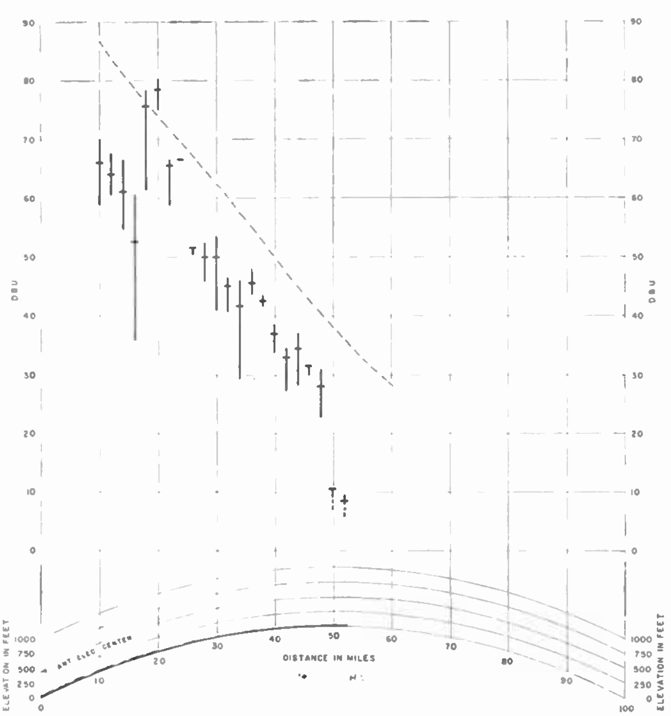

Fig. 8—Measured UHF strengths vs distance in smooth terrain. The dashed curve is the refractivity corrected smooth earth prediction.

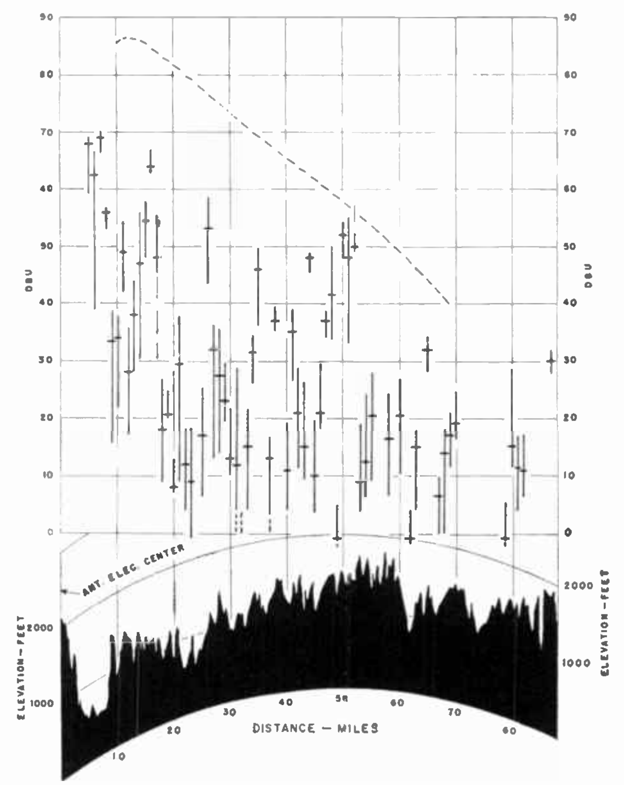

Fig. 10—Measured UHF field strengths vs distance in very rugged terrain. The dashed curve is the refractivity corrected smooth earth prediction.

TABLE III

Summary of Results of Field Strength Measurement

Frequency in mc	H_t in feet	R/λ	P_f	ΔSE in db	Frequency in mc	H_t in feet	R/λ	P_f	ΔSE in db
59.75	890	0.37	98	+0.5	209.75	4500	neg	0	+0.3
59.75	900	.15	94	5.4	493.75	700	19	25	−21.6
59.75	900	.41	35	−0.9	493.75	970	135	32	−30.0
59.75	900	.23	39	−0.6	493.75	420	90	57	−32.2
59.75	910	.39	82	2.2	559.75	490	6.0	98	−29.3
59.75	910	.21	94	0.1	559.75	500	1.4	94	−29.0
59.75	900	.40	70	0.6	559.75	500	6.1	35	−19.7
59.75	880	1.6	62	2.6	559.75	500	2.3	39	−12.9
59.75	230	2.2	25	6.7	559.75	510	3.4	82	−22.2
59.75	670	7.8	32	−2.1	559.75	510	1.7	94	−28.1
59.75	120	10.8	57	12.8	559.75	500	1.8	70	−16.5
59.75	420	0.33	—	2.3	559.75	480	29.0	62	−22.4
61.25	810	2.9	10	1.5	559.75	1975	96.5	50	−37.7
61.25	900	2.0	16	−1.7	559.75	100	74	90	−18.3
61.25	910	2.7	10	−4.3	559.75	360	166	70	−30.8
61.25	900	2.4	10	1.0	559.75	840	91	75	−43.6
61.25	810	5.0	10	−2.7	559.75	650	98	78	−37.0
61.25	620	5.2	21	−1.1	559.75	1330	58	30	−34.4
61.25	1110	6.1	32	−3.6	559.75	1260	187	100	−40.5
61.25	810	6.4	32	−1.6	559.75	1680	128	50	−49.9
90.9	430	7.8	7	−3.0	585.26	690	27.2	10	−12.8
90.9	620	0.45	32	−4.2	585.26	780	18.7	16	−24.7
90.9	480	2.0	70	−4.0	585.26	790	25.5	10	−19.9
90.9	440	2.2	49	−1.8	585.26	780	22.3	10	−21.3
90.9	580	1.0	10	−9.9	585.26	690	47.7	10	−33.0
90.9	390	7.3	25	−10.5	585.26	500	48.7	21	−20.2
90.9	360	12.6	28	−4.4	585.26	990	57	32	−35.2
90.9	570	7.2	25	−8.6	585.26	690	60	32	−36.0
93.1	1245	9.6	100	−8.9	601.74	470	51.5	7	−30.9
93.1	845	24.5	81	−12.4	601.74	660	3.0	32	−14.9
93.1	975	12.3	94	−13.5	601.74	520	13.2	70	−25.0
93.1	1010	14.2	85	−2.8	601.74	480	15.0	49	−21.3
93.1	1080	3.2	67	−5.7	601.74	620	6.4	10	−13.5
93.1	860	15.7	94	−16.0	601.74	430	47.5	25	−33.2
93.1	40	35.8	90	+15.0	601.74	400	82	28	−38.5
93.1	250	31.5	76	−16.1	601.74	610	47.8	25	−24.9
98.5	1920	17.0	50	−14.9	631.75	1275	65	100	−29.4
98.5	40	13.0	90	0.2	631.75	875	166	81	−32.5
98.5	300	29.3	70	6.0	631.75	1005	83.5	94	−30.3
98.5	780	16.0	75	−15.2	631.75	1040	96.5	85	−28.6
98.5	600	17.2	78	−17.7	631.75	1110	21.7	67	−18.6
98.5	1270	10.2	30	−19.0	631.75	890	107	94	−38.5
98.5	1210	33.0	100	−22.1	669.25	4400	neg	0	+1.6
98.5	1620	22.6	50	−19.0	669.25	4400	neg	0	−1.4
193.24	540	13.3	80	−4.0	669.25	4400	neg	0	−1.0
193.24	560	9.7	62	−8.8	789.26	560	55.0	80	−22.0
193.24	690	14.1	76	−2.1	789.26	580	39.7	62	−28.9
193.24	740	14.3	74	−8.9	789.26	710	57.8	76	−21.6
193.24	600	18.2	72	−7.7	789.26	760	58.5	74	−31.7
193.24	610	9.3	78	−8.7	789.26	620	75	72	−28.4
193.24	650	9.2	100	−3.6	789.26	630	38.2	78	−28.1
193.24	430	11.0	80	2.8	789.26	670	38.0	100	−37.1
209.75	4500	neg	0	−1.2	789.26	450	45.0	80	−29.1
209.75	4500	neg	0	−1.6					

for refractivity gradient. In evaluating these results, it should be borne in mind that classical theory predicts considerably higher fields within the radio horizon on the higher frequencies.

Table III provides an indication of the magnitude of the measuring program undertaken. Each line in Table III represents a complete radial series of field strength measurements extending out to the maximum distance to which the signals could be reliably measured. A typical series of radial measurements included 40 or more individual 100-foot mobile runs. The two mobile measuring units employed in taking most of the data traveled a distance of more than 100,000 miles in making these surveys.

Acknowledgment

TASO did not have facilities at its disposal for undertaking actual field work, and all of the measurement data submitted were provided on a voluntary basis by participating organizations. The great bulk of the data supplied, including all of the surveys listed in Table II, was provided through the financial support of the Association of Maximum Service Telecasters, Inc., employing the services of A. D. Ring & Associates. The CBS Television Network, Westinghouse Broadcasting Company, George C. Davis, A. Earl Cullum, Jr., Jansky & Bailey, Inc., and James C. McNary also contributed data.

Forecasting Television Service Fields*

ALFRED H. LaGRONE†, SENIOR MEMBER, IRE

Summary—**The propagation of VHF and UHF television signals over a spherical, irregular surface such as the earth is examined theoretically and experimentally and the principal factors evaluated. The principal factors are found to be frequency, meteorology, terrain and vegetation. It is shown that meteorology, terrain and vegetation vary a significant amount geographically and that local values should be used in forecasting local service fields.**

The principal factors are included in a new empirical method suggested for forecasting the service fields of television stations. The signal forecast by the new method is compared with field-measured signals with good results.

Introduction

THE operation of all television stations in the United States comes under the supervision of the Federal Communications Commission. It is the responsibility of this body to allocate channels, effective radiated power, and location of stations to serve the maximum interest of the public. In this connection, it is of prime importance to the FCC to have accurate information regarding the propagation of radio waves at all television frequencies over a spherical irregular surface such as the earth.

In the early days of television broadcasting, allocations were made on the basis of predicted coverage using conventional propagation theory. This method was used until field reports from operating stations showed it to be inadequate. A study was then made of all available field data in an effort to develop propagation curves that were more reliable. Statistically derived curves were developed from the study for the low VHF and high VHF bands. Curves for the UHF band were not derived because of the lack of sufficient field measured data at the UHF frequencies. However, the limited UHF data available indicated that the low-band VHF curves were in close enough agreement to the UHF measurements to be useful. At a later date, UHF curves were developed but were never generally accepted and were little used.

In 1956, representatives of the television broadcasters and manufacturing industries, at the request of the Federal Communications Commission, established the Television Allocations Study Organization (TASO). It was the purpose of this organization to obtain the best technical advice and information that could be obtained regarding the transmission of a picture from a transmitter to the viewer's screen. The ensuing study by TASO covered all aspects of the television problem, including a re-examination and evaluation of the factors affecting the propagation of television signals and of the propagation curves then in use. This phase of the study yielded a new method for forecasting service fields, including an empirical equation for including terrain effects. This paper is a report on this phase of the TASO propagation study.

Meteorology

Radio waves propagating in the troposphere travel curved paths instead of along straight lines because of the decrease in refractive index with height. Normally, the decrease in refractive index with height is not sufficient at VHF and low UHF to accomplish total trapping; however, some strong gradients do exist at times and partial trapping occurs. These are regarded as anomalous conditions. The normal decrease in refractive index with height causes the wave to bend considerably less than that required for total trapping but it is sufficient to require consideration when computing service fields for a given transmitter. It is customary to take the bending effect into account by modifying the earth's radius "a" to "ka" in the propagation equations.[1] This modification is based on a so-called standard atmosphere which gives a value of four-thirds to the coefficient "k." The product "ka" is referred to as the modified earth radius.

The four-thirds earth radius has been used for many years in computing radio signal strengths and is still useful in the absence of more specific information. A program of regular radiosonde measurements at distributed stations over the Continental United States by the U. S. Weather Bureau can now provide specific information on the amplitude distribution of the refractive index with height at the various stations, so that it is possible to obtain more accurate information on the modified earth radius to be used at given locations. Figs. 1 and 2 show contours of "k" in the United States for the winter and summer periods obtained from the Weather Bureau data.[2]

An examination of the contours of "k" in Figs. 1 and 2 shows larger values of "k" in the Gulf Coast area and along the Atlantic seaboard than in the interior areas. Broadcasters have long recognized the better broadcast conditions in this region and have labeled it Zone 3 which indicates greater service area for the same facilities. Figs. 1 and 2 also show that average propagation conditions along individual radials for a given transmitter may differ by a significant amount.

* Original manuscript received by the IRE January 25, 1960. This is a report of TASO Committee 5.4 on Forecasting Television Service Fields.

† Bureau of Engrg. Res., The University of Texas, Austin, Tex.

[1] J. C. Schelleng, C. R. Burrows, and E. B. Ferrell, "Ultra short wave propagation," Proc. IRE, vol. 21, p. 427; March 1933.

[2] These are preliminary curves drawn from data supplied by Mr. Bradford Bean of the National Bureau of Standards, Boulder, Colo. Mr. Bean will publish his report at a later date.

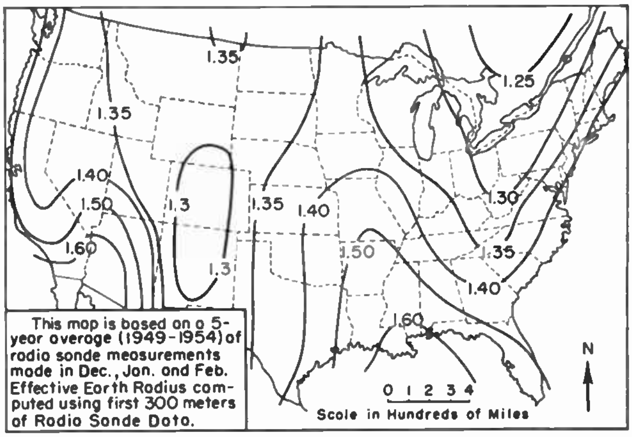

Fig. 1—Effective earth radius contours for winter.

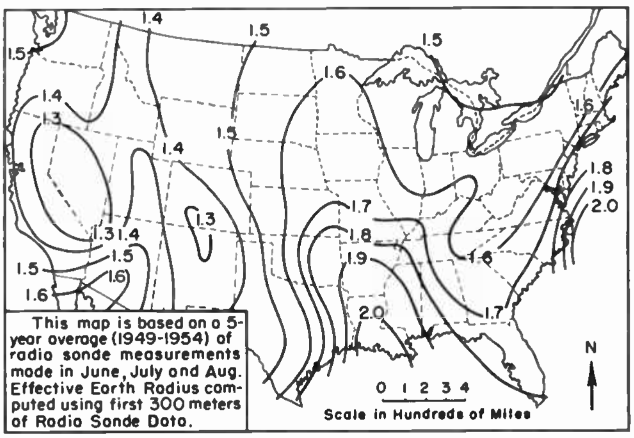

Fig. 2—Effective earth radius contours for summer.

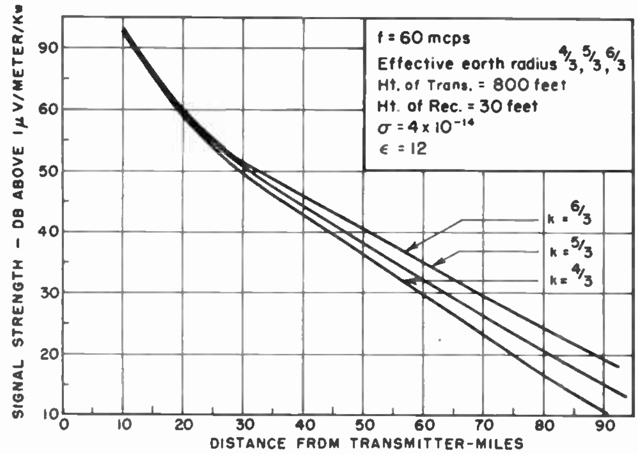

Fig. 3—Signal strength vs distance for different effective earth radii.

The effect of changes in diffraction on signal strength as a function of distance from the transmitter is shown in Fig. 3. The most important changes are observed to take place in the distant field. The magnitude of signal-strength change indicates that area meteorological conditions must be considered in determining the service and interference areas of VHF and UHF transmitters. Recognition should also be made of the large seasonal and diurnal variations found in some locations.

Effective Antenna Height

The effective height of an antenna is a propagation parameter used in determining the signal level in both the optical and diffraction regions of a given transmitter installation. Since no ordinary terrain is perfectly smooth, the average elevation of the two-to-ten mile section along a given radial is generally used as the reference in determining the effective antenna height. There are, of course, an infinite number of cases in mountainous regions where this approximation is inadequate. Such complex terrain must be treated as special cases and conventional methods used in point-to-point analysis.

One example of complex terrain that occurs frequently enough to warrant special mention is that of the path that undergoes one or two major changes in elevation but is otherwise relatively smooth. Such a path might run across a valley for the first twenty miles, then rise suddenly to a plateau several hundred feet above the valley floor. The two-to-ten mile average would provide an excellent reference for the first twenty miles but would hardly be adequate for the remainder of the path. In such cases, it seems appropriate to use two effective antenna heights: one measured from the two-to-ten mile average and one measured from the average elevation of the plateau. A theoretical smooth-earth curve for the path would then be computed in two parts and joined together with a smooth transition in the vicinity of the major elevation change at twenty miles.

The diffracted field beyond the radio horizon for very rough paths is so complex that no practical methods for computing them are known. Theoretically, the diffracted field depends on the phase and amplitude distribution of all the Huygen sources in a plane passing through the diffracting edge. Practically, the field in the shadow region is determined by the phase and amplitude distribution of the Huygen sources in the first few Fresnel zones near the diffracting edge. Thus, it seems reasonable to examine the path profile for the most likely source of a reflected wave that will disturb the Huygen sources in the first few Fresnel zones. This, in most cases, is the terrain near the diffracting edge. On the basis of this argument, it is recommended that the elevation of the five-mile sector, beginning at the radio horizon and extending back toward the transmitter, be averaged and used as the reference for determining the effective transmitter height for propagation beyond the horizon.

Theoretical signal-strength curves show that the signal level becomes less sensitive to changes in transmitter height as the height increases. This means that a fairly rough path can be averaged to obtain the effective antenna height for antennas over 500 feet high with an error of not more than a few db. The two-to-ten mile rule should then be found to apply to terrain that does not vary over ± 10 per cent of the effective antenna height. For terrain rougher than this, it is suggested that the path elevations from two miles out to the radio horizon be averaged and used as the reference, or that the path be treated as a special problem and conventional methods used in a point-to-point analysis.

Frequency Considerations

The signal strength as a function of frequency is shown in Fig. 4. The relationship demonstrated in the example is maintained in most cases of interest in the VHF and UHF television broadcast bands. The important observation to be made from studying the curves is that the near field increases with frequency while the distant field decreases with frequency.

It is not likely that one could go out and measure the exact fields predicted by theory developed for a smooth spherical earth at television frequencies. Vegetation and terrain irregularities would have to be considered. Vegetation affects the received television signal in two principal ways: The effective terminal heights are reduced because the wave is reflected off the vegetation instead of the ground, and the signal is attenuated on passing through vegetation. Both effects vary with frequency and density of vegetation.

The reflection coefficient for an area of vegetation of uniform height approaches -1 at low VHF for angles near grazing incidence.[3] At 1000 mc, the same vegetation may have a reflection coefficient of -0.3 for angles near grazing. The apparent roughness is a function of frequency and can be estimated by application of Rayleigh's criterion.[4] The height at which the wave appears to be reflected is near the top of the vegetation as grazing incidence is approached. At larger angles, the wave penetrates to a depth that depends on the angle, the thickness and uniformity of height of the vegetation, and the frequency of the signal. The depth of penetration can be only approximated, as no measurements at television frequencies are known to the author that provide any useful information on the subject.

Television signals are absorbed by trees in varying amounts depending on the frequency and polarization of the signal and the density and state of the trees.[3] For moderately thick trees in full leaf with the antenna below tree-top level, the average attenuation at 30 mc is 2 to 3 db for vertical polarization and 0 db for horizontal polarization. At 100 mc, the average attenuation is 5 to 10 db for vertical polarization and 2 to 3 db for horizontal polarization. As the frequency increases, the average attenuation increases. At 1000 mc, trees that block vision are almost opaque to the radio signal. Signals reaching the receiver must then diffract over or around the trees. Above 300 to 500 mc, there is little difference in the attenuation for vertical and horizontal polarization.

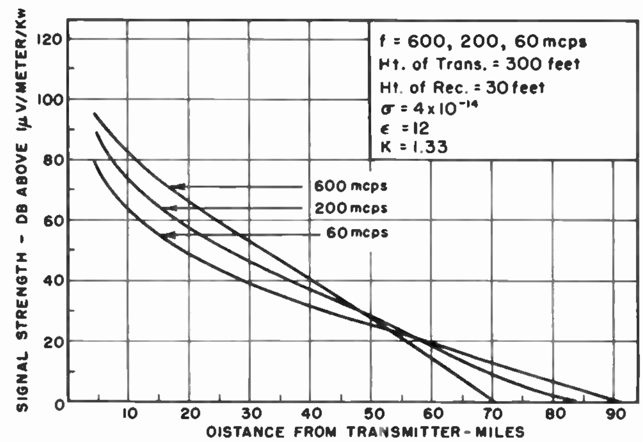

Fig. 4—Theoretical curve as functions of frequency.

Measurements of attenuation through woods in full leaf have been reported for 500 mc by B. Trevor,[5] for 100, 540 and 1200 mc by Saxton and Lane,[6] and for 3260 mc by McPetrie and Ford.[7] Their findings can be represented approximately by the following:

$$\text{db/meter} = 1.29 \times 10^{-3}(f_{mc})^{0.77}$$

where

$$\text{db/meter} = \text{attenuation}$$

$$f_{mc} = \text{frequency in mcps.}$$

No such information is available at the above frequencies for deciduous trees without leaves, although some measurements made by Trevor[5] at 500 mc indicate the attenuation to be significantly less. Trevor found that the attenuation at 500 mc dropped from 0.12 db/meter for trees in full leaf, for both vertical and horizontal polarization, to 0.1 and 0.08 db/meter, respectively, for the same trees leafless.

Fig. 5 shows the effect of trees between the receiver and the transmitter with the receiver in the clear at varying distances. It is interesting to note the clearance distance required for a significant recovery in the signal and the extremely poor signal close by the woods. The measurements were made at 485 mc near Salisbury, Md. by A. D. Ring and Associates, Consulting Engineers, of Washington, D. C.

Earth Constants

Normal changes in earth constants for different geographical areas do not significantly affect radio propagation at television frequencies presently in use.

[3] D. G. Fink, "Television Engineering Handbook," McGraw-Hill Book Co., Inc., New York, N. Y.; 1957.

[4] D. E. Kerr, "Propagation of Short Radio Waves," M.I.T. Rad. Lab. Ser., McGraw-Hill Book Co., Inc., New York, N. Y., vol. 13; 1951.

[5] B. Trevor, "Ultra-high-frequency propagation through woods and underbrush," *RCA Rev.*, vol. 5, pp. 97–100; July, 1940.

[6] J. A. Saxton and J. A. Lane, "VHF and UHF reception," *Wireless World*, vol. 61, pp. 229–232; May, 1955.

[7] J. S. McPetrie and L. H. Ford, "Experiments on propagation of 9.2 cm wavelengths, especially on the effects of obstacles," *J. IEE (London)*, vol. 93, pt. 3A, p. 531; March, 1946.

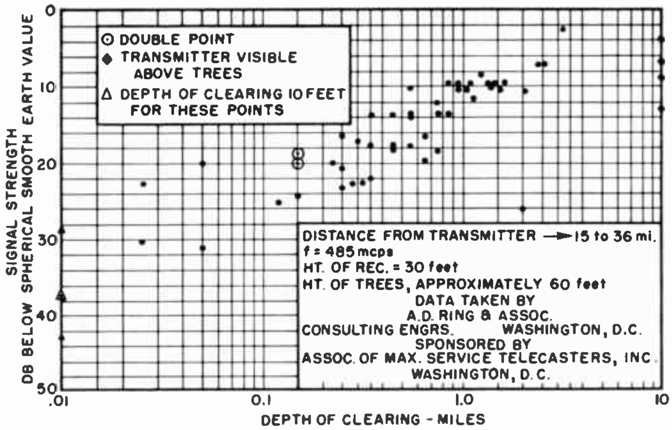

Fig. 5—Measured UHF signal strength vs depth of clearing to tall trees on radio path.

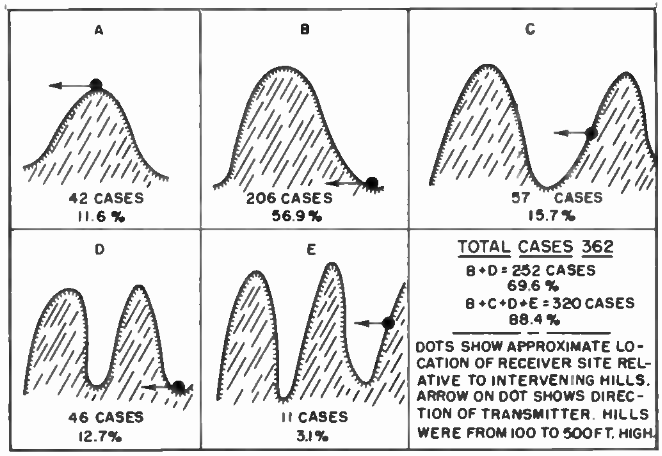

Fig. 6—Pictorial tabulation of receiver site distribution at Wilkes-Barre, Pa.

Prediction Techniques

Median Curves

The theoretical field over a smooth spherical earth provides a first approximation of the median signal. If local earth constants and effective earth radius are used, the computed signal should be very close to the measured signal for reasonably smooth and clear terrain.

A first approximation of the median signal can also be obtained by statistical analysis of a large quantity of field-measured data. The median signal obtained in this manner differs from the theoretical smooth-earth median because the field-measured signal is influenced by factors not considered in the smooth-earth equations. One important factor in the field-measured median is the location of the measuring site. In rough country, for example, field-measured data are taken along existing roads that invariably run in valleys, of which, some are quite deep. Fig. 6 is a pictorial distribution of the measuring sites for such an area in the TASO study. The area in question is that of Wilkes-Barre, Pa. The effect of the hills is clearly apparent in the measured signals shown in Figs. 7 and 8. When such data are included in an over-all field study it lowers the field-derived median such as the FCC's F(50, 50) and Appendix A curves. In reasonably flat or gently rolling terrain, the location of a road is not so greatly influenced by a hill and the measured median signal does not have so large a negative bias as found in the more rugged areas.

Vegetation is also an important factor is field-measured data at some television frequencies, as previously noted. At low VHF, it was found to be negligible, but at high VHF, trees and tall grasses were found to absorb a significant amount of the signal. This results in a lower median signal in the measured data. As a consequence, the signal derived from such data is lower than the median signal predicted by smooth-earth equations at the higher VHF.

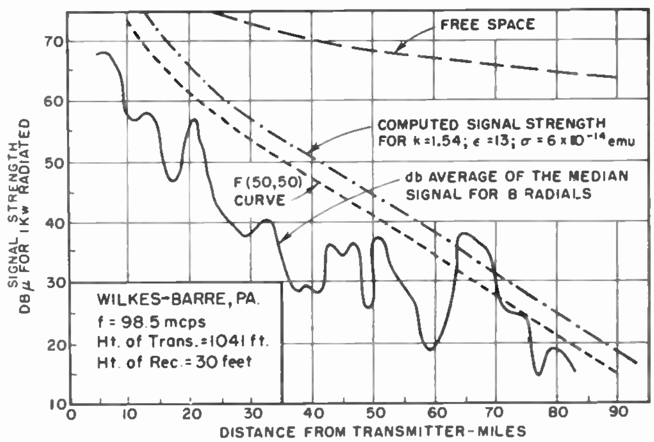

Fig. 7—Field measured average signal strength vs distance.

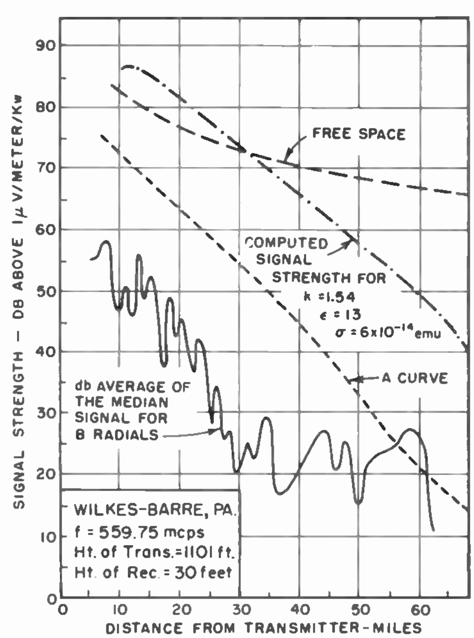

Fig. 8—Field measured average signal strength vs distance

The absorption of radio waves by trees and grasses noted at the higher VHF was found to be considerably more at UHF. Previously, it was noted that trees thick enough to block vision were essentially opaque at 1000 mcps. A receiver on a road beside or in such a forest would then receive its signal principally by diffraction over the trees and the signal would be considerably weakened. A median curve derived from such field-measured data at UHF would then be significantly lower than that predicted by smooth-earth theory.

Another factor to be considered in a median derived from field-measured data is the effective earth radius. Data taken over a large geographical area tend to average out local values, so that the effective earth radius in the derived median is, to a first approximation, the geographical average.

The effects discussed above appear to be the major reasons why a median signal derived from field-measured data differs from the smooth-earth median. The same effects are present in varying degrees on all paths, so a median derived from field-measured data would naturally fit the measured data better in some cases than the theoretical smooth-earth median.

In determining the best method to use for predicting the median field in a given area, it is well to consider both the smooth-earth median and the statistically-derived median in arriving at a decision. A re-examination of Fig. 3, for example, shows that the smooth-earth field increases considerably with increased atmospheric refraction at distances beyond the radio horizon. Fig. 4 shows that the smooth-earth field increases with frequency in the optical region and decreases with frequency in the diffraction region. It seems logical to assume that these same parameters will affect the television signal in the same manner for a rough, vegetation-covered earth. The possibility, then, of being able to use a single statistically-derived median such as the FCC's F(50, 50) and Appendix A curves to predict the median signal for a band of frequencies is poor.

Figs. 9–11 show three cases of field-measured average signals plotted as a function of distance from the transmitter. Included are the FCC's F(50, 50) or Appendix A curves and the theoretical curve for comparison. The theoretical curve is computed for the frequency, terminal heights, effective earth radius and earth constants, as determined for the case and area involved.

An examination of the curve in Fig. 9 shows that there is very little to choose between the F(50, 50) and the computed curve in as far as a fit with the measured data is concerned. From studying this curve and others similar to it, however, it is recommended that one use the theoretical median at low VHF and lower it 1 db over its entire range. This decision incorporates in the predicted median the local meteorological conditions, the gross terrain features, the different characteristics of the near and far fields as a function of frequency, and

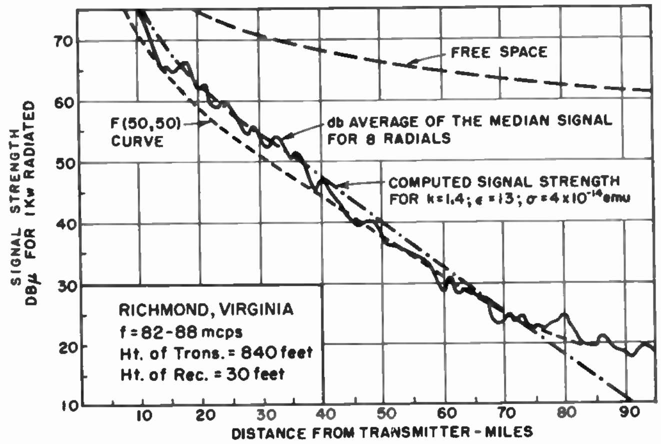

Fig. 9—Field measured average signal strength vs distance.

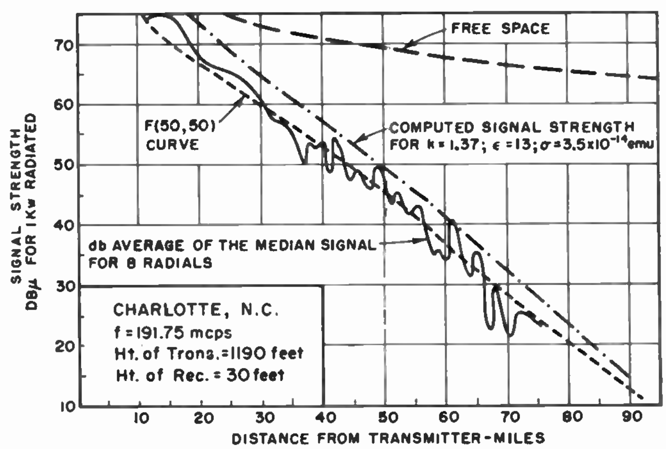

Fig. 10—Field measured average signal strength vs distance.

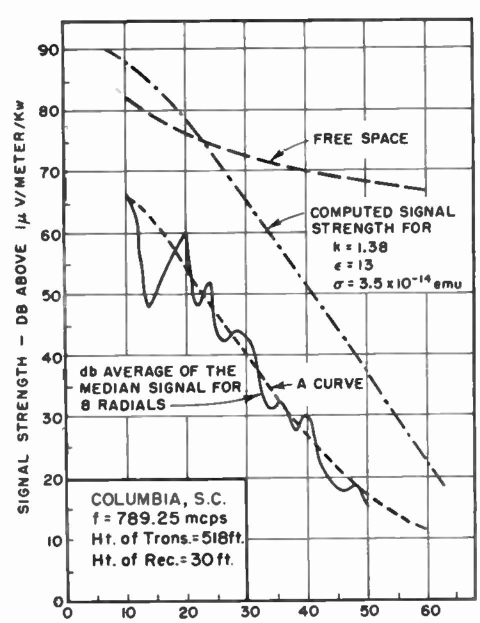

Fig. 11—Field measured average signal strength vs distance.

the small average amount of absorption noted at low VHF.

Fig. 10 is a signal strength curve in the high VHF band. A study of this and similar curves shows clearly that the F(50, 50) curve is a better fit than the theoretical curve. This is a strong argument for adopting the F(50, 50) curve as the median for this band of frequencies. A close look at the theoretical curve, however, will show just as good a fit with the measured data, if not a little better, if we lower the theoretical curve by 4 db. Based on information available to date, this appears to be the average attenuation caused by all factors at high VHF. By use of the theoretical curve instead of the F(50, 50) curve, the local meteorological conditions, the gross terrain features, and the frequency differences in propagation can also be considered. Since these are significant, the theoretical curve lowered 4 db is recommended as the predicted median.

Fig. 11 is a signal-strength curve in the UHF band. An examination of this and similar curves reveals a wide gap between the theoretical and the measured curves. The Appendix A curve, being derived from field-measured data, fits the field-measured data better than the theoretical curve. The Appendix A curve, however, is not flexible and therefore cannot be used as the predicted median for all cases. The theoretical curve considers all propagation parameters in the area and thus is the logical choice as the predicted median. Based on measurements reported to date, the average attenuation at all ranges at UHF appears to be about 22 db. This figure might be slightly larger at the higher frequencies in the UHF band. Accordingly, the theoretical curve for a smooth spherical earth lowered 22 db is recommended as the predicted median to be used at UHF.

Departure of Signal from Median

Equations are available in reference books for computing the field diffracted over objects of simple design such as spheres, cylinders and straight edges, and multiples or combinations of the above. Methods are also available for approximating the field diffracted over one or two simple hills.[3,8,9] Such methods can usually be applied with success on ridges and hills that approximate the models, but there are many cases that are too complex for these methods to be very useful.

An empirical method for obtaining the field strength is presented here that is based on the predicted median and the estimated departure of the signal from the median. The departure signal is an estimate of the effects of diffraction. Terrain and distance are the principal factors considered. Absorption, caused by vegetation, is included in establishing the median. Other local factors that might affect the signal require an on-the-spot evaluation, and such information is not usually obtainable from a topographical map.

In developing the equation for estimating the effects of diffraction, the theory of diffraction was studied and a large number of field-measured cases were examined. The study revealed that a quick estimate of the effect of a hill could be obtained by taking the square root of the height of the hill above the receiver site. The figure thus obtained was an approximation of the drop in the signal in decibels below the median. In equation form,

$$\text{db} = -\sqrt{h_1 - h_r}, \tag{1}$$

where

h_1 = elevation of hill top in feet above mean sea level [Fig. 12(A)],

h_r = elevation of receiver site in feet above mean sea level [Fig. 12(A)].

An improvement in (1) was made by including the distance of the receiver from the hillside, the height of the receiver above the intervening valley, if there was one, and including the effects of other hills between the receiver and the transmitter. Eq. (1) was then modified as follows:

$$\text{db} = c\left[-\left|h_1 - h_2\right|^{1/2}e^{-d_{1r}} - \left|h_2 - h_3\right|^{1/2}e^{-d_{2r}} + \left|h_3 - h_r\right|^{1/2}e^{-d_{3r}}\right], \tag{2}$$

where

the sign of the term is the same as the slope between the two points involved, and (2) is set up for the profile shown in Fig. 12(G),

h_2 and h_3 are elevations in feet above mean sea level [Fig. 12(G)],

d_{1r}, d_{2r} and d_{3r} are distance in miles as measured in Fig. 12(G),

$c \cong 1.6$ for VHF,

$c \cong 2.2$ for UHF.

Fig. 12 shows several other samples of terrain and illustrates the method used in measuring the various path parameters used in (2). It was not possible to illustrate every possible path configuration that could arise; however, it is felt that those shown are sufficient to illustrate the method properly. For the terrain in examples (A) and (B) of Fig. 12, for instance, the equation contains a single term. For examples (C), (D), (E), and (F), the equation contains two terms.

[8] A. N. Kalinin, "Approximate Methods of Calculating the Field Strength of Ultra Short Radio Waves, Taking Into Consideration the Influence of the Local Terrain," Natl. Bur. of Standards, Washington, D. C., translated from Russian by J. W. Herbstreit and K. Warren, transl. no. 6005; September, 1958.

[9] J. Epstein and D. W. Peterson, "A method of predicting the coverage of a television station," *RCA Rev.*, vol. 17, pp. 571–582; December, 1956.

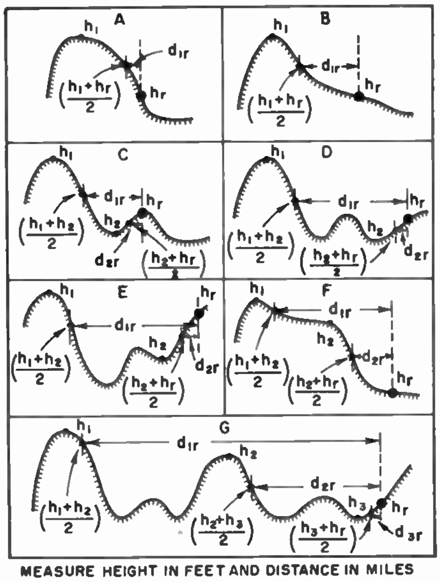

Fig. 12—Sample cases of terrain.

Forecast and Measured Signal-Strength Curves

Three sample curves are shown in Figs. 13 and 14, comparing the forecast with the measured signal strength at VHF and at UHF. The correlation is found to be very good in areas where the terrain factors dominate the field strength variations. In relatively smooth areas, local factors not included in the departure equation produce variations that are not included in the forecast signal. Some of these variations could probably be accounted for in field data obtained specifically for such a study as made here.

Conclusion

The following recommendations or presentations are made on the basis of theory or on the basis of field-measured data analyzed to date:

1) Meteorological effects on the propagation of television signals are significant. The average conditions over the Continental United States vary enough to require local consideration in propagation studies.

2) The two-to-ten mile average of the elevation along a given radial is satisfactory in reasonably smooth terrain for determining the effective antenna height for propagation along the radial. In rough terrain, the average of a longer path than the two-to-ten mile section is recommended. For beyond-the-horizon propagation in rough terrain, the average of the five-mile sector from the radio horizon back toward the transmitter is recommended as the reference elevation for determining the effective antenna height. Some paths are so complex that they constitute special problems and must be treated by special methods.

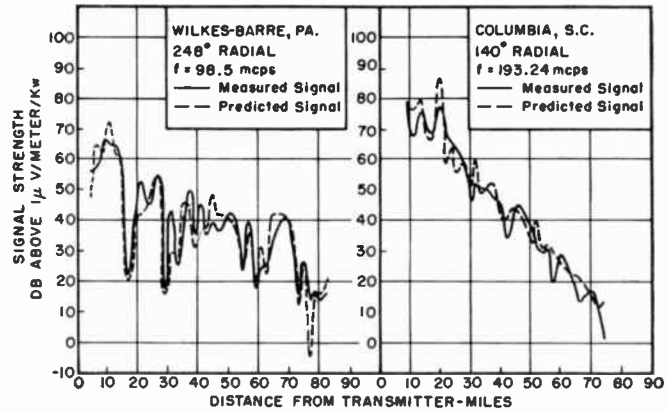

Fig. 13—Predicted and measured signals at low and high VHF television bands.

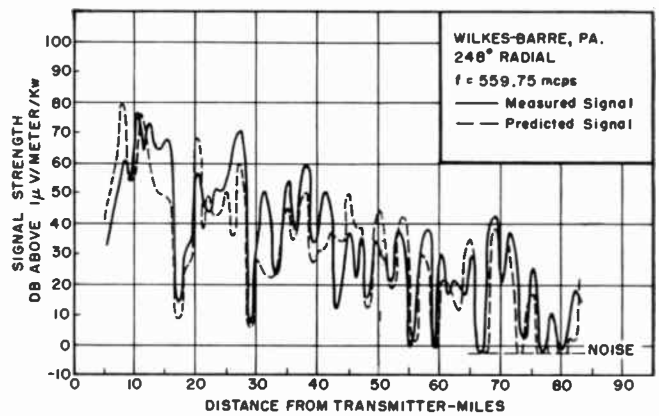

Fig. 14—Predicted and measured signal at the UHF television band.

3) The frequency characteristics of propagation, neglecting absorption, are sufficiently different, even for frequencies in the same band, to require individual consideration for forecasting signal strengths as a function of distance.

4) Normal changes in the earth constants for different geographical areas do not significantly affect radio propagation at television frequencies.

5) The theoretical signal computed at a given frequency using smooth spherical earth equations and considering gross terrain features, local meteorological conditions, and local earth constants, is recommended as the predicted median television signal under the following conditions:

a) at low VHF, the median is lowered 1 db,
b) at high VHF, the median is lowered 4 db,
c) at UHF, the median is lowered 22 db.

6) An empirical method for estimating the departure signal from the median in a given area is presented. The estimated departure combined with the predicted median gives the predicted signal.

The Influence of Trees on Television Field Strengths at Ultra-High Frequencies*

HOWARD T. HEAD†, SENIOR MEMBER, IRE

Summary—**Field studies of UHF wave propagation between television transmitting and receiving antennas indicate that typical woods are essentially opaque at these frequencies. The signal in the presence of woods near the receiving antenna appears to be principally that diffracted over the trees, with a small residual "leakage" field observable where the diffracted fields are very weak.**

The results of measurements are compared with diffraction theory, and the attenuation below free space fields due to the woods is found to be in good agreement with that predicted for a spherical obstacle having a four-thirds earth's radius. The conclusions are applied to the estimation of average losses in large areas.

Introduction

One of the more serious aspects of the problem of providing television service at the ultra-high frequencies has been the failure in many instances to obtain RF field strengths within the service areas as high as predicted by classical propagation theory. It has been generally appreciated that rough terrain and heavy vegetation have depressing effects on the received signal. The recognition of the effects, however, has been mainly qualitative, with no clear understanding of the absolute or relative magnitudes of the respective losses.

Recent work by LaGrone[1] at the University of Texas and others has provided a reasonable quantitative assessment of the influence of rough terrain on the received signal.[2-4] However, even after due allowance has been made for the reduction of signal caused by rough terrain, the observed median field strength is often still substantially below that predicted by classical theory. LaGrone, in his report to the Television Allocations Study Organization, recommends that smooth earth predictions at the ultra-high frequencies (470 mc to 890 mc for television service) be reduced by 22 db to provide basic curves from which further departures due to terrain irregularities are predicted.

* Original manuscript received by the IRE, February 16, 1960 This work was sponsored by the Association of Maximum Service Telecasters, Inc.

† A. D. Ring and Associates, Washington, D.C.

[1] A. H. LaGrone, "Forecasting Television Service Fields," this issue, p. 1009.

[2] K. Bullington, "Radio propagation variations at VHF and UHF," Proc. IRE, vol. 38, pp. 27–32; January, 1950.

[3] D. G. Fink, "Television Engineering Handbook," McGraw-Hill Book Co., Inc., New York, N. Y.; 1957.

[4] J. Epstein and D. W. Peterson, "A method of predicting the coverage of a television station," *RCA Rev.*, vol. 17, pp. 571–582; December, 1956.

Experimental Program

To determine how much UHF signal reduction might be ascribed to the effects of trees, a program of field strength measurements was undertaken in the vicinity of Salisbury, Md., during December, 1958 and January, 1959. This area was selected (see Fig. 1) because the terrain is very flat, because new topographic maps showing woodland cover were available, and because a television transmitting station (WBOC-TV) was in operation with a transmitting antenna height (620 feet above terrain) reasonably characteristic of stations in regular operation. The transmitter operates on television channel 16, which occupies the frequency band from 482 mc to 488 mc. The visual and aural carrier frequencies are 483.26 mc and 487.76 mc, respectively. The radiated power is approximately 20 kw, essentially omnidirectional in the horizontal plane.

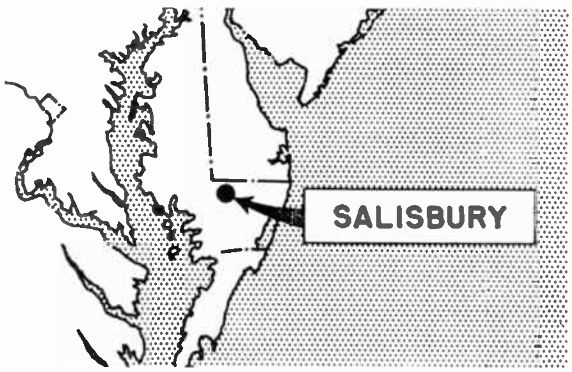

Fig. 1—Field strength measurements to determine the effects of trees were made on WBOC-TV, 482–488 mc, Salisbury, Md.

Field strength measurements on the WBOC-TV signal were made at locations selected to provide transmission under varying conditions over, through, and around woods. At each location selected for measurement, the field strengths were measured using a short, mobile run in accordance with the measuring technique specified by Panel 4 (Propagation Data) of the Television Allocations Study Organization. In a few instances where the mobile run was impractical, a "cluster" of spot measurements was substituted. The use of the mobile run or "cluster" technique introduces an averaging process which tends to smooth out small-area variations caused by standing wave patterns or other local influences.

All of the measurements were made with a receiving antenna height of 30 feet above ground. The details of the equipment and technique utilized in making these measurements have been described in a previous article.[5]

Measurements were made over transmission paths which fall into three general categories:

1) unobstructed ray paths between transmitting and receiving antennas;
2) ray paths obstructed by groups of trees sufficiently small that the signal would be propagated principally through, rather than around, the trees (these are referred to as "thin screens" of trees);
3) ray paths obstructed by groups of trees sufficiently large that the signal would be propagated principally around, rather than through, the trees (these are referred to as "thick screens" of trees).

Measuring locations in this last category were chosen so that the obstructing mass of trees occurred at varying distances from the receiving antenna in the direction of the transmitting antenna. The distance from the receiving antenna to the woods is referred to as the "clearing depth" (see Fig. 2).

Discussion of Results

A survey of the literature reveals only scant references to the effect of trees and foliage on the received signal at the ultra-high frequencies. Trevor[6] in the United States and Saxton and Lane[7] in Great Britain have published results showing the attenuation of the signal when the transmission path is entirely through vegetation. Some classified NDRC reports from World War II include similar data. The available data are reasonably consistent and show relatively severe attenuation of signals at these frequencies when the transmission path lies entirely through trees and underbrush. The conclusions, as summarized by Saxton and Lane, are shown in Fig. 3.

Measurements were made at thirteen locations in the Salisbury area of the attenuation of the signal in passing through thin screens of trees ranging in thickness from 8 meters to 480 meters. The results of these measurements are in reasonably good agreement with the conclusions of Saxton and Lane, but the rate of attenuation shows a decreasing trend with increasing woods thickness. This variation is probably due principally to the fact that the typical television transmission path is basically different from that for the condition where both the transmitting and receiving antennas are surrounded by trees.

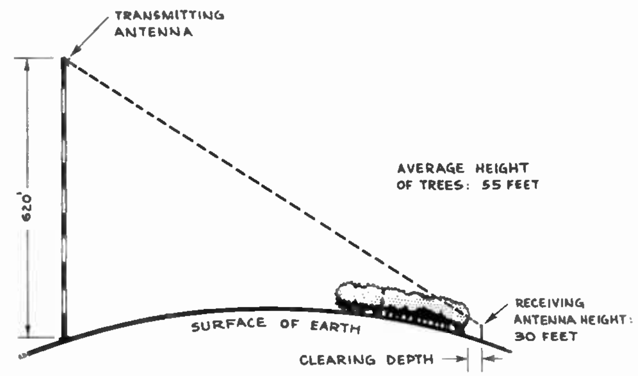

Fig. 2—The typical television transmission path is basically different from that in which both transmitting and receiving antennas are surrounded by trees.

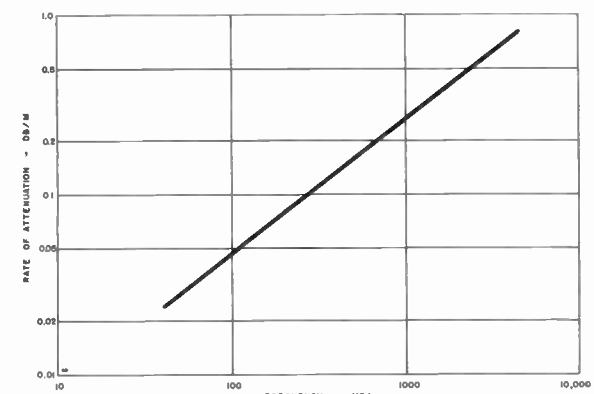

Fig. 3—Rate of attenuation in woods with trees in leaf as a function of frequency (after Saxon and Lane).

In the latter situation, the entire ray path must pass through the obstructing vegetation. For typical television transmission, however, only a small part of the transmission path may pass through trees and underbrush. The transmitting antenna is usually several hundred feet high, and only within a few miles of the receiving antenna is the signal obliged to cope with trees and underbrush near the ground. This is illustrated in Fig. 2, which shows a typical ray path for transmission between television transmitting and receiving antennas. For a path such as that shown, substantial amounts of the signal may be diffracted over and around the trees. The presence of the diffracted signal is most noticeable when the vegetation is dense enough to reduce the signal transmitted through the trees to a very low value.

The first measurements made in the Salisbury area were intended to permit a determination of the signal arriving at the receiving antenna in terms of the at-

[5] H. T. Head, "Measurement of television field strength," *Elec. Engrg.*, vol. 77, pp. 298–302; April, 1958.

[6] B. Trevor, "Ultra-h gh frequency propagation through woods and underbrush," *RCA Rev.*, vol. 5, pp. 97–100; July, 1940.

[7] J. A. Saxton and J. A. Lane, "VHF and UHF reception—effects of trees and other obstacles," *Wireless World*, vol. 61, pp. 229–232; May, 1955.

tenuation in passing through various thicknesses of woods. Examination of the first results, however, showed little correlation with woods thickness, and a comparison with the Saxton and Lane curve (Fig. 3) revealed that the thicknesses being employed were so great that the signal arriving through the woods should be well below the noise level of the measuring equipment; nevertheless, measurable signals were being received. A further study of the measurements showed that the relative signal levels were lowest when the receiving antenna was closest to the edge of the woods between the transmitting and receiving antennas, increasing as the clearing depth (see Fig. 2) increased.

A preliminary analysis showed the signal to increase approximately in proportion to the logarithm of the clearing depth for clearing depths greater than approximately 0.01 mile, but at very close distances to the woods the signal level appeared to be more or less unrelated to the clearing depth. This is illustrated by Fig. 4, which shows the difference between the smooth-earth predictions and the actual observations plotted vs the logarithm of the clearing depth. The straight line is a least-squares fit to the data points beyond 0.01 mile. The standard deviation from the line is 4.1 db.

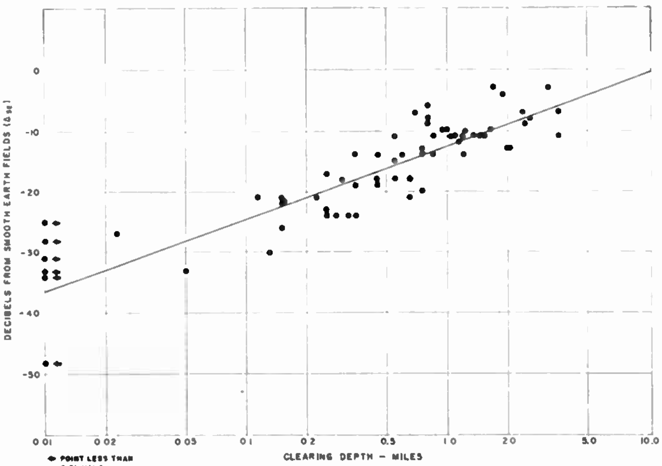

Fig. 4—Depression of signal below smooth-earth values as a function of clearing depth.

Comparison with Diffraction Theory

The basic theory of the diffraction of electromagnetic energy around the edge of a partially or completely opaque object is well established. Particular solutions, however, have been obtained only for a number of special cases, and the typical practical problem may bear little resemblance to the idealized situations for which theoretical solutions have been derived. Also, it is often difficult to foretell from the geometry of the practical case which of the particular theoretical solutions represents the model most closely resembling actual transmission conditions.

The Salisbury data were separated into two groups. In the first group were the thin screen measurements, in which it appeared that the received signals represented so complex a combination of transmitted and diffracted signals that they would have little value in a diffraction analysis. The remaining measurements, consisting of the thick screen measurements and unobstructed ray path measurements, were grouped together and tabulated. For each observation, there was determined the depression of the measured field below the smooth-earth value (Δ_{SE}), the depression of the field below the free-space value (Δ_{FS}), and the ratio of the obstruction of the trees in the first Fresnel zone to the radius of the zone at the point of maximum obstruction (H/H_0). Graphs of these values were plotted and compared with attenuation curves representing various modes of diffraction.[8,9]

A plot of Δ_{SE} vs H/H_0 does not exhibit particularly good correlation with the theoretical diffraction curves. However, a plot of Δ_{FS} vs H/H_0 shows that for Fresnel zone clearances greater than about -1.0, the points tend to fall in the general region of the theoretical curves for diffraction around a smooth sphere. Fig. 5 is a plot of this relationship showing a comparison with theoretical diffraction around a smooth spherical obstacle for a reflection coefficient $R=-1$ and a value of Bullington's parameter M of $M=300$.

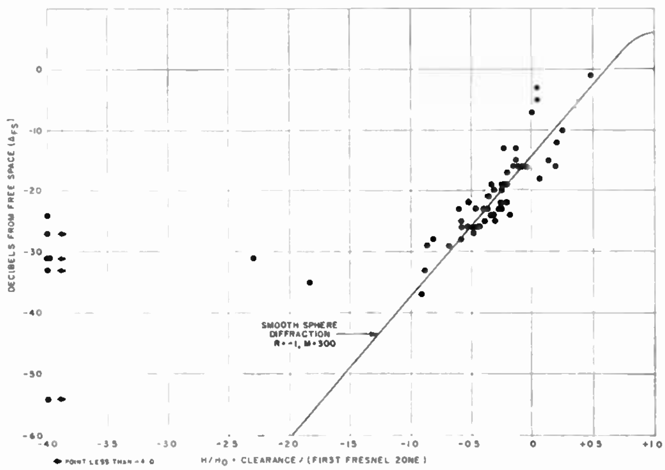

Fig. 5—Depression of signal below free-space values as a function of Fresnel zone clearance for 55-foot trees.

The parameter M is a function of transmitting and receiving antenna heights, frequency and radius of the spherical obstacle. For the heights and frequency at Salisbury, a value of $M=300$ corresponds to a smooth sphere having a radius of 24 miles. The standard deviation of the observed values from the theoretical curve is 3.4 db for Fresnel zone clearances in excess of -1.0.

The observed data were next compared with diffraction theory making the assumption that the trees ex-

[8] K. Bullington, "Radio propagation fundamentals," *Bell Sys. Tech. J.*, vol. 36, pp. 593–626; May, 1957.

[9] A. I. Kalinin, "Approximate methods of computing the field strength of ultra short waves with consideration of terrain relief," *Radiotekhnika (Moscow)*, vol. 12, pp. 13–26; 1957.

hibit some sort of "edge effect," due to the thinness of the upper branches, the small diameter of the top of the trunks, or other causes. Most of the tree heights for the transmission paths at Salisbury had been determined by actual measurements with a Matthews Teleheight, and the average tree heights were approximately 55 feet. The actual tops of the trees were thus some 25 feet above the receiving antenna height of 30 feet above ground.

The values of H/H_0 were redetermined assuming the existence of an "edge effect" of 10 feet; this would result in an apparent average height of the trees of 45 feet above ground, or 15 feet above the receiving antenna. The redetermined values of H/H_0 were then plotted against Δ_{FS} and the plot compared with the theoretical diffraction curves.

Fig. 6 shows a comparison of the observed values for the redetermined values of H/H_0 with the theoretical smooth-sphere diffraction prediction for $M=50$. This value of M corresponds to diffraction around a sphere having a radius equal to four-thirds of the earth's radius, the value customarily assumed in classical theory for propagation through a standard atmosphere. The standard deviation of the observed values from the theoretical curve is 2.9 db for Fresnel zone clearances greater than -0.6.

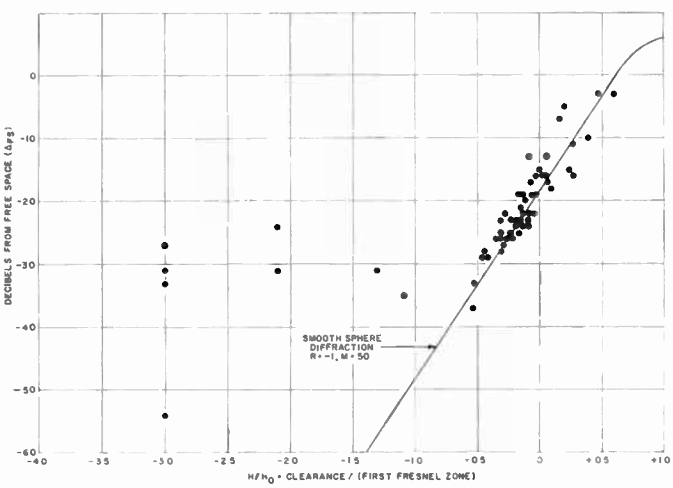

Fig. 6—Depression of signal below free-space values as a function of Fresnel zone clearance for assumed 45-foot trees.

It will be noted from Fig. 6 that the attenuation is substantially less than predicted on the basis of smooth-sphere diffraction for Fresnel zone clearance less than approximately -0.6. These values of Fresnel zone clearance represent locations where the receiving antenna was very close to the obstructing mass of trees, generally within 100 feet or less. In several instances, the receiving antenna was within 10 feet of the nearest edge of the woods.

In this region, the attenuation exhibits little correlation with any of the parameters influencing the other fields. It appears likely that the field received near the edge of the woods arrives at the receiving antenna principally through the tops of the woods and over a number of irregular paths. In making this portion of the measurements, it was frequently observed that the receiving antenna did not exhibit any clear maximum and minimum response as the antenna was rotated; in many instances it was not possible to identify the direction toward the transmitter from the orientation of the receiving antenna. The signal arriving under these conditions has been referred to as the "leakage field" (F_l) because it appears to leak through the tops of the trees, often in a rather erratic fashion.

The measurements which were considered to represent principally leakage field were analyzed for any evident trends. An examination of eight observations of leakage field at distances ranging from 12.0 miles to 22.5 miles from the transmitter indicated the average signal level below the calculated smooth-earth field to be more or less independent of distance. For these eight points, the average depression of the field below the smooth-earth field was approximately 30 db, with a standard deviation of 3.3 db.

Extension of Theory

These observations and conclusions provide a basis for predicting loss of UHF signal strength where the loss is due primarily to the effects of trees. Consider a transmission path such as shown in Fig. 7(a). Between the transmitting antenna and the first woods at the distance D_1 there is no obstruction, and the received fields in this region are those predicted by smooth-earth theory. Beyond D_1, in the woods, the received signals are primarily those arriving through the woods, and the attenuation increases rapidly with woods thickness until the leakage field level is reached (D_2). The attenuation cannot exceed that corresponding to the leakage level, and thus any additional woods thickness does not result in further depression of the signal.

Beyond the distance D_3, where the far edge of the woods is reached, the received signals recover with distance in an approximately logarithmic fashion until the clearing depth is sufficient that the smooth-earth values are once again approached. This logarithmic recovery, which is noted in Fig. 4, can be shown to follow as a consequence of diffraction; the relationship is determined by the geometry associated with the distance between transmitter and receiver.

This model of the behavior of the field permits drawing some interesting conclusions. First, in an area completely covered with trees, or essentially so, the received signal would be largely governed by the leakage level. This level is probably a function of frequency and also of the type of vegetation. If this latter is the case, as seems likely, the leakage fields would be expected to be lower in the spring and summer than in the fall and winter. It seems probable that the relationship of the leakage field to the frequency would be similar to that

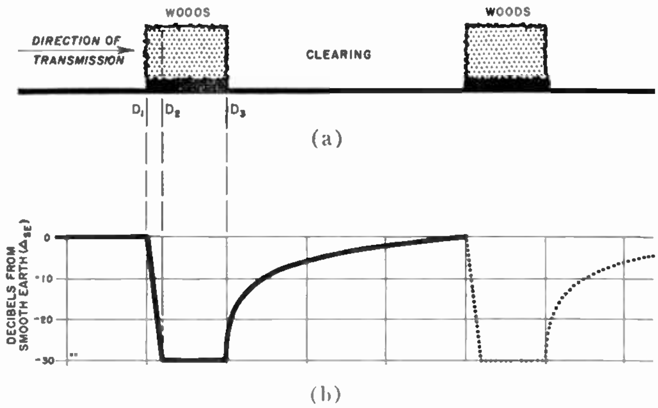

Fig. 7—(a) Model of woods and clearing for estimating average woods attenuation. (b) Depression of signal below smooth-earth values vs distance for the model of Fig. 7(a).

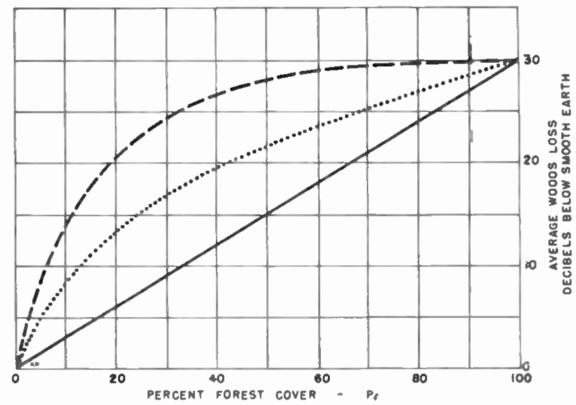

Fig. 8—Estimated average signal depression below smooth-earth value as a function of percentage forest cover P_f.

for attenuation in passing through thin screens of trees as shown in Fig. 3.

If the forest cover is less than 100 per cent, some receiving locations will be closely surrounded by trees and others partly in the clear. Theoretical models of the type shown in Fig. 7(b) were set up, and the effects of various sequences of woods and clearing were determined on the basis of the processes suggested. These studies showed that the average attenuation in an area with P_f per cent forest cover, in which the leakage field is denoted by F_l, cannot be less than $P_f F_l/100$ for any sequences of woods and clearing reasonably to be expected. For unfavorable sequences, the attenuation may be higher than this value, but an upper limit of attenuation is set by the relationship between the decay and recovery characteristics shown in Fig. 7(b). The average attenuation as a function of per cent forest cover based on this model of the behavior of the field is shown in Fig. 8. The straight line corresponds to the least attenuation of the signal for the most favorable sequence of woods and clearing, and the dashed line to the highest attenuation to be expected for the most unfavorable sequence for a given percentage of forest cover. The dotted line shown in Fig. 8 is an average attenuation curve falling between the two limits.

Conclusions

Using Fig. 8, an estimate can be made of the average attenuation of the UHF signal due to the effect of trees, provided that an estimate of the percentage of forest cover can be made. Although some modifications will probably be required for other frequencies and for vegetation under other conditions, it can be seen that the average attenuation due to the trees is on the order of the 22 db below smooth-earth values employed by LaGrone. It appears likely, based on these findings and the model of attenuation derived from them, that forest attenuation may be one of the most significant factors responsible for the average loss in signal at the higher frequencies.

Tropospheric Fields and Their Long-Term Variability as Reported by TASO*

PHILIP L. RICE†, MEMBER, IRE

Summary—**This report presents data from long-term recordings of radio field strength over a large number of propagation paths, and presents curves for predicting field strength over a smooth earth for frequencies between 40 megacycles and 1000 megacycles per second. The basic data provided for the Television Allocations Study Organization during 1957 and 1958 include recordings made in several parts of the world and over various types of terrain and were supplied by numerous sources.**

OVER the past decade, long-distance propagation in the bands above 40 megacycles per second has been carefully studied by government and private laboratories in a number of experimental programs. During 1957 and 1958, Committee 4.2 of Panel 4 of the Television Allocations Study Organization compared available data with theories of diffraction and forward scatter, and under the chairmanship of George C. Davis prepared a paper which is included as part of the final TASO report, "Engineering Aspects of Television Allocations."[1] The committee report, slightly revised and with a few additions, is presented here.

This report presents data from long-term recordings of radio field strength over a large number of propagation paths, and presents curves for predicting field strength over a smooth earth for frequencies between 40 megacycles and 1000 megacycles per second. After pointing out the extremely large variance of the actual fields received over irregular terrain relative to any set of prediction curves using distance as a parameter, and the bias of such curves arising from site selection problems, reference is made to a method which makes possible the prediction of either the service or the interference fields over specific paths for which terrain profile information is available.[2]

The basic data provided to Committee 4.2 consist of a vast number of recordings of field intensities which were made in various parts of the world and over various types of terrain. This information was supplied by numerous sources, including the Federal Communications Commission and the National Bureau of Standards. Fig. 1(a) shows median field strength, $E(50) + 10 \log_{10} d$, plotted vs the four-thirds earth distance between radio horizons, $d_s = d - \sqrt{2h_{te}} - \sqrt{2h_{re}}$ miles, for more than 600 paths in various parts of the world; d is the total propagation path distance in statute miles and $\sqrt{2h_{te}}$, $\sqrt{2h_{re}}$ are the smooth earth horizon distances where h_{te} and h_{re} are effective transmitting and receiving antenna heights in feet. A point is plotted on Fig. 1(a) for each year during which data were recorded over each path; there are, in all, 645 data points for 546 nonoptical paths and fewer data points for line-of-sight paths. One hundred and eighty-five medians correspond strictly to the period 6 P.M. to midnight, and the remainder of the data are period-of-record medians, with a few cases of duplication. The number of paths represented in each of several frequency ranges is indicated on Fig. 1(b) through 1(f).

The scatter of these data over a range of 70 decibels is due mainly to the wide variety of terrain profiles involved, and not primarily to differences in region, climate, period of record, frequency, or antenna height. Although some variance with frequency is expected, most of the paths on Fig. 1(a) correspond to frequencies near 100 megacycles per second, and thus most of the variance of these data must be attributed to terrain effects, including some variance associated with the rather arbitrary method of allowing for the effect of antenna height. Plotting these data vs distance, without any allowance at all for antenna height, the scatter would be greater.

Superimposed on the data of Fig. 1(b) through 1(f) are solid curves which represent the theoretical value of smooth earth tropospheric fields, as determined by the methods used earlier[2] for antenna heights, bracketing those represented by the data in each frequency range.

The dashed curves in each of Fig. 1(b) through 1(f) were drawn through overland U. S. data only; without a theoretical curve to follow, the dashed curve in Fig. 1(f) could not, of course, have been drawn. A considerable fraction of the data in Fig. 1(c) were biased, as will be explained later, in the direction of higher field strengths than would be expected with randomly selected receiving locations. At all frequencies the median curves through the data appear to indicate more transmission loss than would be expected over a smooth earth.

* Original manuscript received by the IRE, January 22, 1960.
† National Bureau of Standards, Boulder, Colo.
[1] Report of the Television Allocations Study Organization to the Federal Communications Commission, "Engineering Aspects of Television Allocations," March 16, 1959. (Obtainable from Dr. G. R. Town, Ames, Iowa, at a cost of $10.00.)
[2] P. L. Rice, A. G. Longley, and K. A. Norton, "Prediction of the cumulative distribution with time of ground wave and tropospheric wave transmission loss," NBS Tech. Note No. 15; July, 1959. (Available at a cost of $1.50 from the Office of Technical Services, U. S. Department of Commerce, Washington, D. C. Foreign remittances must be in U. S. exchange and must include one-fourth of the publication price to cover mailing costs.)

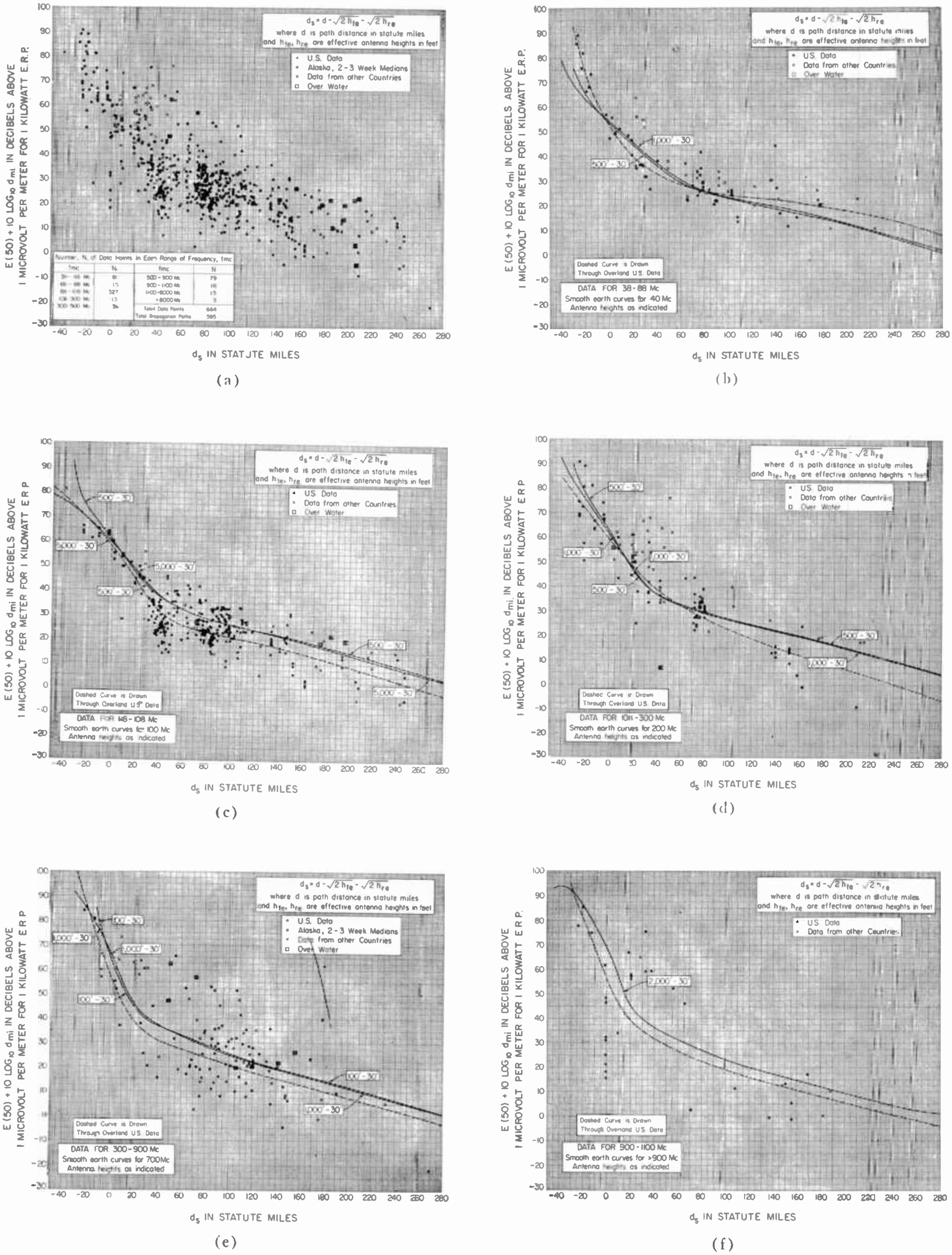

Fig. 1—Median field strength $E(50)$.

Fig. 2 shows $E(50)+10 \log_{10} d$ vs d_s as calculated for a smooth earth with the assumption that the radio refractive index decreases linearly with height for the first kilometer above ground and then decreases exponentially with height.[3] These theoretical smooth earth curves happen to lie very nearly in the middle of the mass plot of data shown in Fig. 1(a). We conclude from this that the terrain irregularities over these paths are just about as likely to increase the expected field as to decrease it, at least in the frequency range in the neighborhood of 100 mc. There is some evidence at higher frequencies, however, that the median effect of the terrain is a decrease in the received field. We will see later that the medians of the fields received at randomly selected receiving sites lie well below the smooth earth curves even at 100 mc. The increase of field strength above smooth earth values in some terrain situations is associated with the phenomenon of "obstacle gain." A theory of obstacle gain is given in another paper published earlier.[4] Also, in this same paper, a method based on four different curvatures of the earth is given for calculating diffracted fields for any degree of terrain roughness, and this provides the explanation for the fact that the fields are sometimes stronger and sometimes weaker than the smooth earth values.

Fig. 3 shows all-day, all-year median field strength plotted vs distance for four frequencies and for transmitting and receiving antenna heights of 500 feet and 30 feet, respectively, using methods described earlier,[2] and assuming a smooth earth and a winter afternoon value of surface refractivity $N_s=301$ corresponding to the usual 4/3 earth. In the optical region and slightly beyond, the estimates of the difference between winter afternoons and all hours given as a function of the angular distance, θ, in the earlier work[2] are here modified slightly to allow for differences in antenna height. As the curves in Fig. 3 show, frequency does not have a large influence on the fields received over a smooth earth beyond the radio horizon.

Figs. 4–10, smooth earth curves, show all-day, all-year median field strengths at 40, 70, 100, 200, 400, 700, and 1000 megacycles per second, with one antenna height fixed at 30 feet and the other antenna height set at 100, 200, 500, 1000, 2000, or 5000 feet. The order of procedure in preparing these curves was as follows: More than a million hours were recorded over two to three hundred propagation paths. A forward scatter theory and a diffraction theory were developed. These theories were found to agree with data in all frequency ranges, for essentially any terrain and for any antenna heights. The smooth earth curves of Figs. 2–10 were prepared using these methods, as described in detail earlier.[2] On specific paths where terrain profile information and surface meteorological data are available, it is advisable to use the prediction methods directly rather than assuming a smooth earth; in this way the standard error of prediction can be reduced to a value of the order of 6 db in the diffraction region and to less than 5 db in the scatter region. The variation with frequency shown by the smooth-earth curves on Figs. 2 and 3 is smaller than that expected over a rough earth. Also, the variation with antenna height at a given frequency (illustrated in Figs. 4–10 for a smooth earth) should be taken into account in television allocations studies.

It should be noted at this point that the selection of the receiving site has a very large influence on the received median fields at large distances in this frequency range, as might be expected from the very large variance of the data illustrated on Fig. 1(a).

Another presentation of data is shown in Fig. 11, this time restricted to data which the prediction methods[2] indicate is more representative of the forward scatter (and layer reflection) propagation mechanisms than of diffraction.

Observed median values of attenuation relative to free space are plotted vs distance in Fig. 11 for a large, heterogeneous sample of data, obtained in most cases with broad beam antennas. No normalization for the effects of frequency, antenna height, loss of antenna gain, terrain or meteorological parameters is included. Almost all recordings were made in the wintertime, and correspond to conditions where tropospheric forward scatter is expected to be the dominant propagation mechanism. Two points are indicated where ionospheric rather than tropospheric scatter may have been recorded at 100 mc. No data are included for cases where diffraction is expected to be more important than forward scatter, such as short paths where the angular distance is small.

Fig. 11 also shows deviations of data from the point-to-point transmission loss prediction method;[2] these deviations are plotted vs distance, using the same data and the same scale. The NRL over-water 50-minute medians shown in Fig. 11 were excluded in calculating the rms deviation of 6.75 db from the empirical curve and the rms deviation of 5.77 db from the theoretical values.

The data include 80 paths from a special experiment conducted in Ohio with randomly selected receiving sites at 85 and 125 miles. For these paths, long-term median observed transmission loss is slightly greater than when antenna sites are carefully selected to be unobstructed. The prediction method in this report indicates an increase in transmission loss of about 12 db per degree of increase in horizon elevation angles, and

[3] B. R. Bean and G. D. Thayer, "On models of the atmospheric radio refractive index," Proc. IRE, vol. 47, pp. 740–755; May, 1959.

[4] K. A. Norton, P. L. Rice and L. E. Vogler, "The use of angular distance in estimating transmission loss and fading range for propagation through a turbulent atmosphere over irregular terrain," Proc. IRE, vol. 43, pp. 1488–1526; October, 1955. See especially Figs. 20 and 21 and the accompanying diagram.

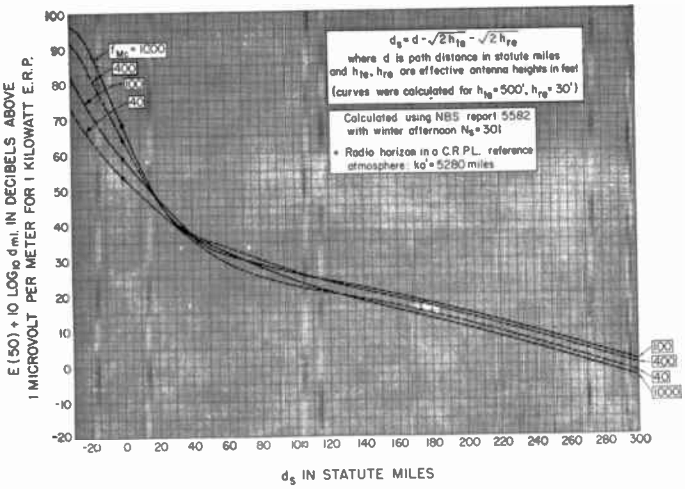

Fig. 2—All-day, all-year median field strength for paths over smooth earth.

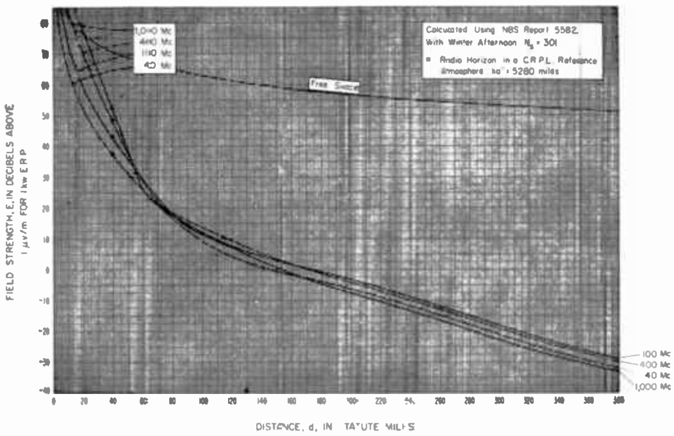

Fig. 3—All-day, all-year median field strength for paths over a smooth earth; antenna heights are 500 feet and 30 feet, frequencies are indicated.

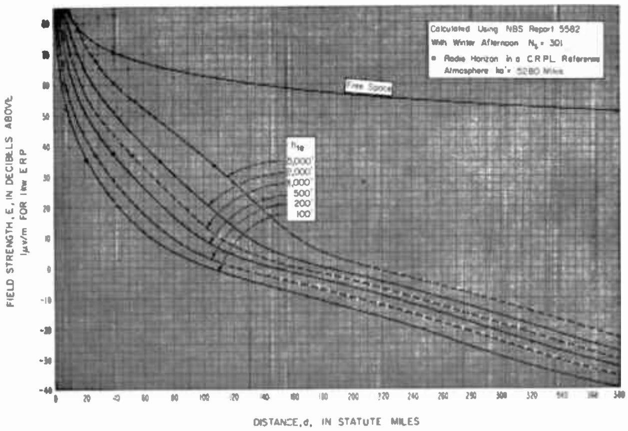

Fig. 4—All-day, all-year median field strength for paths over a smooth earth; frequency = 40 mc, one antenna height = 30 feet, other antenna height as indicated.

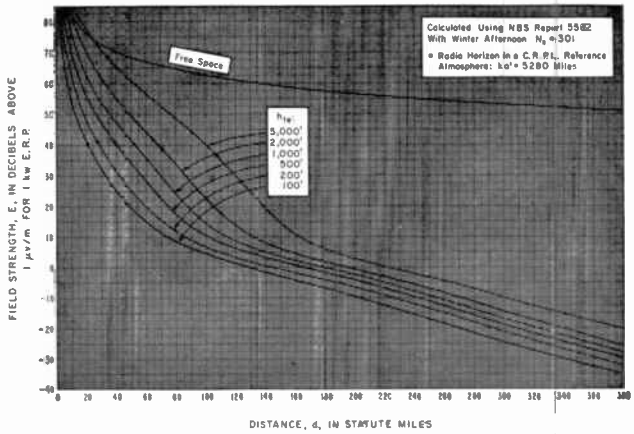

Fig. 5—All-day, all-year median field strength for paths over a smooth earth; frequency = 70 mc, one antenna height = 30 feet, other antenna height as indicated.

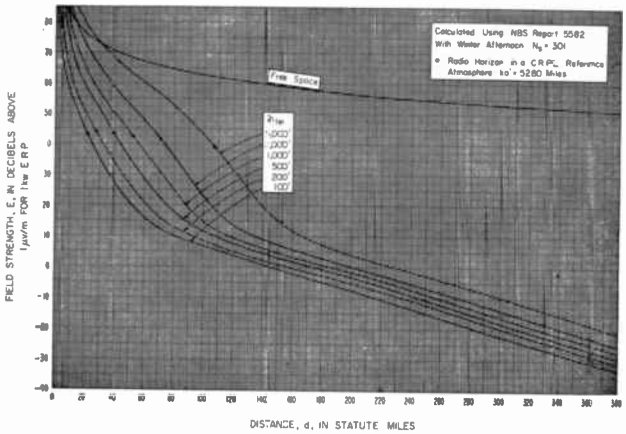

Fig. 6—All-day, all-year median field strength for paths over a smooth earth; frequency = 100 mc, one antenna height = 30 feet, other antenna height as indicated.

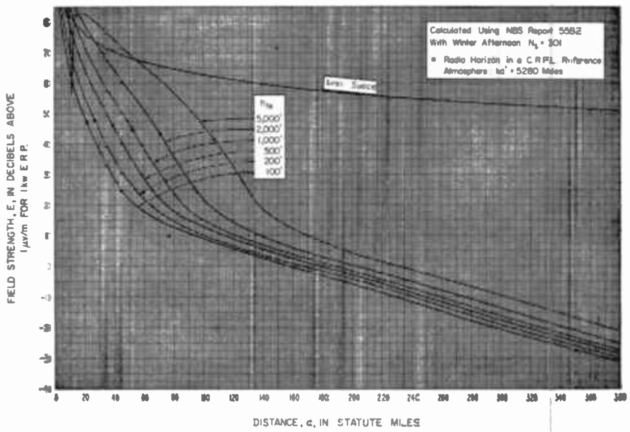

Fig. 7—All-day, all-year median field strength for paths over a smooth earth; frequency = 200 mc, one antenna height = 30 feet, other antenna height as indicated.

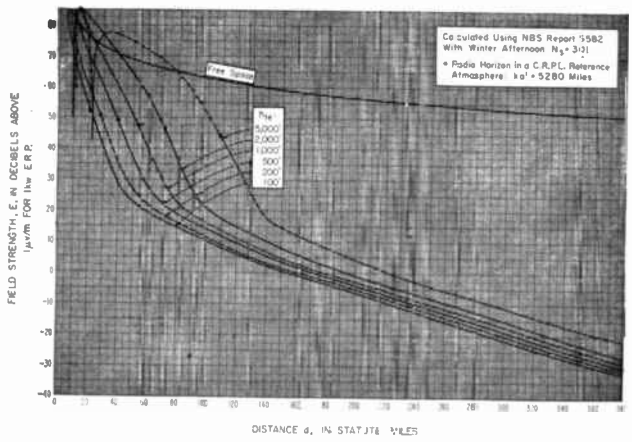

Fig. 8—All-day, all-year median field strength for paths over a smooth earth: frequency = 400 mc, one antenna height = 30 feet, other antenna height as indicated.

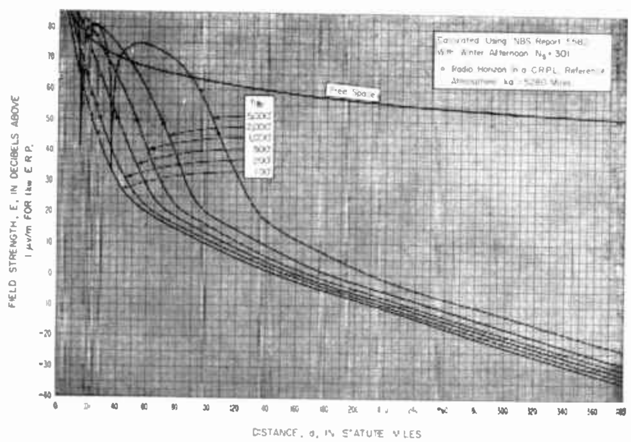

Fig. 9—All-day, all-year median field strength for paths over a smooth earth; frequency = 700 mc, one antenna height = 30 feet, other antenna height as indicated.

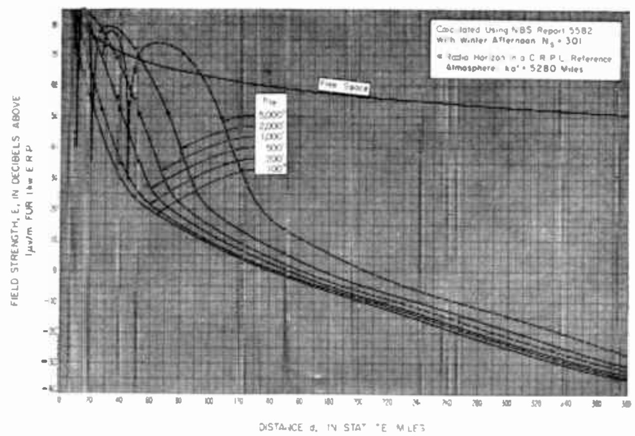

Fig. 10—All-day, all-year median field strength for paths over a smooth earth; frequency = 1000 mc, one antenna height = 30 feet, other antenna height as indicated.

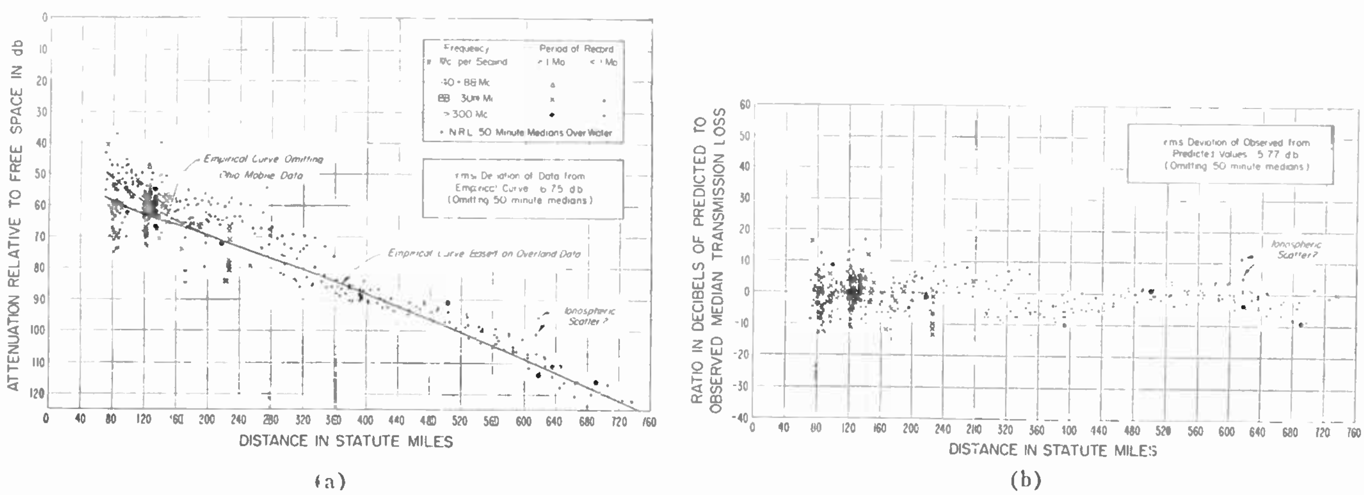

Fig. 11—(a) Median forward scatter radio transmission loss relative to free space corresponding to winter afternoon conditions. (b) Deviation of medians recorded in (a) from values predicted for an exponential atmosphere using NBS Technical Note 15.

these angles were often large for the randomly selected "Ohio mobile" receiving sites.

An experiment conducted in Ohio between 1951 and 1953 by James S. Hill and Carl E. Smith, then of the United Broadcasting Company, monitored two FM transmitters for a year at 20 randomly selected sites at 85 miles, and 20 more sites at 125 miles and showed field strengths well below the average of the 100 mc data on Fig. 11. The 40 receiving sites were chosen without regard to the usual criteria used in selecting receiving sites for long term recordings (namely, in open, relatively flat terrain with no nearby trees or overhead wires), but were chosen instead as nearly as possible on a preset lattice with separations between locations large enough to make the correlation of the received fields for adjacent receiving points negligible. This insured randomness with respect to terrain effects and efficiency in the recording program. Some compromise with the grid was naturally necessary in order to find sites at which power would be available and for which the property owner's access rights were available. The recordings were made over a two-year period from July 3, 1951 to June 30, 1953, and represent all-day, all-year conditions. The recordings were made in mobile laboratories which were moved frequently from one site to the next in order to obtain a good sampling of the seasonal and diurnal effects at each of the 40 receiving locations. A sufficient number of hours of recording were available so that fields $E(1)$, representative of the highest 1 per cent of the hours, could be determined for each path. The recording pen went off scale some of the time, and, as indicated in Table I, the $E(1)$ values were greater in a few instances than the recorded values. Thus, the true mean 1 per cent values are also greater than tabulated values of $\overline{E(1)+10 \log_{10} d}$. In order to obtain a measure of this possible bias, medians of $E(1)+10 \log_{10} d$ are also listed; it appears that the bias is negligible.

Receiving antennas were always 30 feet above the local terrain, while the transmitting antenna effective heights were obtained by finding the height of the transmitting antenna relative to a parabolic curve fit to the central 0.8 of the terrain between the transmitting antenna and its standard atmosphere (4/3 earth radius) horizon.

Table I lists 12 estimates of the variance s_T^2 of the 20 values of $E(T)+10 \log_{10} d$ available for each of two distance ranges, two frequencies, and three percentage values $T=1$ per cent, $T=10$ per cent, $T=50$ per cent. In order to allow for the effects of antenna height, it was assumed that $E(T) + 10 \log_{10} d$ is a function of $d_s = d - \sqrt{2h_{te}} - \sqrt{2h_{re}}$. Thus, since $\sqrt{2h_{te}} + \sqrt{2h_{re}} = 39.4$ miles when $h_{te} = 500$ feet and $h_{re} = 30$ feet, $E(T)+10 \log^{10} d - 10 \log_{10} (d_s + 39.4)$ should be related to the distance $d = d_s + 39.4$ for each station.

Analysis of the Ohio mobile data indicates that *any* overland E vs d prediction curves, obtained simply by averaging data, may involve a substantial bias away from estimates appropriate for television allocation. When receiving sites are randomly chosen in hilly terrain, there will be biases in 1) median location, median time fields, 2) variability due to location, and 3) time variability, relative to overland prediction curves determined by averaging data. The effects of these biases may be largely eliminated by using prediction methods appropriate for the specific paths. This has been established for the data in Table I by comparing observed cumulative distributions on the 80 "Ohio mobile paths" with those predicted earlier.[2]

Most available VHF and UHF long term recordings (British, French, German, and U. S.) correspond to unobstructed antenna sites for which the relationship between distance and angular distance is on the average that which would be expected over a smooth earth. At UHF, a small departure from an average smooth earth may result in considerably decreased field strengths.

TABLE I
OHIO MOBILE DATA
Polarization: Horizontal; Receiving Antenna Heights: $h_{re}=30$ Feet

Station	WCOL	WHKC	WCOL	WHKC
Frequency (mc/s)	92.3	98.7	92.3	98.7
Number of Paths	20	20	20	20
Distance Range (statute miles)	76.0–86.7	80.9–88.9	117.7–123.3	119.3–125.7
Height Range of h_{te} (feet)	318–520	619–820	382–547	728–821
Range in hours of observation	87–125	66–186	149–291	120–310
$\bar{d}_s$ (statute miles)	44.32	38.63	83.06	76.61
Range of d_s (statute miles)	40.8–48.1	33.4–42.3	77.4–85.3	71.6–79.3
$\overline{E(50)+10 \log_{10} d}$ (db)	22.3±1.0	26.0±1.0	20.0±0.7	23.6±0.6
$\overline{E(10)+10 \log_{10} d}$ (db)	33.7±1.4	35.6±1.1	29.0±0.8	31.8±0.8
$\overline{E(1)+10 \log_{10} d}$ (db)	>41.6±1.2	>45.2±1.4	>38.5±1.4	>40.0±1.4
Number of Paths with an Uncertain $E(1)$	5	4	4	2
Median of $\{E(1)+10 \log_{10} d\}$ (db)	42.3	45.75	37.1	37.5
s_{50}^2 in db²	20.08	19.78	8.37	6.49
s_{10}^2 in db²	36.98	25.80	11.32	11.43
s_1^2 in db²	29.93	40.37	36.41	36.79

This frequency terrain roughness effect may be accurately accounted for only by methods appropriate for point-to-point prediction using terrain profile information.

In order to make proper use of propagation curves in allocation, it is necessary that a time-fading factor be associated with them. Another paper[2] predicts time variability where terrain profile data is available. A forthcoming report will give estimates of time fading based on antenna heights and distance.[5] Such estimates are presently available in FCC Report T.R.R. 2.4.16, by Fine and Taff.[6]

Fig. 12(a) to 12(g) present empirical estimates of the time-fading factor $E(10)-E(50)$ vs distance and antenna height for each frequency for which a smooth earth $E(50)$ curve is available. The Appendix, written by W. R. Burns, explains how these estimates were obtained from the data. A paragraph at the end of the Appendix indicates how the newer estimates now being prepared differ from those in this report.

The time-fading factors given in Fig. 12(a) through 12(g) are to be applied to the dashed ("best-fit") curves of Fig. 1(b) through 1(f); they do not apply to the smooth earth curves on the same figures. The data show that $E(1)-E(50)$ is very nearly equal to $2[E(10)-E(50)]$ for any distance, antenna height, or frequency; so separate curves of $E(1)-E(50)$ have not been drawn.

In conclusion, the feasibility of tentative television station assignments in particular areas can be established by making proper allowance for the terrain characteristics in the areas under consideration. This determination may be made for each station pair in the proposed allocation by testing it for mutual interference at a selected set of receiving locations suitably chosen within the service areas of the proposed stations by an efficient statistical sampling scheme. This testing may be accomplished by determining the terrain profiles of both the desired and undesired stations from each of the randomly chosen receiving locations and then calculating the two cumulative distributions with time of the transmission losses corresponding to the desired and undesired transmission paths. Using these distributions of transmission loss, it is easy to obtain the expected distribution of the ratio of desired to undesired signals at the terminals of the receiving atenna. The use of these methods will automatically provide allowance for 1) the effects on the expected median field of the actual terrain in the area under consideration, 2) the expected distribution with time of the fields from both the desired and the undesired station, 3) the effect on these time distributions of the particular terrain in the area under consideration, 4) climatological effects in different parts of the country, and 5) the correlation of the desired and the undesired fields with changes in the receiving location. From such an analysis determination can be made of the percentage of receiving locations which should receive a satisfactory signal, but which are expected to be interfered with by the undesired station.

[5] P. L. Rice, A. G. Longley and K. A. Norton, "Prediction of tropospheric wave transmission loss and its long-term variability," to be submitted for publication in *J. Res. NBS*, pt. D (Radio Propagation), sometime in 1961.

[6] Harry Fine and John M. Taff, "Propagation Data and Service Calculation Procedures used for the Rescinded Appendix A of Report and Order (Docket 11532) Released June 26, 1956," FCC Rept. T.R.R. 2.4.16; October 22, 1956.

Appendix[7]

Empirical Estimates of Long-Term Variability

The data selected for this study were CRPL and FCC data, satisfying the two conditions:

1) Measurements of $E(10)$ were selected from data corresponding to the period 6:00 P.M.–midnight, all year, if more than 114 hourly medians or 20 days of data were available, and from period of record data, if the period of record was equal to or greater than one month.

2) Measurements of $E(1)$ were selected from data corresponding to the period 6:00 P.M.–midnight, all year, if more than 240 hours or 40 days of data were available, and from period of record data, if the period of record was equal to or greater than 60 days.

These data were separated into groups by frequency, and the fading ratios $y(10)=E(10)-E(50)$ and $y(1)=E(1)-E(50)$ were computed and plotted vs distance for each frequency group.

Data for which 15 miles$\leq d_s \leq$200 miles were classified into the 7 frequency intervals 38–66, 66–88, 88–108, 108–300, 300–500, 500–900, 900–1100 megacycles, and the mean values of $y(1)$, $y(10)$, $\log f_{mc}$ were determined for each interval. These 7 values $\overline{y(1)}$, $\overline{y(10)}$, $\overline{\log f_{mc}}$ were compared with the two-linear function of $\log f_{mc}$ given for $y(10)$ and $y(1)$ by FCC T.R.R.2.4.16[6] for a corresponding set of data $(15\leq d_s \leq 200)$; the comparison shows somewhat less frequency dependence than is indicated by Fine and Taff.

Data were next separated into the 6 frequency groups 38–88, 88–108, 108–300, 300–500, 500–900, 900–1100 mc. The distance dependence of $y(10)$ and $y(1)$ was determined for distances greater than 100 miles by linear regressions, first using data for all the frequency groups combined. The expressions for $y(10)$ and $y(1)$ so determined were:

$$y(10) = k(10) - (d - 100)b(10) \text{ db}, \quad b(10) = 0.0268 \quad (1)$$

$$y(1) = k(1) - (d - 100)b(1) \text{ db}, \quad b(1) = 0.0480. \quad (2)$$

[7] Written by W. R. Burns, National Bureau of Standards, Boulder, Colo.

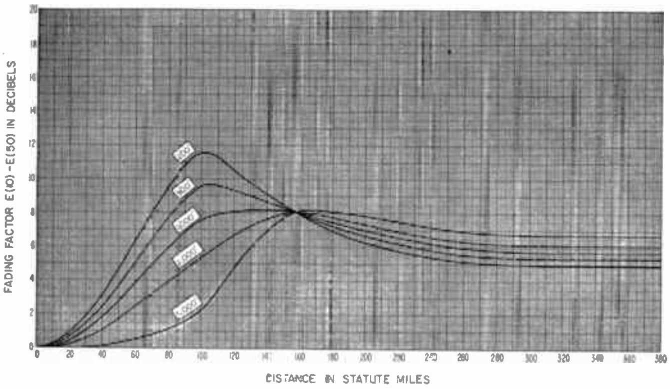

(a)

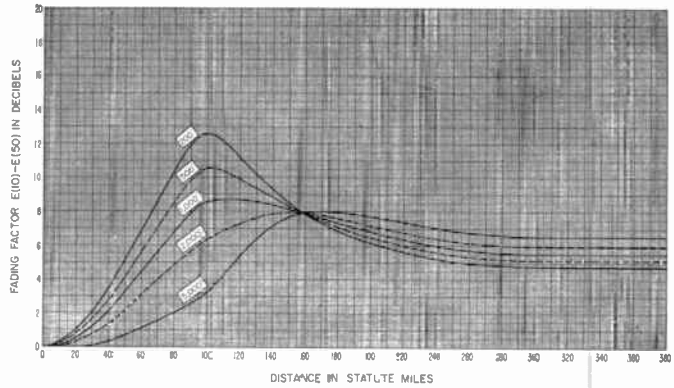

(b)

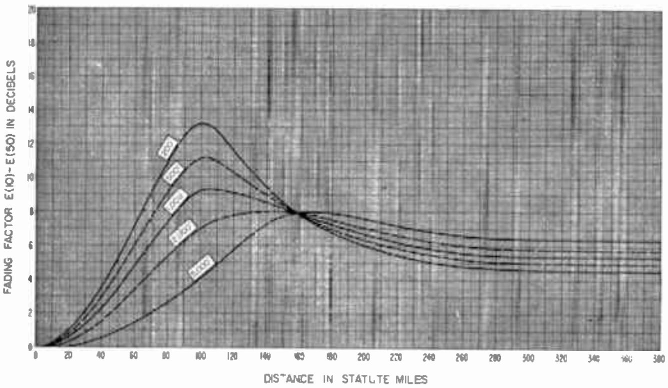

(c)

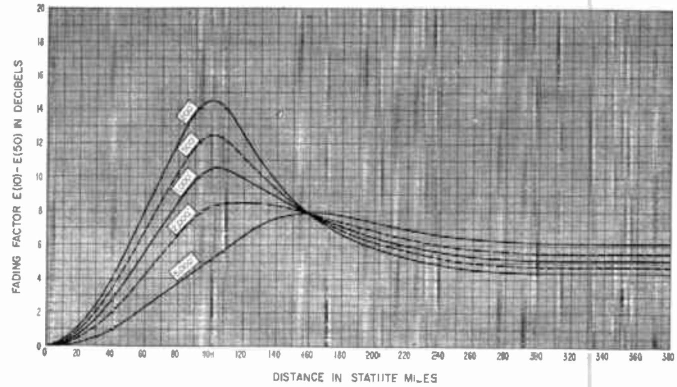

(d)

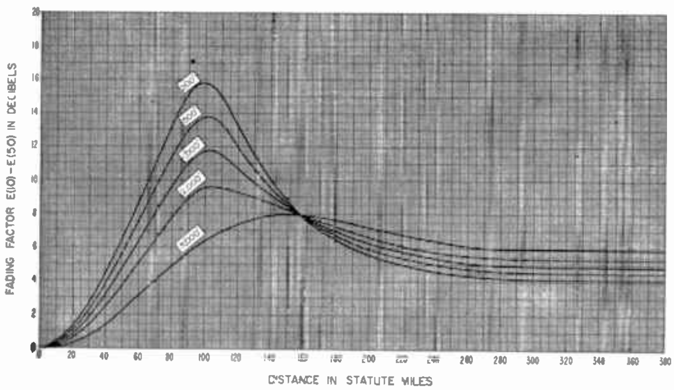

(e)

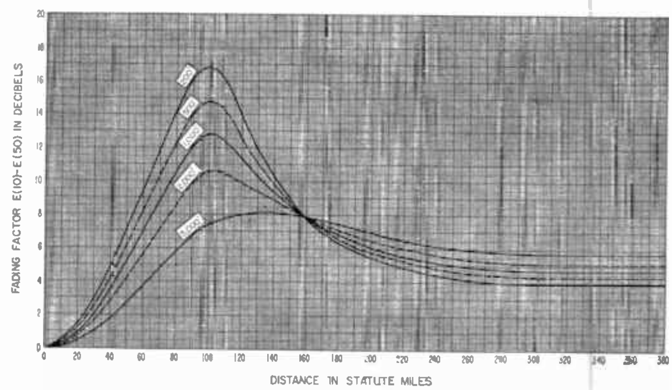

(f)

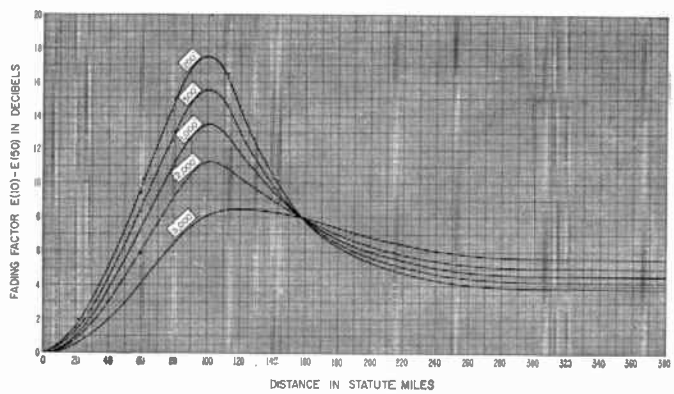

(g)

Fig. 12—Long-term fading factor $E(10)-E(50)$ in decibles vs distance and antenna height at (a) 40 mc, (b) 70 mc, (c) 100 mc, (d) 200 mc, (e) 400 mc, (f) 700 mc, (g) 1000 mc. One antenna at 30 feet, the other as indicated. $E(1)-E(50)=2E(10)-E(50)$.

The weighted average of the six values of the ratio $k(1)/k(10)$ for the corresponding six frequency groups, as determined with b fixed, was approximately two. As a check, both k and b were determined separately, for each of three frequency groups.

Next, linear regressions of $k(10)$ and $k(1)$ on $\log f_{mc}$ were found, using the values of $k(10)$ and $k(1)$ for each of the above six frequency groups and the corresponding values of $\overline{\log f_{mc}}$ for those groups. The expressions for $k(10)$ and $k(1)$ so determined were

$$k(10) = 7.09 + 1.42 \log f_{mc} \tag{3}$$

$$k(1) = 11.43 + 4.10 \log f_{mc}. \tag{4}$$

The distance and frequency dependence of $y(10)$ and $y(1)$ for $d<100$ miles was determined as above, except that only the data with low antenna heights—$h_{te} \leq 1000'$ and $h_{re} \leq 50'$—were used. The linear dependence of $y(10)$ and $y(1)$ upon frequency, at $d=50$ miles was compared with earlier work.[6] Also, the comparison was made for $y(10)$ and $y(1)$ at $d=100$ miles. Our determinations still showed a smaller frequency dependence of $y(10)$ and $y(1)$.

For data in the 88–108 mc frequency group with $h_{re} \leq 50'$, $y(10)$ and $y(1)$ were plotted against d, coding for antenna height (see Fig. 13). The curves in Fig. 13 were obtained from Fig. 12(c).

It appears that $y(1)$ is approximately equal to $2y(10)$. The distance dependence of $y(10)$ for $d>100$ miles was originally determined by drawing a curve through median values of data corresponding to overlapping distance intervals; for $d<100$ miles the curve was made to agree closely with the linear regression given by (1). Next, deviations $\delta y(10)$ of $y(10)$ from this curve were calculated for the data in the 88–108 mc frequency group and satisfying the conditions that $h_{re} \leq 50$ feet and $d<100$ miles. A linear regression of δy on $\log h_{te}$ for these data was determined. Also, the median value of d in the range $0<d<100$ miles was found. The same process was carried through for data with $d>100$ miles combined with the data described above.

A plot of δy vs $\log h_{te}$, for $d<100$ miles, $88<f_{mc}<108$ mc, $h_{re} \leq 50$ feet, seemed to indicate that the equation $\delta y(10) = a - b \log h_{te}$, corresponding to this set of data, should be restricted to the interval 200 feet $\leq h_{te} \leq 5000$ feet. A family of $y(10)$ vs d curves was constructed. The different curves of the family were blended together at about $d=160$ miles. It was decided to further restrict the data to be used by the conditions that $h_{te}<2000$ feet if $d<20$ miles and $h_{te}<5000$ feet, if $d<60$ miles; since the above family of curves was constructed using only those data satisfying these conditions. From this family of y vs d curves, a function $b(d)$ was determined and the following formula was now assumed for $y(10)$ and $\frac{1}{2}y(1)$:

$$\frac{1}{2} y(1) = y(10) = a(d) - b(d) \log \frac{h_{te}}{500} + cb(d) \log \frac{f_{mc}}{100}, \tag{5}$$

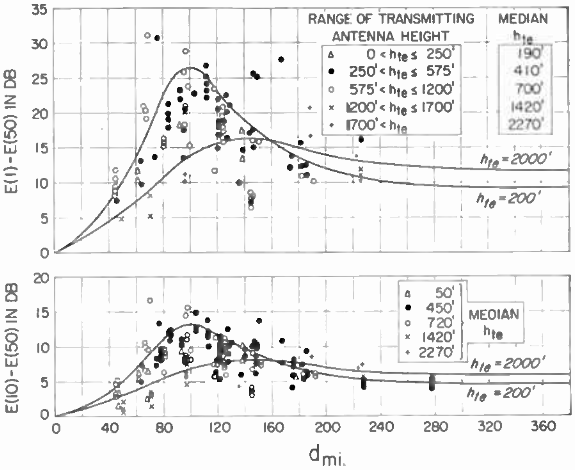

Fig. 13—Long-term variability at 100 mc (88 mc $\leq f_{mc} \leq$ 108 mc).

After examining how well the data could be made to agree with an empirical function of the form given by (5) and fixing on a value of 0.5 for c, it was decided to take into account the variations of h_{re}, and to use the additional data with $h_{re}>50$ feet, by means of the formula

$$\frac{1}{2} y(1) = y(10)$$

$$= a(d) - b(d) \log \left[\frac{(h_{te}+200)(h_{re}+200)}{(500+200)(30+200)}\right]$$

$$+ b(d) \log \sqrt{f_{mc}/100} \tag{6}$$

where $a(d)$ is the estimate of $y(10)$ for 100 megacycles and a 500 foot-30 foot antenna height combination. Finally, $b(d)$ was determined by least squares through all of the data available in each of several distance ranges, and the curves in Figs. 12(a) through 12(g) were drawn using graphs of $a(d)$ and $b(d)$ and using the empirical relation (6).

Subsequent work on this problem indicates that at 100 megacycles per second the long-term variability estimates of another paper[2] are better than the TASO estimates for angular distances beyond ten milliradians, and that for smaller distances the TASO estimates are better. Maximum values of y occur where theoretical diffraction and forward scatter fields are equal; it follows that the angular distance at which such a maximum is expected should be inversely proportional to the cube root of the frequency.

Acknowledgment

Most of the organization and descriptive analysis of data, the comparison of data with theory, and the computation of theoretical curves was done by members of the Tropospheric Analysis Section of the Central Radio Propagation Laboratory, under the direct supervision of Mrs. Mary A. Schafer and with the guidance of Mrs. A. G. Longley.

Picture Quality—Procedures for Evaluating Subjective Effects of Interference*

GORDON L. FREDENDALL†, FELLOW, IRE AND WILLIAM L. BEHREND†, SENIOR MEMBER, IRE

Summary—**In 1958, Panel 6 (Levels of Picture Quality) of the Television Allocations Study Organization conducted a comprehensive study of the subjective effects on picture quality of a number of types of interfering signals and noise, as functions of the levels of interference. These tests were designed and carried out by teams of engineers and experimental psychologists using a selective group of lay observers. This paper deals with the design of the tests and with the laboratory facilities used in the tests.**

THE charge of Panel 6 was stated as follows: "The Panel on Levels of Picture Quality shall determine the numerical specifications of the various objective measures of picture quality which result in specified degrees of subjective viewer satisfaction when television pictures are viewed in the presence of various types of interference."

Television reception is susceptible to interference from many sources which cause degradation of picture quality. Sources which were not considered as relevant in an allocation plan were dismissed by the Panel. Subjective testing was carried out with the following sources of interference: random noise, co-channel interference, upper adjacent channel interference, lower adjacent channel interference, and simultaneous random noise and co-channel interference.

Observations under 63 test conditions were made for monochrome and color reception. A total of approximately 200 observers participated, and 38,000 individual assessments of picture quality were recorded. This paper is intended to present the plan and conduct of the test. The report[1] of the Television Allocations Study Organization to the Federal Communications Commission and the report[2] of Panel 6 should be consulted for a complete account. A résumé of the test data is presented in a companion paper.[3]

Test Personnel and Test Environment

The design of the tests was dictated by the requirement that the test results should be a satisfactory sample of the reaction of the population of home television viewers to pictures accompanied by interference.

The lack of experimental flexibility in private residences with off-the-air signals restricted the choice of a test site to a fixed location at which signal-to-interference ratios could be varied at will and be reproduced. In the opinion of the Panel, the lack of a home atmosphere would be an entirely negligible factor. A large room at the David Sarnoff Research Center of the Radio Corporation of America was selected for the tests.

The plan of the Panel during the early months of activity envisioned the testing of three classes of observers, namely, metropolitan, suburban, and rural, on the basis that individuals from different areas have different criteria as a result of being accustomed to different signal levels and types of interference. As specific test plans developed, it proved impracticable to maintain this distinction. Also, the work already done by Panel 3 indicated that the distinction was probably unnecessary, their experience having been that viewers in unfavorable receiving locations were aware of the poor quality and that judgments of the three classes of observers were substantially alike.

Diversity was exercised in selecting male and female observers with a range of ages from approximately 18–65 years. In all, over 200 observers were recruited from college students and community organizations in the Princeton, N. J. area.

It was concluded that conventional commercial television receivers were the only unquestionably valid display devices for observation by viewers. The question of whether the receivers should be selected from high, medium, or low quality design was resolved by the considered opinion of the Panel that it would be a mistake to use the poorest quality from available models, and that the choice should be made among the higher grade commercial offerings. The selection of five 21-inch receivers, two color and three monochrome, was made by TASO. Placement of the receivers and observers is shown in Figs. 1 and 2.

The average room illumination was 0.6 foot-candle (as reflected from a horizontal magnesium oxide disk) of well-diffused overhead lighting and the highlight screen luminance of the receiver was 20 foot-lamberts.

Test Pictures and Rating Scale for Evaluation of Picture Quality

All television pictures viewed during the tests originated from colored slides. Still subject matter was selected in preference to moving subjects since it is generally acknowledged that observers are less critical of the latter. A television system must be capable of handling the more critical type of subject matter.

A psychological study to determine a scale of picture

* Original manuscript received by the IRE, February 15, 1960.
† RCA Labs., Princeton, N. J.
[1] "Engineering Aspects of Television Allocations"; March 16, 1959.
[2] "Report of Panel 6, Levels of Picture Quality"; January, 1959.
[3] C. E. Dean, "Measurements of the subjective effects of interference in television reception," this issue, p. 1035.

Fig. 1—Viewing room.

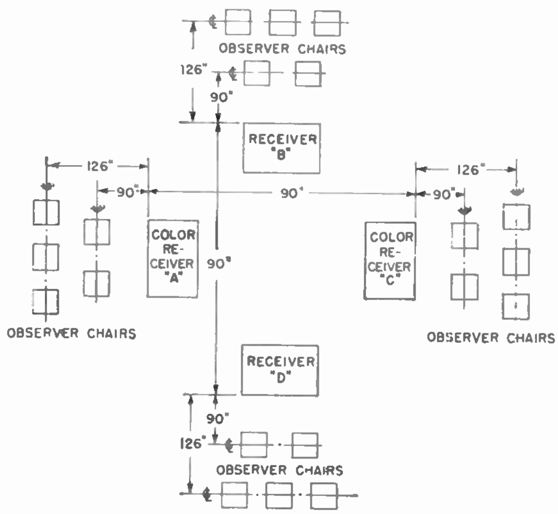

Fig. 2—Viewing arrangement.

quality suitable for lay observers resulted in the following scale and word description:

Number	*Name*	*Description*
1	Excellent	The picture is of extremely high quality, as good as you could desire.
2	Fine	The picture is of high quality providing enjoyable viewing. Interference is perceptible.
3	Passable	The picture is of acceptable quality. Interference is not objectionable.
4	Marginal	The picture is poor in quality and you wish you could improve it. Interference is somewhat objectionable.
5	Inferior	The picture is very poor but you could watch it. Definitely objectionable interference is present.
6	Unusable	The picture is so bad that you could not watch it.

This scale and the accompanying definitions were incorporated into the scoring sheet (Fig. 3) on which the observer recorded his impression of each picture.

TELEVISION ALLOCATIONS STUDY ORGANIZATION
PANEL 6
LEVELS OF PICTURE QUALITY

TEST NO. ________ TV SET ________ OBSERVER ________

EXCELLENT. THE PICTURE IS OF EXTREMELY HIGH QUALITY AS GOOD AS YOU COULD DESIRE.

0 1 2 3 4 5 6 7 8 9 10 11 12 13 14 15 16 17 18 19 20

FINE. THE PICTURE IS OF HIGH QUALITY PROVIDING ENJOYABLE VIEWING. INTERFERENCE IS PERCEPTIBLE.

0 1 2 3 4 5 6 7 8 9 10 11 12 13 14 15 16 17 18 19 20

PASSABLE. THE PICTURE IS OF ACCEPTABLE QUALITY. INTERFERENCE IS NOT OBJECTIONABLE.

0 1 2 3 4 5 6 7 8 9 10 11 12 13 14 15 16 17 18 19 20

MARGINAL. THE PICTURE IS POOR IN QUALITY AND YOU WISH YOU COULD IMPROVE IT. INTERFERENCE IS SOMEWHAT OBJECTIONABLE.

0 1 2 3 4 5 6 7 8 9 10 11 12 13 14 15 16 17 18 19 20

INFERIOR. THE PICTURE IS VERY POOR BUT YOU COULD WATCH IT. DEFINITELY OBJECTIONABLE INTERFERENCE IS PRESENT.

0 1 2 3 4 5 6 7 8 9 10 11 12 13 14 15 16 17 18 19 20

UNUSABLE. THE PICTURE IS SO BAD THAT YOU COULD NOT WATCH IT.

0 1 2 3 4 5 6 7 8 9 10 11 12 13 14 15 16 17 18 19 20

Fig. 3—Observer's scoring sheet.

Conduct of the Tests

A picture accompanied by a certain type of interference was reproduced on each of the four receivers simultaneously for 5 seconds and then removed for 10 seconds to permit rating by the observer on his individual rating sheet before the next presentation was made. Observers were instructed to encircle the number of the presentation under the quality rating dictated by their first impression of the picture. Observers were advised not to vacillate or "reason" in reaching a judgment. Each run consisted of 20 showings of the same subject with 10 different signal-to-interference ratios each repeated 2 times in a random order. The range of ratios extended from severe interference to no interference.

Observers moved as a group to a different receiver at the conclusion of each test run.

Receiver Characteristics

The susceptibility of a receiver to interfering signals on the adjacent channels is determined by the attenuation at the upper adjacent picture carrier and the lower adjacent sound carrier. Attenuation data are given in Table I.

TABLE I

LEVEL IN DB RELATIVE TO PIX CARRIER

Receiver	Pop-up*	Adj. Sound	Band Center	Color Sub-carrier	Sound	Pop-up*	Adj. Pix
1 (color)	−37	< −60	+6	0	< −60	−31	−48
2 (mono)	−33	−51	+5	−1	−22†	−23	−33
3 (color)	−34	< −60	+6	0	−58	−31	−50
4 (mono)	−28	−54	+7	0	−26	−24	−43
5 (mono)	−24	−48	+8	0	−20	−10	−25

* Pop-up refers to the frequency and attenuation at the minimum attenuation point beyond the frequency of the sound trap.
† Sound trap measured −24 but was shifted ¼ mc high (at RF).

TV SIGNAL GENERATING APPARATUS

In these simulated transmissions, the FCC requirements for color transmission were observed in all essential respects. A block diagram of the laboratory apparatus is given in Fig. 4 and a photograph of the equipment in Fig. 5. Testing expediency called for duplication of equipment at several points so that the desire of Panel 6 to test one group of observers on a number of different type tests could be fulfilled. Test conditions could be changed for many of the tests within a few minutes.

In all tests, the picture carrier was modulated to place full white at 15 per cent of the sync-tip carrier voltage, and all sound signals were deviated approximately ±7.5 kc at 400 cycles.

The equipment was located in a separate room not visible to the observers. However, there were visual and verbal communications between the equipment operators and the psychologists conducting the tests.

A. Co-Channel Interference

A simplified block diagram of the test apparatus for co-channel interference is given in Fig. 6 (p. 1034). The frequency offsets between the picture carriers were accurately kept by automatic frequency control circuits at the frequencies of reference signals provided by stable oscillators. An oscilloscope monitored the frequency lock and a counter measured the offset frequency.

A resistive distribution system provided identical signals to the monitoring facilities and the receivers. The desired signal was maintained at a constant level, and the level of the interfering signal was varied to provide the signal-interference ratios used for the subjective tests.

B. Random Noise

In the random-noise tests, the noise was combined at RF with a high-level desired signal, as shown in the simplified diagram of Fig. 6. The noise spectrum was flat within ±3 db over TV Channel 4 (66–72 mc); over the more important frequency band, from the picture carrier to the color subcarrier sideband, the spectrum was flat within ±1 db.

Signal-to-interference ratios for various presentations were produced by maintaining the desired signal at a constant level and varying the noise level.

C. Adjacent Channel

Fig. 7 is a simplified diagram of the apparatus for adjacent-channel interference tests. Channel 4 was the desired channel for lower adjacent channel interference and Channel 3 was the desired channel for upper adjacent channel interference.

The frequency response of Channel 4 from the output of the low-power transmitter to the output of the distribution system is given in Fig. 8. Video frequencies in excess of 4.2 mc were strongly attenuated at the input of the transmitter in accordance with standard practice. The filter characteristic is given in Fig. 9.

An attempt was made to operate with the maximum levels of unwanted sidebands allowed by the standards of the Federal Communications Commission. However, it was not feasible to meet this criterion in all cases. The standards state "the lower sideband . . . , shall not be greater than −20 db for a modulating frequency of 1.25 mc or greater and in addition, for color, shall not be greater than −42 db for a modulating frequency of 3.579545 mc (the color subcarrier frequency)." Referring to the response of the interfering upper channel (Fig. 8), it is seen that for modulating frequencies from 1.25 mc to 2.25 mc the lower sidebands were 2 db below the maximum level allowed by the standards. Sidebands due to modulating frequencies greater than 2.25 mc were below the maximum allowable level. However, the energy in these sidebands is small except around the color subcarrier sideband (63.65 mc), where the response is only 1 db less than the maximum allowed by the standards.

The carrier frequencies were measured before each test by a counter which had an accuracy of 3 parts in 10^6. For the lower adjacent channel (Channel 3) interference tests, the receivers were tuned to remove the lower adjacent sound carrier. A different technique was used to tune the receivers for the upper adjacent (Channel 4) interference tests since a well-defined null was not present in all receivers. The receivers were tuned to WRC-TV (Channel 3) and the fine-tuning adjusted for minimum interference from WCBS-TV (Channel 2) sound carrier and picture carrier of WRCA-TV (Channel 4). This procedure insured that the tuning would be correct after restoration of the test carrier signals.

Signal ratios were changed by varying the desired signal level; the interfering signal level remained constant.

D. Simultaneous Co-Channel and Random-Noise Interference

In each of the simultaneous co-channel and random-noise interference tests, the amount of the desired signal and the amount of the random noise were fixed. The interfering co-channel signal was varied over the same range of levels as the levels used for the co-channel interference tests.

The diagram of test apparatus is the same as Fig. 6, except that noise is added to the two television signals at a separate input to the adder.

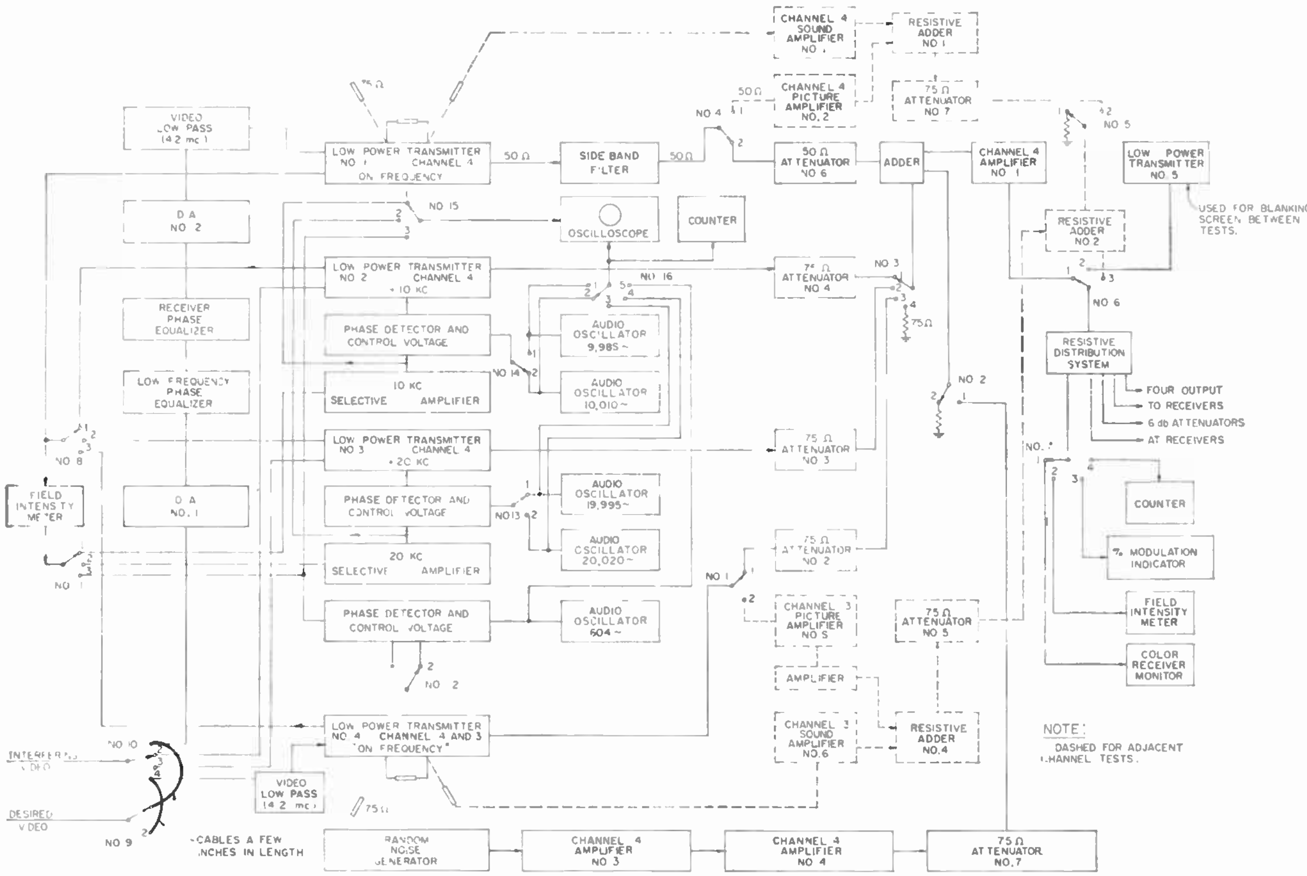

Fig. 4—Laboratory apparatus.

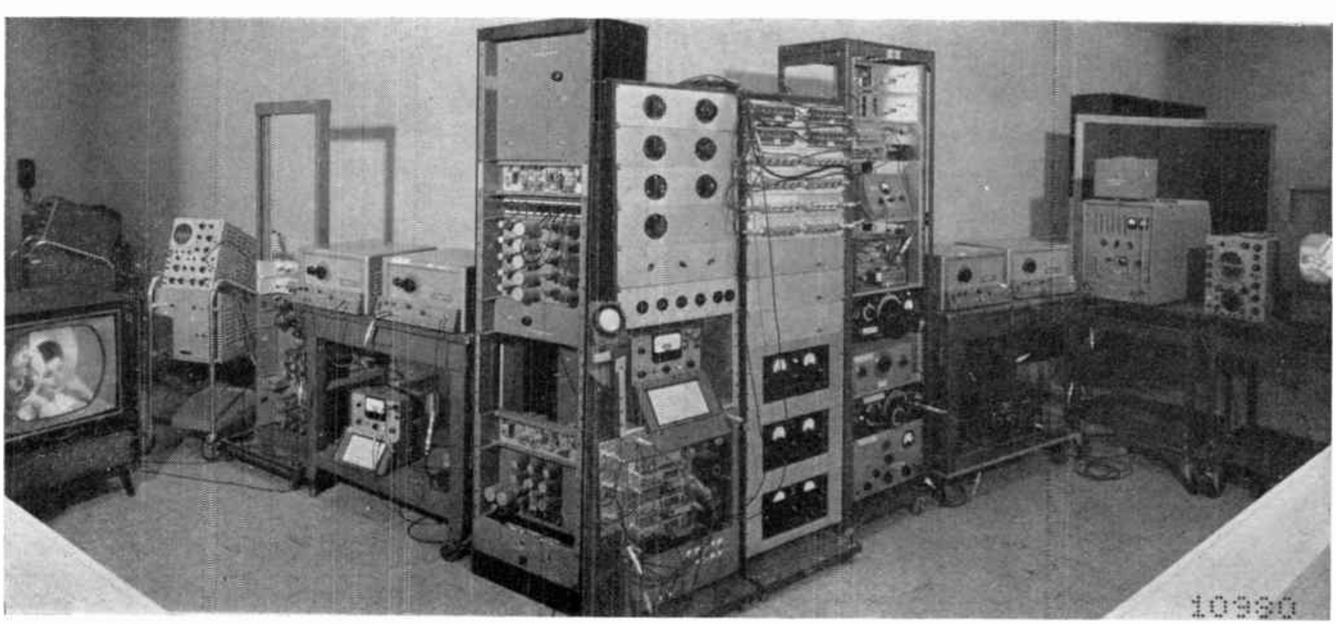

Fig. 5—Equipment setup.

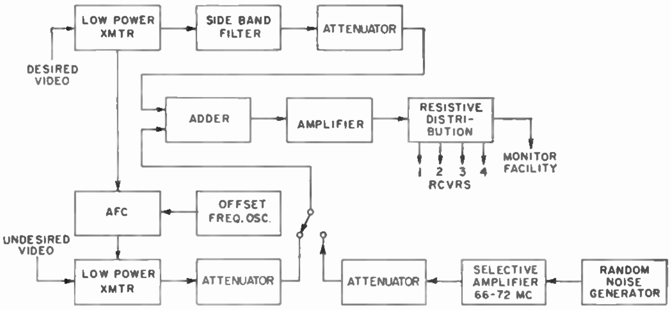

Fig. 6—Simplified diagram of co-channel tests and random noise tests.

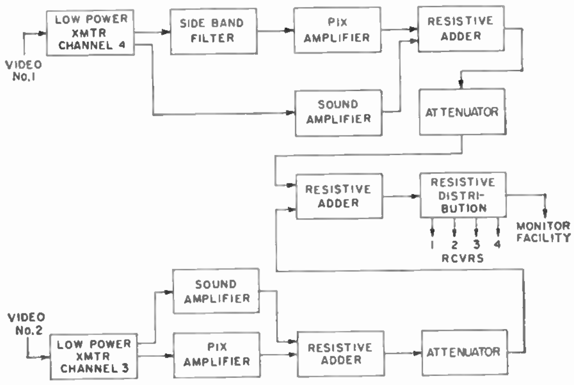

Fig. 7—Simplified diagram of adjacent channel tests.

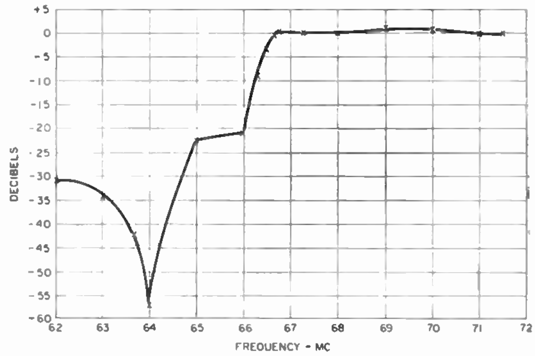

Fig. 8—Channel 4 frequency response.

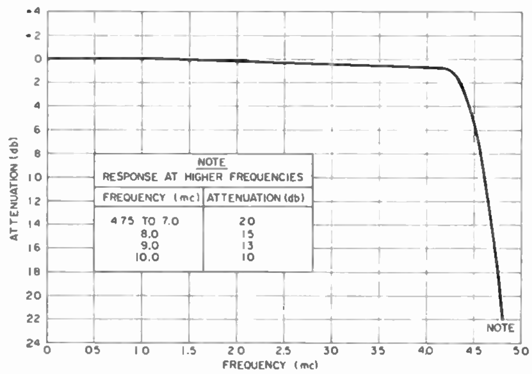

Fig. 9—Amplitude response characteristics of video low pass filter.

Measurements of the Subjective Effects of Interference in Television Reception*

CHARLES E. DEAN†, FELLOW IRE

Summary—**A measurement program was conducted in which almost 200 observers made about 38,000 rating observations on color and monochrome stationary television pictures impaired by various known amounts of interference. Separate tests were made for the following types of interference: upper adjacent channel, lower adjacent channel, random noise, co-channel with each of six carrier-frequency separations, and simultaneous random noise and co-channel. Six rating grades were used as follows: 1) Excellent, 2) Fine, 3) Passable, 4) Marginal, 5) Inferior, and 6) Unusable. The observations were handled on a statistical cumulative frequency basis and plotted on probability paper. Commercial monochrome and color receivers were used, and the tests were made with laboratory signal-generating equipment on the lower VHF television channels.**

As representative results, a picture impaired by upper-adjacent-channel intereference (with 6-mc channels) was rated by 50 per cent of the observers as Passable or better for −27-db ratio of signal to interference. For the lower adjacent case a similar value was found, this result being explained as due to better traps in the medium-high-grade receivers of the test than in many receivers in use by the public. For random-noise interference the requirement for Passable or better rating by 50 per cent of the observers was +27 db on the basis of RMS sync amplitude to RMS noise over the 6-mc channel. The co-channel tests gave the following requirements for the Passable or better rating by 50 per cent of the observers: 22 db for 360 cycles offset, 41 db for 604, 24 db for 9985, 17 db for 10,010, 29 db for 19,995, and 17 db for 20,020. Data for simultaneous co-channel and random-noise interference were taken for 14 combinations of test conditions.

Introduction

At an early point in the Television Allocations Study Organization (TASO) activity it was realized that the five panels then existing should be supplemented by a sixth, in order to obtain data on the physical qualities of television pictures necessary for given grades of viewer satisfaction. Panel 6 was therefore established and proceeded to plan and carry out a suitable program of experimental tests. The equipment and procedures were chosen with care and are described in the companion paper by Fredendall and Behrend.[1]

The many possible combinations of conditions for which tests could be made, especially when it is realized that more than one type of interference can be present simultaneously, made it desirable to take as many data as possible, but also necessitated that careful selection be made of the conditions to be used. The test program which was carried out consisted of 63 test conditions and included participation by nearly 200 persons, who made about 38,000 individual assessments of picture quality.

The results which are considered of the greatest importance are reported in the present paper, chiefly in the form of plotted curves. A more complete account of the work is included in the general TASO report,[2] and extensive additional data are given in the mimeographed Panel 6 report.[3] The original data sheets, the IBM punched cards to which the original data were transcribed, and tabulations made from the cards, have been forwarded to the Federal Communications Commission, where they are available for any desired future studies.

List of Test Conditions

The 63 test conditions which were used consisted of 12 with adjacent-channel interference, 8 with random noise, 29 with various types of co-channel interference, and 14 with combinations of co-channel and random-noise interference. All these are listed in Table I, where the general type of interference is shown in the first column. The next column states whether the interfering frame rate was 29.27 or 30 per second, representative of interference from a color or a monochrome transmission. The following columns give the desired picture, the number and sex of the observers, and the identifying test numbers. All tests were performed at Princeton, but the test numbers assigned here were supplemented by additional numbers in the data processing at Rochester, giving the two sets of test numbers in the last two columns.

Accuracy of Results

Two methods were used to get information on the accuracy of the results of the tests. The first utilized the fact that numerous individuals made assessments on a picture of given technical quality, so that a standard deviation between individuals was obtainable. The second method utilized the fact that, in most of the tests, there was among the presentations of different signal-to-interference ratios in random order a repetition of each ratio, unknown to the observer, so that a measure was obtained of the consistency with which an observer repeated a previous assessment. The conclusion from these considerations is that the findings from the tests are accurate within a standard deviation of approximately ±1 decibel in the signal-to-interference ratio. This is on the basis of the test procedure consisting of assessments of pictures by the observers without

* Original manuscript received by the IRE, February 23, 1960; revised manuscript received, March 29, 1960.

† Hazeltine Research Corp., Little Neck, N. Y.

[1] G. L. Fredendall and W. L. Behrend, "Picture quality—procedures for evaluating subjective effects of interference," this issue, p. 1030.

[2] "Engineering Aspects of Television Allocations," TASO Rept. to the Federal Communications Commission; March 16, 1959.

[3] "Levels of Picture Quality," TASO Rept., Panel 6; January, 1959.

TABLE I
TESTS MADE BY TASO PANEL 6 IN MAY AND JUNE 1958

Type of Interference	Interfering Frame Rate*	Desired Picture	Observers No.	Observers Sex	Test Numbers† Princeton	Test Numbers† Rochester
Adjacent-Channel Tests						
Upper Adjacent Channel	29.97	Miss Taso	18	F	1	1M
Same	29.97	Kitchen	21	F	1K	39J
Same	30	Miss Taso	36	M	1A	2M
Same	30	Kitchen	21	F	1AK	40J
Lower Adjacent Channel (Sound at normal level of 3 db below picture)	29.97	Miss Tsao	18	F	2	3M
Same	29.97	Kitchen	21	F	2K	41J
Same	30	Kitchen	21	F	2AK	43J
Same	30	Miss Taso	18	M	2A	4M
Lower Adjacent Channel (Sound at 10 db below picture)	29.97	Miss Taso	18	F	3	6M
Same	29.97	Kitchen	21	F	3K	42J
Same	30	Miss Taso	18	M	3A	7M
Same	30	Kitchen	21	F	3AK	44J
Random Noise Tests Including Observations with Several Scenes						
Random Noise	Not applicable	Miss Taso	38	F	9	19M
			38	M	9	19M&34J
Same	Not applicable	Cat held by girl	16	F	9C	53J
Same	Not applicable	Drapes and flowers	16	F	9D	52J
Same	Not applicable	Bowl of fruit	16	F	9F	49J
Same	Not applicable	House with horse and carriage	16	F	9H	54J
Same	Not applicable	Kitchen	16	F	9K	48J
Same	Not applicable	Boy & girl holding sail	16	F	9S	50J
Same	Not applicable	Tug of war	16	F	9T	51J
Co-Channel Tests						
Co-channel (604-cycle offset)	30	Miss Taso	18	F	4	9M
Same	30	Kitchen	21	F	4K	45J
Same	29.97	Kitchen	21	F	4AK	46J
Same	29.97	Miss Taso	18	M	4A	10M
Co-channel (360-cycle offset)	29.97	Kitchen	21	F	29K	47J
Co-channel (9985-cycle offset)	30	Miss Taso	38	F	5	11M & 14J
Same	29.97	Miss Taso	18	M	5A	12M
			17	F	5A	2J
Same	30	Kitchen	21	F	5K	16J
			20	M	5K	26J
Same	29.97	Kitchen	17	F	5AK	4J
			20	M	5AK	31J
Co-channel (10,010-cycle offset)	29.97	Miss Taso	33	F	6	13M & 1J
Same	30	Miss Taso	37	F	6A & 6AR	13J & 25J
Same	29.97	Kitchen	17	F	6K	3J
			20	M	6K	30J
Same	30	Kitchen	20	F	6AK	15J
			20	M	6AK	27J
Co-channel (switched between 10,010- and 9985-cycle offset)	29.97	Miss Taso	37	F	14	24M & 5J
Same	29.97	Kitchen	37	F	15	25M & 6J
Same	30	Miss Taso	41	F	18	28M & 17J
Same	30	Kitchen	41	F	19	29M & 18J
Co-channel (19,995-cycle offset)	30	Miss Taso	39	F	7	15M & 23J
Same	29.97	Miss Taso	15	F	7A	11J
			18	M	7A	16M
Same	30	Kitchen	21	F	7K	19J
			20	M	7K	28J
Same	92.97	Kitchen	17	F	7AK	7J
			20	M	7AK	32J
Co-channel (20,020-cycle offset)	92.97	Miss Taso	33	F	8	17M & 12J
			18	M	8	12J
Same	30	Miss Taso	20	F	8A	24J
Same	29.97	Kitchen	17	F	8K	8J
			20	M	8K	33J
Same	30	Kitchen	21	F	8AK	20J
			20	M	8AK	29J
Co-channel (switched between 19,995- and 20,020-cycle offset)	29.97	Miss Taso	37	F	16	26M & 9J
Same	29.97	Kitchen	35	F	17	27M & 10J
Same	30	Miss Taso	41	F	20	30M & 21J
Same	30	Kitchen	41	F	21	31M & 22J

* The two interfering frame rates, 30 and 29.97 cycles per second, give data on the basis of interference coming from a monochrome or color station respectively.

† The K in Princeton test numbers designates the Kitchen Scene. The M in Rochester test numbers designates the May series of tests and similarly J the June series. All tests were made at Princeton, but were assigned separate series of test numbers at Princeton and Rochester.

TABLE I (*continued*)

Type of Interference	Interfering Frame Rate*	Desired Picture	Observers		Test Numbers†	
			No.	Sex	Princeton	Rochester
Tests with Simultaneous Co-channel Interference and Random Noise						
Co-channel and random noise (9985-cycle offset and 38-db ratio of desired signal to random noise)	30	Miss Taso	18	M	11	21M
Same but 32-db ratio of desired signal-to-noise	30	Miss Taso	18	M	10	20M
Same	29.97	Kitchen	20	M	28K	35J
Same but 20-db ratio of desired signal-to-noise	29.97	Miss Taso	18	M	22	32M
Co-channel and random noise (10,010-cycle offset and 38-db ratio of desired signal to random noise)	29.97	Miss Taso	18	M	13	23M
Same but 32-db ratio of desired signal-to-noise	29.97	Miss Taso	18	M	12	22M
Same	29.79	Kitchen	20	M	12K	36J
Same but 20-db ratio of desired signal-to-noise	29.97	Miss Taso	18	M	23	33M
Co-channel and random noise (19,995-cycle offset and 32-db ratio of desired signal-to-noise)	29.97	Miss Taso	18	M	24	34M
Same	29.97	Kitchen	20	M	24K	37J
Same but 20-db ratio of desired signal-to-noise	29.97	Miss Taso	18	M	25	35M
Co-channel and random noise (20,020-cycle offset and 32-db ratio of desired signal-to-noise)	29.97	Miss Taso	18	M	26	36M
Same	29.97	Kitchen	20	M	26K	38J
Same but 20-db ratio of desired signal-to-noise	29.97	Miss Taso	18	M	27	37M

the benefit of any simultaneous comparison. (That is, the tests were not on the basis of comparing two pictures and stating which is better, nor on the basis of one picture being adjustable so that it could be varied to equal the other.)

Choice of Scene

Preliminary observations by panel members using various scenes produced the impression that the character of the scene had little effect on the assigned ratings. The first main series of tests, made during May, 1958, were therefore mostly with one scene, namely the "Miss TASO" picture shown in Fig. 1. It was then realized that other scenes, especially those where the picture detail is of greater interest than the general effect, might be rated more severely by the observers. In the June tests, therefore, numerous conditions were repeated but with the substitution of the "Kitchen Scene," shown in Fig. 2, where the attention is shared by foliage, grapes, apples, bananas, etc. A comparison of the data revealed that the observers did, in fact, make more severe judgements in the case of the Kitchen Scene to the extent of 0.3 grade, or a spread of ± 0.15 grade from the average of the two scenes. (The grade as a unit here is on the basis of the scale of assessment with 1 for Excellent, 2 for Fine, etc., through 6 for Unusable.)

A further study of the effect of scene was made using random-noise interference. Eight of these tests were made, differing only in the change of scene. Included were the scenes of Figs. 1 and 2 and six other assorted scenes. The spread of the assigned grades in the important intermediate range of signal-to-noise ratios averaged 0.6 grade, or ± 0.3 grade. The curves for Figs. 1 and 2 were approximately parallel to each other, and were well situated in the center of the total spread. It is considered, therefore, that the bulk of the general data, obtained by averaging the test results with Miss TASO and the Kitchen Scene, is well representative of the range of scenes used in television broadcasting.

In the tests of adjacent-channel and co-channel interference, the picture on the interfering signal was the Sailboat Scene shown in Fig. 3.

Effect of Sex

The 63 test conditions varied with respect to the general type of interference, the interfering frame rate, and the desired scene. Of these 63, a total of 14 test conditions were employed with separate all-men and all-women groups, so that data were available for comparing men and women as television observers. Analysis of the results of these 14 conditions indicated that: 1) women appear to be more critical of technical picture quality to the extent of about 0.3 grade; 2) there is slightly more variation in rating from woman to woman for a given picture than from man to man, the standard deviations being 1.1 and 0.9 grades respectively; and 3) the two sexes are equally consistent in making a second rating on a given picture, the two viewings being in random order among pictures of other signal-to-interference values—the correlation coefficient between the two ratings was 0.80 for both sexes.

This indication that women are slightly more critical viewers is subject to some qualification on account of the fact that about two-thirds of the men tested were undergraduate college students while the women were older, being chiefly members of women's clubs or parent-teacher associations. An age differential and/or a difference in time devoted to television viewing might therefore have influenced the result. However, the result is supported by tests made several years earlier by McIlwain,[4] in which women typically required 390 kc of color video (the signal above this frequency being only mixed highs) while the men required only 320 kc.

On account of the small magnitude of the differences of the data for men and women, and also the practical

[4] K. McIlwain, "Requisite color bandwidth for simultaneous color-television systems," Proc. IRE, vol. 40, pp. 909–912; August, 1952.

Fig 1—Miss TASO picture used as desired scene in numerous tests.

Fig. 2—Kitchen Scene used as alternative desired scene in various tests.

Fig. 3—Sailboat Scene used as interfering scene in adjacent-channel and co-channel tests.

point that television broadcasting is intended for service to the general population, it is considered that this question can normally be disregarded. No adjustment for sex has been applied to the data obtained in the program of tests.

Effect of Frame Rate

The 12 adjacent-channel and the 29 co-channel test conditions were almost equally divided between frame rates of 30 and 29.97 pictures per second, these corresponding respectively to interference from a monochrome and from a color transmission. Comparison of the data for the two frame rates showed that the benefit of precise-offset co-channel operation (at 10,010 or 20,020 cycles rather than 9985 or 19,995 cycles) is somewhat greater when the interference is at 29.97 than when it is at 30 per second. In other tests, frame rate had little effect and it is therefore thought that in allocations matters other than precise offset it will not be an important factor.

Color vs Monochrome

In all tests, the observers were divided into four groups of about five subjects each, two of the groups observing color receivers while the other two observed monochrome receivers. Equal quantities of data were therefore obtained for color and monochrome reception. Comparisons of the data for the two cases have been made in a few instances and revealed little difference, with a suggestion of a slightly greater tolerance for interference when receiving a color picture. The data for color and monochrome reception are therefore pooled in most of the numerous plots giving the Panel findings.

Methods of Data Handling

At least three methods are available for the reduction of data characterized as here by 1) numerous observers, 2) a number of reasonably closely spaced signal-to-interference ratios, and 3) a choice of several merit ratings which have been intended to constitute equal steps of subjective picture quality. Two of the three methods were used in the analysis of the Panel 6 data, and the third has often been used in other studies of this kind.

The first method can be said to employ a cumulative frequency distribution, the term "frequency" being used here in the statisticians' sense of the number of times a particular test value is obtained. With this method, attention is directed to the data obtained with a particular signal-to-interference ratio in a given test and the distribution of ratings by all the observers in the test is determined. With this frequency distribution in hand, the values can then be added up to obtain the cumulative frequency curve (the statisticians' ogive curve). Such data are naturally plotted on a special type of cross-section paper having a "probability scale" in one of the coordinate directions and a linear scale in the other, since on such paper a statistical normal cumulative distribution appears as a straight line and other distributions show more natural shapes than would be the case with other conventional types of plotting paper. The use of this type of data reduction and plotting by Panel 6 was requested by the Federal Communications Commission (FCC); accordingly, plots of this kind were predominantly used. This method is referred to as "Method I."

The second available method of data handling again directs attention to the results for a particular signal-to-interference ratio, but instead of determining the distribution of ratings, it merely includes an averaging of them. This is called "Method II." In comparison with Method I, it has two disadvantages, *viz.*, 1) the grade steps are necessarily assumed equal in Method II, whereas there is no such requirement in Method I, and 2) the original distribution of grades cannot be recovered by going backward from a Method II plot, whereas they can be in Method I. However, Method II has an advantage in that plots made by this method are much more easily understood by lay and semitechnical readers, since the curves clearly show poor grades assigned to low signal-to-interference values and favorable grades to high signal-to-interference values. Various Method II plots are included in the TASO[2] and Panel 6[3] reports, but because of space limitations none are given in the present account.

Method III was not used in the Panel 6 work, but it is listed because it has been used in various investigations heretofore made in this field. This method consists in directing attention to a particular grade of service and then mathematically handling (*e.g.*, averaging) the values of signal-to-interference ratio which the various observers found necessary for this grade of service.

While for some purposes in using the Panel 6 data it may well be unnecessary to give particular attention to the method of data reduction, the reader is cautioned that the different methods do not necessarily give identical results, so that in important applications careful attention should be given to this matter.

Following previous practice of the FCC, the Method I plots of the data have the signal-to-interference ratio on a linear scale of decibels as ordinates and have as abscissas the probability scale indicating the fraction of the viewers assessing the picture to be of a particular grade or better. Five curves are plotted on the sheet, one each for Grades 1 through 5. No sixth curve is shown because 100 per cent of the observers necessarily considered all pictures to be Unusable or better. With the greater signal-to-interference values plotted upward, the Grade 1 (or Excellent) curve is above all the other curves, the Grade 2 (Fine) curve next below, etc. The meaning of any point of any one of these curves is that at the particular signal-to-interference ratio (the ordinate), the indicated percentage of the viewers (the abscissa) rates the picture as of the stated grade or better. Attention may be concentrated, if desired, on values for 50 per cent of the observers, for 90 per cent, or for any other specified percentage.

The cumulative calculation by which these curves on probability paper are obtained may advantageously be described by a simple example. Suppose a picture of a certain signal-to-interference ratio is judged by numerous observers and that the grades assigned are as follows: 5 per cent of the viewers call the picture Excellent (Grade 1), 25 per cent call it Fine (Grade 2), 50 per cent call it Passable (Grade 3), and the remaining 20 per cent call it Marginal (Grade 4). The cumulative operation consists of adding these up, with a result which can be stated as follows: 5 per cent of the viewers call the picture Excellent, 30 per cent call it Fine or better (*i.e.*, Fine or Excellent), 80 per cent call it Passable or better, and 100 per cent call it Marginal or better. These cumulative values are the points on the plotting sheet where the various curves cross the horizontal line corresponding to the signal-to-interference ratio of the picture. In the same way, data for other signal-to-interference ratios are handled and the points plotted, so that sufficient information is obtained to draw in the desired curves. As an example of a Method I plot, see Fig. 4.

In all these plots giving the results of the Panel 6 tests, the plotted points show the data, with the curves drawn in to indicate the general trends.

Upper-Adjacent-Channel Interference

The desired signal in all tests was according to the FCC color standards, including a frame rate of 29.97 per second. Interference from an upper-adjacent-channel transmission, therefore, appeared as a slowly moving picture if the interference was nominally at 29.97, since the two sync generating chains were independent. If the interfering frame rate was 30 (using 60-cycle power-line synchronization), the interfering picture was completely unsynchronized. The cause of the interference was readily seen to be the picture carrier and sidebands of the upper-adjacent signal, with no effect from the interfering color subcarrier and sidebands or the sound signal.

Plots of the upper-adjacent data, pooling the Miss TASO and Kitchen Scene observations, are shown in Figs. 4 and 5 (p. 1041) for the 29.97 and 30 interfering frame rates, respectively. In the area of chief interest (having grades of Fine (2), Passable (3), and Marginal (4), and 20 per cent to 80 per cent of the observers), the two plots are in good agreement. For the 50 per cent abscissa, as an example of the results, the required signal-to-interference values are −22 db for Fine or better, −27 db for Passable or better, and −31 db for Marginal or better. These values are negative because the receiver selectivity permits the interference to be much stronger than the desired signal at the antenna terminals.

Lower-Adjacent-Channel Interference

Interference from the lower-adjacent channel appears predominantly as an FM bar pattern of 1.5 mc average frequency, which is the difference between the desired picture carrier and the interfering sound carrier.

Tests of lower-adjacent interference were made with the normal 3-db amplitude relation between sound and picture signals of the interfering transmission, and also with 7 db less sound, that is, with the interfering sound power 10 db below the interfering picture power. The stated signal-to-interference ratios in all cases are the values of desired picture to undesired picture, and are, therefore, on the same basis as the upper-adjacent and the co-channel tests. The lower-adjacent-channel test results are shown in Figs. 6 and 7. It can be seen that the 7-db lowering of the interfering sound signal produced changes of about 5 db in the curves. It may be conjectured that the discrepancy of 2 db indicates the appearance of a small amount of interference due to the lower adjacent color subcarrier.

A comparison of Fig. 4 or 5 with Fig. 6 shows the ratios for upper and lower adjacent interference to be much alike, the requirement for 50 per cent of the observers to assess the picture as Passable or better being −26 db or −27 db in both cases. This varies from the general experience of broadcast engineers, who have normally found interference on the lower-adjacent channel to be more objectionable than interference on the upper-adjacent channel. The present data, showing approximately equal effects, appear to be associated with better traps against the lower-adjacent channel in the receivers used by Panel 6 than are provided in many receivers now in service. The data of Panel 6 were taken with receivers which had lower adjacent sound rejections exceeding their upper-adjacent picture rejections on the average by 14 db. This is substantially different from approximate equality reported by the Receiving Equipment Panel (No. 2) for these two rejection values. The Panel 6 data are therefore considered to be a normal result of the decision of Panel 6 to use medium-high-grade receivers in its test program.

Random-Noise Interference

On account of the unique character of random noise, it was considered of special importance, and tests utilizing five groups of observers, totaling 92 persons, were therefore made. Various scenes were used, as listed in Table I.

The results of these tests are plotted in Figs. 8 and 9. In addition to affording random-noise data, these tests indicated the effect of choice of scene, as already discussed. As representative values of the effect of random noise, 50 per cent of the observers required a 23-db ratio for Marginal or better and a 27-db ratio for Passable or better. The present findings are in general agreement with results found by others.[5–8]

[5] R. N. Jackson, "Subjective Assessments of Noise in Television Pictures," Mullard Res. Labs., Redhill, Eng., Rept. Np. 308; July, 1959.

[6] L. E. Weaver, "Subjective impairment of television pictures," *Elec. and Radio Engrg.*, vol. 36 pp. 170–179; May, 1959.

[7] T. Kilvington, "Effects of noise in television transmission," *J. TV Soc.*, vol. 9, pp. 26–31; January, 1959.

[8] R. D. A. Maurice, *et al.*, "The Visibility of Noise in Television," BBC Engineering Division Monograph No. 3 Kingswood Warren, Surrey, Eng.; October, 1955.

The signal-to-interference ratio in the random-noise tests is the ratio of radio-frequency RMS signal during sync peaks divided by the RMS noise voltage over a 6-mc channel.

Co-Channel Interference

The Panel took special interest in the subject of co-channel interference and conducted numerous tests in this area. Tests were made for various offset frequencies, the Miss TASO and Kitchen Scene pictures, and the two frame rates. In addition, the benefit of precise offset was measured with special accuracy by "switched" tests in which at each observation the offset was changed between the best and the worst, such as from 10,010 cycles (best) to 9985 cycles (worst) in the neighborhood of 10 kilocycles.

The lowest offset frequencies used were 360 and 604 cycles, which are respectively a very good value and a very bad value in the low-frequency range and are representative of the performance which may be obtained with very precise carrier-frequency offset operation.[9] A Method I comparison of the data at these two offsets showed a benefit at the 50 per cent abscissa of about 24 db for Fine, 19 db for Passable, and 13 db for Marginal.

The interference at 360 cycles offset consists of a stationary interfering picture. The data which were taken for this offset consisted of a single test with the 29.97 frame rate and the Kitchen Scene, using 21 female observers. The results are given in Fig. 10. The vertical slopes of the upper portions of the Excellent, Fine and Passable curves here suggest that some pictorial aspects of the picture, such as definition, color rendition, subject matter, etc., influenced the ratings and prevented the assignment of a better grade when the interference was weak or imperceptible.

The 604-cycle offset produces slowly moving, widely spaced, horizontal bars. Data with this offset were taken for the four combinations of the two frame rates and the usual two desired pictures. Pooling these four tests gives the curves in Fig. 11.

Co-channel carrier-frequency offsets of 9985 and 19,995 cycles are two of the more objectionable offsets near 10 kc and 20 kc for the frame rate of 29.97 cycles used for the desired picture. These offsets produce a visual effect of slowly moving, narrow, horizontal bars. These are slightly wider for the 19,995-cycle offset. Offsets of 10,010 and 20,020 cycles are two of the more desirable offsets near 10 kc and 20 kc for a frame rate of 29.97 cycles for the desired picture. A visual interlace effect in these cases leads to a finer bar structure and thus reduces the visibility of the interference. In standard offset operation, the frequency difference may range over an interval of ±1 kc from the nominal separation, passing through favorable and unfavorable pre-

[9] L. C. Middlekamp, "Reduction of co-channel television interference by very precise offset carrier frequency," IRE Trans. on Broadcast Transmission Systems, vol. BTS-12, pp. 5–10; December, 1958.

cise-offset conditions.[10,11] An unfavorable condition may last for an appreciable length of time and therefore is regarded as the determining factor in the grade of station service.

The Panel 6 test conditions, as listed in Table I, included 32 on 10-kc and 20-kc precise offset, covering all combinations of four offsets, two scenes, two frame rates, and two methods of test (direct and switched). Individual plots were made for these 32 combinations and are given in the panel report.[3] Five values read from each of these 32 curve sheets are tabulated in Table II. For the present account the eight plots for 29.97 frames per second and the direct test method seem to be of the most value and are therefore given as Figs. 12 through 19.

Comparing the appropriate values in Table II and pooling the data for the two scenes, we find the benefit of precise offset at 10 kc (*i.e.*, 10,010 cycles vs 9985) to average 7.4 db for the 29.97 frame rate and 4.0 db for the 30 frame rate. Similarly at 20 kc the benefit is 10.6 db for 29.97 and 9.4 db for 30.

Considering only the data for the 29.97 frame rate and the Kitchen Scene, as given in Figs. 13, 15, 17 and 19, and computing separately for the various signal-to-interference values, we obtain the curves of Fig. 20. It is seen that the precise-offset improvement is substantial, especially for the higher grades of picture quality afforded by greater signal-to-interference values.

[10] W. L. Behrend, "Reduction of co-channel interference by precise frequency control of television picture carriers," *RCA Rev.*, vol. 17, pp. 443–459, December, 1956; vol. 20, pp. 349–364, June, 1959.
[11] E. W. Chapin, L. C. Middlekamp and W. K. Roberts, "Co-channel television interference and its reduction," IRE Trans. on Broadcast Transmission Systems, vol. BTS-10, pp. 3–24; June, 1958.

A comparison for the six offset frequencies of the signal-to-interference values at which 50 per cent of the observers rate the picture as Passable or better is given in Table III and affords a convenient condensed summary of the effect of the various offsets.

Simultaneous Co-Channel and Random-Noise Interference

Among the many possible cases of two sources of interference acting simultaneously to impair television reception, the Panel chose that of co-channel interference and random noise as most in need of study because of its importance and the absence of previous research attention.[12] Fourteen test conditions were used, of which two were with a 30-cycle interfering frame rate and the remainder with 29.97. In each test, the amount of the desired signal and the amount of the random noise were fixed. The amount of the interfering co-channel signal was varied over a wide range, and in conjunction with the fixed desired-signal intensity determined the stated and plotted db values of signal-to-interference ratio; *i.e.*, the ordinates do not include the effect of the random noise. In some tests, the amount of random noise was substantial, the ratio of the desired signal to the noise being only 20 db; in other tests, this ratio was 32 db, and in others it was 38 db.

Co-channel and random-noise interference in combination produce a visual effect of narrow horizontal bars moving through a "snowy" picture. The contrast of the bars is proportional to the level of co-channel

[12] "Offset Frequencies for TV Emission: Part III, Multiple Co-channel Interference," FCC Lab. Division, Rept. on Project 222,926; December 13, 1956.

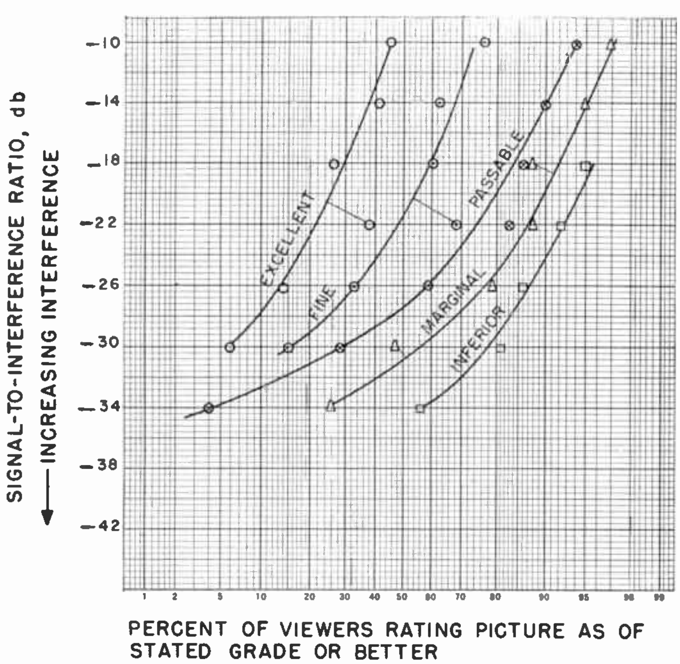

Fig. 4—Upper-adjacent-channel interference with 29.97-cycle interfering frame rate and pooled Miss TASO and Kitchen Scene pictures. Tests 1 (1M) and 1K (39J), using 39 female observers.

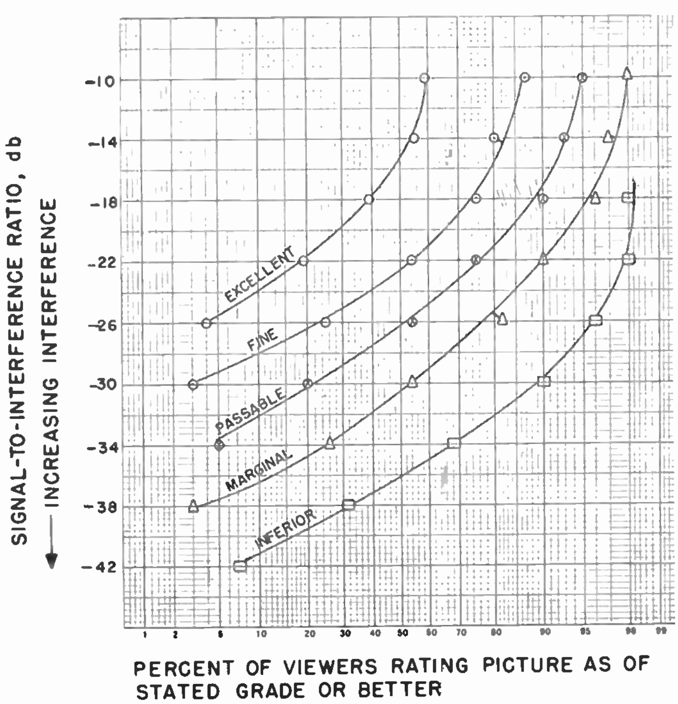

Fig. 5—Same as Fig. 4, but with 30-frame interference. Tests 1A (2M) and 1AK (40J), using 36 male and 21 female observers.

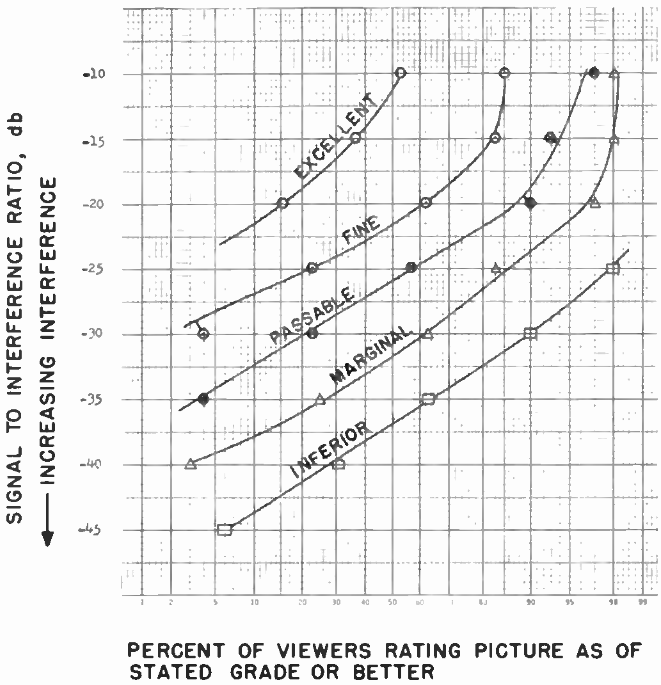

Fig. 6—Lower-adjacent-channel interference with pooled frame rates and pooled Miss TASO and Kitchen Scene pictures. Normal relation of sound and picture power. Tests 2AK (43J), 2A (4M), 2K (41J), and 2 (3M), using 18 male and 60 female observers.

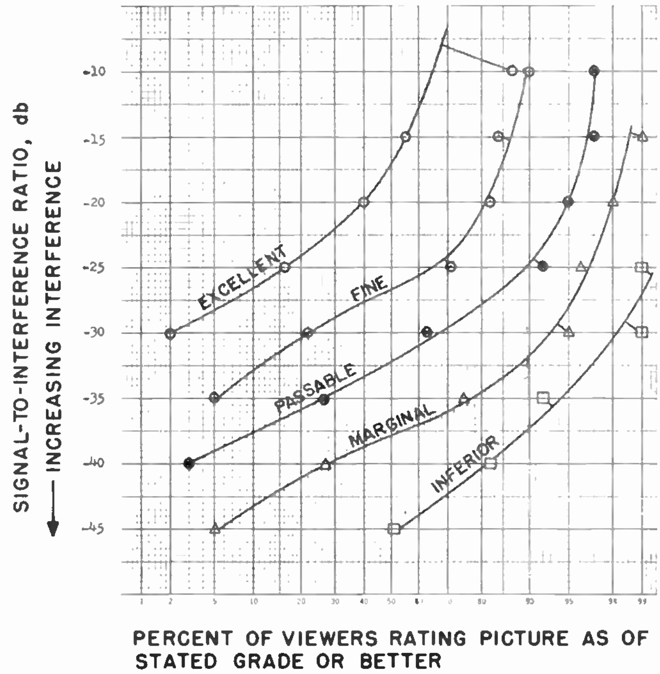

Fig. 7—Same as Fig. 6, but with interfering sound-picture ratio 7 db below normal. Tests 3 (6M), 3K (42J), 3A (7M), and 3 AK (44J), using 18 male and 60 female observers.

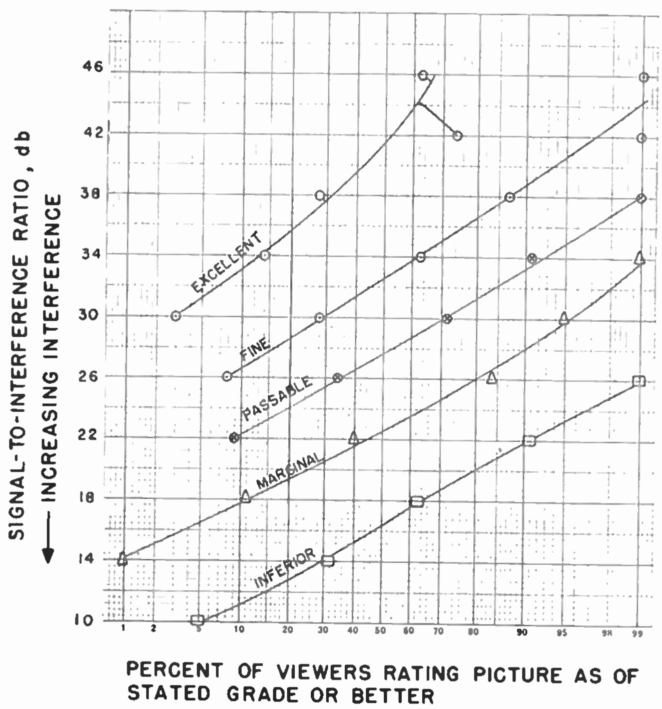

Fig. 8—Random-noise interference with Miss TASO picture. Test 9 (19M and 34J), using 38 male and 38 female observers.

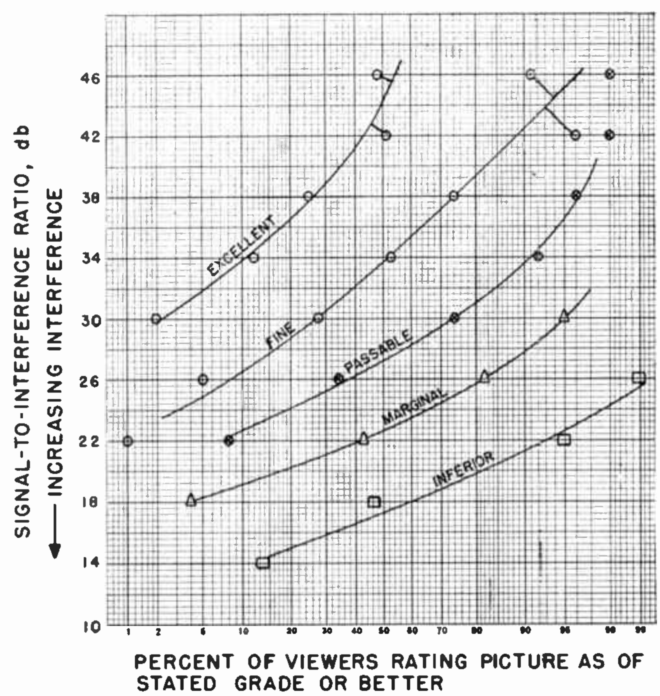

Fig. 9—Random-noise interference, averaging the results from seven scenes not including Miss TASO. Observers were 16 women who participated in all seven tests.

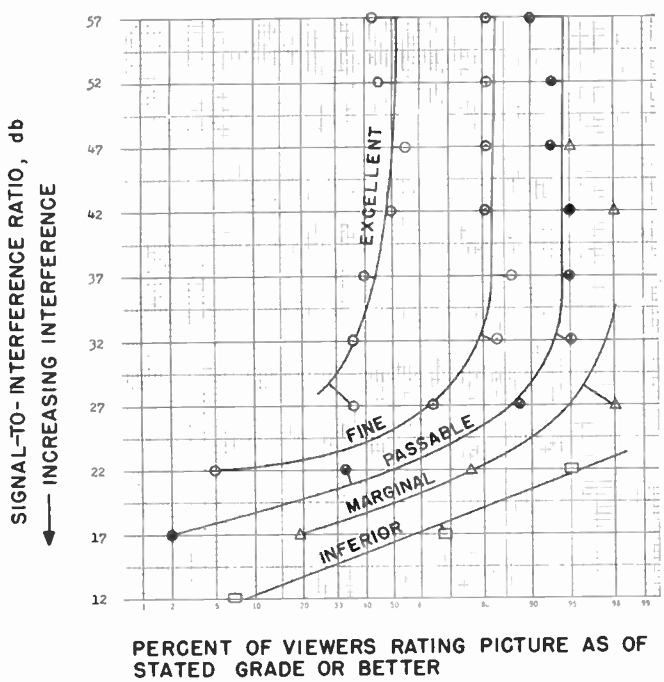

Fig. 10—Co-channel interference with carriers separated by 360 cycles, representative of very precise offset operation. Test was made with 29.97-cycle interfering frame frequency and the Kitchen Scene as the desired picture. The observers were 21 women. Test number 29K (47J).

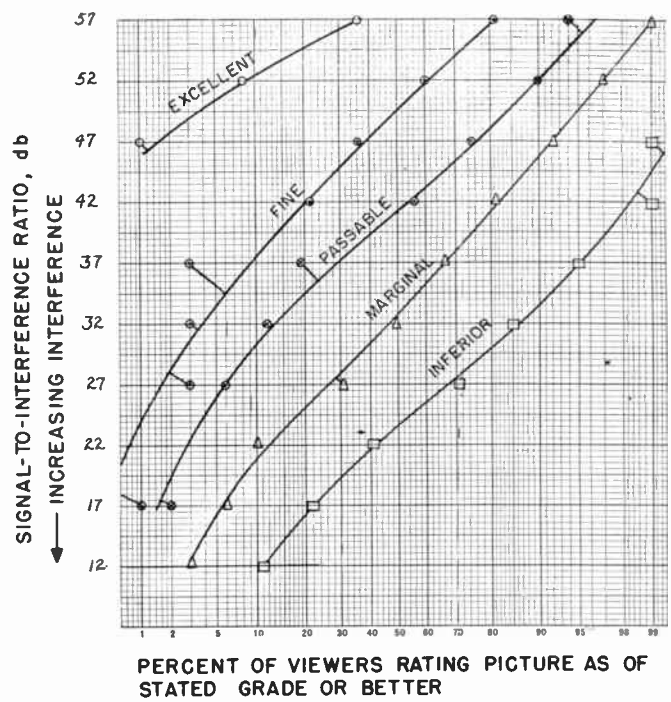

Fig. 11—Co-channel interference with 604-cycle carrier separation, representative of worst relation in region of near-synchronous operation. The data are averages of four tests with the two frame rates and Miss TASO and Kitchen Scene pictures. The observers were 20 men and 58 women. Test numbers 4 (9M), 4K (45J), 4AK (46J), and 4A (10M).

TABLE II

Signal-to-Interference Ratios in Decibels Read from Curves for Co-Channel Intefrerence with Offsets Near 10 and 20 Kilocycles

Offset (cps)	Scene	F. R. (cps)	Switched 50 Per Cent Passable or Better	Direct 50 Per Cent Passable or Better	Switched 80 Per Cent Passable or Better	Direct 80 Per Cent Passable or Better	Switched 50 Per Cent Fine or Better	Direct 50 Per Cent Fine or Better	Switched 80 Per Cent Fine or Better	Direct 80 Per Cent Fine or Better	Switched 40 Per Cent Excellent	Direct 40 Per Cent Excellent
9985	TASO	29.97	20.2	21.2	25.0	27.8	28.0	28.1	35.5	33.5	38.5	38.4
9985	Kitch	29.97	25.5	24.0	34.0	31.7	31.5	30.7	41.8	37.3	42.5	38.5
9985	TASO	30	21.8	19.2	25.0	25.3	25.5	24.6	32.0	30.8	34.2	30.6
9985	Kitch	30	24.2	18.2	30.0	23.0	30.3	24.4	37.7	29.6	35.5	32.0
10,010	TASO	29.97	17.8	16.5	21.6	20.3	21.8	22.1	29.0	28.4	25.3	28.5
10,010	Kitch	29.97	19.5	16.6	24.2	21.2	24.2	21.7	31.7	29.4	32.0	33.4
10,010	TASO	30	21.3	17.3	25.7	20.1	22.1	20.7	26.5	24.9	26.8	26.8
10,010	Kitch	30	20.4	18.4	23.5	21.4	25.2	22.1	30.4	25.4	27.7	27.9
19,995	TASO	29.97	25.5	23.1	30.7	28.8	30.8	31.7	37.4	37.4	42.6	41.6
19,995	Kitch	29.97	30.2	29.0	37.2	34.5	35.8	34.2	42.6	41.4	45.7	47.3
19,995	TASO	30	23.6	25.6	28.0	33.7	29.8	34.5	36.2	42.2	41.2	45.8
19,995	Kitch	30	27.4	26.0	31.6	32.4	32.6	32.8	37.4	40.6	39.2	42.9
20,020	TASO	29.97	16.0	16.9	23.0	20.7	23.5	21.3	29.7	25.3	27.2	27.0
20,020	Kitch	29.97	16.0	17.0	23.6	22.5	24.4	22.9	39.6	29.4	42.0	28.5
20,020	TASO	30	19.7	18.6	22.4	21.1	23.8	20.8	26.7	23.1	30.3	30.2
20,020	Kitch	30	23.0	18.1	27.0	22.3	26.6	23.1	30.4	28.5	32.5	29.8

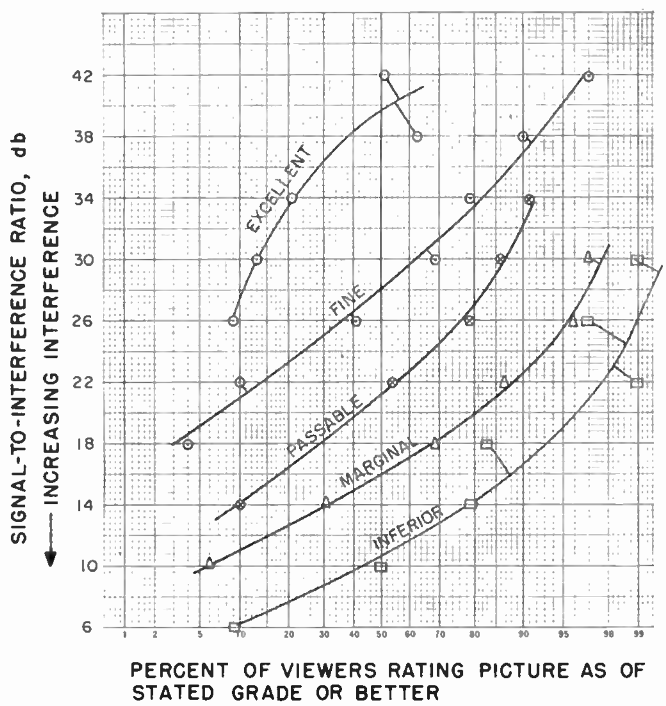

Fig. 12—Co-channel interference with 9985-cycle separation, 29.97 frame rate, and Miss TASO scene. This offset is a very poor one in the vicinity of 10 kc. The observers were 18 men and 17 women. Tests 5A (12M and 2J).

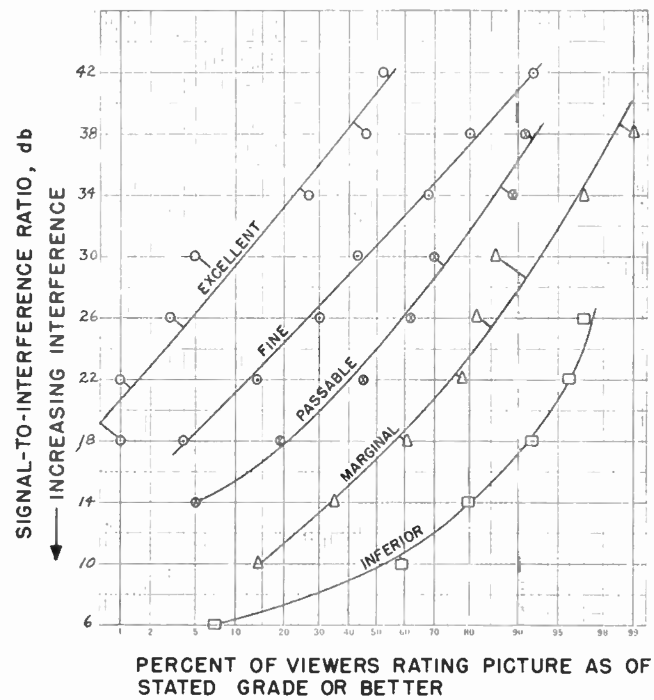

Fig. 13—Co-channel interference for same conditions as Fig. 12 except use of Kitchen Scene. The observers were 20 men and 17 women. Tests 5AK (4J and 31J).

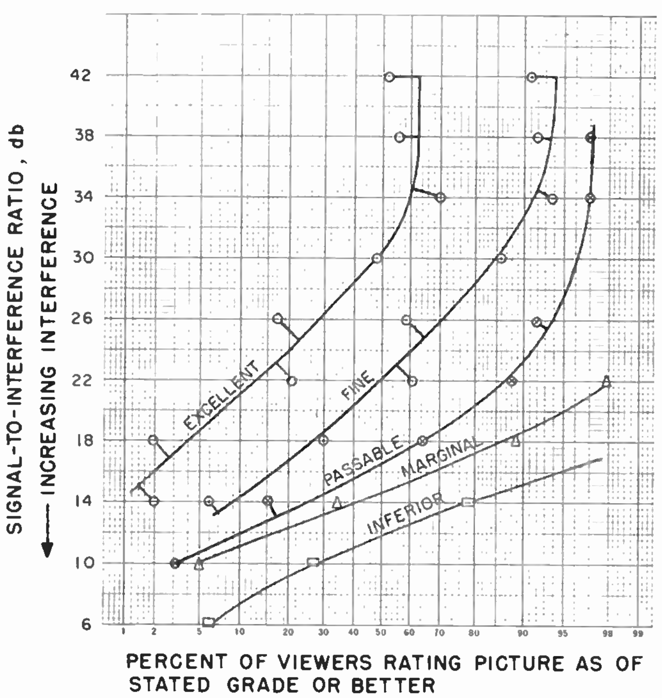

Fig. 14—Co-channel interference with 10,010-cycle separation, 29.97 frame rate, and Miss TASO scene. This offset is a very good one in the vicinity of 10 kc. The observers were 33 women. Tests 6 (13M and 1J).

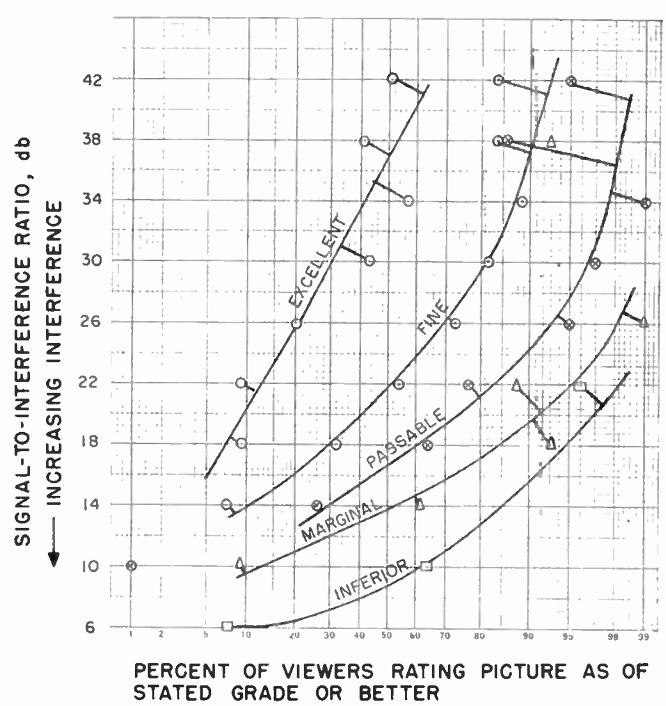

Fig. 15—Co-channel interference for same conditions as Fig. 14 except use of Kitchen Scene. The observers were 20 men and 17 women. Tests 6K (3J and 30J).

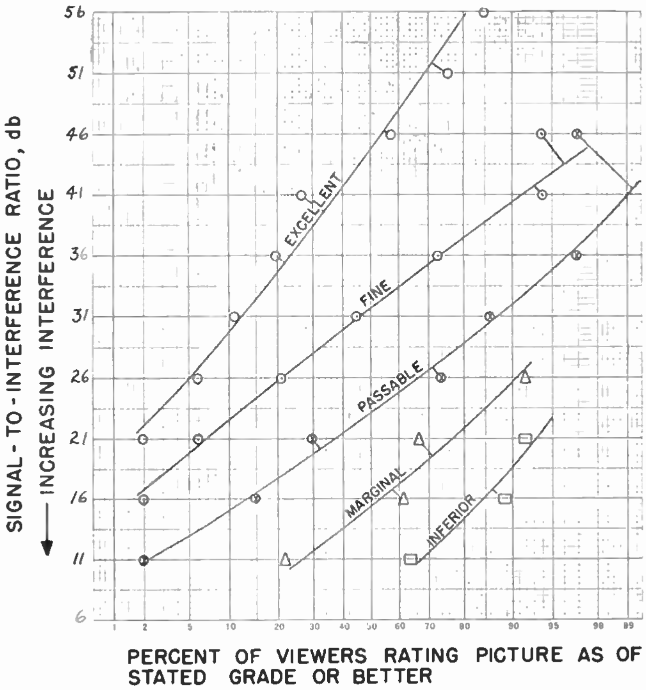

Fig. 16—Co-channel interference with 19,995-cycle separation, 29.97 frame rate, and Miss TASO scene. This offset is a very poor one in the vicinity of 20 kc. The observers were 18 men and 15 women. Tests 7A (16M and 11J).

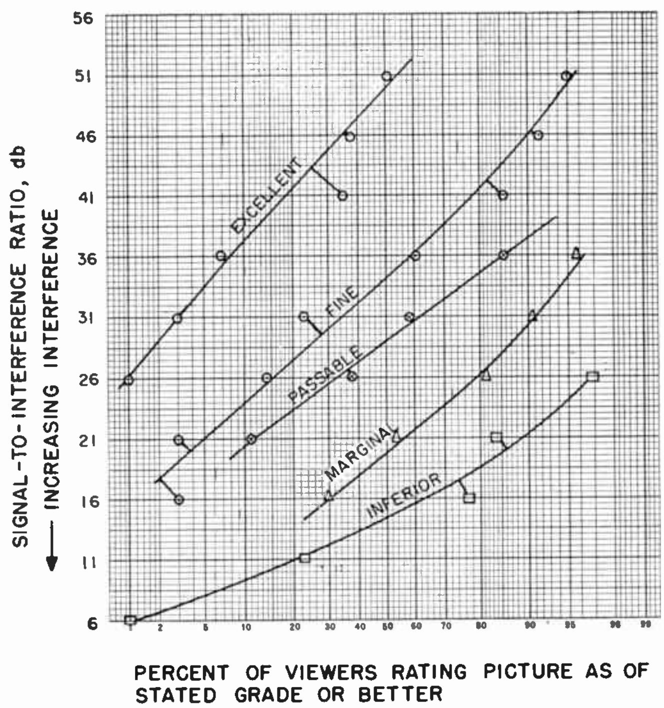

Fig. 17—Co-channel interference for same conditions as Fig. 16 except use of Kitchen Scene. The observers were 20 men and 17 women. Tests 7AK (7J and 32J).

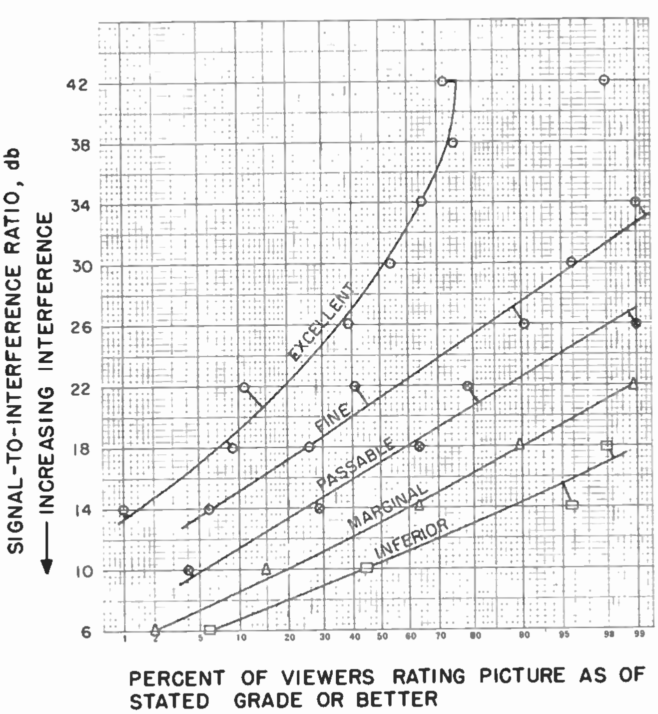

Fig. 18—Co-channel interference with 20,020-cycle separation, 29.97 frame rate, and Miss TASO scene. This offset is a very good one in the vicinity of 20 kc. The observers were 18 men and 33 women. Tests 8 (17M and 12J).

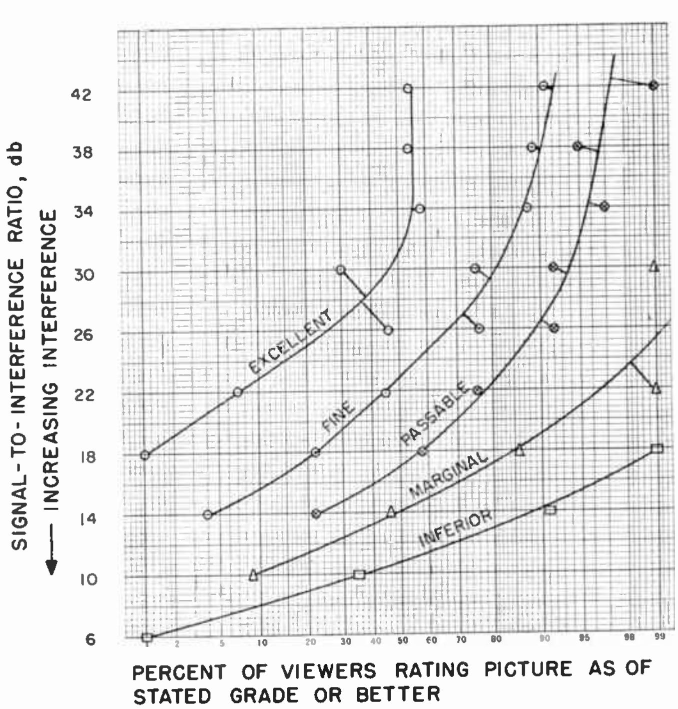

Fig. 19—Co-channel interference for same conditions as Fig. 18 except use of Kitchen Scene. The observers were 20 men and 17 women. Tests 8K (8J and 33J).

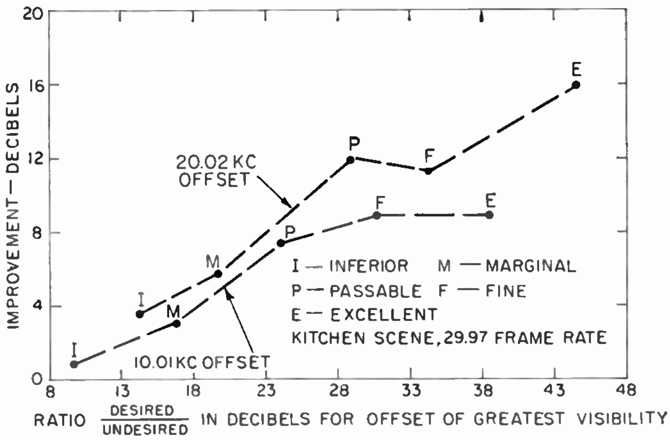

Fig. 20—Improvement afforded by precise-offset operation, computed from Figs. 13, 15, 17 and 19.

interference, and the "snowiness" is proportional to the magnitude of the random noise. The more favorable offsets lead to a finer line structure and reduced visibility of the bar pattern.

It seems likely that in the future considerable effort will be devoted to devising formulas which will give accurately the combined effect of any given amounts of two or more types of interference acting simultaneously. For this reason it appears desirable to give a fairly complete account of the data which the Panel took in this area. The results of the twelve tests at the 29.97 frame rate are therefore shown in Figs. 21–32.

TABLE III

Comparison of Offset Frequencies*

Amount of Carrier Offset	Signal-to-Interference Ratio at which 50 Per Cent of Observers Rate Picture as Passable or Better
360 cycles	22 db
604 cycles	41 db
9985 cycles	24 db
10,010 cycles	17 db
19,995 cycles	29 db
20,020 cycles	17 db

* Conditions: 29.97 frame rate and Kitchen Scene.

An analysis of Figs. 21–32 was made by noting the required signal-to-interference ratios for ratings of Passable or better and Marginal or better and comparing these with the corresponding values for tests with the same types and amounts of co-channel interference but no random noise. In this way, the effect of adding the random noise was obtained. The interesting result was found that in about half the cases the two types of interference (one producing horizontal bars and the other producing general varying mottled effects) seemed to "help" each other, the combination being more acceptable than the co-channel interference alone. This phenomenon was observed in various cases having the 38-db or the 32-db ratio of signal-to-noise, but it was not observed with the greatest noise value corresponding to the 20-db ratio of signal-to-noise.

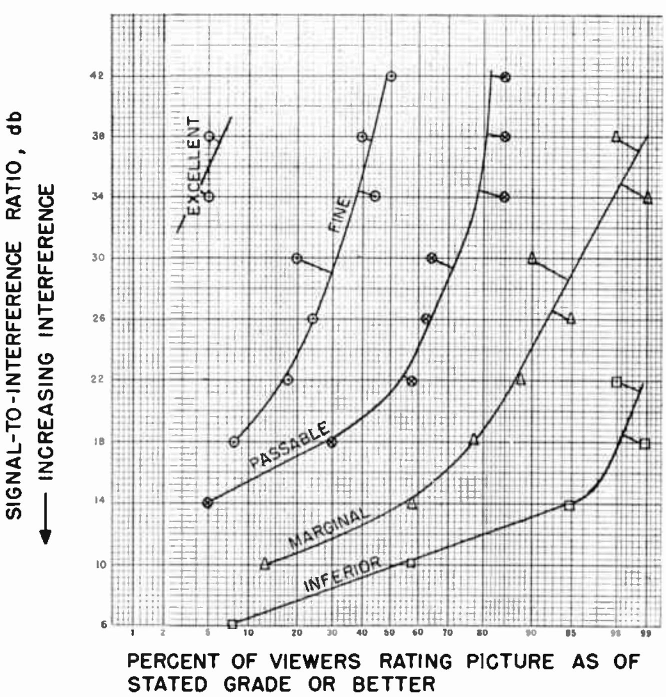

Fig. 21—Simultaneous 9985-cycle co-channel and random-noise interference. The desired signal was at fixed level, 32 db above the fixed random noise. Ordinates give decibel ratio of desired signal to the adjustable-level co-channel interference. Frame rate 29.97 and Kitchen Scene. Observers were 20 men. Test 28K (35J).

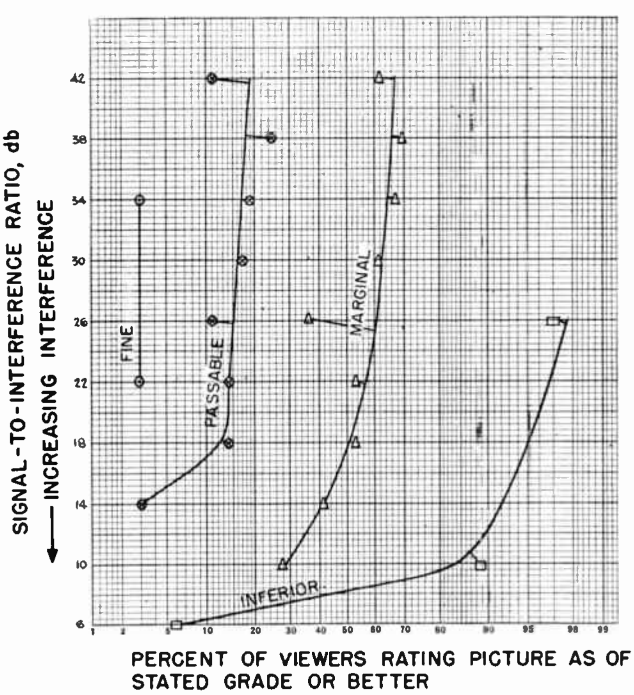

Fig. 22—Same as Fig. 21 except 20-db ratio of desired signal to random noise and use of Miss TASO scene. Observers were 18 men. Test 22 (32M).

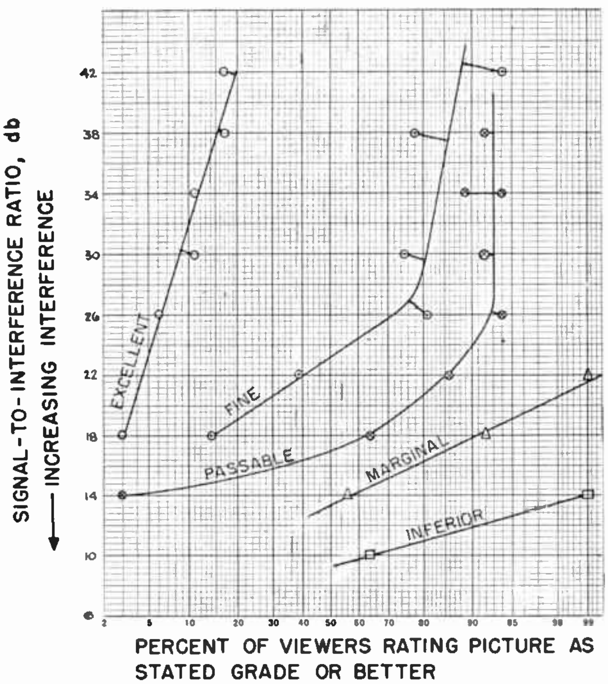

Fig. 23—Simultaneous 10,010-cycle co-channel and random-noise interference with desired signal 38 db above random noise. Frame rate 29.97 and Miss TASO scene. Observers were 18 men. Test 13 (23M).

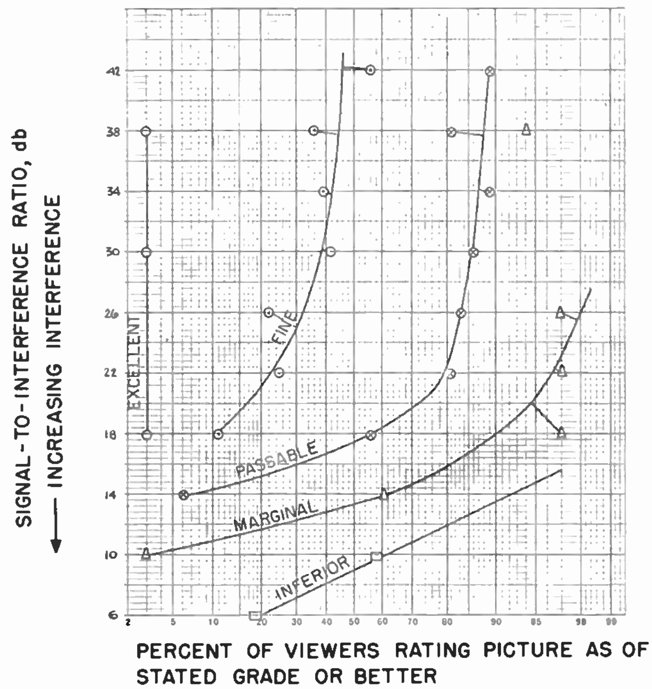

Fig. 24—Same as Fig. 23 except desired signal 32 db above random noise. Observers were 18 men. Test 12 (22M).

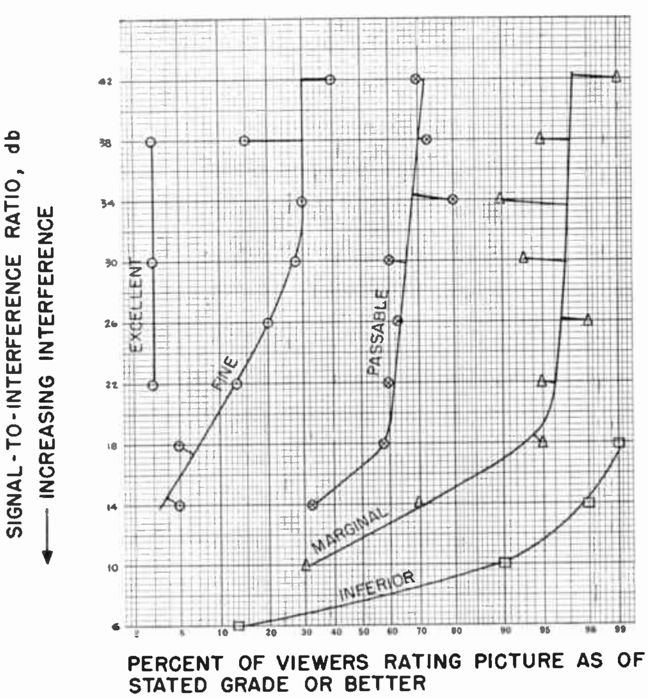

Fig. 25—Same as Fig. 24 except Kitchen Scene. Observers were 20 men. Test 12K (36J).

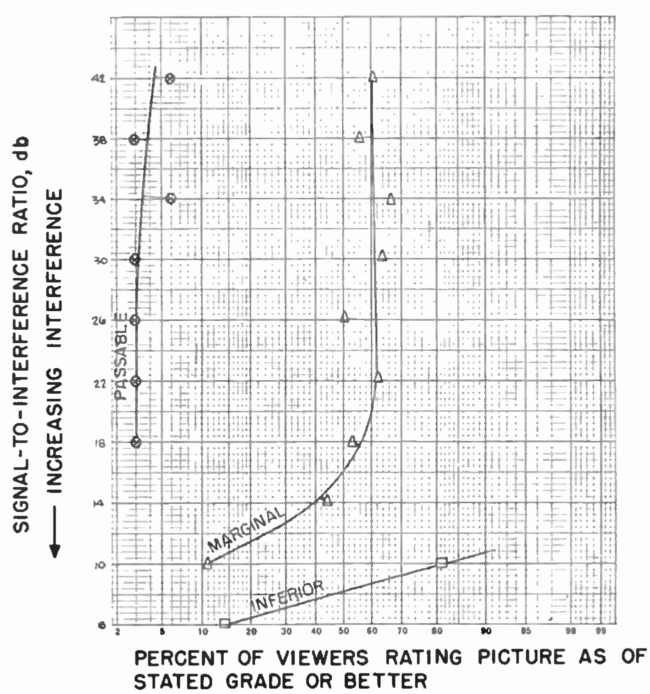

Fig. 26—Same as Figs. 23 and 24 except desired signal 20 db above random noise. Observers were 18 men. Test 23 (33M).

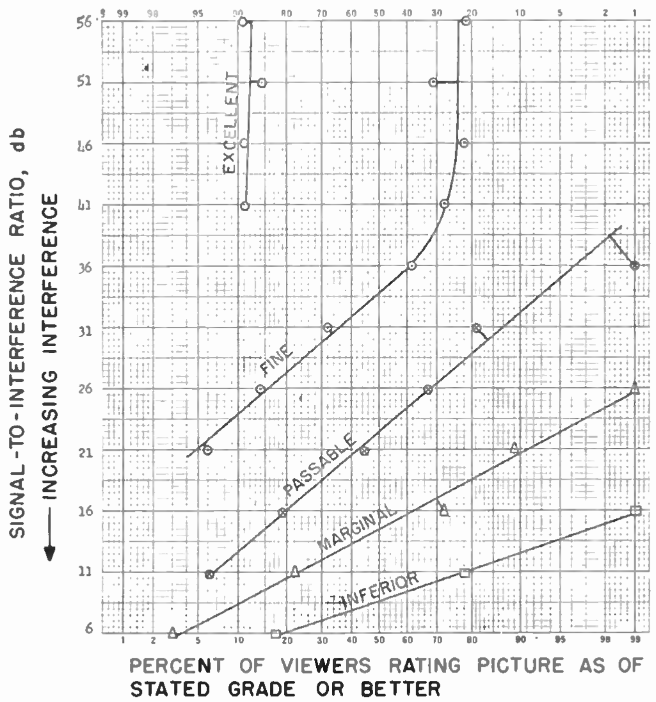

Fig. 27—Simultaneous 19,995-cycle co-channel and random-noise interference with desired signal 32 db above random noise. Frame rate 29.97 and Miss TASO scene. Observers were 18 men. Test 24 (34M).

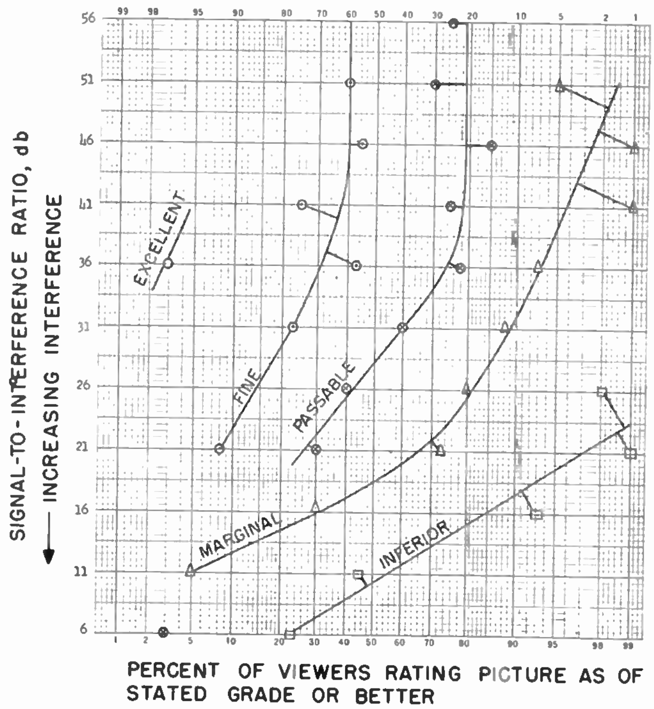

Fig. 28—Same as Fig. 27 except use of Kitchen Scene. Observers were 20 men. Test 24K (37J).

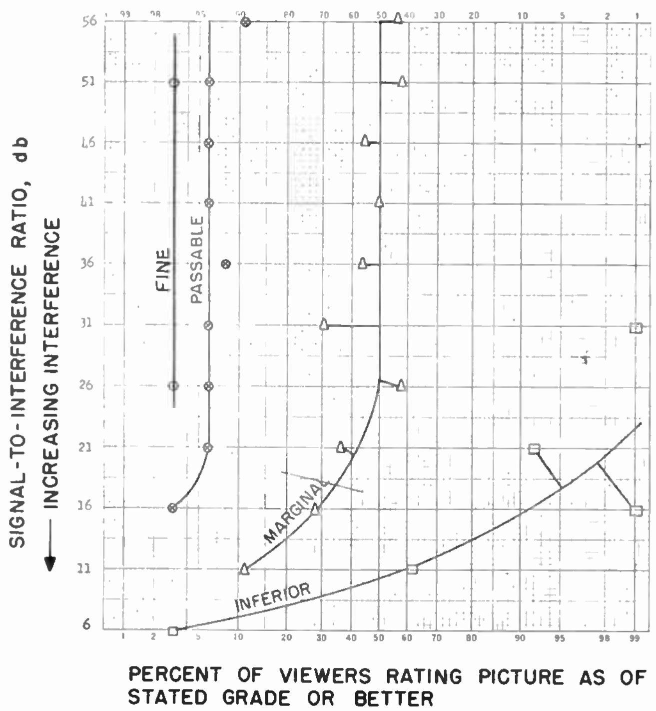

Fig. 29—Same as Fig. 27 except desired signal 20 db above random noise. Observers were 18 men. Test 25 (35M).

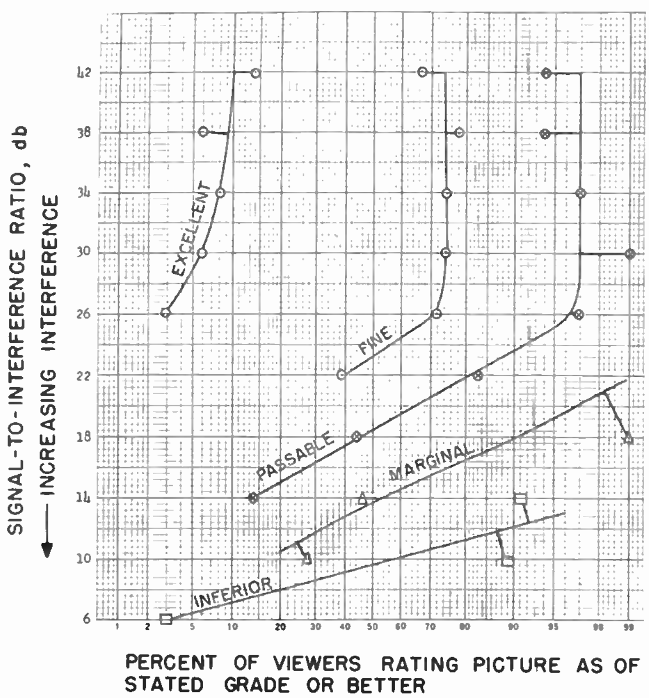

Fig. 30—Simultaneous 20,020-cycle co-channel and random-noise interference with desired signal 32 db above random noise. Frame rate 29.97 and Miss TASO scene. Observers were 18 men. Test 26 (36M).

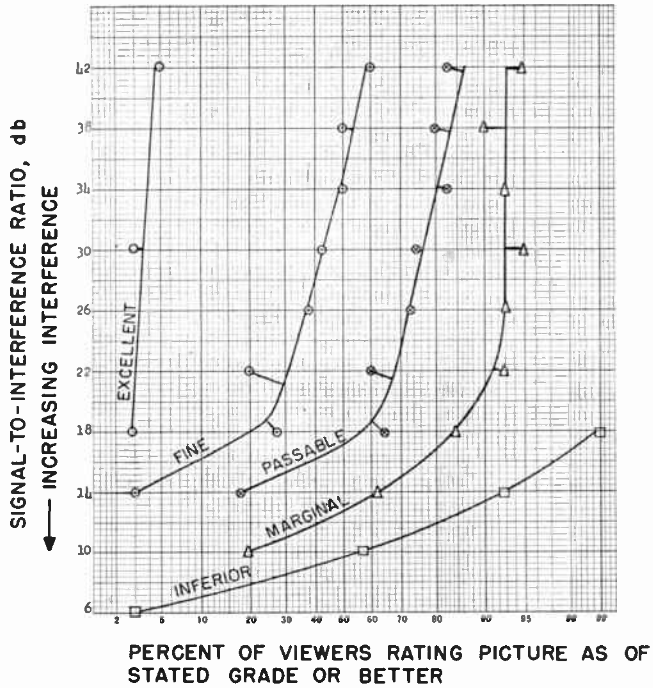

Fig. 31—Same as Fig. 30 except use of Kitchen Scene. Observers were 20 men. Test 26K (38J).

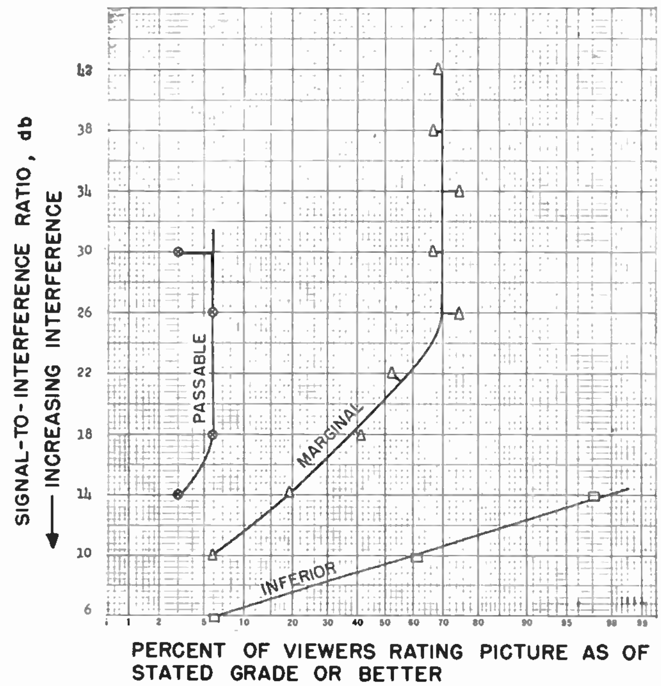

Fig. 32—Same as Fig. 30 except desired signal 20 db above random noise. Observers were 18 men. Test 27 (37M).

Utilization of the Data

The Panel gave a broad interpretation to the scope of its duties in that several grades of viewer satisfaction were taken into consideration and determinations were made of the physical television-picture characteristics necessary for each grade. In particular, six grades were chosen, so that the tests yielded data in terms of these grades or ratings. On the individual subject's scoring sheet these were given as the choices among which each observer selected in making each observation. These six grades, already given, were 1) Excellent, 2) Fine, 3) Passable, 4) Marginal, 5) Inferior, and 6) Unusable.

In utilizing the Panel data, therefore, a direct method is to choose the grade of service to be taken as a criterion, and then to consult the detailed Panel findings for the signal-to-interference ratio required. Should uncertainty be felt in choosing the grade of interest, reference should be made to the sentence descriptions of the six grades given on the observers' data sheets and available in the companion paper.[1] Weight should also be given to the scale used by Panel 3 in the field tests, and by the NTSC in 1950–53, since the Panel 6 scale was designed to be the same except for names and definitions better suited for tests involving the lay public.

When the grade to be taken as the criterion for service has been chosen, the data of Panel 6 are available for determining the required signal-to-interference ratio for various types of interference.

The data of the Panel can also be used in the opposite direction, *i.e.*, to determine for assumed conditions of signal and interference what degree of viewer satisfaction would be experienced.

A study of the Panel 6 data has been made recently by H. Fine of the Federal Communications Commission, including new proposed methods of application. It is expected that this work will be published in the near future.

One aspect of the Panel 6 tests, which should be of value, is that they afford results on various types of interference taken under fairly closely comparable conditions. For example, the question can be answered as to how much random-noise interference is equivalent to a given amount of upper-adjacent-channel interference.

It should be emphasized that extensive analyses of the data beyond those performed by the Panel are possible and should give useful conclusions. This seems a fertile field for doctoral research by graduate students. The original observers' data sheets, the punched IBM cards, and machine-made tabulations are being preserved by the Federal Communications Commission so as to be available for further study.

Acknowledgment

The author especially wishes to acknowledge the interest and the contributions of time and ideas by the members, alternates, and observers of Panel 6. It is regretted that these individuals were so numerous that it is impractical to list them here.

The author also acknowledges the support of the various organizations represented was invaluable. Notable among these were the David Sarnoff Research Center, RCA, Princeton, N. J., and the Eastman Kodak Company, Rochester, N. Y.

Studies of Correlation Between Picture Quality and Field Strength in the United States*

C. M. BRAUM†, SENIOR MEMBER, IRE AND W. L. HUGHES‡, MEMBER, IRE

Summary—**The purpose of this paper is to present data which correlate a given level of picture quality with some corresponding level of measured field strength. The data were gathered by actual house-to-house surveys in conjunction with field strength measurements. This procedure was followed rather than making laboratory tests on new receivers because it was desired to evaluate coverage as it actually was, not as it ought to be. Particular attention was paid to differences between UHF and VHF channels with respect to receiver and antenna performance in given field strengths. The ranges of field strengths required for a passable picture quality are fairly well established for each band of television channels.**

Background

FOR many years, the accepted procedure for arriving at television coverage has been to make field strength measurements in the prospective coverage area of a given television station. These measurements were then coupled with assumed performances of the average home receiver and antenna installation to arrive at some scale of television service coverage. It is necessary to point out that no quarrel is taken with this method. Ultimately, for any given station or market, it is the only foreseeable method that will continue to be used. The difficulty with this approach thus far is that there are many factors which, if ignored, may cause the method to give false conclusions. It is probably expedient to point out some of these factors.

1) The effects of multipath are not accounted for in field strength readings. In turn, this will determine the nature of the antenna installation required for a good television picture. Inherent in this problem is the question about the effort and expense to which people will go to eliminate undesirable ghosts, and how bad such ghosts need to be before they become subjectively important.
2) The evaluation of variations between the performance of receivers of different types and sensitivities, and perhaps what is more important, the degradation of receiver performance with age.
3) The effects of variation in the quality of antenna installations, and the rate of performance deterioration of the antenna installation with weathering and age.
4) The effects of rough terrain as opposed to smooth terrain on signal strength and standing wave patterns within the structure of the general field distribution.
5) The effects of foliage and seasonal variations on propagation, and therefore on picture quality and uniformity throughout the year.
6) The effects of short term variation of weather conditions on picture quality and uniformity. This is of interest not only because of propagation effects, but also because of the equally important factor of degradation of average receiver antenna performance when the antennas and lead-ins are wet and dirty.
7) The effects on service degradation occurring because the receiver owner does not operate his set properly.
8) The effects of the competence level of servicemen.

It goes without saying that all of the above factors vary with the frequency of transmission, be it VHF or UHF. This factor must be considered critically in all of the difficulties listed. It has seemed to some qualified individuals that to evaluate the effects of all of these difficulties is a hopeless task. It is certainly hopeless if one tries to separate and assign numbers to all of the factors by means of objective measurements alone. It does not follow, however, that objective aggregate information on all of the factors cannot be obtained by a combination of objective field strength measurements and subjective house-to-house surveys on over-all picture quality for representative television service areas over the nation.[1] This was the attack taken by Committee 3.3, of which the authors of this paper were co-chairmen, at the direction of the Television Allocations Study Organization (TASO), Panel 3, on field tests. Once such information is obtained, it can be correlated to find not only aggregate effects but also some individual effects of the degrading factors listed.

Procedure of the Surveys

The fundamental problem of evaluating the aforementioned factors in television coverage might be restated in a manner which more properly describes the tests which were made. This problem was to correlate

* Original manuscript received by the IRE, February 1, 1960.
† Joint Council on Educational Television, Washington, D. C.
‡ College of Electrical Engineering, Iowa State University, Ames.

[1] Early work in this area was done by Raymond F. Guy of the National Broadcasting Company. See R. F. Guy, "Investigation of ultra high frequency television transmission and reception in the Bridgeport, Connecticut area," *RCA Rev.*, pp. 98–142; March, 1951. Direct comparisons between Mr. Guy's work and the work of Committee 3.3 are difficult to make because of different data-taking procedures, but such comparisons show no apparent inconsistencies.

picture quality observed in an area with field strength readings taken in that area. Such a correlation study provides the aggregate effects. In addition, certain questions were asked at each home to assist in separating the aggregate effects into some of their component parts. The surveys were made in different types of terrain and in locations all over the country. Surveys were made in the following general areas:

1) Baton Rouge, La.,
2) Madison, Wis.,
3) Albany, Schenectady, and Troy, N. Y.,
4) Fresno, Calif.,
5) Bakersfield, Calif.,
6) Columbia, S. C.,
7) Harrisburg, Pa.,
8) Connecticut Valley Area, New England,
9) Buffalo, N. Y.,
10) New Orleans, La.,
11) Northern Minnesota Area.

All but two of these areas were chosen because of their primary television service. At the time the survey came from both UHF and VHF, so that direct comparisons were possible. The two exceptions were Northern Minnesota and the Albany-Schenectady-Troy area. No facilities were available for simultaneous measurement of the UHF and VHF at Albany-Schenectady-Troy. Therefore, UHF only was measured. Minnesota was chosen as the last test area because it had become apparent that more data were needed for rather weak VHF television signals. Three of the areas have essentially smooth terrain (Baton Rouge, New Orleans, and Columbia). One combined area (Fresno and Bakersfield) has terrain which represents both the smoothest (San Joaquin Valley) and the roughest (Sierra Mountains) terrain that was surveyed. Three of the areas have moderately smooth terrain with a certain amount of rolling hills (Madison, Buffalo, and Minnesota). Three of the areas have moderately rough terrain but not as rough as the Sierras (Albany-Schenectady-Troy, Connecticut Valley, and Harrisburg).

In each area surveyed, station wagons were equipped with field measuring equipment and trained operating personnel. The equipment used on each survey was owned by one of the following: Association of Maximum Service Telecasters, the CBS Television Network, the Federal Communications Commission, or Jansky and Bailey, Inc. personnel to make the house-to-house surveys were provided by the participating television stations in each area. In every case the house survey team was composed of competent television technicians or engineers. At the beginning of each study, the Chairman or Co-chairman of TASO Committee 3.3 visited the area to instruct the survey crew, and to spend a few days in the field with them. Each house survey team was made up of at least two men. Except for two cases, at least one of the men was from a VHF station and one was from a UHF station. This arrangement was deliberate, to avoid unconscious bias factors in the answers. It is the opinion of these authors, at least, that the dual arrangement was probably necessary for the avoidance of later criticism, but that the quality and integrity of the men in the survey teams was such that no bias would have been introduced except in perhaps a negative manner. It was never necessary to restrain a man from boosting his own station, but on occasion it was necessary to insist that each man make his ratings as objective as possible, and that he not lean over backwards in favor of another station.

The field test procedure was uniform throughout the country. Two types of general surveys were run. These two types will be termed *urban clusters* and *rural arcs.* In the urban cluster type of survey, a series of up to thirteen points was chosen in a given measurement location covering an area of approximately one square mile. Urban areas of varying population density were chosen at distances ranging fron five to one hundred and twenty miles from the transmitters of interest. These urban areas were scattered around the transmitter locations as evenly as was possible and consistent with the requirement that all major types of terrain in the area were to be sampled. Further, it was attempted to lay out the geometric pattern of the measurement points in any given urban measurement location in such a way that local terrain variations and urban characteristics were all represented, *i.e.*, river bottoms, hill tops, plateaus, business districts, residential districts, etc. The rural arcs were laid out on topographic maps in such a way that measurement points were approximately equidistant from the transmitters and were separated from each other by two or three miles. In this way it was possible to obtain information that was of use to Committee 3.3 while simultaneously gathering propagation information for other TASO panels.

The general procedure at individual measurement points was as follows. At each point, field strength readings were made on two (or in one case three) calibrating stations. Except for the Minnesota and Albany-Schenectady-Troy surveys, one of the calibrating stations was a major VHF station in the area, and the other was a major UHF station in the same area. Field strength measurements were made at ten and thirty feet for both visual and aural carriers of each calibrating station. In addition, field strength readings of visual and aural carriers were made (at thirty feet only) for other stations which were received in the area. In many cases, continuous ten-foot recordings of field strength were made at both UHF and VHF along the routes covered by the survey teams.

The questions asked of the householder are given on the survey sheet of Fig. 1. It will be noted that this sheet is simply a tabulation of the type of questions raised at the beginning of this paper. The rating of picture quality was carried out with the six point scale common to the NTSC testing programs carried out some years ago. The six possible ratings were *Excellent*, *Good*, *Passable*, *Not Quite Passable*, *Poor*, and *Not Usable*. The index column on the survey sheet is really the column for the engineer's rating of picture quality. It was not expedient to put the engineer's opinion in one column and the owner's opinion in another column, particularly if they did not agree, and the owner happened to see the survey sheet. Therefore, the engineer's opinion was coded. After carrying out the survey one or two times, the engineer's opinion was recorded after leaving the house, so this piece of subterfuge was probably not as necessary as was first thought.

The receiver was always operated by the householder. The survey teams were specifically instructed not to touch the receiver. Each member of the survey team had a special identification card, and a mimeographed letter of thanks on a TASO letterhead was given to each householder on the departure of the survey team. These arrangements and precautions were apparently sufficient because little difficulty was experienced in getting into the house for individual surveys.

Eleven surveys were run in all. There were an average of perhaps nine measurement locations per survey, each requiring a full day, and an average of eleven interviews

CONFIDENTIAL—FOR USE OF FIELD TEST PANEL—CONFIDENTIAL
TELEVISION ALLOCATIONS STUDY ORGANIZATION
Questionnaire for UHF/VHF Television Reception Study

Date ____________ Time ____________ Weather ____________

Location ____________

Description of Site (urban, rolling country, hill top, etc.) ____________

____

Name of Receiver Owner ____________ Address ____________

ANTENNA

Channel	Height	Age	Orientation	Type

TRANSMISSION LINE

VHF ____________ UHF ____________ Separate (yes or no) ____________

RECEIVER

Type and size of receiver ____________ Age of receiver ____________ When last service call ____________

TUNER

Type of tuner ____________ Separate converter (yes or no) ____________

RELATIVE PICTURE QUANLITY

Channel	Index	Owner's Opinion	Comments

OTHER COMMENTS

____

____

Who operated receiver? ____________ Engineer's name ____________

Fig. 1.

per measurement location, making a total of around 1100 interviews. There was an average of about three measurements of field strength per measurement point, and there were usually one or two more measurements than interviews in a given location, so the number of individual measurements is in excess of 3500. Since there were about five men involved in each survey (at least two interviewers, a driver, the measuring engineer and often a TASO member), the effort expended equals well over one and a half man years. This includes field work only. It does not include time for panel and committee meetings and data analysis.

Presentation of Data

One of the major objectives of this program was to obtain correlation information between field strength and picture quality that could be later used by the FCC for channel allocations purposes. As such, it would seem that a point-by-point correlation of picture quality and field strength on some sort of graph would be in order. This type of data analysis was attempted on both an individual point and a statistical basis, but was found to be useless for reasons that were obvious after several areas were surveyed. The combination of variability in receiver performance plus the effects of standing wave patterns in the field strength distribution made it unreasonable to expect a good point-by-point correlation. A more reasonable and more productive approach proved to be to plot the median field strength for a given measurement location against the median picture quality observed in that location. The picture quality rating was obtained by averaging the opinions of the householders and the engineers making the survey. The average difference between the nationwide householder and engineer opinions was 0.43 point on the six point scale, the engineers' opinion usually being lower than that of the householder's. Positive and negative differences averaged out to some extent, and thus in the aggregate, the engineers' opinion averaged only 0.13 point lower than that of the householder. Fig. 2 is a plot of all the median data. Each point represents the median field strength (visual carrier at 30 feet only) vs the median picture quality for one mesaurement location (*i.e.*, the medians of some ten or twelve observations). The picture rating scale was apportioned such that 1 = Excellent, 2 = Good, 3 = Passable, 4 = Not Quite Passable, 5 = Poor, and 6 = Not Usable. The points marked with an X represent VHF observations, and those marked with an O represent UHF observations. Field strength is measured in dbu which means db above one microvolt per meter.

It will be noted in Fig. 2 that some of the points are marked with a star. These particular points were deleted from a revised figure (Fig. 3), because, in each of the measurement locations represented, there was a special anomolous situation that made the data unrepresentative. In addition, three points were added on Fig. 3 that did not appear on Fig. 2. The explanation of each of these deleted and added points is listed below.

1. In preparing Fig. 3, the following points (which appear in Fig. 2) were deleted. These are indicated by stars in Fig. 2.
   a) Channel 10, $Q_m = 6$; $E_m = 40.5$ dbu. Only one observation of picture quality was made. At that location, the householder's antenna was pointed approximately 180 degrees away from the station on Channel 19.
   b) Channel 19, $Q_m = 6$; $E_m = 59.5$ dbu. All receiving antennas were pointed approximately 180 degrees away from the station on Channel 19.
   c) Channel 17, $Q_m = 3.5$; $E_m = 41$ dbu. There were only four operable UHF receivers in this measurement location. The area is obviously not served by Channel 17. Median picture rating was abnormally high due to the presence of two or three excellent antenna installations and the resulting good pictures. $Q_m = 3.5$ does not properly represent the Channel 17 service in this area.

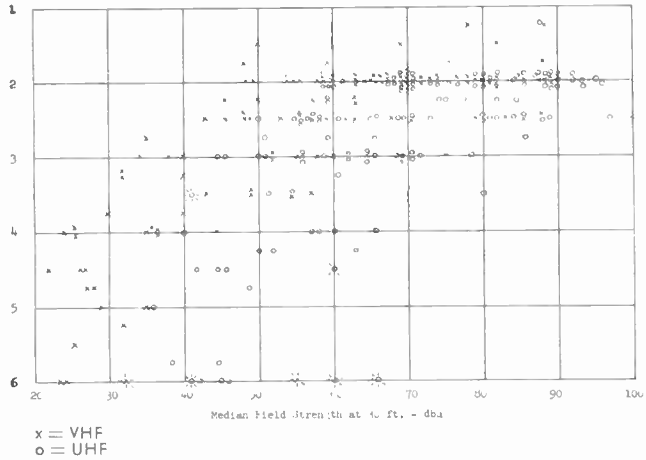

Fig. 2—All UHF and VHF original data.

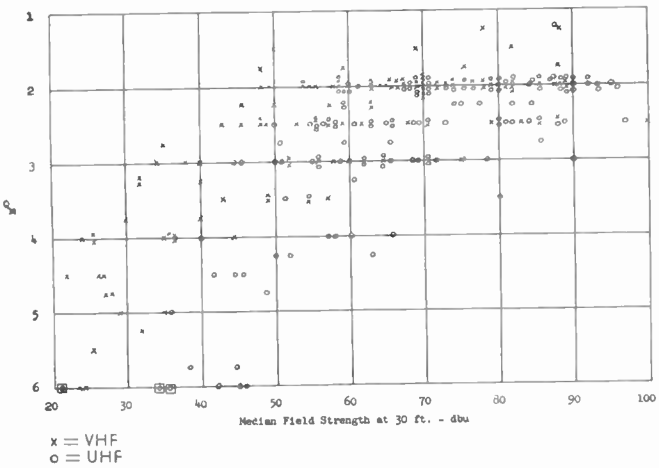

Fig. 3—All UHF and VHF valid data.

d) Channel 12, $Q_m=6$; $E_m=55$dbu. Antennas were all pointed toward another station.
e) Channel 24, $Q_m=4.5$; $E_m=59.5$ dbu. Antennas were all pointed toward another station.
f) Channel 10, $Q_m=6$; $E_m=32.5$ dbu. Only one observation on this station, and antenna was pointed in the wrong direction.
g) Channel 67, $Q_m=6$; $E_m=66$ dbu. Another closer station on VHF carried the same network and UHF receivers and antennas were no longer used.

2. In preparing Fig. 3, the following points (which do not appear in Fig. 2) were added. These are shown as circles in boxes in Fig. 3.
a) Channel 17, $Q_m=6$ (added); $E_m=33.5$ dbu.
b) Channel 28, $Q_m=6$ (added); $E_m=36.5$ dbu.
c) Channel 67, $Q_m=6$ (added); $E_m=22$ dbu.

In each of these three measurement locations, there was no evidence of any service from the stations listed, and it was felt that a picture rating of 6 properly represented the facts.

For purposes of analysis and discussion it is interesting to split the data of Fig. 3 still further. Fig. 4 is a plot of the low channel 30-foot VHF data alone. Fig. 5 is a plot of the high channel 30-foot VHF data. Fig. 6 is a plot of low channel 30-foot UHF data, and Fig. 7 is a plot of the middle and high channel 30-foot UHF data. A low UHF channel will be defined as Channel 40 and below. Anything above Channel 40 will be considered a middle and high UHF channel. Fig. 8 is a plot of all of the 30-foot VHF data, and Fig. 9 is a plot of all the 30-foot UHF data.

It may be wondered by some readers how the figures could have half and quarter steps between the individual six points of the judging scale. The half steps arise because the median of an even number of observations is the average between the two middle observations. In addition, the quarter steps arise because each point has a picture rating determined by the average between the median engineer's opinion and the median householder's opinion.

One of the purposes of these tests was to examine the correlation between picture and field strength, with measurements being made at both a ten foot antenna height and a thirty foot antenna height. All of the data presented thus far were for field strengths at thirty feet. Fig. 10 presents all valid median data for an antenna height of ten feet. Fig. 11 is a plot of low channel ten-foot VHF data. Fig. 12 is a plot of high channel ten-foot VHF data. Fig. 13 is a plot of low channel ten-foot UHF data. Fig. 14 is a plot of medium and high channel ten-foot UHF data. Fig. 15 is a plot of all of the VHF ten-foot data, and Fig. 16 is a plot of all of the UHF ten-foot data. Only valid data are plotted in the ten-foot data figures. That is, anomalous points mentioned earlier have been removed.

The significance of these figures is discussed in the next section on data analysis.

Analysis and Discussion of Data

The differences in performance of television receiving equipment (receivers and antenna installations) operating in the various allocated bands are rather apparent from Figs. 2 through 16. Figs. 3 and 10 illustrate the over-all difference between VHF and UHF. Further, it is possible to subdivide clearly the performance differences between low and high VHF, as well as between VHF and UHF. Comparison of Figs. 4 and 5, as well as 11 and 12, shows degradation of receiving performance from low VHF to high VHF. Comparison of Figs. 6 and 7 (and Figs. 13 and 14 to a lesser extent) shows deterioration from low UHF to middle and high UHF. Most important, Figs. 8 and 9, as well as Figs. 15 and 16, show the over-all degradation from VHF to UHF. It should be noted that, for any given field strength, UHF receiving installations suffer in comparison with VHF installations in at least three important respects—lower antenna conversion factor, higher transmission line loss, and inferior receiver performance, especially with respect to noise factor and sensitivity. These are discussed in detail in the report of Panel 2, and in the paper in this issue by W. O. Swinyard.[2]

Some comment on a comparison of 10- and 30-foot measurements is in order. At the VHF channels, comparison of low channel VHF data (Figs. 4 and 11) indicates that the scattering of points is comparable, but that the 10-foot signal is lower. Comparison of high channel VHF data (Figs. 5 and 12) leads to somewhat similar conclusions. Comparison of low channel UHF data (Figs. 6 and 13) is more difficult because of the absence of low signal data and the scattering of existing data. This is partly due to the fact that the UHF signal disappears much more rapidly with distance over the horizon. Further, standing wave field patterns tend to be more severe at the UHF channels. Comparison of medium and high UHF data (Figs. 7 and 14) suffers from similar problems. In all cases, however, the differences in receiving performance are clearly marked for either 10- or 30-foot field strengths.

It must be remembered that these differences in receiving performance (antennas, transmission lines, and receivers) are due to two fundamental causes. The first can be classified as "state of the art" difficulties. This includes transmission line losses and receiver noise figure. The second has to do with problems of fundamental physics. The most important of these is the lower antenna capture area of antennas of the same type as the frequency is increased.

[2] W. O. Swinyard, "VHF and UHF television receiving equipment," this issue, p. 1066.

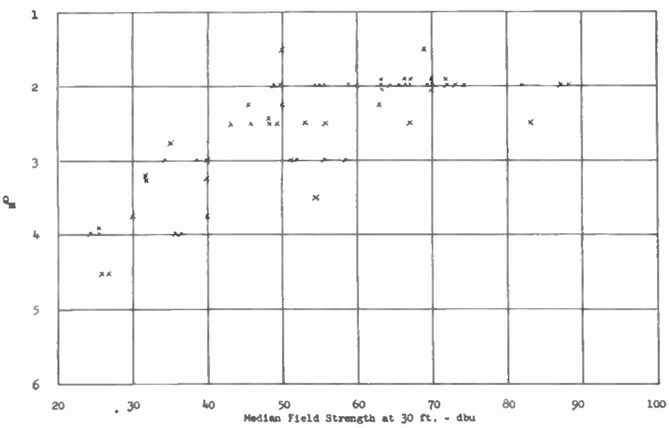

Fig. 4—Low VHF data—Channels 2–6.

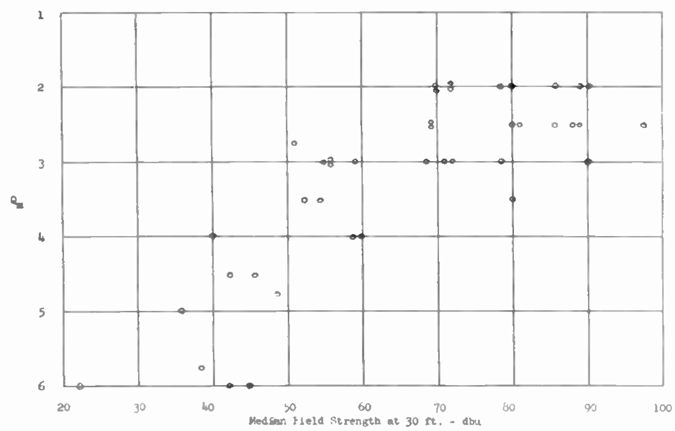

Fig. 7—Middle and high UHF data—Channels 41–83 (primarily middle UHF).

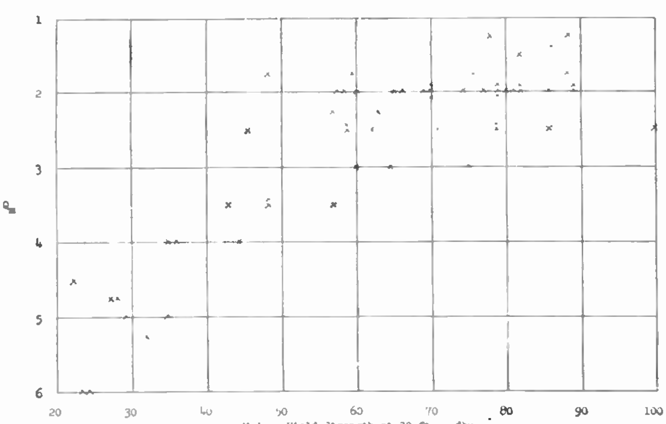

Fig. 5—High VHF data—Channels 7–13.

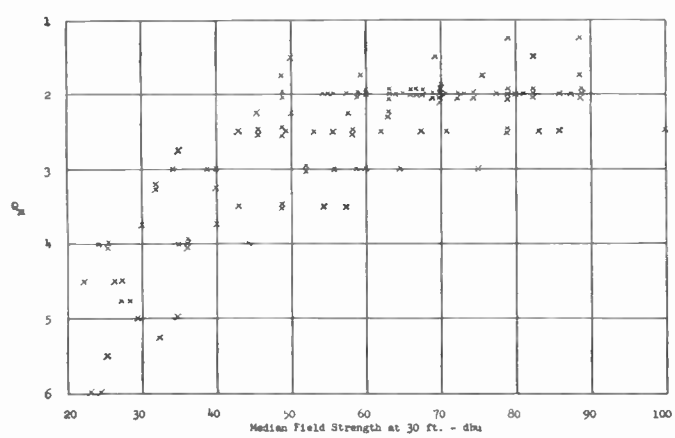

Fig. 8—All VHF data—Channels 2–13.

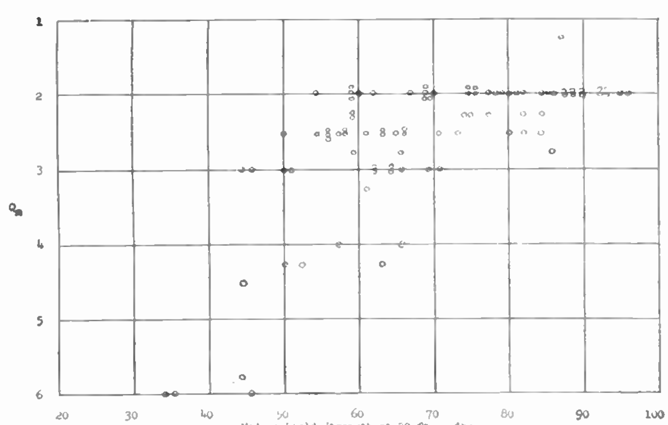

Fig. 6—Low UHF data—Channels 14–40.

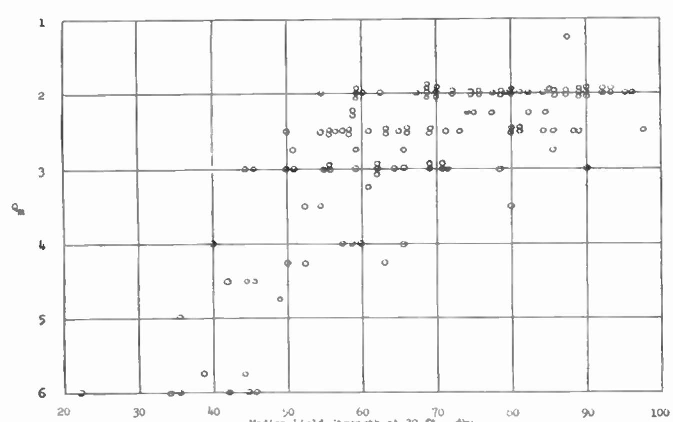

Fig. 9—All UHF data—Channels 14–83.

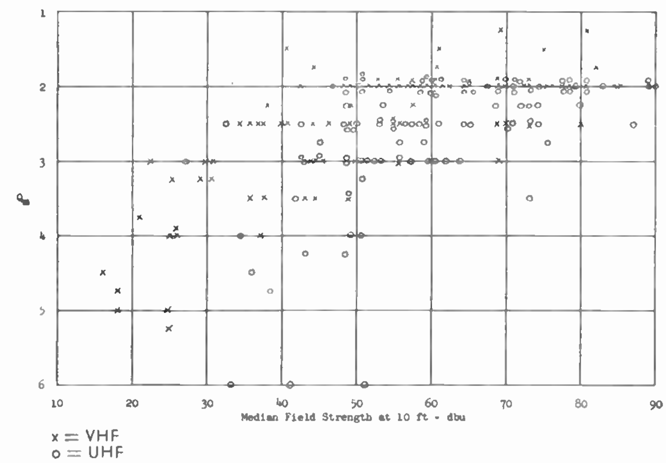

Fig. 10—All UHF and VHF valid data.

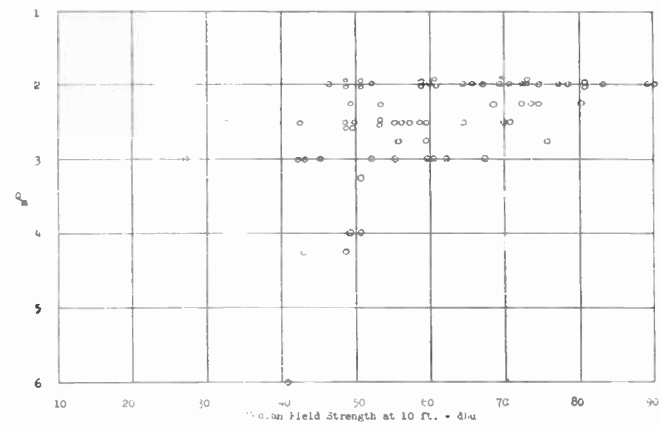

Fig. 13—Low UHF data—Channels 14–40.

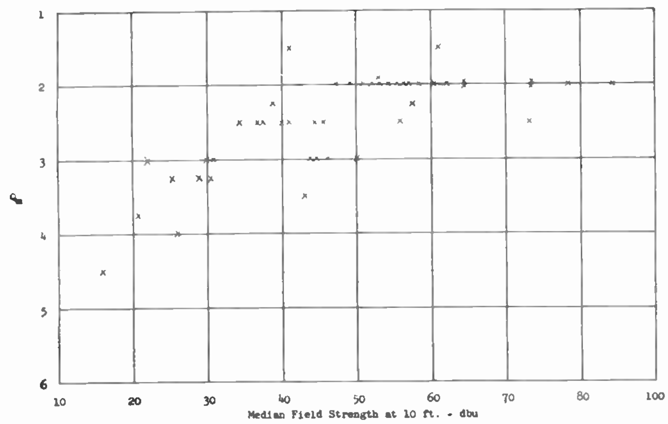

Fig. 11—Low VHF data—Channels 2–6.

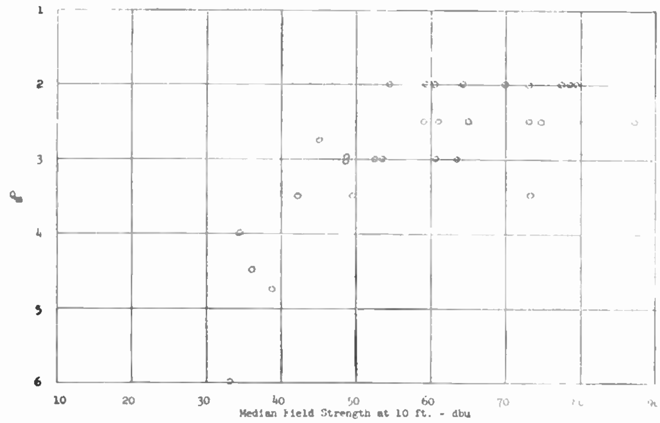

Fig. 14—Middle and high UHF data—Channels 41–83 (primarily middle UHF).

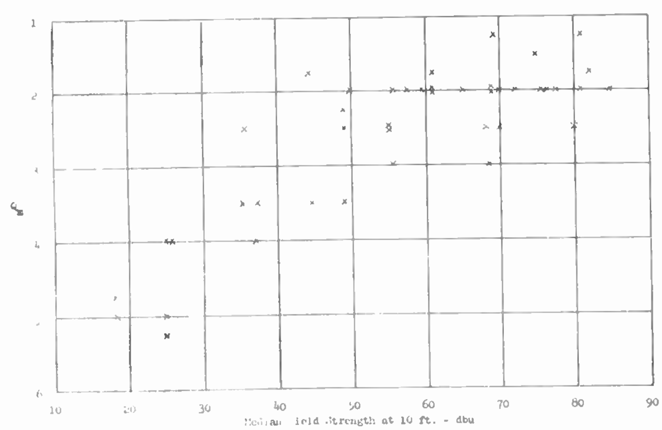

Fig. 12—High VHF data—Channels 7–13.

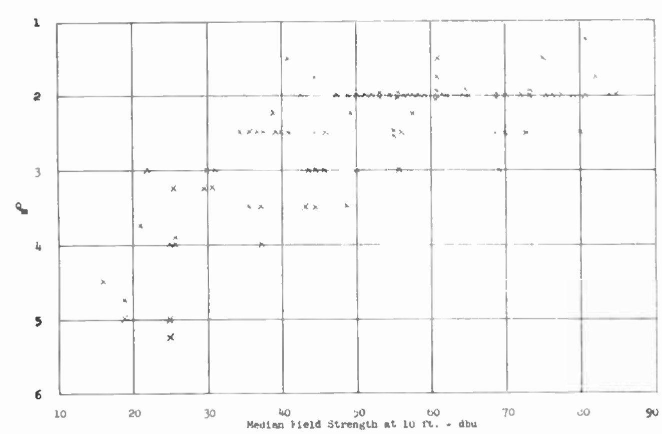

Fig. 15—All VHF data—Channels 2–13.

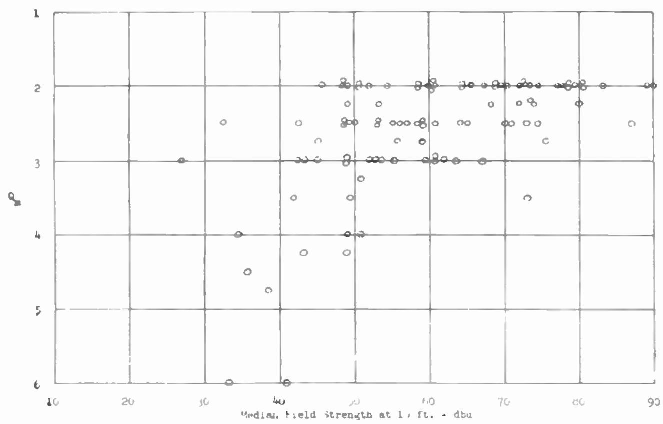

Fig. 16—All UHF data—Channels 14–83.

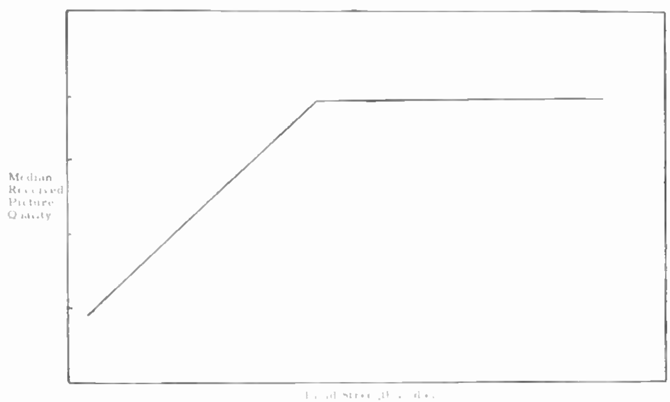

Fig. 17—Idealized picture quality—field strength characteristic.

The over-all nature of Figs. 2 through 16 seems to indicate a general performance characteristic that might be expected. This characteristic is idealized in Fig. 17.

First, in high signal areas, it would be expected that some variation in receiver performance would be encountered due to the variation of receiver and antenna degradation, variations of service quality, etc. The average receiver performance, however, would be relatively independent of field strength as indicated by the horizontal part of the sketch. It is important to note from Figs. 4 through 7, as well as from Figs. 11 through 14, that the variability in this high signal performance is apparently more extensive as the frequency is increased. A second type of performance characteristic to be expected is that, as the signal becomes weaker, the set performance becomes more and more dependent upon signal strength as indicated by the sloping part of the sketch. Presumably, the other variables are still present. One interesting situation was noted throughout the survey. That is, the general quality of receiver installation and state of repair of the average receiver improved as the distance from the transmitter increased, since a fringe receiver must be in better condition to give a usable picture than a receiver close to the transmitter. This "feed-back with distance" characteristic was sometimes so pronounced that average picture quality (particularly at VHF) improved as distance increased out to perhaps twenty or thirty miles. As the signal gets very weak, however, the received picture obviously degrades, and degradation unquestionably goes up with frequency.

Some other interesting points can be obtained from the interview sheets. These are summarized here. It is interesting to examine the UHF conversion figures on an over-all basis. These are given in Table I for a total of 396 homes which had UHF conversion.

TABLE I

Distance from Transmitter (Miles)	Total Homes Visited Having Television in a Mixed VHF-UHF Service Area	Total Television Sets Converted to UHF	Per Cent Conversion
0–10	61	51	84
11–20	160	122	76
21–30	155	108	70
31–40	168	98	58
41–50	32	13	41
51–60	25	4	16

It is interesting to note that of these 396 television sets, 41, or slightly over ten per cent, were inoperative on UHF while they were operative on VHF. No receivers are included in this tabulation which were inoperative on both UHF and VHF. Due to the technical nature of the UHF tuners, no sets were found which were operative on UHF but not on VHF. It should be pointed out that the Fresno, California, data are not included in Table I. This is because the transmitter antenna heights are such that UHF propagation is not representative of conditions in the remainder of the country. In Fresno, good UHF as well as VHF pictures were received at distances as high as 100 miles from the transmitters. This was essentially line-of-sight transmission, of course.

It was found that very few external converters are used for UHF. Further, these are used only in old UHF areas, and are rapidly being replaced with internal units as the old television sets are replaced. Most combination UHF-VHF installations use separate transmission lines, and the usual line for UHF is round twin lead, whereas flat twin lead is almost universally used for VHF.

The average time to the last service call over the country, as determined by this survey at least, is $6\frac{1}{2}$ months. This figure varied widely from area to area, of course. The quality of television service observed varied from area to area. In some communities, for example, almost every television receiver observed was in good operating condition. In others, almost all were in bad operating condition. All degrees in between the extremes were observed. The same general statement, although perhaps to a lesser degree, could be made of antenna installations. The reports from the survey teams indicate that the average television service level throughout the country needs considerable improvement. Generally, more deficiencies in receiver operation were noted due to such things as alignment, than to antenna and receiver installation. This is probably to be expected, since to remedy the former difficulty needs much higher skill on the part of a serviceman than to remedy the latter. Further, a large percentage of service shops are inadequately equipped with test equipment.

General Conclusions

Some general conclusions can be drawn based on the preceding material, and also on some general observations made during the survey.

With certain obvious exceptions, down to a field strength of 60–70 dbu on the average, the best and the worst pictures observed in a measurement location were both UHF pictures. (This statement holds, of course, only for areas served by both UHF and VHF.) These field strengths correspond generally to distance ranges roughly out to the optical line-of-sight. Thereafter, UHF field strength and picture quality deteriorate rapidly while good VHF service holds for considerably greater distances. The rapid deterioration of UHF over VHF is apparently an over-the-horizon propagation problem. In areas where UHF line-of-sight is 75 to 100 miles, UHF service holds up almost comparably with VHF to those distances. This fact was brought out quite forcibly in the Fresno, California, survey. The statement about the best and the worst pictures both being UHF pictures is not difficult to explain. In areas of *adequate* signal strength, UHF does not appear to be subject to ignition noise, airplane flutter, and so forth. Thus the "best" picture is explained. The "worst" picture is explained by the fact that for any given median signal strength in an area, the gamut of receiver performance at UHF is much wider than at VHF.

It was interesting to note that for the most part, the householder did a fairly competent job of operating the receiver. There were exceptions, of course, but in perhaps 75 per cent of the cases, the engineer would not have done much better.

It was definitely noted that, as the distance from the transmitter increased, the average quality of antenna installation improved, and the average service condition of the receiver improved. A much higher percentage of misaligned or otherwise improperly operating receivers was noted close to the transmitters than was noted at considerable distance away (20 miles and above).

Although there is considerable room for individual judgment, Figs. 4 through 7 would seem to indicate that for a *Passable* picture the following mean field strengths at thirty feet in a measurement location are required.

Low VHF	40–45 dbu,
High VHF	50–55 dbu,
Low UHF	55–60 dbu,
Middle and High UHF	62–67 dbu.

There were not enough data to separate middle and high UHF.

It is important to realize that this does not mean that these figures at a receiving antenna will give a passable picture. Rather, they mean that when these figures represent the mean field strength at thirty feet, the height of receiver antennas and quality of receiver performance and installations will be such that median picture quality in that measurement location will be passable. The reader may choose appropriate figures from the ten foot data by examining Figs. 11 through 14, if he desires.

For a *Good* or better picture, the following values of field strength appear to be adequate at thirty feet.

Low VHF	50 dbu and above,
High VHF	60 dbu and above,
Low UHF	65 dbu and above,
Middle and High UHF	72 dbu and above.

It should be noted that the preponderance of low signal VHF data was taken in the northern Minnesota area. This does not detract from the validity of the data as far as correlation between picture quality and field strength is concerned, but may restrict the generality of any conclusions that might be drawn about the receiving antenna height-gain function.

Relative Performance of Receiving Equipment as Reported by Television Servicemen*

HOLMES W. TAYLOR†

Summary—**Incorporate with the over-all study conducted by TASO, Panel 3 (Field Tests) in its study of reception problems conceived a six-page questionnaire which was circulated to that segment of the industry most closely associated with these problem areas—the television servicemen in communities across the nation. The questionnaire dealt with reception conditions, antennas, transmission lines, receivers and allied questions on both VHF and UHF covering both color and monochrome. The statistical compilation of answers received from the cooperating TV servicemen is included in this paper.**

In conjunction with the Television Allocation Study Organization, Panel 3 (Field Tests) brought Committee 3.4 (Analysis of Questionnaires) into being at its 10th Meeting in March, 1958.

This committee was charged with the responsibility of reducing the data obtained from the television servicemen's questionnaires to a form suitable for summarization and analysis. While the questionnaire is not reproduced in this paper, all of the pertinent questions head the various tabulations of the results. All original data, including that generated by the Committee, have been turned over to the FCC.

The Committee received 730 completed questionnaires. Since it was decided to transfer pertinent data from the questionnaires to punched cards, the questionnaires were sorted alphabetically by state and by cities within the state. In this way, the serial number of a questionnaire allowed ready reference to geographical information. The questionnaire data were reduced to numerical alphabetical codes which greatly simplified the summary work and reduced punched card volume.

It became apparent during the preparation of format sheets prior to actually preparing the cards that some of the data had been subject to local interpretations or appeared to be erroneous. After checking through a number of cases, it also became apparent that a certain amount of inconsistency would be averaged out as part of the normal statistical analysis. In addition, the Committee felt that, in the area of interpretation, it should not attempt to reinterpret data since this in itself would tend to disqualify them. However, certain basic ground rules were followed. Data with no meaningful significance (*i.e.*, a question either left blank or answered in such a way that it could not be resolved), were omitted from the summaries. Furthermore, those few areas which called for written comments covered such a wide field of answers that it was decided in the summary only to indicate whether or not the question had been answered.

Finally, in picking the maximum quantity size for various parameters, some answers beyond the capacity chosen were discovered. These were so few that they were included at the maximum number and it was felt that this would not disturb the relative relationship of the final results.

Before presenting the results of the analysis, there are several points which should be considered. The data presented reflect the results of the servicemen's experiences and consequently the receiver information is limited to those sets which have required professional servicing. Thus, in interpreting the results, one must keep in mind that there were undoubtedly a number of receivers which either required no servicing or were serviced by the owner. For example, in the table where it is indicated that the average number of calls per set per year is approximately three, the figure would be reduced if the number of unserviced sets within the average serviceman's area of endeavor were known. While this is a fairly obvious point, it is sometimes overlooked in reviewing data of this nature. In order to place the results of this survey back into the same perspective originally intended, the results are tabulated in the same order as the questions were presented in the questionnaire and divided into six sections:

A. General Information;

B. Receiving Antennas;

C. Receivers;

D. Multipath (Ghost) Problems;

E. Interference;

F. Color Reception.

The actual question from the survey questionnaire has been repeated, and heads each tabulation.

A. General Information

The first three questions in this section of the questionnaire were not summarized, since these questions were used to establish identification and area location of the reporting serviceman. This information for each questionnaire, along with its individual identification number, appears on the punch cards that were used.

* Original manuscript received by the IRE, February 11, 1960.

† Res. Center, Burroughs Corp., Paoli, Pa.

The state and city address of the serviceman was used to establish in which FCC Zone (*i.e.*, I, II or III) he was located, and the following data were established from the information:

a) That questionnaires were returned from 46 of the 48 states (Delaware and Vermont abstaining).

b) That 44 per cent of the questionnaires came from Zone I.

c) That 44 per cent of the questionnaires came from Zone II.

d) That 12 per cent of the questionnaires came from Zone III.

4(a). Please estimate the number of calls per year you make on the following types of receivers:

	Survey Totals	Average Total per Questionnaire	Aggregate Response
VHF	2,975,031	4605	89 per cent
UHF Converter Sets	145,187	621	32
UHF Single-Channel Sets	1762	28	9
All-Channel Sets	392,869	1224	44
Strip-Tuner-Equipped Sets	336,342	998	46
Community-TV Sets	25,686	299	12
Centralized-Receiver-Systems Equipment	2382	21	16

4(b). Please estimate the number of service calls you make PER SET PER YEAR on the following types of receivers:

	Survey Totals	Average Total per Questionnaire	Aggregate Response
VHF	1911	3.11	84 per cent
UHF Converter Sets	856	3.93	30
UHF Single-Channel Sets	153	2.94	7
All-Channel Sets	1139	3.93	40
Strip-Tuner-Equipped Sets	948	3.27	40
Community-TV Systems Sets	242	2.99	11
Centralized-Receiver-Systems Equipment	290	3.15	13

5. For the area you service, please indicate the number of TV antennas you have installed:

	Survey Totals	Average Total Per Questionnaire	Aggregate Response
VHF Indoor Antennas	538,443	1213	61 per cent
UHF Indoor Antennas	78,010	441	24
VHF Rooftop Antennas	829,538	1440	79
UHF Rooftop Antennas	148,932	532	38

Based on the above data, dividing the total calls by the average number of calls per set for a given receiver, furnishes this tabulation of receiver sets serviced per year.

	Receiver Sets
VHF Receivers	957,000
UHF Converter Sets	37,100
UHF Single-Channel Sets	600
All-Channel Sets	100,000
Strip-Tuner-Equipped Sets	103,000
Community-TV Systems Sets	8580
Centralized-Receiver-Systems Equipment	755

Thus, excluding the centralized and community systems, the survey indicates a total of 1,197,000 serviced receivers with VHF capabilities and 240,700 serviced receivers with UHF capabilities. It is interesting to note that the percentage responding for VHF is approximately twice that for UHF. This trend, which shows that about half of the areas responding did not have UHF service, is found throughout the results.

6. Please indicate YES or NO to each of the following descriptions of your area:

	Survey Totals	Percentage Breakdown	Aggregate Response
a)			
Flat	266	38 per cent	
Hilly	220	31	
Flat and hilly	130	18	
Mountainous	16	2	
Flat and Mountainous	1	*	
Hilly and Mountainous	48	7	
Flat, Hilly and Mountainous	31	4	
			Over-all 97 per cent
b)			
Industrial	8	1	
Residential	92	13	
Industrial and Residential	99	14	
Rural	10	2	
Industrial and Rural	1	*	
Residential and Rural	94	13	
Industrial, Residential and Rural	405	57	

* Less than ½ of 1 per cent.

7. Please list in the columns below, the TV stations which provide service to your area. For comments on the usual grade of service, use E for Excellent, G for Good, F for Fair and P for Poor. (This refers to technical performance only, not programming.)

The original data were, of course, by station including call letters and channel numbers; however, in the summarization the channels have been grouped in the following way:

Low VHF	2–6
High VHF	7–13
Low UHF	14–40
Medium and High UHF	41–83.

The latter group was combined because of the low density of stations in this category. The tabulation below is of average distance in miles to the transmitting antenna and is organized by channel groups and grade of service. Response in this area was over 95 per cent.

Channel Group	Grade of Service			
	Excellent	Good	Fair	Poor
2–6	22 miles	37 miles	67 miles	76 miles
7–13	22	31	55	71
14–40	15	18	16	27
41–83	11	13	15	22

The data for average power used by the transmitting stations and the average relative height (vertical distance from top of transmitting tower to serviceman's area) were obtained from the "Television Digest Factbook" and a reference book on height above sea level for numerous locations in the United States. The averages for both power and transmitting height were based on averaging the total number of stations reported for each channel group. Since servicemen reported on the same stations in a number of cases, the average then is multiple station rather than single station average. The average transmitter height is perhaps greater than expected because of the occurrence of stations like WMTW, Poland Spring, Me., where the vertical distance from a serviceman in Portland to the top of the transmitting antenna was 6375 feet. These large heights tended, of course, to bring up the average. Finally, the over-all average, again on a multiple station basis, was 1210 feet.

Channel Group	Average Transmitting Station Power	Relative Antenna Transmitting Height
2–6	88 kw	1272 feet
7–13	240	1235
14–40	350	735
41–83	330	1179

A different analysis showed that there were 444 individual stations covered by the survey (includes six in Canada and one in Mexico). Due to overlap reporting, some of these stations were reported as many as 48 times. The nontranslator stations of this group are 427 and the total United States station density is 541. This survey then represents a 79 per cent coverage.

B. Receiving Antennas

1(a). In your area, how would you rate the performance of a typical rooftop antenna?

1(b). In your area, how would you rate the performance of a typical indoor antenna?

Performance	Rooftop Antenna		Indoor Antenna	
	VHF	UHF	VHF	UHF
Excellent	51 per cent	35 per cent	7 per cent	2 per cent
Good	38	32	28	10
Fair	7	19	32	24
Poor	4	14	33	64
Aggregate Response	97	47	95	54

Note again that the response for VHF is approximately twice that for UHF.

2(a). In a strong-signal area, what are the minimum, average, and maximum outdoor receiving antenna heights you have observed? (Enter height estimates in feet above street level.)

2(b). In a weak-signal area, what are the minimum, average, and maximum outdoor receiving antenna heights you have observed?

Antenna Heights	Strong Signal Area	Weak Signal Area
Minimum	22 feet	29 feet
Average	32	40
Maximum	68	74

3. Selection of the location for an outdoor receiving antenna.

3(a). In weak-signal areas, do you explore the rooftop area for locations of maximum signal intensity?

	Yes	No	Aggregate Response
VHF	53 per cent	47 per cent	89 per cent
UHF	81	19	

3(b). Have you observed seasonal changes in the optimum location of outdoor antennas?

	Yes	No	Aggregate Response
VHF	43 per cent	57 per cent	92 per cent
UHF	63	37	

4. What proportion of receiver installations in your area receive less than optimum picture quality because the owner does not erect an outside antenna?

Proportions of Installations	Aggregate Response
30 Per Cent	95 Per Cent

5. What types of transmission lines are most often used?

Type of Area	Coax	Tubular	Flat	Aggregate Response
Strong Signal VHF	1 per cent	5 per cent	94 per cent	91 per cent
Strong Signal UHF	4	83	13	40
Weak Signal VHF	3	15	82	83
Weak Signal UHF	6	87	7	37

6. Is the transmission line length and/or installation ordinarily a factor in the choice between an indoor and an outdoor antenna?

	Yes	No	Aggregate Response
VHF	12 per cent	88 per cent	94 per cent
UHF	18	82	

Rhombics
Folded or double V
Traveling-Wave
Yagis

For purposes of the analysis, the antenna types used in the table were reduced to five. These five represented a total usage of 80 to 95 per cent, while the use of the others was comparatively small.

Antenna Types

Reception Type	Area Type	Corner Reflectors	Conicals	Dipoles	Yagis	Bow-ties	Aggregate Response
Monochrome	Weak VHF	—	25 per cent	10 per cent	60 per cent	—	76 per cent
	Weak UHF	35 per cent	—	—	28	26 per cent	35
	Strong VHF	—	40	30	24	—	80
	Strong UHF	28	—	—	13	43	36
Color	Weak VHF	—	24	16	53	—	43
	Weak UHF	33	—	—	23	26	11
	Strong VHF	—	36	28	29	—	51
	Strong UHF	33	—	—	13	36	13

7. Do you usually use separate VHF and UHF transmission lines to the receiver?

Yes	No	Aggregate Response
60 per cent	40 per cent	48 per cent

8. Please list your estimate of the minimum, average and maximum lengths of transmission line used for outdoor antennas in strong and weak signal areas at VHF and UHF:

	Strong	Weak	Aggregate Response Strong	Aggregate Response Weak
VHF Minimum	29 feet	36 feet	75 per cent	62 per cent
Average	50	57	81	70
Maximum	115	127	75	65
UHF Minimum	26	31	31	27
Average	44	50	34	29
Maximum	86	90	32	28

9. What type of outdoor antenna have you found most acceptable for MONOCHROME reception: dipoles, yagis, conicals, bow-ties, stacked combinations, corner reflectors, rhombics, others?

10. What type of outdoor antenna have you found most acceptable for COLOR reception: dipoles, yagis, conicals, bow-ties, stacked combinations, corner reflectors, rhombics, others?

The servicemen indicated in the questionnaire that the following types of outdoor antenna were used:

Bow-ties
Conicals
Dipoles
Corner reflectors
Helix
Inline, colinear, colateral
Parabolic

Note that here again the UHF responses are about 50 per cent of the VHF and that the area having color service was about 50 per cent of the UHF and VHF respectively.

C. Receivers

1. What proportion of receiver installations are unsatisfactory?

	Percentage Unsatisfactory	Aggregate Response
VHF	15 per cent	95 per cent
UHF	11	83

In the following list, check reasons for this that have occurred in your experience. Opposite any troubles that are especially frequent, put several check marks.

The number of check marks have been analyzed for each of the performance problems within the specific receiver type only (*i.e.*, no correlation was attempted between receivers). The percentage response to this question, as a whole, was 84 per cent and was based on the fact that a man indicated at least one check mark for a particular trouble under at least one receiver type (this was the only method which determined that a man actually read and considered the question). There were a few cases where there were no check marks, but the part of the question allowing for other reasons had some notation. Those cases were considered valid. Although some of the blank remaining forms may have indicated no troubles, it is hard to bebelieve that a serviceman could have any experience to report on without having to service a receiver.

Performance Difficulty	VHF Receivers	UHF Converters	UHF Strip-Tuner Equipped Receivers	UHF Single-Channel Receivers	All Channel Receivers
Oscillator Drift	10 per cent	19 per cent	23 per cent	22 per cent	18 per cent
Difficulty in Tuning, Tuning too Critical	11	18	16	18	18
Short Tube Life	30	25	19	30	32
Dissatisfaction with External Boxes	3	12	3	3	2
Failure of Beating Oscillator to Cover the Range	3	3	4	4	3
Inadequate Dial Channel Identification Markings	7	6	6	5	8
High Noise Level	20	7	15	8	8
Beat Notes	11	6	9	6	6
Self Oscillation	5	4	5	5	5
Other Reasons	Of the 84 per cent responding to the question as a whole, 33 per cent of this group indicated scattered reasons other than those specified.				

2. If you do business in a mixed VHF-UHF area, is it your experience that new receivers purchased are almost always, usually, or seldom, of the all-channel (UHF and VHF) type?

Purchase Frequency	Percentage Breakdown	Aggregate Response
Always	43 per cent	Over-all 42 per cent
Usually	28	
Seldom	29	

3. Has it been your experience that owners of combination VHF-UHF receivers know how to tune in either MONOCHROME VHF or UHF stations equally well?

Yes	No	Aggregate Response
55 per cent	45 per cent	46 per cent

4. Has it been your experience that owners of combination VHF-UHF receivers know how to tune in either COLOR VHF or UHF stations equally well?

Yes	No	Aggregate Response
55 per cent	65 per cent	30 per cent

D. Multipath (Ghost) Problems

1. What proportion of the total number of sets in your area suffer from ghosts?

	Percentage of Ghosts	Aggregate Response
VHF	12 per cent	83 per cent
UHF	19	23

2. Are ghosts more objectionable on VHF or UHF?

VHF	UHF	VHF and UHF	Aggregate Response
69 per cent	18 per cent	13 per cent	44 per cent

E. Interference

1(a). Listed below are some sources of interference. In the table, check the sources of interference which you have found to exist in your service area at UHF and VHF.

1(b). Please note in the table below the sources of interference you have found to be troublesome in the areas indicated.

The percentage response to this question as a whole was 98 per cent. In analyzing the interference data, the table has been organized such that percentages within the group responding for a particular interference are listed for VHF, UHF, or a combination of both. In addition, the percentage distribution which indicated the most troublesome areas is also shown within the framework of the response for a given type of interference. Since the area group, namely, business-industrial, residential, and rural, can receive either individual or composite checks, there results seven possibilities ranging from each one individually to all three combined. For analysis purposes we have selected the four most prevalent combinations which are business-industrial (B); residential (R); business-industrial and residential (BR); and business-industrial, residential, and rural (BRR). On this basis (4 out of 7), the percentages, when added across, will not necessarily total 100 per cent. Under the aggregate response column, the figure associated with VHF indicates the actual response to the area portion of the question for a given interference as a part of the total (*i.e.*, 98 per cent) response. The statement is similar for UHF. The third response figure represents that portion of the total response which indicated a check mark at UHF, VHF or both for a given interference.

	Band		B	R	BR	BRR	Aggregate Response
Motor Vehicle Ignition Systems	VHF UHF Both	92 per cent 1 7	28 per cent 36 —	14 per cent 10 —	33 per cent 26 —	16 per cent 18 —	68 per cent 6 86
Diathermy Machines	VHF UHF Both	95 * 5	59 54 —	19 8 —	20 38 —	2 0 —	30 2 50
Power Distribution Systems	VHF UHF Both	89 1 10	31 20 —	9 0 —	14 25 —	21 25 —	35 3 45
Neon Signs	VHF UHF Both	94 1 5	86 84 —	4 11 —	9 0 —	1 5 —	40 3 58
TV Receiver Radiation	VHF UHF Both	81 7 12	9 21 —	60 33 —	18 33 —	4 8 —	20 3 44
Standard AM Receiver Radiation	VHF UHF Both	85 7 8	0 0 —	86 0 —	7 0 —	7 — —	2 * 9
FM Receiver Radiation	VHF UHF Both	87 7 6	7 50 —	56 25 —	11 0 —	11 0 —	8 1 21
Electrical Household Devices	VHF UHF Both	88 2 10	4 4 —	47 27 —	9 4 —	9 19 —	44 4 70
AM-FM Broadcast Station Radiation	VHF UHF Both	86 6 8	10 0 —	45 40 —	21 40 —	11 10 —	16 1 29
Shortwave Station Radiation	VHF UHF Both	91 3 6	15 7 —	54 57 —	10 7 —	7 14 —	12 2 29
Amateur Radio Stations	VHF UHF Both	92 2 6	3 0 —	68 58 —	4 17 —	5 21 —	38 3 63
Police Radio	VHF UHF Both	78 10 12	26 10 —	36 37 —	17 23 —	8 13 —	19 4 38
Special Service Communication Systems	VHF UHF Both	73 11 16	33 27 —	28 20 —	17 40 —	9 13 —	12 2 26

* Less than ½ of 1 per cent.
Note: 14 per cent of those responding specified other types of interference.

2. Do you find adjacent channel interference on VHF or UHF?

	Yes	No	Aggregate Response
VHF UHF	55 per cent 7	45 per cent 93	Over-all 87 per cent

3. Do you find co-channel interference on VHF or UHF?

	Yes	No	Aggregate Response
VHF UHF	58 per cent 4	42 per cent 96	Over-all 86 per cent

Note, however, that no duty factor was associated with these questions [E(2), E(3)]. Thus, effects could be of short irregular duration or only at special times of day or season.

F. Color Reception

1. Does color TV seem to work better at VHF, at UHF, or does it work equally well at both bands?

Better at VHF	Better at UHF	Equally Well	Aggregate Response
61 per cent	18 per cent	21 per cent	25 per cent

2. If there are any differences between color reception at VHF and UHF, can you give any reason for these differences?

Of the group responding to F(1), 44 per cent provided written remarks in conjunction with F(2).

General Comments

In analyzing the original and final data which were obtained as part of the TASO survey, there are a number of highlights which are worth mentioning.

A close study of the servicemen's questionnaire indicated that those men who took the time to answer the questionnaire were quite thorough. We received very few questionnaires incompletely filled out. There were, of course, a number of unanswered questions for those areas that had neither UHF nor color service, and this is the reason for the reduced response in those areas. In cross-checking the total results of various sections of the questionnaire, those which dealt basically with the same problem areas showed a very close correlation. Therefore, we believe this indicates that the serviceman did not just make haphazard guesses but was particularly reliable in the way he went about answering the questions.

It is important to remember several things; one, that the sample size, which was 730, represents a small percentage of the total television servicemen throughout the country. In addition, it represents their knowledge as it pertains to receivers that have required attention. No attempt was made to try to derive a figure representing the number of receivers that might be considered as within the area of operation of the serviceman reporting. The accumulated data, of course, are in line with the purpose of the survey which was aimed at finding out just what the problems were, and we feel that many of the sets that have not been repaired by the serviceman have, statistically, somewhat the same problems with respect to ghosts and interferences.

Then, as previously mentioned, there is no doubt that a number of sets were repaired by the owner. The coverage resulting from the survey is particularly gratifying. For example, of the three FCC Zones, the two larger each returned 44 per cent of the data, while the third and smaller zone returned 12 per cent of the total. Also, 46 out of 48 states were represented. In addition, it is a significant fact that out of the 541 individually operating television transmitting stations in this country, this survey covered 427, which represented 79 per cent. These facts greatly increase the importance of the data obtained because they indicate that although the sample may have been small, the coverage was large and quite complete.

It was not the prerogative of this committee to draw definite conclusions from the data presented; however, this report is annotated in several places to point out results that seem to be of particular interest, and in addition, many conclusions are self-evident based on the data themselves.

Acknowledgment

Much of the credit for the effectiveness of this work must be given to the members of Panel 3 who consulted and aided our Committee. The efforts of H. E. Rhea, Director of Engineering, Radio & TV Division, Triangle Publications, Inc.; G. B. Frankenfield, Supervisor Programming Section, Research Center, Burroughs Corporation; and E. H. Boden, Senior Engineer, Sylvania Electric Products, Inc., who served as members of this committee, made it possible to accomplish this work. Special credit is due Sylvania Electric Products, Inc., who completed all final tabulations for the committee.

VHF and UHF Television Receiving Equipment*

WILLIAM O. SWINYARD†, FELLOW, IRE

Summary—This paper covers a study of various types of VHF and UHF television receiving equipment made by TASO Panel 2 and reported October 3, 1958. Information and performance data are given for antennas, transmission lines and television receivers. RF amplifier and oscillator electron devices (tubes and semiconductors) used in television tuners for both VHF and UHF are discussed and tables showing relative performance data for devices of various types are included.

In addition to this study of home television receiving equipment, TASO Panel 2 made studies of 1) community television antenna and distribution systems, and 2) the effects of transmitter sound power reduction on television receiver performance. Results of these studies are also included.

In general, data collected by Panel 2 show that performance of VHF equipment is markedly superior to that of UHF equipment and that a reduction in sound power of television transmitters is harmful to television reception, particularly in fringe areas.

Introduction

TASO Panel 2 was charged with the task of securing reliable information, on both theoretical and practical bases, for the purpose of appraising the present performance of television receiving equipment (monochrome and color) for both VHF and UHF broadcasting on all presently allocated channels. The presently allocated VHF channels are 2–6 in the frequency band of 54–88 mc and 7–13 in the 174–216-mc band. The UHF band is continuous in coverage from 470–890 mc and includes 70 channels numbered 14–84. All channels, both VHF and UHF, are 6 mc wide.

Performance data on antennas, transmission lines and television receivers were obtained by Committee 2.4 directly from the manufacturers of the equipment. Forms for use in recording the data were worked out and sent to the manufacturers along with specific instructions regarding the measurement methods to be used. In the case of antennas, the measurement standard, where applicable, was Electronic Industries Association (EIA) Standard REC-141, "VHF Antenna Performance Presentation and Measurement," which was used for both VHF and UHF antennas. In the case of television receivers, since no up-to-date measurement standard was available, a comprehensive manual, "Measurement Methods," was compiled. This was based on the experience of those skilled in the field and included methods of measurement which were considered to be the best available.

The antenna and transmission line questionnaires were mailed to 52 manufacturers of antennas, 11 manufacturers of transmission lines, and 37 manufacturers of television receivers. After follow-up letters, seven questionnaires were returned with data, five of which provided fairly complete data on the material manufactured by the sources. The data received in reply to the questionnaires, along with valuable data from three other sources, were analyzed and the results appear in this paper.

The television receiver questionnaires, manual of "Measurement Methods" and instructions were sent by Committee 2.1 to all known manufacturers of television receivers and tuners. Replies and data were received from 16 receiver manufacturers, and three tuner manufacturers, covering 78 different receiver chassis and nine tuners. These data were analyzed, the performance characteristics averaged, and the results are presented herein.

All electron devices (tubes and semiconductors) now being used by tuner and set manufacturers were reviewed by Committee 2.7 and tables of data considered important to the performance of these devices as they are used in television tuners were derived and are presented in this paper. In addition, tubes designed for VHF and UHF applications, but whose commercial usage has not yet developed, were added to the lists in order to give an up-to-date picture of their performance capabilities.

Information on community antennas and distribution systems was obtained directly from the operators by Committee 2.5. Answers to questionnaires were received from operators of 125 community television systems.

The effects of transmitter sound power reduction were studied by Committee 2.6. Tests were made in the laboratories of committee members using representative receivers under conditions closely simulating those actually encountered in the field.

Antennas and Transmission Lines

Data on antennas and transmission lines received from seven manufacturers, supplemented by data received from The Association of Maximum Service Telecasters (AMST) and the RCA Service Company were analyzed.

The questionnaire data which were sent in by seven of the 52 manufacturers to whom the questionnaires were sent contain data on 26 VHF and four UHF antennas. Although only seven of the 52 manufacturers sent in data, it is believed that the data are representative since they came from the larger manufacturers.

The AMST data cover 13 all-channel VHF antennas and two special Yagi antennas. The RCA Service Company data cover nine all-channel VHF antennas, one high VHF channel antenna and one Yagi single-channel antenna; they also cover six all-channel UHF

* Original manuscript received by the IRE, January 11, 1960.
† Hazeltine Research, Inc., Chicago, Ill.

antennas and two Yagi antennas designed for specific channels.

Data on transmission lines were received from three of the 11 companies to whom the questionnaire was sent. These companies, however, are the larger ones in the field and for this reason it is felt that significant conclusions may be drawn from the data.

Table I summarizes the more important characteristics of antennas and transmission lines. It can be seen that the gain of UHF antennas is somewhat higher than the gain of VHF antennas when it is measured with respect to a half-wave folded dipole antenna. However, as the frequency increases the reference dipole becomes shorter; hence, it is not as effective in picking up signal at UHF as it is at VHF frequencies. The effectiveness is inversely proportional to frequency, and this fact must be taken into consideration when comparing the gain of VHF and UHF antennas. The dipole constant λ/π shown in Table II takes cognizance of this fact. The dipole constant, in db[1] (also called the antenna lambda factor) added algebraically to the antenna gain, in db, with respect to a half-wave dipole gives the relationship between the incident field intensity and voltage at the receiver input terminals, neglecting transmission line loss.

Theoretically it is possible for the antenna to deliver a constant voltage to the load on all television channels if the field strength is the same for all channels. This requires a constant capture area for all channels.[2] The capture area (sometimes called the effective area or aperture) is $G_1\lambda^2/4\pi$, where G_1 is the power gain as a transmitting antenna relative to an isotropic radiator.[3] For a half-wave dipole G_1 is 1.64 and the capture area is $0.130\lambda^2$. The capture area for a dipole resonant at the center frequency of channel 2 is 38.5 square feet. To maintain this area for all channels requires the use of some sort of high-gain directional antenna at the higher frequencies and particularly at UHF where, for example, a dipole, or dipoles, mounted at the focal point of a parabolic reflector might be used. However, such an antenna has not come into general use in television reception.

It can be seen from Table II that for practicable antennas, and assuming uniform field strength at all frequencies, the signal delivered by the antenna to the input of the transmission line is −5.9 db and −15.6 db at high VHF and UHF, respectively, with reference to low VHF. This loss is further increased by losses in the transmission line. The net result is shown in the last two columns of data in Table II. These data show that in an

[1] The dipole constant is the ratio of the voltage at the transmission line terminals of the dipole antenna to the uniform field strength of the field in which the dipole is located. Its dimensions are therefore those of voltage/field strength or volts/(volts/meter) = meters. By definition, a db is a dimensionless quantity, being proportional to the logarithm of the ratio of two quantities having the same dimensions; therefore, it is not rigorously correct to express the dipole constant as so many db. Since all other quantities entering into this discussion are correctly expressed in db, it is convenient also to express the dipole constant on a logarithmic scale so that the gains (or losses) of all elements may be added to give the over-all gain (or loss) of the system as a whole. The dipole constant has therefore been expressed as

$$K_d \text{ (in db)} = 20 \log_{10} \frac{\text{voltage (in volts)}}{\text{field strength (in volts per meter)}}$$

with the knowledge that the expression is convenient rather than rigorously correct, and that the numerical result can be used only when the voltage and the field strength are expressed in units such that their ratio has the dimension of meters.

[2] G. H. Brown, J. Epstein, and D. W. Peterson, "Comparative propagation measurements: television transmitters at 67.25, 288, 510 and 910 megacycles," *RCA Rev.*, vol. 9, pp. 177–201; June, 1948.

[3] F. E. Terman, "Radio Engineering," McGraw-Hill Book Co., Inc., New York, N. Y., Third ed., p. 729; 1947.

TABLE I

SUMMARY OF CHARACTERISTICS OF ANTENNAS AND TRANSMISSION LINES

TV Band	Gain, db[1]			Front/Back Signal Ratio, db			Horizontal Beamwidth (6 db), Degrees			Transmission Line Loss (100 feet), db					
										New, Dry			5 Years Old, Wet		
	Min	Av	Max	Min	Av	Max	Min	Av	Max	Min	Av	Max	Min	Av	Max
Low VHF	−7.0	3.7	11	0	11.6	30.4	55	109	360	0.7	0.9	1.2	2.1	5.1	8.0
High VHF	−2.5	6.8	12.8	2.2	10.6	26	24	59	210	1.5	1.7	1.9	4.2	9.7	14
UHF	−0.2	7.7	13.5	2.7	15.1	25	30	65	120	2.8	3.6	4.5	7.5	20.0	31

[1] Referred to a tuned, folded dipole.

TABLE II

RELATIONSHIP BETWEEN INCIDENT FIELD STRENGTH AND VOLTAGE AT RECEIVER INPUT TERMINALS

TV Band	Average Antenna Gain	Dipole Constant, K_d (Lambda Factor)	Ratio of Voltage at Transmission Line Input to Incident Field Strength	Average Transmission Line Loss (30 feet)		Ratio of Voltage at Receiver Terminals to Incident Field Strength	
				New, Dry	5 Years Old, Wet	New Dry Line	5-Year Old Wet Line
Low VHF	3.7 db	2.9 db	6.6 db	0.3 db	1.5 db	6.3 db	5.1 db
High VHF	6.8	− 6.1	0.7	0.5	2.9	0.2	− 2.2
UHF	7.7	−16.7	−9.0	1.1	6.0	−10.1	−15.0

average installation the signal delivered by the antenna to the receiver input terminals greatly favors the VHF receiver, and especially the low-frequency channels. The signal delivered to the receiver input terminals is -6.1 db and -16.4 db for the high VHF and UHF bands, respectively, with reference to the low VHF band, assuming equal field strength in all cases and new, dry transmission line. For old, wet transmission line the corresponding figures are -7.3 db and -20.1 db.

Although UHF antennas have been shown to deliver far less voltage to the receiver antenna terminals than VHF antennas, for a given field strength, there is some advantage in their generally smaller physical size.

Receivers

Information concerning the more important circuit and performance characteristics of UHF and VHF receivers, including their susceptibility to various types of interfering signals, was supplied by 16 receiver manufacturers and three tuner manufacturers, covering 78 different receiver chassis and nine tuners. This represents a sufficiently large sampling of the industry to justify some rather general conclusions concerning the important circuit features and performance characteristics of present-day UHF and VHF receivers.

Consideration will be given first to the circuit features of UHF and VHF receivers. Most receivers employ a single transmission line input and are designed to receive VHF signals only. A few UHF/VHF receivers employ a single transmission line input with an internal crossover network. Most combination UHF/VHF receivers have dual inputs.

All VHF receivers reported have provision for reception of 12 channels which are selected by means of a switch having a detent mechanism. Provision is made for "fine-tuning" the selected channel for the best compromise of picture and sound. Most UHF receivers employ continuous tuning from channels 14 through 83, although a few divide the band into segments which can be selected by means of a switch and provide sufficient "fine-tuning" range to tune through each segment, thus covering the entire UHF band in discrete steps.

All VHF receivers employ an RF amplifier stage. Vacuum tubes are employed in the tuner and three tuned RF circuits are used in most cases. On the other hand, UHF receivers do not employ an RF amplifier stage. This matter will be discussed later. All UHF receivers have vacuum tube oscillators and crystal diode mixers, and most of them employ two RF tuned circuits.

All receivers reported, both VHF and UHF/VHF, employ the EIA standard video carrier IF of 45.75 mc. In combination UHF/VHF receivers the VHF tuner circuits are usually employed as IF amplifiers for UHF reception, thereby partially compensating for the losses in the UHF tuner.

Existing VHF television receivers can be adapted to receive UHF signals by means of a converter which, in conjunction with the receiver, operates on a double superheterodyne principle and uses one of the VHF channels as the converter intermediate frequency. No data on UHF converters were reported.

An important characteristic of a UHF converter is its ability to amplify weak signals to a usable level with a good signal-to-noise ratio. Most UHF converters employ a circuit consisting of a tuned preselector, an oscillator, a crystal diode mixer, an IF amplifier, and a power supply. The over-all noise factor of such a converter in combination with a VHF receiver is determined mainly by the following three characteristics:[4]

1) the losses in the preselector and crystal mixer circuits,
2) the noise factor of the converter IF amplifier, and
3) the noise factor of the VHF receiver.

The combined noise factor of the VHF receiver and converter IF amplifier is found usually to be only slightly higher than the noise factor of the converter IF amplifier alone, which may be assumed to be 6 or 7 db. This, combined with an assumed loss of about 10 db in the preselector and mixer circuits together, gives an over-all noise factor of about 16 to 17 db.

Other important converter characteristics are good oscillator stability, adequate selectivity, sufficient bandwidth and low oscillator radiation. A well-designed present-day converter can satisfy all of these requirements.

Converters may reasonably be considered as interim devices. Better results can be secured by using UHF receivers or combination UHF/VHF receivers.

The more important receiver performance characteristics are summarized in Table III. This shows the poorest, average and best results for each of the characteristics listed. It can be seen that the UHF receiver suffers in comparison with the VHF receiver in four major respects: 1) noise factor, 2) image ratio, 3) tuner bandwidth, and 4) oscillator stability. Average VHF noise factors are 6.5–8.5 db and average UHF noise factors are 12.8–13.8 db, a difference of about 6 db in favor of VHF. The image ratio performance is much poorer in UHF receivers. This is due to the practice of using a common IF for UHF and VHF receivers. This IF is as high as it can be for VHF but is too low for UHF; however, it seems to be a good compromise and no change is recommended. The RF bandwidth is much more favorable for VHF than for UHF, leading to fewer interference problems in VHF receivers. Oscillator drift is significantly less in VHF receivers. While the average drift in present UHF receivers is tolerable for monochrome reception, it is doubtful if it is sufficiently low for satisfactory color reception without retuning. Most receivers with remote tuning devices are also critically

[4] W. Y. Pan, "Some design considerations of ultra-high-frequency converters," *RCA Rev.*, vol. 11, pp. 377–398; September, 1950.

TABLE III

RECEIVER PERFORMANCE CHARACTERISTICS

Channel	2–6			7–13			14–40			41–65			66–83		
Characteristic[1]	P	A	B	P	A	B	P	A	B	P	A	B	P	A	B
Noise Factor, db	9.7	6.5	4.6	12.2	8.5	6.5	16.7	12.8	10.5	18.2	13.2	10.0	19.0	13.8	9.5
Sensitivity, uv	150	40	4	270	57	6	360	79	10	280	76	8.5	300	81	11
Image Ratio, db	41	73+	80.5	45	68+	80	14	32	46	10	29	44	6	26	46
IF Interference Ratio, db	36	57+	76	53.5	68+	91	43	64+	88	43	65+	82	43	66+	86
Tuner Bandwidth[2] 3 db down, mc	10.5	7.5	4.0	14.0	9.4	3.5	37.0	17.5	8.0	34.0	18.5	9.0	60.0	25.4	10.0
Tuner Bandwidth[2] 20 db down, mc	22.5	14.8	6.0	37.0	23	8.0	125	48	15	178	59	16	247	74	18
Five-Minute Warmup Drift, mc	0.52	0.09	0.015	0.65	0.14	0.017	0.458	0.17	0.09	0.50	0.22	0.06	0.70	0.28	0.03
One-Hour Warmup Drift, mc	0.45	0.21	0.03	0.40	0.23	0.035	1.25	0.45	0.12	2.5	0.61	0.14	1.142	0.63	0.16
Input VSWR	6.0	2.7	1.0	6.0	2.4	1.0	5.0	2.4	1.0	5.0	2.4	1.0	5.0	2.5	1.0
Adj. Lwr. Snd.[3] Car. Atten., db	14	40	60	20	38	60	16	39	58	16	41	58	16	41	60
Adj. Upr. Pic.[4] Car. Atten., db	26	40	56	24	39	52	20	40	77	24	42	80	20	41	<80

[1] P, A, and B stand for poorest, average and best, respectively.
[2] In general, the broadest bandwidth is considered poorest and the narrowest is considered best. A lower number is generally more favorable down to about 6 mc.
[3] Channels used: 3–6; 8–13; 15–40; 41–65; 66–83.
[4] Channels used: 2–5; 7–12; 14–40; 41–65; 66–82.

dependent on oscillator stability. While VHF receivers are being sold in increasingly large numbers with remote tuning devices, at present such devices are not in widespread use in UHF receivers.

With respect to other performance characteristics for which data were obtained, the difference between UHF and VHF receivers is not significant.

Of the four points mentioned, wherein the performance of UHF receivers suffers by comparison to that of VHF receivers, the most important is the noise factor. The lack of a suitable low-cost RF amplifier tube for use in UHF tuners accounts for the relatively high UHF noise factors.

Not immediately apparent in the data is the fact that UHF receivers fall short with respect to amplification. It has been pointed out previously that this shortcoming in amplification in UHF tuners is at least partially compensated in combination UHF/VHF receivers by using the VHF tuner circuits to provide additional IF amplification. However, in receivers built for UHF reception only, provision would have to be made in the IF amplifier for this additional gain. This probably would require one, or possibly two, extra IF amplifier stages as compared with a VHF receiver. If an RF amplifier stage were used for improvement in noise factors, one additional IF amplifier stage would probably suffice because of the amplification supplied by the RF stage. The provision for additional IF gain for UHF reception in UHF/VHF receivers results in UHF sensitivity, which, while it is slightly poorer than that of VHF receivers, appears to be adequate considering the noise factors.

Table IV shows the reduction in receiver input terminal voltage for the high VHF band and UHF band relative to the low VHF band. The data in columns one and two were derived from the last two columns in Table II and assume the use of a 30-foot length of transmission line as in an average installation. Table IV, columns 3 and 4, shows how these figures are modified, as far as the

TABLE IV

REDUCTION IN RECEIVER INPUT TERMINAL VOLTAGE AND IN SIGNAL-TO-NOISE RATIOS FOR HIGH VHF AND UHF BANDS RELATIVE TO LOW VHF BAND, FOR EQUAL FIELD STRENGTHS[1]

TV Band	Reduction in Receiver Input Terminal Voltage[2]		Reduction in Signal-to-Noise Ratio[3]	
	Transmission Line New, Dry	Transmission Line 5 Years Old, Wet	Transmission Line New, Dry	Transmission Line 5 Years Old, Wet
High VHF	6.1 db	7.3 db	8.1 db	9.3 db
UHF	16.4	20.1	23.2	26.9

[1] Based on average noise factors as follows: Low VHF, 6.5 db; High VHF, 8.5 db; UHF, 13.3 db.
[2] Figures derived from last two columns in Table II.
[3] These figures were obtained by adding to the figures in columns 1 and 2 the average noise factors relative to low VHF, which are as follows: high VHF, 2.0 db; UHF, 6.8 db.

signal-to-noise ratio in the picture is concerned, by the receiver noise factors. In fringe area installation the antenna usually is mounted on a tower high above the roof. In such cases the length of transmission line required might well be 60–100 feet. For a 60-foot length of transmission line the figures in column 3 of Table IV would be 8.3 db and 24.0 db; those in column 4 would be 10.7 db and 31.4 db. For a 100-foot length of line the figures in column 3 of Table IV would be 8.7 db and 25.1 db; those in column 4 would be 12.5 db and 37.3 db. Thus it can be seen that the UHF receiver is under a heavy handicap as compared with a VHF receiver from the standpoint of signal-to-noise ratio in the picture. This could be offset by increasing the UHF antenna gain and decreasing the transmission line losses. However, the margin for improvement in these respects does not seem to be especially significant considering the magnitude of the required improvement. A decrease in UHF receiver noise factors would be equally effective in improving the performance. However, data obtained on tubes and other electron devices, to be discussed later, show that the magnitude of the possible improvement which could be obtained by using an RF amplifier tube is sufficient to provide only a small part of the required improvement.

There is little difference between VHF and UHF receivers with respect to cross-modulation, as is shown in Figs. 1 and 2.

On the positive side, it should be mentioned that experience has shown that UHF receivers are less susceptible to airplane flutter and to various types of electrical disturbances, both natural and man-made, than are VHF receivers.

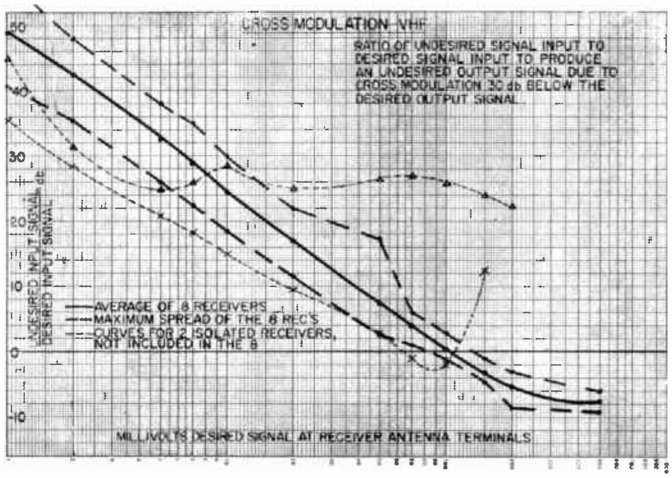

Fig. 1.

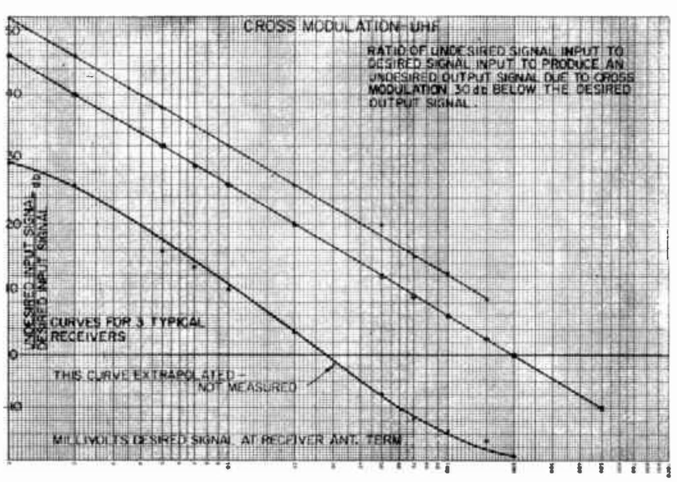

Fig. 2.

Electron Devices for Television Tuners

All of the tubes and semiconductors now being used by TV tuner and set manufacturers were reviewed and tables of data considered pertinent to the performance of these devices in their functional applications were derived. Accordingly, tables were composed listing every tube type now being used in volume in new tuners. In addition, tubes designed for tuner applications at UHF and VHF, but whose commercial TV usage has not yet developed, were added to the lists in order to give an up-to-date picture of the performance capabilities of these devices. The tables are as follows:

Table V.—VHF RF Amplifiers
Table VI.—VHF Oscillator-Mixers
Table VII.—UHF Oscillators
Table VIII.—UHF RF Amplifiers
Table IX.—UHF Mixers
Table X.—UHF Semiconductor Mixers.

These six classifications cover the functional application areas of electron devices used in tuners, and for the purposes of the performance descriptions of products were considered adequate.

Performance Criteria and Technical Data

In the performance tables no attempt was made to provide complete technical information regarding the various electron devices listed since such information is widely available in detail far beyond the scope of this paper. Rather, those electrical characteristics believed to have the greatest significance to the functional applications described in the table headings were selected. In some cases, measurements were made and data presented under "typical" operating conditions rather than under the more normal "rated" conditions for the electron devices under consideration. For example, VHF-RF amplifier tubes were all tested for transconductance (G_m) under typical tuner operating conditions rather than at standard "rated" values of E_b, E_{c2}, I_b and $-E_{c1}$. Thus the relative transconductances and calculated performances derived from these data are considered to represent actual "in-tuner" performance more closely than might otherwise be the case.

The following is a summary of the performance characteristics to be found in Tables V through X:

1) *VHF-RF amplifiers (data in Table V)*:

a) Gain-bandwidth figure of merit. This is determined by calculation from the formula

$$\text{G. B.} = \frac{G_m}{2\sqrt{C_{in} \times C_{out}}}$$

where G_m is the low frequency transconductance, C_{in} is the capacitance from G_1 to $K+H$, and C_{out} is the capacitance from P to $K+H$. It should be noted that this figure of merit does not involve frequency-sensitive parameters and consequently can be misinterpreted. This relative value is valid only when the frequency of operation is such that the input resistance of the tube is high. *In this column larger numbers generally indicate better performance.*

b) Theoretical noise factor—at 50 mc and 200 mc. The theoretical noise factor of a vacuum tube is an expression of the irreducible noise generated by the noncorrelated flow of electrons within the tube. This factor, expressed in db, represents the power ratio of the noise produced by the device being tested to that obtained from an ideal "noiseless" amplifier. In our case, we have

TABLE V

VHF RF Amplifiers

Tube Types in Current Usage	Type Class				Cutoff		Heater Current Versions Available				VHF Characteristics								Static Characteristics	With Shield			Catalog Price
	Cascode	Triode	Tetrode	Pentode	Sharp	Remote	6 Volt I_f in ma	300 ma	450 ma	600 ma	Gain Bandwidth[2]	Theoretical Noise Factor at 50 mc-db[3,7]	Theoretical Noise Factor at 200 mc-db[3,7]	Input Resist. 50 mc-ohms[4]	Input Resist. 200 mc-ohms[4]	Equivalent Noise Resist. ohms	Feed Through Cap.-$\mu\mu f$ (with shield)[5]	Upper Freq. Limit-mc[6]	G_m-μmhos[7]	G to ($K+H$)-$\mu\mu f$ Capacitance	P to ($K+H$)-$\mu\mu f$ Capacitance	G to P-$\mu\mu f$ Capacitance	
6BC5				X	X			X		X	735	3.8	7.4	7,100	500	1,025	0.02	360	7,500	6.6	2.6	0.02	1.17
6BC8	X					X	400			X	2,650	1.7	3.6	10,000	835	340	0.008	500	9,600	2.5	1.3	1.4	2.01
6BK7A	X				X				X	X	2,040	1.8	4.8	6,900	400	355	0.004	380	8,690	3.0	1.5	1.8	1.76
6BK7B	X				X				X		2,040	1.8	4.8	6,900	300	355	0.0043	320	8,700	3.0	1.5	1.8	1.76
6BN4		X			X		200		X	X	1,606	2.0	5.3	9,400	800	460	1.2	530	9,000	3.2	1.4	1.2	1.23
6BQ7A	X				X		400			X	2,410	1.9	5.0	9,400	800	460	0.005	510	8,520	2.6	1.2	1.2	1.98
6BS8	X				X		400			X	2,610	1.7	4.7	6,300	665	345	0.014	520	9,820	2.6	1.35	1.15	1.96
6BZ7	X				X		400			X	2,480	1.9	5.0	9,300	850	420	0.0045	530	8,780	2.6	1.2	1.2	2.01
6BZ8	X					X	400			X	2,520	2.0	5.2	7,400	480	385	0.015	390	9,980	2.8	1.4	1.3	2.37
6CY5			X		X				X	X	1,090	2.7	6.4	11,000	1,070	835	0.03	710	8,100	4.5	3.0	0.03	1.40
PCC88[1]	X				X						2,495	1.6	4.4	7,000	380	190	0.0012	—	13,700	3.5	1.8	1.4	
E-180F[1]				X	X						1,738	2.3	5.9	4,700	170	320	0.019	—	13,500	7.5	3.0	0.03	

[1] European types with possible future usage.

[2] Gain Bandwidth—a figure of merit defined by formula

$$\frac{G_m}{2\sqrt{C_{in} \times C_{out}}}$$

This figure becomes deficient when input resistance becomes low. See Paragraph a), page 1070.

[3] For tube only.

[4] Short circuit input resistance.

[5] Input grid to output plate capacitance.

[6] A relative indication of highest frequency of operation attainable. See Paragraph f), page 1073.

[7] Conditions: $E_{c1} = -1\,V(R_k = 68 \text{ ohms})$. E_b or E_{c2} adjusted for 15 ma I_k and with plate dissipation within rating. These conditions are for comparison on a common basis.

TABLE VI

VHF Oscillator-Mixers

Tube Types in Current Usage	Type Class			Heater Current Versions Available			VHF Characteristics as Oscillators and Mixers			Static Characteristics: Triode[4]				Static Characteristics: Pentode or Tetrode[4]				Catalog Price
	Triode Pentode	Triode Tetrode	Common Cathode	6 Volt I_f in ma	300 ma	600 ma	Resonant Frequency (mc) Measured[1]	Relative Mixer Gain Zero-Bias G_m (μmhos)[2]	Loading (Feed-back) ($\mu\mu f$)[3]	G_m (μmhos)	G to ($K+H$) Capacitance ($\mu\mu f$)	P to ($K+H$) Capacitance ($\mu\mu f$)	G_1 to P ($\mu\mu f$)	G_m (μmhos)	G to ($K+H$) Capacitance ($\mu\mu f$)	P to ($K+H$) Capacitance ($\mu\mu f$)	G_1 to P Capacitance ($\mu\mu f$)	
6AT8A	X		X	450		X	930	5,700	0.06	6,500	2.4	1.0	1.5	5,500	4.8	1.6	0.06	1.62
6BR8A	X			450		X	772	5,500	0.008	8,500	2.5	1.0	1.8	5,200	5.0	3.5	0.008	1.65
6CG8A	X		X	450		X	870	5,700	0.02	6,500	2.4	1.0	1.5	5,500	4.8	1.6	0.02	1.62
6CL8A		X		450		X	794	6,500	0.01	8,000	2.7	1.2	1.8	6,400	5.0	3.4	0.01	1.62
6CQ8		X				X	671	5,800	0.015	8,000	2.7	1.2	1.8	5,800	5.0	3.3	0.015	1.65
6EA8	X			450		X	694	7,300	0.01	8,500	3.2	1.1	1.7	6,400	5.0	3.4	0.01	
6EH8	X			450			708	6,100	0.012	7,500	2.8	2.2	1.8	6,000	4.8	3.2	0.012	
6U8A	X			450		X	694	5,500	0.006	7,500	2.5	1.0	1.8	5,000	5.0	3.5	0.006	1.65
6X8	X		X	450		X	990	5,700	0.06	6,500	2.4	1.0	1.5	5,500	4.8	1.6	0.06	1.62
6EU8[5]	X			450		X	694	7,300	0.01	8,500	3.2	1.1	1.7	6,400	5.0	3.3	0.015	

[1] A relative indication of the highest frequency of operation attainable (in oscillator section).

[2] G_m measured at zero bias considered significant. Conditions: $E_{c1}=0$, $E_{c2}=70$ volts, $E_b=100$ volts.

[3] Considered as a function of capacitance between the input signal grid and output plate.

[4] Capacitances measured with external shield.

[5] The 6EU8 differs from the 6EA8 in base connections.

TABLE VII

UHF OSCILLATORS

Tube Types in Current Usage	Type Class	Heater Current Versions Available			Oscillator Characteristics	Static Characteristics				Catalog Price
	Triode	225 ma 6 volt	450 ma	600 ma	Resonant Frequency[1] (mc)	G_m (µmhos)	Input Capacitance[2] G_1 to $(K+H)$ (µµf)	Grid-Plate Capacitance[2] (µµf)	Output Capacitance[2] P to $(K+H)$ (µµf)	
6AF4	X	X	X	X	1,345	6,500	2.2	1.9	1.4	2.01
6AF4A	X	X	X	X	1,408	6,500	2.2	1.9	1.4	2.01
6T4	X	X			1,343	7,000	3.3	1.7	1.8	2.01

[1] Cold line test. Considered a relative indication of the highest frequency of operation but not necessarily the highest attainable.
[2] Capacitance measured with external shield.

TABLE VIII

UHF RF AMPLIFIERS

Tube Types Considered[1]	Type Class	UHF Characteristics						VHF 200 mc Characteristics		Static Characteristics				Catalog Price
	Triode	Power Gain—db (measured) (500 mc)[2]	Power Gain—db (measured) (900 mc)[2]	Noise Factor—db (500 mc) (measured)	Noise Factor—db (900 mc) (measured)	Approximate Input Resist. (ohms) Grounded Grid (900 mc)	Equivalent Noise Resistance (ohms)	Noise Factor—db	Power Gain—db	G_m (µmhos)	Grid to $(K+H)$ Capacitance (µµf)[3]	P to G Capacitance (µµf)[3]	P to $(K+H)$ Capacitance (µµf)[3]	
6AM4	X	7.1	7.0	13.2	14.0	100	340	8.1	12.0	9,800	3.2	2.2	0.22	2.99
6AN4	X	12.0	10.0	12.0	14.0	100[4]	300	6.5	14.0	10,000	2.6	1.7	0.18	2.54
6BC4	X	10.0	6.0	11.5	14.5	100[4]	300[4]			10,000	2.9	1.6	0.26	2.49
6BY4	X	15.0	15.0	7.5	8.5	180	500	4.2	14.0	6,000	1.2	0.7	0.007	—
6299	X	15.5	15.0	5.5	8.0	100	175	3.7	16.0	12,000	3.5	1.7	0.015	56.00
6BA4	X	14.0	14.0	8.0	11.0	125	400[4]			8,000	2.4	1.4	0.02	39.25
5876	X	11.7	14.0	9.4	12.5	150	500			6,500	2.5	1.4	0.035	13.55
7077	X	14.5	14.5	5.5	7.5	150	350	2.7	14.5	9,000	1.9	1.0	0.01	—

[1] Types shown are not in current usage. The list is being retained to provide technical information to TASO.
[2] Gain measurements with the minimum of 10-mc bandwidth.
[3] Capacitances as published with grounded-grid connection.
[4] Calculated. Data shown for other types are measured.

TABLE IX

UHF MIXERS

Tube Types Considered[1]	Type Class	Static Characteristics				Catalog Price
	Triode	G_m (µmhos)	G to $(K+H)$ Capacitance (µµf)	P to G Capacitance (µµf)	P to $(K+H)$ Capacitance[2] (µµf)	
6AM4	X	9,800	3.2	2.2	0.22	2.99
6AN4	X	10,000	2.6	1.7	0.18	2.54
6BC4	X	10,000	2.9	1.6	0.26	2.49
6BY4	X	6,000	1.2	0.7	0.007	

[1] Types shown are not in current usage. The list is included to provide technical information.
[2] Grounded-grid with shield.

TABLE X

UHF SEMICONDUCTOR MIXERS

Types in Current Usage	750-mc Over-all Noise Figure (NF_{if}=3.5 db)	Conversion Loss	Output IF Impedance at 40 mc	Catalog Price
1N82A	13.0 db	8.0 db	400 ohms	0.98
1N72	13.0 db	8.0 db	400 ohms	0.87
1N124A	13.0 db	8.0 db	400 ohms	
1N147	13.0 db	8.0 db	400 ohms	

NOTE: Crystal Current = approximately 0.75 ma. These data are presented as family characteristics. See Paragraph 6), page 1074.

followed the method of Rothe[5] to make measurements,[6] at 90 mc, of the noise parameters of the tubes listed in the table. From these the noise factors can be calculated. The values shown in the tables are the lowest values of noise factor one may obtain from each of the types listed under the test conditions specified. *Low noise factor is regarded to be desirable for RF amplifier applications.* It should be noted that in practical applications the over-all tuner noise factor is generally 2 to 3 db greater than the values shown in the table because of circuit limitations. Noise factor is sensitive to operating conditions. The data presented are not necessarily under optimized conditions.

In a practical case it should be noted that the correlated noise usually cannot be eliminated completely, at least with today's techniques. For this reason, the theoretical noise factor listed in Table V will not be realized. In combination with other parameters, a listing of tubes in order of merit may be somewhat different when considering correlated noise than when not considering it.

c) Input resistance—at 50 mc and 200 mc. This important parameter is an indication of the apparent elec-

[5] H. Rothe and W. Dahlke, "Theory of noisy fourpoles," PROC. IRE, vol. 44, pp. 811–818; June, 1956.
[6] C. Metelmann, "Noise Measurements by the Rothe Method," presented at the AIEE Winter General Meeting, New Hork, N. Y.; January 21, 1957.

trical resistance one may measure between the input grid and cathode at the frequency indicated. Since this value of resistance appears as a loading factor on the tuned circuits usually associated with RF amplifier stages, *a high value of input resistance, i.e., least loading of tuned circuit, is considered desirable*. Values of input resistance shown in Table V were measured under "rated" operating conditions given in the tube manuals. The values shown are averages obtained from measurements made on tubes manufactured by several different companies. This characteristic is quite dependent upon operating point (I_b, E_b, $-E_{c1}$) and frequency. (Input resistance is approximately proportional to $1/(\text{frequency})^2$ in the UHF and VHF range.)

d) Equivalent noise resistance. This value of resistance referred to the input network is one of the parameters by which the noisiness of an electron device can be described. This value of resistance, which can be determined experimentally by the use of Rothe's theory,[5] will produce the same noise energy at room temperature as the electron device being measured. Tubes having *low values of R_{eq} are generally better* than those having high values. An approximate method for calculating an equivalent noise resistance for triodes is given by the formula

$$R_{eq} = \frac{2.5}{g_m}.$$

Experience has shown that this figure is sometimes seriously in error, and considerable care must be taken in applying calculated values.

The Rothe method for determining the R_{eq} has been applied to the measurements in Table V because it has been determined to give accurate results.

e) Feedthrough. This is a value of capacitance measured from output plate to input grid of the RF amplifier. This capacitive reactance provides a coupling path for oscillator voltage to appear on the input tuned circuits. Therefore, the *feedthrough capacitance should be as small as possible* for best results in TV applications.

f) Upper frequency limit. This is a calculated value of the frequency at which the product of the input resistance and the transconductance equals unity, $G_m \times R_{in}(f) = 1$. Since the input resistance is proportional to $1/f^2$ approximately, this calculation for frequency can be made by simple arithmetic if the G_m is known and an accurate value of R_{in} at some frequency has been determined.

One must recognize that this upper frequency limit is an expression of considerable significance. The numbers shown here are probably somewhat higher than could be realized in practical tuners. *High values of upper frequency limit are desirable.*

g) G_m—transconductance. This characteristic is regarded as one of the more significant of amplifier tube parameters. The data reported in Table V were determined by operating the tubes under operating conditions typical of TV tuner applications rather than under "rated" conditions specified by the tube industry. In order to compare tube types, measurements were made under the same operating conditions.

All G_m measurements (1000 cps) listed in this column were made at $I_p = 15$ ma; $R_k = 68$ ohms (yielding a bias of -1.02 volts); and E_b adjusted to give the proper I_b. The tetrodes and pentodes were operated at $I_K = 15$ ma with the screen grid at plate potential. The transconductance of the cascode triodes was measured in a series-cascode connection with G_m of the input section being measured and recorded. *High values of G_m are desirable.*

h) Catalog price. In each of the tables a column of catalog price is included to enable the reviewer to determine the relative "net" price for which these tubes can be purchased. The committee arbitrarily selected a widely distributed 1958 catalog as the source of this information. Wherever price information is not included, no price was available from the catalog chosen.

2) *VHF oscillator mixers (data in Table VI).* Current practice in VHF tuner design is to employ a triode-pentode or triode-tetrode tube as a single-tube oscillator-mixer. The triode section of the tube functions as the local oscillator which supplies a signal to the other section of the tube for the purpose of converting the VHF signal to an intermediate frequency, usually 40 mc. In the performance evaluation of these electron tubes, the following characteristics are considered as definitive:

a) Resonant frequency measurement. This is the frequency at which the internal structure, including the base leads, becomes resonant. While this frequency is not necessarily the highest frequency at which the tube can be made to oscillate by the use of appropriate circuit components, the values indicated in Table VI provide relative indications of the maximum frequencies of these tubes. *A high resonant frequency is desirable.*

b) Gain—relative. This figure is an indication of the relative mixer section gain which may be realized from the tube under test. This measurement is a static, rather than a dynamic, test of the zero-bias transconductance of the mixer section. The mixer conversion transconductances, obtained under dynamic conditions, are approximately one-fourth of the values shown here. *A high value of zero-bias G_m is desirable.*

c) Loading (feedback). This value of capacitance represents the undesirable coupling which exists between the output plate of the mixer and its input grid. *A low value of loading is desirable.*

d) Static characteristics. The static characteristics of VHF oscillator-mixers deemed most significant are listed under this heading. *In general, high transconductances (G_m) and low interelectrode capacitances are the desirable features of these tubes.*

3) *UHF oscillators (data in Table VII).* Only three tubes are in current usage as UHF oscillators. These are all triodes and are characterized by a high resonant frequency. These tubes are physically small in order to keep capacitance and lead inductance low, and are re-

quired to supply a few milliwatts of power to the mixer stage of UHF tuners.

4) *UHF-RF amplifiers (data in Table VIII).* None of the tube types listed is being used in TV tuners for home use at the present time. The first three tubes on this table are of miniature construction, while the remaining tubes employ special construction techniques designed to yield superior UHF performance.

a) Gain measurements—at 500 and 900 mc. These figures are expressed in decibels for the condition of power matched impedances. Since the circuit and the tube are so intimately related at UHF, no attempt has been made in this table to separate the performance characteristics of each as was done at VHF. A number of different circuit configurations of the grounded-grid type were used. *A high value of power gain is desirable.*

b) Noise factor. This is an expression, in db, of the noisiness of the amplifier stage under test. The noise factor is determined primarily by the characteristics of the electron device being used. Since the UHF tube or semiconductor employed acts as a generator of unwanted noise signals, the basic UHF performance of the equipment, that is, its ability to receive weak signals, is dependent upon this factor to a considerable extent. Methods of measuring this characteristic are complex; however, by using a calibrated noise generator, such as a noise diode or argon discharge lamp and a calibrated amplifier, a relatively accurate determination of noise factor can be made. It should be noted that noise factors at UHF were measured at the frequencies stated. This is different from the VHF noise factors which were calculated. *Low values of noise factor are desirable.*

c) Approximate grounded-grid input resistance. All of the triode tubes listed are intended for application in grounded-grid circuits. Accordingly, the approximate input resistance of the stage is determined by the transconductance of the tube and is nearly $1/G_m$. Maximum power gain is obtained when the source resistance is approximately equal to this value. Minimum noise factor may be obtained at some other values of source resistance.

d) VHF characteristics of UHF tubes. It should be noted that all UHF triodes are capable of very effective operation at VHF.

e) Catalog price. The last five types shown in Table VIII, employing special construction, are somewhat more costly than the more conventional types.

5) *UHF mixers—vacuum tube.* No UHF vacuum tube mixers are now being used for TV (home use) tuners. The types listed in Table IX have been tested in laboratories and have been found to be applicable to this type of circuit.

6) *UHF Mixers—semiconductor.* The types in current usage are listed in Table X. In addition to these types, a few others are known to be in limited use. The performance figures shown represent average crystal mixers in average tuners. *All UHF-TV tuners in current production use crystal mixers.* A wide variety of applications, some involving double conversion, or harmonic oscillator drive, have been noted in addition to the usual single conversion (to 40 mc) applications. Semiconductor mixers have a conversion loss of about 8 db as noted and provide low impedance drive to the IF amplifier.

Interpretation of Data

It is evident from the foregoing discussion and the data contained in the tables that a great many factors enter into the selection and application of electron tubes and semiconductors for TV tuners. The most salient technical characteristics have been covered to some extent. Nonetheless, other factors should be considered in weighing this technical information. One could generalize and state that the functional requirements of electron devices for TV tuners appear in the following possible order of importance:

1) Noise factor—should be low.
2) Amplification (sensitivity)—should be high.
3) Oscillator stability—frequency of oscillation should be constant.
4) Dynamic range.
   a) Gain control—should be widely variable without introduction of distortion or increase of over-all signal-to-noise ratio.
   b) Cross-modulation—low so that desired weak signals are not distorted in presence of undesired strong signals.
5) Efficiency of operation—should be high to minimize power input requirements.

Fig. 3 is a plot of noise factor vs frequency in which the theoretical noise factors for electron devices, as reported in the appropriate tables, and the measured noise factors of receivers are given. It should be recognized that these data represent laboratory measurements in which the effects of galactic noise and noise from other sources, such as ignition noise, radiation effects from industrial equipment, lighting devices, etc., have been excluded. Since most of these sources of noise exhibit decreasing output as frequency increases, the effective performance of receivers, particularly in the VHF region, may deviate greatly from the values shown in Fig. 3. Two reports demonstrating the frequency sensitive nature of these types of noise[7,8] were considered in detail and reported to TASO Panel 2 for additional consideration by the TASO organization. When these additional noise sources are considered, it is apparent that the items listed above may not be in the order of greatest importance for all receiving locations. Nevertheless, these five items are regarded to be the major technical areas of consideration in the application of electron devices to TV tuners.

[7] K. Bullington, "Radio propagation fundamentals," *Bell Sys. Tech. J.*, vol. 36, pp. 593–626; May, 1957.

[8] D. V. Carlson, "Galactic Noise—An Important Design Consideration of VHF Television Tuners," RCA Industry Service Lab., Rept. No. LB-1068; April 4, 1957.

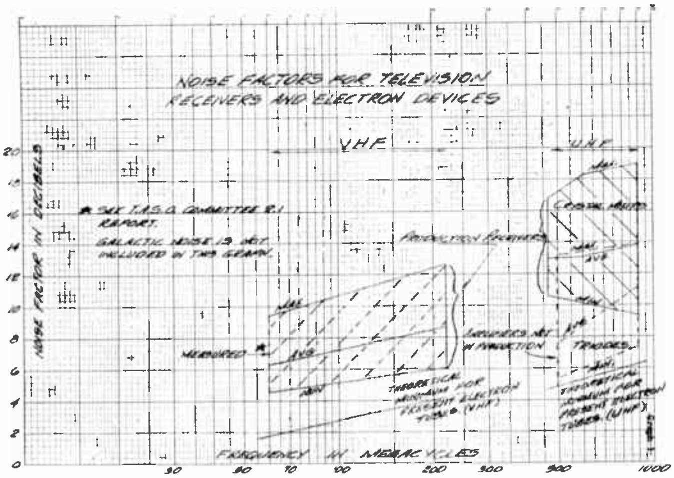

Fig. 3.

It should be recognized that some characteristics of electron devices, combined with circuit elements of the tuners in which they are used, account for important performance attributes of these tuners. In most cases, the data reported in the foregoing tables do not include parameters which are normally associated with circuit design considerations such as capacitance from heater to cathode. As was mentioned earlier in this paper, only those characteristics completely identifiable with the electron device being evaluated are listed, and distinct efforts have been made to prevent these data from reflecting circuit considerations which are outside the control of the tube or diode manufacturer.

In summary, it appears that in the VHF region available vacuum tubes are capable of providing generally adequate tuner performance in at least the first three technical areas listed above. In the UHF region, electron devices are available to perform the functional requirements of tuner operation; however, present practice embodies only the use of vacuum tube oscillators and crystal mixers with performance results as shown in Fig. 3. By employing vacuum tubes designed for UHF applications as RF amplifiers, considerable performance improvement could be realized. However, it should be noted that tubes capable of providing this improved performance are relatively very expensive and for some time have been regarded as lacking economic justification for consumer product applications.

At UHF, oscillator stability has been recognized as one of the major technical problems to be solved. Engineering work has been done on both the tubes and the circuits in which they are used, and improvements have been made by the various manufacturers in both of these areas. Although long-term life test data were not available in sufficient quantity to draw industry-wide conclusions, it was recognized that somewhat higher cathode loading, leading potentially to shorter operating life, is required from UHF oscillator tubes than from VHF oscillator tubes.

Data presented in the tables show that the performance/price ratios for tubes used at VHF are higher than those for tubes designed for UHF applications. Where economic factors must be given consideration, it is reasonable to consider the present status of the performance/price ratios as reflecting the inherently more costly nature of high-performance UHF tubes. It is beyond the scope of this paper to speculate on the changes which might be anticipated in this situation should wider interest develop in UHF applications.

Regarding transistors, there is no commercial use of transistors in TV tuners at VHF or UHF. Laboratory tuners using transistors have been built and tested which would receive VHF signals and convert them to IF for further amplification. No similar work at UHF was discovered. No performance information on VHF applications was available.

Community Antennas and Distribution Systems

Community antenna and distribution systems provide television service to communities spreading across the entire country. These communities range in population from a few hundred to about 50,000.

According to a recent report,[9] there were 610 community antenna systems in operation. Not all operators reported the number of homes they serve, but those giving figures reported a total of 492,345 subscribers, with a potential of 934,864. The number of subscribers per system averages 1056, with a potential average of 2068. One system with 900 subscribers and a potential of 1500 was in operation in Alaska.

Information collected from the field shows that of the 125 community television systems providing information on the number of channels received and the distances to the transmitters, 24 systems reported the reception of UHF signals and seven received some of their signals via microwave relay. Fig. 4 shows the distribution of distances over which the 125 systems receive the signals which they use—VHF, UHF and microwave relay.

Fig. 5 was based on the data on UHF signals reported by the 24 systems and shows the distribution of transmission distances involved. It is hoped that a comparison of these data with data obtained by TASO committees involved in propagation studies might be useful in determining distances over which satisfactory UHF signals might be received for Community Antenna Television (CATV) use. In this connection it should be observed that there are some differences between the forms of the propagation data which would be applicable to the CATV reception problem and to the usual service area or interference area. Such data are often presented in the form using the statistical parameters $A(B, C)$ where A is a field strength, quite low in interference areas and moderate to high in service areas; B represents a percentage of locations at which this field strength is exceeded C per cent of the time. Both B and C are relatively high in service areas (50 per cent and

[9] *Television Digest*, vol. 14, p. 2; September 20, 1958.

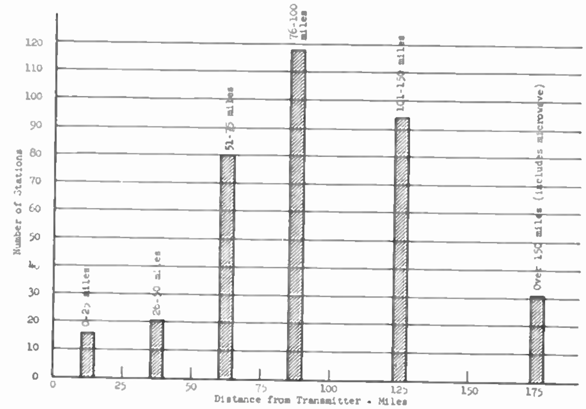

Fig. 4—Total number of stations (VHF, UHF and microwave relay) used by 125 community antenna television systems vs distance.

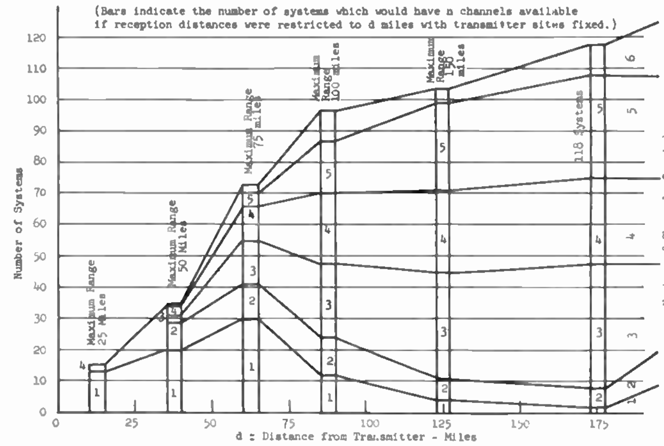

Fig. 6—Chart indicating effect on 125 community antenna television systems if reception distance were restricted.

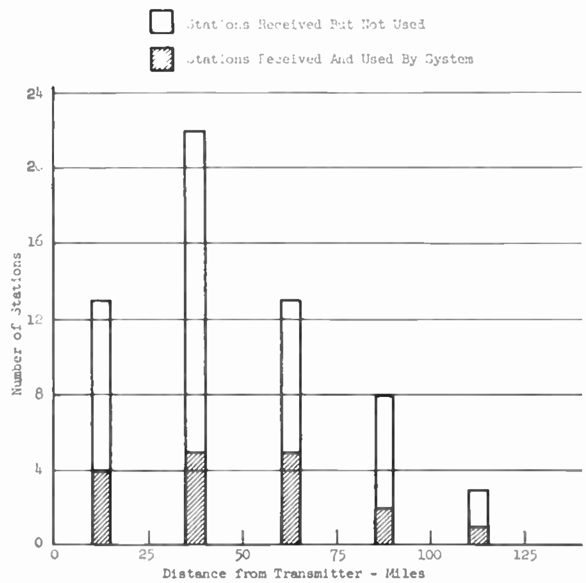

Fig. 5—Number of UHF stations reported received by 24 community antenna television systems vs distance.

higher for *B* and 90 per cent for *C*) and low in interference areas.

In the locations where CATV systems are likely to fill a need, the values of these parameters are somewhat different. For example, *A* needs to be moderate, *B* is likely to be quite low, and *C* should be high.

The data presented in Figs. 4 and 5 indicate that reception distances for this type of signal area for UHF are likely to be considerably less than for VHF operations, although exact numerical data might be difficult to obtain. To some degree, the difference in reception distances may be due to the fact that most community TV systems have relied largely on VHF signals up to now.

In order to determine the possible impact of a restriction in reception range, the data provided in the questionnaire were assembled as shown in Fig. 6. In this figure, the original data were arranged to show what would happen to the 118 systems using off-air reception entirely if the usable range of the stations which are presently used were dropped to specific distances of 25, 50, 75, 100 and 150 miles. It will be noted that there would be a continuous decrease in the number of systems which could receive any signals at all, as well as an increase in the number which would be restricted to carrying only one or two channels. Since the economics of system operation depends in some cases on the number of channels available for distribution, this could represent a more rapid decrease in the number of systems which it might be feasible to operate. The most rapid decrease occurs in the region of a 75-mile maximum range which coincides very closely with the most rapid decrease in UHF reception reported.

The data appear to indicate that a shift in frequency of the transmitters involved would have a considerable impact on the operation of community antenna systems. A large number of communities would lose service entirely and the operations of another large group would be severely restricted. This impact could probably be reduced somewhat by recourse to microwave relay or similar service to obtain signals. However, economic factors here are fairly complicated. It appears likely that a large number of the systems first affected by a reduction of transmission range would be the smaller systems serving communities of a few hundred. The cost of relay service would be out of the question for many of these unless a service, common carrier or private, using less expensive installations were made available.

Effects of Transmitter Sound Power Reduction on Receiver Performance

Tests were made on representative television receivers to determine the effects of a reduction in sound power on the performance of television receivers. The receivers used in these tests included the various types of sound detector circuits currently in use; the results obtained are therefore felt to be representative of those which can be expected in the field using new, aligned receivers of modern design, properly installed.

The following types of tests were made in order to determine the extent to which receiver performance was affected or modified by a reduction in transmitter sound power below the value currently standardized, *i.e.*, between 50 and 70 per cent of the peak visual power:

Thermal noise (signal-to-noise ratio)
Impulse noise rejection.

Additionally, consideration was given to the problem with respect to:

Loss of service area
Adjacent-channel interference
Fine-tuning characteristics
Fading
Co-channel interference
Sound vs picture performance.

It has been the experience of receiver manufacturers since receivers were first put on the market that there has been an ever-present demand for greater sensitivity. Users in fringe areas are, in many cases, willing to install receivers at considerable expense provided a good, reliable sound signal can be obtained even though the picture performance may be subject to fading, interference, impulse or thermal noise of a magnitude such as to cause serious picture degradation, or even a loss of picture from time to time. In such areas a reduction in sound power would result in serious impairment of service and in many cases a complete loss of service.

Thermal Noise Performance

A reduction in transmitted aural power will result in poorer receiver signal-to-thermal-noise ratio which will, by reduction of receiver fringe area sound performance, reduce the sound coverage of any given transmitter. To obtain experimental verification of the reduction of sound channel thermal noise performance, measurements were made on nine different receivers. Four different types of FM detector systems are represented in these receivers covering every type in use today. In all cases, measurements are for one of the lower VHF channels. Fig. 7 presents the data of one of these receivers which is typical of the group. Sound channel signal-to-noise ratio is plotted as a function of picture-to-sound ratio for a number of picture carrier signal levels. It can be seen that for each signal level there is a threshold value of picture-to-sound ratio below which the signal-to-noise ratio degrades rapidly. Fig. 8 presents a summary of these data for all the measured receivers. The loss of sound channel signal-to-noise ratio per unit reduction in sound carrier is plotted as a function of

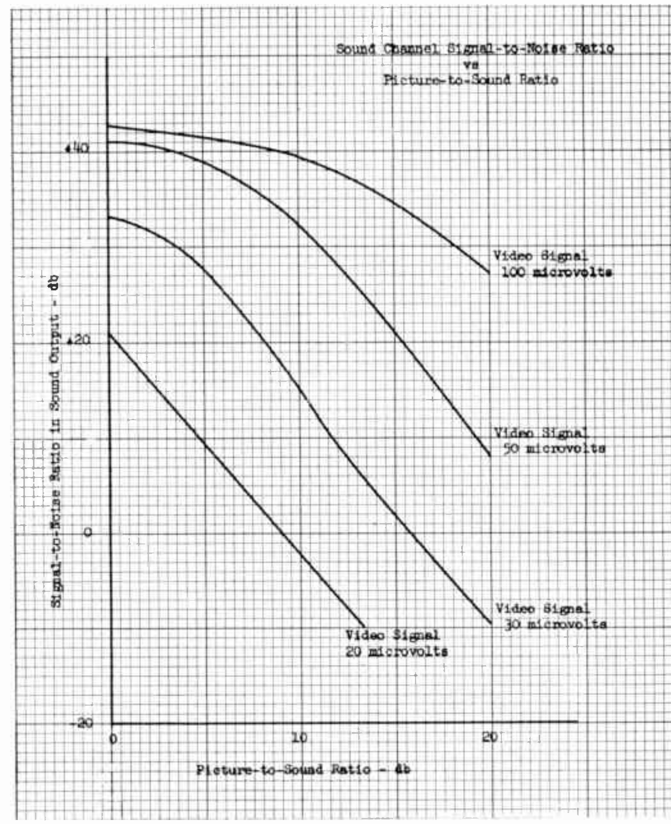

Fig. 7.

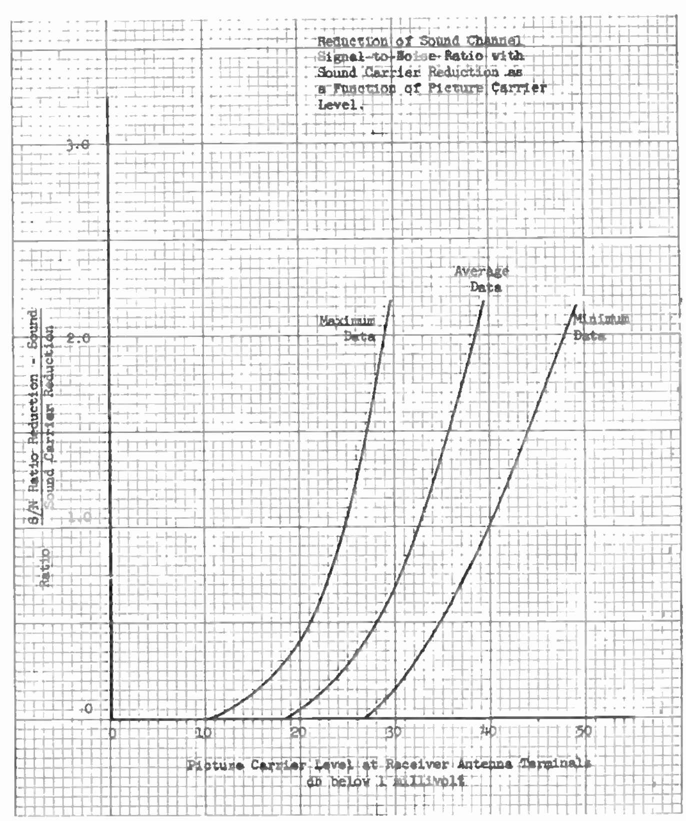

Fig. 8.

picture carrier level. In these data the average of all the receivers is presented and the data for the measured extremes are also plotted. As an example, from this curve it can be seen that with 20 microvolts (−34 db) of picture signal (open-circuit antenna voltage delivered through a 300-ohm dummy antenna to the receiver), an average loss of about 1.5 db in signal-to-noise ratio will occur for each db of aural carrier power reduction. These data are for new, aligned receivers of modern design. If we add the losses expected due to misalignment, tube aging and antenna orientation and mismatch, as well as transmission line losses, it is reasonable to expect that this type of signal-to-noise ratio loss would occur in the 100 to 200 microvolts-per-meter range of signal strength in a substantial number of receivers currently in the hands of the public.

Sound quieting sensitivity, which takes into account only thermal noise considerations, is 30 microvolts for the typical receiver in the group used to obtain these data. As can be seen from Table III, the picture sensitivity for 78 receivers reported varied from four to 150 microvolts. The distribution of sensitivity shows:

12.8 per cent—less than 10 microvolts
34.6 per cent—between 10 and 20 microvolts
19.2 per cent—between 20 and 30 microvolts
11.5 per cent—between 30 and 50 microvolts
9.1 per cent—between 50 and 100 microvolts
12.8 per cent—greater than 100 microvolts.

The importance of fringe area performance may be judged by the fact that more than 66 per cent of the receivers reported picture sensitivities better than 30 microvolts.

Impulse Noise Rejection Performance

A common form of noise interference in the sound channel is that caused by automotive ignition noise, electric motor commutator noise (shavers, mixers, vacuum cleaners, etc.), arcing switches, and lightning. This form of noise is usually lumped under the general heading of impulse noise. In order to measure the effect of aural carrier power reduction on receiver performance in the presence of this form of noise, an interference source, such as a nonsynchronous 60-cps rotating arc device, was coupled through a variable attenuator into the antenna circuit of the test receiver in parallel with the desired standard visual and aural television signal. The interference noise signal input to the receiver was increased until its presence was noted in the sound output of the receiver either by aural or measured output detection. The aural signal was then reduced in steps and at each step the change in noise interference required to restore the original condition was recorded. Data were obtained on seven different commercial receivers. Data for a typical receiver are plotted in Fig. 9 for visual signal input levels ranging from 50 to 10,000 microvolts. Fig. 10 presents a plot of data for the relative impulse noise level for constant audible interference as a function of sound-picture ratio. This is the average of all data for all seven receivers measured. A loss of tolerance

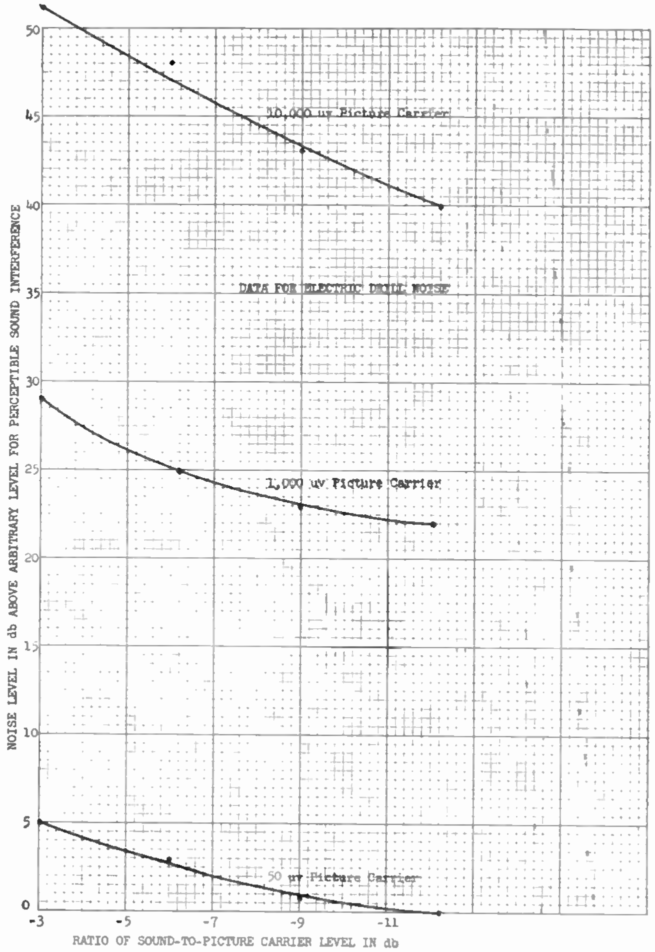

Fig. 9.

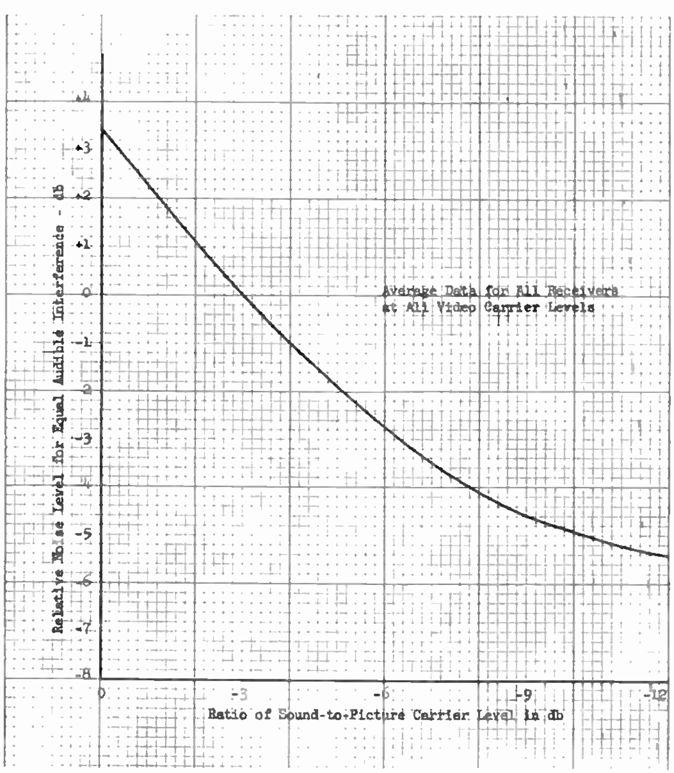

Fig. 10.

to impulse noise of about 1 db for every db of reduction in aural power is noted. This performance loss occurs at strong signals as well as weak; the performance loss with reduction of aural power is as great at 10,000 microvolts as it is at 50 microvolts. As in the previous case for thermal noise, these data are for new, aligned receivers of modern design.

Loss of Service Area

In order to show the loss of service area resulting from a reduction of sound power, the required field strength in db above 1 μv/meter to produce 30 db quieting was determined by measurement of the quieting sensitivity for representative TV receivers under existing transmission standards and calculation of the equivalent field strength. The average figures for antenna gain and transmission line losses were used for channels 4 and 10, which are about in the middle of the two frequency ranges. The required increase in video and sound signal levels to compensate for a reduction in sound power with respect to video power was determined to be 0.57 db for each db drop in sound power. This was obtained from the average degradation in signal-to-noise ratio at the 30-db level in data furnished by the members of this Committee.

Finally, the reception range and loss of service area was determined from the FCC curves of expected field strength, assuming maximum authorized power in the TV transmitter, and representative antenna heights.

Figs. 11 and 12 show the loss of service area for VHF channels 2–6 and 7–13 resulting from a reduction of sound power below the present minimum of 3 db below the peak video power. The service area is reduced about 20 per cent on the low VHF channels and about 10 per cent on the high VHF channels if a 7-db reduction in sound power is made.

Adjacent Channel Interference

A reduction in transmitted aural power would reduce the lower adjacent channel sound interference in those areas where it now exists by an amount equal to the sound power reduction. Examination of the data in Table III shows that receiver attenuations for the lower adjacent channel sound signal vary widely, ranging from 14 db to 60 db. The attenuations are distributed as follows:

11.8 per cent—less than 30 db
42.1 per cent—between 30 and 40 db
13.2 per cent—between 40 and 50 db
32.9 per cent—greater than 50 db.

This wide variation is reflection of the fact that this performance characteristic is determined by competitive pressure in particular areas rather than by a universal requirement.

The fact that competitive pressure determines receiver adjacent channel rejection capabilities in most cases means that for any small variation in adjacent channel interference, such as would be accomplished by a 7-db reduction in sound power, the net improvement

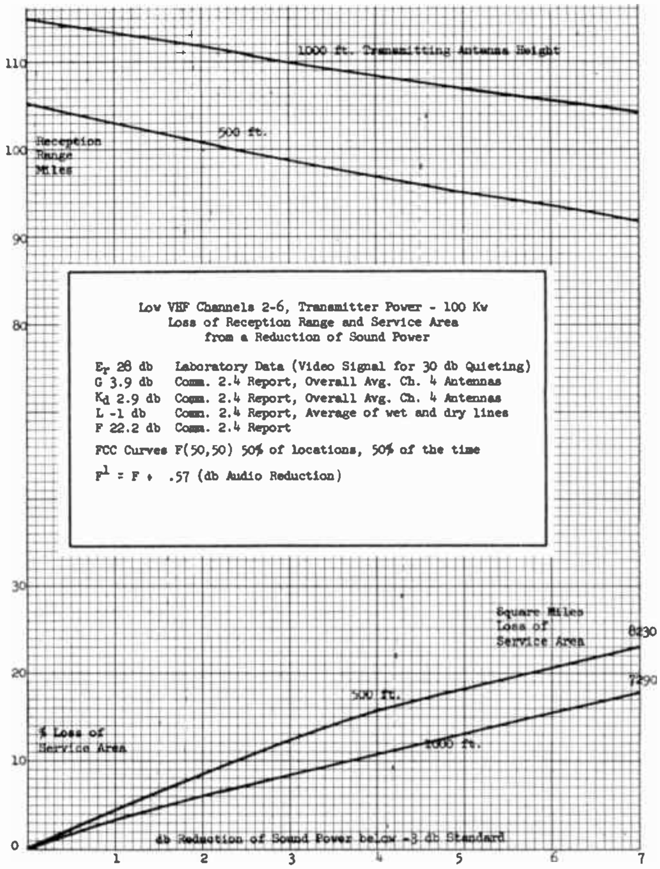

Fig. 11.

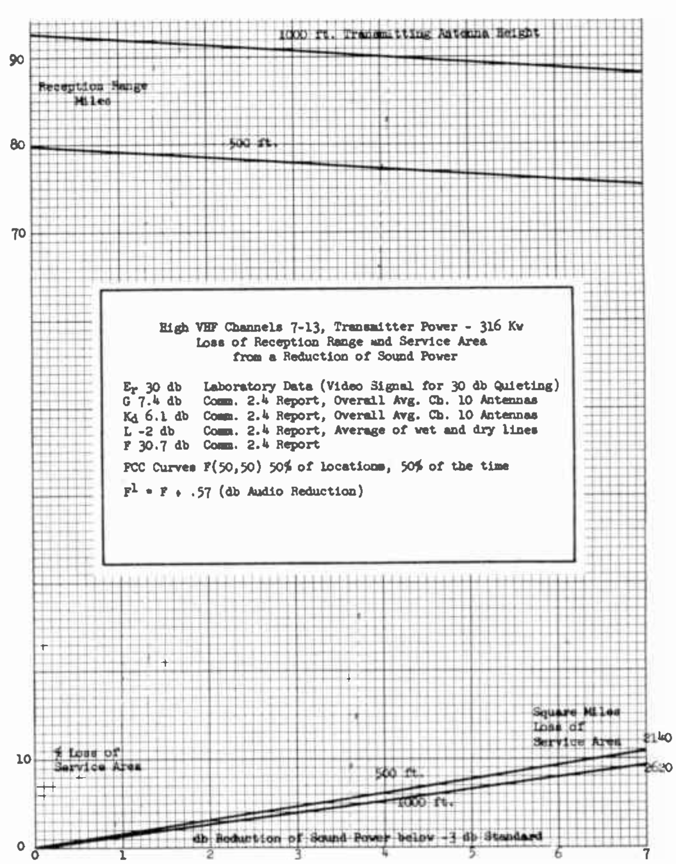

Fig. 12.

would be relatively short-lived, as new designs under economic pressure would tend to seek the same competitive level as is now considered satisfactory. Conversely, any increase in adjacent channel interference, such as might result from a permitted increase in both picture and sound power, might result in no long-term degradation in adjacent channel performance, as competitive pressure would force receiver manufacturers to build more adjacent channel rejection in receivers.

Other factors which are of importance but less susceptible to a quantitative analysis include the following.

Fine Tuning

A reduction in transmitted sound power will result in a more critical requirement for fine tuning in weak signal areas, thus increasing the need for skill and judgment in adjusting the fine tuning control, a function in which most consumers are presently inept.

Fading

A reduction in transmitted sound power will aggravate the effects of fading, either natural or man-made, such as airplane flutter, on the sound performance of the TV receiver.

Co-Channel Interference

In some locations at present both picture and sound reception is limited by co-channel interference. Co-channel picture interference can be considerably improved by operation of all transmitters on the proposed super-accurate offset. In the event of improved picture channel performance by the use of these techniques, reduction of sound channel coverage might nullify the improved picture coverage.

Sound vs Picture Performance

It is the emphatic experience of all television receiver manufacturers that the public will tolerate and be entertained by extremely marginal picture signals provided satisfactory sound signals are available. In the report of the first NTSC in 1941, it is stated, "... a given amount of interference is more disturbing in the sound than in the picture. The service area of the television system will be determined by the acceptability of the service with respect to the noise interference."

Future System Development

Technological advances and improvements could conceivably make use of the sound channel to transmit additional information. A reduction of aural power could obstruct such possible future benefits.

It is considered beyond the proper scope of this paper to hypothesize what design changes might be made by commercial television receiver manufacturers in the future in the event of any change in transmission standards; however, it can be stated that the factors cited with regard to thermal and impulse noise considerations are fundamental to all receiver designs.

In summary, any proposals for sound power reduction should weigh what appears to be a minor and probably short-lived advantage of adjacent channel sound interference reduction against the disadvantage of the fundamental reduction of system capability and coverage.

Acknowledgment

The data and other pertinent information presented in this paper were collected by the members of TASO Panel 2 and its several committees, comprising a total membership of 75 industry engineers. A debt of gratitude is owed to these men.

In particular, appreciation is expressed to the following Panel 2 officers and Committee Chairmen:

G. W. Fyler, Zenith Radio Corporation
K. A. Chittick, Radio Corporation of America
S. P. Ronzheimer, Hazeltine Research, Inc.
D. W. Pugsley, General Electric Company (now with Ramo-Wooldridge Corporation)
R. S. Yoder, Motorola, Inc.
A. W. Bridgett, Spencer Kennedy Laboratories
G. G. Edlen, Entron, Inc.
D. Sillman, Westinghouse Electric Corporation
A. P. Haase, General Electric Company
J. F. McAllister, Jr., General Electric Company
W. P. Boothroyd, Philco Corporation
S. Napolin, Granco Products, Inc.

Findings of TASO Panel I on Television Transmitting Equipment*

H. G. TOWLSON†, SENIOR MEMBER, IRE, AND J. E. YOUNG‡, SENIOR MEMBER, IRE

Summary—**TASO made a thorough study of the characteristics, performance and cost of television transmitters, antennas and transmission lines, and translators. The results of these studies gives a clear picture of the technical and economic factors involved in operating television transmitters in the VHF and UHF bands. This paper summarizes some of these studies which are reported in detail in the TASO Report, "Engineering Aspects of Television Allocations."[1]**

Introduction

Any study of the frequency allocation of television broadcasting involves many parameters. It was the purpose of TASO Panel I to study those having to do with transmitting equipment—to accumulate information for the purpose of appraising both present and potential performance of television transmitters, antennas and transmission lines, translators and other transmitting equipment for both VHF and UHF broadcasting.

At the date of the Panel 1 report there were 448 VHF and 93 UHF broadcast stations in operation, and the cost data developed and presented by Panel 1 show that each of these 541 stations has a considerable capital investment in its plant. Since each plant, if it is to continue operating, must be either immediately or potentially profitable, any study of allocations must include economic as well as technical factors. The first portions of this paper will deal mostly with the cost factors and the latter portions with the technical performance characteristics.

Organization of Panel 1

Representation on the Panel was secured by invitation to known manufacturers of transmitting equipment and to networks and broadcasting stations, as well as by press releases from TASO headquarters announcing the formation of the panels and inviting participation by interested persons. The committee organization of Panel 1 was set up as follows:

1.1 Committee on Standard Transmitters—charged with studying the characteristics (cost, performance, reliability) of standard TV transmitters, both VHF and UHF.

1.2 Committee on Repeater Transmitters—charged with the investigation of the performance of repeater transmitters.

1.3 Committee on Antennas—charged with the study of the characteristics of antennas, towers and transmission lines.

1.4 Committee on Systems—charged with the study of the applicability of new techniques in transmitter operation.

Attention is called to the term "repeater" transmitters in the title of Committee 1.2. "Repeater" is used to include satellites, translators and boosters. The regular Television Broadcasting Station was classed as a "standard" transmitter under Committee 1.1.

Methods of Obtaining Cost Information

To obtain reliable first hand information considerable use was made of questionnaires. Committee 1.1 sent questionnaires to 490 operating stations to obtain transmitting plant information on their initial and operating costs as well as information on technical performance, outages, etc. Committee 1.3 sent questionnaires to 475 stations to obtain antenna plant information, and the response to these questionnaires was about 55 per cent. Committee 1.2 obtained information on facilities and operating data for translators by means of a questionnaire sent to all translators and to all translated television stations.

Prices on current TV equipment, tube costs, operating powers, etc. were obtained directly from the catalogues of the manufacturers of transmitting equipment. At first, Panel 1 proposed to report on potential power outputs and costs. As such information had to come from the manufacturers themselves, to avoid any possibility of antitrust action, all requests for information were channeled through the Federal Communications Commission. The manufacturer supplied the information to the FCC where it was digested. The composite data was then forwarded to TASO with all identification of the manufacturers removed. However, the data had such wide cost variations that it was considered inconclusive and was deleted from the Panel Report.

Considerable technical information was made available to Panel 1 through the fine cooperation of the FCC. This included information from its Mobile Monitoring Service on frequency stability, maintenance of power output, modulation characteristics, compliance with FCC rules and required maintenance time.

Initial Costs—Transmitter Selling Prices

Fig. 1 is a plot showing the average selling prices of VHF and UHF transmitters as obtained from the manu-

* Original manuscript received by the IRE, February 24, 1960.
† General Electric Co., Syracuse, N. Y.
‡ Radio Corp. of America, Camden, N. J.
[1] "Engineering Aspects of Television Allocations," TASO Rept.; March 16, 1959.

facturers. The connecting lines have been drawn between the values merely to better indicate the trend between VHF and UHF. However, it should be noted that transmitters are usually available for only the rated powers as indicated by the points themselves, and the intermediate powers would not necessarily be available at the prices indicated by the graph. It would normally be necessary, if an intermediate power is required, to employ a transmitter of the next higher standard rating. The VHF selling price averages include both low channel and high channel facilities inasmuch as their differences were not great. The VHF prices all include one set of operating tubes. However, the UHF prices, except for powers of 1 kw and lower, do not include tubes so the UHF curve would actually be somewhat higher than indicated. The VHF prices for 20-kw and 35-kw ratings were reported together so this average was plotted at the intermediate $27\frac{1}{2}$-kw rating. The UHF 20-kw and 25-kw prices were likewise averaged together at the $22\frac{1}{2}$-kw rating.

Fig. 1 indicates that for a given transmitter peak power output, the UHF transmitter price is considerably greater than for VHF. However, it must be borne in mind that the higher effective radiated powers (ERP) at UHF are obtained largely through use of the higher gain antennas which are quite feasible at the higher frequencies. The result is that lower power transmitters are usually used at UHF than at VHF so the actual initial transmitter costs, at typical installations, are probably not greatly different.

The selling prices given in Fig. 1 were for transmitters designed for the normal 2/1 ratio of visual power/aural power. For use in discussions regarding possible higher ratios, it was estimated that if a VHF transmitter were specifically designed for a 4/1 ratio it would have a price about 15 per cent lower, and one designed for 10/1 ratio about 25 per cent lower, than the values of Fig. 1. The corresponding reductions for UHF were estimated at about 10 per cent and 20 per cent.

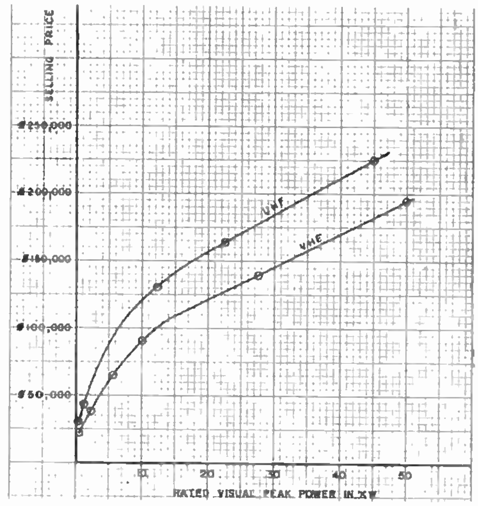

Fig. 1—Comparison of selling prices of VHF and UHF TV transmitters (January, 1958).

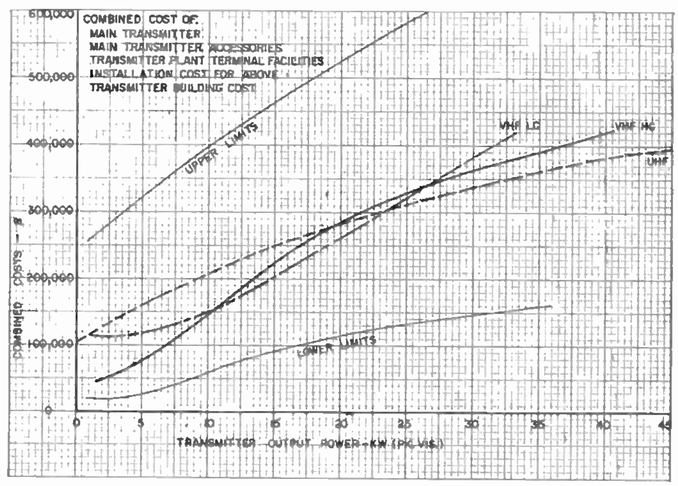

Fig. 2—TV transmitting plant costs.

Transmitting Plant Costs

The "transmitting plant costs" were obtained from the questionnaires to the broadcasters. It should be noted that the term "transmitting plant" as used above includes the main transmitter, the main transmitter accessories, and the transmitter plant terminal facilities, plus installation and transmitter building costs.

The data which came back had tremendous spreads in their values. Some installations must have been very plush indeed, and others equally austere! A method of presentation was arrived at, however, which produced a meaningful display. The data were grouped, for each band, into five groups of visual transmitter peak powers. For the VHF low channels the groupings were from 0 to 2 kw inclusive, 2 to 6 kw, 6 to 12 kw, 12 to 25 kw, and over 25 kw to 35 kw inclusive. For the VHF high channels the groupings were from 0 to 2 kw inclusive, 2 to 6 kw, 6 to 12 kw, 12 to 20 kw, and over 20 kw to 50 kw inclusive. For UHF the groupings were 1 kw, 5 kw, 12.5 kw, 25 kw, 45 kw. In the TASO Report complete charts are included for each band showing the maximum, minimum, and the average costs reported for each grouping, and the numbers of stations whose data were included.

Fig. 2 shows the curves obtained by joining, for each band, the average cost points of each grouping to show the comparison between VHF and UHF. The upper and lower limits are shown to indicate the magnitude of spread of the original data. From Fig. 2 it is seen that, comparing the average costs of low channel VHF and high channel VHF, no significant difference was found for transmitter power outputs of 7.5 kw and higher. The average cost of a high power UHF transmitting plant (say 25 kw and above) was found to be a little less than that of the average VHF plant. At lower powers, however, the UHF plant averaged substantially higher in cost than VHF plants.

Considering the spread of the initial data itself, we can see that the differences in transmitting plant costs between the three bands are not great.

Antenna Plant Costs

Information on the selling prices of antennas for the various power ratings and gains was obtained from three manufacturers. Antennas were listed only for the standard power gains (1, 2, 3, 4, 5, 6, 8, 10 etc.); however, the values were connected together as a curve to highlight the relations between VHF and UHF prices. A fairly linear relation was noted between selling price and power gain as indicated in Fig. 3. These graphs show the average selling prices (but for standard ratings only) for low channel VHF, for high channel VHF, and for UHF. For a given gain, the VHF high channel antennas are less costly than are the VHF low channel units, and for UHF antennas are much less costly than for VHF. However, again, it should be pointed out that higher gain antennas are normally used at UHF than at VHF, and for VHF high channel than for VHF low channel, so the typical antennas that might be used would probably not differ greatly in price.

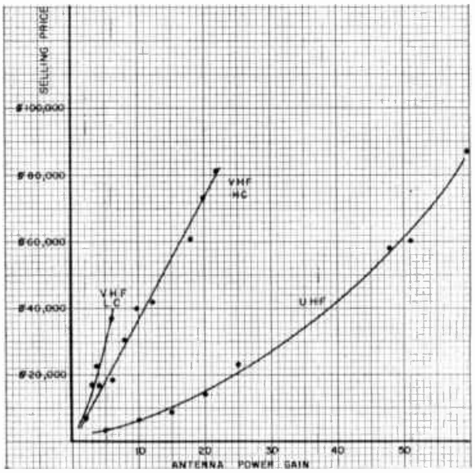

Fig. 3—Average selling prices of TV transmitting antennas (January, 1958).

Comparison of Antenna Plant Costs

A more meaningful comparison is the one of typical antenna plant costs which includes not only the cost of the antenna but also the costs of the diplexer, transmission line, tower and erection. These data were obtained from the questionnaires to the stations.

The data had very great spreads of costs as reference to the complete TASO report will show. After some experimentation in plotting the information it was found that, due to the predominant effect of the tower height, costs vs tower height produced a meaningful display. To avoid confusion the VHF low channel information was limited to stations operating at 100-kw ERP, and VHF high channel to stations operating at 316 kw. Due to the smaller number of returns, all UHF data was included.

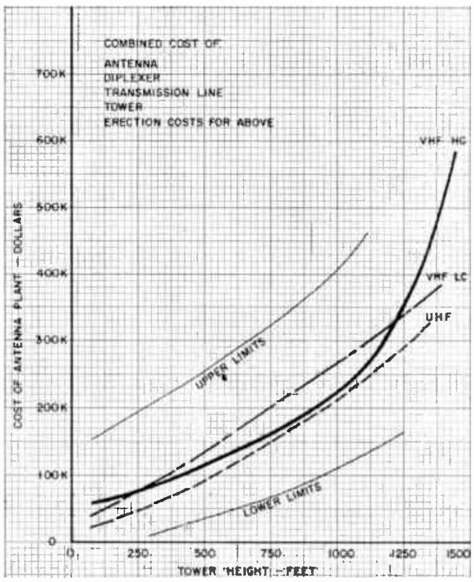

Fig. 4—Average antenna plant costs.

Fig. 4 shows average curves only taken from the TASO report. To indicate the spread of the original data, approximate lower and upper limits are indicated. It is seen that the average curves are fairly linear—at least out to about 1000-foot tower height. The differences of antenna plant costs for the three bands are not great—although the UHF antenna costs tend to average somewhat less than those for VHF.

Total Cost of Transmitting Plant

The total cost of a transmitting plant includes the costs of the transmitting plant and the antenna plant. Because of the various manners in which transmitter, accessories, antennas, transmission lines, towers, etc. are combined in different stations, it was not felt correct to merely add the data of Fig. 2 (as obtained by one committee) to the data of Fig. 4 (as obtained by another committee). Rather, the information on the total cost of the transmitting plant was solicited directly from the stations.

Again, the spread of received data was very great and again the predominant effect of the tower height was evident. In Fig. 5 the averages of the TASO Report data are plotted to show the trends between the three bands. On the average, maximum power VHF high channel stations seem to cost about 25 per cent more than maximum power low channel VHF stations. UHF stations operating at powers up through 300-kw ERP seem to cost about 10 per cent less than the VHF low channel stations. Little information was obtained regarding 500- and 1000-kw ERP UHF stations, but it appeared that their costs were comparable to those of maximum power VHF low channel stations.

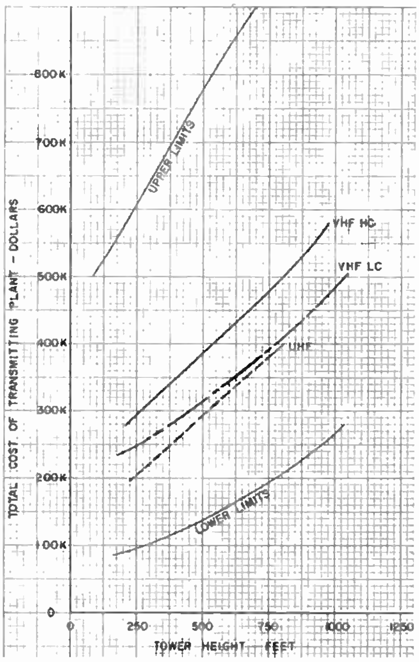

Fig. 5—Average total cost of transmitting plant.

Monthly Operating Costs

Values of the power input figures and estimated operating tube costs per hour were received from the transmitter manufacturers, and these are included in the full TASO report. They indicate that a UHF transmitter consumes more primary power, for a given peak power output, than does a VHF transmitter, and for a given peak power output the tube cost per hour is greater for UHF. Some savings in both areas would result from a higher ratio of visual/aural power.

For more meaningful information on the monthly operating costs, the data received back from the broadcasters was analyzed, and this is summarized in Fig. 6. These monthly operating costs include only primary power costs, tube costs, and maintenance parts. All figures were normalized to a common base of 455 hours per month of operation.

The data were assembled, for each band, into groups by visual transmitter peak powers. For VHF low channels the groupings were from 0 to 2 kw inclusive, 2 to 6 kw, 6 to 12 kw, 12 to 25 kw, and over 25 to 35 kw inclusive. For VHF high channels the groupings were 0 to 2 kw inclusive, 2 to 6 kw, 6 to 12 kw, 12 to 20 kw, and over 20 to 50 kw inclusive. For UHF, the groupings were 1 kw, 12.5 kw, 25 kw, 45 kw. In the TASO Report complete charts are included for each band showing maximum, minimum and average operating costs as reported for each grouping, as well as the number of stations for which data is included.

Fig. 6 shows the curves produced by joining, for each band, the average operating costs points of each grouping to indicate the trend between VHF and UHF. The upper and lower limits indicate the amount of spread in the original data. These curves show that, for a given

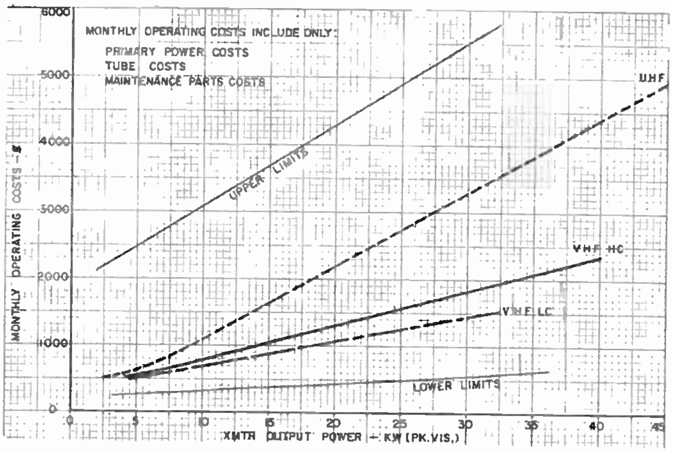

Fig. 6—Monthly operating costs.

power output, the average operating costs for high channel VHF stations average about 15 per cent higher than those of low channel VHF stations. For UHF stations the operating costs varied from about 20 per cent higher than for low channel VHF stations for the lowest powers to 100 per cent higher for transmitter power outputs above 15 kw.

However, if we consider that lower power transmitters are more often used at UHF than at VHF (because of the use of the higher gain antennas) it is probable that the differences in operating costs at typical installations are not very great.

Reliability

For information on characteristics of television broadcast stations which, taken together, measure reliability, the committee turned to the files of the FCC. The characteristics deemed important, and the variation between VHF and UHF follow:

1) Frequency stability—Reports of off-frequency operation, both of the visual transmitter and the intercarrier difference between visual and sound, occurred in more than half the UHF stations sampled, while the number of high VHF and low VHF channel stations off frequency was less than twenty per cent and ten per cent, respectively, of those sampled. This variation results at least partly from the greater use of outside frequency measuring services by the VHF stations—in over 90 per cent of the stations sampled compared to 51.2 per cent of the UHF stations. There appeared to be a general lack of frequency measuring service available to UHF stations due to the shorter transmission range of UHF stations and the lack of UHF measuring equipment.
2) Modulation characteristics—The VHF visual transmitters were generally better than UHF units, particularly with respect to linearity. This is believed to be at least partly due to a tendency to continue to operate tubes to the point of degradation of output at UHF to minimize operating cost.

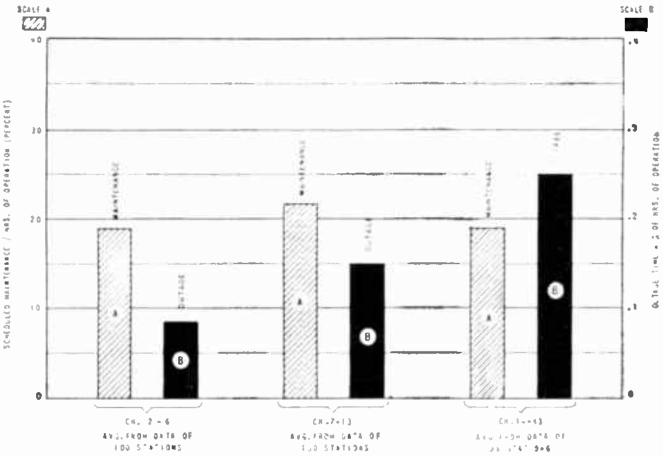

Fig. 7—Comparison of transmitter maintenance and outage time.

3) Maintenance and outage time—Fig. 7 compares low VHF, high VHF and UHF stations. Outage time, although relatively low for all three groups of stations, is clearly greatest for the UHF group despite comparable maintenance effort.
4) Tube life—Tube life at UHF was found to be generally shorter than VHF. This was reflected in the higher operating cost per hour on UHF.
5) Avenues of needed improvement—There are two general areas where the committee found improvement needed under present FCC standards. The first, improvement in tube life, was mainly a problem at UHF. The second, improved frequency stability and measurement, was needed to a degree in all three bands, most at UHF, least in the low VHF band. Table I shows the visual carrier frequency stability required. The first column shows the present FCC standard; the second, that needed if precise frequency control is to be used to reduce co-channel interference; and the third, the still greater stability needed for very precise frequency control to achieve maximum reduction of co-channel interference.

Table II shows the possible accuracy of frequency monitoring by several different methods.

It will be noted that WWV transmissions may be used to check the frequency of low VHF stations operating under the precise standards. For very precise frequency stability at low and high band VHF, and precise stability at UHF the atomic resonance standard is adequate. Even this is hardly sufficient to achieve the needed stability for very precise operation at UHF. Fortunately, the large number of channels available in the UHF band makes the need for very precise stability unlikely.

In addition to the more complicated monitoring means required for improvement in frequency stability, the frequency control used to drive the transmitter must also be improved if the need for continual checking against the standard is to be avoided.

TABLE I

Required Visual Carrier Frequency Stability[2]

	FCC	Precise	Very Precise
Low VHF	±1000 cycles	5 parts in 10^8	1 part in 10^8
High VHF	±1000 cycles	2 parts in 10^8	4 parts in 10^9
UHF	±1000 cycles	5 parts in 10^9	1 part in 10^9

TABLE II

Means of Frequency Measurement

Present TV frequency monitors ±500 cycles[3]	(±5 parts in 10^7)
Monitoring by use of WWV transmissions	5 parts in 10^8
Monitoring by use of VLF transmissions (not presently available)	2 parts in 10^9
Monitoring by use of atomic resonance standard	1 part in 10^9

Antennas

In addition to the cost studies discussed earlier in this paper, the Committee on Television Antennas gathered information on transmission lines and towers. Its chairman also chaired the Task Group on Directional Antenna Tests. Out of the work of this group grew the directional antenna tests reported in another paper. A summary of information obtained on transmission lines and towers follows:

Transmission Lines

To develop cost data on the transmission lines used at UHF and VHF, the committee laid out typical 1000-foot runs of co-axial transmission lines, and waveguides including elbows, gas barriers, etc. This information is summarized in Fig. 8.

Towers

The effect of height of the supporting tower on cost was developed from cost data solicited from a number of manufacturers. The relation between cost and height is shown in Fig. 9. Insufficient data were received for tower heights between 1250 and 1600 feet, but they have been included in the dashed portion of the curve. A medium-sized antenna was assumed in these calculations. The effect of size of the antenna on the cost of a 1000-foot, 50 pound per square inch tower is shown in Fig. 10, and the effect of variation in design wind pressure is shown in Fig. 11.

Of these parameters, only the antenna size affects the relative cost of UHF and VHF installations. Because of the higher effective radiated power required at UHF an antenna having a higher wind load is required. The increase is modest however, amounting to an average of perhaps 15 per cent.

[2] *Ibid.*, see Sect. 24.4.3.

[3] Includes check against a standard frequency or measuring service at intervals varying from a few months at low VHF to a few weeks at UHF.

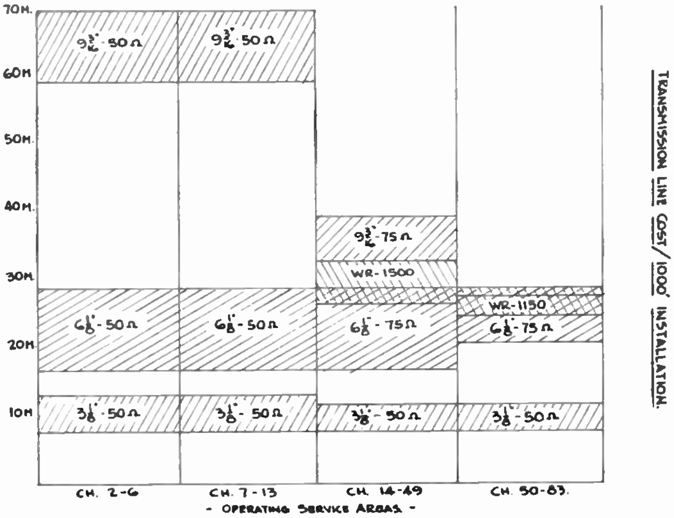

Fig. 8—Equipment cost information.

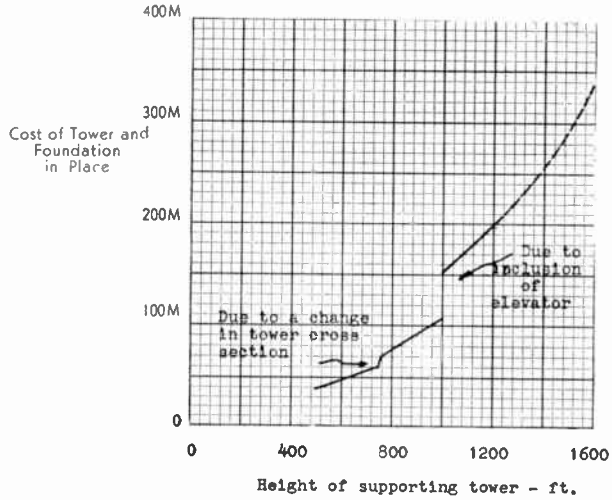

Specification: EIA Standard TR-116
Wind Pressure: 40 lbs/sq. ft. for under 1000 ft.
50 lbs/sq. ft. for over 1000 ft.
Antenna: Med. size (100 sq. ft. project area at 50 ft.)
Transmission line: 12 in. total width
Elevator: In towers over 1000 ft.
All towers guyed.
Cost does not include antenna or transmission line.

Fig. 9—Cost of tower vs height.

Data on permissible deflection of antennas under the action of wind were solicited from several manufacturers. A tabulation of these angles for wind pressure of 10 pounds per square foot, for various types of antennas, is included in the committee report. These data may be summarized here by stating that a well designed guyed tower should have a maximum deflection of 0.17 degrees at a wind pressure of 10 pounds per square foot at the base of the antenna.

Repeater Transmitters

The committee found need for definitions of the several terms used to define satellites, translators and boosters. Table III (opposite) was, therefore, prepared.

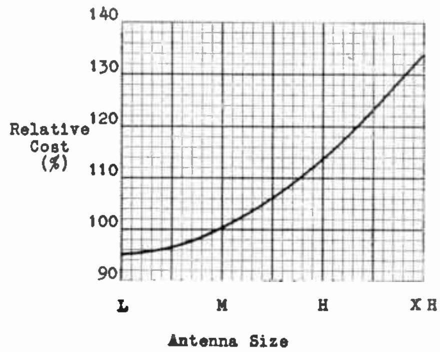

L—4-bay superturnstile Ch. 4–6
6-bay superturnstile Ch. 7–13
2-bay slotted ring
M—6-bay superturnstile Ch. 2–6
12-bay superturnstile Ch. 7–13
3–5-bay slotted ring
3-bay helical high band
H—12-bay superturnstile Ch. 4–6
high gain UHF—slotted cylinder, helical, high gain
XH—12-bay superturnstile Ch. 2–3
Tower—1000 ft. high, 50 lbs/sq. ft. design

Fig. 10—Relative cost of tower vs antenna size.

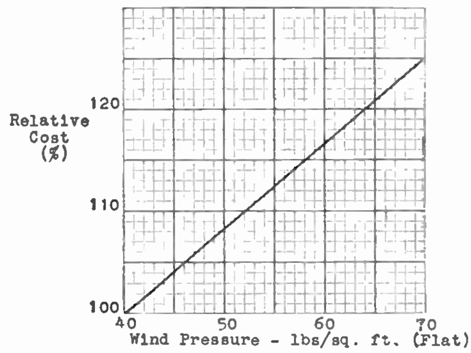

Specification

Tower: 1000 feet high
No elevator
Transmission Line 12 in. total width per ft. of height
Antenna: Medium size (100 sq. ft. project area at 50 feet)

Fig. 11—Relative cost of tower vs wind pressure.

The generic term "repeater" was selected as being applicable to all three classes of nonoriginating stations.

General Repeater Performance

The committee, in its report, found that generally satisfactory reception of television translators had been reported. In fact, it was noted that they were operating with aural power levels at least 6 db below the peak visual power, and that a number of translators were known to be operating with aural power 10 db below the standard ratio. In view of this history the committee recommended that the ratio of visual to aural power be changed from the present standard of 2:1 to 4:1.

UHF Booster Tests

A series of measurements and observations were outlined by the committee for the UHF booster already in operation at Waterbury, Conn. Much of this work

TABLE III

DESCRIPTION OF VARIOUS TYPES OF TELEVISION BROADCAST STATIONS

	Standard	Satellite	Translator	Booster
1. Presently provided for in rules	x	x	x	(a) (b)
2. Limited by rules to UHF broadcast channel only			x	(a)
3. UHF and VHF channels	x	x	(b)	(b)
4. Cannot originate programs			x	x
5. Does not ordinarily originate programs		x		
6. Can originate programs	x	x		
7. Must repeat program on same channel				x
8. Must repeat program on another channel			x	
9. Programmed only by off-air pickup			x	x
10. Programmed by line relay or off-air pickup	x	x		
11. Maintains standard mileage separations	x	x	x_1	
12. Licensed on non-interference basis			x(a)	(a) (b)
13. Maximum power limited by technical factors				x
14. Maximum ERP/height limited by rules	x	x		(a)
15. Remote control operation now permitted			x	(a) (b)
16. Maximum transmitter power limited by rules	x	x	x(c)	(a) (b)
17. Unlimited directional antenna permitted by rules			x	(a) (b)

x_1 = With respect to regular and satellite stations only.
(a) = Presently proposed in Docket No. 11331 ("On Channel" Booster Stations—UHF only).
(b) = Presently proposed in Docket No. 12116 (Low Power Repeater Stations).
(c) = Presently limited to 10 watts by rules but increase to 100 watts proposed in Docket No. 12567, and approved for adoption by the FCC effective December 26, 1958.

could not be completed in time to be included in the TASO report.

The following two paragraphs are quoted from the tentative conclusions of the interim report on the Waterbury tests:

> Thus far it is indicated that there are locations where interference between main station and repeater station cannot be reduced by simple antenna orientation techniques. Further investigation is required, particularly in the use of such methods as cross-polarization to obtain a better discrimination of wanted to unwanted signals. It is planned to conduct tests using two matched re-transmitting antennas at the output of the repeater. One will be mounted for horizontal polarization and the other for vertical.
>
> The only assuring procedure so far for discriminating against an undesired signal in favor of the desired signal for ghost elimination, where both signals are arriving at the receiver test sight at small angles, is the use of low elevations (a few feet above the ground) to reduce or eliminate the signal from the unwanted source. Shielding one signal with a car or house has also shown some promise. This technique will also be investigated further.

Survey of UHF Translators

A task force of the committee surveyed translator licensees and television stations being rebroadcast, by questionnaire. Data thus obtained were compared with information in FCC files. Table IV presents some of the results.

Much significant data were obtained which cannot be reproduced here for lack of space.[4]

[4] *Op. cit.*, "Engineering Aspects of Television Allocations," The interested reader is referred to Sec. 1.2.6 in which all of the information is included.

TABLE IV

	TASO Data[5]	TASO and FCC Data[5]
No. of areas served by TV translators	41	92
No. of individual communities	65	132
No. of individual TV translators authorized	60	156
No. of areas using 1 translator	25	53
No. of areas using 2 translators	12	23
No. of areas using 3 translators	4	15
No. of areas using more than 3 translators	—	1
Total population in areas served by translators	321,150	717,893
Total no. of homes in areas served	83,896	187,500[6]
Total no. of UHF receivers in use	37,641	84,500[6]
Per cent of homes equipped for UHF reception	45%	45%[6]
Total investment in translator installations	$375,655	$892,764
Average cost of a 1-channel system	$ 6,212	$ 5,380
Average cost of a 2-channel system	$ 13,040	$ 11,977
Average cost of a 3-channel system	$ 20,764	$ 18,820
Cost of one 5-channel system	—	$ 60,681[7]
No. of installations costing less than $4,000 per channel	3	13
No. of installations costing $4,000–$6,000 per channel	21	49
No. of installations costing $6,000–$8,000 per channel	7	15
No. of installations costing $8,000–$10,000 per channel	6	9
No. of installations costing over $10,000 per channel	3	5
Annual operating cost of all translators	$ 52,638	$162,661
Average annual operating cost of 1-channel system	$ 1,161	$ 1,149
Average annual operating cost of 2-channel system	$ 1,990	$ 3,140
Average annual operating cost of 3-channel system	$ 2,210	$ 2,720
No. supported by public funds		14
No. supported by private funds		8
No. supported by TV broadcast stations		5
No. supported by public subscription		66
Average ERP employed		189 watts
Average height of antenna above community		1,515 feet
Average maximum distance served	22 miles	

[5] See text for explanation
[6] Extrapolated.
[7] Unusual installation employing a high tower.

Determining the Operational Patterns of Directional TV Antennas*

F. G. KEAR†, FELLOW, IRE, AND S. W. KERSHNER‡, MEMBER, IRE

Summary—**In January, 1959, the Television Allocations Study Organization authorized its Committee on Directional Antennas to conduct field tests on directional TV antennas looking toward development of a means whereby the operational antenna pattern could be determined and to explore the effect of reflections and anomalous propagation on the degree of directivity actually obtained as compared with that calculated.**

Tests were subsequently carried out at WBZ-TV in Boston, Massachusetts, and at WKY-TV in Oklahoma City, Oklahoma, with special directional antenna systems possessing various degrees of directivity. Measurements were made at distances varying from a few miles from the transmitter to well over 100 miles from the transmitter. Within the limits imposed upon the tests by the choice of sites, nature of the terrain, and a limited period of observation, it was found that propagation conditions did not materially affect the directivity of the array, even at distances where the scatter fields were of appreciable magnitude.

In the course of these measurements and tests, a procedure was developed whereby the operational antenna pattern could not only be determined, but also rechecked at suitable intervals thereafter.

Introduction

In the field of television broadcasting, vertical directivity of the transmitting antenna system has long been employed in order to make the most efficient use of the available radiated power. However, with few exceptions, directivity in the horizontal plane has been avoided. Two of the factors behind this reluctance to use directional antennas for TV were: 1) the absence of a tested and acceptable procedure for proving the performance of a TV antenna pattern and for making subsequent checks on it, and 2) uncertainty as to the extent to which the directivity could be maintained in the suppression area under conditions of serious local reflections or tropospheric scatter.

In its study of the over-all problems of television allocations, it became evident to the members of TASO that antennas with horizontal directivity would be useful in allocation if dependence could be placed upon their performance. It was apparent that, in the limited time available to TASO, it would be impossible to make an exhaustive study of all of the factors affecting the performance of directional antennas under all combinations of local and distant terrain conditions. However, it was agreed that even a limited amount of information would be valuable, and a special group was appointed to review the problem and make recommendations as to the best possible procedure.

* Original manuscript received by the IRE, February 15, 1960.
† Kear and Kennedy, Washington, D. C.
‡ A. D. Ring and Associates, Washington, D. C.

This initial study led to the formation of a "Committee on Directional Antenna Tests," which was charged with preparing a program of tests on directional antennas, the results of which may be expected:

> First, to form the basis for establishing procedures for determining the extent to which the operational antenna pattern corresponds (1) with the antenna pattern as measured at the antenna test site, and (2) with the antenna pattern previously calculated or otherwise determined to be required for the site in question.
>
> Second, to provide corroborative detail on the extent to which the behavior of the distant field (100 km or more) from a TV directional antenna is determined by the directivity of the operational antenna pattern.

During this same period the Association of Maximum Service Telecasters had independently decided to conduct tests on directional TV antennas, and upon the formation of the Directional Antenna Committee the tests which AMST had proposed were made a part of the TASO program.

The Westinghouse Broadcasting Company, Inc., indicated their willingness to make the facilities of television station WBZ-TV available for some of these tests and the licensee of WKY-TV in Oklahoma City also agreed to cooperate in the project. WJMR-TV in New Orleans offered the use of their experimental operation on Channel 12, but the experimental authorization was terminated prior to initiation of the tests.

WBZ-TV possessed a unique advantage in that it employed separate antennas for visual and aural transmission. This meant that the aural pattern could be directionalized to some extent without seriously affecting the over-all television service rendered by the station. It provided maximum power-height (FCC Zone I) so that observations could be conducted over substantial distances in order to observe the effect of diffraction and scatter.

WKY-TV was a valuable acquisition since the station had proposed to purchase a new antenna for emergency use and now agreed that it could be modified to permit rotation while installed. An additional calibrating or reference antenna could also be added to this structure and the over-all performance of the combination could be measured carefully on the test range before delivery to WKY-TV. Measurements made at the site after installation of the antenna would therefore permit comparison between the antenna patterns measured at the test range and the performance after erection at the transmitter site.

The program of tests finally proposed by the Committee was approved by the appropriate body of TASO and funds for the test program were allocated. The tests at WBZ-TV were made during the early part of 1959, terminating in time to move the measuring equipment and personnel to Oklahoma City for the tests at WKY-TV. These tests were conducted during the fall of 1959 and were concluded in December of that year. A description of the tests and the results obtained follow.

Measurement of the Performance of the Antenna at Television Station WBZ-TV

The antenna installation for WBZ-TV consists of two three-section superturnstile antennas mounted one above the other on a 1107-foot tower which is located approximately eight miles southwest of Boston, Massachusetts. For the purposes of this test the upper antenna was used as an experimental directional antenna for aural transmissions on 71.74 mc.

Separate transmission lines were installed to connect the north-south and east-west superturnstile elements to a special power dividing network installed in the transmitter building. This network was designed to provide either "nondirectional" operation with normal 50-50 power division or directional operation with a power ratio of 20 db between the two sets of superturnstile elements. For both modes of operation the normal 90° phase relationship was maintained. The high power elements were oriented at a true bearing of approximately 351.5° and this was the expected direction of minimum radiation from the directional antenna. During the period of the field measurements, the power dividing network was switched to provide alternate 15-minute periods of nondirectional and directional operation with the same power input from the aural transmitter. Fig. 1 shows the expected radiation patterns in terms of relative voltage based on pattern shapes for single superturnstile elements supplied by RCA.

The field measuring program consisted of obtaining three types of measurements. Fig. 2 is a map showing the expected direction of minimum signal and the locations at which the field measurements were obtained. The first type of measurements comprised field strength measurements for both directional and nondirectional operation made along four radial routes from the transmitter, at distances ranging from 9.0 to 50.4 miles. At each measuring location, a continuous mobile recording of the signal was made over a distance of approximately 100 feet. These measurements were made with a half-wave dipole receiving antenna mounted 30 feet above the road surface. At each location, recordings were obtained over the same path for both directional and nondirectional operation during adjacent 15-minute periods.

The second type of measurements consisted of field strength measurements made at locations traversing a "cross minimum" route at distances ranging from 18.6 to 21.8 miles. These measurements were made in the same manner as described above for the radial field strength measurements.

The third type of measurements consisted of time recordings of signal strengths at several fixed locations over periods ranging from 7 to 18 days. At each location, the signal was recorded for alternating 15-minute periods of nondirectional and directional operation.

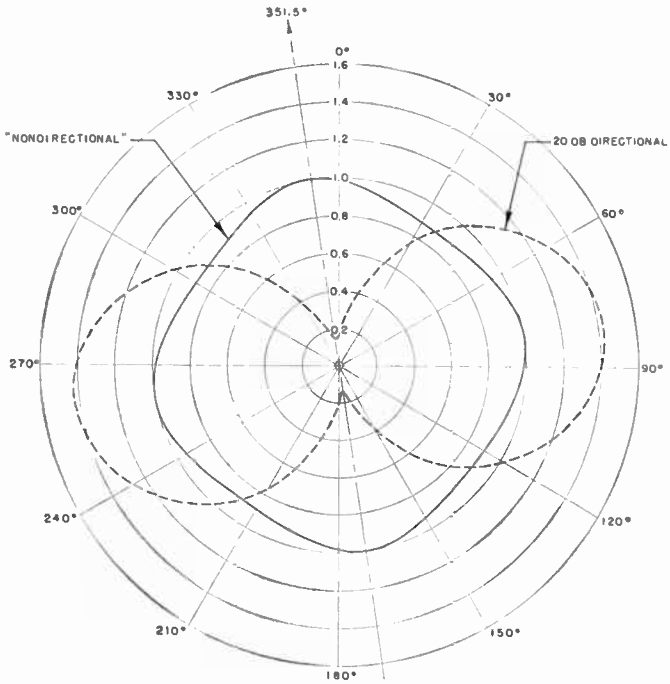

Fig. 1—Computed horizontal radiation patterns of WBZ-TV antenna.

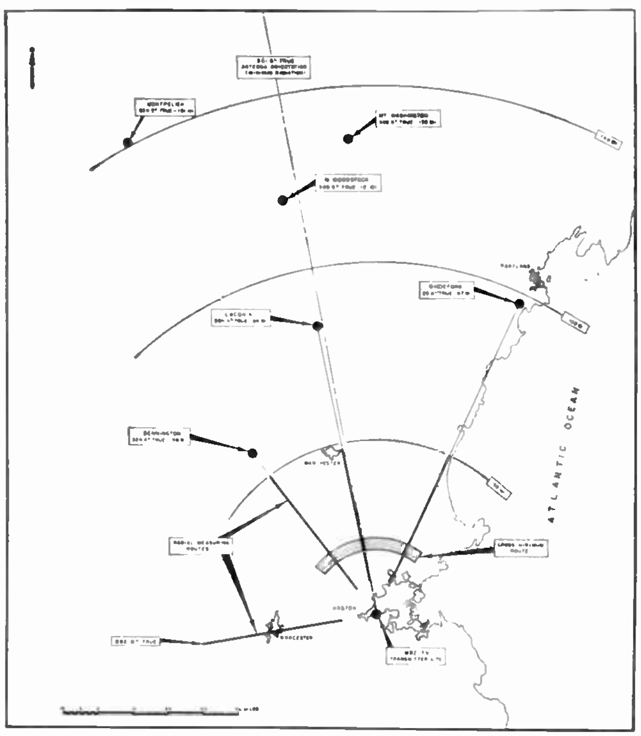

Fig. 2—Map showing WBZ-TV transmitter site and measuring locations.

Fig. 3 shows the results of the measurements made along the four radial paths from the transmitter. For each location the median signal levels were determined from the recorder charts for directional and nondirectional measurements along the same path. The ratio of these median values expressed in db is plotted vs distance from the transmitter station. The average ratio and the standard deviation for each direction are indicated on the graphs. The standard deviation was less than 0.8 db for all four radial directions.

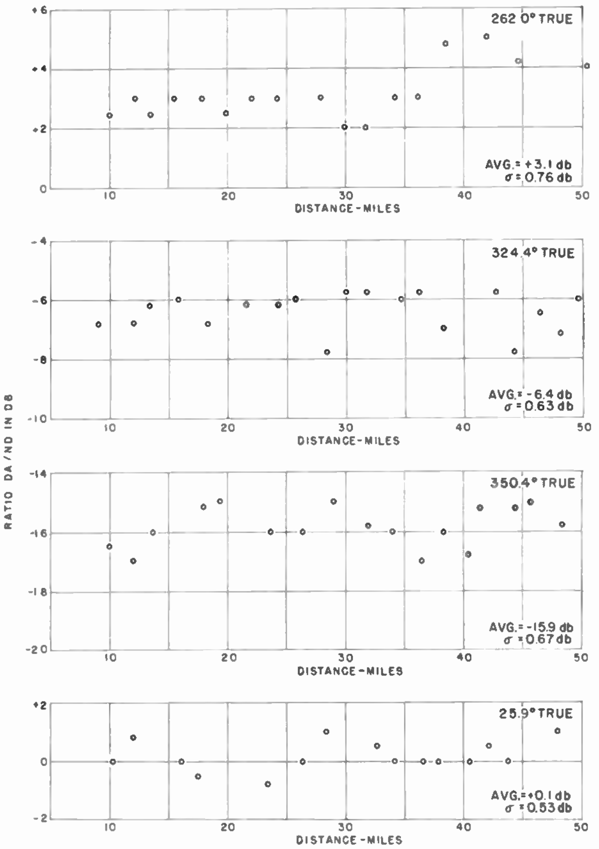

Fig. 3—Radial ratio measurements, WBZ-TV.

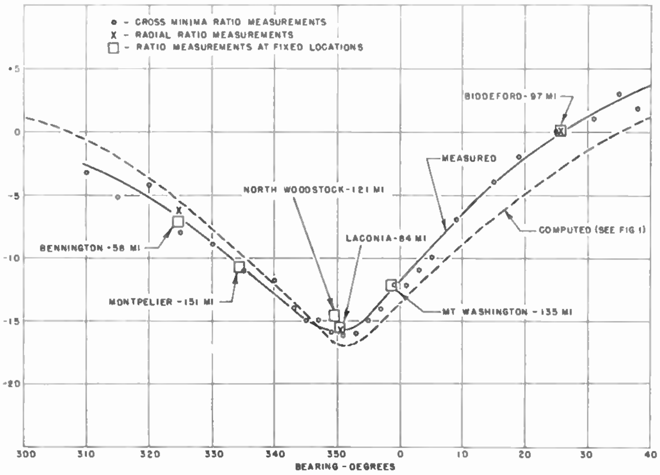

Fig. 4—Measured and computed ratios, WBZ-TV.

Fig. 4 shows the ratios obtained from the cross minimum measurements along with the average ratios obtained from the radial measurements and the average ratios obtained at the six fixed measuring points. The solid curve shows the average of the measured data, and the dashed curve shows the expected ratio based on the computed antenna patterns of Fig. 1. It should be noted that the expected ratio (DA/ND) in the direction of minimum radiation is 17 db instead of 20 db because the maximum radiation from the directional antenna is 3 db greater than from the nondirectional antenna.

Table I summarizes the results of the measurements obtained at the six fixed locations where time recordings of the signals were made.

TABLE I

Summary of Results of Recordings Made at Fixed Measuring Locations

Location	Bearing	Distance, Mi.	Number of Recording Periods	Average Ratio DA/ND
Bennington, N. H.	324.4°	58	190	− 7.1 db
Montpelier, Vt.	334.2	151	27	−10.9
North Woodstock, N. H.	349.5	121	35	−14.7
Laconia, N. H.	350.4	84	175	−15.5
Mt. Washington, N. H.	358.6	135	67	−12.4
Biddeford, Me.	25.9	97	185	+ 0.2

The number of periods for which 15-minute records of both nondirectional and directional signals were obtained is indicated for each location along with the average ratio of the signals. Comparison of the results as plotted in Fig. 4 shows close agreement between the ratios obtained at the fixed locations and the ratios obtained from the radial and cross minimum measurements made at closer locations. It should be noted, however, that the results obtained at 121 miles (349.5° true) indicate one or two db less suppression than the measurements made at closer locations. This effect may be due to scatter propagation modes which tend to "fill in" the minimum of the pattern.

With the exception of the Mt. Washington and Montpelier locations, the fixed locations were selected to represent typical rural receiving locations for the terrain involved. The Mt. Washington recordings were made at the site of television station WMTW-TV at an elevation of approximately 6300 feet above sea level. The Montpelier recordings were obtained at the Montpelier Community Television receiving site located on the southwest side of a mountain at an elevation of 1125 feet above sea level.

The equipment used at the fixed locations consisted of high-gain fringe-type antennas mounted at heights of 30 to 40 feet. Baluns and coaxial transmission lines were used to connect the antennas to crystal-controlled receivers which were connected to the recording meters. The receivers were calibrated on a daily basis with laboratory-type signal generators.

Figs. 5 and 6 show the distributions of the median signal levels for all 15-minute periods of nondirectional and directional operation recorded at the two fixed recording locations in the direction of maximum suppression. Smooth lines were drawn through the measured points, and the ratios of the signals exceeded for 50 per cent and 10 per cent of the time are indicated. These data do not indicate any consistent trend between the 50 per cent and the 10 per cent signal ratios.

Measurement of the Performance of the Antenna at Television Station WKY-TV

An extensive program of measurements was undertaken to determine the performance of a special experimental directional antenna installed by television station WKY-TV at their transmitting site five miles north of Oklahoma City, Oklahoma. Careful control of the antenna design was possible because the management of station WKY-TV agreed to incorporate the directional antenna project into the installation of a new standby antenna system.

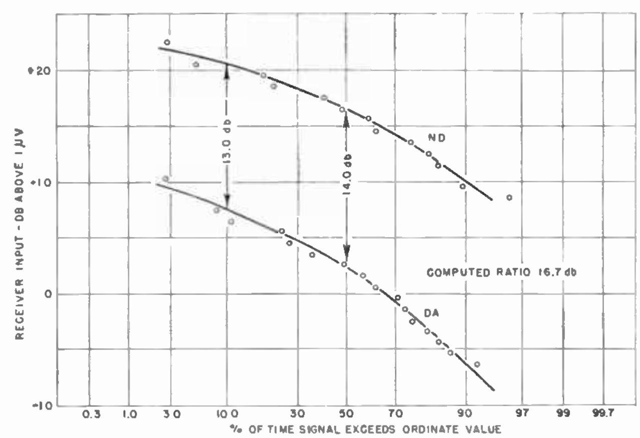

Fig. 5—Results of recordings made at North Woodstock, 349.5° true, 121 miles.

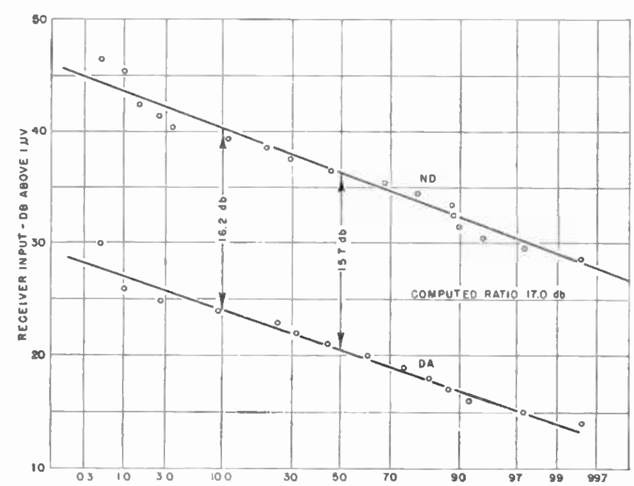

Fig. 6—Results of recordings made at Laconia, 350.4° true, 84 miles.

The directional antenna consisted of a modified RCA Type TF-3EM three-section superturnstile designed for operation on television Channel 4. Fig. 7 is a photograph showing the main antenna and the special reference antenna which is mounted some twenty feet above the upper superturnstile elements. The reference antenna consists of two folded half-wave dipoles mounted in the same horizontal plane with the spacing and phasing arranged to provide a "figure 8" type pattern and low coupling to the superturnstile antenna elements. Both the superturnstile antenna and the reference antenna

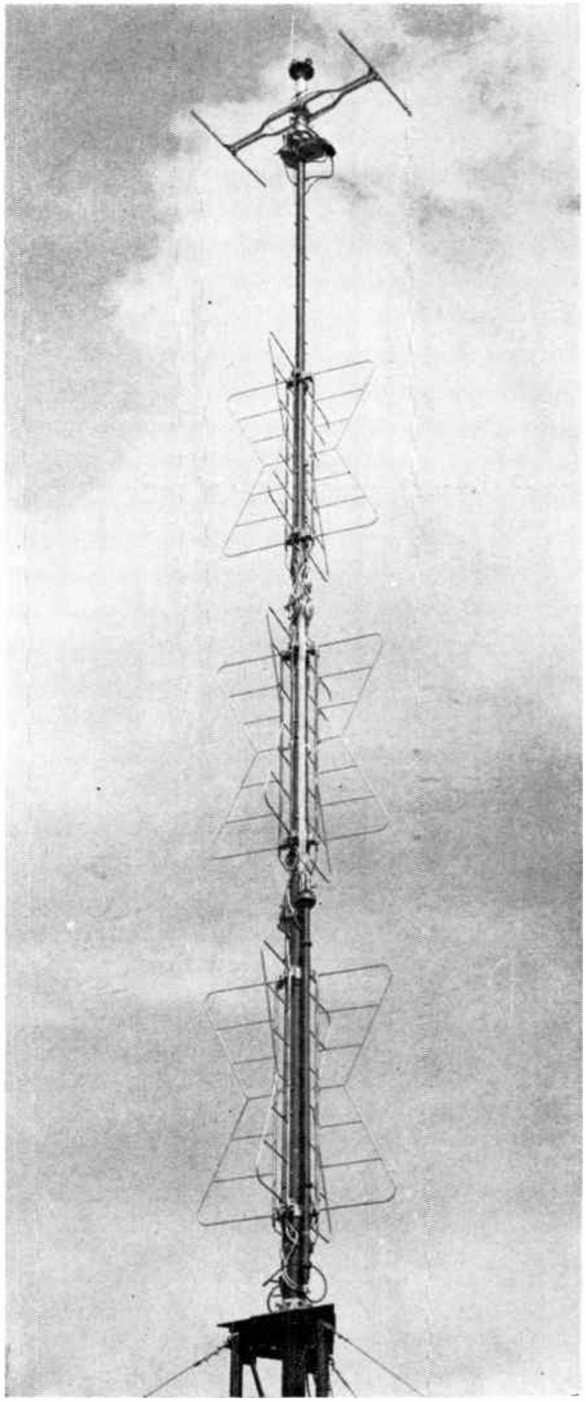

Fig. 7—Photograph of WKY-TV directional antenna system, showing main and reference antennas.

were equipped with motor drive mechanisms and remote control and bearing indicator systems so that the antennas could be independently positioned to any desired orientations. Flexible RG-117/U coaxial transmission lines provided connections between the antenna elements and the rigid $3\frac{1}{8}$-inch transmission lines used to connect the antennas to the transmitter. Three interchangeable power-dividing tees provided power ratios of 0, 10, or 20 db between the two sets of superturnstile elements. Motor-driven coaxial switches permitted switching the transmitter to either the superturnstile antenna or the reference antenna.

The special directional antenna and reference antenna were assembled by RCA and a complete set of pattern measurements was made at the Gibbsboro, New Jersey, test site of RCA. Fig. 8 shows measured horizontal patterns for the three modes of operation as made at Gibbsboro with the reference antenna removed. Similar pattern measurements were made at the aural carrier frequency, and pattern measurements were also made with the reference antenna in place. Analysis of these measurements showed that the reference antenna had only a small effect on the pattern of the main antenna.

The antenna was then shipped to Oklahoma City and installed on a 263-foot supporting tower located some 800 feet from the 969-foot main antenna tower of station WKY-TV. The field measurements made after installation included measurement of pertinent details of the radiation patterns at the visual carrier frequency, aural carrier frequency, and at sideband frequencies 2.0 and 3.6 mc above the visual carrier frequency. All measurements were made during the early morning experimental hours following sign-off of the regular WKY-TV program. Three basic types of measurements were made. The first type employed the reference antenna method for which measurements were made of the signals received from the main antenna and the reference antenna, with the reference antenna oriented for maximum signal at the measuring location. Measurements by the reference antenna method were made along four radial routes from the transmitter and along one cross minimum route, as shown by Fig. 9. These measurements were made with a half-wave dipole receiving antenna mounted at a height of 10 feet.

The second type of measurements utilized the rotation method. The signal received from the main antenna was observed as the main antenna was rotated. Measurements were made by this method at locations along the 90° radial route from the transmitter employing a receiving antenna height of 10 feet.

The third type of measurements consisted of recordings made for extended periods of time over two paths of 65 and 206 miles (see Fig. 9). Measurements were made on the visual carrier frequency at Bristow, Oklahoma, with the main antenna set at specific orientations for alternate 10-minute periods. Measurements were also made of the visual signal received from the KRLD-TV transmitter located near Dallas, Texas, with the WKY-TV directional antenna used as a receiving antenna.

The portion of the pattern providing minimum radiation (maximum suppression) was considered to be the most important area for exploration, and the "90° minimum" portion of the pattern (see Fig. 8) was selected for detailed study. The "0° maximum" was used as the reference for establishing suppression ratios.

Fig. 10 shows the results of the measurements of the 20-db pattern made by the reference antenna method along four radial routes. At each location, measurements were made of the signals from both the main antenna and the reference antenna at three cluster points spaced

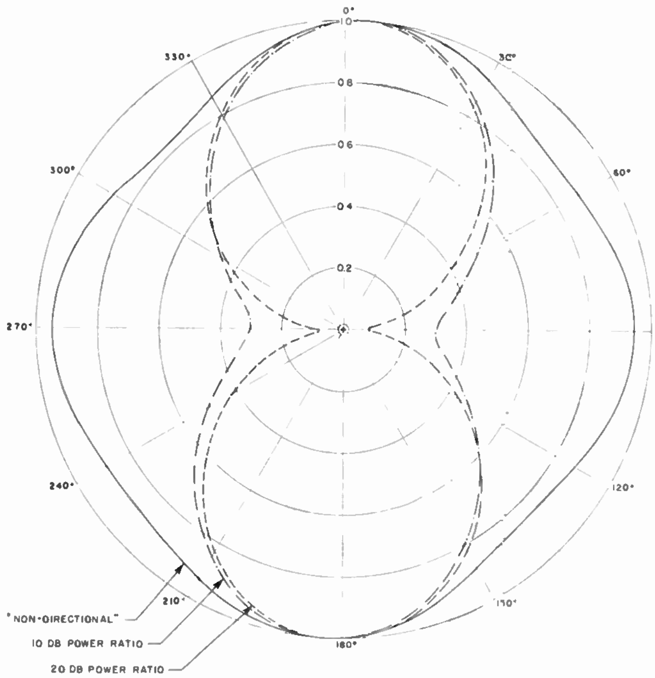

Fig. 8—Horizontal radiation patterns measured by RCA, 67.5 mc, reference antenna removed.

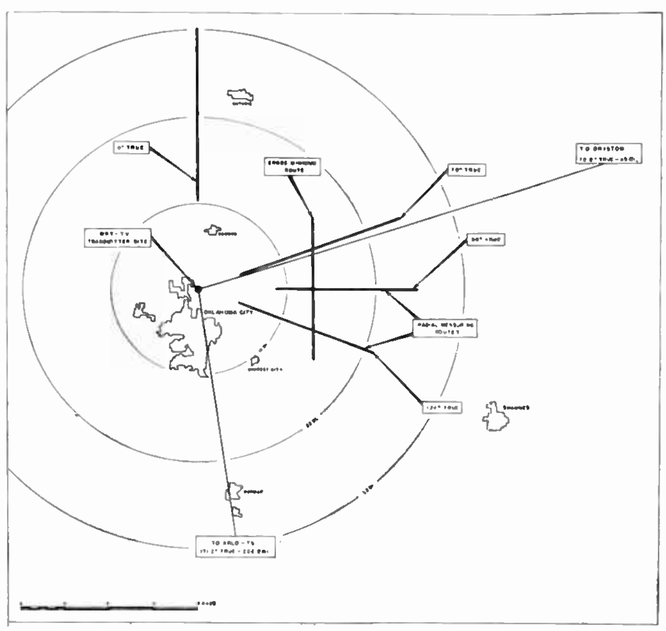

Fig. 9—Map showing WKY-TV transmitter site and measuring locations.

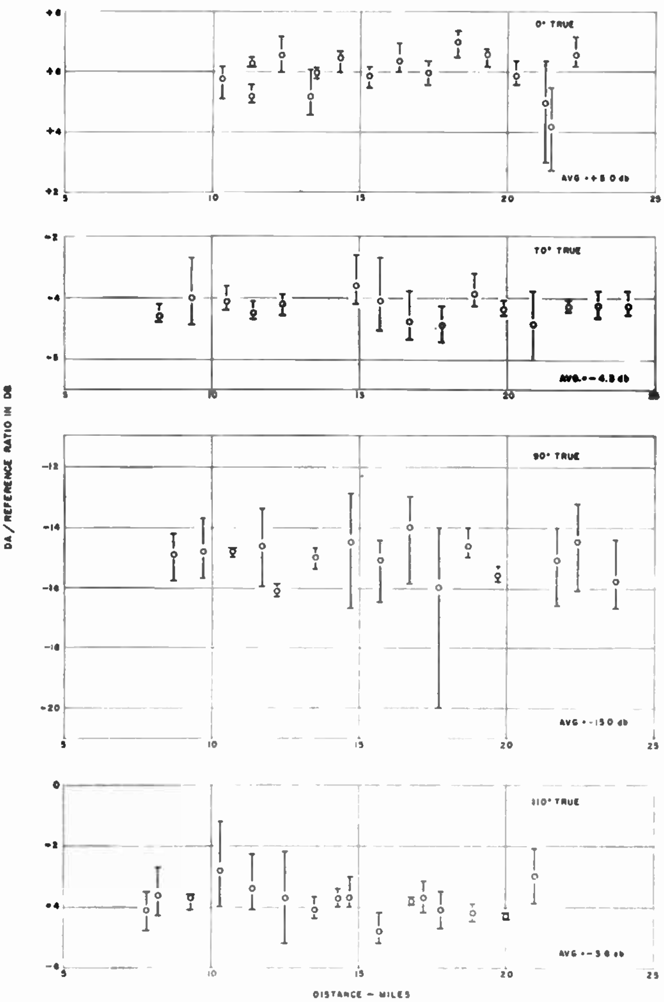

Fig. 10—Results of reference antenna ratio measurements made along radial routes, 20-db power ratio, visual carrier.

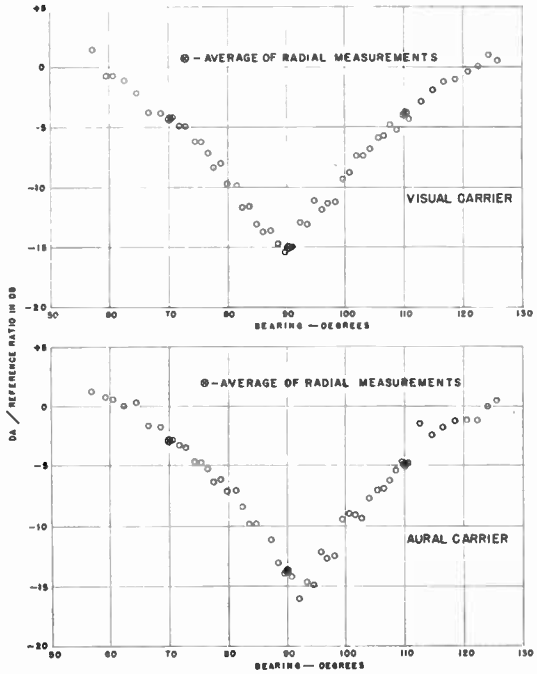

Fig. 11—Reference antenna ratio measurements along cross-minimum route, 20-db power ratio.

at 50-foot intervals along the road. The main antenna orientation remained fixed with the "north" elements aligned with true north, and the reference antenna was oriented for maximum received signal. The graphs show the minimum, average and maximum ratios for each measuring location.

Fig. 11 shows the results of the cross-minimum ratio measurements of the 20-db pattern made using the reference antenna method. Each point plotted on the graphs represents the ratio observed at a single measuring point along the cross-minimum route. The average results of the radial measurements are also shown.

Fig. 12 shows the results of measurements made at the aural and visual carrier frequencies and sideband frequencies using the point-by-point rotation method.

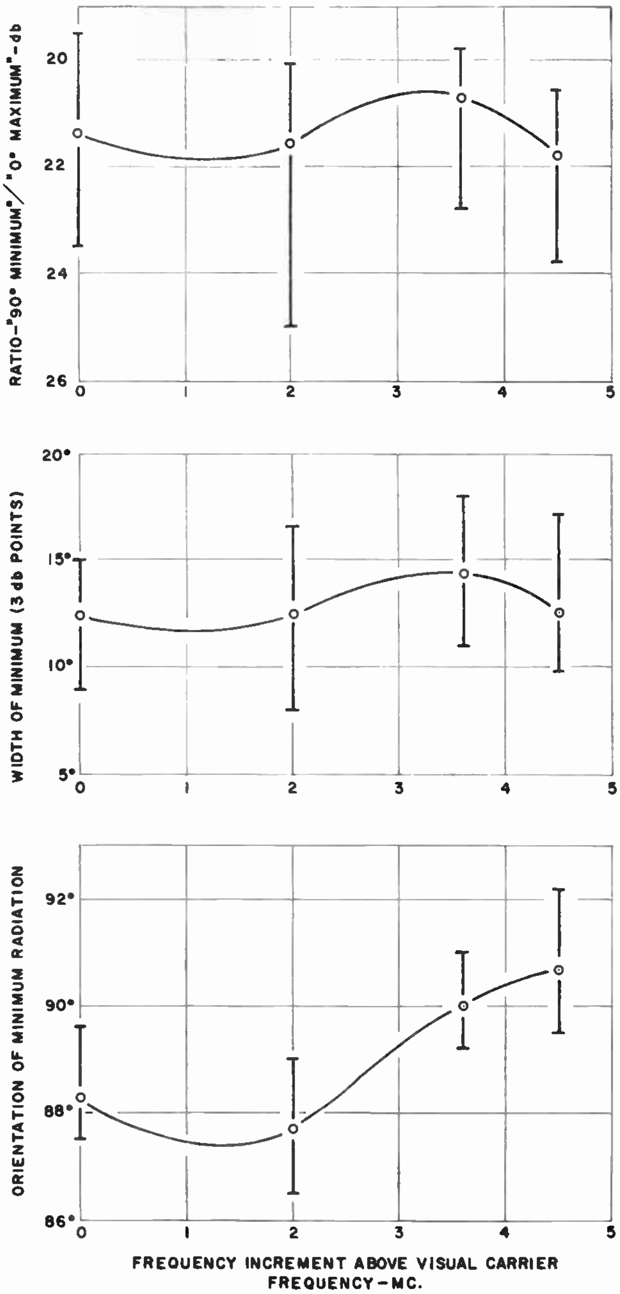

Fig. 12—Results of measurements made using point-by-point rotation method, 20-db power ratio.

Measurements were made at 17 locations along the 90° radial route, and the graphs of Fig. 12 show the minimum, average and maximum values observed. At each location, the received signal was measured as the antenna was rotated point-by-point over the sector required to provide details of the position and width of the 90° minimum of the radiation pattern. The signal obtained from the 0° maximum of the radiation pattern was also measured in order to obtain the ratio of minimum to maximum signal. Analysis of the data obtained by the rotation method indicates that the depth, orientation and width of the minimum of the radiation pattern vary as a function of both location and frequency. Substantial variations in the pattern parameters occurred at different locations in the same radial direction and even at locations spaced about 100 feet apart along the same road. These variations are believed to be caused by scattering of the signal caused by terrain irregularities. The test data indicate that the results of a large number of measurements made at different locations must be averaged to obtain an accurate operational radiation pattern.

Measurements of the 20-db pattern were made at Bristow during the early morning experimental hours for the period of October 7 through October 11, 1959. The measuring equipment was set up in a downtown hotel room and the signal was received by means of a fringe area type antenna mounted on the roof of the hotel. The visual signal was recorded for 30-minute periods, and the average results are given in Table II. During each period the signal was recorded both for the indicated orientation and with the 0° maximum towards Bristow, and the ratio of the median signals was established.

TABLE II

Results of Bristow Measurements (73.2° True—65 Miles)

Orientation of Path Measured Clockwise from North Antenna Elements	Number of Recording Periods	Average Ratio of Signals Referred to 0° Maximum
80°	12	−16.6 db
90°	29	−20.6 db
100°	10	−14.4 db

Table III shows the results of measurements of the 20-db pattern made by employing the WKY-TV directional antenna as a receiving antenna to pick up visual signals transmitted by station KRLD-TV which operates in Dallas, on television Channel 4. The use of this reciprocal technique permitted obtaining data over a relatively long path (206 miles). The measurements were made between the hours of 1 A.M. and 5 A.M. from November 30 to December 12, 1959.

During the first ten minutes of each half-hour period the signal was recorded with the antenna oriented for maximum pickup from KRLD-TV (north superturnstile element towards KRLD-TV). During the next 10-minute period, the signal was recorded with the indicated orientation. The remaining time of each half-hour period was used to calibrate the receiving equipment and to record the noise level and any other signals present with the KRLD-TV transmitter shut down. The analysis of these periods of noise recordings showed the absence of significant signals arriving from other sources.

The median signal values (db above 1 μv at input to the receiver) for the ten-minute periods were determined and the average ratios for each day's recordings are given in Table III. The antenna orientations given are corrected for an error of 0.8° in the bearing indicator system which was discovered after the measurements were made.

TABLE III

Summary of Results, KRLD-TV Measurements

Date	Number of Periods	Average Ratio of Signals Referred to 0° Maximum		
		80.8°	90.8°	100.8°
Nov. 30	8		−19.9 db	
Dec. 2	8			−12.5 db
Dec. 3	8	−15.8 db		
Dec. 4	8		−19.8	
Dec. 5	8		−19.3	
Dec. 7	7		−22.7	
Dec. 9	8			−15.3
Dec. 10	8	−19.3		
Dec. 11	8		−22.2	
Dec. 12	4			−15.1
	4	−18.5		
Weighted Average		−17.7 db	−20.7 db	−14.1 db

Fig. 13 shows the results of the measurements of the 90° minimum portion of the 20-db radiation pattern by the several methods employed. Data are shown for operation at both the visual and aural carrier frequencies, and the dashed lines provide a comparison with the pattern measurements made before installation. The results show close agreement for the pattern measurements made after installation by different methods, and there is no great difference between the patterns measured before and after installation.

Fig. 14 shows the results of measurements of the 10-db directional antenna pattern before and after installation. Measurements of the 10-db pattern were not made at the two distant recording locations, but the measurements made by the reference antenna method and the rotation method are in close agreement.

Fig. 15 shows photographs of test patterns made at four locations between 4.9 and 6.7 miles from the transmitter with the 20-db antenna pattern employed. Fig. 15(a) shows the test pattern as received with the antenna oriented for maximum signal at the receiver. Figs. 15(b)–15(d) show the signals received with the antenna oriented for either minimum signal at the receiver or 10° from the position of minimum signal, as indicated. These photographs were selected as typical of test pattern observations made at locations in all eight

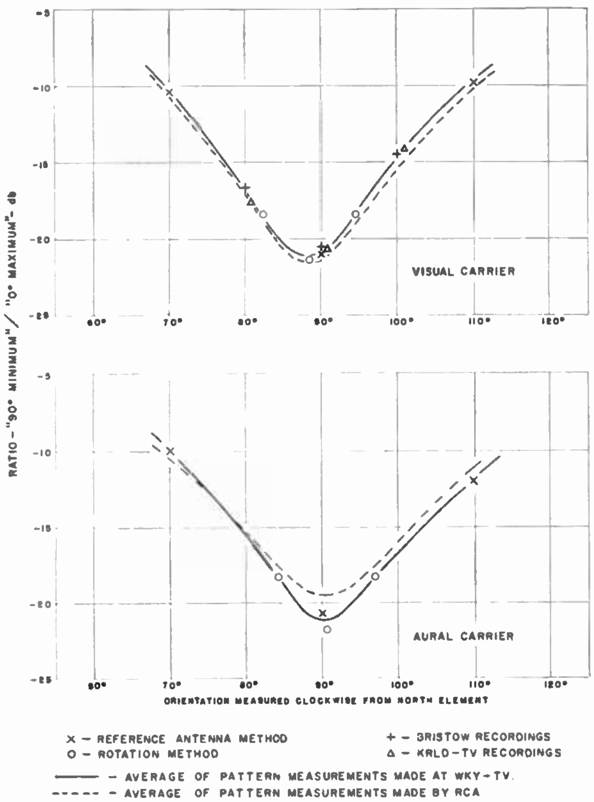

Fig. 13—Results of measurements of the 90° minimum portion of the pattern, 20-db power ratio.

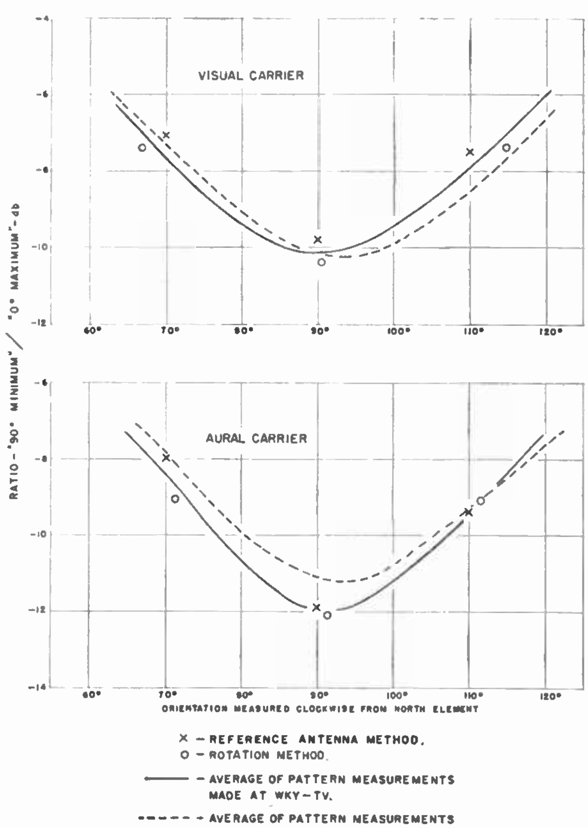

Fig. 14—Results of measurements of the 90° minimum portion of the pattern, 10-db power ratio.

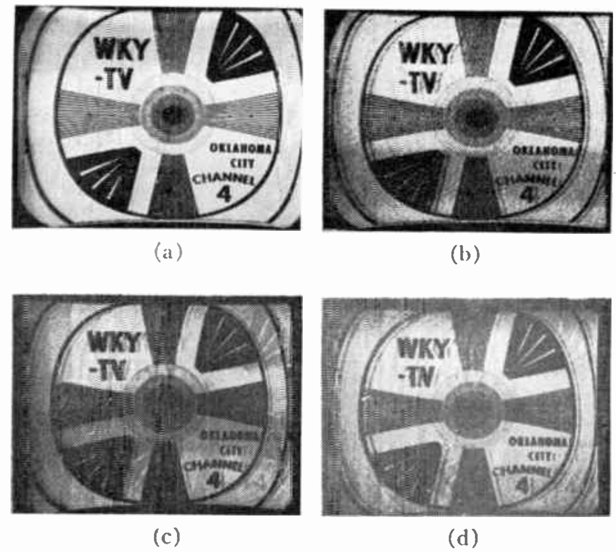

Fig. 15—Photographs of test patterns, 20-db power ratio. (a) 6.2 miles west, antenna oriented for maximum signal. (b) 6.2 miles west, antenna oriented for minimum signal. (c) 5.8 miles southwest, antenna oriented for minimum signal. (d) 5.8 miles southwest, antenna oriented 10° from minimum.

directions from the transmitter. In all cases, ghosts ranging from moderate to severe were evident when the antenna was oriented for minimum received signal. In some cases, ghosts were still quite noticeable with the antenna oriented 10° from the minimum position. A limited number of test pattern observations made with the 10-db pattern indicated negligible to slight ghost problems in the directions of minimum radiation.

Recommended Method of Measuring the Operational Antenna Pattern of a Television Antenna

On the basis of the results obtained and described in this paper, it is considered that the most practical way of measuring the operational antenna pattern is the reference antenna method. The directional antenna should incorporate a rotatable reference antenna designed to operate on the visual, color subcarrier and aural frequencies. The coupling between the reference antenna and the main antenna or other nearby objects must be low enough to minimize errors due to radiation effects. The test transmitter may be of lower power than the transmitter normally used, but should have sufficient power to provide signals of adequate strength at the required measuring locations. The power into the antennas must be accurately determined and maintained. Controls should be available at the transmitter for rotating the reference antenna.

Field strength measurements should be made along at least eight radial paths from the transmitting antenna. These paths should include the direction(s) of maximum radiation, the direction(s) toward stations requiring protection, and at least two additional directions toward the service area of each station requiring appreciable protection. For each direction, measurements of the signals received from the main and reference antennas should be obtained in at least eight measuring locations at distances between 10 and 30 miles. The measuring locations should be selected so as to provide a clear, unobstructed path to the transmitting antenna, and the reference antenna should be rotated for maximum received signal. The ratio of the signals from the reference and main antennas should be established either by means of short mobile runs made by the continuous recording technique, or on the basis of the average results of four cluster measurements at points located at least 50 feet apart.

Measurements should be made at the visual carrier frequency at each measuring location. At approximately half of the measuring locations, measurements should also be made at the color subcarrier frequency and at the aural carrier frequency. Field strength measurements may be made with a receiving antenna height of approximately 10 feet.

Measurements should also be obtained at the visual carrier frequency along cross minimum routes through those arcs which include the service area(s) of other station(s) where suppression is required. These should be made at distances between 10 and 30 miles, and point ratio measurements should be obtained at intervals ranging from three to four degrees in the case of suppressions on the order of 10 db to 1 or 2 degrees for suppression on the order of 17 db. At all measuring points, the reference antenna should be positioned for maximum received signal and measurements should be made of the signals from both the reference antenna and the main antenna.

The operational antenna pattern should be established by analysis of the ratio measurements using the average or median ratio obtained for each radial direction. The ratios for each radial direction should be plotted vs distance and the resulting graphs should show no significant correlation with distance, except as expected because of the difference in vertical patterns of the two antennas. The radiation determined for each direction should be referred to the radiation in the direction of maximum radiation.

The suppression obtained at visual carrier frequency should meet the requirements set forth under the Conclusions to this paper. It is suggested that suppression at the color subcarrier and aural frequencies be within ± 2 db of the suppression measured at the visual carrier frequency.

Monitoring points should be selected in each critical direction. These points should provide unobstructed paths to the transmitting antenna. If the cluster measuring method is employed, at least six points should be measured and the exact location of each of the cluster measuring points should be permanently established. Ratio measurements should be made at the monitoring points at monthly intervals to insure that the operational pattern is properly maintained.

Conclusions

Factors beyond the control of TASO and the Directional Antenna Committee made it necessary to restrict the tests to measurements which were expected to provide an answer to the two problems set forth in the terms of reference of the Committee previously quoted. Tests were conducted at only two sites employing only one basic type of directional antenna, and any conclusions which are drawn must be made with full appreciation of the limitations thus imposed. Measurements made upon directional antennas of other types or having a more complicated structure and/or located in rough terrain or large metropolitan centers might show greater deviation from the expected results. However, the uniformity of the results obtained in these tests would tend to indicate that if sufficient care is employed in using directional antennas as an instrument of allocation, the antennas can be depended upon to perform in the manner intended. From the experience gained from future operation of directional antennas by operating television stations, it is to be expected that the limited conclusions reported here can be expanded and augmented in the same fashion as this information was obtained by the operation of directional antennas in the standard broadcast band.

Based upon the results of the tests just described and keeping in mind the limitations thereon, the following conclusions have been reached.

1) The operational antenna pattern, that is to say, the pattern measured with the antenna installed on its supporting structure at the transmitter site, can be accurately established after installation by field measurements, using either the reference antenna or rotational techniques.
2) Measurement of the operational antenna pattern after final installation is considered essential to insure that the suppression intended is actually obtained. Such measurements will not only show the influence of nearby objects on the operational pattern, but will also permit correction of any possible irregularities in the antenna pattern caused by damage during installation or improper connections and adjustments.
3) The reference antenna method is probably more practical and feasible than the rotational method in the case of actual operating antennas. For accurate results, the reference antenna must be designed to insure low coupling to the main antenna elements, tower structure and guy wires. Utilization of the rotational reference antenna eliminates the necessity for an accurate radiation pattern of this antenna.
4) The methods employed in these tests are not suitable for determining the vertical directivity of the operational antenna pattern, although a small but important sector thereof can be studied by an analysis of ratio measurements made over a limited range of distances by the reference antenna meth-

od. Because of this limitation, the antenna manufacturer must be relied upon to provide information on the vertical pattern characteristics. In making measurements on antennas with unusual heights or large beam tilts, the effect of the vertical plane pattern on the measured ratios at various distances should be considered when selecting the range of distances over which the measurements are to be made.

The question of the amount of fill in the directions of maximum suppression is of course most important. This fill is a function not only of the depth of the suppression but also of the steepness of the sides of the pattern. As applied to the Television Allocations problem, suppression will generally be required over a relatively wide arc. Consequently, the use of directional antennas with high degrees of suppression and steep sides is not likely.

The observations at WKY-TV showed that with a suppression of 20 db in the operational pattern at considerable distances from the transmitter, measured suppression of 16 to 17 db could be counted upon, and the average over a long period of time approximated the calculated 20-db value. It would appear that for the present, at least, a suppression of 20 db is too great to be used with confidence that the intended suppression would be obtained in practice. On the other hand, suppressions on the order of 10 db appear to present no problem.

Until further experience is gained, we believe that directional antennas should not be used to provide protections greater than 15 db (ratio of major lobe to minimum). To provide for possible propagation "fill in" effects, the operational pattern should indicate somewhat greater suppression than that required to meet the protection requirements. Until further knowledge is available, it is suggested that a "fill in factor" of 2 db be used for suppressions in the order of 15 db and that the factor be reduced to zero for suppressions less than 10 db. For example, if calculations indicate that a suppression of 15 db is required, the directional antenna should be designed for 17 db and this figure should be obtained in the operational pattern.

Distinct from this problem is the appearance of ghosts when the radiation is suppressed to the order of 20 db as, for example, in the WKY-TV case. Reflections of the main beam from nearby objects may reach a magnitude equal to, or greater than, the direct signal. In selecting a site for a television station which would require a directional antenna having a high degree of directivity, it would be desirable to locate the transmitter so that the suppressed direction is toward the area of lowest population density.

The conclusions expressed herein are those of the authors of this paper, and they do not necessarily reflect the conclusions of the Directional Antenna Committee or of TASO.

Sound-to-Picture Power Ratio*

K. McILWAIN†, FELLOW, IRE

Summary—**During the Television Allocations Study Organization's deliberations the question of lowering the television sound-to-picture power ratio from 50 per cent to 10 per cent was raised to determine its effect on allocation policy. The transmitter engineers favored it as simplifying the transmitter and reducing its price. The receiver engineers opposed it as reducing the useful range of the receiver and complicating its design. While TASO made no recommendation on the question, it is the author's personal opinion that it is best to leave well enough alone.**

WHILE the consideration of a reduction in the sound-to-picture power ratio of the United States Standard Broadcast television system had been discussed before, serious action on this subject in TASO was triggered off by a statement by E. W. Allen, Chief Engineer of the Federal Communications Commission, that he believed that the choice of this ratio could have an influence on allocations. This is because the usual limitation on adjacent channel spacing is the interference from the undesired sound signal in the lower frequency channel adjacent to the desired channel. Lowering the sound power might well extend the range of the higher frequency channel.

This remark stirred up considerable activity in both Panel 1, Transmitters and Panel 2, Receivers. Some interest was also generated in Panel 3, Field Tests and in Panel 5, Analysis and Theory. This paper is the history of the subsequent controversy as it developed in TASO.

The original sound-to-picture power ratio allowed in the FCC monochrome regulations ranged from 50 to 150 per cent. In the color television regulations this range was reduced to 50 to 70 per cent. This made little

* Original manuscript received by the IRE, February 3, 1960; revised manuscript received March 1, 1960.
† Research Center, Burroughs Corp., Paoli, Pa.

practical difference since almost all stations were then operating near the 50 per cent limit. It was suggested that the ratio be lowered to 10 per cent—a decrease of 7 db.

There is no question that the 50 per cent figure gives an aural range considerably greater than the picture range and that this increased range is used. The author has seen receivers at Riverhead, Long Island, N. Y., reaching 70 miles to pick up New York City. The pictures were, at best, ghostly outlines, but the sound was fine and the people watched and listened. A. J. Ebel "can report from three years viewing experience with inferior signal that so long as the sound level was maintained much enjoyment and/or information could be obtained from TV programs even though the picture was of very poor quality or faded out completely. On the other hand, when the sound would fade, the content of the program was lost even though the picture held." Our experience with radio has trained us to fill in, while the television performers are not, in general, skilled pantomimists. Since the system is used under these conditions let us now examine the effects of making a change in the present standards.

As far as TASO is concerned, the three ratios discussed were the present 50 per cent, 20 per cent, and a lower limit of 10 per cent.

Several criteria of comparison have been put forward. Let us examine them one by one, starting with the less controversial (if there are any).

Receiver Interference

The report of Committee 1.4 of TASO points out at least two forms of interference which would be decreased, namely sound into video and the 900-kc beat in color reception. Obviously for a given design, for less sound power there would be less sound interference.

The TASO Committee 2.6 report points out, however, effects in the receiver which they regard as much more serious. The effects of a reduction in transmitted aural power from present standards on typical modern television receivers will now be considered.

Thermal Noise Performance[1]

A reduction in transmitted aural power will result in poorer receiver signal-to-thermal-noise ratio which will, by reduction of receiver fringe area sound performance, reduce the sound coverage of any given transmitter. To obtain experimental verification of the reduction of sound channel thermal noise performance, measurements were made on nine different receivers in the engineering laboratories of some of the members of TASO Panel 2. Four different types of FM detector systems are represented in these receivers covering every type in use today. In all cases, measurements are for one of the lower VHF channels. Fig. 1 presents the data of one of these receivers which is typical of the group. Sound channel signal-to-noise output ratio is plotted as a function of picture-to-sound input ratio for a number of picture carrier signal levels. It can be seen that for each signal level there is a threshold value of picture-to-sound ratio below which the signal-to-noise ratio degrades rapidly. Fig. 2 presents a summary of these data for all the measured receivers. The loss of sound channel signal-to-noise ratio per unit reduction in sound carrier is plotted as a function of picture carrier level. In these data the average of all the receivers is presented and the data for the measured extremes are also plotted. As an example, from this curve it can be seen that with 20 microvolts (−34 db) of picture signal (open circuit antenna voltage delivered through a 300-ohm dummy antenna to the receiver), an average loss of about 1.5 db in signal-to-noise ratio will occur for each db of aural carrier power reduction. These data are for new, aligned receivers of modern design. If we add the losses expected due to misalignment, tube aging and antenna orientation and mismatch, as well as transmission line losses, it is reasonable to expect that this type of signal-to-noise ratio loss would occur in the 100- to 200-microvolts-per-meter range of signal strength in a substantial number of receivers currently in the hands of the public.

Sound quieting sensitivity which takes into account only thermal noise considerations is 30 microvolts for the typical receiver in the group used to obtain these data. In the report on receivers prepared by Committee 2.1 of Panel 2, the reported picture sensitivity for 78 receivers in the low VHF channels varied from 4 to 150 microvolts.[2] The distribution of sensitivity shows:

12.8 per cent less than 10 microvolts
34.6 per cent between 10 and 20 microvolts
19.2 per cent between 20 and 30 microvolts
11.5 per cent between 30 and 50 microvolts
9.1 per cent between 50 and 100 microvolts
12.8 per cent greater than 100 microvolts.

The importance of fringe area performance may be judged by the fact that more than 66 per cent of the receivers reported picture sensitivities better than 30 microvolts.

Impulse Noise Rejection Performance[1]

A common form of noise interference in the sound channel is that caused by automotive ignition noise, electric motor commutator noise (shavers, mixers, vacuum cleaners, etc.), arcing switches, and lightning. This form of noise is usually lumped under the general heading of impulse noise. In order to measure the effect of aural carrier power reduction on receiver performance in the presence of this form of noise, an interference source, such as a nonsynchronous 60-cps rotating arc device, was coupled through a variable attenuator into

[1] The text and figures in this section are taken from the report of TASO Committee 2.6.

[2] See Table III of W. O. Swinyard, "VHF and UHF television receiving equipment," this issue, p. 1069.

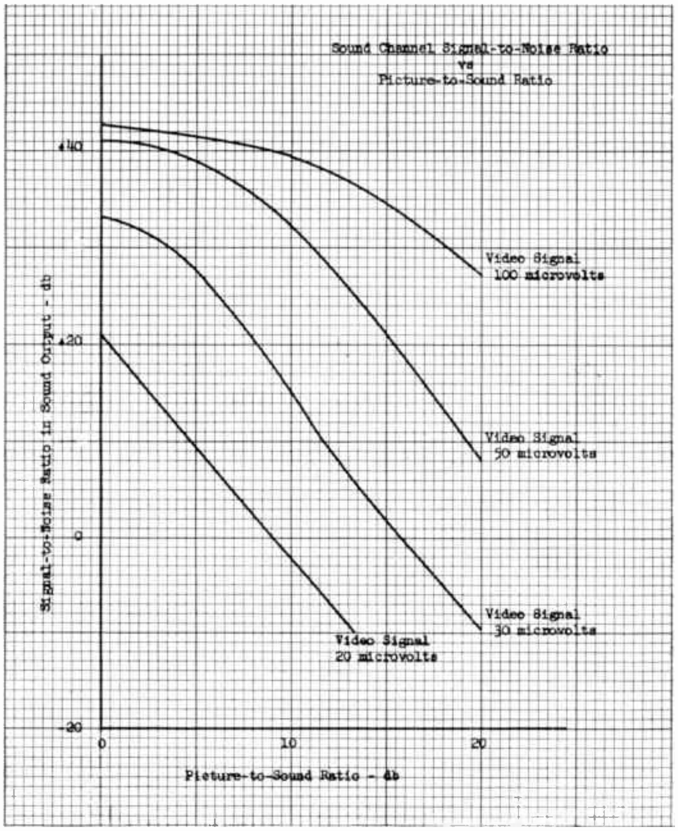

Fig. 1.

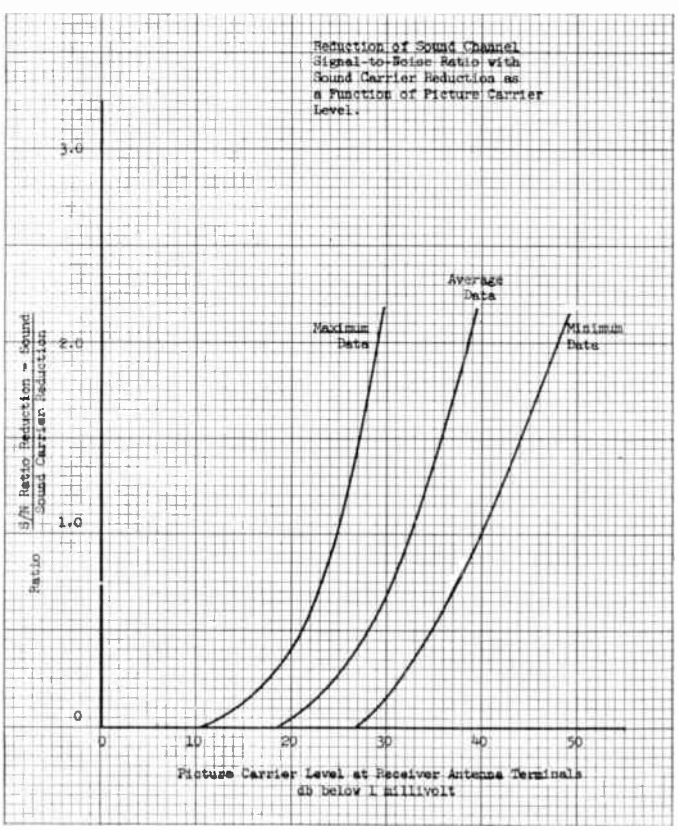

Fig. 2.

the antenna circuit of the test receiver in parallel with the desired standard visual and aural television signal. The interference noise signal input to the receiver was increased until its presence was noted in the sound output of the receiver either by aural or measured output detection. The aural signal was then reduced in steps and at each step the change in noise interference required to restore the original condition was recorded. Data were obtained on seven different commercial receivers, independently measured in the laboratories of Panel 2 members, and data for a typical receiver are plotted in Fig. 3 for visual signal input levels ranging from 50 to 10,000 microvolts. Fig. 4 presents a plot of data for the relative impulse noise level for constant audible interference as a function of sound-to-picture power ratio. This is the average of all data for all seven receivers measured. A loss of tolerance to impulse noise of about 1 db for every decibel of reduction in aural power is noted. This performance loss occurs at strong signals as well as weak; the performance loss with reduction of aural power is as great at 10,000 microvolts as it is at 50 microvolts. As in the previous case for thermal noise, these data are for new, aligned receivers of modern design.

Costs

The transmitter engineers report that the cost savings of from 10 per cent to 40 per cent resulting from a change of picture-to-sound power ratio from 2:1 to 10:1 may be of importance to a television station. The approximate savings, based upon the Committee 1.1 report, for the 10:1 ratio are as follows:

VHF	
½ kw visual power rating	27 per cent
5 kw visual power rating	30 per cent
10 kw visual power rating	30 per cent
25 kw visual power rating	40 per cent
50 kw visual power rating	40 per cent
UHF	
$\frac{1}{10}$ kw visual power rating	10 per cent
1 kw visual power rating	10 per cent
12 kw visual power rating	30 per cent
25 kw visual power rating	10 per cent
45 kw visual power rating	20 per cent

Loss of Service Area[1]

The savings in cost of operation must of course be measured against the decreased population the transmitter will serve even though partially. In order to show the loss of aural service area resulting from a reduction of sound power, the required field strength in decibels above 1 μv/meter to produce 30-db quieting was determined by measurement of the quieting sensitivity for representative TV receivers under existing transmission standards and calculation of the equivalent field strength using the formula and data presented in TASO Committee 2.4's report. The average figures for antenna gain and transmission line losses were used for channels 4 and 10 which are about in the middle of the two fre-

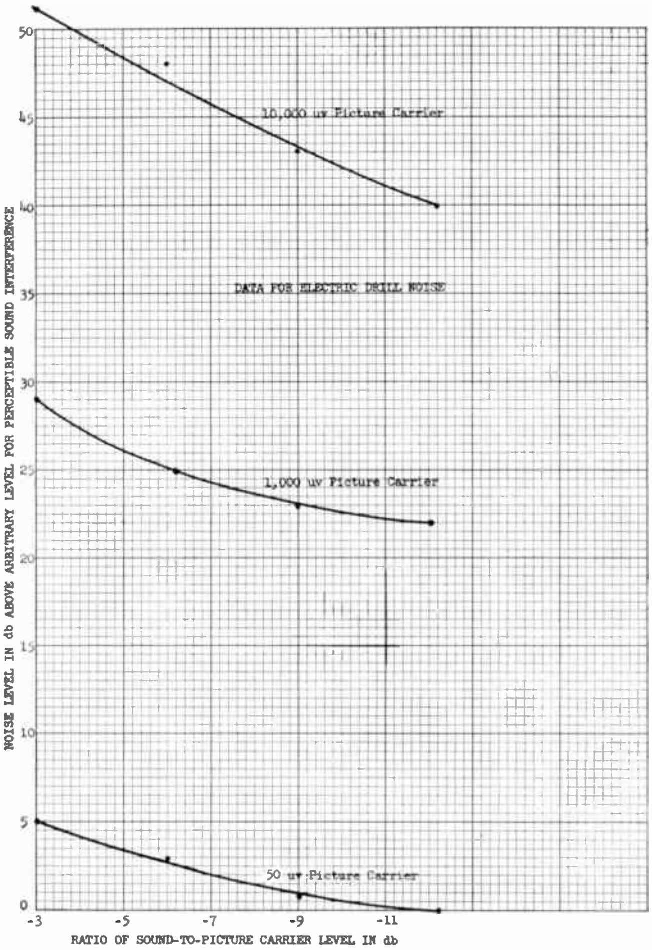

Fig. 3.

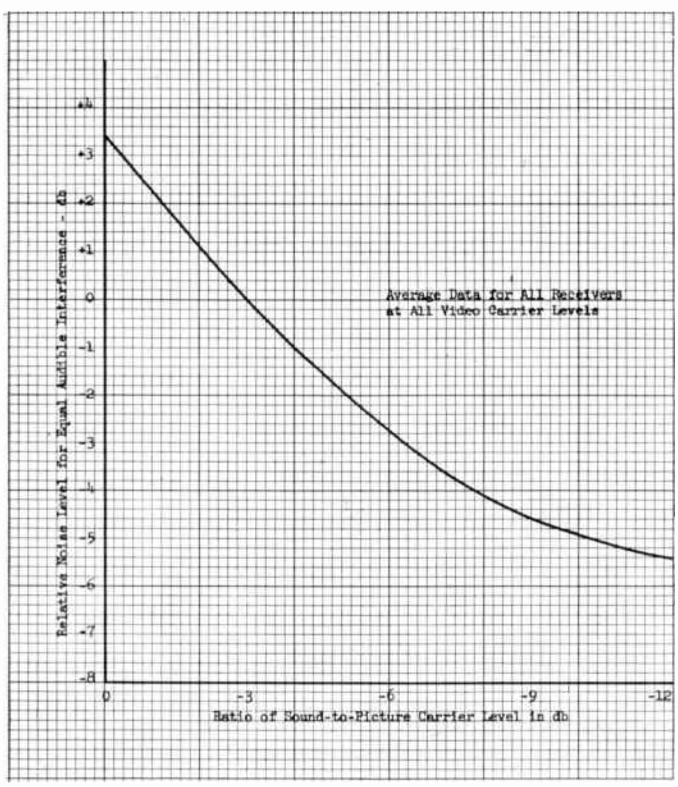

Fig. 4.

quency ranges. The required increase in video and sound signal levels to compensate for a reduction in sound power with respect to video power was determined to be 0.57 db for each decibel drop in sound power. This was obtained from the average degradation in signal-to-noise ratio at the 30-db level in data furnished by members of Committee 2.6.

Finally, the reception range and loss of service area were determined from the FCC curves of expected field strength, assuming maximum authorized power in the TV transmitter, and representative antenna heights. Figs. 5 and 6 show the loss of service area for VHF channels 2–6 and 7–13 resulting from a reduction of sound power below the present minimum of 3 db below the peak video power. The service area is reduced about 20 per cent on the low VHF channels and about 10 per cent on the high VHF channels if a 7-db reduction in sound power is made. This assumes that service area is limited by the signal-to-thermal-noise ratio.

First NTSC

Both sides quote the first NTSC report. The reduced sound adherents quote that the first NTSC Panel 4 originally recommended visual-to-aural ratio of 4:1 to 8:1.

The unreduced sound adherents point out that the first NTSC recognized that the public will tolerate and be entertained by extremely marginal picture signals provided satisfactory sound signals are available. In the report of the first NTSC in 1941, it is stated, "a given amount of interference is more disturbing in the sound than in the picture. The service area of the television system will be determined by the acceptability of the service with respect to the noise interference."

Since the first NTSC reported almost twenty years ago and its members were not endowed with second sight, the quotation of these opinions looks like grasping for straws.

Elimination of Equipment Consideration

All of the arguments listed above seem to this reviewer largely to cancel out; moreover, it had been agreed by TASO to reject economic arguments unless related to the problem of allocations. In fact, the interim report of Panel 5 states: "Though there would be some savings possible to broadcasters through equipment simplifications and some reduction in power cost, it has been agreed in TASO that this is not significant to allocations and is therefore not a consideration."

Adjacent Channel Interference[1]

One consideration which seems at first blush to have an influence on allocations is the interference in the picture from the nearby sound signal of the next lower channel (exists on channels 3, 4, 6, and 8 through 13). The interfering sound carrier is only $1\frac{1}{2}$ megacycles from the desired picture carrier.

The unreduced sound power adherents counter with this argument. Granted that a reduction in transmitted

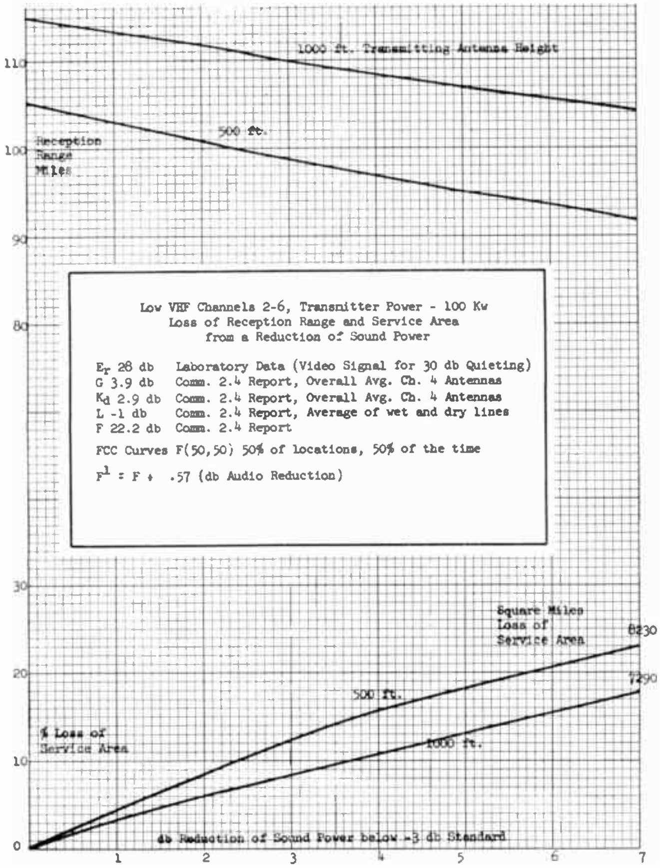

Fig. 5.

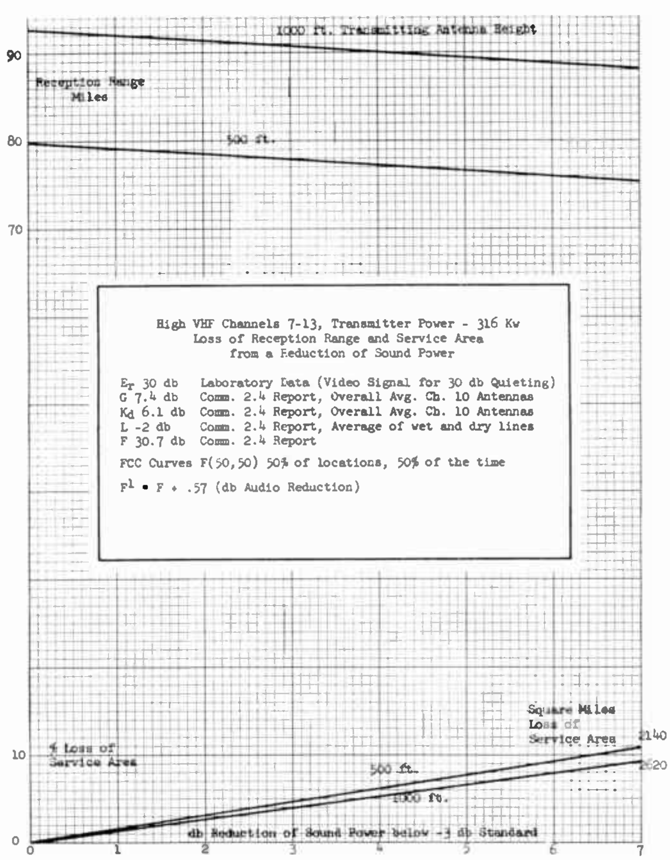

Fig. 6.

aural power would reduce the lower adjacent channel sound interference in those areas where it now exists by an amount equal to the sound power reduction. Examination of the receiver report of Committee 2.1 of Panel 2 shows that receiver attenuations for the lower adjacent channel sound signal vary widely, ranging from 14 db to 60 db, distributed as follows:[2]

11.8 per cent less than 30 db
42.1 per cent between 30 and 40 db
13.1 per cent between 40 and 50 db
32.9 per cent greater than 50 db.

This wide variation is a reflection of the fact that this performance characteristic is determined by competitive pressure in particular areas rather than by a universal requirement.

The fact that competitive pressure determines receiver adjacent channel rejection capabilities in most cases means that for any small variation in adjacent channel interference, such as would be accomplished by a 7-db reduction in sound power, the net improvement could be relatively short lived, as new designs under economic pressure would tend to seek the same competitive level as is now considered satisfactory. Conversely, any increase in adjacent channel interference, such as might result from a permitted *increase* to *both* picture and sound power might result in no long term degradation in adjacent channel performance as competitive pressure would force receiver manufacturers to build more adjacent channel rejection in receivers.

Surveys

Several surveys were conducted under various conditions ranging from asking servicemen to make two measurements a day while three stations voluntarily varied picture-to-sound power ratios at random all the way from 2:1 to 10:1, to one station which had to run at reduced power because of antenna difficulties but experienced no customer complaints. There was no clear indication from any of these. People are prone to turn up the volume control, to lay difficulties to a change in the weather, or just not to remember. A trained observer turning immediately from one simple sound to compare it with a similar sound can discriminate about 1 db. Whether an untrained observer, after a time interval, and comparing one complex sound with an entirely different one can remember a difference of 5 db is doubtful, except where it makes the difference of being able to understand or not. Suffice it to say, there is no proof that anyone noticed the degraded service and protested. It is not, however, certain that at the fringe area, the percentage of usable broadcasts was or was not decreased.

We know that a usable signal for any individual is determined by his judgment of whether it is worth the effort to try to read it. The strong sound folk have shown that a decrease in the strength of the sound inevitably makes the signal-to-noise ratio worse and therefore makes the signal harder to read.

Since present receivers have been designed to eliminate largely the various interferences and, therefore, are practically noise-limited, and since, with respect to this characteristic, at least the good receivers are working at the limitation of the state of the art it would appear to this reviewer that less harm would be done by leaving the sound level near what it is and devoting our time to improving noise figure and other qualities of the receiver.

Bibliography

[1] "Rules Governing Radio Broadcasting Services," issued by the Federal Communications Commission, Washington, D. C.

[2] D. G. Fink, "Television Standards and Practice," McGraw-Hill Book Co., Inc., New York, N. Y.; 1943.

[3] V. K. Zworykin and G. A. Morton, "Television," John Wiley and Sons, Inc., New York, N. Y.; 1940, 1954.

[4] K. McIlwain and C. E. Dean, "Principles of Color Television," John Wiley and Sons, Inc., New York, N. Y.; 1956.

[5] D. G. Fink, "Color Television Standards," McGraw-Hill Book Co., Inc., New York, N. Y.; 1955.

[6] Television Allocation Study Organization, minutes of Panel Coordinating Committee:
p. 3 (D278PCC24); December 4, 1957.
p. 2 (D314PCC26); January 8, 1958.
pp. 1, 2 (D378PCC30); March 5, 1958.
pp. 1, 2 (D413PCC32); April 2, 1958.
p. 3 (D447PCC34); May 7, 1958.
p. 2 (D478PCC36); June 3, 1958.
p. 2 (D505PCC40); July 2, 1958.

Attachment: "Memorandum re Sound-to-Picture Power Ratio," (D497-2PCC39); July 2, 1958.

[7] Final Report of TASO Panel 1, Committee 1.4 (D722P1.76); August 28, 1958.

[8] Final Report of TASO Panel 2, Committee 2.6, "Sound-to-Picture Power Ratio" (D659P2.47).

[9] Final Report of TASO Panel 3, Committee 3.3, Part II, "A Study of Television Aural-to-Visual Power Ratio at VHF," p. 41 (D579-1P3.38); Date.

[10] Interim Report of TASO Panel 5, Section I, pp. 362–363; January 8, 1959.

Presentation of Coverage Information*

DONALD C. LIVINGSTON†, SENIOR MEMBER, IRE

Summary—**Two methods for calculating the locations of boundary contours defining the limits for various grades of television service are described and discussed. The first is the location probability method, which has been used by the Federal Communications Commission for the past ten years in its allocation and channel assignment operations. The second is the newly developed acceptance ratio method, which emerged from the work of the Television Allocations Study Organization.**

Introduction

THROUGHOUT the life of a television broadcasting station, occasions arise when it is desirable that means exist for estimating how large an area can be reached by its programs and how this area is disposed geographically. It is also of interest to know how quality of reception varies over this area. These questions have been of particular interest to the Federal Communications Commission because of its responsibility for assigning television channels in such a way as to provide a maximum amount of service to a maximum number of people. It is also of interest to individual broadcasters since their ability to attract sponsors for their programs is a function of the number of people who can be reached by their commercial messages.

In 1949, a method for developing such information was deduced by a special committee of the Federal Communications Commission.[1] Since then, the method has been used by the Commission to assist in the determination of whether the licensing of a proposed new station will be consistent with the over-all allocation plan. Within the past several years, the method has been examined by the Television Allocations Study Organization (TASO) in its studies on television coverage presentation methods and has been endorsed as the best method available. At the same time, TASO regarded the method as too complicated mathematically, particularly in view of the admitted deficiencies in certain experimental data with which use of the method was necessarily coupled. It seemed worth while to attempt to develop a new method which had a simpler mathematical form and which would avoid the use of experimental data of questionable accuracy. In the course of an effort to accomplish this purpose, a new method was conceived by Dr. Bowie[2] and studied in detail by TASO Panel 5.[3] Although it was concluded that the new method represented a restricted special case of the old one and would be inapplicable in many actual situa-

* Original manuscript received by the IRE, February 16, 1960.
† General Telephone and Electronics Labs., Inc., Bayside, N. Y.

[1] "FCC, Report of Ad Hoc Committee for Evaluation of Radio Propagation Factors Concerning Television and Frequency Modulation Broadcasting Services in Frequency Range Between 50 and 250 Mc," FCC, Washington, D.C., vol. I, May 31, 1949; vol. II, July 7, 1950.

[2] R. M. Bowie, "The television system from the allocation engineering point of view," this issue, p. 1112.

[3] "Engineering Aspects of Television Allocations," Rept. of TASO to FCC, pp. 359–362 and 366–368; March 16, 1959.

tions, it was nevertheless considered to possess features of mathematical simplicity more consistent with the accuracy of the available experimental data with which it would be used than was the old method. In short, it was considered that both methods would be of value under appropriate circumstances.

Until the present time, neither method has been adequately described and explained in the readily accessible technical literature. The purpose of the present paper is to overcome this deficiency. The technical discussion will begin with a description of the older of the two methods, known as the location probability method. This will be followed by a similar treatment for the new method, which has come to be known as the acceptance ratio method.

Location Probability Method

Discussion of the location probability method conveniently begins with introduction of the concept of a *cell*. A cell will be defined as an area on the ground in the field of a transmitting antenna radiating a desired signal. The cell will be required to have dimensions which permit it to satisfy simultaneously the following two conditions:

1) The dimensions must be small enough so that the locations of all points within the cell relative to the transmitting antenna can be described to an acceptable first approximation by the same distance and direction angle. In essence, this means that the linear dimensions of the cell must be small compared with the distance between the transmitting antenna and any selected point within the cell. It follows that cells near the transmitter must be quite small while those further away can be larger in direct proportion to their distances.

2) A cell must have large enough dimensions to permit it to enclose a population of uncorrelated receiving sites from which statistically representative samples, small compared with the total population, can be taken by random selection. By "uncorrelated" is meant that detailed knowledge of the reception conditions at one site does not permit one to infer in detail the reception conditions at any other site in the population. By "statistically representative samples" are meant assemblages of sites yielding distributions of receiving conditions having essentially the same median values and standard deviations as those for the full population.

It is to be noted that these two requirements are necessarily mutually exclusive at locations within some critical distance of the transmitting antenna. That is, when the cell is small enough to satisfy the first condition mentioned above, it may be too small to satisfy the second condition. Thus, there is always a region of indefinite extent around the antenna which cannot be divided into cells. Within this region, the concepts to be developed in this paper cannot be applied without some modification in the basic philosophical approach, but it will eventually be seen that this consideration is of only academic interest.

Consider the field $E(t)$ at an individual arbitrarily selected site within some given cell. This field is likely to vary with time in some such manner as shown in Fig. 1. Over any relatively short interval of time, the field strength may tend to fluctuate in a random manner about a fairly well-defined median value. This is the case for the interval depicted in Fig. 1. When longer intervals are considered, however, it is likely to be revealed that the short-term median value is itself a function of time, being lowest during the afternoon hours and increasing steadily after sunset. Thus, the short-term median field shows a diurnal variation. Similarly, it shows a seasonal variation, tending to be higher during the summer than during the winter.

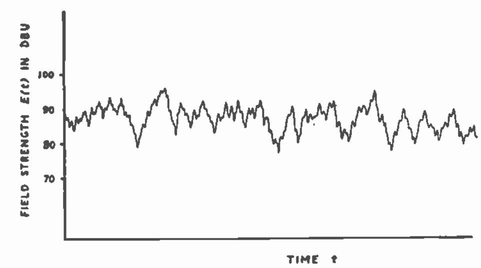

Fig. 1—Typical time variation of field strength $E(t)$.

When $E(t)$ data for the field at the selected site are available for an interval of time long enough to permit the averaging out of components due to diurnal and seasonal variations, it becomes possible to construct from the $E(t)$ data a new function $F'(T)$ which is fully independent of time. This new function is to be defined so that the symbol $F'(T)$ represents that value of field strength which is exceeded at the given site for exactly T per cent of the above-specified sufficiently long interval of time. It then follows, for example, that $F'(50)$ represents the long-term median field strength. It also follows that the smaller the value of T, the higher is the value of $F'(T)$. Although this point is of only academic interest, it will also be noted that the values associated with the symbols $F'(0)$ and $F'(100)$ cannot be unique unless special qualifications are placed on their definitions. Suppose, for example, that the lowest field ever encountered at the given site is $F'_{\min}$. Then, according to the definition already given, the symbol $F'(100)$ might be applicable to any field strength less than $F'_{\min}$. In the same way, any field strength greater than $F'_{\max}$ might be denoted by the symbol $F'(0)$. This multiplicity is readily eliminated by the adoption of a pair of special definitions $F'(0) \equiv F'_{\max}$ and $F'(100) \equiv F'_{\min}$.

When $F'(T)$ is plotted as a function of T, the result is a curve such as that shown in Fig. 2. Although this curve may show considerable variation in form for data from different receiving sites, its slope is always negative along its entire length. It is instructive to note that the same curve could have been derived from the same data in another way. First, the abscissa and ordinate scales in Fig. 1 would be subdivided into large numbers of narrow intervals with the number of intervals in the abscissa scale greatly exceeding that in the ordinate scale. The two sets of intervals would define a rectangular grid subdividing the curve into a large number of short segments. Each segment would be characterized by a pair of ordinate and abscissa values referring to the pair of scale intervals within which it occurred. A new curve would next be drawn, showing the number of segments falling within each ordinate interval as a function of the ordinate value belonging to that interval. This plot would be a frequency function indicating the relative frequency with which any given field strength occurred, and might appear as in Fig. 3. Finally, a graph would be drawn to display as a function of the abscissa values in Fig. 3 the area lying under the curve and to the right of each abscissa. The abscissa values in Fig. 3 would be plotted along the ordinate scale in the new diagram, and the areas would be plotted along the abscissa scale in terms of the parameter T, which represents the area in question divided by the total area under the entire curve in Fig. 3. The resulting curve will be recognized as representing a cumulative distribution function. This curve is also identical with that in Fig. 2.

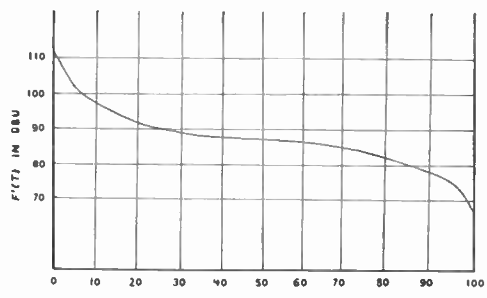

Fig. 2—Function $F'(T)$ corresponding to $E(t)$ in Fig. 1.

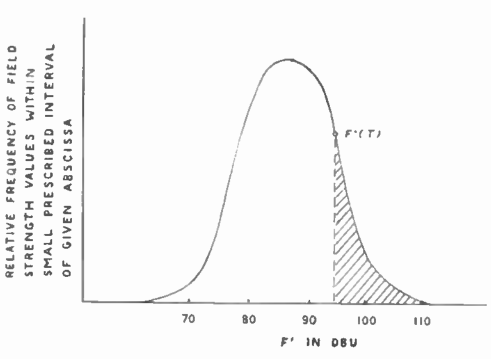

Fig. 3—Frequency distribution corresponding to Fig. 1. Shaded area is T per cent of total area under curve.

In what follows, a field strength value which is exceeded at a given site for exactly T per cent of a suitably long period of time as defined above will be called a *T per cent field*. Thus, $F'(T)$ denotes a T per cent field, and it would become meaningful, for example, to speak of 60 dbu[4] as being the 70 per cent field at a given site. Now consider not just one site within a given cell but all of the sites in a statistically representative sample of the population of uncorrelated sites in the cell. Let $E_i(t)$ and $F_i(T)$ be the field strength and the T per cent fields, respectively, at the ith site in the cell. Corresponding to any arbitrarily selected value of T, there exists a definite value of $F_i(T)$ at every site, and it is to be expected that the value at one site will generally differ somewhat from that at another site in the same cell unless the terrain around and within the cell is flat and the corresponding air space unobstructed. The distribution of values of $F_i(T)$ corresponding to a given value of T would be expected to be a function of the terrain roughness, and it is intuitively reasonable to expect the median value of $F_i(T)$ in the distribution to be primarily a function of distance to the cell from the transmitting antenna, contour of the intervening terrain, effective height of the transmitting antenna, etc., and to expect the standard deviation of values about this median to increase with the roughness of the terrain in and around the cell in question.

It will shortly become necessary that some sort of assumption be made about the manner in which the $F_i(T)$ values for a given value of T are distributed about their median. In both the original Ad Hoc Committee Report[1] and a more recently published discussion[5] of the location probability method, the mathematical formulation was patterned in a way which tacitly assumed a normal distribution. This, however, does not mean that some other form of distribution could not be used just as readily in the formulation. Published data show that a normal distribution is indeed approached when the cell is expanded along a circular arc with the transmitting antenna at its center. But this type of cell, since it does not comply with the definition given earlier in this paper, will not be considered further. In the case of cells of the type defined in this paper, there appears to be a scarcity of published data on which to base a reliable determination of what type of distribution is more likely to be encountered, but the available data seem to suggest that a Rayleigh distribution is more likely to provide a satisfactory fit with the data than is a normal distribution. There is also theoretical reason for expecting that this might tend to be the case.

Next to be constructed is a graphical representation of the distribution. This construction begins with selection of a suitable interval $\Delta F'$ in the range of F' values. A coordinate system is then laid out with the scale of F' values arranged along the abscissa axis. A smooth curve is then drawn in such a way that its ordinate at each point approximates the number of $F_i'(T)$ values lying within the selected interval $\Delta F'$ of the abscissa of

[4] DBU denotes decibels above a field strength of 1 μv per meter.
[5] E. W. Allen, "Wave propagation, radiation, and absorption," in "Television Engineering Handbook," D. G. Fink, Ed., McGraw-Hill Book Co., Inc., New York, N. Y., ch. 14, pp. 26–32; 1957.

the point. If $\Delta F'$ has been chosen small enough, the curve will represent the frequency function for $F_i'(T)$ corresponding to the specified value of T. It might appear as shown in Fig. 4, which depicts the distribution of $F_i'(40)$ values among a set of sites in a given cell. As the value of T is varied, it is to be expected that the form and position of the curve might shift. It is clear from what has preceded that increasing the value of T will cause the position of the curve to shift to the left. The effect on the shape of the curve cannot be inferred at this point.

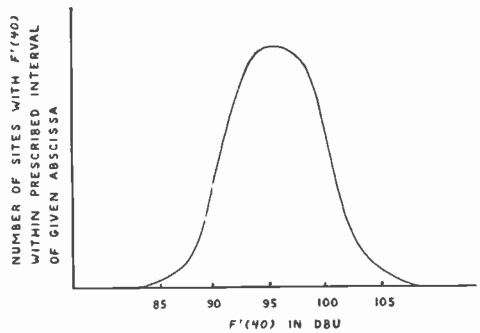

Fig. 4—Typical distribution of $F_i(40)$ values over sites in given sample.

At this point, the requirement that the data are to be taken at a statistically representative set of uncorrelated sites is to be invoked. From this requirement and from the definition of a cell, it follows that the forms of the distributions of the type shown in Fig. 4 should not be sensitive to the method used in choosing the set of statistically representative sites and should not even vary significantly from one cell to an adjacent one. In fact, the entire concept of a cell with finite area could be abandoned at this point. Instead of dealing with sets of sites in cells and calculating median fields and considering frequency functions relating to sets of data taken from discrete uncorrelated sites, one might now deal instead with probability functions for the field at a given site. The appropriate probability function would have the same form as did the corresponding frequency function for the statistical assemblage. The median field would be replaced by the most probable field if the frequency function is symmetrical, and the uncertainty in the prediction would be measured by the standard deviation in the frequency function. At a later point in this development, it will be desirable to adopt the probability approach for values at a single point. For the present, however, the purposes of clarity will best be served by retaining the statistical point of view involving cells and sets of uncorrelated sites.

The purpose of the next step in the development of the location probability method is to provide means for determining the answer to this question: Given a particular cell and given a particular statistically representative set of receiving sites in that cell, what percentage L of the sites in this set can be expected to exhibit fields which exceed some prescribed field strength level F' for at least some preassigned percentage T of the time? To answer this question, one can begin by determining the T per cent fields $F_i'(T)$ at all of the sites, T being the preassigned percentage T of the time, and continue by constructing from these values a frequency curve of the type shown in Fig. 4. There can then be constructed at the abscissa corresponding to the prescribed field strength level F' a vertical line which divides the area under the frequency curve into two parts. Now the total area under the curve represents the total number of sites in the given sample, the area to the right of the vertical line represents the number of sites having $F_i'(T)$ values larger than F', and the area to the left represents the number having values smaller than F'. From the meaning of the quantity $F_i'(T)$ as illustrated in Fig. 2, it should be intuitively clear that if the T per cent field at a given site is larger than F', then there exists some T' larger than T such that the prescribed level F' coincides with the T' per cent field corresponding to T'. For example, let F' be 80 dbu, and let $T=40$ per cent. For the case shown in Fig. 2, the $F'(40)$ field has a value of about 88 dbu. However, there exists a value of T larger than 40 per cent such that the corresponding $F'(T)$ level equals the prescribed 80 dbu. This larger T value is seen in Fig. 2 to be $T=86$ per cent. It follows that all of the sites represented by the area to the right of the vertical line have fields which exceed the value F' for *at least* T per cent of the time. Exactly analogous reasoning reveals that all of the sites represented by the area to the left of the line have fields exceeding F' for less than T per cent of the time. Thus, the desired percentage L of the sites having fields exceeding level F' for at least T per cent of the time is the ratio of the area to the right of the vertical line to the entire area under the curve. Hereafter, the symbol F' will be replaced by the symbol $F'(L, T)$ to denote that it is a function of both L and T.

$F'(L, T)$ can be plotted as a function of L for any fixed value of T by constructing the previously described vertical line at various abscissa positions on the $F_i'(T)$ frequency curve and plotting these abscissas as a function of the corresponding area ratios. The resulting curve is a cumulative distribution function similar to that in Fig. 2, the shape of the plot arising in any given case depending, of course, on the particular form of the $F_i'(T)$ function for that case. Through suitable application of nonlinearity to the abscissa scale of such a graph, one can easily test the data to determine to what type of distribution they belong. It has been most customary to assume a normal distribution for such data, for which the corresponding test involves the use of *probability coordinates*. Coordinates of this type are shown in Fig. 5 with the $F'(L, 40)$ distribution derived from Fig. 4 plotted against them. The solid curve represents the actual data, while the dotted straight line represents the normal distribution which fits it most closely. In the event that the $F'(L, T)$ data do not yield a nearly linear plot on probability coordinates, a reasonable next guess at the form of the distribution involved would often be a Rayleigh distribution. This hypothesis could be tested by replotting the data against a corresponding set of nonlinear coordinates.

It has usually been customary in working with the location probability method to assume that the $F'(L, T)$ values are normally distributed. This assumption can be expressed analytically by the formula

$$F'(L, T) = F'(50, T) + kN(L), \tag{1}$$

in which $N(L)$ is a prescribed standard cumulative normal distribution such that $N(50)=0$ dbu and $N(10)=20.5$ dbu. Being a cumulative normal distribution, $N(L)$ has a straight-line plot on probability coordinates and is therefore fully determined by the above two specified values. The quantity k is a constant with numerical values given by Allen[6] as 0.53 for VHF fields and 0.75 for UHF fields. $N(L)$ is shown in Fig. 6. In the event that the distribution under consideration is not normal, the standard reference distribution $N(L)$ for a cumulative normal distribution would be replaced by a corresponding function appropriate to the actual type of distribution. The ensuing Figs. 5 and 6 would then appear the same as in this paper except that the nonlinearity in the abscissa scales would assume a different form from that shown.

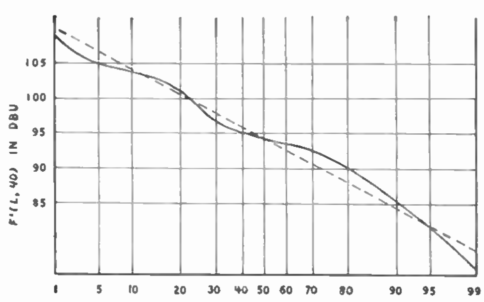

Fig. 5—Function $F'(L, 40)$ corresponding to distribution in Fig. 4.

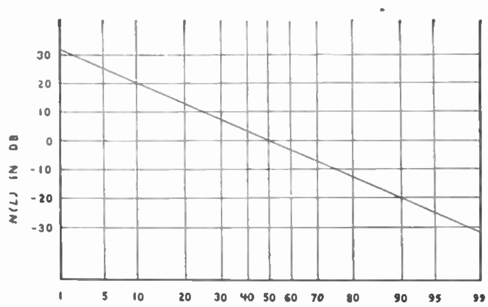

Fig. 6—Standard normal distribution function $N(L)$.

[6] *Ibid.*, p. 31.

Just as the location probability method employs (1) to describe the distribution of $F'(L, T)$ in L in terms of a well-defined standard distribution law, it also employs a corresponding relation to similarly describe the distribution of $F'(L, T)$ in T in terms of a similar distribution law. Thus, (1) can be generalized, in the case of normal distributions in both L and T, to

$$F'(L, T) = F'(50, 50) + kN(L) + M(T), \tag{2}$$

in which $M(T)$ is a cumulative normal distribution such that $M(50)=0$ dbu, thereby making it a constant multiple of the standard cumulative normal distribution $N(T)$. $N(T)$, of course, is simply the previously introduced standard function $N(L)$ with the variable L replaced by the variable T. Before (2) can be used, means must be provided for determining values of $M(T)$ other than $M(50)$. The procedure supplied in the location probability method is based on the relation

$$M(T) = M(T_0)\,\frac{N(T)}{N(T_0)}, \tag{3}$$

which follows directly from consideration of similar triangles in Fig. 7, representing T_0 as having the value 10 per cent, although any other value would be equally usable. The curve $N(T)$ in Fig. 7 is the same as that in Fig. 6 except for the change in variable, and the curve $M(T)$ represents the straight-line approximation to the function $F'(50, T)$ which coincides with it at $T=T_0$ and at $T=50$ per cent.

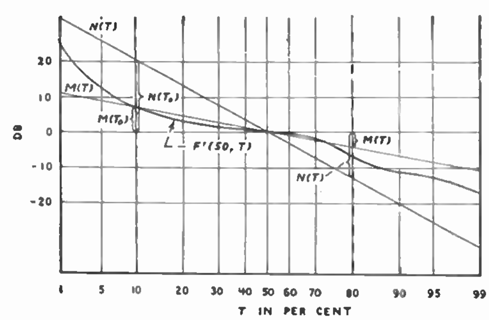

Fig. 7—Graphical interpretation of (3).

Eq. (3) by itself is not sufficient for the determination of $M(T)$, for this relation eliminates $M(T)$ only by exchanging it for the new quantity $M(T_0)$. In order to evaluate $M(T_0)$, one can set $L=50$ per cent and $T=T_0$ in (2) and solve for $M(T_0)$. The result is

$$M(T_0) = F'(50, T_0) - F'(50, 50). \tag{4}$$

Thus, evaluation of $M(T_0)$ requires knowledge of $F'(50, 50)$ along with $F'(50, T_0)$.

At this point, it is convenient to introduce the symbol $F(L, T)$, defined through the relation

$$F'(L, T) = P + F(L, T), \tag{5}$$

in which P is the effective radiated power of the transmitter. $F(L, T)$ is a normalized quantity which is conveniently presented through a family of curves. Curves for $F(50, 50)$ and $F(50, 10)$ are presented by Allen.[5] If T_0 is placed equal to 10 per cent in (4) and if (5) is then substituted into (4), one obtains

$$M(10) = F(50, 10) - F(50, 50), \tag{6}$$

which is readily evaluated through use of the above-mentioned curves. It is thus seen that, in the course of several steps, it becomes possible to deduce numerical values for any field strength level $F'(L, T)$ through (2), (3), and (6). Or, by altering the sequence of operations, one can solve for L after $F'(L, T)$ and T have been specified. As will be seen shortly, this latter procedure is the one which must be used in establishing service area boundary contours in accordance with the present FCC specifications for service of various grades.

The formulation as thus far developed is sufficient for application of the location probability method in the absence of interfering signals generated outside the receiving plant itself. It will therefore be convenient to interrupt the orderly evolution of the formulation at this point to describe how it is used in determining the limits of service of various grades in the absence of interfering signals.

In addition to the mathematical formulation already described, specifications must be provided for defining the performance characteristics of at least one, and perhaps more than one, standard reference receiving plant. It has been customary to base allocations and assignments on analyses involving the use of a single standard reference receiving plant at all distances from the transmitting antenna. However, there is no inherent limitation in the location probability method which compels such a procedure, and one could, if he so desired, carry out the procedure with different standard reference receiving plants for each of the different grades of service. In any event, one specification which must be provided for a standard reference receiving plant is the minimum field strength which must prevail at the antenna to provide a picture with acceptable signal-to-noise ratio. This ratio is called the *signal-to-noise acceptance ratio* and must be determined by subjective testing of a representative group of observers. No unique value for this ratio will arise from such tests, for different observers will exhibit different tolerance levels for noise in the picture. What the tests will yield is a distribution of acceptance ratios. The ratio, thereafter to be regarded as *the* signal-to-noise acceptance ratio, would then be defined as that tolerated by some prescribed percentage of the observers. If $F'(T)$ is now used to denote the field strength level at which the actual signal-to-noise ratio is just equal to the acceptance ratio at a given site, then T is called the *time availability of service* at that site. This name is based on the concept that *service* is said to be available at the given site as long as the signal-to-noise level is not less than the signal-to-noise acceptance ratio for the standard reference receiving plant. T in the present instance, of course, is the percentage of time for which the signal-to-noise ratio is not less than the signal-to-noise acceptance ratio and is therefore the percentage of time for which service is available.

Consider now the cell in which the given site is located. Because of the way in which the function $F'(L, T)$ has been defined, not only does there exist a definite numerical value in dbu for this function corresponding to any given pair of values for the parameters L and T, but there also exists a definite value of L corresponding to any given pair of values for the parameter T and the function $F'(L, T)$. In other words, one can regard L as a function of T and $F'(L, T)$ and can determine the value of L corresponding to specified values of T and $F'(L, T)$ if the form of the functional relation is known. This is what is done in determining what grade of service is available in a given cell. When T is the time availability of service and $F'(L, T)$ is the acceptance ratio for noise-limited service, then L is called the *location probability* for noise-limited service with time availability T. As currently defined, grade A service prevails in a given cell if the signal-to-noise acceptance ratio is exceeded for 90 per cent of the time at not less than 70 per cent of the sites. Grade B service prevails if this same ratio is exceeded at between 50 and 70 per cent of the sites for 90 per cent of the time.

The service area around a transmitter can thus be mapped by the above method into Grade A and Grade B areas if no interfering signals are present. The procedure would involve determining L for specified T and $F'(L, T)$ at each cell, designating as the Grade A and B service areas the assemblages of cells for which L equals or exceeds 70 per cent and for which L is less than 70 per cent but not less than 50 per cent, respectively. Such a map might appear as in Fig. 8 if the terrain around the transmitting antenna is only moderately rough. If the terrain is rougher, the resulting map would show a more tortuous contour accompanied by a larger number of enclaves and exclaves, both large and small. In such a case, arbitrary conventions might be adopted to simplify the contours, but this subject lies outside the domain of the present discussion.

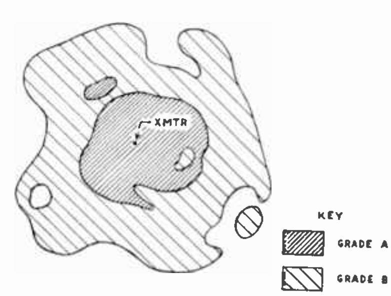

Fig. 8—Hypothetical contours for Grades A and B service.

Time availability and location probability have thus far been defined as attributes collectively held by all of the sites in a cell of finite dimensions. It is also possible to consider them as attributes of individual sites. This is accomplished by invoking the considerations cited earlier for arriving at the conclusion that one could abandon the concept of cells and deal on a probability basis with values at individual sites instead of on a statistical basis with values at an assemblage of uncorrelated sites within a given cell. When this is done, the distribution of field strengths actually observed among the assemblage of sites can be regarded as a *probability density distribution* for the field strength at any given site in the cell. Thus, the area lying under the frequency curve and bounded by a prescribed pair of abscissas represents the probability that the field at the given site lies in the range between the limits corresponding to the prescribed abscissas.

Next to be determined is the procedure for determining the availability of service when the degrading influence is contributed by interfering signals from another transmitter rather than by locally generated thermal noise. There are now two signal fields to deal with, a desired field and an undesired field, and each can be described in terms of its own $F'(L, T)$ functions in the manner already described. These functions will be designated as $F_d'(L_d, T_d)$ and $F_u'(L_u, T_u)$, respectively. Moreover, it will be supposed that the desired signal is always strong enough to override noise, so that service interruption occurs only when the desired signal fails to override the interfering signal by a sufficient amount. It now becomes necessary to define what amount is sufficient. This involves subjective evaluation of pictures which result when various ratios exist between the levels of desired and undesired signals at the receiver input terminals. The minimum such ratio which results in an acceptable picture is defined as the *acceptance ratio for the pertinent type of interfering signal.* Thus, there are co-channel, upper-adjacent channel, lower-adjacent channel, image frequency acceptance ratios and others, depending upon the natures of the interfering signals and the frequency ranges in which they lie.

When service is limited by interfering signals, the angle between the directions of arrival of the desired and undesired signals becomes of importance, and this brings the directivity characteristics of the receiving antenna into the discussion. Specifically, it becomes necessary to translate the acceptance ratio, measured as a ratio of voltages at the receiver input terminals, back through the antenna transmission line and through the antenna into a ratio of local radiation fields at the antenna. Let the strengths of the desired and undesired fields at the antenna at the ith site in a given cell be $E_{di}(t)$ and $E_{ui}(t)$, respectively, and let the gains of the antenna in the directions from which these fields arrive be G_d and G_u, respectively. Then the corresponding signal voltages $V_{di}(t)$ and $V_{ui}(t)$, respectively, at the receiver input terminals are

$$V_{di}(t) = E_{di}(t) + G_d + K_d \tag{7a}$$

$$V_{ui}(t) = E_{ui}(t) + G_u + K_d \tag{7b}$$

when all quantities are expressed in decibels. K_d is the dipole constant of the antenna, representing the conversion factor between strength of the field at the antenna and the output voltage at its terminals. The ratio $R_i(t)$ of desired to undesired signal voltage is then

$$R_i(t) = E_{di}(t) - E_{ui}(t) + G_d - G_u. \tag{8}$$

Eq. (8) represents instantaneous conditions which vary with the passage of time. As was true in the earlier treatment, it is possible to deal with field strength levels exceeded for specified percentages of the time. Then the time-dependent quantities in (8) can be replaced by frequency functions. If $E_{di}(t)$ and $E_{ui}(t)$ are uncorrelated, that is, if knowledge of the time variation of $E_{di}(t)$ does not permit one to correctly predict the time variation of $E_{ui}(t)$, then the median value $A_i(50)$ of the voltage ratio $R_i(t)$ will be given by

$$A_i(50) = F_{di}'(50) - F_{ui}'(50) + G_d - G_u. \tag{9}$$

The assumption that $E_{di}(t)$ and $E_{ui}(t)$ are uncorrelated seems likely to be valid when the desired and undesired fields do not both arrive from nearly the same direction, thereby subjecting both fields to the same terrain effects. However, in the event that the arrival directions are nearly alike, it seems unlikely that lack of correlation can safely be assumed. In general, the symbol $A_i(T)$ designates that value of $R_i(t)$ which is exceeded for T per cent of a long period of time at the ith site.

When all of the other sites in a statistically representative sample of the sites in the given cell are considered, distributions $A(L, T)$, $F_d'(L_d, T_d)$, and $F_u'(L_u, T_u)$, are obtained, each having its own median and standard deviation. The medians, of course, are $A(50, 50)$, and $F_d'(50, 50)$, and $F_u'(50, 50)$, respectively. Since the sites are assumed to be uncorrelated, one can write the relation

$$A(50, 50) = F_d'(50, 50) - F_u'(50, 50) + G_d - G_u \tag{10}$$

by applying (9) to all of the sites in the sample and generating the cumulative distribution functions in the same manner described earlier for forming $F'(L, T)$ from a set of $F_i'(T)$ values.

By analogy with (2), one can also write

$$A(L, T) = A(50, 50) + n'(L) + M'(T), \tag{11}$$

in which $n'(L)$ and $M'(T)$ are proportional to the standard deviations of the distributions of $A(L, T)$ in L and T, respectively. Now a well-established theorem in statistics states that the standard deviation of a distribution consisting of the differences between corresponding values in a pair of uncorrelated distributions is equal to the square root of the sum of the squares of the standard deviations of the component distributions. The component distributions in the present case can be described by the relations

$$F_d'(L_d, T_d) = F_d'(50, 50) + k_d N(L_d) + M_d(T_d) \quad (12a)$$

$$F_u'(L_u, T_u) = F_u'(50, 50) + k_u N(L_u) + M_u(T_u) \quad (12b)$$

through comparison with (2). Thus, $n'(L)$ and $M'(T)$ in (11) are given by

$$n'(L) = N(L)\sqrt{k_d^2 + k_u^2} \quad (13a)$$

$$M'(T) = \sqrt{\overline{M_d(T)}^2 + \overline{M_u(T)}^2}. \quad (13b)$$

For present purposes, however, it will be convenient to leave $n'(L)$ unchanged. Substitution of (10) and (13b) into (11) yields

$$A(L, T) = F_d'(50, 50) - F_u'(50, 50) + G_d - G_u + n'(L) + \sqrt{\overline{M_d(T)}^2 + \overline{M_u(T)}^2} \quad (14)$$

This is the basic relation used in determining the limits for each grade of service under interference-limited conditions. $A(L, T)$ is the voltage ratio of desired signal to undesired signal which is exceeded at the input terminals of L per cent of the standard receivers in a given cell for at least T per cent of the time. Setting $T=90$ per cent, setting $A(L, T)$ equal to the acceptance ratio for the prevailing type of interference, and solving (14) for L will yield the percentage of standard receiving plants in the given cell which will have service for at least 90 per cent of the time when one such plant is located at each site in a statistically representative sample of the population of uncorrelated sites in the cell. The parameters G_d and G_u may be regarded as constants throughout any given cell, values for $F_d'(50, 50)$ and $F_u'(50, 50)$ may be taken from standard curves such as those given by Allen,[5] and the constants $M_d(90)$ and $M_u(90)$ may be determined through the use of (3) in the manner described earlier.

In the special case in which the desired field can be regarded as independent of time, or when fading of the desired signal can be regarded as negligible in comparison with that of the undesired signal, $M_d(90)$ can be placed equal to zero in (14). The result is that

$$A(L, 90) = F_d'(50, 50) - F_u'(50, 50) + G_d - G_u + n'(L) + M_u(90). \quad (15)$$

Then, upon noting that

$$M_u(90) = - M_u(10) \quad (16)$$

because of the antisymmetry of the $M(T)$ functions about the $T=50$ per cent line, as is evident in Fig. 7, one can use the relation

$$F_u'(50, 10) = F_u'(50, 50) + M_u(10) \quad (17)$$

which follows from (12b) to reduce (15) to

$$A(L, 90) = F_d'(50, 50) - F_u'(50, 10) + G_d - G_u + n'(L). \quad (18)$$

Eq. (18) is an approximation to (14) which can be used in place of it whenever the desired field can be regarded as having negligible time variation. Values for $F_u'(50, 10)$ can be taken from standard curves such as those given by Allen.[5]

This concludes the description of the location probability method. It has consisted of three principal parts: 1) Introduction of the concept of a cell and presentation of the basic cell statistics, involving the time-dependent field strength $E_i(t)$ and the time-invariant T per cent fields $F_i'(T)$ for all values of T at each site in the cell, and finally, the cumulative distributions $F'(L, T)$ for all of the sites in a statistically representative sample of the population of uncorrelated sites in the cell; 2) introduction of the concepts of a standard reference receiving plant, of a signal-to-noise acceptance ratio, of service, time availability of service, of location probability, and finally, description of the procedure for constructing a service map through the use of the $F'(50, 50)$ data and the standard cumulative distribution function $N(L)$; and 3) introduction of the concept of signal-to-interfering signal acceptance ratios, formation of the $A(L, T)$ functions and description of the procedures for relating them to the standard $F'(50, 50)$, $F'(50, 10)$, and $N(L)$ data, and description of the procedure for using these functions in the construction of service maps. A corresponding treatment will now be given for the acceptance ratio method.

Acceptance Ratio Method

The acceptance ratio method, like the location probability method, involves subdividing the area around the desired transmitting antenna into cells, the same criteria for specifying the size of a cell being applicable to both methods. The acceptance ratio method was conceived as a replacement for the location probability method on the ground that the available knowledge about the field distributions in space and time over typical terrain did not seem sufficiently precise to justify the use of such an elaborate mathematical framework as has been built up around the location probability method. To be more specific, it was considered that the procedures which had been provided for evaluating the quantities $F'(L, T)$ for desired and undesired fields rested on assumptions the validity of which could not readily be assessed on the basis of available data. As was pointed out earlier, the procedure requires that some specific form be assumed for the distribution of $F'(L, T)$ in both L and T. It is evident that whatever form of distribution is assumed, there will remain uncertainty regarding the basic suitability of the chosen form for the physical situation being considered. Even if the form is appropriate, that is, even if a normal distribution is a better choice then, say, a Rayleigh distribution, there still remains the problem of assigning numerical values to the constants which define the particular normal distribution to be used. Thus, numerical values must be assigned to k, $M(T_0)$, and $F'(50, 50)$ before (2) can be applied in the noise-limited case, and corresponding assignments must be made before the interference-limited case can be treated.

It is the objective of the acceptance ratio method to arrive at a specification of what grade of service is available within a given cell purely on the basis of $F'(50, 50)$ levels for the desired field and of $F'(50, T_0)$ levels for the dominant interfering field without recourse to assumptions concerning the way in which the $F'(L, T)$ functions vary with L and T. Thus, standard $F(50, 50)$ and $F(50, T_0)$ data would be required, but no use would be made of cumulative normal distribution functions. In order to realize this objective, the acceptance ratio method defines the limit for any given grade of service not in terms of the percentage of locations within a given cell at which a designated field strength level is exceeded for a specified percentage of the time, but simply in terms of whether the median field over the cell is large enough to override noise and interfering signals. The minimum acceptable desired field is determined by the noise characteristics of a specified standard reference receiving plant in the noise-limited case and by the strength of interfering signals arriving in the cell from various directions in the interference-limited case.

In addition to avoiding the use of assumptions concerning the form of the distribution of $F'(L, T)$ in L and T, the acceptance ratio method also seeks to provide for the demarkation of service grade limits solely on the basis of the new data developed during the period of operation of TASO. These data are of two principal kinds. One is the system of median curves and deviation formulas developed from the TASO data by Dr. LaGrone.[7] The other is a set of median curves and time-fading curves developed by the Bureau of Standards from a separate body of data. It has been proposed as part of the procedure for the acceptance ratio method that the field strengths obtained through the application of the TASO median curves and deviation formulas be regarded as $F'(50, 50)$ values for the desired field and that the Bureau of Standards curves be used to provide $F'(50, T_0)$ values for fields due to interfering stations when the latter are too remote from the cell in question to permit application of the LaGrone method.

Up until this point, discussion of the acceptance ratio method has been in general terms in order to outline the essential features of the philosophy on which it is based. Next to be presented is a detailed description of the method itself. Whereas an analysis in terms of the location probability method was ordinarily built around a single standard reference receiving plant so that only a single set of acceptance ratios would be encountered, the acceptance ratio method proposes to use a different reference receiving plant for each grade of service. TASO has recommended the use of three grades of service, to be designated Principal City, Urban, and Rural, and so the acceptance ratio method proposes the use of three reference receiving plants. The suggested characteristics of these plants would be derived from the TASO Panel 2 data on the characteristics of actual receiving plants observed in the field, and this would be done in a manner intended to establish for each grade of service a reference receiving plant whose characteristics would especially suit that plant for use in the prevailing environment and at the same time permit that plant to be assembled from a judiciously chosen but readily available selection of components. Thus, a receiver used as a standard reference receiver for rural service would be equipped to perform more satisfactorily with a weak signal from the desired station than would one designed as a standard receiver for principal-city service. This would mean that it would have higher sensitivity and lower noise factor. Similarly, it would be equipped with a high-gain antenna to which it would be connected by a transmission line which was laid out and maintained with more meticulous care than would be necessary or worthwhile in a principal-city installation. In the same way, this receiver would be provided with above-average capability for rejecting adjacent-channel and co-channel television signals because of the relatively high likelihood that such interfering signals might be present in sufficient strength to compete seriously with the desired signal.

It is thus to be considered that three standard receiving plants have been specified. Consider first the use of the principal-city standard receiving plant in arriving at the boundary contour determining the limit of the principal-city service area. It is assumed that the desired signal is sufficiently strong throughout the region receiving principal-city service so that any interfering signals which may be present can usually be safely ignored and the boundary fixed solely on the basis of the signal-to-noise acceptance ratio for the standard receiver. Since the noise factor and input noise level of the standard receiver are to be specified initially, and since a signal-to-noise acceptance ratio for principal-city viewers is also to be determined from subjective tests, the minimum acceptable level of desired signal for the standard receiver can be deduced. The $F'(50, 50)$ contour corresponding to this field strength level then becomes the boundary of the principal-city service area.

Next, consider location of the outer boundary of the urban service area. This, according to the acceptance ratio method, is to be the contour on one side of which the urban standard receiving plant gives satisfactory service and on the other side of which it does not. Service on the other side may fail to be satisfactory for either of two reasons. One is that the signal-to-noise ratio may be below the signal-to-noise acceptance ratio, and the other is that the signal-to-interference ratio may be below the signal-to-interference acceptance

[7] A. H. LaGrone, "Forecasting television service fields," this issue, p. 1009.

ratio. The desired contour is to be located by considering each type of signal degradation separately and then taking appropriate account of which influence is predominant in each individual cell. This will give rise to two separate contours. One contour will be that along which the $F'(50, 50)$ level of the desired signal is just high enough to permit the signal-to-noise acceptance ratio to be exceeded. This would then be the outer boundary of the urban service area if no interfering signals were present. The other contour will be that along which the $F'(50, 50)$ level of the desired signal and the $F'(50, T_0)$ level of the interfering signal are in such ratios that the ratios of the resulting signal voltages at the receiver input terminals just barely exceed the signal-to-interference acceptance ratio appropriate to the particular type of interfering signal under consideration. This ratio of field strength levels, of course, would need to be determined through consideration of the ability of the receiving antenna to discriminate against the interfering signal by virtue of the fact that the desired and the interfering signals generally arrive from different directions. The acceptance ratio method in the form most recently described[3] thus yields a contour for constant signal-to-interference voltage ratio at the receiver input terminals determined by a constantly varying ratio of desired-to-undesired signal field strengths at the receiver antenna. The variability of the latter ratio, of course, is attributable to the fact that the desired and interfering signals are arriving from directions with constantly varying angles of separation between them.

Returning to the two contours which would be found through the above procedures as the outer boundaries of areas receiving noise-limited and interference-limited service, respectively, it is next necessary to construct from these contours a single contour representing the unqualified outer boundary of urban service. This is to be done by constructing a new contour around the area which is simultaneously enclosed by *both* of the previous contours, so that both acceptance ratios will be exceeded in all cells enclosed by the new contour. In other words, the new contour will follow in every direction from the transmitting antenna whichever contour lies closer to the antenna. This procedure for establishing the location of the boundary for urban service will certainly be valid if the desired signal is constant in time. In the event that this constancy does not exist, the acceptance ratio method would propose to assume a tendency for positive and negative excursions in the fields to cancel each other, thereby permitting the median fields $F_d'(50, 50)$ and $F_u'(50, 50)$ to be used, where the subscripts d and u have the same meanings employed in describing the location probability method.

In the location of the boundary contour marking the outer limit of rural service, exactly the same procedure used in the case for urban service would be repeated, the standard rural receiving plant now being used as the basis for arriving at the appropriate acceptance ratios.

The following criticism has been leveled at the acceptance ratio method: As has been seen, the proposed method for fixing the boundary of an area receiving a given grade of service is such as to make the median field strength of desired signal on one side of the boundary just high enough to override noise and interference, while the median field on the other side is just short of being high enough. Some distance inside this boundary, that is, on the side toward the transmitter, the median field will evidently be appreciably greater than the value which yields a barely acceptable picture. Similarly, some distance outside this boundary the median field will be appreciably less than this minimum value. However, the acceptance ratio method provides no means for arriving at a number representing the percentage of time that an acceptable picture can be expected when the median field has any particular value. At the boundary itself, the picture will be acceptable only 50 per cent of the time. This, presumably, is too small a percentage of time to permit the service to be regarded as satisfactory. Some distance closer to the transmitter the percentage is higher, but the acceptance ratio method offers no means for determining how much higher. At some particular distance closer to the transmitter, the percentage will be just high enough to permit service to be regarded as barely satisfactory; but no means are provided for determining this distance, and hence, a contour cannot be constructed through such points. Such a contour, it would seem, should logically be used as a service boundary rather than that given by the acceptance ratio method. Defenders of the acceptance ratio method argue, on the other hand, that because of the uncertainty in the time dependence of the data which must be used with the location probability method, the location of iso-service contours for time availabilities other than 50 per cent is necessarily more subject to error than is that for those of 50 per cent.

Summary and Conclusion

To the casual reader, it will be plain at this point that use of the location probability method necessarily involves very extensive mathematical manipulation, and that relatively few mathematical operations are involved in using the acceptance ratio method. Presumably, he will wonder if the location probability method offers sufficient advantage over the acceptance ratio method to justify the use of the former in spite of the greater mathematical complexity of the operations involved. He might first recognize the obvious fact that no advantage will be gained at all if use of a more elaborate method does not lead to a result superior to that available from the acceptance ratio method. As has been seen, application of the location probability method involves the use of previously available experimental field strength data. If these data are not properly suited to the situation under consideration, then it would seem difficult to justify the additional mathematical labor involved. The Ad Hoc Committee itself, at the very time when it was developing the location probability method, recognized and called attention to the inadequacy of the data with which it had to work. For the next ten years after the development of the location probability method, users of this technique nevertheless had little choice but to use these admittedly inadequate data if they were to use the method at all. One of the most valuable results of the work of TASO was the generation of a new set of experimental data which promised to be more generally valid than were the data with which the Ad Hoc Committee had to work. It is not at all certain, however, that even these data are capable of providing as much information on the time and location variability of the fields as would be desirable for use with the location probability method. The great sensitivity of the location probability method to these time and location variability data is connected with (2). It will be recalled that this equation, in order to yield values for $F'(L, T)$, must have substituted into it suitable values for $N(L)$ and $M(T)$. It will be recalled that these two quantities were specified in (2) as representing cumulative normal distributions, but that they might under appropriate circumstances be replaced by cumulative distribution functions of other forms. One of the most important purposes which must be served by the standard data used with the location probability method is that of providing for the determination of the appropriate forms for these functions.

On the basis of these considerations, it might appear that the acceptance ratio method ought to be used in preference to the location probability method. This, however, is not necessarily a safe conclusion in view of the fact that, inadequate as the standard data are, they may still provide with the probability location method a high enough degree of precision to offset the best accuracy that the acceptance ratio method can offer.

Another very strong argument is available for the location probability method. It has been seen that this method provides measures of the percentage of locations in a given cell which are able to obtain satisfactory service. On the basis of such a number in combination with data on the population density in a cell, it becomes readily possible to calculate the number of people who have service in a given cell for any given value of L. In the case of the acceptance ratio method, on the other hand, it is possible to arrive at a numerical measure for the number of people per unit area capable of receiving satisfactory service only on the boundary contours between regions having different grades of service, since only along these contours can a value be found for L.

In conclusion, it seems that neither method is always clearly superior to the other. In the long run, it seems certain that the location probability method must prove superior, but this can happen only after suitable experimental data are available for use in conjunction with it. In the meantime, when determinations of the types given by these methods are to be made, it seems appropriate that both techniques be considered.

The Television System from the Allocation Engineering Point of View*

ROBERT M. BOWIE†

Summary—**Television allocation is technically dependent upon the properties of the television system comprising, in sequence, the transmitter plant, the propagation path, the receiver plant and the observer. Performance is limited either by receiver noise or by noise and undesired signals entering by way of the receiver antenna. Analysis of this system and its components has led to criteria by means of which service may be defined. These criteria have been incorporated in a procedure for producing maps portraying selected isoservice contours applicable as defining boundaries of the several grades of service. Precision of portrayal is limited essentially by the uncertainty of measurement or prediction of propagation which has led to the use of quasistatistical methods of treatment. Some resulting limitations are pointed out.**

* Original manuscript received by the IRE, February 12, 1960.
† General Telephone & Electronics Labs. Inc., Bayside, N. Y.

THE United States has for some time been confronted with an unresolved television allocation problem arising, not from the lack of assignable spectrum, but rather from significant differences in signal propagation and equipment performance over the wide frequency spectrum assigned to television.

These differences are not astonishing when one recalls that the assigned spectrum extends over almost four octaves.

This great breadth of spectrum is increased considerably over that required to accommodate the 82 channels by the assignment of gaps between the low and high VHF and between the VHF and the UHF. These gaps are equivalent to 55 channels.

Experience during the decade since the UHF band was added to television has demonstrated that the differences in propagation over the broad television spectrum cannot be disregarded, and that ten years have not been sufficient time to reduce the disparity in equipment performance over this spectrum appreciably. It has been pointed out that even with a substantial improvement in performance of UHF transmitters and receivers relative to VHF equipment, such as by the use of parametric amplifiers in the receiver, there will remain at least a 15-db advantage to the VHF in fringe-area performance because of propagation differences alone, while phase anomalies in the UHF wavefront at the receiver antenna site appear likely to preclude the use of UHF antennas having an effective aperture or signal-gathering ability equal to that of VHF antennas. It has become evident, however, that television service must be economically competitive in any one locality. A number of technical approaches to the resolution of this problem are now in various stages of study, evaluation or use, although as yet the FCC has not completed its study and finalized its choice among them. They are listed:

1) "Deintermixing" of VHF and UHF assignments.
2) A two-class allocation plan involving limited broad-area, high-power VHF stations interspersed with less restricted local UHF stations.
3) Shifting all television to UHF.
4) Shifting all television to VHF and
   a) using close-packed allocation principles [1] under which a station's service area would be limited by interference from its neighbor, and not by receiver noise;
   b) obtaining a larger VHF spectrum by trading UHF spectrum to the military.
5) Multicasting, particularly in the UHF, wherein more than one transmitter at the same, or possibly at another frequency, is operated by one station using closed-link interconnection.
6) Rebroadcasting (regardless of ownership of rebroadcast equipment)
   a) at some frequency (boosters);
   b) at another frequency (translators).
7) Employing very-precise-carrier frequency control, particularly with the close-packed allocation plan.
8) The using of directional transmitter antennas, such as with multicasting.
9) Employing cross-polarization of transmissions such as with close-packed allocation, multicasting and boosters.
10) Increasing transmitter power—particularly at UHF.
11) Increasing transmitter antenna heights—particularly at UHF.
12) Reducing aural-to-visual transmitter power ratio,
   a) by increasing visual power;
   b) by decreasing aural power, particularly with close-packed allocations.
13) Improving receiving plant performance in the UHF such as with parametric amplifiers and lower-loss lead-in lines. (The performance of high-quality VHF receiver plants is probably a practical limit here which leaves at least some 15-db poorer fringe area propagation in the UHF relative to the VHF.)
14) Improving receiver plant discrimination against television interference, particularly when close-packed allocation is extensively used, both in UHF and VHF.
15) Satellite transmissions or reflections (not imminent).

It is interesting to note in the above listing that some nine items are concerned with propagation; four are essentially instrumental and two involve both. This points up clearly the critical importance of propagation in the preparation of any sound television allocation plan. The relationship of this factor to the others constituting a television service can best be seen by reference to the Systems Concept Chart of Fig. 1.

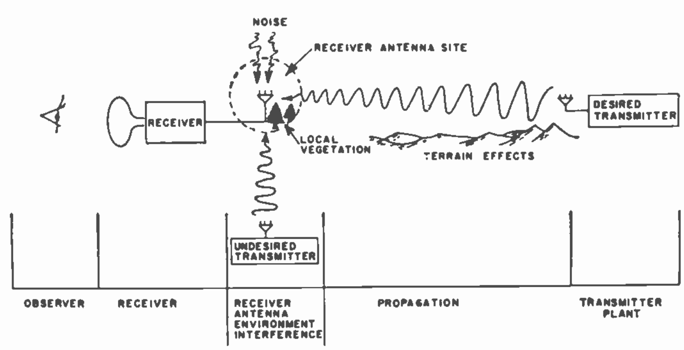

Fig. 1—System concept chart.

I. Systems Concept

The Systems Concept Chart [2] was originally developed by TASO Panel 5, but was tacitly employed earlier by the Ad Hoc Committee [3] in its reports of 1949 and 1950, and by the FCC [4] in its Third and Sixth Reports.

The equipment and propagation paths by means of which a television program is conveyed from a studio into a viewer's consciousness can be regarded, for the desired signal, as a sequential system. Furthermore, with the exception of receiver noise, the interference and undesired signals all enter this sequence at essentially one point, the receiver antenna. The sequentiality with interference entering essentially at one point considerably simplifies the analysis of the system. The process of analysis is not unlike that for a transmission line in which the transfer characteristics of the line elements are known. One can start at either end of the system, and using the characteristics of each element in sequence, can compute at each step the characteristics for the system as seen looking back along the path of computation.

If one starts with the observer, he needs to know the human reaction to varying degrees of picture degradation produced by each of the various types of interference to be expected. This information has been obtained in a consistent manner for all of the major types of interference by TASO Panel 6 (Levels of Picture Quality). As an example of its findings, a curve providing this kind of information for lower adjacent-channel interference is shown in Fig. 2. There are, of course, similar curves for the other forms of interference.

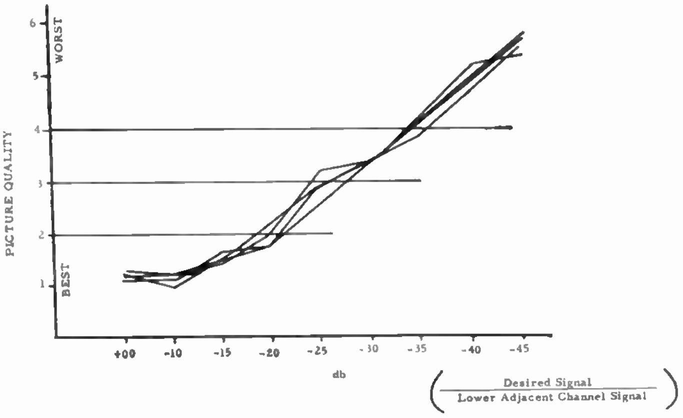

Fig. 2—Graph of picture quality vs ratio of desired signal to lower adjacent-channel interference (from report of Panel 6).

The ordinate, picture quality, is a statistically obtained measure of human satisfaction, while the desired-signal-to-lower-adjacent-channel-signal ratio is expressed in db. Similar curves have been prepared for upper adjacent channel, random noise and various forms of co-channel interferences. In all cases the ratios apply at the input terminals of the receivers used in the tests. Thus, to transform the curves to apply at the receiver antenna location, it is necessary only to have available the characteristics of the lead-in line and the antenna. The latter must include the directional properties of the antenna, because the desired and undesired stations will usually have different bearings from the receiver location.

Actually, it is not necessary for allocation purposes to transform each curve in its entirety, but merely to transform certain critical or limiting numbers to the antenna location. If the FCC were to specify the three grades of television service recommended by Committee 5.3 of TASO Panel 5—namely, Principal City, Urban, and Rural—then the Commission would first need to select the lower limit of picture quality applicable to each grade of service. For illustrative purposes here, these limits have been chosen to be as 2, 3 and 4, respectively, on the picture quality scale. If one now considers the case of lower adjacent channel interference, the undesired signal cannot exceed the desired one by more than 20, 26 and 34 db, respectively, for the three grades of service. These values have been read from the curve of Fig. 2. The reason for permitting the undesired lower adjacent-channel signal to be much stronger than the desired signal for an acceptable picture is that television receivers have strong rejection against lower adjacent channel signals built into them. Using the method just described, one can develop three limiting ratios corresponding to the three grades of service for each of the various types of interference for which the Commission wishes to set limits. These limiting ratios, expressed in db, could be tabulated in the following manner where the blank spaces would be filled in with figures applicable at the receiver input for the qualities of picture specified by the FCC.

	Principal City	Urban	Rural
Upper adjacent channel			
Lower adjacent channel			
Co-channel			
Image			
External random noise			

To transform these limiting ratios as tabulated to apply at the receiver antenna site, it is necessary to know, for each grade of service, what quality of typical receiver plant the Commission wishes to specify. When the Commission specifies a typical receiver plant for a grade of service, it would, in essence, be specifying the transfer characteristics of the antenna, lead line [5] and receiver. In the TASO Report [6], such typical transfer characteristics have been selected for illustrative purposes and the computations have been carried out yielding, for the lower adjacent-channel case, interference ratios applicable at the receiver antenna site. The resulting ratios are 12, 32 and 59 db, respectively. These, then, are the factors expressed as db ratios by which the lower adjacent channel signal may exceed the desired signal for a just acceptable picture as defined earlier. These db ratios at the antenna location then become "the critical numbers" for television allocations.

To carry out the calculations, it was necessary to assume that the FCC had selected fixed values for the antenna's discrimination against undesired signals arising from the directional characteristics of the antenna. Otherwise, different sets of ratios would apply in different directions about the receiver antenna. Later in this report, that simplification is removed.

The "transfer" characteristics of the receiver plant include such receiver and antenna characteristics as the adjacent-channel rejection ratios, image rejection, receiver noise factor, lead-line loss and antenna aperture or λ factor and gain. In general, the antenna characteristics are functions of both azimuth angle and channel number. To assist the FCC in its selection of typical receiver plant characteristics, TASO Panel 2 compiled comprehensive tabulations based upon extensive surveys of sets and antennas in manufacture [6] in 1958.

II. Critical Numbers

By the process just described, it is possible for the FCC to arrive at a set of critical numbers for each grade of service and to specify, in terms of field strength ratios [7] at the receiver antenna location, what signal is deemed necessary to render a particular grade of service. The critical numbers now become the terms in which to express the three limiting isoservice contours that define the boundaries of the three grades of service. More will be said of these contours later.

III. Prediction of Propagation

The most elusive and probably, therefore, the most critical task of TASO has been to provide means for predicting, with useful accuracy, where and how much television service will be rendered. The critical numbers just described provide means for defining service in terms of field requirements at a site. What is needed beyond this are means for predicting the propagation of the desired and the undesired signals from their respective transmitters to arbitrary receiver sites in the service area. Unfortunately, this cannot be done with meaningful accuracy for any one receiver site because propagation is subject to variation with frequency, terrain, gradient of the index of refraction of the atmosphere, the time of day and year, and the vegetation in the vicinity of the receiving antenna. Theoretical formulas exist for propagation over a smooth earth of arbitrary conductivity as a function of frequency, taking into account different gradients of the atmospheric index of refraction. However, basic theory and mathematics for coping adequately with irregular terrain and local clutter do not exist. It has been found necessary, therefore, to treat propagation on a statistical basis for both time and location. This means that one cannot predict precisely what desired and undesired fields will be laid down at a receiver antenna site, but rather can predict the probabilities of laying down these fields. Diurnal variations in field strength at a point near or beyond the radio horizon may, for example, be of the order of 15 to 20 db, while seasonal variations are of the same order. In like manner, the fields experienced at various locations in a given locality can vary by even greater amounts, particularly if the terrain is rough. It is customary to denote by $F'(L, T)$ that field which can be expected to be exceeded in L per cent of locations in a locality for T per cent of the time by a specified transmitter plant. For example the $F'(50, 50)$ field will be exceeded in half of the randomly selected receiver sites in the locality for half of the time. The term "locality" is somewhat vague for lack of any clear-cut criterion for its size. It must be large enough so that readings are not related to each other as they might be if taken on adjacent house tops, yet it must not be so large as to contain excessive variations with distance from the transmitter or with major changes in terrain. The principal dimensions of such a locality are of the order of a few miles to a few tens of miles. More will be said of this later in discussing portrayal of coverage. Suffice it to say here that this vagueness does not destroy the usefulness of the concept and provides a very necessary smoothing factor in mapping the fields about a transmitter for allocation or assignment purposes. Allocation, or even assignment, is a "broad-brush" type of task from which local detail must be omitted in the interest of broad comprehension and decision.

Since $F'(L, T)$ fields such as $F'(50, 50)$ fields cannot be calculated by purely theoretical means, various methods of obtaining them empirically have been developed. Probably the best known of these are the 1952 $F(50, 50)$ curves [8] contained in the Rules and Regulations of the Commission (Section 3699 of these Rules). They were obtained by averaging available propagation data for all parts of the country at all times of the year; hence, they are too general for the study of specific station assignments. They have been recommended as Type I curves by Committee 5.4 of TASO Panel 5, as have also those of the FCC-TRR Report No. 2.4.16.

Committee 5.4 foresaw [9] need for three successively more exact and detailed methods for predicting television service field strengths; these were designated Type I, II and III.

Briefly, a Type-I curve is an average empirical propagation curve to be applied on a country-wide basis for broad or preliminary purposes. A Type-II curve would take into account average large area effects such as terrain roughness and meteorology and is believed suitable for allocations and assignments purposes except in rugged terrain. A Type-III curve would permit the prediction of field strength in relatively small areas for specific conditions of terrain and meteorology. It would be useful for allocation and assignments in rugged terrain and for detail studies of assignments in rolling terrain.

A Type-II method or curve should be capable of yielding $F'(50, 50)$ fields on a locality basis throughout the service area of the transmitter. One such method was developed by Howard T. Head [10] and submitted to Committee 5.4. It is of the type in which empirical corrections are made to theoretical propagation curves based on a standard smooth-earth formula. Standard atmosphere is also assumed. A suitable number of radii from the transmitter are laid out on a large-scale contour map and elevations are read at exactly two-mile intervals on each radius. These elevations are plotted on Cartesian coordinates, as shown in Fig. 3, and a best-fit "least squares" straight line is drawn. The intercept on the ordinate establishes the effective antenna height for that radius, while the rms deviation of the points from the line in feet yields the roughness factor R. By analysis of the field data gathered by Panel 4, it has been established empirically that the loss in db relative to the smooth-earth fields is approximately $3.6\sqrt{R/\lambda}$, where λ is the free-space wavelength. This empirical relation was found to hold for both VHF and UHF,

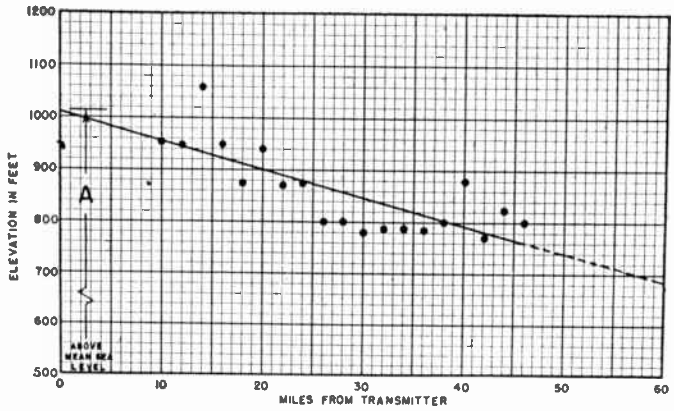

Fig. 3—Elevation sample points and least squares fit.

though better results at UHF can be obtained by also taking forestation [11] into account. The resulting empirical equation involving the percentage of forestation P_f is

$$\text{Loss (db)} = \frac{30P_f + 3.6(100 - P_f)\sqrt{R/\lambda}}{100}.$$

The method has the advantage of relative simplicity, but provides no character along a radius other than a uniformly degraded smooth-earth curve. Committee 5.4 has recommended consideration of this method for allocation purposes, based on further test to gain experience.

Committee 5.4 has recommended for consideration as a Type-III method that developed by Prof. A. H. LaGrone [12] of the University of Texas under contract to TASO. His method provides for the making of empirical corrections to theoretical smooth-earth propagation curves, modified, however, to account for the effect of local clutter at the receiver site. The smooth-earth calculations are made by using local Weather Bureau average data for the gradient of the atmosphere's index of refraction; this gradient affects the effective radius of the earth.

During the development of the empirical formula, it was noted that as the terrain being studied approached the ideal smooth-earth, there remained an unaccounted degradation which appeared to bear some relation to the level of forestation or local clutter at the receiver site. By the preceding method, Dr. LaGrone estimated this form of degradation to be -1 db for the lower VHF, -4 db for the upper VHF and -22 db for the UHF. This modification to the smooth-earth formula is applied before computing the further degradation in the field at a point due to the effect of the terrain intervening between the point and the transmitter. The determination of field strength is made for a point in the service area of the transmitter by drawing an accurate radial profile through the point and applying the following empirical formula to find the degradation from the modified smooth-earth curve:

$$\begin{aligned}\text{Loss (db)} &= C\left[-\left|h_1 - h_2\right|^{\frac{1}{2}}(\exp - d_{1r}) - \left|h_2 - h_3\right|^{\frac{1}{2}}(\exp - d_{2r})\right.\\ &\qquad \left. + \left|h_3 - h_r\right|^{\frac{1}{2}}(\exp - d_{3r})\right]\end{aligned}$$

where

h_1, h_2, h_3 and h_r are elevations in feet above mean sea level,
d_{1r}, d_{2r}, and d_{3r} are distances in miles as defined in Fig. 4,
$C \cong 1.6$ for VHF, and
$C \cong 2.2$ for UHF.

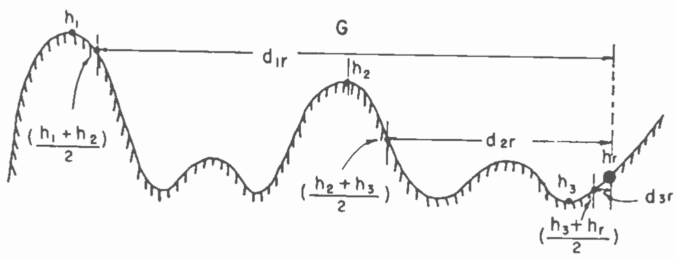

Fig. 4—Sample cases of terrain (measure height in feet and distance in miles).

The second part of Reference [12] contains additional typical hill configurations together with appropriate modifications of the empirical formula. The presentation here is not intended to be complete and the reader is commended to the reference for full information.

Unfortunately, this method has been derived using only about half of the Panel 4 data. However, cross-correlations as high as 0.8 have been obtained in making comparisons of computed fields with Panel 4 data for rough terrain. Further experience with this method is proposed before its full adoption for allocation and assignment purposes. It should be noted that this method yields more specific and detailed field information than the method described earlier, but at the cost of greater computational effort.

IV. Specification of Service

From the standpoint of the receiver plant, service can be defined, for the purpose of this report, as the transform of the level of picture quality into the corresponding desired field strength and interference ratios at the receiver antenna site. The transformation is brought about through the use of the characteristic of the receiver plant and, hence, service is explicitly dependent upon a stipulated receiver plant. It is necessary at this point to give special attention to the receiver antenna pattern, since this is one of the essential characteristics of the receiver plant. If it is assumed that the antenna maximum is directed toward the desired signal, the relative bearing of an undesired signal must be considered in computing the corresponding interference ratio. Thus, each interference ratio is a vector quantity and could take the form of a polar plot.

If a particular level of picture quality is now set as the limit for a given grade of service such as Urban, then the corresponding limiting service required by the receiver antenna can be expressed in terms of a set of criteria. This set will include a value of desired signal strength and values for each of the interference ratios such as co-channel, lower adjacent channel, image and so on.

At this stage, the location of the receiver site relative to the desired and undesired transmitter is arbitrary; hence, as before, each criterion (except desired signal) is really a polar plot. However, for ease of manipulation, values for several selected directions could be tabulated as illustrated below.

yields the corresponding interference ratio could be replaced directly by the median, or $F_d'(50, 50)$ and $F_u'(50, 50)$ fields where the subscripts d and u denote desired and undesired signal [13], respectively.

The extension of the principle that the effects of small excursions about a mean are self-compensating to the case of wide excursions is fraught with some uncertainty. However, because of the lack of data on which to base a better choice, there seems to be no obviously superior alternative. Proceeding then with the use of median fields, the limit of a grade of service such as Urban would consist of a set of criteria as before, but with the median field values replacing the former steady-state fields.

It has been the practice of the FCC to express the limits of service in terms of field probabilities other than 50 per cent. For example, Grade A service requires that

	Principal City				Urban				Rural			
	0°	60°	120°	180°	0°	60°	120°	180°	0°	60°	120°	180°
Desired field strength												
Lower adjacent-channel interference ratio												
Upper adjacent-channel interference ratio												
Co-channel interference ratio												
Etc.												

Thus far, service has been considered only under steady-state conditions. Since these do not prevail in practice, the statistical nature of the service rendered at a receiver site must be introduced. It is obvious that each field at the receiver antenna site may vary quite independently in such a manner that the actual interference ratios experienced in the locality of the receiver site will vary both with time and from site to site in the locality. It is difficult to give quantitative figures for the effect of such variations upon service because they are dependent upon viewer reaction to both picture quality fluctuations and inhomogeneity of receiving conditions in a locality. To obtain meaningful figures here, one would need to conduct statistical viewer tests on the effects of various types of fading and upon the sociological effect of inferior and superior sites in the locality. Lacking these, one might make a beginning by stating that for mild excursions from the mean in both time and location, the effect of positive excursions would be substantially offset by negative ones. Under this condition, the desired field and the interfering field whose quotient

pictures of acceptable quality be obtained in the best 70 per cent of sites in a locality for at least 90 per cent of the time. It is clear, of course, that if the time and location distribution functions for the various desired and undesired fields involved are known, one can always find from the median field values other sets of field values that will yield the desired quality of picture for other percentages of locations and times. This is essentially what is done in the location probability method as employed by the Commission [14]. For a mathematical treatment of this subject, the reader is referred to the companion paper by D. C. Livingston [15].

Two disadvantages of using nonmedian field values are that they have a greater uncertainty than the 50-per cent values and the labor of computation is greater. Probably the major attraction lies in an intuitive feeling that the specification of service in terms of field probabilities higher than 50 per cent is more realistic.

It has been the practice with the location probability method to employ a single specified receiver plant for both currently specified grades of service and to distinguish between them by requiring a higher level of location probability for the better grade of service. Thus, for Grade A service, an acceptable picture must be available in the best 70 per cent of locations for at least 90 per cent of the time while for Grade B, an acceptable picture is to be expected in only the best 50 per cent of locations for 90 per cent of the time. However, the location probability method, in its broadest interpretation such as evolved during the life of TASO, need not be limited to a single specified receiver plant for all grades of service [16].

Also during the life of TASO, a simplifying modification of the location probability method of specifying the limit of service was evolved which became known as the acceptance ratio method. It employs median-service fields and also different standard receiver plant for each grade of service.

In both methods, for lack of better data, it has been found expedient to employ the field data as though having a 50-per cent time probability. The usual practice is to take data during daytime hours only and at such times of the year as meet measurement schedules; hence, such data are not truly time-median values. Further, it is recommended that field strength measurements be made along roads using a 30-foot antenna height. Hence, the field data contain a "road" bias as well as the "temporal" bias. These same biases exist in the Head and LaGrone methods of field prediction, as both are empirically dependent on the data of Panel 4 which were taken in this manner. It was felt by Committee 4.1 of TASO Panel 4 that steps should be taken to reduce these sources of uncertainty [18].

Regardless of whether the location probability or the acceptance ratio method were used, the set of "critical numbers" employed in specifying the limits of the grades of service would continue to look like the tabulation given earlier in Section IV, but with the spaces filled in with db ratios that take into account the statistical nature of television service.

V. Isoservice Contour and Portrayal of Coverage

The last technical step in the preparation of data for use in allocation or assignment is the production of a map (or maps) of the area about a transmitter showing where service is available and how much. The map should be reasonably unique so that maps prepared by different engineers from the same basic data will not exhibit major differences. Such a map must be capable of showing two or more grades of service and must be fine grained enough to show the relative coverage in different directions from the transmitter and in different areas. Finally, it must be possible to draw the map in a straightforward manner with reasonable effort by means of suitable propagation curves and data, and to confirm the predicted areas from a reasonable number of field-strength measurements taken in an appropriate manner.

Though there was not evinced in TASO a full unanimity regarding a suitable method of portrayal, there was a consensus favoring a method of the type about to be described It is believed that this method satisfies the criteria just set forth which have been derived from those in the Report of Committee 5.3 [19].

It appears desirable and proper that the limit of a grade of service be an isoservice contour. Since it is recommended that there be three grades of service, there would then be three corresponding outer limiting isoservice contours. Disregarding minor enclaves and exclaves, it is evident that the grades of service will lie one outside the other with the Principal City grade at the center. About the latter will be the Urban grade as an annular ring and beyond that another annular ring representing the Rural service area. The inner boundary of each such annular service area will be set by the outer limit of the next higher grade of service while the outer limiting isoservice contour will be established by the criteria for the grade of service directly involved.

Since service, as previously defined, depends on the specified receiver plant, then, if a different receiver plant were specified for each of the three grades of service recommended by TASO, there would be three sets of limiting isoservice contours. In such a set, there would be a separate isoservice contour for the desired signal and for each form of interference. A simplified set of such isoservice contour, using only three contours, is shown in Fig. 5.

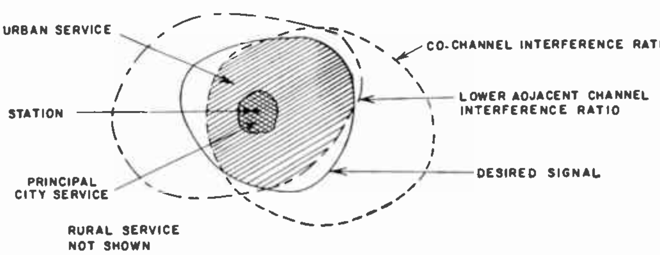

Fig. 5—Examples of the manner in which a service area is bounded by overlapping contours of constant desired signal strength and interference ratios.

In general, these various limiting isoservice contours would not be expected to agree. The service area as shown cross-hatched in Fig. 5 is that area which is within all of the contours, excluding, however, the areas of the higher grades of service. In Fig. 5 the Principal City service area is so excluded.

The drawing of any contour on a map first requires the plotting of points having the appropriate value for that contour. This is to be done for the limiting isoservice contour associated with each form of interference. Because of the great variability in individual field strength measurements and the necessity to hold down the labor required to obtain the necessary data, Committee 4.1 of TASO Panel 4 has proposed the following method for obtaining the points for plotting [20].

Draw on the map of the area about the transmitter a series of concentric circles ranging in radius from five to ten miles less than the expected Principal City contour to slightly beyond the expected Rural contour. There should not be less than three or more than five such circles, and their radii should be chosen in 10- to 15-mile steps. Divide the area about the transmitter into eight 45° sectors. This plan is shown for a typical VHF station in Fig. 6. The total number of data points should be equal to about 80 times the number of circles, but distributed approximately as the square roots of the radii of the various circles. Note on Fig. 6 that these radii and circles constitute the center lines of cells such as the one cross-hatched in the figure. A cell can now be defined as a locality with definite boundaries. The computations proceed on a cell basis.

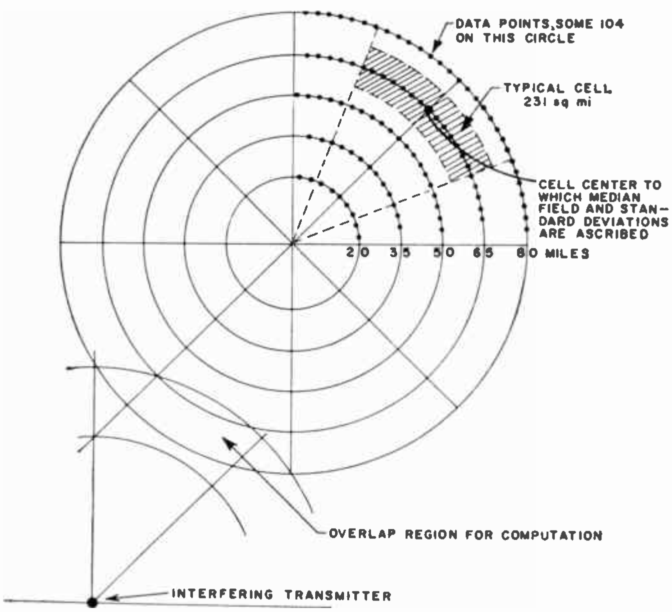

Fig. 6—The cell layout about a transmitter.

Up to this point, it has not been made clear whether the field strength data at the points on the circles are to be computed or measured. The plan was drawn for field measurements, but with some modifications to line up the data points along radials, computation could be used conveniently. The median field is then determined for each cell and the median value ascribed to the center point of the cell. The standard deviation is also determined for the cell and ascribed to its center. The procedure as described is intended to apply particularly for the service field. However, with a little care, similar but intersecting circles could be drawn about nearby interfering transmitters as shown in Fig. 6 and the interfering fields computed (or measured) for the overlapping, interfering cells. If, however, the interfering transmitter is remote enough to be in the tropospheric transmission range, resort may be had to the tropospheric propagation curves provided to Committee 4.2 of TASO Panel 4 by The Central Propagation Laboratory of the Bureau of Standards at Boulder, Colorado [21].

From this procedure there would result a full set of desired and interfering field values ascribed to the center of each cell about the desired transmitter. Sets of interference ratios could then be computed at each cell center. However, these interference ratios would generally not be exactly the desired ones for the limiting isoservice contours. This is because of the coarseness of the cell structure. The desired points for the various interference ratios can then be located along each 45° radial by linear interpolation from the values at the adjacent cell centers. The particular limiting isoservice contours associated with various interference ratios can then be sketched.

VI. Selection of "Critical Numbers" for Limit Contours

It is believed that valuable information can be gained from the observations of TASO Panel 3 that would be useful in the selection of "critical numbers" for specifying the limiting isoservice contours. Panel 3 observed [17] that as one recedes from the transmitter through the service area, the quality of the receiver plant tends to improve in such a manner that the received picture quality is substantially constant out to the point at which it becomes economically prohibitive to make further improvements. One of the curves prepared from the Panel 3 data is reproduced here as Fig. 7. Examination of this curve and the others in Reference [17] shows a substantially constant level of picture quality, with only the expected statistical spread, out to the point at which the curve appears to break downward. This is the point at which further receiver plant improvement becomes uneconomical. It would seem logical, therefore, to select a single level of picture quality for the first two grades of service. The evidence from the findings of Panel 3 indicate that public reaction would place the limit at $2\frac{1}{2}$ or 3.

It is interesting, also, to examine the data that define the break downward in the level of picture quality vs distance curves. As Panel 3 has pointed out in its report (TASO Rept., p. 221), this break appears to come, for the lower VHF, at the point at which the field strength for the desired signal drops to 40–45 dbu. For the upper VHF the figure appears to be 50–55 dbu. These figures appear worthy of consideration in the setting of limits of service for cases in which the limit is expected to be set by receiver noise.

For the outer or Rural Grade of service, one is operating on the declining portion of the curve. From Fig. 8, taken from page 208 of the report of Panel 3, it is evident that the density of points falls off with decreasing level of picture quality at a value of about 4.5, though the drop in density is not sharp. Examination of the Panel 3 curves (TASO Report, pp. 208–215) shows that for the low VHF the corresponding field strength to

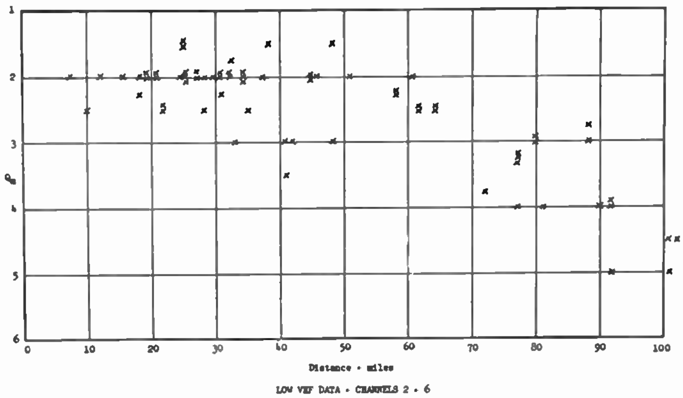

Fig. 7—The VHF data—Channel 2–6.

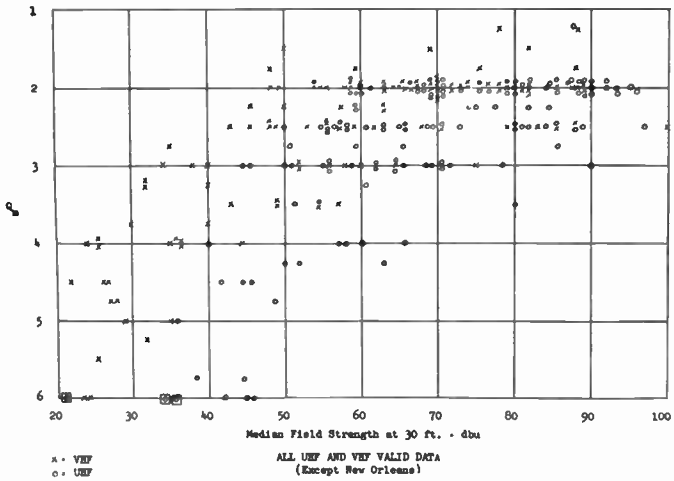

Fig. 8—All UHF-VHF valid data (except New Orleans).

be about 25 dbu. At the high VHF it is about 30 dbu and for the UHF about 50 dbu. These figures probably chiefly represent reception limited by receiver noise, as the observations were made in the daytime when television interference tends to be at a minimum; hence, they would be of interest in selecting the critical number to define the outer limiting contour for desired signal strength.

Concluding Remarks

Though TASO has contributed extensively to the available body of data on television service and to the orderly understanding of the mechanisms of allocation, there remain points on which continued elucidation and improvement are needed. Some of these are listed here to stimulate further attention.

1) It has been pointed out that temporal biases exist in the recommended method of taking data and in the two proposed formulas for field prediction. Some worthwhile correction could probably be made to new field strength data obtained by the method of Committee 4.1 if note were taken of the time of day and year for each measurement and if generalized correction curves were worked out to show how much the field at various times of day and year can be expected to vary from the all-time mean. It is possible, also, that correction factors could be worked out for the field computation methods of LaGrone and Head, since they are based on Panel 4 data.
2) The use of interference field data from the curves of Committee 4.2 in computing interference ratios introduces another minor source of error because the data were taken too well. In general, the receiving sites were selected to be quite free of local clutter of the type encountered in most television reception locations. No doubt degradation factors can be worked out for frequency, possibly for topographical roughness and for forestation. It should be borne in mind, also, that these are all-day, all-year medians and their use with uncorrected daytime, seasonal field data introduces some error.
3) The "road-bias" problem remains unresolved. Either the median or $F'(70, 90)$ field strength value computed for a cell really represents the probability of achieving the specified field or better in road measurements, and not necessarily in randomly located receiver plants of the specified quality. Some satisfaction might be gained by examining the data on the level of picture quality vs field strength compiled by Panel 3 (TASO Rept. [6], pp. 208–215). That Panel found, however, that detailed correlations between roadside measurements and adjacent home observations could not be made. Furthermore, the tendency for the receiver plant improvement to compensate for field strength degradation would mask any correlation, since grades of receiver plants were not reported. Additional study needs to be given to this matter.
4) It is recognized that, in general, limits of areas of service will be somewhat distorted circles about the transmitter. Since each limit is actually a selected isoservice contour, this means that the direction of maximum gradient or rate of change of service is perpendicular to this contour, and, hence, is chiefly radial in direction. Accordingly, to be able to set the limit contours most accurately, one needs to have the greater knowledge about the radial, rather than the circumferential, field variation. Presently, however. items of data are planned to be three times as dense circumferentially as radially. Further, for UHF stations, as presently proposed, there could be as few as three data circles about the transmitter to set three service limit contours. This comment points up

the need for some further study of means for improving radial detail, even at the expense of circumferential if necessary. Study is suggested in the following three areas: a) a Type-II method of field prediction having radial variations responsive to terrain; b) the laying out of the cell structure about the transmitter so as to improve radial detail; c) the development of a procedure for taking proof-of-performance field data yielding greater radial detail.

5) The evaluation of the effect of local clutter near the receiver antenna site has been recognized as needing serious attention. Some definite progress on the effect of forestation has been made, but the work needs extension, and it should be pointed out that little is yet understood about the effects of such obstructions as power lines and adjacent buildings.

It is believed that the work of TASO has provided a consistent over-all approach to the technical problems of allocation and station assignment. The salient features of this approach are outlined in the following:

1) The first consistent set of human reaction curves was evolved. These relate picture quality to signal degradation resulting from each of the important forms of interference such that meaningful correlations can now be drawn among the effects of the various forms of interference. Thus, it is now possible to state, for example, the level of lower adjacent channel interfering signal that is equivalent to a stated level of co-channel interfering signal. This is essential in drawing isoservice contours.
2) Sets of television service field data taken from extensive field measurement made in a consistent manner for the entire television spectrum and for the various forms of terrain throughout the United States were compiled. These data have served, and may continue to serve, as the basis of new empirical procedures for predicting service fields.
3) Two partially empirical procedures of service field predictions, applicable in all parts of the country, were developed and recommended for further study.
4) The pertinent characteristics of television receiver plants in production in 1958, from which typical receiver plant specifications may be drawn for allocation purposes, were analyzed and tabulated.
5) Transmitter plant characteristics and costs suitable for use in determining the economic feasibility of various allocation plans were compiled.
6) A philosophy of, and procedures for, the specification of service, the prediction of performance and the portrayal of coverage were set forth.

Through the deliberation of TASO, there have been evolved a broader interpretation of the location probability method of specifying service and a simplified form of this method. The latter reduces the labor of calculation with no significant reduction in the meaningfulness of the results.

Bibliography

[1] Reference [6], p. 362—referred to as "Interference Limited," Principles of Allocation.
[2] R. M. Bowie, "Systems approach to the determination of television coverage," *Elec. Engrg.*, vol. 77, pp. 129–132; February, 1958.
[3] Ad Hoc Committee for the Evaluation of the Radio Propagation Factors Concerning the Television and Frequency Modulation Broadcast Service in the Frequency Range Between 50 and 250 mc, vol. I, FCC Rept. No. 36830; May 31, 1949; vol. II, FCC Rept. No. 54382; July 7, 1950.
[4] "Television Broadcast Service—Third Notice of Further Proposed Rule Making," FCC Rept. No. 47 CFR, pt. 3 (Docket Nos. 8736, 8975, 8976, 9175), March 21, 1951; "Sixth Report and Order," FCC Rept. No. 52-294, 74219 (Docket Nos. 8736, 3975, 9175, 8976), April 14, 1952.
[5] Since the interference ratios of Panel 6 apply at the receiver input, one needs only the antenna and lead line characteristics to transform the limit ratios to the antenna site. However, to use a different receiver as might be specified for another grade of service, the receiver characteristics would be required.
[6] "Engineering Aspects of Television Allocations," Rept. of the Television Allocations Study Organization to the Federal Communications Commission; March 16, 1959.
[7] Since receiver noise is actually generated in the receiver and not introduced at the antenna, its effect is slightly different. Here the FCC would have to specify the minimum field strength of desired signal at the receiver antenna site for each of the three grades of service.
[8] $F(50, 50)$ is a normalized field strength for 1-kw effective radiated power in the direction of the measurement point. $F'(L, T)$ is not normalized and is for a specified transmitter plant.
[9] Reference [6], pp. 403–412.
[10] "A Method of Predicting Average Field Strengths at Television Broadcast Frequencies," Appendix to Final Rept. of Committee 5.4 contained in the Final Rept. of TASO Panel 5.
[11] Howard T. Head, "The Influence of Trees on Television Field Strengths at Ultra High Frequencies," Appendix to Final Rept. of Committee 5.4 in Final Rept. of TASO Panel 5.
[12] A. H. LaGrone, "Forecasting Television Service Fields," Reference [6], pp. 413–447; and A. H. LaGrone, "Empirical Method for Determining the Effect of Uneven Terrain on the Television Signal at a Given Location," Appendix to Final Rept. of Committee 5.4, in Final Rept. of TASO Panel 5.
[13] In taking the quotient, there are other statistical requirements which, however, appear to be reasonably well satisfied in practice. The various $F_u'(50, 50)$ fields must not be correlated and the corresponding field distribution functions must be reasonably symmetrical about the mean.
[14] See also D. G. Fink, "Television Engineering Handbook," McGraw-Hill Book Co., Inc., New York, N. Y., pp. 14-26–14-32; 1957.
[15] D. C. Livingston, "Presentation of coverage information," this issue, p. 1102.
[16] "Report of Committee 5.3 Television Coverage Operator," Reference [6], Figs. 392–396. Also see Final Rept. of Panel 5—Analysis and Theory, Television Allocation Study Organization, the Final Rept. of Committee 5.3 including "Minority Report of TASO Committee 5.3," by Robert S. Kesby, attached thereto and the "Portrayal of Coverage" under "The Overall Technical Task of TASO."
[17] Reference [6], pp. 216–221, 356, 360 and 572–578.
[18] Reference [6], p. 287. See "Concluding Comments on Validity, Accuracy and Extensions," under "The Overall Technical Task of TASO," Final Rept. of Panel 5—Analysis and Theory, Television Allocation Study Organization.
[19] Reference [6], p. 393.
[20] Reference [6], p. 281.
[21] Reference [6], pp. 302–322.

Correction

Britton Chance, author of "Electron Transfer in Biological Systems," which appeared on pages 1821–1840 of the November, 1959, issue of PROCEEDINGS, has requested another and more satisfactory reproduction of Fig. 31 (p. 1838), which appears below.

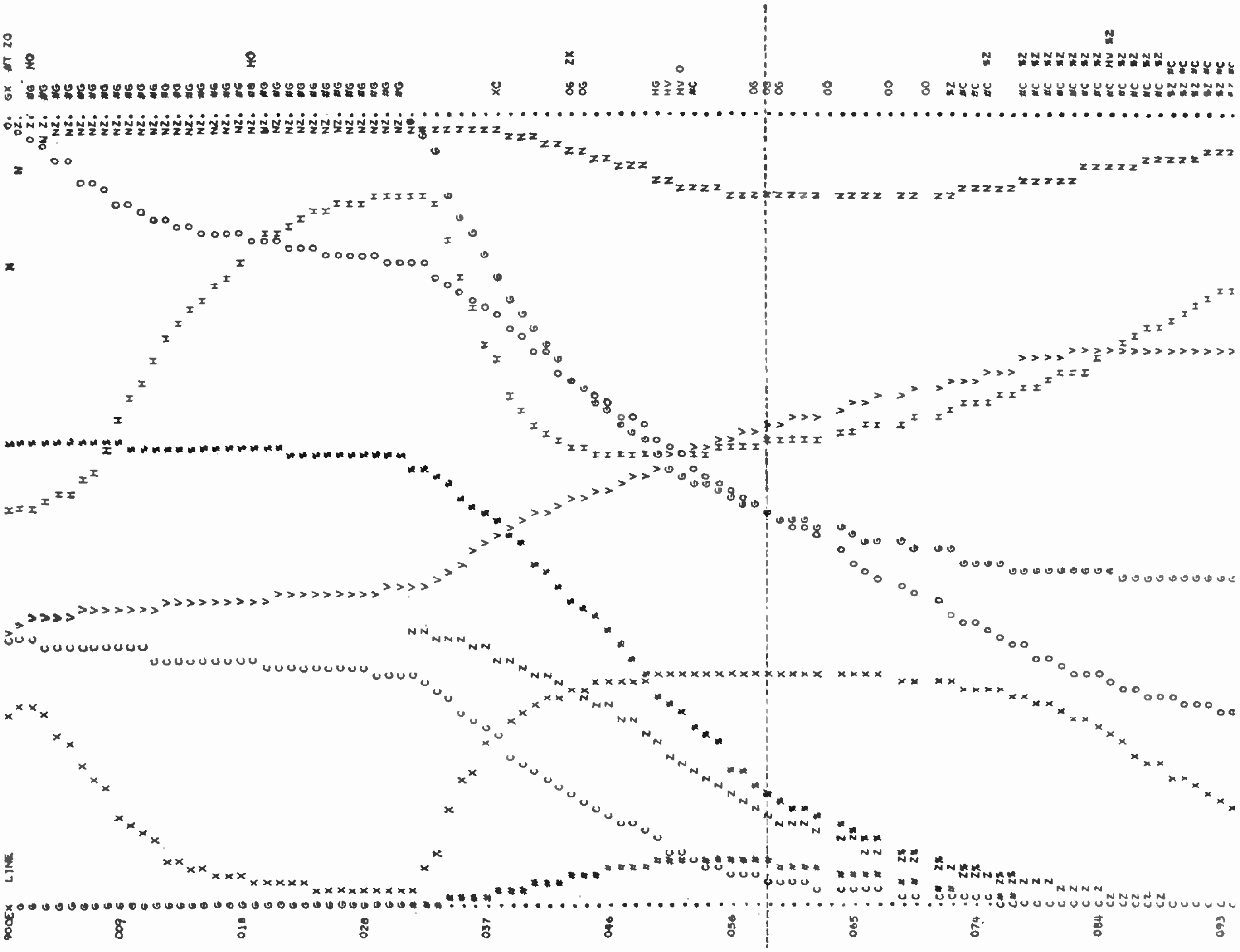

Fig. 31—High-speed printer record of the kinetics of ten intermediates in metabolic control systems of Figs. 29 and 30. The identification of the chemicals is given in Table II. The identification of the time scale at the bottom of the graph, the normalization of the concentrations for the variables and the key to the crossing over of the traces at the top of the graph, are explained in the text (DC-4). (Data obtained with Univac 1, with the aid of the University of Pennsylvania, Computer Center.)

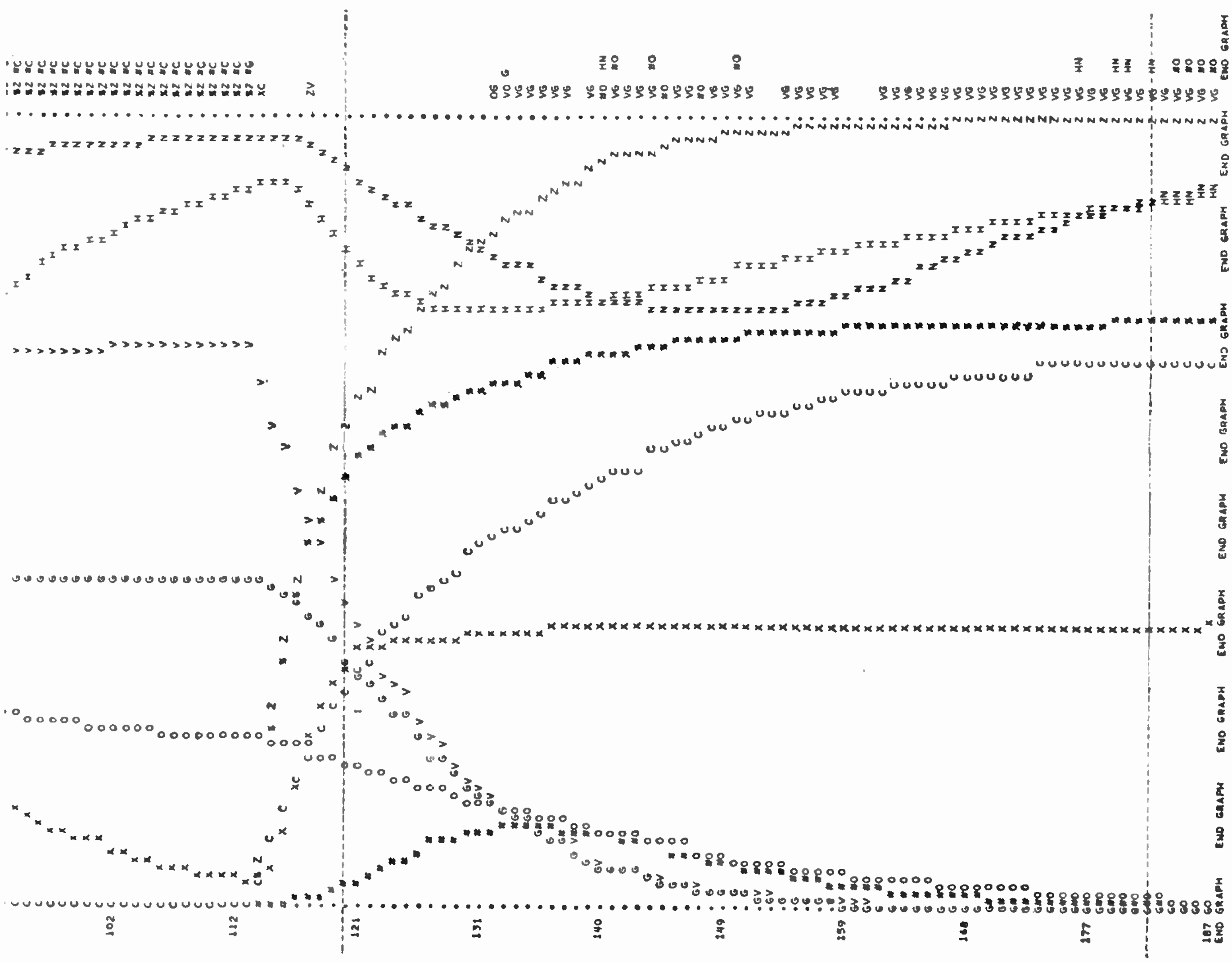

IRE Standards on Television: Methods of Testing Monochrome Television Broadcast Receivers, 1960*

60 IRE 17. S1

COMMITTEE PERSONNEL

Subcommittee on Television Receivers—1952–1956

W. O. SWINYARD, *Chairman*

W. R. Alexander
J. Avins
J. Bell
C. E. Dean
E. C. Floyd
E. C. Freeland
W. J. Gruen
W. R. Koch
C. O. Marsh, Jr.
I. J. Melman
B. S. Parmet
G. A. Rogers
S. P. Ronzheimer

Editing Subcommittee—1952–1956

S. P. RONZHEIMER, *Chairman*

J. Bell
C. E. Dean
G. A. Rogers

Ad Hoc Review Committee—1957–1960

J. AVINS, *Chairman*

E. C. Freeland
W. R. Koch
K. M. St. John
J. P. VanDuyne

Committee on Radio Receivers

G. S. LEY, *Chairman* 1958–1960
D. E. HARNETT, *Chairman* 1956–1958
J. AVINS, *Chairman* 1951–1955
W. P. BOOTHROYD, *Vice-Chairman* 1958–1960
W. O. SWINYARD, *Vice-Chairman* 1956–1958

J. Avins 1956–1960
K. A. Chittick 1956–1960
L. E. Closson 1956–1959
A. S. Goldsmith 1958–1960
D. E. Harnett 1958–1960
D. J. Healey, III 1956–1960
J. J. Hopkins 1956–1959
K. W. Jarvis 1956–1959
J. K. Johnson 1956–1960
W. R. Koch 1956–1960
G. S. Ley 1957–1958
I. J. Melman 1956–1959
G. Mountjoy 1956–1959
J. N. Phillips 1956–1959
L. Riebman 1956–1959
J. D. Reid 1956–1959
L. M. Rodgers 1956–1960
G. A. Schupp 1957–1960
S. W. Seeley 1956–1959
C. L. Spencer 1959–1960
W. O. Swinyard 1958–1960
F. B. Uphoff 1956–1960
R. S. Yoder 1956–1959

Committee on Standards—1959–1960

R. F. SHEA, *Chairman*

L. G. CUMMING, *Vice-Chairman*
J. G. KREER, JR., *Vice-Chairman*
C. H. PAGE, *Vice-Chairman*

J. Avins
W. F. Bailey
M. W. Baldwin, Jr.
J. T. Bangert
W. R. Bennett
J. G. Brainerd
P. S. Carter
A. G. Clavier
S. Doba, Jr.
R. D. Elbourn
P. Elias
G. A. Espersen
R. J. Farber
D. G. Fink
G. L. Fredendall
E. A. Gerber
A. B. Glenn
V. M. Graham
R. A. Hackbusch
R. T. Haviland
A. G. Jensen
R. W. Johnston
I. Kerney
A. E. Kerwien
G. S. Ley
W. Mason
D. E. Maxwell
P. Mertz
H. I. Metz
H. R. Mimno
E. Mittlemann
L. H. Montgomery, Jr.
G. A. Morton
R. C. Moyer
J. H. Mulligan, Jr.
A. A. Oliner
M. L. Phillips
R. L. Pritchard
P. A. Redhead
R. Serrell
W. A. Shipman
H. R. Terhune
E. Weber
R. B. Wilcox
W. T. Wintringham

Measurements Coordinator

J. G. KREER, JR.

* Approved by the IRE Standards Committee, November 19, 1959. Reprints of this Standard 60 IRE 17. S1, may be purchased while available from the Institute of Radio Engineers, 1 East 79th Street, New York, N. Y., at $1.00 per copy. A 20 per cent discount will be allowed for 100 or more copies mailed to one address.

Part 1—INTRODUCTION

Chapter 1—General

1.1 Object

THIS standard replaces IRE Standard 48 IRE 22. S1, "Standards on Television: Methods of Testing Television Receivers, 1948."

At a later date, a standard for color television receivers will be introduced. Reference will be made in that standard to many portions of the present standard which are applicable to color television receivers as well as to monochrome receivers.

1.2 Scope

This standard describes procedures for measurement of the performance characteristics of the picture and sound sections of television receivers. Where specific test conditions are stated, these apply to home broadcast receivers designed to receive transmissions in accordance with the specifications of the United States Federal Communications Commission.[1] Where other conditions apply, appropriate modifications must be made.[2]

Emphasis is placed on over-all receiver performance. Internal characteristics such as the gains and bandwidths of individual stages are not generally considered.

1.3 Standard Test Frequencies

The range of standard test frequencies includes all of the allocated television channels. The present television channel allocations, where A includes frequencies from $470+6(C\text{-}14)$ to $470+6(C\text{-}13)$, and

$$P = 471.25 + 6(C\text{-}14)$$

$$S = 475.75 + 6(C\text{-}14),$$

are as follows:

Channel No.	Channel Allocation mc	Picture Carrier Frequency mc	Sound Carrier Frequency mc
2	54–60	55.25	59.75
3	60–66	61.25	65.75
4	66–72	67.25	71.75
5	76–82	77.25	81.75
6	82–88	83.25	87.75
7	174–180	175.25	179.75
8	180–186	181.25	185.75
9	186–192	187.25	191.75
10	192–198	193.25	197.75
11	198–204	199.25	203.75
12	204–210	205.25	209.75
13	210–216	211.25	215.75
14	470–476	471.25	475.75
15	476–482	477.25	481.75
⋮	⋮	⋮	⋮
C	A	P	S
⋮	⋮	⋮	⋮
82	878–884	879.25	883.75
83	884–890	885.25	889.75

When measurements are not performed on all VHF channels, they should be made on Channels 4 and 10. The picture and sound carriers of these two channels are referred to as the *VHF standard test frequencies.*

Receivers which cover the entire UHF range should be measured on Channels 18, 48 and 79. The picture and sound carriers of these three channels are referred to as the *UHF standard test frequencies.*

1.4 Standard Test Input Levels

Input signal levels may be expressed in either of two ways:

a) In terms of available power (Section 1.4.1), in which case the input is preferably expressed in decibels below one watt.

b) In terms of input voltage, in which case the input is frequently expressed in microvolts or in decibels below one volt and the intended source resistance is stated.

When a standard composite picture signal is used, input level refers to the value during the synchronizing pulse interval. Where a picture carrier with sine-wave modulation is used, the input level is the value of the carrier in the absence of modulation.

Normally, two signal generators will be used so as to to supply both the sound and picture carriers. Unless otherwise specified, the outputs of these generators will be maintained equal.

1.4.1 Available Power. The available power is the power delivered by a generator to a matched load. It is equal to $E^2/(4R)$, where E is the rms open-circuit voltage of the generator and R is the internal resistance of the generator (including the dummy-antenna resistance). It is preferably expressed in decibels below 1 watt. The signal generator may be calibrated in terms of the available signal power and used on that basis, even though not matched exactly by the load impedance. If a signal generator is to be used with various values of dummy-antenna resistance, it should be calibrated in terms of the open-circuit voltage and the available power should be calculated from the above formula. When reference is made to values of power input, it is understood that the available power is meant.

1.4.2 Input Voltage. Input level in terms of voltage refers to the open-circuit voltage of a generator with an internal resistance, including the dummy-antenna resistance (Section 1.7), equal to the nominal input resistance of the receiver. By this definition, when the receiver input impedance is a resistance equal to the nominal input resistance, the input voltage (open-circuit voltage) is twice the voltage appearing across the antenna terminals of the receiver.

[1] Rules and regulations of the Federal Communications Commission, pt. 3, Sec. 3.682.

[2] A related IEC Standard, "Recommended Methods of Measurement on Receivers for Television Broadcast Transmissions," is published by the International Electrotechnical Commission, 39, rue de Malagnou, Geneva, Switzerland.

Since the input impedance of television receivers built in the United States has been standardized at a value of 300 ohms, it has become common practice to express the input in microvolts, or in decibels below one volt. However, voltage measurements made on receivers designed for a different input impedance will not be directly comparable to those made on receivers designed for the standard 300-ohm impedance unless correction is made for the difference in input impedance.

1.4.3 Values of Standard Test Input Levels. Standard input levels are specified in Table I. Corresponding to these values of available power, which are independent of the receiver input impedance, are shown the approximate equivalent values of open-circuit voltage for the standard impedance level of 300 ohms.

TABLE I

Available Power, db below 1 watt	Approximate Equivalent Input Voltage for $R=300$ Ohms	
	microvolts	db below 1 volt
131	10	100
121	32	90
111	100	80
101	320	70
91	1000	60
81	3200	50
71	10,000	40
61	32,000	30
51	100,000	20

1.4.4 Standard Mean-Signal Input Power. The standard mean-signal input power is 81 db below 1 watt, corresponding to 3200 μv at 300 ohms.

1.5 Standard Picture Test Modulation

1.5.1 Sine Wave. The standard test modulation for sine-wave modulated signals shall be 30 per cent amplitude modulation at 400 cps.

1.5.2 White-Pattern Modulation. The standard test modulation envelope for white-pattern modulation shall be an RF signal modulated by the waveform standardized by the Federal Communications Commission and shown in Fig. 1.5.2 with the picture portion of the signal constant at 15 per cent of the carrier level during the synchronizing peaks.

1.5.3 Gray-Pattern Modulation. The standard test modulation envelope for gray-pattern modulation shall be an RF signal modulated by the synchronizing waveform of Fig. 1.5.2 with the picture portion of the signal constant at 40 per cent of the carrier level during the synchronizing peaks.

1.5.4 Test-Pattern Modulation. The standard for test-pattern modulation shall be an RF signal modulated by the EIA (Electronic Industries Association) test pattern (Fig. 1.5.4) with the white peaks at 15 per cent of the carrier level during the synchronizing peaks.

1.6 Standard Sound Test Modulation

Standard test modulation of the sound carrier is frequency modulation at 400 cps with a deviation of 7.5 kc; this is 30 per cent of the maximum system deviation of 25 kc.

The standard transmitter pre-emphasis provided by a time constant of 75 μsec is normally not employed in fidelity testing of the sound channel. Instead, the corresponding standard de-emphasis characteristic, shown in Fig. 1.6, is applied as a compensating correction to the amplitude-vs-frequency response. This procedure is described in Section 10.2.2.

1.7 Standard Dummy Antenna

The standard dummy antenna presents a balanced, resistive, 300-ohm source impedance to the antenna terminals of the television receiver. Signal generators that do not have these properties must be provided with an external network which may consist of resistors or of a balun.

The resistors used should have negligible reactive components, and in the case of two or more generators, the resistance networks should be located at the signal generators with a 300-ohm balanced line to the receiver. Most of the networks used with two or more signal generators require a correction factor for determining the open-circuit voltage from the generator voltage.

If a balun is used in place of a resistance network, its voltage transformation and impedance characteristics must be known with respect to frequency. If either of these characteristics is not reasonably flat, an iterative resistance attenuator network may be used to minimize departures from uniform transmission or termination.

The effect of reversing the connections to the receiver antenna terminals and reversing the power-line connections of either the signal generator or the receiver or both should be noted. A change in the receiver output is an indication of unbalance in the dummy-antenna system; however, no change in receiver output does not necessarily indicate a balanced dummy-antenna system.

When more than one signal generator is used, a comparison should be made of the relative receiver output as each signal generator is tuned in turn to the same frequency, to obtain the appropriate correction.

The following paragraphs describe several examples of dummy-antenna configurations. In many instances, balun transformers can be used advantageously, particularly where it is desirable to effect impedance matching with a minimum power loss, or when the receiver has little unbalanced signal rejection.

1.7.1 Single Balanced Signal Generator. The network consists of two resistors of equal value, one connected in series with each terminal of the signal generator and of such value that the total output impedance, including the signal generator, is 300 ohms.

1.7.2 Single Unbalanced Signal Generator. The network consists of two resistors, a 150-ohm resistor connected in series with the "ground" terminal of the signal generator and a resistor (equal to 150 ohms minus

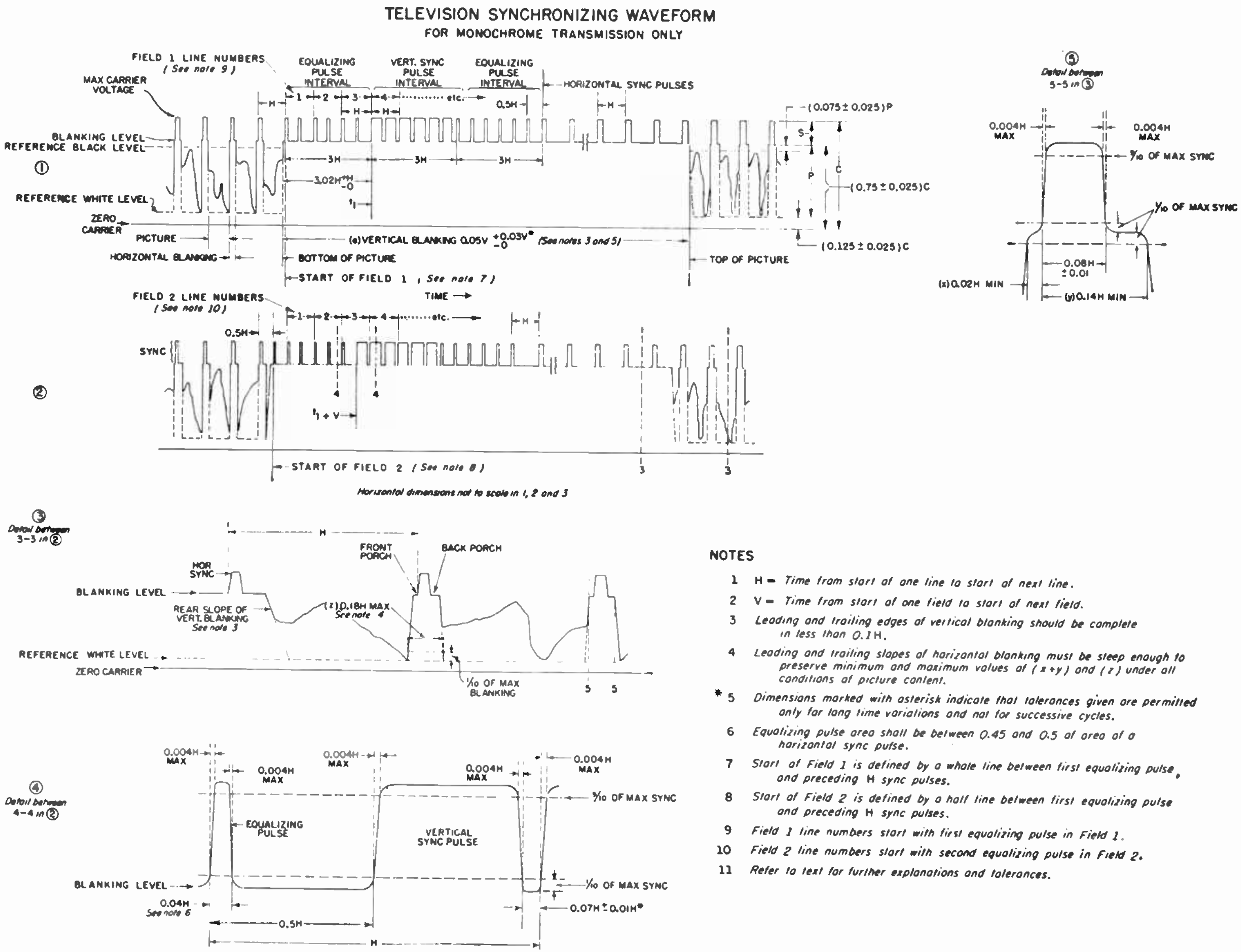

Fig. 1.5.2—Television synchronizing waveform for monochrome transmission.

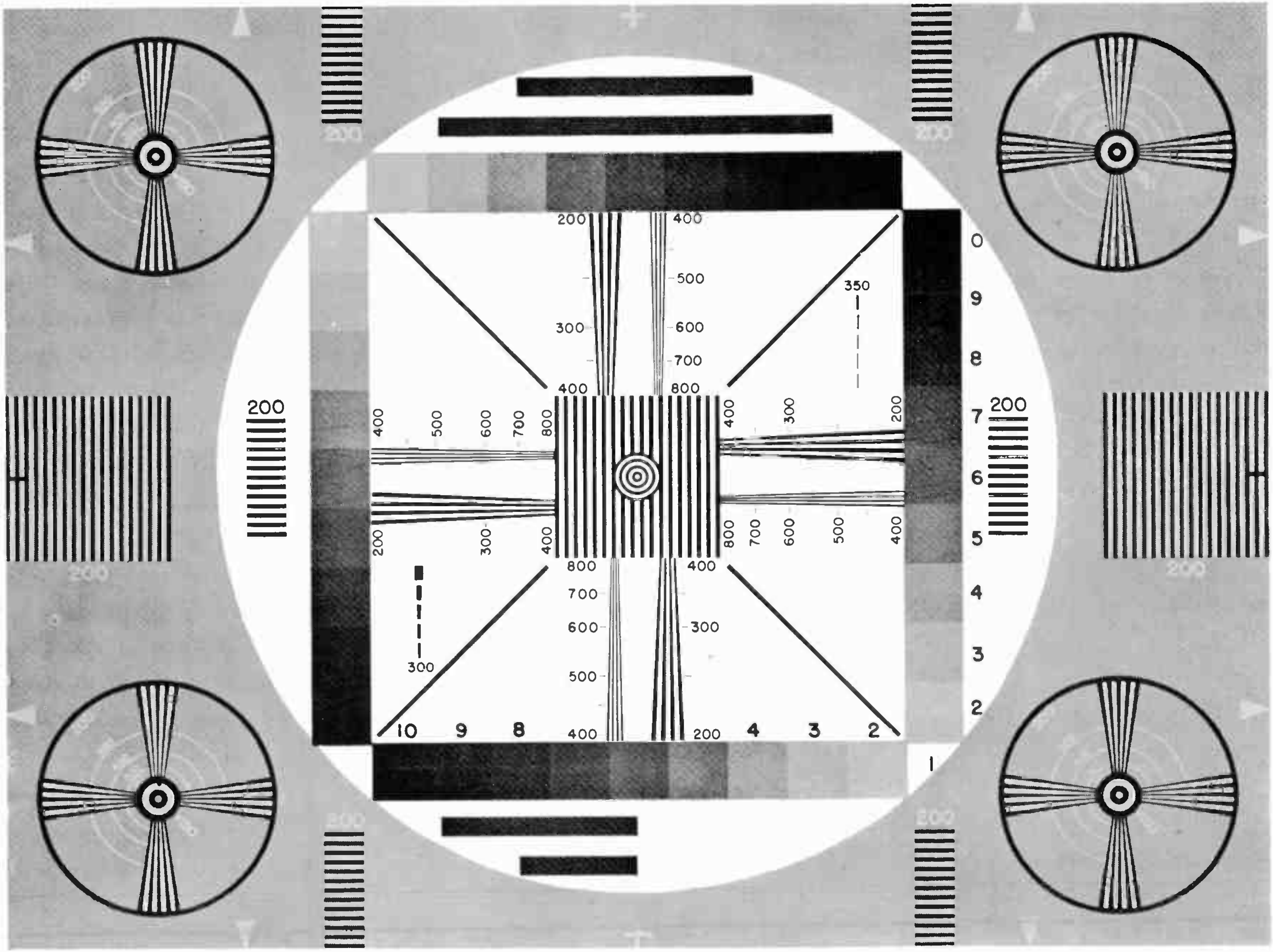

Fig. 1.5.4—EIA resolution chart.

the generator output impedance) in series with the output terminal of the signal generator.

1.7.3 Two Signal Generators. Separate picture and sound signal generators may be connected as shown in Fig. 1.7.3. The open-circuit voltages obtained from the connections of Fig. 1.7.3(a) and 1.7.3(c) are one-half the generator open-circuit voltages.

Fig. 1.7.3(c) illustrates a special case in which signal generators with 300-ohm output impedance are employed. The dummy-antenna network provides an impedance match to the signal generator outputs as well as the required source impedance to the receiver

1.7.4 Three Signal Generators. For certain measurements, a third signal generator may be required. The two connections shown in Fig. 1.7.4 provide an open-circuit voltage that is one-third the generator open-circuit voltage.

Fig. 1.7.4(b) illustrates a special case in which signal generators with 300-ohm output impedance are employed and the dummy-antenna network provides an impedance match to the generator output.

1.8 Standard Picture Test Output

The standard picture test output as delivered by the receiver to the controlled element of the picture tube shall have an amplitude of 20 volts between blanking level and white, as determined by a cathode-ray oscilloscope when using the standard white-pattern modu-

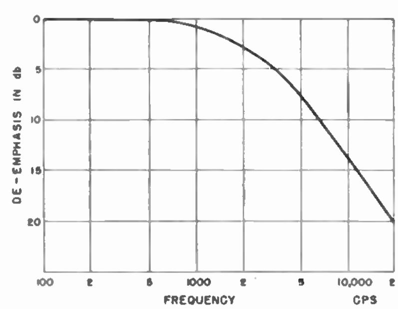

Fig. 1.6—Standard de-emphasis curve.

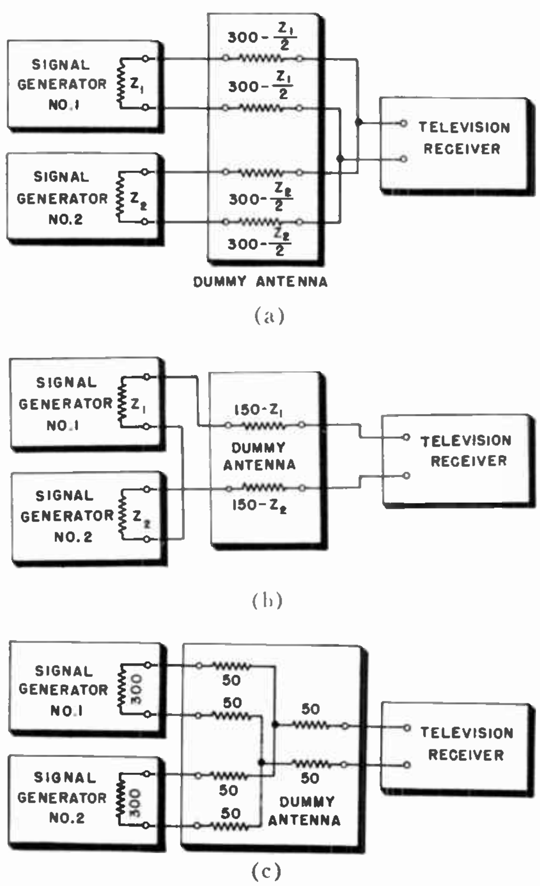

Fig. 1.7.3—Dummy-antenna connections for two signal generators. (a) Two signal generators in parallel. (b) Two signal generators in series. (c) Two 300-ohm signal generators in parallel.

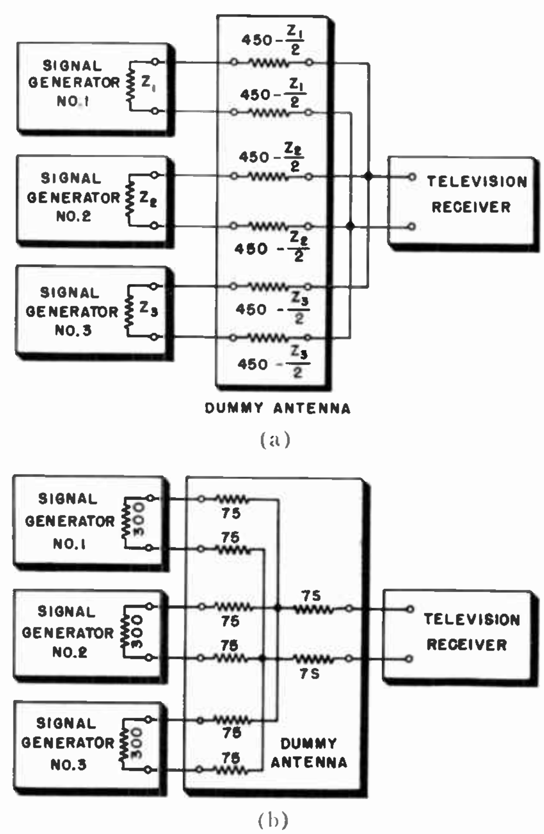

Fig. 1.7.4—Dummy-antenna connections for three signal generators. (a) Three signal generators in parallel. (b) Three 300-ohm signal generators in parallel.

lation (Section 1.5.2). When using symmetrical sine-wave modulation (Section 1.5.1), the standard output shall be 20 volts peak-to-peak. These outputs are equivalent for a receiver having a linear relationship between input and output over the amplitudes involved, as shown in Fig. 1.8. If the particular receiver being measured has been designed to operate with a picture device whose operating voltage requirements are so different from the conventional picture tube as to make the above value of 20 volts unsuitable, a value should be chosen to be approximately one-half of the normal maximum input voltage for the particular picture device being used. The value so chosen should be included in the data.

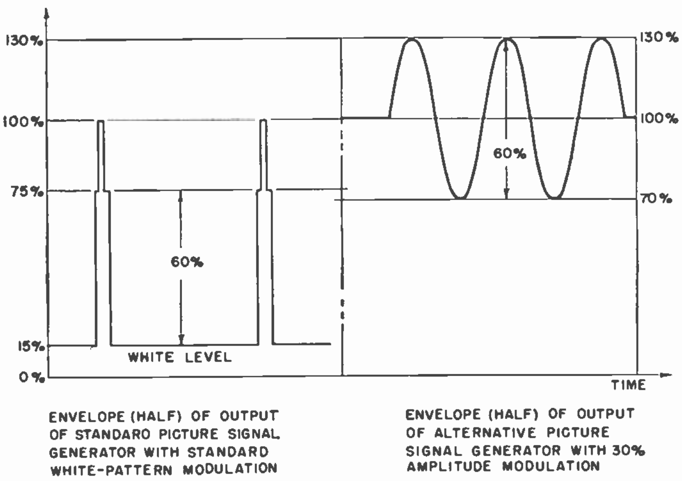

Fig. 1.8—Equivalence of output from standard white-pattern modulation and alternate 30 per cent amplitude modulation.

1.9 Standard Sound Test Output

1.9.1 Standard Test Output. For receivers capable of delivering at least 1 watt at 10 per cent distortion (Section 10.3), the standard test output is an audio-frequency power of 0.5 watt delivered to a standard dummy load. For receivers capable of delivering 0.1 watt but less than 1 watt at 10 per cent distortion, the standard test output is 0.05 watt of audio-frequency power delivered to a standard dummy load. When this latter value is used, it should be specified.

1.9.2 Standard Dummy Load. Output measurements of the sound section of a television receiver are made in terms of the power delivered to a standard dummy load substituted for the loudspeaker, except in special cases where other terminations are specified. The standard dummy load is a pure resistance whose value is equal to the absolute value of the 400-cps impedance of the loudspeaker. Where an output transformer is connected between the receiver and the loudspeaker, the output transformer is treated as part of the receiver.

1.10 Standard Test Conditions

1.10.1 General. It is assumed that the following standard test conditions are in effect during all tests unless noted otherwise.

1.10.2 Power Supply. Receiver measurements are made at the supply voltage for which the receiver is designed. Mean values of voltage and frequency are arbitrarily selected, such as 117 volts and 60 cps for ac operated receivers. Certain receiver characteristics may be desired at other than standard supply voltages and frequencies, or over a range of operating values. Tests should be made to check whether the receiver operates satisfactorily over the range of operating voltage and frequency likely to be encountered in service.

1.10.3 Ambient Temperature and Humidity. The ambient temperature should be between 20° and 35° C, and the relative humidity should be below 90 per cent.

1.10.4 Electron Devices. The electron tubes or other devices used should have standard rated values of those characteristics which significantly affect the performance of the receiver.

1.10.5 Television Receiver Adjustments.

1.10.5.1 General. All control settings not otherwise specified should be adjusted for normal reception. The synchronizing controls are adjusted for proper synchronization and best interlace. The contrast control is adjusted for maximum focused luminance (Section 3.9), unless otherwise stated, and the brightness control is set so that the line structure just disappears in the darkest portion of the gray scale. The scanning linearity, the scanning amplitude, and the focus adjustments are optimized.

1.10.5.2 Tuning adjustments. The receiver is normally tuned so that the local oscillator operates at the correct frequency, corresponding to the selected channel. This adjustment can be made by measuring either the local oscillator frequency or the picture carrier intermediate frequency (nominally 45.75 mc) with a frequency meter.

When measuring peak picture and peak sound sensitivity, the receiver is tuned as described for these tests (Sections 4.3 and 8.4).

Chapter 2—Requirements and Characteristics of Test Apparatus

2.1 Standard Picture Signal Generator

The standard picture signal generator should provide a signal with the following characteristics:

a) The generator should be capable of modulation by the waveform of Fig. 1.5.2 to produce a modulated signal whose characteristics are in accordance with the Rules and Regulations of the Federal Communications Commission.[1]

b) The amplitude-vs-frequency characteristic should display less than 0.5-db response difference for any two modulating frequencies in the range from 30 cps to 4.5 mc. The time-delay errors should be negligible within this frequency band. Ideally a vestigial-sideband filter is required; however, most receiver tests can be made without this filter (Section 6.2.2).

c) The output voltage should be adjustable to any value over the range between 1 and at least 200,000 μv. Higher outputs up to 2 volts are desirable. The output-level indicator should measure the output during synchronizing peaks.

d) Incidental phase modulation of the carrier should not exceed 10 degrees swing at full video modulation at any carrier frequency.

e) Extraneous frequency modulation (hum) of the carrier should be negligible with respect to the characteristic under observation, especially when the generator is to be used in connection with the sound signal generator (Section 2.3) for tests on the sound channel.

2.2 Alternative Picture Signal Generator

Although the complete performance testing of the picture section cannot be accomplished without the use of a standard picture signal generator and a pattern generator, as described in Sections 2.1 and 2.4, many tests can be made with a standard signal generator producing a sine-wave 30 per cent amplitude-modulated signal. Furthermore, certain of the standard tests can be facilitated by the use of this type of signal generator. This generator should have a frequency range extending from below the intermediate frequency up to the highest television channel plus twice the intermediate frequency of the receiver under test, should be capable of amplitude modulation at 400 cps, and should have a variable output voltage up to at least 200,000 μv and preferably 2 volts.

Extraneous frequency modulation of the carrier should be negligible with respect to the characteristic under observation, especially when the generator is to be used in connection with the sound signal generator (Section 2.3) for tests on the sound channel. The carrier frequency stability should be consistent with the requirement of Section 2.3(d).

2.3 Sound Signal Generator

The sound signal generator should have the following characteristics:

a) The output should be calibrated from 1 to 200,000 μv with a constant source impedance.

b) It should be capable of frequency modulation at rates of 30 to 15,000 cps to a deviation of at least 25 kc and preferably to 50 kc with negligible distortion, and negligible incidental amplitude modulation.

c) Amplitude and frequency modulation at power-line frequencies should be negligibly small.

d) The carrier frequency should be sufficiently stable to maintain an accuracy of ± 5 kc in the 4.5-mc difference frequency between the sound and picture carriers.

2.4 Pattern Generator

This equipment, which supplies a modulating signal to the picture signal generator, must contain means for generating a composite signal which will contain not only those picture elements which comprise a test pattern, but also correctly timed blanking and synchronizing pulses. The characteristics of the standard synchronizing waveforms are given in Fig. 1.5.2.

The pattern generator must be provided with the necessary controls and monitoring means to assure the correct levels of the various components of the composite picture signal. It must be free of hum, noise, and other extraneous components.

In addition to the standard synchronizing-signal waveforms, the pattern generator should be capable of providing the following composite picture test patterns:

a) The white-pattern modulation of Section 1.5.2.

b) Gray-pattern modulation of Section 1.5.3.

c) Sine-wave modulation for frequencies of 100 kc to 4.5 mc.

d) Square-wave modulation of variable repetition rate capable of being synchronized with the sweep frequencies.

e) Staircase patterns arranged to appear as vertical stripes and to be movable over the entire picture.

f) The monoscope type of test pattern (Fig. 1.5.4).

g) A cross-hatch pattern in which the video component consists of two sets of synchronized narrow rectangular pulses at time intervals equal respectively to not more than $\frac{1}{16}$ of the vertical and horizontal scanning intervals. These pulses produce a cross-hatch pattern of stationary vertical and horizontal lines.

2.5 Wide-Band Cathode-Ray Oscilloscope

A calibrated wide-band oscilloscope is required for testing the performance of the picture circuits of a television receiver. Its phase and amplitude response must be such as to avoid significant distortion of any waveform of interest; the major requirements are that the deflection sensitivity difference between any two frequencies from 30 cps to 4.5 mc should be less than 0.5 db and that the time-delay error be negligible.

The input impedance should be high enough so that the performance of the circuits to which the oscilloscope is connected is not affected by the resistance or capacitance of the oscilloscope input circuits.

2.6 Audio-Output and Distortion-Measuring Devices

Apparatus for the measurement of audio output and distortion is the same as that required for the testing of frequency-modulation receivers.[3] The output meter should measure true rms values.

2.7 Measurement of Luminance

The photometer used in all luminance measurements should be capable of operating over a small area of the image. An instrument having an acceptance angle of 1

[3] See Section 3 of IRE Standards, 47 IRE 17. S1, "Standards of Radio Receivers: Methods of Testing Frequency-Modulation Broadcast Receivers, 1947."

degree operated at a distance from the image equal to four times the picture height is suitable. The instrument should preferably be of the objective type and should simulate the color response of the average human eye. If the instrument is of the subjective matching type, a calibrated filter should be fitted to secure optimum color match.

Since ambient lighting is variable, the effect of this should be assessed separately. Ambient lighting includes reflections of the television picture from surrounding objects, and a check should be made with the receiver operating at maximum brightness to verify that the luminance of the light reflected from any object does not exceed 0.2 foot-lambert.

When subjective methods are used, sufficient time should elapse before measurements are taken in order to condition the eye to the low level of ambient illumination. Unless otherwise stated, all luminance measurements should be taken at the center of the relevant area in a direction parallel to the optical axis of the picture screen.

2.8 Shielded Enclosure

A shielded enclosure is required for some television receiver measurements in order to attenuate external signals that might otherwise affect the measurements.

Part II—PICTURE SECTION OF RECEIVER

Chapter 3—Picture Quality

3.1 General Considerations

Picture quality depends on characteristics which include size, resolution, contrast range, transfer characteristic, geometric distortion, interlace, luminance, and focus. These may be measured or evaluated by viewing the image of suitably designed test charts. One test chart recommended for this purpose is shown in Fig. 1.5.4 and is described in Standard RS-170 of the Electronic Industries Association. Other useful charts are described under the applicable sections of this standard.

The pattern generator (Section 2.4) makes use of a camera or scanner focused on the chart, or a monoscope containing a copy of the chart. The modulation level of the picture signal generator is set with the whitest portion of the gray scale of the chart at reference white level (15 per cent) and the darkest portion of the gray scale at reference black level (Fig. 1.5.2).

The receiver is tuned in accordance with Section 1.10.5.2 with standard mean-signal input, and the controls are adjusted as in Section 1.10.5.1.

3.2 Picture Size

3.2.1 Definition. The picture size is described by four projected quantities: Picture diagonal, maximum picture height, maximum picture width and picture area. Linear dimensions are specified in inches and area in square inches.

3.2.2 Method of Measurement. The projected dimensions are determined by means of a sliding gauge or other suitable device. Another method consists of photographing the picture area from a point situated on the optical axis of the area at a distance equal to at least five times the maximum picture height. From this photograph, the projected dimensions, as well as the picture area, are determined.

3.3 Curvature of Picture Screen

3.3.1 Definition. The curvature of the picture screen is defined by the ratio between the picture depth and the maximum picture height. The picture depth is defined as the distance between two geometrical planes, both perpendicular to the optical axis, one going through the image point nearest to the observer and the other going through the most distant image points of the picture area.

3.3.2 Method of Measurement. The picture depth is measured with the aid of a traveling microscope or other suitable means.

3.4 Geometric Distortion

In the television transmitter, the coordinates of the picture elements are translated into time differences in the television signal. In the receiver the reverse process must take place in order to obtain undistorted reproduction. Any deviation from the desired linear relationship between timing and position due to the receiver is defined as geometric distortion.

Geometric distortion is measured by using an electrical time pattern generator [Section 2.4(g)] in which the video information consists of two sets of synchronized pulses, at equidistant time intervals, representing a cross-hatch pattern of horizontal and vertical lines. Detailed procedures for measuring geometric distortion are given in IRE Standards, 54 IRE 23. S1.[4]

3.5 Nonlinearity

3.5.1 Definition. Scanning nonlinearity is defined in terms of the pattern of horizontal and vertical lines produced by the cross-hatch pattern generator [Section 2.4(g)]. The horizontal nonlinearity is the departure of the spacing between any two adjacent vertical lines from the mean spacing between the lines expressed as a percentage of the mean spacing between the lines. Vertical nonlinearity is defined similarly. Both horizontal and vertical nonlinearities are measured along projected horizontal and vertical lines through the center of the picture area.

3.5.2 Method of Measurement. A cross-hatch pattern generator is used [Section 2.4(g)]. To determine the nonlinearity, a photograph of the reproduced pattern may be taken as in Section 3.2. Alternatively, a traveling

[4] "IRE Standards on Television: Methods of Measurement of Aspect Ratio and Geometric Distortion," Proc. IRE, vol. 42, pp. 1098–1103; July, 1954.

microscope or other suitable means may be used to measure the distance between adjacent intersection points of the projected pattern.

3.5.3 Presentation of Data. The nonlinearity is plotted on a linear time scale as abscissa and a linear percentage scale as ordinate. The equal time intervals corresponding to the divisions of the picture area as transmitted are marked on the abscissa.

The difference between the mean distance and the distance between adjacent points is plotted as a percentage of the mean distance, at the center of each time interval. Graphs are plotted for both vertical and horizontal nonlinearity.

Short-time nonlinearity of scanning, such as results from yoke ringing, may not appear. To measure such deviations a more closely spaced pattern is necessary.

3.6 Raster Distortion

3.6.1 Definition. Raster distortion is the deviation from a true rectangle of the largest completely visible contour of approximately the correct aspect ratio formed by the test pattern.

3.6.2 Method of Measurement. An electrically generated cross-hatch test pattern [Section 2.4(g)] is used.

A photograph of the reproduced pattern may be taken under the same conditions as specified in Section 3.2.

On this photograph, or a similar projection of the reproduced pattern on a plane perpendicular to the optical axis, the distorted reproduction of the contour of the largest completely visible rectangle formed by the test pattern and having approximately the correct aspect ratio is traced (Fig. 3.6.2). This contour is normally an adequate description of raster distortion.

If one form of distortion predominates, it may be measured in accordance with the following methods. Fig. 3.6.2 represents a generalized contour. The corner points A, B, C and D are marked, and the auxiliary lines AB, BC, CD, DA, KF and HE are then drawn so that $AE=EB$, $BF=FC$, $CH=HD$, $DK=KA$.

The greatest distance between the line AB and the contour section between A and B lying outside the quadrangle $ABCD$ is called a_2.

The distance between AB and the point of the contour section lying farthest away from AB inside the quadrangle $ABCD$ is called a_1. The distances b_1, b_2, c_1, c_2, d_1 and d_2 are similarly defined.

The following distortion percentages are specified:

Horizontal Trapezoid Distortion

$$T_H = \frac{AD - BC}{AD + BC} \cdot 100 \text{ per cent}$$

and

Vertical Trapezoid Distortion

$$T_V = \frac{AB - DC}{AB + DC} \cdot 100 \text{ per cent.}$$

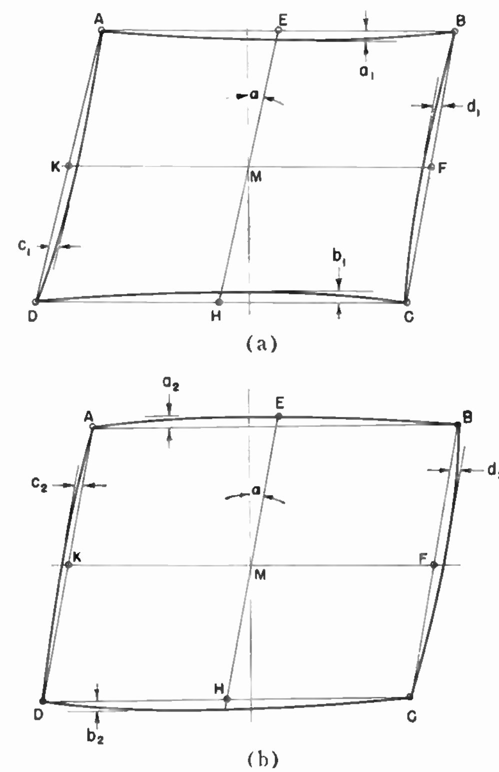

Fig. 3.6.2—Raster distortion measurements. (a) Pincushion distortion. (b) Barrel distortion.

If the contour sections AB as well as DC lie completely *outside* the quadrangle $ABCD$, the

Horizontal Barrel Distortion

$$B_H = 2\frac{a_2 - b_2}{AD + BC} \cdot 100 \text{ per cent.}$$

If the contour sections AB as well as DC lie completely *within* the quadrangle $ABCD$, the

Horizontal Pinchushion Distortion

$$C_H = 2\frac{a_1 + b_1}{AD + BC} \cdot 100 \text{ per cent.}$$

Similarly, the

Vertical Barrel Distortion

$$B_V = 2\frac{c_2 + d_2}{AB + CD} \cdot 100 \text{ per cent}$$

and the

Vertical Pincushion Distortion

$$B_V = 2\frac{c_1 + d_1}{AB + CD} \cdot 100 \text{ per cent.}$$

Parallelogram Distortion is expressed by the angle in degrees.

Ripple Distortion of the contour is present when the raster contour sections AB, CD, BC, DA show undulations. The peak-to-peak value of such undulations may be expressed as a percentage of raster height or width.

3.7 Influence of Hum on Geometric Distortion and Brightness

Geometric distortion and brightness irregularities may occur as a result of power-supply voltages and power-supply magnetic and electric fields. These effects can be distinguished by operating the receiver from a supply having a frequency differing slightly (*e.g.*, 1 cps) from the field frequency. Alternatively, if the receiver uses a power supply to which the picture synchronizing-signal generator is locked, the necessary relative phase changes may be obtained by rotating a suitable manual phase shifter in the lock-in circuit of the synchronizing-signal generator through 360 degrees.

With respect to geometric distortion, the excursion of the points in the picture which have the greatest vertical and horizontal movements are noted. The picture center should be offset (and the background brightness increased) so that the raster edges can be observed. This enables a determination of the degree of raster motion and synchronizing timing variation.

Brightness variations normally appear as moving horizontal bands. The receiver contrast and brightness controls may be adjusted to produce a gray background to facilitate observation of the shading.

The faults observed in this section are described together with the conditions of measurement.

3.8 Luminance

For a specified set of conditions, the maximum luminance of a television picture may be limited by factors which include deterioration of focus, geometric or size distortion, inadequate video drive, and the relative area of the picture at the peak white level. Flicker, which is generally not a limiting factor, is not considered here. See Section 2.7 for method of measurement.

3.9 Maximum Focused Luminance

3.9.1 Definition. This is the maximum luminance at which the focus is sufficient to resolve the line structure.

3.9.2 Method of Measurement. Apply to the receiver the standard test-chart modulated signal (Fig. 1.5.4) at mean-signal input level. Increase the luminance level to obtain the maximum luminance at which the focus is still sufficiently good to show line structure in maximum luminance areas near the center of the raster, with the focus control optimized.

3.9.3 Presentation of Data. The luminance is expressed in foot-lamberts, together with a description of the uniformity of focus over the raster.

3.10 Maximum Usable Luminance

The maximum usable luminance is measured with the same setup used to measure maximum focused luminance (Section 3.9.2). The luminance level is increased until significant degradation of the picture occurs for reasons other than defocusing. This luminance value is recorded as the maximum usable luminance together with a statement of the limiting condition.

3.11 Contrast

3.11.1 Introduction. Contrast is the ratio of the luminance of a peak white area of the picture screen to the luminance of a black area of the picture screen. Contrast may be limited by halation effects in the display device, by ambient illumination, or by severe nonlinearity in the luminance transfer characteristic. The first two are considered in this section and the third in Section 3.14.

3.11.2 Halation-Limited Contrast. The degree to which contrast is limited by halation effects is influenced by the following factors:

a) The relative size of black and white areas. In general, contrast decreases as a greater portion of the screen is excited by electrons. See Fig. 3.11.2(a).

b) The relative distance between points at which contrasting luminances are measured. In general, the contrast decreases as the distance between the measurement points decreases. See Fig. 3.11.2(b).

c) The presence of high luminance areas at the corners or edges of the picture. Scattering of electrons from the neck or sides of the picture tube may limit contrast. See Fig. 3.11.2(c).

3.11.2.1 Method of measurement of halation-limited contrast. Halation-limited and electron-scattering contrast are measured using the test charts shown in Fig. 3.11.2. The picture-tube beam current must be cut off in the black (shaded) areas of the picture. The white areas of the picture are at maximum focused luminance. The ambient illumination should be negligible.

a) Halation-limited large area contrast (α_l) is measured with the test chart shown in Fig. 3.11.2(a):

$$\alpha_l = \frac{2L_2}{L_1 + L_3}.$$

b) Halation-limited detail contrast (α_d) is measured with the test chart of Fig. 3.11.2(b):

$$\alpha_d = \frac{L_2 + L_3 + L_4 + L_5}{4L_1}.$$

c) Electron-scattering-limited large area contrast (α_s) is measured with the test chart of Fig. 3.11.2(c):

$$\alpha_s = \frac{L_2 + L_3 + L_4 + L_5}{4L_1}.$$

3.11.3 Contrast Limited by Ambient Illumination. With ambient illumination the luminance values of the black and white areas of the picture are increased by an equal amount, thus reducing the contrast. If, without ambient illumination, the luminance of a black area is L_b and the luminance of a white area is L_w, the large area contrast is

$$\alpha_l = \frac{L_w}{L_b}.$$

With ambient illumination, an amount L_r is added to

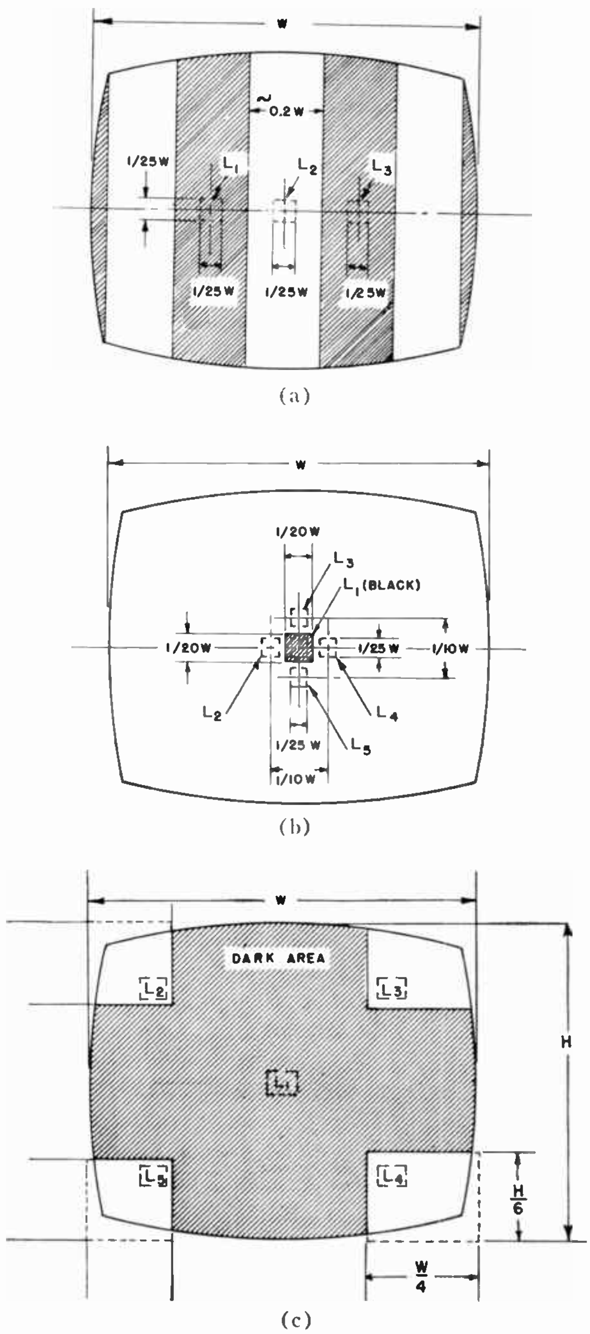

Fig. 3.11.2—(a) Test pattern for measurement of halation-limited large-area contrast. (b) Test pattern for measurement of halation-limited detail contrast. (c) Test chart for measurement of electron-scattering-limited large-area contrast.

L_b and L_w. L_r is the luminance due to the ambient light reflected by the picture screen. If ρ is the reflection coefficient of the picture screen (Section 3.11.4) and L_0 is the luminance caused by the ambient illumination with $\rho = 1$, then

$$L_r = \rho L_0.$$

Thus the contrast with ambient illumination (α_i) becomes

$$\alpha_i = \frac{L_w + L_r}{L_b + L_r} = \frac{L_w + \rho L_0}{L_b + \rho L_0}.$$

3.11.4 Reflection Characteristic of the Picture Screen.

3.11.4.1 Definitions. The reflection characteristic of the picture screen is the luminance value in the direction of the optical axis as a function of the angle of incidence of the ambient illumination relative to the luminance value of an ideally diffuse surface with the same ambient illumination, the receiver being switched off.

3.11.4.2 Method of measurement. The front of the receiver is illuminated by a source of light equivalent to Standard Illuminant *C*. A magnesium carbonate block is placed on the optical axis in contact with and in front of the optical surface nearest to the viewer.

The luminance values of the magnesium carbonate block and the face of the receiver adjacent to the carbonate block are measured. The measurement is repeated as the angle of incidence of the light is varied.

3.11.4.3 Presentation of data. The results are expressed as the ratio between the luminance of the face of the receiver and that of the magnesium carbonate block corrected for its known reflectance. This ratio is plotted as a function of the angle of incidence.

3.12 Resolution and Focus

3.12.1 Definition. The vertical and the horizontal resolution is expressed as the maximum number of lines which can be resolved in the vertical and the horizontal directions as read from the resolution wedges on a reproduction of the standard test chart, Fig. 1.5.4.

3.12.2 Method of Measurement. The receiver is set up as in Section 3.1 with standard test-chart modulation. The focus should be adjusted in such a manner that the best over-all compromise is obtained. The nominal resolution is read at the point along the converging lines beyond which each individual line cannot be recognized with certainty. The resolution is recorded in the center and in the four corners of the picture. The highlight luminance should be specified.

3.13 Electrical Fidelity

The electrical fidelity is measured in Chapter 6, which describes measurement of the high-frequency step response (Section 6.4) and the line and field-rate step responses (Section 6.5). These data should be supplemented by a description of the test-chart reproduction, with the receiver adjusted as in Section 3.1. Ringing, overshoot, smear, and line or field shading should be described qualitatively.

3.14 Luminance Transfer Characteristic

3.14.1 Definition. The luminance transfer characteristic represents the relationship between the luminance and the corresponding picture modulation percentage.

3.14.2 Method of Measurement. A television signal at standard mean-signal level, modulated with the staircase pattern of Section 2.4(e) consisting of vertical bars equally distributed through the gray scale, is applied to the receiver terminals. The dimensions of the gray scale pattern should be approximately one-fourth of the respective picture dimensions. The modulation is adjusted so that the lightest bar corresponds to 15 per cent of the carrier level during the synchronizing peaks and the darkest bar to black level. Black level is defined as 70 per cent of peak-synchronizing amplitude for this test only. The contrast and brightness controls of the receiver are adjusted so that the scanning lines just disappear in the darkest bar and the lightest bar is at maximum focused luminance (Section 3.9). The luminance of each bar is measured with the gray scale pattern centered in the picture. The measurements should be repeated with the gray scale at the sides and corners of the picture and may also be repeated with higher or lower background brightness.

3.14.3 Presentation of Data. The luminance of each bar is plotted against the modulation level expressed as a percentage of the blanking level to peak white amplitude. 8.3 per cent on the abscissa corresponds to black level (70 per cent of the peak-synchronizing amplitude) and 100 per cent corresponds to reference white level (15 per cent of the peak-synchronizing amplitude). Logarithmic scales are used. See Fig. 3.14.3 for typical data.

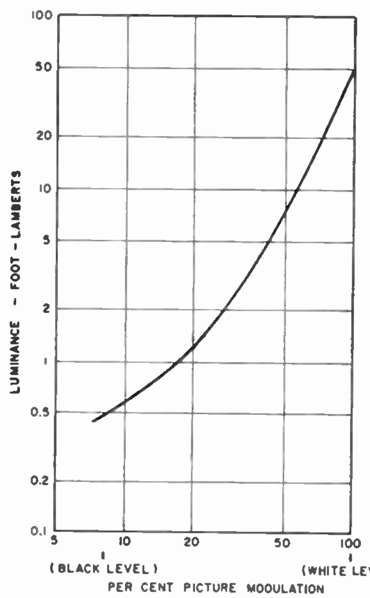

Fig. 3.14.3—Luminance transfer characteristic.

3.15 Interlace

The quality of the interlace is described by the ratio of the distances between one scanning line and the two lines adjacent to it which belong to the interlaced field, each expressed as a percentage of the distance between two consecutive lines in a single field (Fig. 3.15). A test should be made to determine whether the interlace is affected by the vertical hold control, the type of picture modulation, or other control settings, and the results noted in the data.

3.16 Effect of Vertical Synchronizing Pulse on Horizontal Synchronization

Rotation of the horizontal hold control may produce a relative displacement of the upper part of the picture. This effect is described by noting the deformation of a vertical line, as described by δ_1 and δ_2 in Fig. 3.16, as the horizontal hold control is rotated through the pull-in range. The resulting displacements are expressed as a percentage of the picture dimensions:

$$\frac{\delta_1}{w} \times 100 \quad \text{and} \quad \frac{\delta_2}{h} \times 100.$$

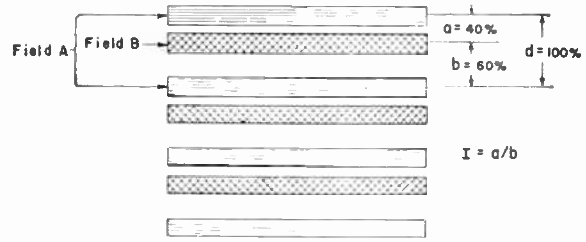

Fig. 3.15—Quality of interlace.

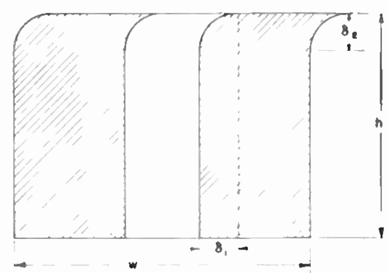

Fig. 3.16—Pulling on vertical synchronizing pulses.

3.17 Effects of Picture Information on Synchronization

Picture information in the form of large area black-to-white transitions frequently has adverse effects on synchronization. These effects may be measured by the use of a test chart as shown in Fig. 3.17(a). The receiver is adjusted as in Section 1.10.5. The resulting displacements [Fig. 3.17(b)] are expressed as a percentage of the picture width:

$$\text{Pulling on picture content} = \frac{d}{w} \times 100.$$

If no displacements result, the synchronizing-signal amplitude is reduced until measurable displacements occur. The data must include a statement of the reduction in synchronizing signal used.

Other test charts than the one shown in Fig. 3.17(a) may be used to advantage. For example, the polarity of Fig. 3.17(a) may be reversed, or the relative black and white areas varied. Due to the subjective nature of these data, the results are best reported as a side-by-side comparison, rather than as absolute data.

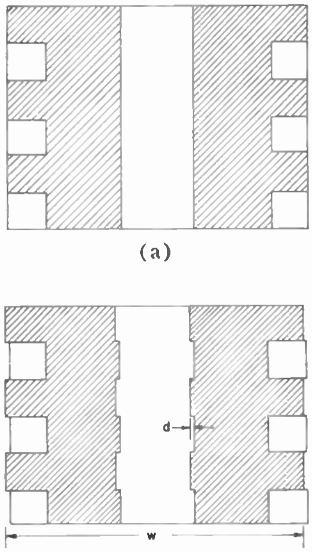

(a)

(b)

Fig. 3.17—Effects of picture on synchronization. (a) Test chart. (b) Typical results.

3.18 Subjective Examination of Picture Quality

Degradations of picture quality which are not described by the tests specified in this standard may be detected by subjectively examining the picture over a wide range of operating conditions. Particular emphasis should be given to the effect of variations in the settings of the receiver controls.

The following types of degradation should be looked for:

a) Luminance irregularities due to extraneous signals at the picture device control electrode, scanning velocity variation, or fold-over.

b) Interference generated internally such as extraneous oscillations in the deflection system (Barkhausen or other retarding field oscillations), shock excitation of incidental resonant circuits by sudden start or cessation of deflection currents, or crosstalk of sound into the picture.

c) Unstable synchronization, characterized as jumping, jittering, rolling, etc.

The above conditions can frequently be described best by a photograph of the phenomenon. When this is not possible, a subjective description of the extent, direction, size, shape, frequency and seriousness of the fault should be given.

Chapter 4—Sensitivity, Picture

4.1 Picture Sensitivity

The sensitivity of the picture channel may be limited either by the available gain or by internal (thermal-agitation) noise originating principally in the tuner.

The "nominal sensitivity" and the "peak sensitivity" describe the extent to which the receiver performance is limited by the available gain. The "noise factor" is a measure of the internal receiver noise.

The nominal sensitivity (Section 4.2) is a measure of the receiver gain when the receiver is tuned normally to produce the nominal picture carrier intermediate frequency.

The peak sensitivity (Section 4.3) is a measure of the receiver gain when the receiver is retuned so that it has maximum gain at the picture carrier frequency. The sound channel performance and the adjacent-channel selectivity under this retuned condition are dependent upon the required amount of retuning of the local oscillator and the amount of shift in the IF amplifier selectivity as a function of AGC voltage.

In actual use, the receiver may be tuned to achieve a compromise between picture sensitivity, sound sensitivity and adjacent-channel rejection, depending on local conditions. This yields an effective value of receiver sensitivity which depends upon how closely the nominal sensitivity approaches the peak sensitivity.

In addition to gain and internal receiver noise, the effective receiver sensitivity is influenced by other characteristics such as weak-signal IF selectivity, transient response, gamma, contrast, luminance, screen persistence, clipping levels, and synchronizing performance.

4.2 Nominal Picture Sensitivity

4.2.1 Definition. The nominal picture sensitivity is the lowest input signal which results in standard picture test output when the receiver is tuned to produce the nominal picture intermediate frequency (Section 1.10.5.2).

4.2.2 Method of Measurement. The picture signal generator is connected to the receiver as described in Section 1.7. Standard white-pattern modulation (Section 1.5.2) is used. The receiver is tuned to produce the nominal intermediate frequency (Section 1.10.5.2) and the receiver controls are adjusted for maximum sensitivity.

The input signal is increased until the standard picture test output (Section 1.8) is obtained. This value is the nominal picture sensitivity.

If the video output is obscured by noise, sufficient filtering should be added so that the blanking level and peak white are delineated.

Where a television signal generator is not available, a 30 per cent sine-wave modulated signal (Section 1.5.1) can be used. This alternative procedure requires that the normal AGC voltage which would be produced by standard white-pattern modulation be simulated. A low-pass filter is used to reject thermal noise, and the input level is adjusted to produce standard test output.

4.2.3 Presentation of Data. The sensitivity is measured on the channels of interest and the results expressed in microvolts or in decibels below 1 volt.

4.3 Peak Picture Sensitivity

4.3.1 Definition. The peak picture sensitivity is the lowest input signal which results in standard picture test output when the receiver is tuned for maximum picture output.

4.3.2 Method of Measurement. The procedure is the same as in Section 4.2.2 except that the receiver is detuned the minimum amount required to produce peak output in the vicinity of the normal tuning position; if the output continues to increase as the receiver is detuned from the normal setting (as defined in Section 1.10.5.2), the peak sensitivity is measured with the receiver tuned so that the intermediate frequency produced is 1.5 mc lower than the nominal value.

4.3.3 Sound Sensitivity. The peak sound sensitivity, as described in Chapter 8, is measured for the same receiver tuning used in measuring the peak picture sensitivity.

4.4 Noise-Limited Sensitivity—Noise Factor

4.4.1 Introduction. Provided a receiver has sufficient gain, its usable sensitivity is primarily limited by its noise factor.[5] The noise factor is a significant and reproducible measure of the noise performance of the input portion of the receiver, as compared with that of an ideal noise-free receiver. Other factors influence the noise-limited sensitivity as described in Section 4.1.

4.4.2 Definition of "Noise Factor (Noise Figure), Average. Of a linear system, the ratio of (1) the total noise power delivered by the system into its output termination when the noise temperature of its input termination is standard (290°K) at all frequencies, to (2) the portion thereof engendered by the input termination. For heterodyne systems, portion (2) includes only that noise from the input termination which appears in the output via the principal frequency transformation of the system and does not include spurious contributions such as those from image-frequency transformations."[6]

4.4.3 Method of Measurement. A random noise generator, which usually consists of a temperature-limited thermionic diode, is employed as a calibrated source of random noise. This noise generator is matched to the nominal 300-ohm input impedance of the receiver.

In order to compare the receiver noise with that of an ideal receiver, the receiver detector is linearized by injecting an auxiliary unmodulated signal at either the signal or the intermediate frequency. The noise factor is then determined by noting the amount of noise which must be added by the noise generator to produce a 3-db increase in the noise measured at the detector output.

The detailed measurement procedure is given below:

a) The test equipment is connected to the receiver.

b) The receiver is tuned as described in Section 4.3 for measuring peak picture sensitivity.

c) The AGC voltage applied to the first amplifier in the receiver is replaced by a fixed bias equal to that existing at the amplifier when the input is connected to a standard dummy antenna, with no applied signal. An adjustable bias source is connected to replace the AGC voltages on the later IF amplifier stages. The AGC voltages normally developed in the receiver should be rendered completely ineffective.

d) The waveform at the output of the video detector is examined with an oscilloscope to establish that only noise is present (no hum or other signals). If it is necessary to disable the vertical or horizontal sweep circuits to eliminate interference, the power supply should be loaded so that operating conditions of the rest of the receiver are normal.

e) A high-impedance video voltmeter is connected across the video-detector output to measure the noise output. If an averaging type of meter is used, precaution should be taken that it does not overload on the upper part of the scale because of the high ratio of peak-to-rms value of the noise voltage. The technique outlined in the following steps must be carefully followed so that the noise peaks are not clipped in the receiver itself. To observe whether nonlinearity is present, the video-detector output should be monitored on the oscilloscope throughout the test.

Care should be taken that no regeneration is introduced as a result of connecting the video voltmeter and the oscilloscope to the output of the detector.

f) An unmodulated carrier at either signal or IF frequency is coupled loosely into the receiver. The signal is tuned to the picture carrier frequency (normally the center of the band for this measurement) and its amplitude is increased to the point that *just* produces maximum output reading on the video voltmeter. This amplitude is the amount required to linearize the detector. The reading on the video voltmeter is then observed.

g) The noise generator is then turned on and its output increased until the noise output meter reading increases 3 db above that of step f). The noise factor is then read from the calibrated noise generator scale. If the noise factor for a 3-db increase in receiver noise output is not indicated directly on the instrument, or if the noise factor of the receiver is beyond the range of the instrument, making it impossible to increase the noise output by 3 db, then the following formula for the noise factor is applied:

$$NF \text{ (in db)} = 10 \log_{10} \frac{20IR_a}{M-1}$$

where

I = dc current through the noise diode,
R_a = noise generator source resistance,
M = relative increase in receiver noise output power.

h) The effect of spurious responses, principally the image response, is usually negligible in television receivers, provided the image rejection is greater than 6 db.

i) The noise factor should be measured as a function of input signal level or alternative means should be

[5] This definition is from 57 IRE 7. S2 "Standards on Electron Tubes: Definitions of Terms, 1957," vol. 45, pp. 983–1010; July, 1957.
[6] 53 IRE 7. S1 "Standards on Electron Devices: Methods of Measuring Noise," Proc. IRE, vol. 41, p. 896; July, 1953.

used to establish that the noise factor for maximum sensitivity conditions is indicative of the signal-to-noise ratio at higher signal levels. For example, if shorting the AGC bias applied to the tuner improves the signal-to-noise ratio, this indicates that the noise factor is poorer at the higher signal levels.

4.4.4 Presentation of Data. The noise factor, for each channel measured, is given in decibels. A statement of whether the signal-to-noise ratio is degraded by the AGC voltage is included [see Section 4.4.3 (i)].

4.5 AGC Characteristic and Figure of Merit

4.5.1 Definition.

4.5.1.1 AGC characteristic. The AGC characteristic describes the dependence of the picture output and the sound output levels on the input signal.

4.5.1.2 AGC figure of merit. The picture AGC figure of merit is the number of decibels reduction of the input signal, below 100,000 μv, required to reduce the picture output voltage by 10 db. The sound AGC figure of merit is defined in the same manner.

4.5.2 Method of Measurement. The picture and sound signal generators are connected to the receiver as described in Section 1.7. Standard white-pattern picture modulation (Section 1.5.2) is used. The sound carrier is modulated 30 per cent at 400 cps. The picture-to-sound carrier ratio is unity.

The receiver is tuned to produce the nominal intermediate frequency (Section 1.10.5.2), and the contrast and volume controls adjusted for standard test output with an input signal of 100,000 μv. The input signal is then varied from 10 μv to 2 volts (if available), without altering the controls, and the picture and sound outputs measured as a function of the input level. The measurement is repeated with the controls adjusted for standard test output with input signals of 10,000 and 1000 μv, as in Fig. 4.5.3.1.

If the video output is obscured by noise, sufficient filtering should be added so that the blanking level and peak white are delineated.

If the receiver has a "local-distance" sensitivity switch, its position should be noted. If the sensitivity or contrast controls significantly influence the operation of the AGC circuit, the measurement should be repeated for appropriate settings of the controls.

4.5.3 Presentation of Data.

4.5.3.1 AGC characteristics. This is plotted as in Fig. 4.5.3.1 for picture and sound outputs.

4.5.3.2 AGC figure of merit. This is noted as in Fig. 4.5.3.1 for both the picture and sound outputs.

4.6 Maximum Usable Input Signal

4.6.1 Definition. The maximum usable input signal is the highest level of input signal for which the receiver gives acceptable performance under specified conditions.

4.6.2 Method of Measurement. The same test conditions are used as in Section 4.5.2.

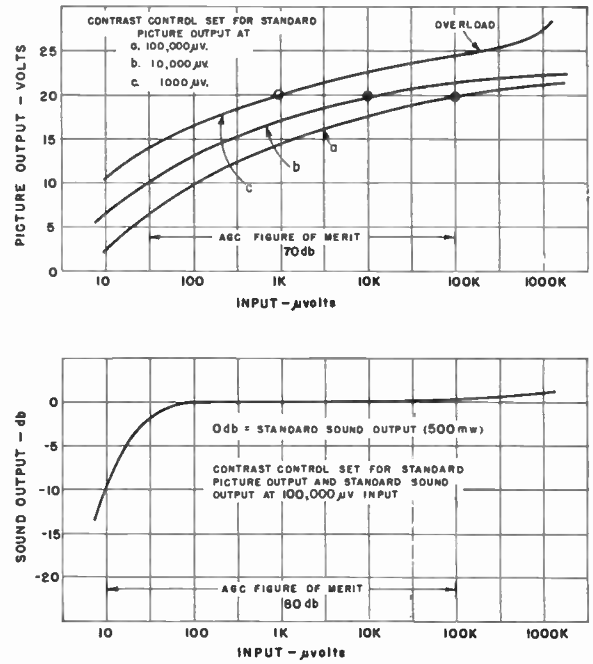

Fig. 4.5.3.1—AGC characteristics for the picture and sound channels.

1) The input level is gradually increased and the receiver controls and switches are adjusted to maintain optimum performance. The highest input signal level for which the performance remains acceptable is noted.

2) The measurement is repeated to find the highest input signal level which will just cause the receiver to operate abnormally (*e.g.*, "lock-out" by AGC blocking) when the channel selector is switched, or when the receiver power is turned on with the input signal applied.

4.6.3 Presentation of Data. The lowest of the values determined in the preceding three tests is recorded with a description of the effect which causes impaired performance.

4.7 AGC Speed

4.7.1 Definition. Amplitude modulation of the composite input signal (airplane flutter) produces amplitude modulation at the picture tube to a degree which depends upon the characteristics of the AGC circuit. The AGC speed is described by a plot of the residual amplitude modulation at the picture tube against the frequency of the amplitude modulation, the per cent modulation of the input signal being maintained at 30 per cent. The AGC speed figure of merit is the frequency at which the per cent modulation of the signal at the picture tube is reduced from 30 per cent to 10 per cent.

4.7.2 Method of Measurement. The picture signal generator is connected to the receiver through an auxiliary RF amplifier, the gain of which can be varied by the application of a sine wave. The percentage modulation is maintained at 30 per cent, while the frequency of modulation is varied from a few cps to several hundred cps. Standard white-pattern modulation (Section 1.5.2) is used. The receiver is tuned to produce the nominal intermediate frequency (Section 1.10.5) and the receiver controls are adjusted for standard test output.

The detector output is observed on an oscilloscope. At each frequency of modulation, the percentage amplitude modulation at the detector output is recorded.

The test is performed at an input level of 3200 μv and 100,000 μv. If the reduction in amplitude modulation percentage is observed to depend significantly on the contrast or AGC controls, the tests are repeated with representative settings of these controls.

4.7.3 Presentation of Data. The amplitude modulation at the picture tube input is plotted against the frequency of the modulation. The AGC speed figure of merit is noted on the curve.

Chapter 5—Interference, Picture

5.1 Introduction

Interfering signals which affect the picture may be generated externally or may be generated by the receiver itself. These undesired signals may enter the receiver through the antenna, the power line, and in some cases, may be picked up directly by the circuit components.

The receiver selectivity characteristics (Section 5.2) indicate the susceptibility of the receiver to undesired signals whose principal path includes the antenna.

Internally generated interference (Section 5.3) can best be measured by observation of the reproduced picture under conditions of controlled input signals.

Separate tests are included for compatibility with color signals (Section 5.4) and the effects of impulse-noise interference (Section 5.5).

5.2 Selectivity Characteristics

5.2.1 Combined Radio-Frequency and Intermediate-Frequency Selectivity Characteristic.

5.2.1.1. Definition. The combined radio-frequency and intermediate-frequency selectivity characteristic is a measure of the relative gain vs frequency from antenna to video detector.

5.2.1.2 Method of measurement. It is desirable to take data under various conditions of receiver gain in order to show possible effects of regeneration and circuit detuning. Since the automatic gain-control circuits are disabled for this measurement, the desired receiver gain conditions are selected initially and the corresponding RF and IF gain-control voltages are measured. The following conditions of receiver gain are suggested:

a) Gain at nominal sensitivity level (Section 4.2.1).

b) Gain with input signal 20 db above nominal sensitivity level.

c) Gain at standard mean-signal level.

The procedure described in Section 4.2.2 is followed and the RF and IF gain-control voltages are measured and recorded for the picture carrier input levels referred to in a), b), and c) above.

The picture carrier modulation is then changed to 30 per cent 400-cps modulation. The gain-control circuits are disabled and RF and IF biases, as determined in the previous measurement at the nominal sensitivity level, are provided from an external source such as a battery. The contrast control remains at its maximum setting for the remainder of the measurements.

The signal generator, with just enough output to give a readable indication at the picture tube, is varied in frequency over the pass band and set at the trap frequency of highest attenuation. At this frequency, the signal generator output is adjusted to give a selected reference level at the picture tube. This reference level should be as high as possible without encountering overload.

The output indicating device may be an oscilloscope or a voltmeter. A 400-cps band-pass filter will prevent thermal noise or hum from affecting the readings.

The signal generator frequency is then varied over the pass band of the receiver and data are taken at enough points to define the selectivity characteristic. At each frequency of measurement, the input level is adjusted to give the previously selected reference output at the picture tube and this input level is recorded.

This procedure is repeated for the receiver gain conditions of b) and c) above with the gain-control biases adjusted to the appropriate values. The same reference output level is used for the three sets of measurements. When making the measurements at reduced receiver gain, it may not be possible to obtain data at the trap frequencies due to overload of the RF or IF circuits.

Because the selectivity is normally measured at an abnormally low detector level to prevent overload, it is desirable to make an additional test to determine whether the response in the pass band changes significantly with detector level.

The selectivity characteristic should be measured on at least one of the standard VHF and one of the standard UHF test channels (Section 1.3).

5.2.1.3 Presentation of data. The combined radio-frequency and intermediate-frequency selectivity characteristic of the receiver is plotted as in Fig. 5.2.1.3.

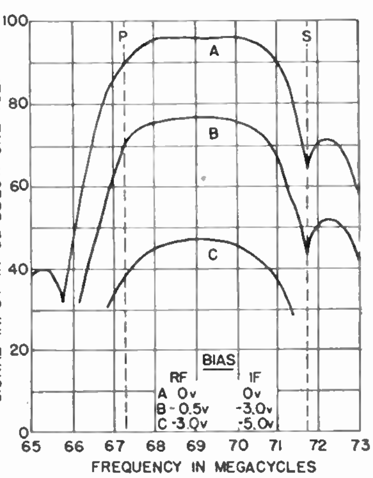

Fig. 5.2.1.3—Typical RF-IF selectivity characteristic.

5.2.2 Intermediate-Frequency Selectivity Characteristic.

5.2.2.1 Definition. The intermediate-frequency selectivity characteristic is a measure of the selectivity of the receiver circuits from the converter input to the video detector.

5.2.2.2 Method of measurement. The procedure of Section 5.2.1.2 is repeated with the signal generator tuned to the intermediate-frequency range and connected to the converter input instead of to the antenna. Measurements are made for the same receiver gain conditions as in Section 5.2.1.2 and the same reference output level is used.

Precautions must be taken to prevent feedback as a result of the signal generator connection.

5.2.2.3 Presentation of data. The intermediate-frequency selectivity is plotted as in Fig. 5.2.1.3 with the appropriate change in the frequency scale.

5.2.3 Rejection of Predictable Off-Channel Signals.

5.2.3.1 Introduction. A television receiver, tuned properly to a desired channel, is subject to interference from a number of specific signals having predictable frequencies. Interference from these signals occurs often enough to warrant individual measurements of the ability of the receiver to reject these specific frequencies. The following measurements are usually made:

1) Lower-Adjacent-Channel Sound-Carrier Rejection Ratio
2) Upper-Adjacent-Channel Picture-Carrier Rejection Ratio
3) Accompanying-Sound-Carrier Rejection Ratio
4) Intermediate-Frequency Rejection Ratio
5) Image Rejection Ratio.

The rejection ratios are ratios of the over-all gain of the receiver at the desired picture carrier frequency to that at the interfering signal frequency of interest.

5.2.3.2 Method of measurement. The test conditions for these measurements are the same as those described in Section 5.2.1.2 except that here the relative gain of the receiver is measured at the picture carrier frequency and at the interfering signal frequency of interest only (as enumerated in Section 5.2.3.1).

In the case of intermediate-frequency and image rejection ratios, the measurements of gain are made at the frequencies within the intermediate- and image-frequency ranges which produce the greatest receiver output.

The intermediate-frequency rejection ratio is usually made for both balanced and unbalanced signal input conditions as follows:

Balanced Input. The signal generator is connected to the receiver through the standard dummy antenna (Section 1.7).

Unbalanced Input. The intermediate-frequency signal is applied unbalanced to the receiver antenna terminals as shown in Fig. 5.2.3.2. However, the desired picture carrier signal is applied balanced through the standard dummy antenna. The unbalanced input voltage is the voltage across the resistor at the output of the resistive pad. When making the unbalanced connection, one should connect the generator ground terminal to a receiver ground terminal which is as near as possible to the antenna connections to the tuner.

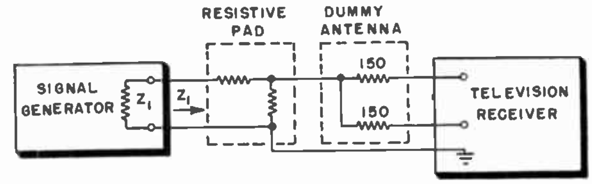

Fig. 5.2.3.2—Connections for unbalanced intermediate-frequency interference ratio measurement.

These rejection ratio measurements are normally made at the receiver gain setting corresponding to nominal sensitivity level.

The measurements should be made on at least one of the standard VHF and one of the standard UHF test frequencies.

5.2.3.3 Presentation of data. The ratio of the input signal level at the interfering frequency of interest to that at the desired picture carrier frequency is expressed in decibels.

5.2.4 Spurious Responses.

5.2.4.1 Introduction. In addition to the interfering signals described in Section 5.2.3, there are other frequencies at which interfering responses may occur. Spurious responses can be caused if external signals or one of their harmonics in combination with the receiver local-oscillator frequency or one of its harmonics produce an interfering signal in the intermediate-frequency pass band. Spurious responses may also be caused by cross modulation.

Because of the extreme frequency range involved, it is generally impractical to test for all possible spurious responses. The test described in Section 5.2.4.2 specifies a limited frequency range which is adequate to cover most of the possibilities likely to be encountered.

In general, the interfering signals existing at the lower end of the frequency range specified in Section 5.2.4.2 will appear as unbalanced signals at the receiver input terminals, while those at the higher end appear as balanced signals. Because the balanced or unbalanced signal condition is a function of many unpredictable factors, the test specifies that measurements be made for both conditions.

5.2.4.2 Method of measurement. For this test a signal source capable of supplying a harmonic-free interfering signal output from 10 μv to at least 2.0 volts is required. This source should cover the frequency range of 0.5 to 1000 mc. To fulfill these requirements, more than one generator may be necessary, and low-pass filters may be required to attenuate harmonics.

The interfering signal generator and the picture and sound signal generator are applied to the receiver in balanced connection through the dummy antenna described in Section 1.7.3. The resolution chart is applied as modulation to the picture signal generator, standard sound modulation is applied to the sound generator, and the interfering signal generator is amplitude-modulated 30 per cent at 1000 cycles. The picture and sound signal generators are adjusted for an input approximately 10 db above the nominal sensitivity input (Section 4.2), the receiver is adjusted for normal operation, and the interfering signal generator is set at maximum output.

The frequency of the interfering signal is varied over the range from 0.5 to 1000 mc while the picture is under observation. Any interference to either picture or sound should be noted together with the frequency at which it occurs. If any interference is noted, the interfering signal level at that frequency is reduced until the interference is just perceptible and this signal level is noted.

The test should be repeated with the picture and sound signal input 10 db below the maximum usable input level (Section 4.6).

These tests should be repeated with the interfering signal applied in the unbalanced connection, as shown in Fig. 5.2.4.2.

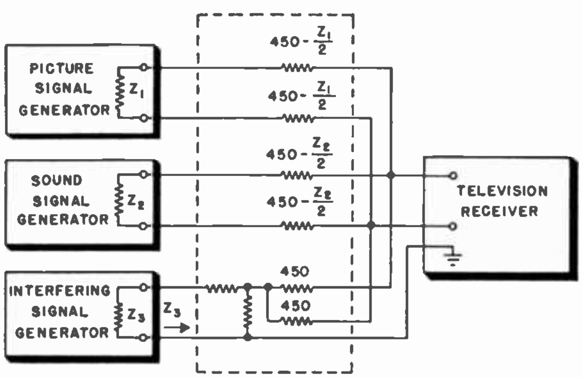

Fig. 5.2.4.2—Generator connections for unbalanced-input spurious-response measurement.

5.2.4.3 Presentation of data. The ratio between the interfering and desired signals in decibels is tabulated where the interference for the condition is just perceptible. The frequency of the interfering signal, the channel to which the receiver is tuned, the level of the desired signal, and the type of interference are noted.

5.3 Internally Generated Interference

5.3.1 Radio-Frequency and Intermediate-Frequency Harmonic Interference.

5.3.1.1 Definition. 1) In a television receiver tuned to accept an RF signal which is a harmonic of the intermediate frequency, the harmonics generated by the IF amplifier may be of sufficient amplitude to be reamplified by the tuner and mixed with the desired RF signal. A beatnote having a frequency equal to the difference between the desired RF carrier and the IF harmonic is produced. If this beat frequency lies within the receiver video pass band, it can be observed on the picture tube screen. This is intermediate-frequency harmonic interference, sometimes referred to as "tweets," and is usually more troublesome with weak input signals.

2) Picture interference may also be caused by harmonics of the desired input signal mixing with harmonics of the local oscillator and producing signals that fall within the intermediate-frequency pass band of the receiver. This interference is more likely to appear with strong input signals.

5.3.1.2 Method of measurement. The picture and sound carrier generators are connected through the standard dummy antenna to the receiver. The picture modulation consists of standard white-pattern modulation and the sound generator is unmodulated. The receiver is adjusted for normal operation.

Observations are made on an oscilloscope connected to the picture tube input. The signal input levels are varied from 10 μv to the maximum usable signal input level (Section 4.6), and the input level and receiver tuning for the most objectionable interference within the usable (neglecting the tweet) picture range are noted. At this level, the peak-to-peak beat output during the picture interval and the blanking level to peak white amplitude are measured.

5.3.1.3 Presentation of data. The peak-to-peak beat output is expressed as a percentage of the blanking level to peak white output and recorded with the input signal level for the channels of interest. Where a subjective evaluation is necessary, a description of the perceptibility of the beat and the effect of receiver tuning should be included with the pertinent test conditions.

5.3.2 Sound into Picture

5.3.2.1 Definition. This type of interference is a result of either the coupling of the sound modulation or 4.5-mc intercarrier signal from the sound channel circuitry to the video circuitry, or intermodulation between sound and picture carriers in the RF or IF circuits. The result is an undesired pattern on the picture tube screen.

5.3.2.2 Method of measurement. The sound and picture signal generators, at standard mean-signal input, are connected to the input of the receiver (Section 1.7.3). The receiver is tuned and adjusted for normal operation (Section 1.10.5). White-pattern modulation (Section 1.5.2) is applied to the picture carrier generator and 100-cps modulation is applied to the sound carrier generator at maximum system deviation. The receiver volume control is adjusted for standard test output (Section 1.9). The speaker should be electrically connected to the receiver and in its normal position with respect to the receiver chassis. The signal source must be free of cross modulation between picture and sound signals.

The sound-to-picture carrier ratio is then increased from unity, maintaining the picture carrier constant, until 100-cps bars are just perceptible on the picture tube screen and the corresponding value of sound-to-picture carrier ratio is recorded.

The test should be repeated with sound modulation removed, and the sound-to-picture carrier ratio increased until the effect of the sound carrier becomes visible in the form of a fine-grain 4.5-mc beat pattern. The corresponding sound-to-picture carrier ratio is recorded.

The preceding tests should be repeated at maximum usable input signal to detect cross-modulation effects.

With unity sound-to-picture carrier ratio at standard mean-signal level, the volume control is advanced until interference is again observed. The power output at which this occurs is noted.

5.3.2.3 Presentation of data. The sound-to-picture carrier ratio in decibels which results in just perceptible interference, together with the picture carrier level, is tabulated for the tests described in Section 5.3.2.2. The sound power output corresponding to just perceptible interference is also noted.

5.3.3 Interference from Horizontal Deflection Circuits.

5.3.3.1 Introduction. This interference is usually caused by bursts of RF energy generated in the horizontal deflection system and coupled into the signal circuits at either the incoming signal frequency or intermediate frequency. The visual effects usually consist of a vertical bar in the picture or horizontal synchronization instability, or both. The interference may appear on one or more channels and is usually more severe at weak signal input levels.

5.3.3.2 Method of measurement. The receiver is tuned to a channel where the interference is noted. The appropriate picture carrier signal with white-pattern modulation (Section 1.5.2) is connected to the receiver through the dummy antenna, and the receiver is tuned normally. The transmission line to the tuner should be in its normal position for this measurement since the results are affected by the location (and the balance) of the input system.

The level of the picture carrier signal is then gradually increased until the interference is no longer perceptible. This signal level is recorded. The test should be repeated for all channels where the interference is noted.

5.4 Compatibility with Color Signal

5.4.1 Introduction. The purpose of this test is to determine subjectively whether the monochrome receiver under test is capable of receiving a color signal without producing undesirable beatnote patterns in the picture.

5.4.2 Method of Measurement. For this test a laboratory-generated color signal is required. The picture and sound carrier signals at standard mean-signal level are connected to the receiver. Standard sound test modulation is applied to the sound carrier and the picture carrier is modulated with video information corresponding to a color bar pattern. It is desirable to have full-purity (or "saturated") color bars corresponding to each of the primary colors as well as the complementary colors, and in addition one white bar. The white bar is transmitted as a peak white signal at full intensity, and the color bars are transmitted at 75 per cent of their maximum possible amplitude in order to avoid over-modulation effects on certain colors. These levels are chosen as representative of the most severe conditions ordinarily found in natural scenes.

With the receiver controls adjusted for normal operation, the picture is observed in each of the bar areas for the presence of spurious patterns resulting from the 3.58-mc chrominance signal, or a 920-kc beatnote between the chrominance signal and the sound carrier. Effects of variations in the tuning should also be noted.

The test should be repeated with the sound carrier level maintained at twice the picture carrier level. A check should be made to determine whether the results vary significantly with signal level.

5.4.3 Presentation of Data. The presence of a 3.58-mc or a 920-kc beat should be recorded, together with the corresponding input signal conditions. The effect of variations in the receiver tuning control should also be noted.

5.5 Impulse Noise Interference Susceptibility

At present no instrument is available which closely simulates the interference generated by automobile ignition systems, vibrators, shavers, and similar sparking devices. Lacking such equipment, receiver performance under impulse-noise conditions is usually evaluated by making comparative performance tests using an actual noise source coupled to the receiver input.

The receiver under test and the comparison receiver are placed in a shielded room and connected through a dummy-antenna network so as to receive equal signals. The noise source is mounted outside the shielded room and coupled to the single cable which feeds both receivers.

The receivers are adjusted for normal operation using standard test-pattern picture modulation and standard sound modulation. Initial tests are made at a level 10 db above nominal sensitivity level.

The susceptibility of the receiver is tested by observing the performance as the interference input level is increased. Observations should be made for the following defects:

a) Disturbance of the luminance during and immediately after the interfering pulses. Note should be made of whether the interference is predominantly black or white, the duration of the interference, the presence of blocking, and AGC disturbance.

b) Disturbance of the horizontal synchronization.

c) Disturbance of the vertical synchronization.

d) Disturbance of the sound output.

The relative performance of the receiver under test with respect to the comparison receiver is described. The observations are repeated at various input signal levels and with various types of noise sources.

Chapter 6—Electrical Fidelity, Picture

6.1 Introduction

The electrical fidelity is the over-all response of the receiver to the electrical variations which make up the signal present at the picture tube input. This involves two broad characteristics:

One is the ability of the receiver circuits, as the scanning spot travels horizontally, to reproduce a transition representing an abrupt change from black to white (or vice versa) and to resolve fine horizontal detail. This ability is dependent on the amplitude and phase response of the receiver to frequencies above 100 kc. In a monochrome receiver the phase response need not be measured directly since adequate information may be obtained from measurement of the amplitude response (Section 6.3) and the step response (Section 6.4).

The other characteristic is the ability to reproduce the electrical variations which correspond to the shading in the picture. This involves the response to frequencies down to the field repetition rate. The information may be obtained by observing the low-frequency square-wave response (Section 6.5) at both the field rate and the line rate.

6.2 General Measuring Techniques

6.2.1 Picture Signal Generator. The signal source for measuring the electrical fidelity must have sufficiently low distortion so as not to interfere with the receiver measurements. In addition to the test modulation, the picture carrier should be provided with composite sync modulation. This is desirable so that the AGC, sync, and dc restorer circuits function normally. If composite sync modulation is not used, these circuits should be biased in such a way that the normal picture signal response is not distorted. For additional requirements of the picture signal generator, refer to Section 2.1.

6.2.2 Vestigial-Sideband Filter. To exactly simulate the television broadcast transmission characteristic requires the use of a vestigial-sideband filter. However, most receivers have sufficient selectivity so that this relatively complex filter can normally be omitted with negligible distortion of the amplitude response and the step response.

6.2.3 Standard Envelope-Delay Predistortion Network. To simulate television broadcast transmissions, a standard envelope-delay predistortion network (Fig. 6.2.3) is inserted ahead of the modulation input of the picture signal generator. (This network is designed to compensate for the high-frequency phase distortion introduced by the relatively sharp cutoff in the picture IF amplifier of color receivers.)

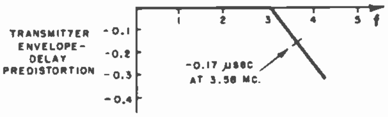

Fig. 6.2.3—Response of the standard transmitter envelope-delay predistortion network.

6.2.4 Receiver Input Connections. The output of the picture signal generator is supplied to the receiver as described in Section 1.7.

6.2.5 Selection of RF Channel. The measurements are normally made on a single channel having a relatively flat RF response.

6.2.6 Receiver Tuning. The receiver must be carefully tuned. If the tuning differs from that in Section 1.10.5.2, the tuning criterion should be described in the data.

6.2.7 Signal Input Level. The standard mean-signal input level is used.

6.2.8 Picture Signal Generator Modulation. The picture signal generator modulation is specifically described for each of the three measurements in Sections 6.3.2, 6.4.2, and 6.5.2.

6.2.9 Test Output Level. The nominal test output level is the standard picture test output (Section 1.8). However, other levels may be used where the modulation percentage or the contrast control has a significant effect on the response.

6.2.10 Adjustment of Receiver Controls. The receiver controls are adjusted for normal operation. In each of the measurements the effect of the contrast control on the response should be observed and, where significant, measurements should be repeated for representative settings of this control. The brightness control should be adjusted for normal operation for each of these contrast control settings so that picture tube overload will not distort the response. Where overload occurs in the video amplifier, it may be necessary to reduce the percentage of the picture signal modulation. Deviations from the specified measuring conditions should be included in the data.

6.2.11 Oscilloscope Connection. The response at the input of the picture tube is observed using a wide-band oscilloscope (Section 2.5). A probe having negligibly small input capacitance may be used; alternatively, the picture tube may be disconnected and its capacitance replaced by that of the oscilloscope in such a way as not to alter the original response.

6.3 Amplitude Response

6.3.1 Definition. The amplitude response is the sine-wave modulation-frequency response characteristic at the picture tube input as a function of the modulation frequency.

6.3.2 Method of Measurement. The picture signal generator is modulated with a composite sync signal and a sine-wave picture signal as shown in Fig. 6.3.2. The sine-wave modulation frequency is varied between 100 kc and 4.5 mc while maintaining the modulation constant at the level where the peaks of the sine waves correspond to 15 per cent and 70 per cent of the synchronizing signal peaks. A video sweep generator may be used for this modulation.

The receiver contrast control is adjusted for standard picture test output at the input of the picture tube for the lowest modulation frequency (100 kc). Where contrast control settings have a significant effect on the response, the response should be measured at several

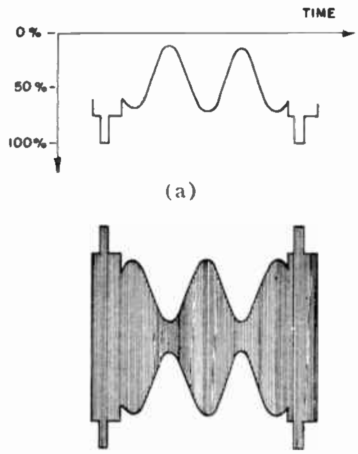

(a)

(b)

Fig. 6.3.2—Sine-wave picture signal used for measuring the amplitude response. (a) Picture-tube signal. (b) Modulated RF picture signal.

representative settings, observing the precautions of Section 6.2.10.

The amplitude response may be dependent on the percentage modulation of the sine-wave picture signal. If the response is observed to change significantly as the percentage modulation is reduced, the measurement should be repeated with the modulation of the sine-wave envelope reduced by 6 db.

6.3.3 Presentation of Data. The amplitude of the sine wave at the input to the picture tube is plotted as a function of the modulation frequency as shown in Fig. 6.3.3.

6.4 Step Response

6.4.1 Definition. The step response is the waveform measured at the picture tube input when the picture modulation is a rectangular pulse having sufficient duration for steady-state to be reached.

6.4.2 Method of Measurement. The standard picture signal generator is modulated with a rectangular pulse and composite sync [Fig. 6.4.2(a)]. The rectangular pulse is synchronized to the line scanning frequency and phased so as to produce a black vertical bar. The step response is described by the waveform at the picture tube input corresponding to the black-to-white and white-to-black transitions. This contains the desired information on rise time, overshoot, ringing, smear, etc., as defined by Fig. 6.4.2(b). (This differs considerably from a typical receiver response.)

The step response may be dependent on the percentage modulation. If the response is observed to change significantly as the percentage modulation is reduced, the measurement should be repeated with the modulation reduced by 6 db.

When the contrast control is observed to have a significant effect on the step response, the measurement should be repeated for representative settings of the contrast control.

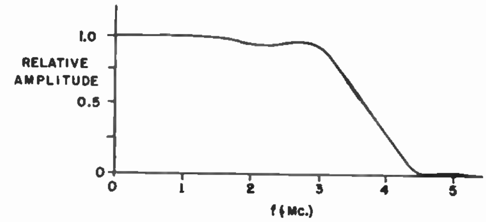

Fig. 6.3.3—Over-all receiver amplitude response.

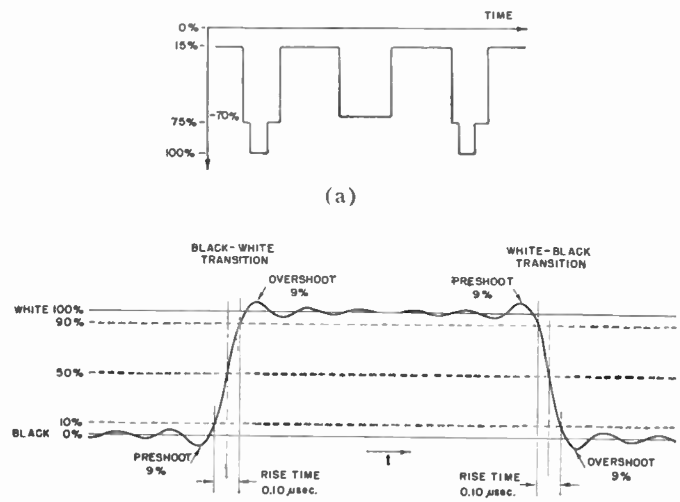

(a)

(b)

Fig. 6.4.2—(a) Rectangular pulse modulation for step-response measurement. (b) Nomenclature for specification of high-frequency square wave (response shown is that of ideal band-pass filter with rectangular cutoff).

6.5 Low-Frequency Square-Wave Response

6.5.1 Definition. The low-frequency square-wave response is the waveform produced at the picture tube input, at the field rate and the line rate, when the input signal modulation corresponds to a pattern the lower half of which is black and the upper half white.

6.5.2 Method of Measurement. The picture signal generator is modulated with white at 15 per cent and black at 70 per cent of the peak of sync. The waveform at the picture tube input and the level shift are observed as in Fig. 6.5.2.

Frequently measurement of the low-frequency square-wave response is complicated by the presence of other low-frequency voltage components at both the grid and cathode of the picture tube, including blanking components. In such instances, the resultant output waveforms must be determined with due consideration for these components.

Hum voltages associated with the power supply may lead to errors in the measurements. These can be identified by operating the receiver from a supply which is asynchronous with the field frequency.

6.5.3 Presentation of Data. The low-frequency square-wave responses, including the white-level shift, are shown as in Fig. 6.5.2(a) for the vertical rate, and Fig. 6.5.2(b) for the horizontal rate. Significant power supply hum components should be noted.

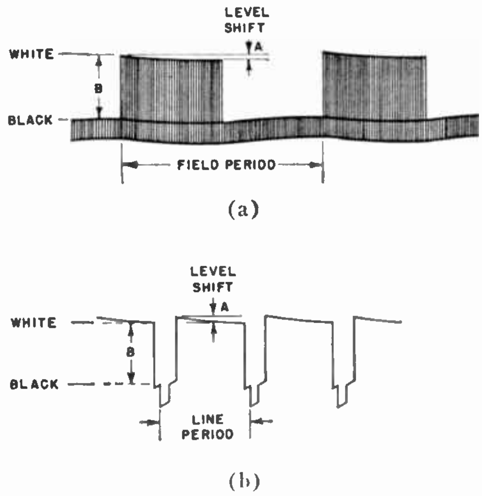

Fig. 6.5.2—(a) White-picture level shift during the field period, and (b) same but during the line period.

6.6 Electrical Transfer Characteristic

The electrical transfer characteristic may be plotted following a procedure similar to that described in Section 3.14 for measuring the luminance transfer characteristic.

Chapter 7—Stability

7.1 Stability of Local Oscillator

7.1.1 Introduction. These tests are designed to show variations in the frequency of the local oscillator of a television receiver resulting from receiver warm-up and changes in line voltage and signal input level.

7.1.2 Warm-up Drift.

7.1.2.1 Introduction. The local-oscillator frequency usually varies with time for a period following receiver turn-on because of slight changes in component values and tube characteristics with rising temperatures. Ideally, this test is made under controlled humidity conditions and a statement of the existing humidity is included with the test data.

7.1.2.2 Method of measurement. Local-oscillator frequency drift can be measured by measuring the variation of the intermediate frequency produced in the receiver when receiving a stable RF signal. If a suitable frequency counter is available, the intermediate frequency is measured directly at the output of the IF amplifier.

Lacking a frequency counter, the measurement may be made by injecting a signal into the IF amplifier from a stable signal generator covering the intermediate-frequency range. The beatnote produced is monitored at the picture tube and measurements are made by reading the signal generator frequency required to maintain zero-beat output.

The RF picture signal is applied at standard mean-signal input on one of the standard test frequencies.

The receiver is turned on and the fine tuning control is quickly adjusted to place the produced IF signal at the nominal picture intermediate frequency of the receiver. In taking the succeeding measurements of local-oscillator drift with time, the fine tuning control is left untouched.

Frequency readings should be started at one minute after turning on the receiver and continued at suitable intervals until the frequency is stabilized.

The test should be repeated for all channels of interest, always allowing sufficient time for the receiver to cool off completely.

7.1.2.3 Presentation of data. Curves of local-oscillator frequency drift with time are plotted as in Fig. 7.1.2.3.

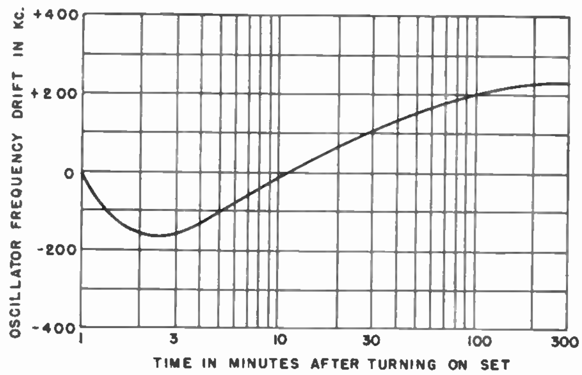

Fig. 7.1.2.3—Local-oscillator warm-up frequency drift characteristic.

7.1.3 Drift with Line-Voltage Variation.

7.1.3.1 Method of measurement. The procedure used to measure drift with line-voltage variation is similar to that described in Section 7.1.2.2. Before this test is begun, however, the receiver should have been in operation long enough to reach temperature stability as determined in Section 7.1.2.2. The fine tuning control is adjusted to produce the nominal oscillator frequency at a line voltage of 117 volts.

The deviation from nominal oscillator frequency is read as the line voltage is varied in 5-volt steps from 105 to 130 volts. Allowance of approximately half a minute should be made after shifting the line voltage so that the cathode temperature stabilizes.

The test should be repeated for all channels of interest.

7.1.3.2 Presentation of data. Curves of frequency drift vs line voltage are plotted as in Fig. 7.1.3.2.

7.1.4 Drift with Variation in Signal Input Level.

7.1.4.1 Introduction. Variations in signal input level may affect the oscillator frequency indirectly by way of the automatic-gain-control circuit. Because of the internal power-supply impedance, variations in AGC voltage may significantly change the dc voltage applied to the oscillator circuit.

7.1.4.2 Method of measurement. The measurement procedure used is similar to that described in Section 7.1.2.2 except that the receiver should have reached

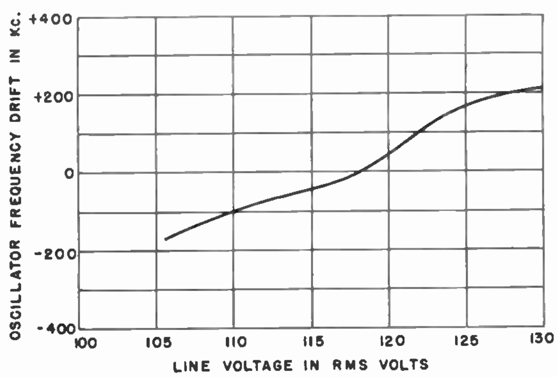

Fig. 7.1.3.2—Local-oscillator frequency drift with line-voltage variation.

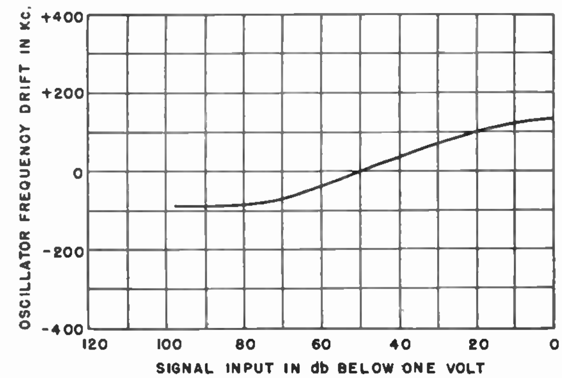

Fig. 7.1.4.3—Local-oscillator frequency drift with signal-input level variation.

temperature stability before readings are taken. The fine tuning control is adjusted to produce the nominal oscillator frequency at a line voltage of 117 volts.

Readings of deviations from nominal oscillator frequency are made as the signal input level is varied from 10 μv to 1 volt.

7.1.4.3 Presentation of data. Curves of local oscillator frequency drift vs signal input level are plotted as in Fig. 7.1.4.3.

7.2 Stability of Deflection Synchronization

7.2.1 Range of Hold Controls.

7.2.1.1 Introduction. It is necessary in the case of automatic-frequency-controlled oscillators to differentiate between pull-in range and hold-in range. Hold-in range is the range of applied frequencies over which the oscillator will hold synchronism once it is synchronized. Pull-in range is the range of applied frequencies over which the oscillator will pull into synchronism as the signal is initially applied. The hold-in range is greater than the pull-in range. Operation of scanning systems beyond the pull-in range but within the hold-in range is normally not satisfactory, since any momentary interruption in the signal will cause the receiver to lose synchronism. Pull-in range is, therefore, the important factor.

With vertical synchronizing circuits, which are usually triggered, the hold-in and pull-in ranges are substantially equal.

7.2.1.2 Method of measurement. For pull-in range measurements, the picture carrier with white-pattern modulation (Section 1.5.2) is applied through the standard dummy antenna to the receiver. The receiver is tuned as described in Section 1.10.5.2. Measurements are made at nominal picture sensitivity level (Section 4.2), standard mean-signal input level, and maximum usable signal level (Section 4.6). The contrast control is set for standard picture test output.

7.2.1.2.1 Horizontal pull-in range. The horizontal hold control is used to throw the receiver out of horizontal synchronism and then is slowly returned to the position where the picture just returns to synchronization. The frequency of the scanning oscillator, just before pull-in occurs, is measured. This measurement is made with the hold control moving in from both sides of center frequency, and the difference of these two frequencies is the horizontal pull-in range.

7.2.1.2.2 Vertical pull-in range. The vertical hold control is used to throw the receiver out of vertical synchronism, and then returned slowly to the position where the picture just returns to synchronization. The synchronizing voltage is then removed from the vertical oscillator, permitting it to free-run, and the frequency of the vertical oscillator is measured. The measurement should be repeated for the other setting of the hold control where synchronization just takes hold. When removing the synchronizing voltage care must be taken that the frequency-determining circuits of the oscillator are not affected.

7.2.1.3 Presentation of data. The frequency difference between the two extremities of the pull-in range is tabulated for the horizontal and vertical pull-in measurements together with the signal input level at which the measurement is made.

7.2.2 Scanning Oscillator Stability.

7.2.2.1 Introduction. These stability tests are designed to show variations in the frequencies of the horizontal and vertical scanning oscillators resulting from receiver warm-up and variations in line voltage.

7.2.2.2 Warm-up drift.

7.2.2.2.1 Method of measurement. For these measurements the synchronizing channel of the receiver is suitably disabled so as to allow the scanning oscillators to run free. An RF input signal is not required for this test but care should be taken that any stray input signals do not change during the measurement.

Frequency measurements of the horizontal and vertical scanning frequencies are made by means of a frequency counter. Alternatively, oscilloscope Lissajous patterns using a calibrated audio-frequency generator and loosely coupled signals from the horizontal and vertical scanning circuits can be used. These measurements are made for the same time interval described in Section 7.1.2.2.

7.2.2.2.2 Presentation of data. The horizontal and vertical scanning oscillator warm-up drifts are plotted as in Fig. 7.1.2.3 with the appropriate changes of the frequency scale.

7.2.2.3 Drift with line-voltage variation.

7.2.2.3.1 Method of measurement. The procedure used to measure scanning oscillator drift with line-voltage variation is similar to that described in Section 7.2.2.2.1 except that the frequency readings are taken as a function of line voltage. The line voltage is varied in 5-volt steps from 105 to 130 volts.

Before this test is begun, the receiver should have reached temperature stability as determined in the measurement of Section 7.2.2.2.1.

7.2.2.3.2 Presentation of data. The horizontal and vertical scanning oscillator frequency drifts are plotted as in Fig. 7.1.3.2 with appropriate changes of the frequency scale.

7.2.3 Static Phase Accuracy of AFC Loop.

7.2.3.1 Definition. The static phase accuracy is a measure of the change in relative phase between input and output of the AFC loop which accompanies a change in either input frequency or local-oscillator frequency.

7.2.3.2 Method of measurement. To measure the static phase accuracy, a picture signal generator, modulated with the resolution chart and having an output amplitude equal to standard mean-signal input level, is applied through the dummy antenna (Section 1.7) to the receiver. The receiver is tuned according to Section 1.10.5. The contrast control is adjusted for standard test output.

The horizontal hold control is moved first clockwise and then counterclockwise to the extremes of the pull-in range as defined in Section 7.2.1. The location of a fixed point of the test pattern is observed on the picture-tube screen and the horizontal displacement of this point is measured as the horizontal hold control is moved through the pull-in range. The static phase accuracy in degrees per cycle per second is given by

$$\frac{\text{Observation Point Displacement (inches)} \times 360 \text{ (degrees)}}{1.15 \times \text{Trace Width (inches)} \times \text{Pull-In Frequency Range (cps)}}.$$

The factor 1.15 in this equation allows for a retrace time of 13 per cent. Trace width refers to the length of horizontal travel of the forward trace of the electron beam. If the scanning width is so great that the picture tube is overscanned, the trace width should include that portion of the trace which lies beyond the edge of the picture tube.

7.2.4 Phase Step Response of AFC Loop.

7.2.4.1 Definition. This test is a measure of the response of the horizontal AFC loop system to a step of input phase. This response is indicative of the system's ability to integrate the incoming synchronizing information over a given period of time. Systems with the same step response will, in general, show comparable performance under the influence of random noise.

7.2.4.2 Method of measurement. Method 1: The horizontal synchronizing signal is phase-modulated at the sync generator with a 30-cps square wave synchronized with the sync generator. The receiver is synchronized both horizontally and vertically and is adjusted for best linearity. The horizontal hold control is set at the center of its pull-in range. A stationary video pulse is transmitted during each horizontal line so that a vertical white line appears in the center of the picture tube screen when the phase modulation is removed from the synchronizing signal. With the phase modulation applied, the white line traces the positive and negative step response of the AFC loop on alternate fields as a stationary pattern on the picture tube screen. In this display the vertical axis is the time axis and the horizontal axis displays the output phase amplitude. A special signal generator has been developed for this test and is described by Gruen.[7] In this method, the synchronizing signal, but not the video pulse, is phase-modulated. To insure linear operation of the AFC loop, the phase-modulation amplitude should not exceed ±30 degrees.

A typical step response is shown in Fig. 7.2.4.2. Rep-

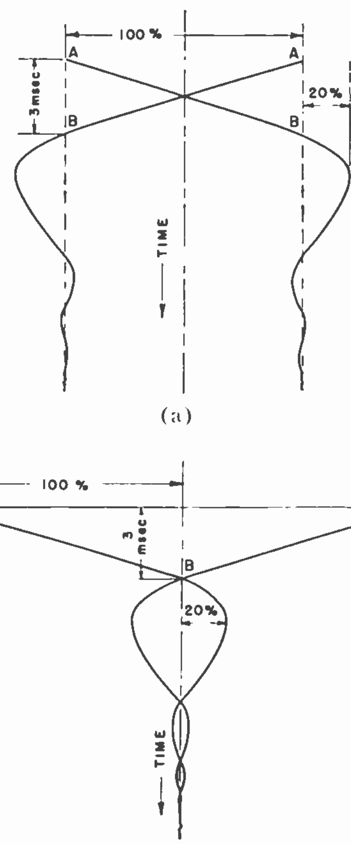

Fig. 7.2.4.2—Typical phase step response of horizontal AFC loop.

[7] W. J. Gruen, "Test generator for horizontal AFC scanning system," IRE Trans. on Broadcast and Television Receivers, vol. PGBTR-5, pp. 36–43; January, 1954.

resentative ranges of values of overshoot are 15–25 per cent, and of rise time from the start of the transient to the first crossover (point *A* to point *B*) are 2–4 msec. The start of the transient should be smooth as shown in the figure; an abrupt change at this point is indicative of direct sync getting into the horizontal oscillator.

Method 2: If the composite sync generator of the picture-signal generating equipment is accessible, a 30-cps square wave may be introduced into the reactance tube of the sync generator to obtain the desired phase modulation. (The sync generator's 31.5-kc oscillator should operate as a locked oscillator controlled by a fixed frequency.) With this method, both the video and sync signals are phase-modulated.

7.2.4.3 Presentation of data. The results of this measurement consist of photographs of, or plots derived from, the picture-tube screen and will be of the form of Fig. 7.2.4.2.

7.2.5 Interference Affecting Synchronization. Receivers are tested for vulnerability to impulse-noise interference as described in Section 5.5.

It is possible for picture or sound information to affect the synchronization. This is checked by subjecting the receiver to a wide range of operating conditions, including operation at minimum and maximum contrast, high brightness, high sound output, etc.

Any impairment of synchronization is reported along with a description of the test conditions.

Part III—SOUND SECTION OF THE RECEIVER

Chapter 8—Sensitivity

8.1 General

This section includes procedures for the measurement of the over-all performance of the sound channel. Receivers employing a separate sound IF channel have not been produced for some years and therefore are not considered.

In all tests, it is assumed that the input signal consists of both the picture and sound signals, and that the ratio of the sound-to-picture carrier is unity, unless otherwise specified. The difference frequency between the carriers must be maintained accurately at 4.5 mc ±5 kc.

All measurements described are on the basis of an over-all test. However, particularly in making design rather than performance measurements, it is frequently advantageous to check the 4.5-mc intercarrier sound channel by breaking into the receiver at the video detector output with a 4.5-mc signal. Adequate isolation is required in this case to prevent loading and regenerative effects.

8.2 Sound Sensitivity

The sensitivity of the sound channel is measured under the same conditions as the nominal picture sensitivity (Section 4.2) and the peak picture sensitivity (Section 4.3). The corresponding sensitivities for the sound channels are termed the nominal sound sensitivity and the peak sound sensitivity, respectively.

8.3 Nominal Sound Sensitivity

8.3.1 Definition. This is the lowest input signal required to produce standard sound test output when the receiver is tuned to produce the nominal intermediate frequency.

8.3.2 Method of Measurement. The receiver under test is connected to the sound and picture signal generators through the standard 300-ohm dummy antenna (Section 1.7.3) and tuned as described in Section 1.10.5.2 to produce the nominal intermediate frequency. Unity ratio is maintained between sound and picture carriers. The sound signal generator is frequency modulated 30 per cent (7.5-kc deviation) at a 400-cps rate. The picture-signal generator is modulated with standard white-pattern modulation (Section 1.5.2), and the receiver controls are adjusted as in measuring the picture sensitivity (Section 4.2). The volume control is at maximum and the tone control is set for maximum 400-cps response. The signal generator outputs are adjusted to obtain standard sound test output (Section 1.9) across the dummy load. The output meter should be connected across the load through a 400-cps bandpass filter to reject the random noise output (Fig. 8.3.2).

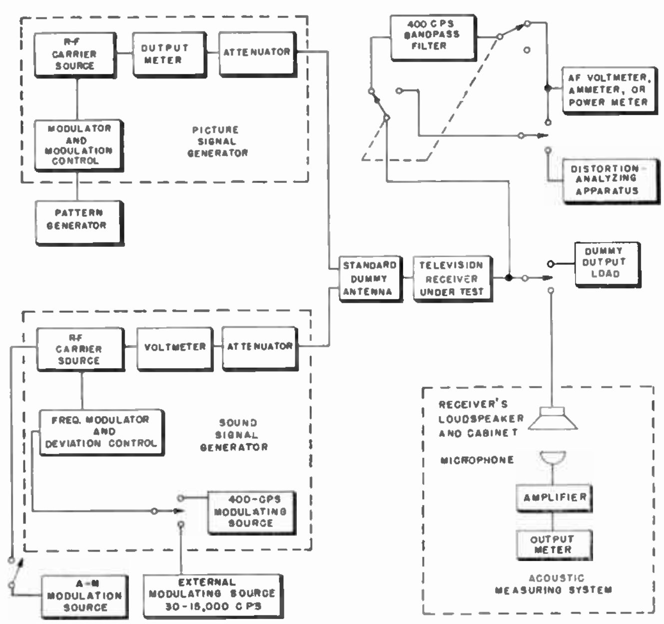

Fig. 8.3.2—Block diagram of equipment for testing the over-all performance of the sound section of a television receiver

8.4 Peak Sound Sensitivity

8.4.1 Definition. This is the lowest input signal required to produce standard sound test output when the receiver is tuned as in measuring peak picture sensitivity (Section 4.3).

8.4.2 Method of Measurement. The procedure is the same as Section 8.3.2 except for the receiver tuning.

8.5 Quieting Sensitivity

8.5.1 Definition. The quieting sensitivity is the lowest input signal required to reduce the noise output to a value which is 30 db below the output obtained when standard test modulation (Section 1.6) is applied to the sound carrier.

8.5.2 Method of Measurement. The procedure is similar to that for measuring nominal sound sensitivity (Section 8.3) except that the volume control is adjusted to maintain standard sound test output (Section 1.9) and the tone controls are adjusted to provide a flat over-all response (allowing for normal transmitter pre-emphasis). The standard sound test modulation is then switched on and off, while the input signal is reduced until a value is reached at which a 30-db difference in indicated output is noted between the modulated and unmodulated conditions. This value of input signal is the quieting sensitivity.

8.6 Signal-to-Noise Ratio

To supplement the quieting sensitivity (Section 8.5), it is desirable to measure the signal-to-noise ratio as a function of input signal. The picture and sound signal generators are connected to the receiver as described in Section 1.7. White-pattern modulation (Section 1.5.2) is used for the picture and 400-cps 30 per cent modulation for the sound. The receiver controls are adjusted for normal operation. At each input level the sound output is observed with the volume control set for standard output and the tone controls adjusted as in Section 8.5.2. A 400-cps band-pass filter should be used to reject noise (Fig. 8.3.2). The modulation is then switched off, the filter removed from the circuit, and the noise output measured. The signal-to-noise ratio is expressed in decibels and plotted as a function of the input signal (Fig. 8.6). Hum, deflection voltage pickup, and video interference should not be included in this noise measurement; these are separately evaluated (Section 10.4).

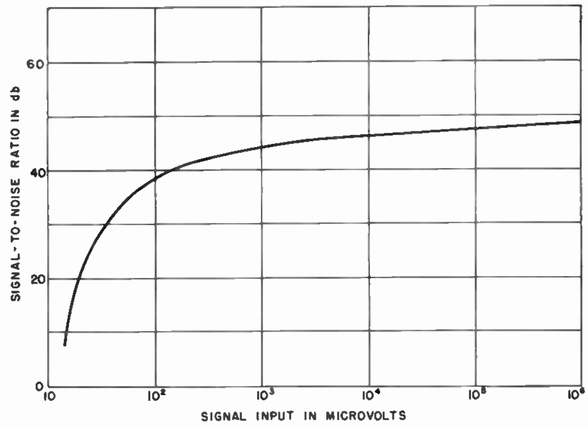

Fig. 8.6—Signal-to-noise ratio.

8.7 AGC Characteristic

Refer to Section 4.5.

8.8 Limiting Characteristic

8.8.1 Introduction. The limiting characteristic shows the variation in the sound output as the sound carrier amplitude is varied, the picture carrier amplitude being maintained constant. The degree of limiting affects the variation in sound output with receiver tuning. It also affects the suppression of amplitude modulation and interference (Section 9.2), although this suppression is accomplished by other than static limiting in many receivers.

8.8.2 Method of Measurement. The limiting characteristic is measured by connecting the picture and sound signal generators as in Section 1.7, using standard mean-signal input level. Standard gray-pattern modulation is used (Section 1.5.3). The sound carrier is 30 per cent modulated at 400 cps, and the volume control is set for standard output at the maximum point on the output characteristic. The sound carrier amplitude is varied below and above the nominal 1:1 sound-to-picture carrier ratio and the sound output is plotted against the sound-to-picture carrier ratio.

Chapter 9—Interference, Sound Section

9.1 Selectivity and Spurious Responses

The over-all selectivity curve (Section 5.2.1) provides a measure of the susceptibility of the sound channel to interference from adjacent-channel signals and other undesired signals. For example, the susceptibility to adjacent-channel picture carrier interference is usually determined by the selectivity for a signal 1.5 mc above the desired sound carrier frequency.

The test procedure used to check spurious responses in the picture channel is applicable to the sound channel as described in Section 5.2.4.

The sound IF circuits which are tuned to the 4.5-mc intercarrier frequency are sufficiently selective with conventional design so that measurement of their selectivity is not normally required.

9.2 Amplitude-Modulation Suppression Ratio

9.2.1 Introduction. The AM suppression ratio is a measure of the ability of the sound channel to reject undesirable amplitude modulation of the sound carrier. This amplitude modulation can occur, for example, as a result of cross-modulation of the sound carrier with the modulated picture carrier.

Two methods are described for measuring the suppression of amplitude modulation: 1) the meter method (Section 9.2.2) and 2) the oscilloscope method (Section 9.2.3). The meter method has the advantage of being more sensitive and providing a more quantitative measure of amplitude-modulation suppression for receivers which have a high degree of suppression. The oscilloscope method, although less sensitive, frequently provides useful design information not directly obtainable from the meter method.

9.2.2 Meter Method. The picture and sound signal generators are connected to the receiver as described in Section 1.7. Standard white-pattern modulation (Section 1.5.2) is used for the picture carrier. The receiver controls are adjusted for normal operation with the generators set at standard mean-signal input level.

The sound carrier is simultaneously frequency- and amplitude-modulated. The sound carrier is 30 per cent frequency-modulated at between 50 and 70 cps and 30 per cent amplitude-modulated at 400 cps. A 400-cps high-pass filter is used to measure the output resulting from the amplitude modulation. This choice of AM and FM frequencies has the advantages that harmonic distortion of the FM output and incidental undesired frequency modulation of either the picture or sound carriers at power-supply frequency are rejected by the high-pass filter.

The sound signal generator must have negligible incidental frequency modulation when it is amplitude-modulated. The picture signal generator must also satisfy this requirement. Unless the equipment is known to have negligible incidental frequency modulation, an external amplitude modulator, adequately isolated, should be used.

The output resulting from the 30 per cent frequency modulation is measured with the amplitude modulation removed. The 30 per cent amplitude modulation is then simultaneously applied to the sound carrier and the 400-cps high-pass filter is used to measure the output resulting from the amplitude modulation. The ratio of the two outputs, corrected for the filter attenuation, and expressed in decibels, is the AM suppression ratio.

The measurement is normally made on one channel for various input signal levels. Repetition of the measurement for higher percentages of amplitude modulation and at other amplitude-modulation frequencies provides useful data.

To eliminate the effect of noise, it is frequently desirable to carry out the measurement at mean-signal level with unity sound picture carrier ratio, and to repeat the measurement with the sound carrier amplitude as the parameter. Alternatively, the measurement can be made at the 4.5-mc intercarrier beat frequency (Section 8.1).

9.2.3 Oscilloscope Method. In the oscilloscope method, the procedure is similar to that for the meter method. However, the sound output is connected to the vertical plates of an oscilloscope, while the AF generator which frequency-modulates the sound carrier is connected to the horizontal plates so as to produce the display shown in Fig. 9.2.3. Correction for phase shift may be required to close the pattern.

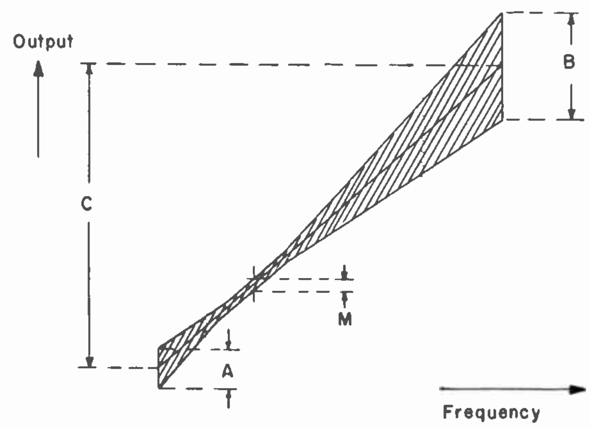

Fig. 9.2.3—Display of amplitude-modulation-suppression ratio on the oscilloscope.

The formulas shown below define an unbalanced suppression ratio, a balanced suppression ratio and a maximum suppression ratio:

$$\text{Unbalanced suppression ratio} = R_u = 2\left|\frac{C}{A-B}\right|$$

$$\text{Balanced suppression ratio} = R_b = 2\left|\frac{C}{A+B}\right|$$

$$\text{Maximum suppression ratio} = R_m = \left|\frac{C}{M}\right|.$$

The expressions for R_u and R_b are applicable only when the pattern is as shown in Fig. 9.2.3. When the cross-over point is outside the displayed pattern, the expressions for R_u and R_b become:

$$R_u = 2\left|\frac{C}{A+B}\right|$$

$$R_b = 2\left|\frac{C}{A-B}\right|$$

The procedure described in connection with the meter method is applicable to the oscilloscope method.

Although 30 per cent frequency modulation is used in measuring these suppression ratios, as in the meter method, it is desirable to increase the frequency modulation to at least 100 per cent in order to view the complete discriminator characteristic.

Chapter 10—Fidelity, Sound Section

10.1 Electric and Acoustic Fidelity

This chapter describes methods for measuring the electric fidelity, including the amplitude-vs-frequency response, harmonic distortion, and power output of the audio signal delivered to the dummy load which replaces the speaker. The acoustic fidelity is measured by applying the same signal generator and receiver procedures, with the speaker in the completely assembled cabinet replacing the artificial load. Acoustic measuring procedures are described in other IRE standards.

10.2 Amplitude-vs-Frequency Response

10.2.1 Definition. The amplitude-vs-frequency response shows the manner in which the electrical output delivered to the dummy load reproduces the modulating audio signal. It takes into account all characteristics of the receiver except those of the loudspeaker.

10.2.2 Method of Measurement. The picture and sound signal generators are connected to the receiver which is adjusted for normal operation as in Section 1.10.5. Mean-signal input level and 30 per cent sound modulation are used. The receiver volume control is adjusted so that the point of maximum response in the audio frequency range gives standard sound test output. The output is observed while the modulation frequency is varied continuously from 30 to 15,000 cps.

If the receiver has one or more tone controls, the response is plotted for the adjustment which gives the maximum bass and treble compensation. The tests should be repeated for minimum and mean settings of the tone controls.

If the response changes substantially with the volume control setting, this test should be repeated at selected power levels.

Since no pre-emphasis is employed in the sound signal generator, the measured power output values should be corrected by adding the values corresponding to the standard receiver de-emphasis curve, which has the absolute values shown in Fig. 1.6.

The presence of overload at any point should be noted.

10.2.3 Presentation of Data. The results are plotted with the frequency as the abscissa on a logarithmic scale and the power output in decibels as the ordinate on a linear scale. The 400-cps output is taken as the 0-db reference level and the corresponding absolute power is noted on the graph.

10.3 Harmonic Distortion

10.3.1 General. The over-all harmonic distortion in the electrical output is measured for a wide variety of signal and operating conditions. From these measurements it is possible to determine the part of the receiver which is responsible for the distortion.

Nonlinear distortion in the signal generating and measuring equipment must be negligible.

10.3.2 Definition. The harmonic distortion is determined by the percentage of the rms value of the harmonics in the output when a pure sinusoidal modulating signal is used, the formula being

$$K = \frac{\sqrt{E_2^2 + E_3^2 + E_4^2 + \cdots}}{\sqrt{E_1^2 + E_2^2 + E_3^2 + E_4^2 + \cdots}} \times 100 \text{ per cent.}$$

E_1 is the fundamental-frequency voltage and E_2, E_3, E_4, etc. are the voltage values of the individual harmonics present across the dummy load.

Hum, deflection, and video components are not included in harmonic distortion.

A distortion analyzer will read the rms value of the total distortion, while a wave analyzer is required if the individual harmonics are of interest.

10.3.3 Method of Measurement. The picture and sound signal generators are connected to the receiver as described in Section 1.7. Standard gray-pattern modulation is used. Unless otherwise specified, standard mean-signal input level is used and the controls are adjusted for normal operation. If interference from either the power supply, video, or deflection system is encountered, suitable precautions are taken so that the harmonic distortion measurement is not affected. A wave analyzer may be used to measure the individual harmonics.

The distortion is measured with the following characteristics as the principal parameters:

10.3.3.1 Distortion vs power output. The modulation is fixed at 30 per cent, the modulation frequency at 400 cps, and the harmonic distortion is plotted as the output is varied by means of the volume control.

The *power output for 10 per cent harmonic distortion* and the *maximum power output* without regard to distortion are individually noted.

The *residual power output* is the output corresponding to minimum setting of the volume control.

10.3.3.2 Distortion vs percentage modulation. The modulation frequency is fixed at 400 cps and the output is maintained at standard test output by adjustment of the volume control (where possible). The harmonic distortion is plotted as the modulation is varied from 10 per cent to 200 per cent.

The procedure is repeated with the output held at a level 10 db below standard test output so that output-stage distortion is minimized.

10.3.3.3 Distortion vs modulation frequency. The modulation is fixed at 30 per cent and the output is maintained at standard test output. The modulation frequency is varied and the harmonic distortion is measured.

The preceding measurements are supplemented where necessary by measurements which show the effect of power output, tone control setting, input signal level, and sound-to-picture carrier ratio. In particular, the presence of distortion due to stray coupling at low volume should be noted.

10.4 Power Supply (Hum), Deflection, and Video Interference

10.4.1 Introduction. The tests in this section are designed to detect interference in the sound output which may arise from causes such as inadequate power supply filtering (hum), coupling to the deflection circuits, and coupling to the video circuits (buzz).

The nuisance value of this interference depends upon its waveform as well as its rms value and the acoustic frequency response of the receiver.

10.4.2 Method of Measurement. The picture and sound signal generators are connected to the receiver as described in Section 1.7. Except where otherwise specified, standard white-pattern picture modulation and 30 per cent 400-cps sound modulation are used, and the receiver controls are adjusted for normal operation. The sound output delivered to the dummy load is observed with both a meter and an oscilloscope.

10.4.2.1 Interference output—volume control at standard test output setting. The volume control is set at the position which produces standard test output and the sound modulation is switched off. The amplitude and waveform of the interference output is noted for the worst setting of the tone controls.

The receiver contrast control and the depth of picture modulation are increased and the conditions resulting in interference are noted.

10.4.2.2 Interference output—volume control at minimum setting. The volume control is set at minimum. The sound modulation is switched off and the interference output is noted.

10.4.2.3 Hum modulation. With the sound modulation on and standard test output, the waveform or spectrum of the sound output is observed to detect the presence of intermodulation, including power supply, hum, deflection, or video components.

10.4.3 Presentation of Data. The amplitude, waveform, and source of the interference should be specified and the conditions of measurement.

These interference measurements in particular should be supplemented by listening tests to evaluate qualitatively the interference under normal operation.

Chapter 11—Radiated and Conducted Emissions

11.1 General Considerations

Television receivers which cause interference to other receivers and services generally have been found to produce it in either of two ways: at higher frequencies by waves radiated from the chassis, transmission line and antenna; and at lower frequencies by waves conducted over the power line.

11.2 Radiated Interference

The method of measurement is given in IRE Standards 51 IRE 17. S1.[8] The results are stated in microvolts per meter at a distance of 100 feet, at each frequency.

11.3 Conducted Interference

The method of measurement is given in IRE Standards 54 IRE 17. S1,[9] in the supplement to these standards 58 IRE 27. S1,[10] and in IRE Standards 56 IRE 27. S1.[11] The results are stated in microvolts, at each measurement frequency, across the standard power-line impedance network.

Chapter 12—Miscellaneous

12.1 Receiver Input Impedance

12.1.1 Introduction. Although the magnitude and phase angle of the complex impedance at the input terminals of the receiver can be measured, it is usually of more interest to know either the voltage standing wave ratio, VSWR, produced in the transmission line, or the absolute value of the reflection coefficient, ρ, which are related as follows:

$$\text{VSWR} = \frac{1 + |\rho|}{1 - |\rho|}.$$

When the imput impedance varies across the channel, the VSWR for frequencies in the region of the picture carrier is of primary interest. The input impedance is often a function of signal level.

12.1.2 Definitions. The voltage standing wave ratio is the ratio of the maximum to the minimum voltage that appears at points along the transmission line. The reflection coefficient is the complex ratio of the voltage of the reflected wave to the voltage of the incident wave.

12.1.3 Method of Measurement. A long transmission line of the specified characteristic impedance is connected to the input terminals of the receiver, which is switched on and tuned to the appropriate channel. The AGC voltage applied to the first amplifier in the receiver should be stabilized at the value corresponding to a weak applied signal. A signal generator is connected to the other end of the transmission line. The generator applies an unmodulated radio-frequency signal of constant voltage (open-circuit) and variable frequency to this end of the transmission line. The strength of the signal at this end is measured with a detector. The combination of the signal generator and the detector must terminate the transmission line accurately with its characteristic impedance [see Fig. 12.1(a)]. The signal strength is plotted as a function of the input signal frequency, first with the receiver end of the transmission line short-circuited and secondly with the receiver end of the transmission line connected to the antenna input terminals of the receiver. From these two curves, the VSWR is derived, using the relation

$$\text{VSWR} = \frac{V_2 + V_1}{V_2 - V_1}.$$

[8] "IRE Standards on Radio Receivers: Open Field Method of Measurement of Spurious Radiation from Frequency Modulation and Television Broadcast Receivers, 1951," Proc. IRE, vol. 39, pp. 803–806; July, 1951.

[9] "IRE Standards on Receivers: Methods of Measurement of Interference Output of Television Receivers in the Range of 300 to 10,000 kc, 1954," vol. 42, pp. 1363–1367; September, 1954.

[10] "Supplement to 'IRE Standards on Receivers: Methods of Measurement of Interference Output of Television Receivers in the Range of 300 to 10,000 kc, 1954,' " vol. 46, pp. 1418–1420; July, 1958.

[11] "IRE Standards on Methods of Measurement of the Conducted Interference Output of Broadcast and Television Receivers in the Range of 300 Kc to 25 Mc, 1956," vol. 44, pp. 1040–1043; August, 1956.

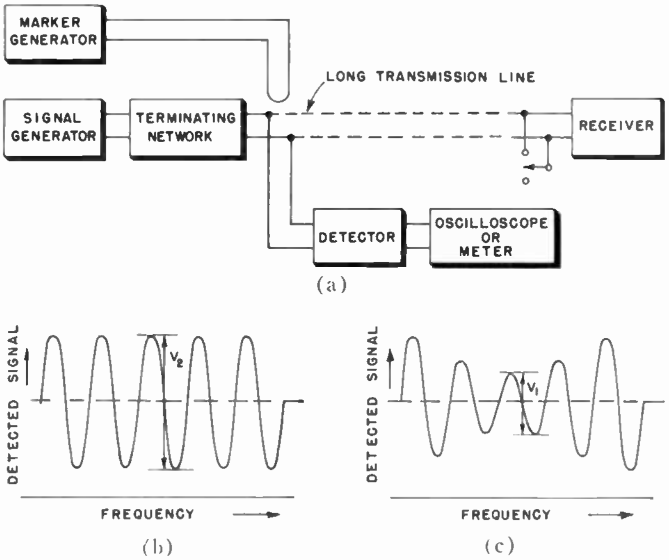

Fig. 12.1—(a) Circuit arrangement for measurement of voltage-standing-wave ratio. (b) Detected signal with receiver end of the transmission line short-circuited. (c) Detected signal with transmission line terminated with the receiver input terminals.

The transmission line must be long enough so that a sufficient number of undulations is recorded within a frequency range corresponding to the pass band of the receiver. The frequency separation between adjacent minima is

$$f = \frac{v}{2l},$$

where

v = velocity of propagation of the transmission line, and

l = length of the transmission line,

when the far end of the transmission line is short-circuited. The attenuation of the transmission line must be low enough so that the undulations are of sufficient amplitude when the far end of the transmission line is short-circuited.

By using a sweep signal generator the detected signal can be displayed on an oscilloscope. If the detector is not linear, a calibration of the indication is necessary. The applied signal should not be so large that the input portion of the receiver is overloaded. The tests should be repeated with the AGC voltage fixed at values corresponding to higher input levels.

12.1.4 Presentation of Data. The VSWR is stated for each channel and input level measured. When the VSWR varies across the channel, the stated value should be for frequencies in the region of the picture carrier.

12.2 Change in Band-Pass by Antenna Mismatch

12.2.1 Definition. The change in band-pass by antenna mismatch is defined as the change in selectivity produced by a 4-to-1 change in the dummy-antenna impedance from the matched value, when the transmission line between the dummy antenna and the receiver is varied in electrical length over a range of one-half wavelength, keeping the amplitude of the response at the picture carrier frequency constant. This measurement is designed to simulate results which are obtained with conventional antennas which cause mistuning and loading of the receiver input circuits.

12.2.2 Method of Measurement. The equipment is arranged to measure the selectivity as in Section 5.2.1, or a sweep oscillator and oscilloscope display may be used, with markers at the picture carrier frequency and at 3 mc higher. Provision is made to change the dummy-antenna impedance to either one-fourth or four times the standard value (300 ohms). The AGC voltage should be stabilized at the value corresponding to the signal level being used. Using the standard dummy antenna, the response at the picture carrier frequency is set to standard test output, and the response at other frequencies of interest measured. The standard dummy antenna is then replaced by the mismatched dummy antenna, and the signal input adjusted to give the same response at the picture carrier frequency. The response at the other frequencies is again measured. The transmission line between the dummy antenna and the receiver is replaced by one having an electrical length of one-eighth wavelength greater, and the process repeated. Several lengths of transmission line, up to one-half wavelength greater electrical length than the original, are substituted.

The tests should be repeated for applied signals of different levels.

12.2.3 Presentation of Data. The maximum change in response at each frequency of interest is given in decibels. The change in response at the frequency corresponding to 3-mc video modulation, and at the sound carrier frequency, should be included.

Correspondence

Operation of an Esaki Diode Microwave Amplifier*

A microwave amplifier using a germanium Esaki diode has been operated at 4.5 kmc with the following results:

Maximum stable gain	$=23$ db;
Voltage gain–bandwidth product (23-db gain at a bandwidth of 20 mc)	$=2.75\times10^{8}$;
Effective source noise temperature (noise figure $=7$ db)	$=1200°$K;
Saturation power output	$\approx1\times10^{-6}$ watt.

The diode peak current was 1.1 ma and the peak-to-valley ratio was 2.5.

The amplifier is shown schematically in Fig. 1. It consists of a single port cavity A, containing the Esaki diode B, which is coupled via an iris to a short section of a waveguide beyond cutoff C, separating it from the main propagating waveguide D. The incident input signal and the reflected (and amplified) output signal are separated by a low-loss circulator.

As with all regenerative amplifiers, sufficient loading must be provided to prevent oscillation from taking place. This was achieved by a dielectric plug, E, which, when completely inserted into the cutoff section, enables the latter to propagate. The depth of insertion is thus used to vary the external coupling of the cavity.[1]

It can be shown that, for high gain, the voltage gain-bandwidth product is given by

$$\sqrt{G}\,\Delta f \approx \frac{1-\dfrac{Q_d}{Q_c}}{\pi RC}. \qquad (1)$$

where Q_d/Q_c is the ratio of the power dissipated inside the cavity to that generated by the negative resistance of the diode. R and c are, respectively, the negative resistance and the capacitance of the diode. G is the power gain while Δf is the separation in cycles/second between the half-power points. The constancy of $\sqrt{G}\Delta f$ was checked at $G=23$ db and $G=17$ db. Since Q_d/Q_c in our experiment was ~0.5, the measured result, $\sqrt{G}\Delta f=2.75\times10^{8}$, represents approximately one half of the asymptotic value attainable according to (1) in the limit of strong overcoupling, $Q_c \gg Q_d$.

The effective source noise temperature T_e[2] is given by the relation

$$T_e = \frac{(\sqrt{G}+1)^2}{G} \cdot \left[T_c\left(\frac{Q_{ex}}{Q_c}\right) + \frac{eI_0R}{2k}\left(\frac{Q_{ex}}{Q_d}\right)\right] \qquad (2)$$

where

T_c is the cavity ambient temperature;

$$\frac{Q_{ex}}{Q_c} = \frac{\text{external "}Q\text{"}}{\text{unloaded "}Q\text{"}}$$

* Received by the IRE, February 16, 1960.

[1] This scheme was first used by J. P. Gordon in a paramagnetic resonance experiment.

[2] T_e is related to the noise figure F by the relation

$$F = 1 + \frac{T_e}{290}.$$

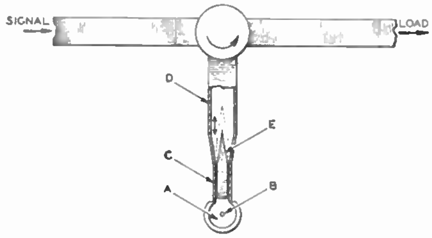

Fig. 1—A schematic view of the Esaki diode amplifier. (The symbols are explained in the text.)

is the ratio of the power lost in the cavity to that delivered to the external load;

Q_{ex}/Q_d is the ratio of the power generated by the diode to that supplied to the load;

I_0 is the dc bias current;

e is the electronic charge;

k is Boltzmann constant; and

$-R$ is the negative resistance of the diode.

The measured noise temperature of 1200°K was approximately twice as high as that expected from (2) in the limit of strong coupling where $Q_{ex} \ll Q_c$. This difference is due to the operation of the cavity near the condition of critical coupling. An increase in coupling was prevented by the amount of parasitic losses inside the cavity, which placed a limit on the maximum loading at which high gain could be obtained. Substantially lower noise temperatures are to be expected from diodes with better peak-to-valley current ratios (where lower values of I_0R can be attained), and from diodes with smaller series resistance. There is also the possibility of intrinsically lower I_0R products with other semiconductors.

The authors wish to express their gratitude to E. Dickten who fabricated and mounted the diode used in the experiment.

A. Yariv
J. S. Cook
P. E. Butzien
Bell Telephone Labs.
Murray Hill, N. J.

Voltage Tuning in Tunnel Diode Oscillators*

During some recent experimental work on microwave tunnel diode oscillators, voltage tuning ranges of up to 12 per cent have been obtained by varying the operating bias of the oscillator. Power output was approximately -30 dbm.

Fig. 1 shows a curve of frequency vs voltage obtained with an oscillator using an Esaki diode, manufactured by Sony Corporation, Japan. The diode was mounted at one end of a low impedance coaxial line, as shown in Fig. 2, and the other end of the line was terminated in a matched load, across which the operating voltage was applied.

* Received by the IRE, February 29, 1960.

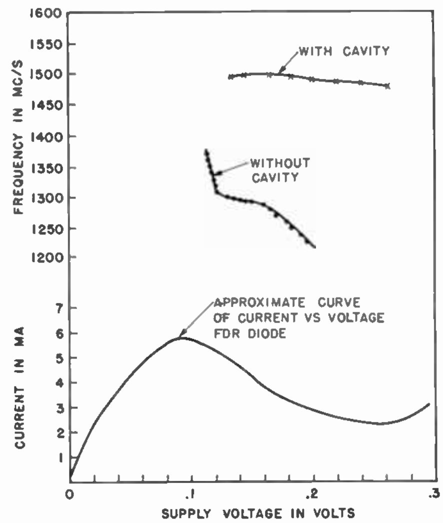

Fig. 1—Voltage tuning curves for tunnel diode oscillator.

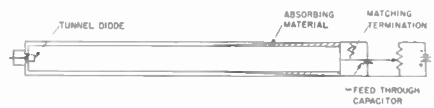

Fig. 2—Tunnel diode oscillator (output was taken from a probe at the diode end).

The dependence of frequency on the operating potential in a voltage-controlled negative resistance oscillator is a well-known phenomenon. The mechanism is particularly clearly explained by Edson.[1] As the diode has a nominal maximum negative resistance of 25 ohms, and the impedance of the coaxial line is 20 ohms, there is quite a wide band near the resonant frequency of the diode package where the diode can oscillate.

By varying the operating voltage, the effective negative resistance of the diode at which the oscillation will reach a steady state may be varied, and thus the frequency will change. The relative amplitude and phase of the harmonics generated will also vary with supply voltage, and, as shown by Edson, this also affects the oscillation frequency. The nonlinearity of frequency vs voltage is thought to be due to resonances at the harmonic frequencies.

By adding a quarter wave re-entrant cavity in the center conductor of the coaxial line, the impedance at the oscillating frequency can be raised, resulting in more power output (approximately -15 dbm) but a voltage tuning range of only about 20 mc at 1500 mc or 1.3 per cent. Both oscillators could be tuned mechanically over a 30 per cent bandwidth with little change in output.

J. K. Pulfer
Radio and Electrical Engineering Division
National Research Council
Ottawa, Ontario, Canada

[1] W. A. Edson, "Vacuum Tube Oscillators," John Wiley and Sons, Inc., New York, N. Y.; 1953.

A Technique for Cascading Tunnel-Diode Amplifiers*

The tunnel diode can often be used as the active element in a conventional amplifier stage. It is at times desirable to cascade such amplifiers. Since the tunnel diode is a two-terminal device it does not supply the isolation of either the vacuum tube or the transistor. Thus, special techniques must be used when cascading tunnel-diode amplifiers. Such a technique is presented here. For convenience, voltage amplification will be discussed although a similar discussion could be applied to current amplification or power amplification.

Let us consider the simple tunnel-diode amplifier shown in Fig. 1. We shall assume that L_1 and L_2 are such that they act as open circuits at all frequencies of interest, while C is such that it acts as a short circuit at all frequencies of interest. The elements L_1, L_2, and C are used to supply direct bias. The equivalent circuit for the tunnel diode can be represented simply by a negative resistance over a wide range of frequencies. This will be done here. The equivalent circuit for this amplifier is shown in Fig. 2. The voltage gain of this circuit is given by

$$K = \frac{E_2}{E_1} = \frac{R}{R - r}. \tag{1}$$

Note that K can be made as large as desired by choosing $-r$ so that $R-r$ is sufficiently small. However, stability requirements usually limit the maximum value of K. If the maximum allowable gain per stage is less than the required over-all gain, then several amplifier stages must be cascaded. As it stands, this amplifier does not lend itself well to cascading. However, the addition of a second tunnel diode, which does not change the voltage gain, results in an amplifier that can be easily cascaded. Such an amplifier and its equivalent circuit are shown in Figs. 3(a) and 3(b), respectively. Note that the negative resistance of TD_1 may be different from that of TD_2. It is assumed that there are tunnel diodes with the required negative resistances. If this is not the case, then the required negative resistance can be obtained by combining a tunnel diode with a positive resistance. The voltage gain of this circuit is the same as that of Fig. 1 and is given by (1). However, the input resistance of the circuit of Fig. 1 is $R-r$, while the input resistance of the circuit of Fig. 2 is given by

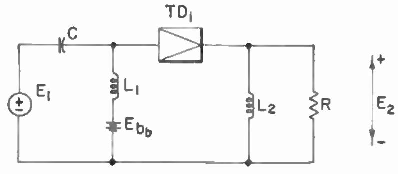

Fig. 1—A simple tunnel-diode amplifier.

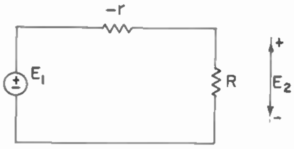

Fig. 2—The equivalent circuit for the simple tunnel-diode amplifier of Fig. 1.

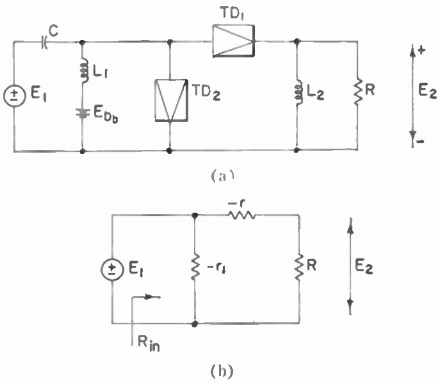

Fig. 3—(a) A tunnel-diode amplifier that can be cascaded; (b) its equivalent circuit.

$$R_{in} = \frac{-r_1(R - r)}{R - r - r_1}. \tag{2}$$

Now let us choose $-r_1$ so that $R_{in} = R$. Then solving (2) for $-r_1$, we obtain

$$-r_1 = \frac{R(R - r)}{-r}. \tag{3}$$

The input resistance of this circuit is now equal to the load resistance, thus this circuit may be used as the "load resistance" of a similar circuit. When several of such stages are cascaded the voltage gain of each will be $K = R/(R-r)$. The over-all gain will, of course, be the product of the individual stage gains. For instance, a typical circuit is shown in Fig. 4(a). The over-all voltage gain of this circuit is K_1K^3, where $K_1 = R/(2R-r)$ is the gain of the first stage. Note that it has been assumed that the internal resistance of the signal source is not zero but is equal to the load resistor R. The equivalent circuit for this amplifier is shown in Fig. 4(b). Pertinent voltages and resistances are indicated in this equivalent circuit. The resistances are "viewed" in the direction shown by the arrow.

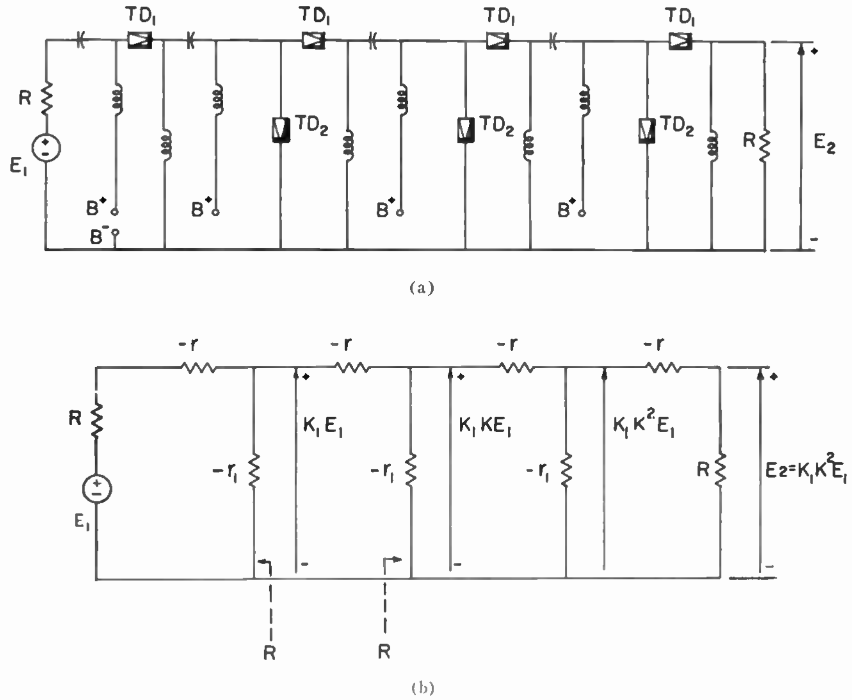

Fig. 4—(a) A typical cascaded tunnel-diode amplifier; (b) its equivalent circuit.

The previous discussion considered the cascading of amplifier stages. Actually, the circuit of Fig. 4 may be viewed as a transmission line connecting the input generator to the output load. In this case, the transmission line is made up of negative resistance elements and, hence, produces a gain rather than a loss. Note that with some minor modification this "transmission line" can start and end with shunt rather than series elements.

If impedances are placed in series with the series tunnel diodes (TD_1) and impedances are placed in shunt with the shunt tunnel diodes (TD_2), then the gain of the amplifier can be made frequency dependent. This must be done with care to insure that the amplifier will be stable.

P. M. Chirlian
Dept. of Electrical Engineering
New York University
New York, N. Y.

* Received by the IRE, February 15, 1960.

Negative L and C in Solid-State Masers*

When a material exhibiting quantum-mechanical resonance absorption is caused to be emissive by producing an inverted population distribution—which is necessary for maser operation—the impedance behavior of the material changes in two ways: not only does the resistive component become negative to provide gain, but the dependence of the reactive component on frequency reverses sign. This second property can be used to obtain gain and bandwidth performance that exceeds the limitations imposed by conventional network analysis. For amplifier design calculations, it is convenient to represent this fact by an equivalent circuit. For example, the permeability of a crystal in the neighborhood of a sharp electron paramagnetic resonance (for a Lorentz-shaped line) is of the form

$$\mu = \mu_0 \left(1 - \frac{j\chi_{\max}''}{1 + jT_2\Delta\omega}\right) \qquad (1)$$

where $\chi_{\max}''$ is the peak value of the absorptive component of complex susceptibility, and T_2 is the reciprocal linewidth. This relation may be represented by the equivalent circuit shown in Fig. 1 with $G=1/(\mu_0\chi_{\max}''\omega_0)$, and $jB=(jT_2\Delta\omega)/(\mu_0\chi_{\max}''\omega_0)$. When the population is inverted, the permeability becomes

$$\mu = \mu_0 \left(1 + \frac{j\chi_{\max}''}{1 + jT_2\Delta\omega}\right),$$

for which the corresponding circuit becomes that shown in Fig. 2, in which all symbols are taken as positive. For a Gaussian-shaped line, the expressions are an approximation that is only valid in the center of the line, but the general conclusions are true.

This result is obtained by solving the equation of motion for the system in question,[1] and it can be readily observed experimentally. When the crystal is incorporated in a cavity resonator, an appropriate circuit suggested is that shown in Fig. 3. When the negative terms in this circuit are large compared with the positive terms (a situation that represents a strong paramagnetic resonance and a large filling factor), the circuit shown in Fig. 4 is suggested. The normal C'' and L'' are used to compensate for the negative L and C of the electron-spin resonance, to achieve increased bandwidth. The circuit of Fig. 4 represents two cascaded cavities with an inverted paramagnetic crystal in the second. In order to achieve significant improvement, L' must be small. The criterion suggested by stored-energy implications is

$$LG \leq \frac{C}{G} \qquad (2)$$

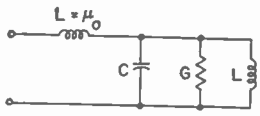

Fig. 1.

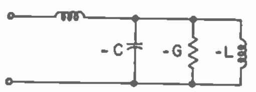

Fig. 2.

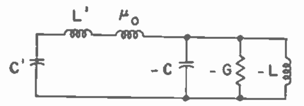

Fig. 3.

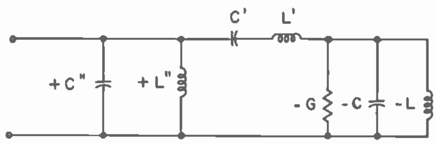

Fig. 4.

and this has been verified by direct calculation.

If a filling factor of 1 is obtained in the active cavity, (2) reduces to

$$\chi_{\max}'' \geq \frac{1}{\omega_0 T_2}, \quad \text{or} \quad \chi_{\max}'' \geq \frac{\Delta\omega_0}{\omega_0}, \qquad (3)$$

where $\Delta\omega_0$ is the full width of the paramagnetic-resonance line. This condition is just about met for "pink" ruby at 9 kmc and at 4.2°K, for which, under typical experimental conditions, $\chi'' \approx 0.01$, and $\Delta\omega_0/\omega_0 \approx 0.005$. Cavity losses, which are usually small under these conditions, were ignored in our analysis. A maser in which these phenomena are utilized has been constructed by Goodwin and Moss.[2]

The gain-bandwidth theory of Fano[3] can be extended to the negative L and C situation. In the high-gain limit, with a single maser crystal, it gives

$$\frac{1}{\pi}\int \ln \mathcal{G}^{1/2} d\omega = \Delta\omega_0 \cdot \left[\left(1 + \frac{3\chi_{\max}''\omega_0}{\Delta\omega_0}\right)^{1/3} - 1\right] \qquad (4)$$

where the integral is over the amplifier bandwidth, and $\mathcal{G}^{1/2}$ is the voltage gain of the cavity maser as a function of frequency.

Increasing the spin concentration augments the effect by increasing χ'', as long as the linewidth $\Delta\omega_0$ does not increase also. Raising the operating frequency augments the effect for a given sample by increasing both χ'' and $\omega_0/\Delta\omega_0$. Lowering the temperature, of course, also helps.

The presence of the negative L and C terms does not materially change the performance of a typical traveling-wave maser because the circuit is too broad-band to introduce sufficient compensating reactance.

Incidentally, these negative L and C properties do not appear in parametric amplifiers. The broad-banding procedures discussed by Seidel and Herrmann,[4] for example, are of a more conventional type.

R. L. Kyhl
Dept. of Electrical Engineering and
Research Laboratory of Electronics
Mass. Inst. Tech.
Cambridge, Mass.

* Received by the IRE, March 2, 1960. This work was supported in part by the U. S. Army (Signal Corps), the U. S. Air Force (Office of Scientific Research, Air Research and Development Command), and the U. S. Navy (Office of Naval Research).

[1] F. Bloch, "Nuclear induction," *Phys. Rev.*, vol. 70, pp. 460–474 (see sec. III); October 1 and 15, 1946; R. Karplus and J. Schwinger, "Saturation in microwave spectroscopy," *Phys. Rev.*, vol. 73, pp. 1020–1026 (see eq. 23); May 1, 1948.

[2] F. E. Goodwin and G. E. Moss, Hughes Aircraft Co., Research Labs., Culver City, Calif., private communication; November 12, 1959.

[3] R. M. Fano, "Theoretical limitations on the broadband matching of arbitrary impedances," *J. Franklin Inst.*, vol. 249, pp. 57–84; January, 1950; vol. 249, pp. 139–154; February, 1950.

[4] H. Seidel and G. F. Herrmann, "Circuit aspects of parametric amplifiers," 1959 IRE WESCON Convention Record, Part 2, pp. 83–91.

Parametric Oscillatory and Rotary Motion*

The semiconductor parametric amplifier belongs to a more general class of devices, in which one or more parameters in the underlying integro-differential equation are periodic time functions. In principle, the reactance variation may equally well be accomplished by ferromagnetic means, so that the inductance becomes a periodic function. The conditions for oscillations are

$$L\frac{di}{dt} + i\frac{dL}{dt} + Ri + \frac{1}{C}\int idt = 0, \qquad (1)$$

$$C\frac{dv}{dt} + v\frac{dC}{dt} + Gv + \frac{1}{L}\int vdt = 0. \qquad (2)$$

Here (2) is the better-known equation, pertaining to a variable-capacitance amplifier with $\beta A = 1$. The second term identifies the opportunity of amplification, offered with C varied at twice signal frequency. The capacitance variation frequency is the pump frequency, at which the capacitance is reduced on every half-cycle of the signal voltage wave, thus giving off energy to the rest of the system. This is the way the stimulance is injected, which in an amplifier almost, but not quite, takes care of the dissipation.

The writer has undertaken to investigate parametric devices with mechanical rather than electrical input signal.[1] Variable inductance devices at low frequency proved to offer the easiest approach, and several mechanical oscillators with equal pump and signal frequencies were successfully constructed. Thus, "the world's simplest servosystem" emerged, with the model adjusted for $\beta A < 1$. With the aid of the second term in (1), $i\,dL/dt$, a small mechanical displacement x was turned into a larger mechanical one, associated with much more power, and it is only logical to expect that a similar servosystem can be designed in accordance

* Received by the IRE, March 1, 1960.

[1] H. P. Knauss and P. R. Zilsel, "Magnetically maintained pendulum," *Amer. J. Phys.*, vol. 19, pp. 318–320; May, 1951.

with (2). Thus a narrow-frequency-range oscillating reed, telephone, or loudspeaker design may be based on either equation, not to mention other devices of this general nature with or without supporting active elements, such as switching transistors.

With the aid of a Mathieu-Hill type of equation solution, it can be shown that the term $i\ dL/dt$ yields a double-valued force function, the explanation for the easily demonstrated fact that sustained oscillations are obtained. To show that nonlinearity is not essential, an additional small-signal model was built without iron, and proved to oscillate. Since in the solution of the equation, the double-valued force function is independent of the sign of the displacement x, the association of the stimulance part of the force function with $-x$ is by no means unique; it could just as well be $+x$. To prove this theoretical point, predicting rotational motion, the "electronics motor" in Fig. 1 was constructed, and true enough it rotated. The favored speed of the model is about 200 rpm. The effect can be enhanced if a switching transistor amplifier of time constant T and with $Z_i \gg Z_\sigma$ is attached, for example, as indicated by the dotted lines. The transistor amplifier is not essential to the operation, nor is the capacitor C_1. This capacitor was introduced because it made the circuit approach resonance conditions, and thus accept a heavier current. It yields the frequency $1/2\pi\sqrt{L_1 C_1}$, or which is lower than the lines frequency. Thus the slope $di/d\omega$ is negative, so that the stimulance part of the force function pertaining to $i\ dL/dt$ is aided by the force function due to $di/d\omega$, in which $\omega = 2\pi f$, with the particular value $f = 60$ designating lines frequency.

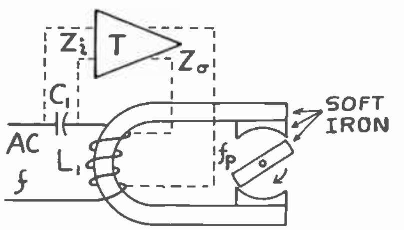

Fig. 1—Principle of the parametric motor. The rotor spins around in either direction, although there are no contacts, no rotor winding, no magnets, no rotational field, and no synchronous speed.

HARRY E. STOCKMAN
Dept. of Elec. Engrg.
Merrimack College
North Andover, Mass.

A Transverse-Field Traveling-Wave Tube*

Recently there has been an urgent interest in traveling-wave parametric amplifiers which utilize an electron beam as the reactive element. One such amplifier which has achieved very-low-noise performance has been described by Adler *et al.*[1] The amplifier uses the fast electron cyclotron wave as the signal and idler modes and a traveling high-frequency electric quadrupole field as the pump mode. In the Adler Tube the pump frequency is set equal to twice the cyclotron frequency of the electrons and the phase velocity of the pump wave is infinite.

There is also a related class of beam-type parametric amplifiers in which the pump mode is at an arbitrarily low frequency including dc and the pump phase velocity is finite including zero. The idler mode is a slow cyclotron wave. These amplifiers are not characterized by extremely low-noise performance, but have other interesting properties as has been shown by Gordon *et al.*[2] It is the purpose of this paper to present preliminary experimental results on an amplifier using a static spatially-varying electric quadrupole field to achieve amplification of the fast cyclotron wave.

The interaction in the static quadrupole field can be understood by reference to Fig. 1 in which an electron in the phase appropri-

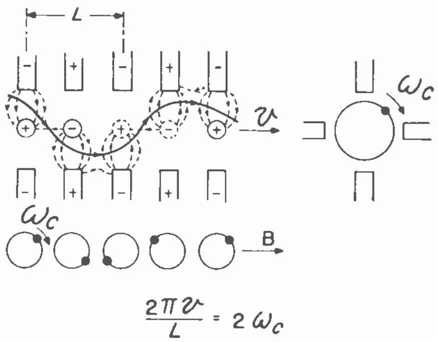

Fig. 1—The energy-gain mechanism.

ate to energy gain is shown. The drifting electron gains rotational energy as it loses drift energy; the quadrupole fields merely serving to deflect the electron. No energy is transferred from the quadrupole fields to the beam. It can be seen, also, that the synchronism condition requires that $2\omega_c = 2\pi v/L$, ω_c being the cyclotron frequency, v the drift velocity and L the periodic spacing of the quadrupole fields. Thus, the drifting electrons experience an apparent pump field of frequency $2\omega_c$.

As in the Adler device, an exponential growth of the orbit occurs which, coupled with a phase focusing induced by the quadrupole fields, leads to a net increase in the kinetic power of the fast cyclotron wave. Since no power is supplied by the pump fields and the drift velocity of the beam is decreased, it follows that the idler wave is a slow wave. Hence the zero pump frequency amplifier also may be compared to the conventional traveling-wave tube in which the corresponding "fast" wave is the electromagnetic wave carried by the slow-wave circuit while the "idler" wave is the slow space-charge wave.

The gain in the quadrupole fields is given by

$$G = 20 \log \cosh gV_q \text{ (db)} \tag{1}$$

in which V_q is the dc voltage applied to the quadrupole plates and g is a geometrical factor proportional to the number of quadrupole sections. Fig. 2 shows the observed

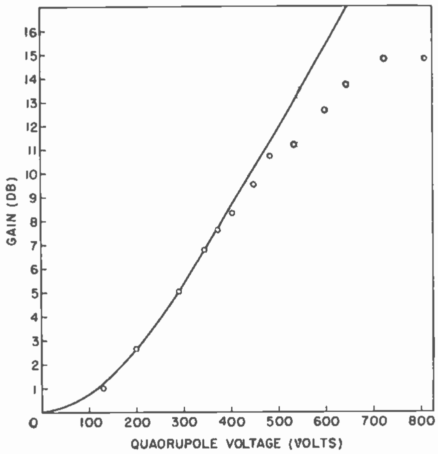

Fig. 2—Gain as a function of quadrupole.

gain minus the insertion loss as a function of the quadrupole voltage with the beam at the synchronous voltage. The solid line is the curve predicted by (1) in which the value of the constant g has been adjusted. The value of the constant is 30 per cent higher than the value calculated from knowledge of the quadrupole geometry. The experimental points depart considerably from the predicted curve for gains above 8 db. At this point, interception on the quadrupole begins. This results from a defect in the electron gun which introduces up to twenty volts of rotational energy onto the beam and is not inherent in the device. The deficit in gain is a result of the interception and the departure from the synchronous condition resulting from the decrease in beam voltage of those electrons with large rotational energy. The beam voltage and current are 800 volts and 2 ma, respectively. The quadrupole structure has a periodicity of 0.25 cm with an inner diameter of 0.20 cm and has 10 periods. The couplers are ridged waveguide cavities with a center-band frequency of 3.25 kmc and a bandwidth of 2 per cent.

A major advantage of the device is the fact that after the fast-wave energy is stripped from the beam in the output coupler, the remaining excitation on the beam is the slow idler wave. Thus, the spent electrons are monoenergetic and can be collected at close-to-cathode potential. As a result, the efficiency of the device can be very high.

No noise measurements have been made as yet, and although the device is not expected to have the extreme low-noise performance of the high-frequency-pumped amplifier, there is every reason to believe that it will compete with the more conventional traveling wave tubes in this respect.

E. I. GORDON
Bell Telephone Labs., Inc.
Murray Hill, N. J.

* Received by the IRE, March 7, 1960.

[1] R. Adler, G. Hrbek, and G. Wade, "The quadrupole amplifier, a low-noise parametric device," PROC. IRE, vol. 47, pp. 1713–1723; October, 1959.

[2] E. I. Gordon, S. J. Buchsbaum, and J. Feinstein, "A Transverse Field Amplifier Employing Cyclotron Resonance Interaction," paper presented at the Seventeenth Conference on Electron Tube Research, Mexico City, Mex.; June, 1959.

WWV and WWVH Standard Frequency and Time Transmissions*

The frequencies of the National Bureau of Standards radio stations WWV and WWVH are kept in agreement with respect to each other and have been maintained as constant as possible with respect to an improved United States Frequency Standard (USFS) since December 1, 1957.

The nominal broadcast frequencies should, for the purpose of highly accurate scientific measurements, or of establishing high uniformity among frequencies, or for removing unavoidable variations in the broadcast frequencies, be corrected to the value of the USFS, as indicated in the table below.

WWV FREQUENCY WITH RESPECT TO U. S. FREQUENCY STANDARD

1960 March 1600 UT	Parts in 10^{10}‡
1	−146
2	−146
3	−146
4	−146
5	−146
6	−145
7	−145
8	−145
9	−145
10	−145
11	−145
12	−144
13	−144
14	−144
15	−144
16	−144
17	−144
18	−145
19	−144
20	−144
21	−144
22	−144
23	−144
24	−144
25	−144
26§	−144
27	−147
28	−147
29	−147
30	−146
31	−146

‡ A minus sign indicates that the broadcast frequency was low.
§ On March 26 the frequency was decreased 3×10^{-10}.

The characteristics of the USFS, and its relation to time scales such as ET and UT2, have been described in a previous issue,[1] to which the reader is referred for a complete discussion.

The WWV and WWVH time signals are also kept in agreement with each other. Also they are locked to the nominal frequency of the transmissions and consequently may depart continuously from UT2. Corrections are determined and published by the U. S. Naval Observatory. The broadcast signals are maintained in close agreement with UT2 by properly offsetting the broadcast frequency from the USFS at the beginning of each year when necessary. This new system was commenced on January 1, 1960. The last time adjustment was a retardation adjustment of 0.02 s on December 16, 1959.

NATIONAL BUREAU OF STANDARDS
Boulder, Colo.

* Received by the IRE, April 25, 1960.
[1] "United States National Standards of Time and Frequency," PROC. IRE, vol. 48, pp. 105–106; January, 1960.

Correction to "On the Regenerative Pulse Generator"*

Viktor Met, author of the above Correspondence, which appeared on pages 363–364 of the March, 1960, issue of PROCEEDINGS, has advised *the Editor* that the drawings of Figs. 2 and 3 were preliminaries, and should have been replaced with ones submitted at a later date. The revised figures are reproduced herewith.

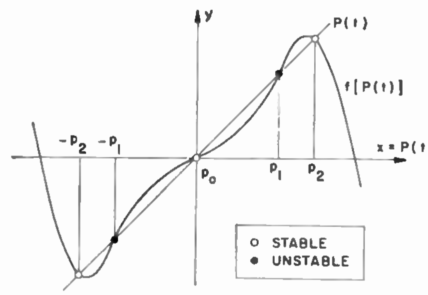

Fig. 2—Graphical solution of the nonlinear difference equation for a fifth-order nonlinearity.

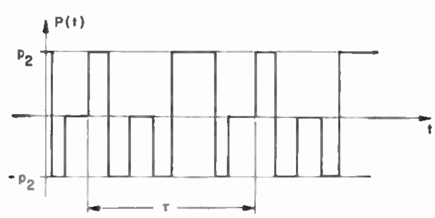

Fig. 3—Step-function, representing the general steady state solution.

* Received by the IRE, March 17, 1960.

Anomalous Reverse Current in Varactor Diodes*

While working on parametric amplifiers and harmonic generators using Varactor diodes, an interesting phenomenon was noticed concerning the direction of average diode current flow when a high-frequency pump source was applied. An appreciable reverse current was measured for dc bias voltages very much closer to forward conduction than to reverse breakdown. Measurements show that the instantaneous diode voltage is not even required to reach the dc breakdown value, and that this abnormal breakdown occurs only when the voltage during the positive-going half cycle is sufficiently large to swing into the forward conduction region. A plausible explanation of this phenomenon is that the large number of minority carriers injected during the forward half cycle are multiplied through collision ionization on the reverse half cycle, yielding a net negative current.[1] This occurs only at high frequencies because the voltage can swing negative before an appreciable number of injected carriers are lost through recombination or diffusion to the junction.

At X band, the effect is quite pronounced with a Bell Laboratories type Si 43 Varactor whose reverse characteristic is "hard" (less than 1-μa reverse current flows until breakdown occurs at −10.5 volts). An applied X band signal causes a reverse current of 20 μa at only −0.5 volt bias, although the diode characteristic is such that forward current of several microamperes occurs at +0.6 volt. For a slightly more positive value of bias, the current passes through zero and becomes positive. The dc bias at which the transition from forward to reverse current occurs was plotted as a function of frequency (Fig. 1). Since the ac drive varied

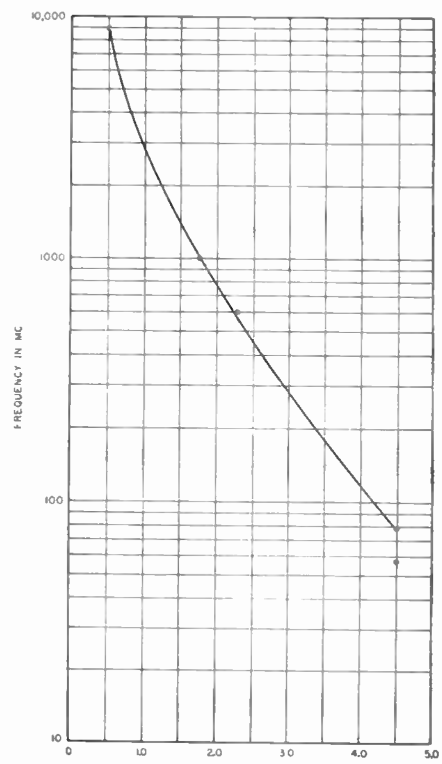

Fig. 1—Trend of effect vs frequency.

over the frequency range, this curve should be regarded only as illustrating a trend. The anomalous effect is seen to be most pronounced for the highest frequencies and disappears below about 60 mc for the above diode. This frequency region agrees with the minority carrier lifetime of 0.05 μsec[2] for these diodes. Since the effect was small or negligible below several hundred megacycles, a direct observation of diode waveforms could not be made.

* Received by the IRE, October 26, 1959. This work was supported under Air Force Contract AF30(602)-1854.

[1] Suggested by A. Uhlir, Jr., in a conversation held at Airborne Instruments Lab.
[2] "Crystal Rectifiers," Bell Telephone Labs., Ninth Interim Tech. Rep., Signal Corps Contract DA-36-039-sc-5589; October 15, 1956.

There are at least two explanations which may describe the above phenomena. One explanation requires that the ac signal be large enough to swing into both forward conduction and dc breakdown. Rectification about the forward characteristic should be poor because of minority carrier storage, and thus breakdown current should counterbalance the forward current at bias levels closer to forward conduction. This effect would be aided by the asymmetry of the waveform of voltage across the diode, which is peaked in the negative direction because of the shape of the C-V curve.

The second explanation is that the voltage does not reach the dc breakdown value, but at high frequencies some new mechanism occurs causing reverse current to flow at a voltage less than the normal dc breakdown voltage. To determine which explanation is correct, we have measured the voltage across the diode under conditions when the anomalous behavior was observed. This was done by two methods. The first method involved determining the amplitude of the various frequency components of the voltage across the diode by the use of a slotted line and reconstructing the waveform under the most pessimistic assumptions about phase. If the relative phases were such that all the peaks added in the negative direction, the maximum reverse voltage would only be 6.6 volts. This is considerably less than the value of 10.5 volts at which dc breakdown occurs.

At this point, we must mention the difference between the voltage we measure at the diode terminals and that which exists at the junction. The diode lead inductance is resonant with the junction capacitance from 3 to 4 kmc depending on the bias. The fundamental frequency was made low enough (470 mc) so that even at the third harmonic the parasitic elements introduce a negligible discrepancy.

For a second independent measurement to determine whether the diode voltage reaches dc breakdown, a high-frequency peak reading voltmeter (HP410B) was mounted in 50-ohm line directly in front of the diode and its coaxial mount. The meter response was flat to the fourth harmonic of the 185-mc signal used here. By reversing the diode and bias polarities with respect to the meter, both forward and reverse peaks were measured. They were +1.4 volts and −7.3 volts respectively. Again we see that the reverse peak does not reach the breakdown level.

Additional enlightenment as to the nature of the reverse conduction process results from a plot of average diode current vs bias for a fixed value of ac drive. (See Fig. 2.) The curve shown is for 370 mc. Similar results were found at other frequencies. The current is seen to be continuous through zero, indicating both forward and reverse current even at small bias levels. After switching from negative to positive it returns to zero for a range of bias values midway between the forward and reverse portions of the dc characteristic. This indicates that the voltage swing is too small to enter either conduction region when biased midway. Therefore, the negative current at small bias levels is not due to a large signal entering dc breakdown, but seems to depend upon forward current being drawn during part of the cycle. A further increase in bias results in breakdown current at −5.8 volts, indicating an ac amplitude of 4.7 volts. When this is added to the bias (2.8v) for the first crossover through zero, negative current is seen to be generated when the instantaneous voltage reaches −7.5 volts.

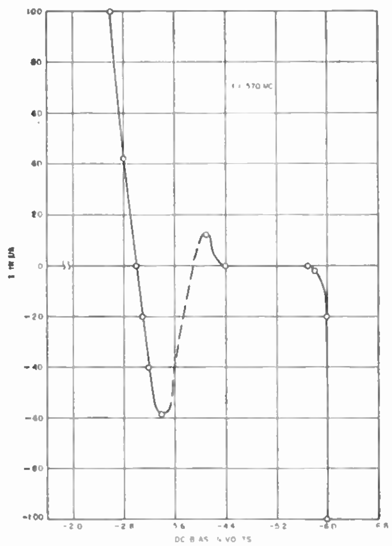

Fig. 2—Average diode current vs dc bias with ac drive (Si-43 No. 33).

The dashed portion of the curve denotes an unstable region, the operating point flipping from one extreme to the other. When biased in this region, a relaxation oscillation existed between these points at about 1 cps.

It should be noted that the circuits used have no structures tuned near the operating frequency, so that the variation of current with bias is not due to resonance effects involving the diode capacitance. The bias lead was suitably bypassed to ac.

Following the high-frequency experiments with the BTL Varactor diodes, the phenomenon was reproduced at low frequencies (15 mc) with a Hoffman 1N138 diode for which the lifetime was measured as about 1 μsec. The ratio of lifetime to RF period is seen to be of the same order of magnitude as in the high-frequency experiment. In addition, the breakdown mechanism is known to be of the avalanche type since this diode also exhibits the random pulse phenomenon described by McKay.[3] An oscilloscope verifies that the voltage is not required to reach dc breakdown, although the difference is not as great as in the high frequency case. A curve of average current vs diode bias similar to that of Fig. 2 was obtained, where the crossover through zero occurs at about −9 volts bias and the dc breakdown voltage is −27 volts.

It seems reasonable to conclude then that at RF periods which are short compared with the minority carrier lifetime, the carriers injected during the forward half cycle are multiplied through collision ionization on the reverse half cycle, resulting in a net reverse current. From the three high-frequency experiments presented, the maximum reverse voltage for anomalous current is about 7 volts. McKay has plotted the multiplication factor M vs V/V_b for a linearly graded silicon junction diode, where V_b is the breakdown voltage. For $V_b = 10.5$, $V/V_b = 0.7$, and the multiplication factor is about 2. Although this is not too much multiplication, the injected carriers represent a large increase in minority carrier density over the steady state level (of the order of 10^6). As a result, even a multiplication of two may yield considerable reverse current.

Conclusions have not yet been reached concerning the magnitude of the effects of this phenomenon on parametric amplifiers and harmonic generators, but it would seem to limit the voltage swing short of forward conduction under the penalty of an additional loss mechanism and some additional noise (even though the net dc current were zero, noise generated on the forward and reverse half cycles would degrade the noise figure of an amplifier). Operation in the nonconductive region between breakdown and forward conduction would avoid this effect, but considerable nonlinearity is probably lost by not driving into the forward region.

The author wishes to thank J. C. Greene, Dr. B. Salzberg and E. W. Sard for helpful discussions and suggestions.

K. Siegel
Airborne Instruments Lab.
Melville, N. Y.

[3] K. G. McKay, "Avalanche breakdown in silicon," *Phys. Rev.*, vol. 94, pp. 877–884; May, 1954.

Relativity and the Scientific Method*

The recent Proceedings article by J. R. Pierce[1] has triggered considerable adverse comment[2] on Einstein's Theory of Relativity. In the maze of detail which was discussed, one very important principle was all but forgotten, *i.e.*, the operation of the scientific method.

The objective of physical science is to provide a theoretical basis for interpretation of the observed behavior of nature. Observations are thus the final and conclusive arbiter of the "correctness" of any physical theory. It follows that a theory may never be "proved," since it is impossible to perform *all* experiments. Conversely, if such proof were possible, there would be no more

* Received by the IRE, October 22, 1959.
[1] J. R. Pierce, "Relativity and space travel," Proc. IRE, vol. 47, pp. 1053–1061; June, 1959.
[2] H. L. Armstrong, "Comment on relativity and space travel," Proc. IRE, vol. 47, p. 1778; October, 1959.

need for the theory itself since the purpose of any theory is to predict the outcome of new experiments. The success of a theory may thus be judged by the manner in which it fulfills this objective. In contrast, only one physical observation is required to disprove a theory. If it can be shown that a prediction of the theory is in clear contradiction to the behavior of nature as observed by a well-performed experiment, the theory must be discarded.

If we are to retain our present concepts of the scientific method, we should treat the Theory of Relativity as any other theory. No amount of belief or disbelief and no lengthy emotional expression of philosophy will substitute for a careful analysis of the observed physical facts in relation to the predictions of the theory. To date, a great number of results predicted by the Theory of Relativity have been experimentally verified. No case of clear contradiction has yet been found. Whether the theory in its present form will continue to enjoy such remarkable success indefinitely is not the subject under discussion here. Few scientists today would be willing to attest to the infallibility of any theory. However, until now the Theory of Relativity has stood the test of many critical experiments which any potential critic would do well to ponder, and until such an experiment demonstrates a clear contradiction, the critic should content himself with devising new experiments.

Irrespective of the eventual outcome of experimental work, the Theory of Relativity will remain the remarkable contribution of a remarkable man and a monument to the ability of the scientific method to bring understanding to an area where there was none.

C. A. Mead
Calif. Inst. of Tech.
Pasadena, Calif.

A Simple General Equation for Attenuation*

The familiar equations for the attenuation of various kinds of transmission media all involve two basic kinds of dependencies. One is the intrinsic electrical properties of the conductors and dielectric; the other is the geometric configuration and scale of the cross section. It may not be generally appreciated that the attenuation of most of the media in which the waves are guided by conductors can be expressed by a single simple equation in which the two kinds of dependencies just mentioned are represented by separate and distinct coefficients. Once the equation is written, its coefficients may be readily evaluated by comparison with the usual equations for those cases for which the wave equations have been solved, or by correlation with experimental data. We believe this concept of a general equation is interesting, and that the equation itself is of considerable engineering usefulness.

* Received by the IRE, October 30, 1959.

One of the writers, Szekely, has produced a mathematical proof, using perturbation techniques, that the equation presented is indeed general and applies to all transmission systems having conducting surfaces parallel to an axis of a general orthogonal curvilinear coordinate system, along which the waves are propagating and in which the wave equations are separable. The proof will not be given here. It is based, however, on the assumption of good conductors and good dielectric materials. The equation applies, for example, to the attenuation per unit length of wire pairs, of coaxial conductors, of all transmission modes of waveguides of any shape of cross section, of strip lines, etc. It even applies to such structures as conical horns if the attenuation is expressed in nepers or decibels per unit length, per unit solid angle.

The attenuation per unit length of any transmission medium in the class just defined is given by

$$\alpha = \frac{M \dfrac{\sqrt{f}}{a}\left[A + B\left(\dfrac{f_c}{f}\right)^2\right] + D}{\sqrt{1 - \left(\dfrac{f_c}{f}\right)^2}}, \qquad (1)$$

where:

D = constant depending only on the intrinsic properties of the dielectric,

M = constant depending only on the intrinsic properties of the dielectric and of the conducting material,

A, B = constants depending on the configuration (but not the scale) of the cross section, and on the transmission mode,

a = a selected linear dimension of the cross section specifying its size or scale, all other dimensions having fixed ratios to a,

f = transmitted frequency, and

f_c = cutoff frequency of the particular transmission mode on the given medium.

The constant D accounts for that part of the attenuation that is due to dissipation in the dielectric. In many cases where the dielectric is air or some other gas, this may be neglected. The remainder of this equation, representing the attenuation due to dissipation in the conductors, can be written in a normalized form:

$$\alpha_m \cdot a^{3/2} = \frac{M\sqrt{af}\left[A + B\left(\dfrac{f_1}{af}\right)^2\right]}{\sqrt{1 - \left(\dfrac{f_1}{af}\right)^2}}. \qquad (2)$$

where $f_1 = af_c$.

A plot of $(\alpha_m \cdot a^{3/2})$ vs (af) gives one curve that is applicable to any scale of cross section, for a given medium of given shape of cross section and a given mode of transmission.

To apply (1) to a particular case, it is necessary to know the values of M, D, A, B and f_1. Since M and D depend only on the conducting and dielectric materials, they can be determined once for all transmission media employing particular materials, say copper and air. Their values are given by

$$D = \frac{\eta\sigma}{2} \qquad (3)$$

$$M = \frac{1}{\eta}\sqrt{\frac{\pi\mu_m}{\sigma_m}}. \qquad (4)$$

In these,

$\eta = \sqrt{\mu/\epsilon}$ = intrinsic impedance of the dielectric, where μ and ϵ are the absolute permeability and dielectric constant of the dielectric,

μ_m = permeability of the conducting material,

σ = conductivity of the dielectric, and

σ_m = conductivity of the conducting material.

For a vacuum and substantially for gases, $\eta = 120\pi = 377$ ohms. For dielectrics having a different dielectric constant than that of a vacuum, $\eta = 377/\sqrt{\epsilon_r}$, where ϵ_r is the relative dielectric constant.

It shall be noted that at frequencies well above cutoff, the portion of the attenuation constant caused by a lossy dielectric is very nearly a frequency independent constant, ($\alpha_D \cong D = \frac{1}{2}\mu\sigma$); this is true for any geometric configuration, scale of cross section, or mode of transmission, provided that the conductance of the dielectric is constant and small. (In some dielectrics such as paper in paper-insulated telephone cables, σ appears to be a function of frequency.)

If rationalized MKS units are used, the attenuation given by (1) will be in terms of nepers per meter. Obviously, the attenuation may be converted to other units by multiplying M and D by suitable factors. Table I gives some values of M for copper conductors ($\sigma_m = 58 \times 10^6$ mhos per meter) and air dielectric, corrected for several combinations of units.

TABLE I
VALUES OF M FOR COPPER CONDUCTORS AND GAS DIELECTRIC

α	a	f in cps.	f in KMC/sec.
Nepers /meter	cm	69.1×10^{-9}	2.19×10^{-3}
db/meter	cm	600×10^{-9}	19×10^{-3}
db/ft	inches	72.1×10^{-9}	2.28×10^{-3}
db/mile	inches	0.38×10^{-3}	12

The constants A, B, and f_1 are obtainable from the equations given in the literature for most cases of interest. For cases not yet explored mathematically, their determination requires the application of electromagnetic wave theory, a process often difficult and too lengthy to discuss here. However,

TABLE II
VALUES OF CONSTANTS DEPENDENT ON CONFIGURATION AND MODE

MEDIUM	MODE	CUTOFF $f_1 = af_c$	CUTOFF $\lambda_1 = \lambda_c/a$	A	B
PAIR OF WIRES 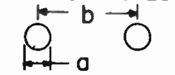	PRINCIPAL	(NOTE 1) 0	∞	$\dfrac{1}{\sqrt{1-(a/b)^2}\cosh^{-1} b/a}$	0
COAXIAL CABLE 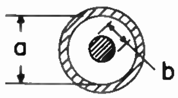	PRINCIPAL	0	∞	$\dfrac{1+a/b}{\log_e a/b}$ MIN = 3.59, WHEN $a/b = 3.59$	0
	NEXT HIGHER	$v/1.95$	1.95 APPROX	—	—
WAVEGUIDE – RECTANGULAR 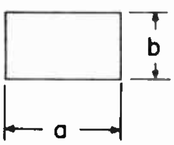	TE_{10}	$\dfrac{v}{2}$	2	$\dfrac{a}{b}$	2
	TE_{mn}	$\dfrac{v}{2}\sqrt{m^2+n^2\dfrac{a^2}{b^2}}$	$\dfrac{2}{\sqrt{m^2+n^2\dfrac{a^2}{b^2}}}$	$\dfrac{a}{b}\cdot\dfrac{m^2+\dfrac{a}{b}n^2}{m^2+\dfrac{a^2}{b^2}n^2}\cdot\dfrac{2}{S_m S_n}$	$2\left(\dfrac{1}{S_m}+\dfrac{a}{bS_n}\right)-A$
				(NOTE: $m=0$, $S_m=2$; $m\neq 0$, $S_m=1$ SIMILARLY FOR S_n)	
	TM_{mn} $(m \geq 1,\ n \geq 1)$	$\dfrac{v}{2}\sqrt{m^2+n^2\dfrac{a^2}{b^2}}$	$\dfrac{2}{\sqrt{m^2+n^2\dfrac{a^2}{b^2}}}$	$2\dfrac{m^2+\dfrac{a^3}{b^3}n^2}{m^2+\dfrac{a^2}{b^2}n^2}$	0
WAVEGUIDE – CIRCULAR 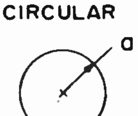	TE_{mn}	$\dfrac{v}{2\pi}r'_{mn}$	$\dfrac{2\pi}{r'_{mn}}$	$\dfrac{m^2}{(r'_{mn})^2-m^2}$	1
	TM_{mn}	$\dfrac{v}{2\pi}r_{mn}$	$\dfrac{2\pi}{r_{mn}}$	1	0
		NOTE: $r_{mn} = n^{th}$ ROOT OF $J_m(r)$; $r'_{mn} = n^{th}$ ROOT OF $J'_m(r)$			

NOTE 1: v = VELOCITY IN UNBOUNDED DIELECTRIC $= 1/\sqrt{\mu\varepsilon} = c/\sqrt{\mu_r\varepsilon_r}$

as stated earlier, we have proved the existence of these constants for all cases in the previously defined class. The values of these constants for several common cases are given in Table II.[1]

It will be observed that (1) and (2) are analogous to the well-known equation,

$$\alpha = \frac{R}{2R_0} + \frac{GR_0}{2} \tag{5}$$

where R is the effective series ac resistance per unit length, G is the effective shunt conductance per unit length, and R_0 is the real part of the characteristic impedance. Obviously D is dimensionally similar to $GR_0/2$; and since $M\sqrt{f}$ is equal to the surface resistance of the conductor divided by η, the first part of the equation is dimensionally similar to $R/2R_0$.

The discussion above probably contains little that is new to those well versed in electromagnetic theory. However, we believe the engineering usefulness of the equation in the form given, plus the realization of its generality, justifies this communication.

D. K. GANNETT
ZOLTAN SZEKELY
Bell Telephone Labs., Inc.
Murray Hill, N. J.

[1] Some of these values were obtained from equations given in G. C. Southworth, "Principles and Applications of Waveguide Transmission," D. Van Nostrand Co., New York, N. Y., pp. 94–95; 1950.

General Properties of the Propagation Constant of a Nonreciprocal Iterated Circuit*

Complementing an effort to introduce nonreciprocal loss into a microwave iterated circuit, a theoretical determination has been made of the behavior of the propagation constant of a general iterated circuit containing nonreciprocal components. This circuit might find use in a traveling-wave tube or parametric amplifier.

The model examined was an infinitely long chain of identical two-port networks, each specified by the matrix

$$(Z) = \begin{pmatrix} z_{11} & z_{12} \\ z_{21} & z_{22} \end{pmatrix},$$

where $z_{12} \neq z_{21}$ since each network contains nonreciprocal components. Voltages (and currents) to the right and left of each network are assumed to be related by the factor $e^{j\Theta}$ and the problem is to examine the nature of Θ.

The voltages and currents of the system are related by

$$\begin{pmatrix} V_n \\ V_{n+1} \end{pmatrix} = (Z)\begin{pmatrix} I_n \\ -I_{n-1} \end{pmatrix} \tag{1}$$

where n refers to the nth network and $e^{j\Theta} = V_{n+1}/V_n = I_{n+1}/I_n$. Eq. (1) may be expanded and put into the form

$$z_{12}e^{j\Theta} + z_{21}e^{-j\Theta} = z_{11} + z_{22}. \tag{2}$$

* Received by the IRE, October 19, 1959.

Use is made of the following definitions

$$\frac{z_{21}}{z_{12}} = e^{2(jb-\psi)},$$

$$\phi = b + (\text{angle of } z_{12}),$$

$$\Theta = \theta + j\chi,$$

$$x = 1/2\,\frac{\operatorname{Im}(z_{11}+z_{22})}{|z_{12}|},$$

$$r = 1/2\,\frac{\operatorname{Re}(z_{11}+z_{22})}{|z_{12}|},$$

$$P_c(x) = e^{\psi}(r\cos\phi + x\sin\phi),$$

$$P_s(x) = e^{\psi}(r\sin\phi - x\cos\phi). \tag{3}$$

After a little algebra, (2) may be written

$$\cos(\theta - b)\cosh(\chi - \psi) = P_c(x)$$

$$\sin(\theta - b)\sinh(\chi - \psi) = P_s(x). \tag{4}$$

Finally, conservation of energy requires that

$$r \geq 1/2\left|1 + e^{2(j\phi-\psi)}\right| \geq 0. \tag{5}$$

Although all quantities are basically a function of frequency, it will be convenient to consider x as an independent variable and r as a parameter. Although specific values of x and r do not determine the other quantities uniquely, they do determine upper and lower bounds on the other quantities. The cases of $r=0$ and $r>0$ will now be treated.

1) $r=0$ (lossless case). From (5), $\psi=0$, $P_c(x)=x$, and $P_s(x)=0$, so that (4) becomes

$$\cos(\theta - b)\cosh\chi = x$$

$$\sin(\theta - b)\sinh\chi = 0. \tag{6}$$

Eq. (6) has the simultaneous solution

$$\left.\begin{aligned}\cos(\theta - b) &= x\\ \chi &= 0\end{aligned}\right\} -1 \le x \le 1,$$

$$\left.\begin{aligned}\theta - b &= m\pi\\ \cosh\chi &= (-1)^m x\end{aligned}\right\} |x| \ge 1.$$

χ and $\theta - b$ are plotted vs x as the solid curves in Figs. 1 and 2 where it is understood that

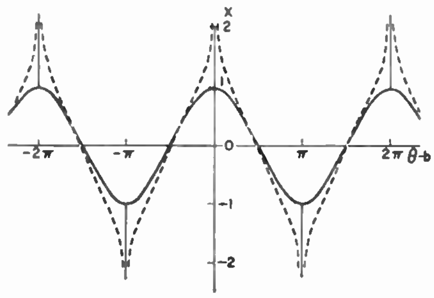

Fig. 1.

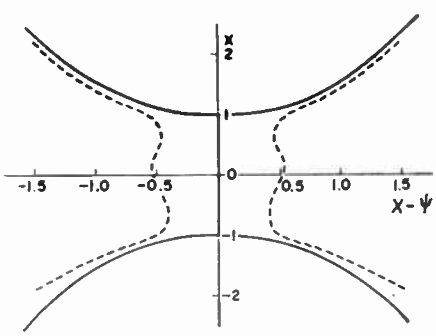

Fig. 2.

$\psi = 0$. The structure has a pass band from $-1 \le x \le 1$. Within this range, the loss parameter χ is zero and the phase parameter θ varies from $m\pi + b$ to $(m \pm 1)\pi + b$. For x above 1 and below -1, the loss parameter is high and the phase parameter is $m\pi + b$. The significant difference between the nonreciprocal and reciprocal cases is that in the latter x is an even function of θ, *i.e.*, $b = 0$. In the former case, this is no longer true. At $\theta = 2\pi m$, x is not 1 but cos b. Thus, for a nonreciprocal circuit, the propagation constants of the space harmonics will depend on the direction of propagation. A plot of x vs θ would look like Fig. 1 except that the curve shown in Fig. 1 would be shifted to the left or right of the ordinate by an amount b. If b is not a constant but a function of x, the situation is further complicated.

2) $r > 0$ (lossy case). For $r > 0$, (5) indicates that it is only possible to determine ϕ and ψ to within a band of values whose upper and lower limits may be calculated. Thus, for specific values of r and x, P_c and P_s may be determined to within a band whose upper and lower limits may be calculated. Nevertheless, from this information, it is possible to predict the general behavior of the loss and phase parameters. Typical plots of these parameters vs x are shown as the dotted curves in Figs. 1 and 2.

As an aid in determining these plots, we write (4) in the form

$$\sin^2(\theta - b) = P_c^2(x)\tan^2(\theta - b) - P_s^2(x),$$

$$\sinh^2(\chi - \psi) = P_c^2(x)\tanh^2(\chi - \psi) + P_s^2(x) \quad (7)$$

and note the intersection of the left and right hand sides of each equation as P_c and P_s are given their extreme values holding r fixed and varying x.

The behavior of χ and θ for $r > 0$ is more or less an expected extension of the $r = 0$ case except that now the loss parameter depends on the direction of propagation since $\psi \ne 0$. A plot of χ vs x would be the plot of Fig. 2 shifted to the left or right of the ordinate by an amount ψ. If ψ is a function of x, the situation is further complicated.

Two points of practical importance should be noted about an iterated nonreciprocal circuit used as a traveling-wave tube circuit. First, in a traveling-wave tube, $\theta = \beta L$ where L is the periodic length. In order to get interaction with the electron beam over a maximum of the pass band (from $x = -1$ to $+1$), at midband (frequency corresponding to $x = 0$) β must be approximately equal to the plasma slow-wave propagation constant and $\theta = \theta_{x=0}$. For the reciprocal case, $\theta_{x=0}$ is very close to an odd multiple of $\pi/2$ so that L is determined. In the nonreciprocal case, $\theta_{x=0} =$ (odd multiple of $\pi/2) + b$ and theoretically may be any angle. Thus, L is not restricted and may be chosen so as to optimize some parameter such as interaction impedance.

Secondly, it can be true that the addition of loss broadens the band of circuit-wave interaction with the electron beam (see Fig. 1, dotted curves). However, the attendant forward-wave loss negates the desirability of doing this. However, in a nonreciprocal circuit, it is theoretically possible to introduce ψ in such a way that the forward loss is small. At the same time, the backward loss increases, which is usually a desirable circuit property.

The author wishes to acknowledge the valuable aid of S. Sensiper of Hughes Aircraft Co. who suggested the problem and who provided subsequent stimulating discussions.

R. N. CARLILE
Dept of Elec. Engrg.
University of California
Berkeley, Calif.
Formerly at Hughes Aircraft Co.
Culver City, Calif.

Parametric Amplifier Antenna*

A number of circuit configurations have been reported[1] for employing voltage variable capacitors as the active element in a parametric amplifier. One form, described by Harris[2] and others, utilizes a coaxial distributed structure to provide, at the same time, appropriate resonant conditions for both the signal and the so-called idler frequency components. In this mode of operation the input signal and the output are at the same frequency f_s. The pumping energy source may be at $2f_s$, $4f_s \cdots$ etc., while the idler will have a corresponding value of f_s, $3f_s \cdots$. A number of advantages can be derived by realizing this circuit in a balanced form and incorporating the resulting structure inside of a half wave dipole as shown in Fig. 1. The amplifier consists of the outer cylinder of length L which serves as an antenna, and an inner coaxial conductor, diameter D', supported at the center by an RF connector and low loss dielectric spacers as shown. Each end of the center conductor is connected to the corresponding end of the antenna through parametric diodes (HPA 2800) at C and C'. The antenna is split at the mid-point to provide dc isolation for the diode bias paths. A thin dielectric layer between the dipole sections and the central supporting sleeve serves as an RF bypass path for antenna currents. The pumping signal is applied to both diodes in phase through the inner conductor at P_1. With the center conductor at dc ground, either through the generator or a suitable transmission line stub, diode bias voltages are applied at $B+$ and $B-$. In operation the interior coaxial region serves as a resonant storage volume for both the signal and idler components. The output is taken at P_2 from loop S through a suitable network which passes f_s while rejecting f_i.

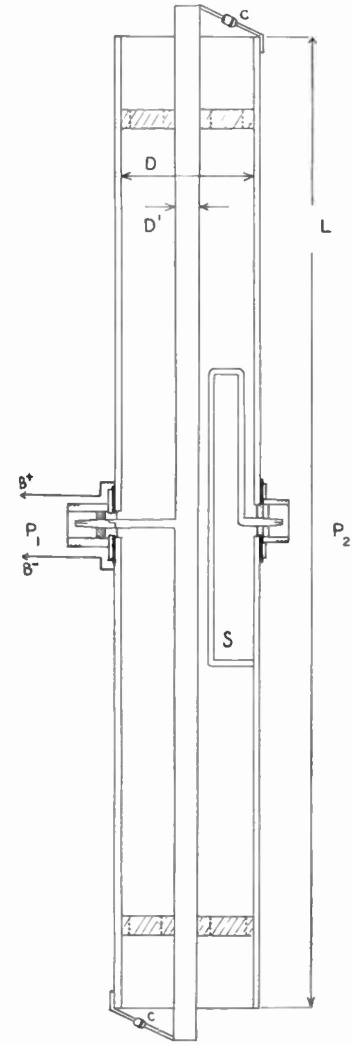

Fig. 1—Cross-sectional view of parametric amplifier antenna or "parant."

Fig. 2 shows the inner construction of a unit designed for use at 220 mc. Fig. 3 is the assembled antenna-amplifier dipole. It is necessary that the physical length of the

* Received by the IRE, October 29, 1959. The work described has been carried out under the sponsorship of the Electronics Research Directorate, Air Force Cambridge Res. Center.

[1] A. Uhlir, Jr., "The potential of semiconductor diodes in high frequency communications," PROC. IRE, vol. 46, pp. 1099–1115; June, 1958.
B. Salzberg and W. E. Sard, "A low-noise wideband reactance amplifier," PROC. IRE, vol. 46, p. 1303; June, 1958.
[2] F. S. Harris, "The parametric amplifier," CQ, vol. 14, November, 1958.

antenna cylinder be adjusted for the desired center operating frequency while at the same time the coaxial system is resonant at f_s and an odd multiple of f_n. Since the free resonant length of an antenna is significantly less than $\lambda/2$ the interior system would appear to have less than its requisite electrical length. It has been found, however, that with the antenna units investigated to date an adjustment of fringing and diode capacitance has been sufficient to achieve the simultaneous resonance conditions without the use of an internal dielectric septum. Antenna-amplifier gain, relative to a passive dipole of the same length and diameter and measured as a function of frequency, is shown in Fig. 4.

In addition to the advantage of a potentially low noise figure such as is common to reactive parametric amplifiers, this arrangement provides a low impedance output at a coaxial connection in the neutral plane of the antenna. Complications in construction arising from the use of a split outer conductor can be avoided by separating the inner conductor into two sections at the center and applying the pumping and bias voltages through a twin coaxial connector instead of the type N as used in this version.

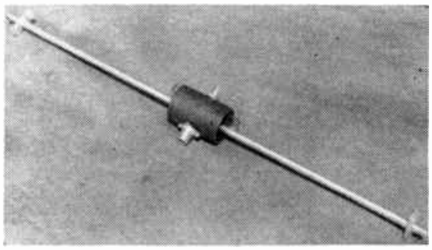

Fig. 2—Antenna center conductor showing output loop and coaxial connectors.

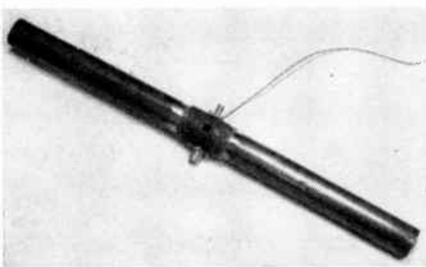

Fig. 3—Assembled antenna amplifier dipole.

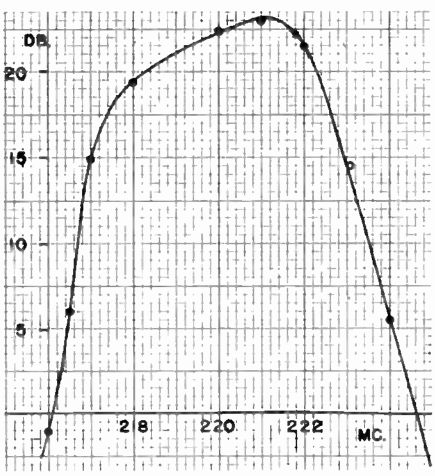

Fig. 4—Antenna amplifier gain relative to passive dipole having the same length and diameter. Pumping source frequency and dc bias adjusted at each point for maximum gain.

ALBERT D. FROST
Antenna Systems Lab.
Dept. of Elec. Engrg.
University of New Hampshire
Durham, N. H.

Superdirectivity*

Kock[1] in his interesting paper on "Related Experiments with Sound Waves and Electromagnetic Waves" credits Schelkunoff[2] with the first discussion of superdirectivity in aerial arrays. Though Dr. Schelkunoff's paper is of basic importance in this field, investigation of the phenomenon commenced much earlier. The first demonstration of the possibility of superdirectivity that we know of was published in 1922 by C. W. Oseen.[3] Reference to four other papers prior to that of Schelkunoff was given by us in a previous paper.[4] In the bibliography appended to that paper, we listed all the work on superdirectivity then known to us; the quite impressive total of twenty-eight items resulted. In view of the continued interest in this subject it may be of value to bring this listing up to date, as attempted in the bibliography below. For the Goward reference [1] we are indebted to Mr. J. D. Lawson of the Atomic Energy Research Establishment at Harwell.

A. BLOCH,
R. G. MEDHURST,
S. D. POOL
Research Laboratories,
The General Electric Co., Ltd.
Wembley, England.

Author's Comment:[5]

I feel that Oseen[3] discussed the possibility of superdirectivity, whereas Schelkunoff[2] and Franz [28] demonstrated a feasible method of approach to its realization. Schelkunoff U. S. Pat. No. 2,286,839 on this subject was applied for on December 20, 1939; it was issued on June 16, 1942. I am indebted to Dr. Franz for the receipt of reprints of two papers of his [28, 30] which appeared during the war and which I failed to reference. The second [30] refers to still another author on superdirectivity: A. Fradin, *J. O. A. Ph.*, Leningrad, Russia, vol. 9, p. 1161; 1939.

WINSTON E. KOCK
Research Laboratories Div.
Bendix Aviation Corp.
Detroit, Mich.

* Received by the IRE, November 4, 1959.
[1] W. E. Kock, "Related experiments with sound waves and electromagnetic waves," PROC. IRE, vol. 47, pp. 1192–1201; July, 1959.
[2] S. A. Schelkunoff, "A mathematical theory of linear arrays," *Bell Sys. Tech. J.*, vol. 22, pp. 80–107; January, 1943.
[3] C. W. Oseen, "Die Einsteinsche, Nadelstichstrahlung und die Maxwellschen Gleichungen," *Ann. der Phys.*, vol. 69, pp. 202–204; 1922.
[4] A. Bloch, R. G. Medhurst, S. D. Pool, "A new approach to the design of super-directive aerial arrays," *Proc. IEE (London)*, pt. III, vol. 100, pp. 303–314; September, 1953.
[5] Received by the IRE, November 25, 1959.

BIBLIOGRAPHY

[1] F. K. Goward, "An improvement in end-fire arrays," *Proc. IEE, (London)*, vol. 94, pp. 415–418; November, 1947.
[2] R. L. Pritchard and M. D. Rosenberg, "Optimum directivity patterns for linear arrays," *J. Acoust. Soc. Amer.*, vol. 20, pp. 594–595; July, 1948.
[3] H. L. Knudsen, "Superforstærkning hos antenner," *Elektrotek Tiddsskr.*, vol. 64, pp. 213–221; June 5, 1951. (In Danish)
[4] G. Sinclair and F. V. Cairns, "Optimum patterns for arrays of non-isotropic sources," IRE TRANS. ON ANTENNAS AND PROPAGATION, vol. AP-1, pp. 50–59; February, 1952.
[5] A. S. Dunbar, "On the theory of antenna beam shaping," *J. Appl. Phys.*, vol. 23, pp. 847–853; August, 1952.
[6] L. L. Bailin and M. J. Ehrlich, "Factors affecting the performance of linear arrays," PROC. IRE, vol. 41, pp. 235–241; February, 1953.
[7] R. H. DuHamel, "Optimum patterns for endfire arrays," PROC. IRE, vol. 41, pp. 652–659; May, 1953.
[8] A. A. Pistolkors, "Use of Mathieu functions for computing field distribution in an antenna to obtain a given directional diagram," *Dokl. Akad. Nauk SSSR*, vol. 89, no. 5, pp. 849–852; April 11, 1953; Natl. Sci. Foundation transl. NSF-tr-113.
[9] L. D. Bakhrakh, "A solution of the integral equation for a linear antenna," *Dokl. Akad. Nauk SSSR*, vol. 92, no. 4, pp. 755–758, October 1, 1953; Natl. Sci. Foundation transl. NSF-tr-211, February. 1954.
[10] R. L. Pritchard, "Optimum directivity patterns for linear point arrays," *J. Acoust. Soc. Amer.*, vol. 25, pp. 879–891; September, 1953.
[11] ———, "Maximum directivity index of a linear point array," *J. Acoust. Soc. Amer.*, vol. 26, pp. 1034–1039; November, 1954.
[12] T. T. Taylor, "Design of line-sources for narrow beamwidth and low side-lobes," IRE TRANS. ON ANTENNAS AND PROPAGATION, vol. AP-3, pp. 16–28; January, 1955.
[13] R. L. Pritchard, "Discussion on optimum patterns for endfire arrays," IRE TRANS. ON ANTENNAS AND PROPAGATION, vol. AP-3, pp. 40–43; January, 1955.
[14] E. N. Gilbert and S. P. Morgan, "Optimum design of directive antenna arrays subject to random variations," *Bell Sys. Tech. J.*, vol. 34, pp. 637–663; May, 1955.
[15] R. Kovács and L. Solymár, "Theory of aperture aerials based on the properties of entire functions of the exponential type," *Acta Phys. Acad. Sci. Hung.*, vol. 6, no. 2, pp. 161–184; 1956.
[16] M. Uzsoky and L. Solymár, "Theory of superdirective linear arrays," *Acta Phys. Acad. Sci. Hung.*, vol. 6, no. 2, pp. 185–205; 1956.
[17] G. T. di Francia, "Directivity, super-gain and information," IRE TRANS. ON ANTENNAS AND PROPAGATION, vol. AP-4, pp. 473–479; July, 1956.
[18] A. Bloch, "N-terminal networks: some theorems with applications to the directive properties of aerial arrays," *Wireless Engr.*, vol. 33, pp. 295–300; December, 1956.
[19] V. L. Pokrovskii, "On the theory of optimal linear antennas," *Radio Engrg. and Electronics*, vol. 2, no. 12, p. 123; 1957.
[20] D. G. Tucker, "Signal/noise performance of super-directive arrays," *Acustica*, vol. 8, no. 2, pp. 112–116; 1958.
[21] L. Solymár, "A reactance theorem for antennas," PROC. IRE, vol. 46, p. 779; April, 1958.
[22] ———, "Maximum gain of a line source antenna if the distribution function is a finite Fourier series," IRE TRANS. ON ANTENNAS AND PROPAGATION, vol. AP-6, pp. 215–219; July, 1958.
[23] R. F. Harrington, "On the gain and beamwidth of directional antennas," IRE TRANS. ON ANTENNAS AND PROPAGATION, vol. AP-6, pp. 219–225; July, 1958.
[24] G. Broussard, "Contribution à l'étude théorique rayonnement," in "Comme. Prés. au Congrès International Circuits et Antennes Hyperfréquences," 1957, vol. 1, pp. 58–62, suppl. to L'Onde Élec.; August, 1958.
[25] N. F. Barber, "Design of 'optimum' arrays for direction-finding," *Elec. and Radio Engr.*, vol. 36, pp. 222–232; June, 1959.
[26] J. D. Lawson, "Electromagnetic wave problems," *Elec. and Radio Engr.*, vol. 36, pp. 332–338; September, 1959.
[27] R. F. Kyle, "Super-gain aerial beam," *Elec. and Radio Engr.*, vol. 36, pp. 338–340; September, 1959.
[28] K. Franz, "Die Verbesserung des Uebertragungswirkungsgrades durch Richtantennen," *Telefunken Mitteilungen*, vol. 21, pp. 3–8; 1940.
[29] J. C. Simon, G. Broussard, and E. Spitz, "Sur la superdirectivité d'une antenne à rayonnement transversal," *Comptes Rend. Acad. Sci.*, vol. 248, pp. 2309–2311; April, 1959.
[30] ———, "Bemerkungen über die Absorptionsflache von Richtantennen," *Hochfr. u. Elektrakustik*, vol. 61, pp. 51–53; 1943.
[31] L. D. Bakrakh, "The maximal directivity coefficient of linear and plane aerials," *Dokl. Acad. Nauk SSSR*, vol. 95, pp. 45–48; March 1, 1954.

Parallel Field Excitation*

AT-cut circular quartz plates or lenses are used for the control of precision oscillators in the range of 500 to 2500 kc.

The major requirements are: high Q, freedom of unwanted responses, and a good frequency-temperature behaviour.

As the inductance of these crystals is low, it is necessary to reduce by all means the resistance of the crystals in order to obtain high Q values. Good crystals, however, have a very low resistance of about one to five ohms. This complicates the design of the oscillator from the point of view of impedance matching.

As a result of recent work performed at the Paris Observatory, as well as at Oscilloquartz Dept. of Ebauches S.A. at Neuchatel, Switzerland, the electric parameters of the crystals were altered by application of an electric field parallel to the major surfaces of the crystal; this is instead of having it normal to the surfaces, as it is usually done for the excitation of thickness-shear vibrations.

There are two main points to consider when the parallel field method is applied:

1) Inductance and resistance are rising, but the former rises quicker than the latter; thus the Q value increases.
2) The resistance of unwanted responses is highly increased, especially that of unwanted face shear modes.

For one-mc fundamental-mode plated lenses of about 27-mm diameter, Q values between 6 and $8\cdot 10^6$ have been obtained. For 0.5-mc fundamental-mode plated lenses of about 38-mm diameter, the Q is approximately 8 to $10\cdot 10^6$. For both types, the resistance has values between 45 and 80 ohms, and the inductance is approximately 50 times higher than the inductance of crystals excited by a field normal to the surfaces.

Much higher Q's are obtained with *non-plated* crystals excited by the parallel field. Depending upon the choice of the geometry of the electrodes and of the air gap, the Q's of 0.5- and 1-mc lenses are approximately $20\cdot 10^6$.

All the measurements mentioned above have been made at room temperature.

V. Ianouchevsky
Observatoire de Paris
Paris, France

Bibliography

R. Bechman, "Filterquarze im Bereich 7 bis to 30 MHz," Arch. Elek. Ubertragung, vol. 13, pp. 90–93; 1959.
R. Bechmann, "Improved High-Precision Quartz Oscillators," Proc. IRE, vol. 48, pp. 367–368; March, 1960.

* Received by the IRE, November 6, 1959.

Theoretical Hysteresis Loops of Thin Magnetic Films*

The theoretical static behavior of single domain thin magnetic films can be determined on the basis of a few hypotheses:

1) The magnetization vector has a constant amplitude M_s.
2) It lies in the plane of the film.
3) The total energy per unit volume of the film is

$$E = K \sin^2 \theta - HM_s \cos (\phi - \theta) \quad (1)$$

The first term in (1) is the uniaxial anisotropy energy, where K is the anisotropy constant and θ the angle between the magnetization vector and the preferred direction of magnetization (easy direction). The second term is the energy of magnetization in the applied field of amplitude H and of direction ϕ.

Magnetization curves obtained from (1) are analyzed as a function of ϕ by Stoner and Wohlfarth[1] and for crossed fields by Smith.[2] Chu and Singer[3] give a graphical method, based on these energy considerations, for the determination of theoretical hysteresis loops. This communication gives a simple analytical method as well as a graphical construction more accurate and easier than the first method, which is sometimes difficult because of the flatness of the energy minimum. As is known, the magnetization assumes the direction in which the total energy E is a minimum.

$$\frac{\partial E}{\partial \theta} = 0; \quad \frac{\partial^2 E}{\partial \theta^2} > 0. \quad (2)$$

Two stable orientations exist for certain values of the field. By a continuous variation of the field vector, a jump occurs when the present minimum disappears; this case is realized when

$$\frac{\partial^2 E}{\partial \theta^2} = 0. \quad (3)$$

An analytical expression for the theoretical hysteresis loop, given by (1) and (2), is easy to obtain. The easy and hard directions are called x and y. The projections H_x and H_y of the field and the projections M_x and M_y of the magnetization are considered. M_x and M_y are related to the angle θ by

$$M_x = M_s \cos \theta; \quad M_y = M_s \sin \theta. \quad (4)$$

Reduced variables can be introduced in order to get dimensionless equations:

$$h_x = \frac{H_x M_s}{2K}; \quad h_y = \frac{H_y M_s}{2K};$$

$$m_x = \frac{M_x}{M_s}; \quad m_y = \frac{M_y}{M_s}. \quad (5)$$

Combination of (1), (2), (4) and (5) gives the system:

$$\boxed{\begin{aligned} m_x^2 + m_y^2 &= 1 \\ \frac{h_x}{m_x} - \frac{h_y}{m_y} &= -1. \end{aligned}} \quad (6)$$

The simplest way to compute hysteresis loops in the easy and hard directions, by means of these equations, is to consider m_x or m_y as the independent variable and h_y or h_x as a parameter, and then to compute h_x or h_y. The four main cases are shown in Fig. 1(a) below, and Fig. 1(b), next page. The jumps in the first two curves occur when $\partial h_x/\partial m_x = 0$ which, combined with (6), gives

[1] E. C. Stoner and E. P. Wohlfarth, "A mechanism of magnetic hysteresis in heterogeneous alloys," *Phil. Trans. Roy. Soc., A*, vol. 240, pp. 599–642; 1948.
[2] D. O. Smith, "Static and dynamic behaviour of thin permalloy films," J. Appl. Phys., vol. 29, pp. 264–273; March, 1958.
[3] K. Chu and J. R. Singer, "Thin film magnetization analysis," Proc. IRE, vol. 47, pp. 1237–1244; July, 1959.

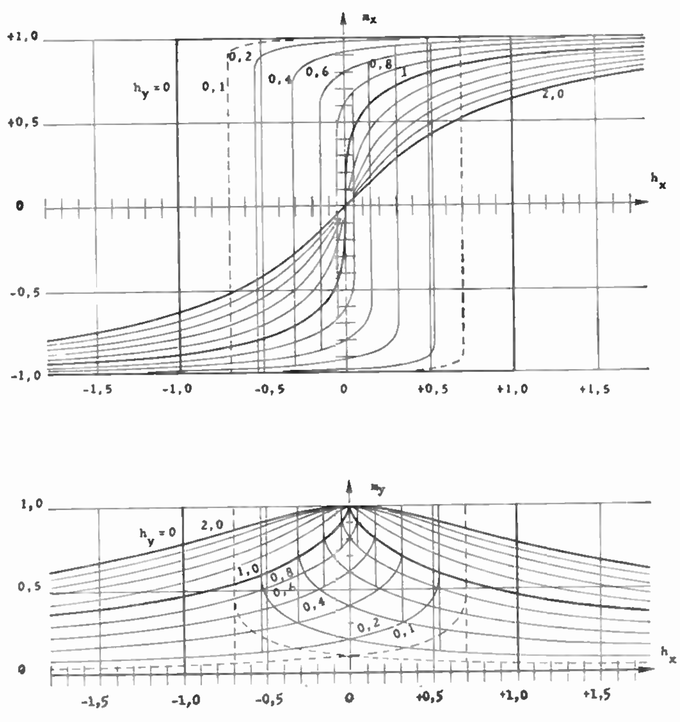

Fig. 1(a)

* Received by the IRE, November 2, 1959.

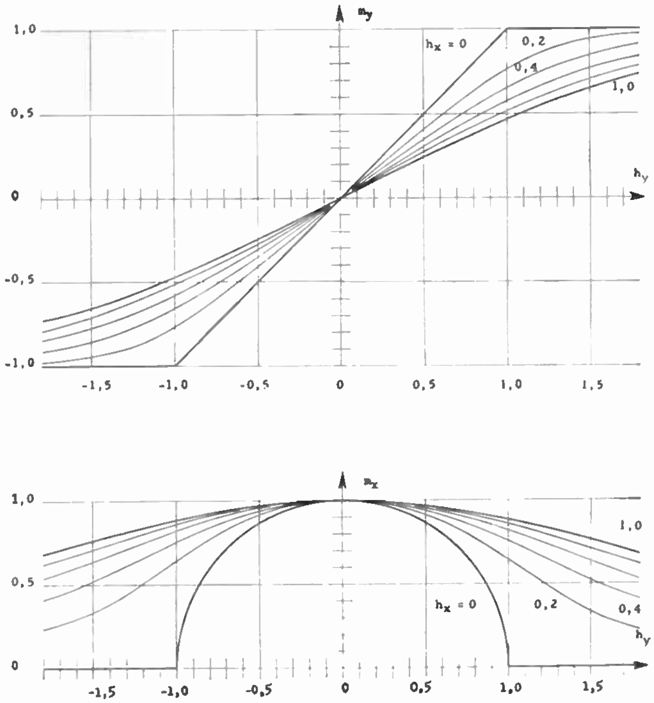

Fig. 1(b)

Fig. 1—Magnetization projection m_x and m_y. (a) As a function of the field h_x in the easy direction and with the field h_y in the hard direction as parameter; (b) as a function of the field h_y in the hard direction and with the field h_x in the easy direction as parameter.

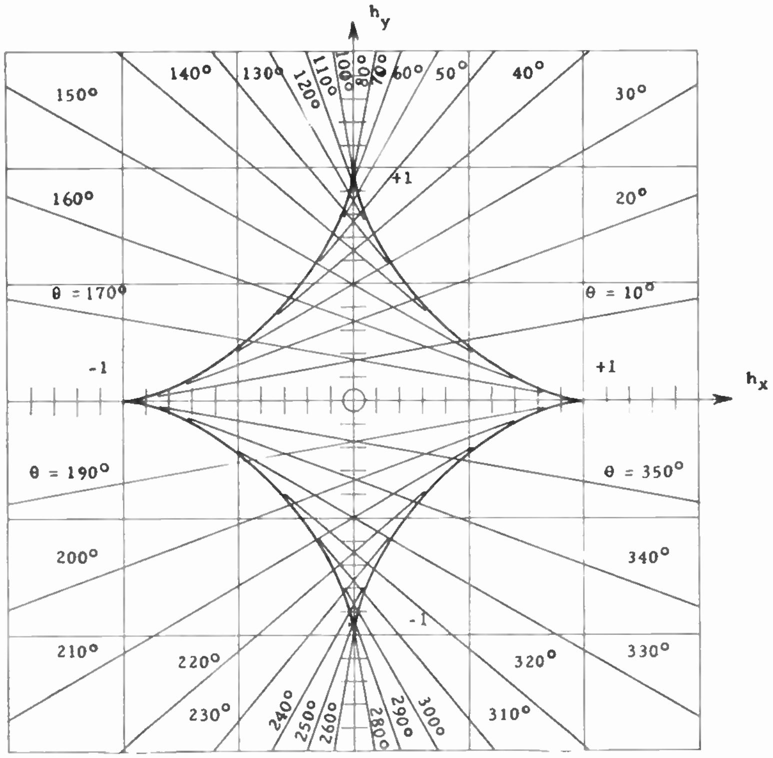

Fig. 2—Critical curve and geometrical construction of the magnetization direction θ.

the relation

$$h_x^{2/3} + h_y^{2/3} = 1. \qquad (7)$$

This equation represents the critical curve. The magnetization just before a jump is

$$m_x = h_x^{1/3}; \qquad m_y = h_y^{1/3}. \qquad (8)$$

In the easy direction, the curves are reversible when $h_y \geq 1$. The initial susceptibility in the reduced curves is then

$$\left.\frac{\partial m_x}{\partial h_x}\right|_{h_x=0} = \frac{1}{h_y - 1}.$$

In the hard direction, the curves are always reversible, and the initial susceptibility is

$$\left.\frac{\partial m_y}{\partial h_y}\right|_{h_y=0} = \frac{1}{h_x + 1}.$$

An essential property of (6) is the linear dependence of h_x and h_y for a given value of m_x, m_y or of the direction θ of the magnetization vector. Furthermore, it can be shown[4] that all the straight lines in the (h_x, h_y) plane are tangential to the critical curve (7). This property can be used for the graphical determination of hysteresis loops under various conditions (Fig. 2), as first proposed by Slonczewski.[5] The straight line going through the point (h_x, h_y) and tangential to the critical curve forms, with the x axis, an angle θ equal to the angle formed by the magnetization vector with the easy direction.

Experimental curves agree very well with the theoretical curves obtained under the simplified initial hypotheses, provided single domain structure and rotational processes only take place. This is the case for the reversible curves shown in Fig. 3.

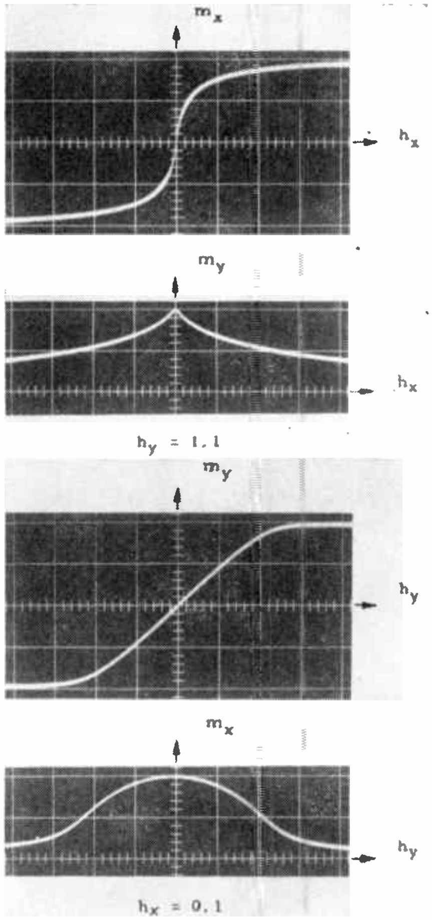

Fig. 3—Experimental M-H loops of a Ni Fe film of about 80-20 composition show rotational and reversible behavior at low frequency (500 cps).

H. J. Oguey
Res. Lab., IBM Corp.
Zurich, Switzerland

[4] P. Franklin, "Advanced Calculus," McGraw Hill Book Co., Inc., New York, N. Y., p. 343; 1944.
[5] J. C. Slonczewski, "Theory of magnetic hysteresis in films and its application to computers," IBM Rept. No. RM 003.111.224, October 1, 1956 (unpublished).

Narrow-Band Filtering of Random Signals*

The misconception that the output of a narrow-band filter is more nearly Gaussian than some corresponding non-Gaussian random input appears to be widespread. The incorrectness of this concept is demonstrated by the following examples.

First, consider the random process consisting of the pure cissoids,

$$x(t) = e^{2\pi j(ft+\phi)}, \quad -\infty < t < \infty,$$

where the frequency f is a random variable with arbitrarily given probability distribution,

$$\Pr\{f \le \lambda\} = F(\lambda), \quad -\infty < \lambda < \infty,$$

and the random phase ϕ is uniformly distributed on the unit interval. The process thus defined[1] is stationary in the wide sense, with autocovariance easily seen to be

$$\langle x(t_1)\overline{x(t_2)}\rangle = \int_{-\infty}^{\infty} e^{2\pi j\lambda(t_1-t_2)}dF(\lambda). \qquad (1)$$

[Note that any (unit power) power spectrum may be thus realized.] If this process is applied as input to a filter with transfer function

$$\begin{aligned} Y(2\pi jf) &= 1 \quad f' < f \le f'', \\ &= 0 \quad \text{otherwise}, \end{aligned} \qquad (2)$$

then the output, renormalized to unit power, has at any fixed time the form,

$$\begin{aligned} &\Delta^{-1/2}e^{2\pi j\theta} \text{ with probability } \Delta, \\ &0 \text{ with probability } 1-\Delta, \end{aligned}$$

where $\Delta = F(f'') - F(f')$, and where θ is a random variable uniformly distributed on the unit interval. This distribution of the output does not approximate the (complex) unit normal distribution in any reasonable sense as $f''-f' \to 0$. The analogous real process and filter also give rise to a non-Gaussian output distribution.

A more striking example is provided by

$$x(t) = n^{-1/2}\sum_{\nu=1}^{n} e^{2\pi j(f_\nu t+\phi_\nu)}, \quad -\infty < t < \infty, \quad (3)$$

where $f_\nu, \phi_\nu, \nu = 1, \cdots, n$ are mutually independent random frequencies and phases, respectively, each distributed as in the example above. The autocovariance of process (3) is given by (1), as before. If n is large, then the distribution of $x(t)$ of (3) at any fixed time will be nearly Gaussian, by the central limit theorem. If now f' and f'' are chosen so that $n\Delta$ is moderately small (say $n\Delta < 0.25$) then the output of filter (2) will have at any fixed time the form (again, renormalized to unit power)

$$\begin{aligned} &0 \text{ with probability } && 1-n\Delta+O((n\Delta)^2) \\ &(n\Delta)^{-1/2}e^{2\pi j\theta} \text{ with probability } && n\Delta+O((n\Delta)^2) \\ &\text{(other) with probability } && O((n\Delta)^2), \end{aligned}$$

with Δ and θ as before. Thus a random signal whose distribution at any fixed time is nearly Gaussian is converted by narrow-band filtering to one whose variables are much less Gaussian.

It may be argued that the processes described above are not ergodic and the author is willing to admit the possibility that narrow-band filtering of a non-Gaussian stationary (wide sense) process which is ergodic in the wide sense[2] might give a process whose variables are individually more nearly Gaussian. However, the above examples indicate that a proof will have to be more delicate than the heuristic arguments usually given. (In these arguments, small correlation is confused with small stochastic dependence.)

S. P. Lloyd
Bell Telephone Labs.
Murray Hill, N. J.

* Received by the IRE, October 22, 1959.

[1] J. L. Doob, "Stochastic Processes," John Wiley and Sons, Inc., New York, N. Y., p. 525; 1953. It is to be emphasized that each sample function of the process is a pure cissoid, of fixed frequency and phase, extending indefinitely in time. The random element is the choice of frequency and phase.

[2] By this we mean a process whose sample function autocorrelations (time average) are equal to the process autocovariance (statistical average) with probability 1; the definition of Doob is different. See J. L. Doob, *op. cit.*, pp. 461–464, 493–497.

Rapid Periodic Fading of Medium Wave Signals*

The occurrence of a peculiar type of rapid fading, called "flutter phenomenon," in broadcast signals have been reported by Subba Rao and Somayajulu.[1] They observed this type of fading regularly on the 41-m and 61-m bands and occasionally on the 19-m band, but never on the medium wave band. Recently, Yeh and Villard[2] reported the occurrence of a more rapid fading of signals in the 41-m band propagating over long paths crossing the magnetic equator.

Using a superheterodyne broadcast receiver, the AVC system of which was disconnected, and a recording millivoltmeter, it has been possible to record the same type of rapid fading of signals on the medium wave as well as short wave bands. A few typical records are reproduced here. The particulars of these records are as follows: Fig. 1(a) shows fading of transmission in the 19-m band from Karachi, received at 1935 hours Indian Standard Time (IST) on March 3, 1959. Fig. 1(b) shows the same in the 61-m band from Madras, received at 1845 hours IST the same day. Fig. 2(a) is a record of such fading of signals at 280.4-m received from Delhi at 2027 hours IST, also the same day. Fig. 2(b) represents another such record of the 280.4-mc signals obtained at 1912 hours IST on March 16, 1959 and

* Received by the IRE, October 22, 1959.

[1] N. S. Subba Rao and V. V. Somayajulu, "A peculiar type of rapid fading in radio reception," *Nature*, vol. 163, p. 442; March, 1949.

[2] K. C. Yeh and O. G. Villard, Jr., "A new type of fading observable on high-frequency radio transmissions propagated over paths crossing the magnetic equator," Proc. IRE, vol. 46, pp. 1968–1970; December, 1958.

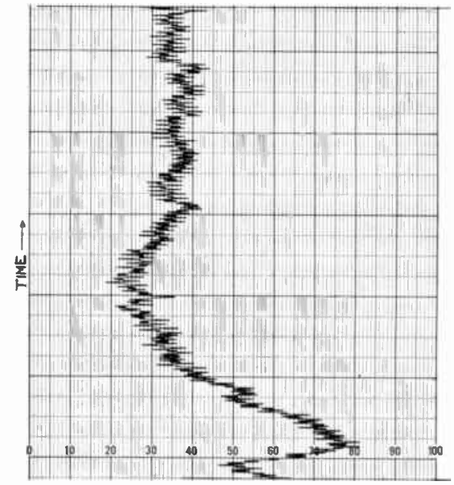

Fig. 1(a)

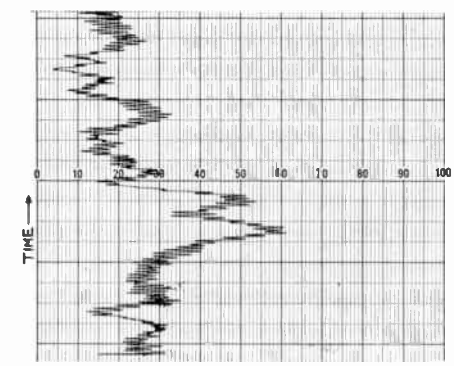

Fig. 1(b)

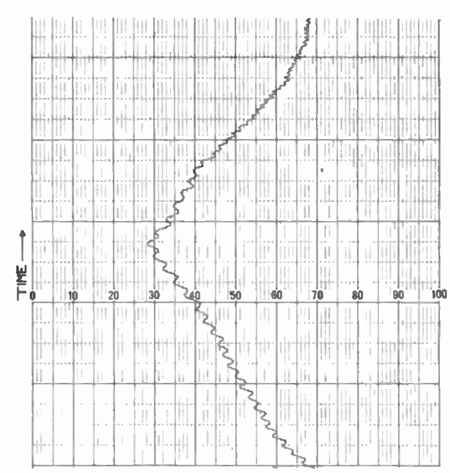

Fig. 2(a)

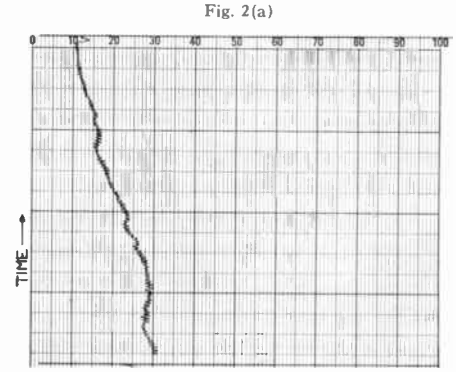

Fig. 2(b)

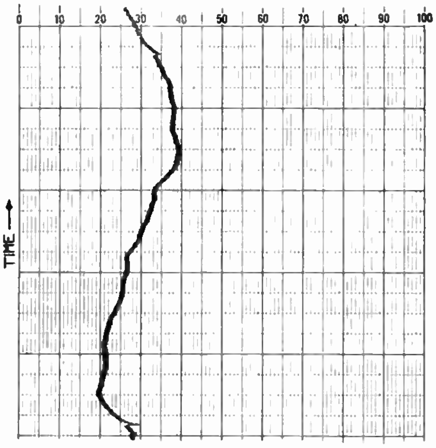

Fig. 2(c)

Fig. 2(c) shows a more rapid fading of the same signals at 1850 hours IST on March 12, 1959. On the time axis, four large divisions represent one minute.

It may be noted that the rate of fading of the medium wave signals is of the same order as that of the short wave signals, namely, about 1.5 to 3 cps. No known mode of propagation can account for such a rate of fading at this wavelength. Further records are being made.

The gift of a Varian type G-10 graphic recorder from the U. S. Government under the India Wheat Loan Educational Exchange Scheme is gratefully acknowledged.

HARIHAR MISRA
Physics Department
Ravenshaw College
Cuttack 3, India

Report on the AGU Study of the Metric System in the United States

The American Geophysical Union's Special Committee for the Study of the Metric System in the United States has noted the recent publication of our "Letter to the Editor" and its accompanying Questionnaire in the PROCEEDINGS.[1]

We wish to express our sincere appreciation for the courtesy of the IRE in presenting this matter to its readers. We wish also to thank your members who aided the Committee by a generous response of completed questionnaires. Many of the replies included letters containing helpful suggestions and offering financial assistance if requested.

Those readers who have access to the September, 1959, *Transactions of the American Geophysical Union* will find there a full report of the Committee, together with an analysis of the replies to the Questionnaire received up to July. At this date, three months later, 1080 have been analyzed. The scientific and engineering field was rather well covered by publication last spring of the Letter or Questionnaire, or both, in eight of the leading journals and magazines of the United States. Briefly, to the most significant question as to whether it would be desirable to replace the English System with the Metric as the "only official system" of weights and measures in the United States, ninety per cent have replied in the affirmative. The average suggested period of transition was about 22 years; this indicates agreement with the Committee on the necessity for a long transition period to avoid economic dislocation through education in the schools, through a normal retirement of presently active older personnel, and through the normal obsolescence of existing equipment.

The Congress of the United States, for the first time in nearly thirty years, is faced with a decision on metric legislation, recently introduced in both Houses. House Bill, HR7401, May, 1959, by Mr. Brooks of Louisiana, and Senate Bill, S2420, July, 1959, by Mr. Neuberger, both call for a feasibility study of the problem by an appropriate Government agency, with fund authorization. A third action of interest is the introduction in July, 1959, by Representative Fulton, of House Concurrent Resolution 364 which would place the Congress on record in favor of the Metric System.

It is apparent that the United States must soon decide whether to change over gradually, during the next generation, to a far simpler and more logical system of weights and measures, or to continue to live in comparative isolation with the remaining ten per cent of the world's population not yet under the Metric System.

FLOYD W. HOUGH
Chairman, Committee for the
Study of the Metric System
in the United States,
American Geophysical Union
1515 Massachusetts Ave., N. W.
Washington 5, D. C.

* Received by the IRE, November 1, 1959.

[1] F. W. Hough, "AGU Committee for the Study of the Metric System in the United States," PROC. IRE, vol. 47, p. 584; April, 1959.

Noise Spectrum of Phase-Locked Oscillators*

The fundamental parameter that best describes a phase-locked klystron is the noise spectrum of the oscillator in the phase-locked condition.[1] Some time ago a program for studying the sources of noise in phase-locked oscillators was established in the Microwave Spectroscopy Laboratory of the Research Laboratory of Electronics, Massachusetts Institute of Technology. The following remarks are a summary of the results of this project at its termination.

Since the first demonstration[2] of the simple utility of phase-locking klystron techniques in the microwave region, there has been considerable concern about the purity and validity of the resulting spectrum. Sources of noise, either amplitude-modulation noise or phase-modulation noise, can arise at many points in the servo-control loop. The importance of the various sources of noise is most convincingly demonstrated by experimental measurement. For this reason, a test facility consisting of two Felch oscillators,[3] at 1 mc and 5 mc, was built; active tube multipliers, multipling to 300 mc and 700 mc, were constructed; and electronic phase-locking equipment for K-band and X-band klystrons was assembled or constructed. The final system is shown in the block diagram of Fig. 1. It consists essentially of a silicon-diode harmonic generator, balanced mixer, 455-kc IF amplifier, phase demodulator, dc amplifier, and phase-correcting network to the klystron repeller. Previous phase-stabilization circuits measured in this laboratory have indicated a carrier noise level of approximately 60 db/cps.[4] It was our intention to use the measurements for comparing the noise amplitude as a function of the multiplication ratio and as a function of the low-frequency crystal-reference oscillator frequency.

Two klystrons were stabilized in this fashion and were beaten against each other in a superheterodyne receiver; the resulting beat note (arising from a small difference in the fundamental crystal-oscillator frequencies) could be displayed on an oscilloscope and the carrier-to-noise ratio could be analyzed with a General Radio harmonic distortion analyzer.

Unfortunately, when the system reached satisfactory operating condition, it was found that even with a frequency multiplication of 10,000 from a low-level Felch crystal oscillator the noise power per frequency interval was much too low to be measured on the distortion analyzer. The clarity of the beat note under these conditions can be seen from Fig. 2. The video bandwidth of the presentation system was 4 mc, so that the photograph shows the total noise signal. Although no definite measurements are available, the noise level must be less than 100 db below carrier per cps.

We conclude that with reasonably decent feedback electronics, the noise arising from the fundamental crystal oscillator or the multiplier chain is negligibly small, even with a frequency multiplication ratio of 10,000. Stated another way, this means that there should be no difficulty in operating a phase stabilizer from a 10-mc crystal in the 100-kmc frequency region, and so on.

There is no doubt that the system as we have operated it is far from optimum. The IF frequency is low. This was governed by a desire to have it less than the fundamental

* Received by the IRE, October 22, 1959. This work was supported in part by the U. S. Army (Signal Corps), the U. S. Air Force (Office of Scientific Research, Air Research and Development Command), and the U. S. Navy (Office of Naval Research).

[1] M. W. P. Strandberg, Letter to the Editor, *Radiotek. i Elektron.*, vol. 3, p. 1220; September, 1958.

[2] M. Peter and M. W. P. Strandberg, "Phase stabilization of microwave oscillators," PROC. IRE, vol. 43, pp. 869–873; July, 1955.

[3] F. P. Felch and J. O. Israel, "A simple circuit for frequency standards employing overtone crystals," PROC. IRE, vol. 43, pp. 596–603; May, 1955.

[4] M. W. P. Strandberg, "Phase stabilization of microwave oscillators," PROC. IRE, vol. 44, p. 696; May, 1956.

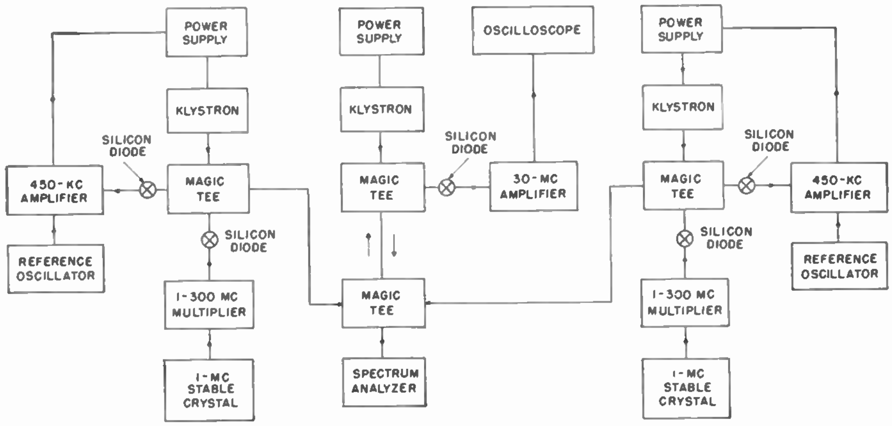

Fig. 1—Phase-locked stabilization of microwave frequencies.

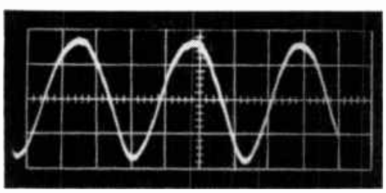

Fig. 2—Beat note of two phase-locked klystrons.

crystal-oscillator frequency. Thus the system was limited to a locking range of less than 0.5 mc; the hold in range, however, was approximately 10^4 mc. Even with this relatively poor design, these experiments have removed any doubt about the feasibility of phase-locking techniques—in the face of the argument that in the process a catastrophic amount of noise will also be generated. There is no doubt that this noise limitation will be met as the multiplication ratio becomes greater. As far as we can foresee, a multiplication ratio of 10,000 should be quite sufficient for most purposes, and should still be adequately remote from the multiplication ratio that would yield a noisy spectrum in the stabilized klystron output.

The over-all, long-time, relative phase stability of the two systems has not been studied because a study of the phase stability of the particular multipliers used would not be of general interest. The secular phase shift in the multiplier output can be reduced by limiting the number of multiplier stages and carefully controlling the input signal, temperature, operating potentials, and so forth. It would seem that a single-stage multiplier would be ideal for this purpose because it would minimize the amount of control that would have to be introduced to remove secular phase drifts from the multiplier chain. These secular drifts would only be evident if two klystrons were stabilized through two multiplier chains to a single crystal reference source, and the relative phase of each klystron with respect to the other determined. Few applications would have such stringent stability requirements. On the other hand, there are advantages in having a simple multiplier chain, simply from the point of view of convenience.

Some investigation of single-stage multipliers is being carried out in the Microwave Spectroscopy Laboratory, M.I.T. In particular, it has been pointed out by Sharpless[5] that gallium arsenide shows no carrier storage effects for switching times of the order of 10^{-10} seconds. Gallium-arsenide crystals, kindly supplied by the Texas Instruments Company, are being investigated under operating conditions in which they are driven hard by a 10-mc potential into the conduction region and into the Zener breakdown region. At 10 mc, with 100-mw power at 10 mc into the crystal, we should be able to obtain 0.1 μw of power at 10,000 mc. This would be more power than is needed to obtain satisfactory low-noise phase-locking.

The author would like to acknowledge the assistance of J. G. Ingersoll in carrying out the phase-locking experiments reported here.

M. W. P. STRANDBERG
Dept. of Physics and Res. Lab. of Electronics
Massachusetts Institute of Technology
Cambridge, Mass.

[5] W. M. Sharpless, "High-frequency gallium arsenide point-contact rectifiers," *Bell Sys. Tech. J.*, vol. 38, pp. 259–269; January, 1959.

Beam Focusing by RF Electric Fields*

It is well known that the periodic electrostatic fields can focus electron beams. One might suppose that the RF electric fields with a distribution similar to those fields can focus the beam. We studied the case of a strip beam passing through a parallel plane waveguide which carries E_{01} mode, and obtained some general conclusions.

Assumptions used are: 1) small perturbation, 2) the contribution of magnetic fields may be neglected, and 3) the term $(dy/dz)dv/dt$ may be neglected. The second assumption is reasonable if $u_0 \ll c$ and if the operating frequency is not near the cutoff points. Following the well-known procedure, one gets the path equation, eliminating t in

* Received by the IRE, October 26, 1959.

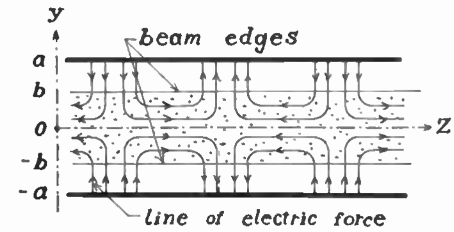

Fig. 1—Electric field distribution between two parallel planes.

the equation of motion.[1] The small perturbation from $y=b$ is expressed by

$$y_1 = q_1 \cos(\alpha z - \delta) + p_1 \sin(\alpha z - \delta),$$

$$\alpha = \frac{\omega}{u_0} + \beta, \qquad \delta = \frac{\omega}{u_0} z_0. \tag{1}$$

Substituting (1) into the path equation, one gets the condition of stability.[2]

It is of interest that the beam can not be focused by forward traveling waves. The power required to focus the beam by backward waves, P_1, is given by

$$P_1 = 8.02 \times 10^5 \frac{I_0}{F_1(\omega) \sin\left(\frac{b}{a}\pi\right)} \text{(watts/m)}$$

$$F_1(\omega) = \frac{(\omega_c/\omega)^2}{1 + \frac{u_0}{c}\sqrt{1-(\omega_c/\omega)^2}} \cdot \left[1 + \frac{u_0}{c}\left\{\frac{\sqrt{1-(\omega_c/\omega)^2}}{1+\frac{u_0}{c}\sqrt{1-(\omega_c/\omega)^2}} - \frac{1}{\sqrt{1-(\omega_c/\omega)^2}}\right\}\right]. \tag{2}$$

The magnitude of perturbation q_1/b is of the order of $3\times 10^{-2} \pm \sqrt{I_0 a}$. In the case of standing wave focusing, the necessary power P_2 (one-directional) is

$$P_2 = 1.01 \times 10^8 \frac{I_0/\sqrt{V_0}}{F_2(\omega) \sin\left(\frac{b}{a}\pi\right)} \text{(watts/m)}$$

$$F_2(\omega) = \left(\frac{\omega_c}{\omega}\right)^2 \frac{\{1-(\omega_c/\omega)^2\}^{3/2}}{1-\left(\frac{u_0}{c}\right)^2\{1-(\omega_c/\omega)^2\}}. \tag{3}$$

q_2/b is of the order of $0.4\times\sqrt{I_0/\sqrt{V_0}}$. P_2 is larger than P_1 because the forward traveling waves have defocusing action. As the magnitudes of $F_1(\omega)$ and $F_2(\omega)$ are of the order of 1, P_1 and P_2 are considerably large for reasonable $I_0(A/m)$ (see Fig. 2). It is noted that P_1 is proportional to I_0, while P_2 to $I_0/\sqrt{V_0}$.

The explanation for defocusing action of forward traveling waves is as follows. The electric field of E_{01} mode is given by

[1] P. K. Tien, "Focusing of a long cylindrical electron stream by means of periodic electrostatic fields," *J. Appl. Phys.*, vol. 25, pp. 1281–1288; October, 1954.

[2] Report presented to the Meeting of the Professional Group on Microwave Tubes of the IEE, Japan; July, 1959.

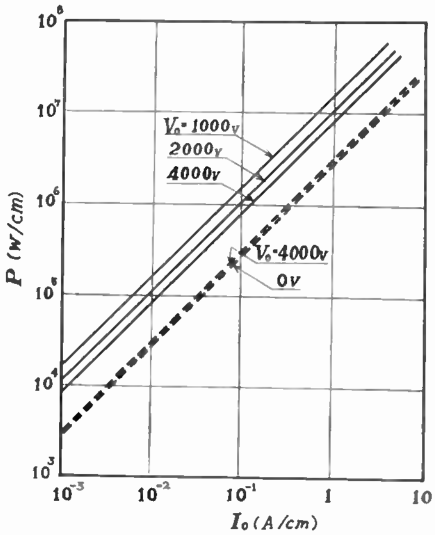

Fig. 2—Power required to focus the beam. Solid lines: power for standing waves. Dotted lines: power for backward traveling waves.

$$E_y = \beta \sin k_y y \cos(\omega t \pm \beta z),$$
$$E_z = \mp k_y \cos k_y y \sin(\omega t \pm \beta z). \qquad (4)$$

Putting $t=0$, (4) becomes

$$E_y = \beta \sin k_y y \cos \beta z,$$
$$E_z = - k_y \cos k_y y \sin \beta z. \qquad (5)$$

The field distributions of both forward and backward traveling waves are identical and similar to periodic electrostatic fields. To clarify the action of those traveling wave fields, it is helpful to see those fields from a moving coordinate that is traveling with a velocity equal to the mean velocity u_0 of electrons. Then $(\omega t \pm \beta z)$ is transformed into $(\omega/u_0 \pm \beta)z - (\omega/u_0)z_0$. The field distribution on the moving coordinates is obtained by substituting $\omega/u_0 \pm \beta$ into β of (5) and shifting the origin of coordinates. There are two cases: 1) $\omega/u_0 \pm \beta$ and β have the same sign or 2) they have the opposite sign. In the former case, the distribution is similar to periodic electrostatic fields. In the latter case, the phase relation between E_y and E_z is opposite to (5); electrons are axially decelerated when they experience outward force and accelerated when they experience inward force, which is contrary to the case of electrostatic lenses. In our E_{01} mode, the backward wave corresponds to the former case and the forward wave to the latter. This means the forward wave has defocusing action.

The phase relation between electric field components in slow wave circuit is the same as (5). In general, one may conclude that backward traveling waves and forward traveling waves which are slower than electrons can focus the beam, but forward traveling waves which are faster than electrons cannot.

E. Sugata
M. Terada
K. Ura
Y. Ikebuchi
Dept. of Electronic Engrg.
Osaka University
Higashinoda, Miyakojima
Osaka, Japan

Determination of Sign of Power Flow in Electron Beam Waves*

The question very often arises of whether a particular electron beam wave carries positive power or negative power[1] This can be particularly perplexing in dealing with transverse waves, because, associated with every transverse wave in an axially flowing electron beam, there are axial wave motions. The total power carried by the wave is, therefore, a combination of axial and transverse components, one of which may be positive and the other one negative. We propose here a method of determining the power flow for any wave, axial or transverse.

The best way to set up a "pure" electron wave of phase velocity v_1, is to couple the beam *loosely* to a circuit capable of carrying a pure wave at the same phase velocity; under this condition the circuit wave will slowly excite the beam wave. For typical electron beams, we need consider only quasi-static fields, where the phase velocity is so low that the electric fields of the wave differ negligibly from the fields of some electrostatic configuration moving at velocity v_1 with respect to a stationary observer. If we imagine ourselves moving at velocity v_1, we see purely static periodic fields. In such fields the radial velocity perturbations imparted (eventually) to the electrons must represent energy which is equal and opposite to the axial energy change experienced by the electrons. That is, as the electrons move through the static periodic fields and develop increasing radial velocities, they have the same increase in radial energy as decrease in axial energy. If, therefore, a radial velocity $\tilde{v}_r$ is imparted to the electrons, an axial velocity change $\tilde{v}_z$ is likewise imparted, in such a way that the total change in the ac energy or power in the beam is zero. The beam in the coordinate system of the wave is moving to the left at velocity $(v_b - v_1)$, where v_b is the beam velocity in the laboratory coordinates. The energy relationship is

$$\tilde{v}_r^2 + (v_b - v_1 + \tilde{v}_z)^2 = (v_b - v_1)^2 \qquad (1)$$

which reduces to

$$\tilde{v}_r^2 + 2\tilde{v}_z(v_b - v_1) + \tilde{v}_z^2 = 0;$$

for small signals,

$$\tilde{v}_r^2 = 2\tilde{v}_z(v_1 - v_b). \qquad (2)$$

Now $\tilde{v}_z$ the axial velocity perturbation and $\tilde{v}_r$ the transverse velocity, are invariant with respect to the transformation from the moving coordinates to the laboratory system. Consequently, in laboratory coordinates, the total ac energy of the electrons is proportional to

$$W_{ac} = \tilde{v}_r^2 + (v_b + \tilde{v}_z)^2 - v_b^2 = \tilde{v}_r^2 + 2v_b\tilde{v}_z \qquad (3)$$

(for small signals) Substituting from (2) we obtain

$$W_{ac} = \tilde{v}_r^2 + \tilde{v}_r^2 \frac{v_b}{v_1 - v_b} = \tilde{v}_r^2 \left(\frac{v_1}{v_1 - v_b}\right). \qquad (4)$$

The "sign" of the ac power carried by the beam will be the same as the sign of W_{ac}. The relative proportion of axial and transverse power can also be obtained from (4). The factor $\tilde{v}_r^2$ is always positive so that the energy imparted to the electrons depends on the factor $(v_1/v_1 - v_b)$. From this factor, one can readily show that the condition for the wave to carry negative power is

$$v_b/v_1 > 1. \qquad (5)$$

The phase velocities of space charge waves and cyclotron waves are given by

$$v_{1\,(\text{space charge})} = \frac{v_b}{1 \pm \dfrac{\omega_p}{\omega}},$$

$$v_{1\,(\text{cyclotron})} = \frac{v_b}{1 \pm \dfrac{\omega_c}{\omega}},$$

where in general, ω_p and ω_c have values depending on the beam geometry, as is well known. From (5), the slow space charge wave and the "slow" cyclotron wave both have negative power flow.

W. R. Beam
Rensselaer Polytech. Inst.
Troy, N. Y.

* Received by the IRE, November 12, 1959.
[1] The "negative power" concept was first introduced by L. J. Chu. It is of great importance in gain and noise considerations.

Response of a Square Aperture to a Thermal Point Source of Radiation*

Antenna patterns are defined for point-source continuous wave targets. In these days of radio astronomy and thermal ground mapping, however, it is of interest to show the effective antenna pattern against a black body point source. It is evident from the start that an increase in bandwidth will receive more power, but produce some progressive pattern change from the familiar cw pattern.

Power radiated from a black body in the radio spectrum is given by the Rayleigh Jeans' approximation to Planks radiation formula.[1]

$$\frac{dP}{A_T d\lambda} = \frac{2\pi ckT}{\lambda^4} \frac{\text{power}}{\text{unit area} \cdot \text{unit wavelength}} \qquad (1)$$

where

A_T = projected area of source visible to antenna
λ = wavelength of radiation
k = Boltzmann's constant energy per degree of temperature
T = absolute temperature
c = velocity of light

An antenna is sensitive to only one polarization and thus can collect only half of this amount of power.

$$\frac{dP}{A_T d\lambda} = \pi ck \frac{T}{\lambda^4} = 1.3 \times 10^{-14} \frac{T}{\lambda^4} \frac{\text{watts}}{\text{meter}^3} \qquad (2)$$

with λ expressed in meters, and T expressed in degrees Kelvin.

An antenna removed from the source a distance ρ and having an effective aperture

* Received by the IRE, November 9, 1959.
[1] R. A. Smith, F. E. Jones, R. P. Chasmar, "The Detection and Measurement of Infrared Radiation," Oxford University Press, London, England, p. 27; 1957.

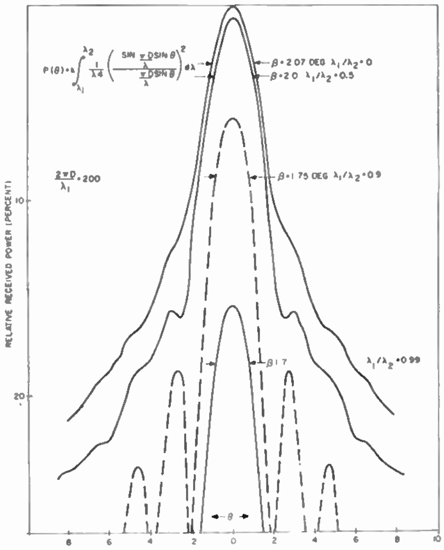

Fig. 1

of A_r receives power,

$$P = \frac{A_T\pi ckT}{4\pi\rho^2}\int_{\lambda_1}^{\lambda_2}\frac{A_r}{\lambda^4}\,d\lambda. \tag{3}$$

The effective area, A_r, is, in general, frequency-sensitive and depends upon the antenna design and target angle relative to the antenna. A square aperture uniformly illuminated would produce[2]

$$A_r(\theta\lambda) = A\left[\frac{\sin\left(\frac{\pi a}{\lambda}\sin\theta\right)}{\left(\frac{\pi a}{\lambda}\sin\theta\right)}\right]^2 \tag{4}$$

where the physical area $A = a^2$.

The reason for the selection of a square aperture is that this allows integration of (3) and just as ably demonstrates the effect as does a circular aperture which must be machine evaluated. Carrying this out, one finds

$$P = \frac{A_TckTA\left[\sin\left(\frac{2\pi a}{\lambda_2}\sin\theta\right) - \frac{2\pi a}{\lambda_2}\sin\theta - \sin\left(\frac{2\pi a}{\lambda_1}\sin\theta\right) + \frac{2\pi a}{\lambda_1}\sin\theta\right]}{4\rho^2\frac{2}{3}[2\pi a\sin\theta]^3}. \tag{5}$$

Notice that in the limit at $\theta\to 0$ (target on the antenna axis)

$$P = \frac{A_TckTA}{4\rho^2}\,\frac{1}{3}\left(\frac{1}{\lambda_1^3}-\frac{1}{\lambda_2^3}\right). \tag{6}$$

Using this as a normalization with $\lambda_2 = \infty$, the relative power pattern may be written

$$p = \frac{\sin\left(\frac{2\pi a}{\lambda_2}\sin\theta\right) - \frac{2\pi a}{\lambda_2}\sin\theta}{\frac{1}{6}\left(\frac{\lambda_2}{\lambda_1}\right)^3\left(\frac{2\pi a}{\lambda_2}\sin\theta\right)^3} - \frac{\sin\left(\frac{2\pi a}{\lambda_1}\sin\theta\right) - \frac{2\pi a}{\lambda_2}\sin\theta}{\frac{1}{6}\left(\frac{2\pi a}{\lambda_1}\sin\theta\right)^3}. \tag{7}$$

[2] S. Silver, "Microwave Antenna Theory and Design," *Radiation Laboratory Series*, vol. 12, McGraw-Hill Book Co., Inc., New York, N. Y.

Eq. (7) is shown in Fig. 1 (on the left) for $\lambda_1/\lambda_2 = 0, 0.5, 0.9, 0.99$ or, to say this another way, for an infinite, octave, ten per cent, one per cent bandwidth. With increasing bandwidth the slightly increasing beamwidth and lowering of the sidelobe level should be noticed. Eventually, the lobes as such disappear. It is also of interest that for a given upper-frequency limit, once an octave bandwidth has been achieved only about 12 per cent more power is available by extending this to zero low frequency limit.

M. S. Wheeler
Air Arm
Westinghouse Electric Corp.
Friendship Internatl. Airport
Box 746, Baltimore 3, Md.

A Dispersionless Dielectric Quarter Wave Plate in Circular Waveguide*

Certain applications of circularly polarized waves at microwave frequencies require that the axial ratio of the wave approach unity (0 db) as closely as possible and maintain this value over a broad band of frequencies. Previous applications had permitted the use of quarter wave plates which generated circularly polarized waves having an axial ratio of as much as 3 db. This note describes an improved dielectric quarter wave plate for circular waveguide which generates a circularly polarized wave with an axial ratio under 0.2 db over the 12 per cent frequency band from 8.5 to 9.6 kmc.

It is well known that a circularly polarized wave can be generated by loading a waveguide of circular or square cross section with a slab of dielectric material in such a manner that equal-amplitude orthogonal waves experience a 90° differential phase shift upon passing through the loaded section of waveguide. The design of this type of a dispersionless differential phase shifter in square waveguide has yielded to rigorous analysis.[1–3] On the other hand designs for use in circular waveguide have been arrived at largely on an empirical basis because of the difficulty in obtaining exact solutions for the circular waveguide case.[1,4]

It is possible, however, to apply analytical techniques to the problem of dispersionless dielectric quarter wave plates if the parameters of desired differential phase shift, frequency limits and waveguide size are fixed and dominant mode propagation is assumed throughout. For these conditions, the solution obtained is specific rather than general and a design must be calculated for each set of parameters of interest. The method evolves from a consideration of the expression of the differential phase shift $\Delta\phi$ in a dielectric slab loaded waveguide

$$\Delta\phi = 2\pi l\left(\frac{1}{\lambda_p}-\frac{1}{\lambda_t}\right), \tag{1}$$

where λ_p is the guide wavelength existing in the waveguide when the slab is parallel to the plane of the E vector, and λ_t is the guide wavelength produced when the slab is transverse to the E vector. Using the definition for guide wavelength

$$\lambda_g = \frac{\lambda}{\sqrt{\epsilon - \left(\frac{\lambda}{\lambda_c}\right)^2}}, \tag{2}$$

(1) may be rewritten

$$\Delta\phi = \frac{2\pi l}{\lambda}\left[\sqrt{\epsilon_p - \left(\frac{\lambda}{\lambda_c}\right)^2} - \sqrt{\epsilon_t - \left(\frac{\lambda}{\lambda_c}\right)^2}\right], \tag{3}$$

where ϵ_p and ϵ_t are effective dielectric constants required to satisfy (2) for measured values of λ_p and λ_t. The effective dielectric constant will be smaller than the dielectric constant of the material employed since a waveguide partially filled with a dielectric material will have the same phase delay as a waveguide completely filled with a material of lower dielectric constant.

The dispersion D in a differential phase shift device may be defined as

$$D = \Delta\phi_1 - \Delta\phi_2, \tag{4}$$

where $\Delta\phi_1$ and $\Delta\phi_2$ are the differential phase shifts occurring, respectively, at f_1 and f_2, the frequency limits of interest. Assuming a given waveguide size and frequency band, and setting $\Delta\phi_1 = 90°$, the expression for dispersion about 90° differential phase shift becomes

$$D_{90^\circ} = \frac{\pi}{2}\left[1 - \frac{\lambda_1}{\lambda_2}\left(\frac{\sqrt{\epsilon_p - (\lambda_2/\lambda_c)^2} - \sqrt{\epsilon_t - (\lambda_2/\lambda_c)^2}}{\sqrt{\epsilon_p - (\lambda_1/\lambda_c)^2} - \sqrt{\epsilon_t - (\lambda_1/\lambda_c)^2}}\right)\right]. \tag{5}$$

Eqs. (3) and (5) were evaluated for the frequency band from 8500 to 9600 mc, assuming a 15/16-inch ID circular waveguide. In order to systematize the computation, ϵ_p and ϵ_t were chosen according to a regular progression of both the mean effective dielectric constant ϵ_m and the ratio of effective dielectric constants ρ where

* Received by the IRE, October 19, 1959.
[1] W. P. Ayres, "Broadband Quarter Wave Plates," Electronic Defense Lab., Mountain View, Calif., Tech. Memo. No. EDL-M46; September 30, 1955.
[2] "Antenna Phenomena Research," Antenna Lab., Dept. of Electrical Engrg., Res. Foundation, Ohio State University, Columbus, Final Engrg. Rept. No. 594-7; November 1, 1955.
[3] H. S. Kirschbaum and S. Chen, "A Method of Producing Broadband Circular Polarization Employing an Anisotropic Dielectric," Antenna Lab., Dept. of Electrical Engrg., Res. Foundation, Ohio State University, Columbus, Engrg. Rept. No. 662-2; July 16, 1956.
[4] R. A. Brown and A. J. Simmons, "Dielectric Quarter Wave and Half Wave Plates in Circular Waveguide," Naval Res. Lab., Washington, D. C., Rept. No. 4218; November 10, 1953.

$$\epsilon_m = \sqrt{\epsilon_p \epsilon_t} \quad \text{and} \quad \rho = \frac{\epsilon_p}{\epsilon_t}. \tag{6}$$

The results of the computations are shown in Figs. 1(a) and 1(b). For the conditions chosen, the differential phase shift turns out to be solely a function of ρ and the dispersion is dependent only upon the value of ϵ_m. These curves, applied to the experimental measurements of ϵ_p and ϵ_t for various thicknesses of both polystyrene and teflon, resulted in plots of differential phase shift [Fig. 2(a)] and dispersion [Fig. 2(b)] as a function of dielectric slab thickness. Note that for the assumed case, minimum dispersion occurs in the region of high differential phase shift.

In designing a dispersionless quarter wave plate on the basis of these curves, consideration must, of course, be given to proper impedance matching. Only a stepped matching structure was considered in order to calculate the dispersion and differential phase shift occurring in the matching section. Using polystyrene of sufficient thickness to give a positive dispersion (3/16 inch in this case), steps were calculated to yield a binomial impedance change in the plane of the slab. Because of the thinness of the slab, it was hoped and borne out by subsequent measurements that no special matching measures would be required in the plane perpendicular to the slab. After calculating the differential phase shift introduced by the matching section, the length of the body of the quarter wave plate was computed to produce an over-all differential phase shift of 90°. Dispersion in the design was calculated to be about 1°.

Model quarter wave plates were constructed according to the calculated dimensions using both polystyrene and Rexolite, a material whose dielectric constant is the same as that of polystyrene. Axial ratios of between 0.2 and 0.3 db over the 12 per cent frequency band were obtained. Subsequent measurements indicated that the differential phase shift was slightly in excess of the desired 90°. By shortening the body of the dielectric element 0.015 inch, the error in the differential phase shift was reduced and a quarter wave plate which generates a circularly polarized wave of less the 0.2-db axial ratio was obtained. This is within 2 per cent of perfect circular polarization. The dimensions of the final model, designed to fit in 15/16-inch ID circular waveguide, are shown in Fig. 3, and the electrical performance characteristics of the unit are shown in Figs. 4(a) and 4(b).

R. D. Tompkins
Radar Division
Naval Research Lab.
Washington 25, D. C.

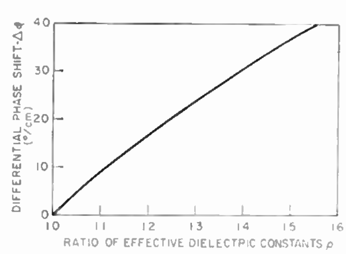

(a)

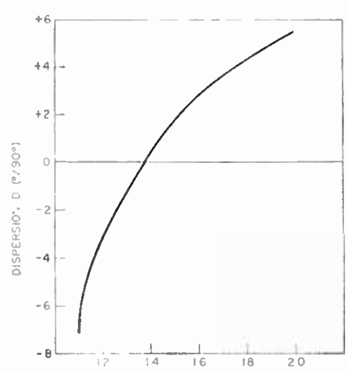

(b)

Fig. 1—(a) Differential phase shift vs ratio of effective dielectric constants for 15/16-inch ID circular waveguide at 8.5 kmc. (b) Dispersion about 90° vs mean effective dielectric constant for 15/16-inch ID circular waveguide in the frequency range 8.5 to 9.6 kmc.

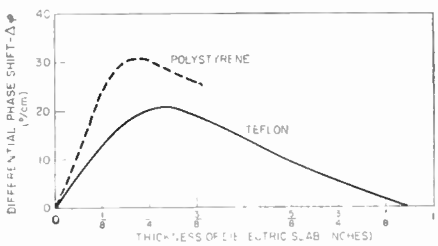

(a)

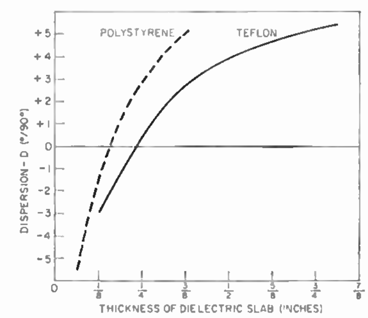

(b)

Fig. 2—(a) Differential phase shift vs thickness of dielectric slab at 8.5 kmc. (b) Dispersion about 90° vs thickness of dielectric slab.

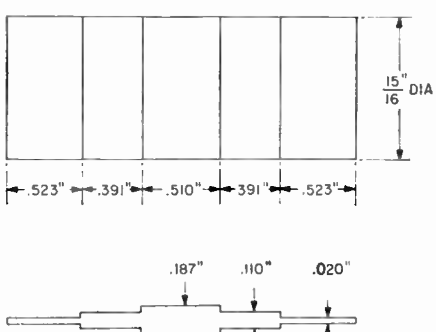

Fig. 3—A dispersionless quarter wave plate showing dimensions in inches. Material is polystyrene.

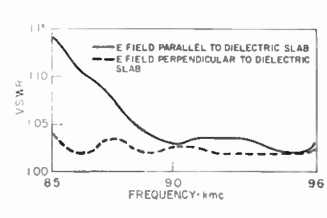

(a)

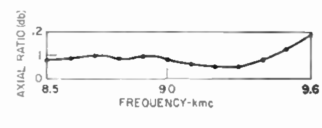

(b)

Fig. 4—(a) VSWR vs frequency for E field parallel and perpendicular to dielectric slab. (b) Output axial ratio of quarter wave plate.

Measuring the Mean Square Amplitude of Fading Signals Using a Selected Quantile Output Device (SQUOD)*

In many experiments it is necessary to measure the mean-square amplitude of a varying signal. The use of a square law detector is obvious. However, if the mean amplitude varies over a wide range, a system of attenuators has to be used, which is a disadvantage in automatic equipment designed to measure the signal over long periods.

The ideal receiver for measuring the amplitude of a signal which may vary over a wide range is one with a logarithmic characteristic such as that described by Chambers and Page.[1] The mean output from such a receiver does not, however, correspond to the root mean square signal. When the fading is completely random, for instance, the mean output is about 9 db in power below that corresponding to the rms signal.

The purpose of this note is to draw attention to the fact that, if the signal input to a nonlinear receiver consists of steady and random components as described by Rice,[2] then the quantile of the output voltages, chosen so that the receiver output is less than the quantile for 60 per cent of the time, is almost equal to the output corresponding to the rms-signal input. This is shown in Fig. 1 where the error in decibels, by which the input signals corresponding to the various quantiles exceed the rms-signal input, is plotted against the ratio of the square of the amplitude of the random component to the mean-square value of the signal, a measure of the depth of fading. It is seen that the quantile chosen leads to an error of less than 0.26 decibel, no matter what the depth of fading.

A device called a "Selected Quantile Output Device," or SQUOD, has been con-

* Received by the IRE, December 1, 1959.
[1] T. H. Chambers and I. H. Page, "The high-accuracy logarithmic receiver," Proc. IRE, vol. 32, pp. 1307–1314; August, 1954.
[2] S. O. Rice, "Mathematical analysis of random noise," *Bell Sys. Tech. J.*, vol. 23, pp. 282–332, July, 1944; and vol. 24, pp. 46–156, January, 1945.

structed for determining the required quantile. The circuit, shown in Fig. 2, includes an amplitude comparator—the first ECC81—between the voltage input from the receiver and output to the recorder. The input voltage is a dc negative-going voltage varying from +20 to −20 volts. The adaption of the circuit to positive-going voltages is obvious.

The comparator operates a relay. With the relay closed or open, the condenser C (12 mf) charges or discharges through the resistance R, at uniform rates determined by the 15-volt or 22-volt batteries respectively, with R_2 (approximately 300 Ω) providing a fine control. The electrometer tube 4066 is used in a circuit basically due to Farmer.[3] The grid current is about 10^{-12} amp, allowing values of R up to about 10^{10} ohms. The voltage on the condenser C is thus transferred to the grid of the last half of the second ECC81, which acts as a cathode follower with a constant current load. As the battery voltages are fixed relative to the output voltage, the charging and discharging rates remain fixed.

The OA81 diode connected to the anode of the first ECC81 insures that, should the input voltage drop and the second half of the tube take all the current, the second anode cannot drop much below 85 volts and cannot force its grid to draw current.

The 4-mf condenser shunts the output of the electrometer tube and removes all ripple caused by fluctuating emission of the filament. This capacative shunt path is taken via the condenser C, in order to minimize phase lag in the control loop. As the electrometer tube has a gain of approximately one, the capacity seen in shunt with C from R is negligible.

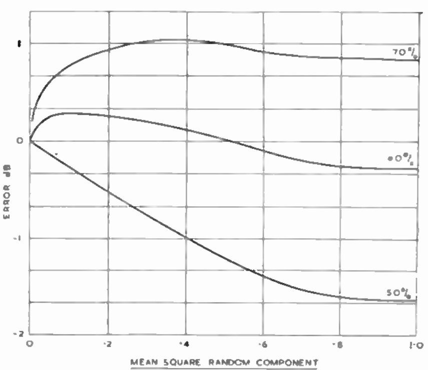

Fig. 1—The error in decibels by which the various quantile exceed the rms value, plotted against the ratio of the mean square value of the random component to the mean square value of the signal when the selected quantile exceeds the signal for 50, 60, and 70 per cent of the time.

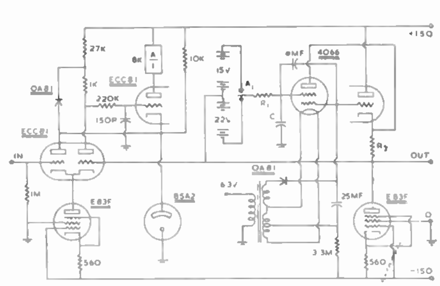

Fig. 2—Circuit of the SQUOD.

[3] F. T. Farmer, "Electrometer for measurement of voltages on small ionization chambers," *Proc. Phys. Soc.*, vol. 54, pp. 435–438; September, 1942.

The device is sensitive to changes of input voltages of 0.05 volt, and has a working range of about 60 volts.

The SQUOD, in conjunction with the logarithmic receiver, is being used fo. automatic and accurate recording of the mean-square amplitude of echoes reflected from the ionosphere, and may be of use in other applications in which quantities to be measured are subject to random fluctuations.

The authors gratefully acknowledge the receipt of research grants from the University of New Zealand.

A. E. Adam
J. D. Whitehead
Physics Department
University of Otago
Dunedin, New Zealand

Observations on Angle Diversity*

Recently several papers have appeared discussing the use of angle diversity[1,2] in a tropospheric scatter system. These papers suggest that, at the upper UHF and SHF bands, angle diversity is much more efficient than any other type of diversity. It is the purpose of this note to attempt to clarify the characteristics of angle diversity, and to point out that it is probably no better than simple space diversity from S/N points of view and that the total real estate required is also the same. Angle diversity, however, will provide greater bandwidth capability because the very narrow beams utilized will cut down multipath delays.

To be specific, let us consider the analysis presented by Vogelman, *et al.*[2] They suggest the use of a very large antenna with multiple feeds at the transmitting end to illuminate the entire effective scatter volume with non-overlapping beams (measured by the 3 db points). By implication, each of the beams would illuminate only a fraction of that volume. Thus, if five feeds were used, each beam would illuminate approximately one-fifth of the effective scatter volume. Let us pursue the implication of this a little further by considering two cases. In each case, the total power output at the transmitter is the same. In one case, the power is split among the several feeds in a large antenna. In the other case, all the power is put into one smaller antenna whose beam fills the same volume as all the beams of the larger antenna do. Since the total power being fed in at the transmitting end is the same for both situations and the volume through which the power flows is also the same the power, density flux through the scatter volume must be the same for both cases. It would appear, therefore, that in general it would be preferable to put all the power into one feed of a smaller antenna than to use a complex arrangement of multiple feeds and multiple frequencies in a large antennas as has been suggested.[2] One qualification must be added. If the required total power output is many times the power output capability of a single tube, then the paralleling of many tubes at the transmitter may also become a difficult problem. However, to offset this difficulty, we have the following advantages: 1) paralleling several tubes is more efficient in terms of radiated power because the off-centering of the multiple feeds involves a loss of probably 3 to 6 db per feed; 2) the alignment of the larger beam associated with the smaller antenna becomes simpler; and (3) much less bandwidth is required.

Now let us consider the receiving end. If multiple feeds are placed in one large antenna, angle diversity could be achieved. However, the same S/N statistics can be achieved by the more conventional means of spaced smaller antennas and, moreover, the total real estate required would be the same for both cases. To make this clear, consider an antenna whose beamwidth just fills the effective scattering volume. In this discussion this antenna will be called the reference antenna. This antenna will realize its full free-space gain. Any larger antenna will suffer an antenna-to-medium coupling loss such that the received signal would be of comparable magnitude to the signal received on the reference antenna. Thus an antenna which has five times the area of the reference antenna will "see" approximately one-fifth of the effective scatter volume. A corollary to this is that phase coherence of the incoming wave is not maintained over the dimensions of this larger antenna. As a matter of fact, the phase of the incoming wave is coherent over an area approximately one-fifth that of the antenna itself. This means that we can place five smaller antennas, each the size of our reference antenna, in a diversity system in the same area occupied by the larger antenna, and as already stated, each of these smaller antennas will receive a signal of magnitude comparable to that received by the larger antenna. Thus, from this example we see that the one large antenna (five times the area of our reference antenna) which utilizes five different feeds arranged for diversity will give the same S/N statistics as five antennas each the size of our reference antenna. Also, the area occupied by either antenna system is the same. As mentioned at the beginning of this letter, the one advantage that a system utilizing a larger antenna with multiple feeds has is greater bandwidth capability. However, to achieve this angle diversity for the purpose of increasing bandwidth capability, one does not have to utilize multiple feeds and multiple frequencies in a large antenna at the transmitting end. One smaller antenna whose beam just fills the effective scatter volume will suffice.

Harold Staras
RCA Labs.
Princeton, N. J.

* Received by the IRE, November 2, 1959.

[1] R. Bolgiano, Jr., N. H. Bryant, and W. E. Gordon, "Diversity Research in Scatter Communications with Emphasis on Angle Diversity," Contract AF 30(602)-1717, Final Rept., pt. 1; January, 1958.

[2] J. H. Vogelman, J. L. Ryerson, and M. H. Bickelhaupt, "Tropospheric scatter system using angle diversity," Proc. IRE, vol. 57, pp. 688–696; May, 1959.

Author's Comment[3]

Mr. Staras in his communication "Observations on Angle Diversity" has assumed that the purpose of this type of diversity is to illuminate the entire scatter volume with a uniform power density flux. I would like to point out that this is not the case. The purpose of angle diversity is to increase the reliability of tropospheric scatter communications. To this end, let me illustrate the advantages of angle diversity with numerical values rather than by pointing out flaws in Mr. Staras' letter.

Using Mr. Staras' illustration, let us compare the following two cases:

Case I. A 30-foot antenna with 4 units arranged for space diversity in the same geographic area as Case II; two antennas over two. Power per reflector is the same as power per feed in Case II. The frequency is 10 kmc.

Case II. A 60-foot antenna with 4 feeds in a row at 0° elevation. Power per feed is the same as power per reflector in Case I. The frequency is 10 kmc.

The distance between transmitter and receiver is 300 miles; Realized Gain[4] per antenna pair (1 receive and 1 transmit) for Case I is 86 db; and Realized Gain per beam pair (1 receive and 1 transmit) for Case II is 89.2, 89.9, 89.9, and 89.2, respectively. Using 50 per cent reliability for one path of Case I, identical transmitter power and receiver sensitivity, the reliabilities for the individual beams of Case II are 75 per cent, 80 per cent, 80 per cent and 75 per cent respectively.[5]

With quadruple space diversity, Case I gives an over-all reliability of 88 per cent or 120 errors per 1000, while 4 feed angle diversity gives in Case II an over-all reliability of 99.7 per cent or 3 errors per thousand.

JOSEPH H. VOGELMAN
Dynamic Electronics Div.
Capehart Corp.
Richmond Hill 18, N. Y.

[3] Received by the IRE, December 4, 1959.
[4] L. P. Yeh, "Tropospheric Scatter System Design," Westinghouse Electric Corp., Baltimore, Md., Tech. Rept. No. 5; October, 1957. See Fig. 4.
[5] *Ibid.*, Fig. 6.

General *N*-Port Synthesis with Negative Resistors*

This note gives an n-port synthesis for any $n\times n$ admittance $[Y(p)]$, impedance $[Z(p)]$, or scattering $[S(p)]$, matrix, in which the matrix elements are general rational functions with real coefficients containing zeros and poles of arbitrary multiplicity anywhere in the complex frequency (p) plane. It will be shown that the synthesis can always be performed with passive elements (R, L, C, gyrators, ideal transformers) and negative resistors. This total group will here be defined as "physical elements."

* Received by the IRE, November 20, 1959. This work was done under Contract AF-18(600)-1505 sponsored by the Army, Navy and Air Force.

First consider the synthesis of $Y(p)$. Express each element $y_{ij}(p)=\sum a_k p^k + y_{ij}^{(0)}(p)$ where $y_{ij}^{(0)}(p)$ is a proper fraction and hence has no poles at ∞. Then $Y(p)=\sum p^k A_k + Y_0(p)$, where the A_k are real constant matrices. Let us consider the synthesis of one of the matrices $p^k A_k$. A_k may be separated into its symmetric (A_k'') and skew symmetric (A_k') parts, and each of these diagonalized by a real congruent transformation. The symmetric part $p^k A_k''$ goes into diag $(p^k, p^k, \cdots, 0_{r+1}, \cdots, 0_n)$ where the rank of A_k'' is r. The skew symmetric part, $p^k A^{k'}$, goes into

$$\operatorname{diag}\cdot\begin{bmatrix}0 & p^{-k}\\ p^k & 0\end{bmatrix},\begin{bmatrix}0 & -p^k\\ p^k & 0\end{bmatrix},\ 0_{m+1},\cdots 0_n$$

where the rank of A_k' is m, an even number. Each 0_j is a scalar zero. We have then merely to show the synthesis of the diagonal elements

$$\pm p^k,\ \begin{bmatrix}0 & -p^k\\ p^k & 0\end{bmatrix},$$

and by appropriate transformers and parallel interconnections[1] $\sum p^k A_k$ may be synthesized as an n-port.

Fig. 1 shows how the admittance element $\pm p^2$ is synthesized; and in conjunction with the negative impedance converter circuit of Fig. 2, it is clear that $\pm p^2$ only requires passive elements and negative resistors. Fig. 3 shows how the admittance $\pm p^{n+1}$ can be synthesized in terms of elements of lower degree. Hence, by induction any p^k may be constructed of physical elements. Fig. 4 shows the realization of the admittance matrix

$$\begin{bmatrix}0 & -p^k\\ p^k & 0\end{bmatrix}$$

in terms of physical elements, where the admittance element $\pm p^k$, synthesized above, is used as a building block.

The next step is to synthesize $Y_0(p)$, whose singularities are all in the finite p plane. Let σ_0 be the positive real part of that pole of $Y_0(p)$ located farthest to the right of $j\omega$ in the complex p plane. Then make the frequency transformation $s=p-\tau$, $\tau>\sigma_0$. The function $Y_0(s)$ is now analytic on $j\omega$ and in the right half p plane, though it need not be passive (*i.e.*, it need not possess a positive quadratic form for internally dissipated power). The synthesis of such a $Y(s)$ has been given previously as a passive network some of whose ports are augmented by series-connected negative resistors.[1] Each coil L in the network for $Y_0(s)$ is now replaced by the series combination of L and a negative resistor $-L\tau$, and each condenser C by C in parallel with negative conductance $-C\tau$. This gives $Y_0(p)$ as a network with physical elements, and the parallel combination of $Y_0(p)$ with $\sum p^k A_k$ completes the synthesis.

[1] H. J. Carlin, "The synthesis of non-reciprocal networks," *Proc. Symp. on Modern Network Synthesis II*, Polytechnic Institute of Brooklyn, Brooklyn, N. Y., vol. 5, pp. 11–44; April, 1955.

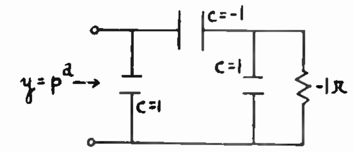

Fig. 1.

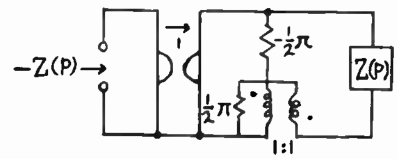

Fig. 2.

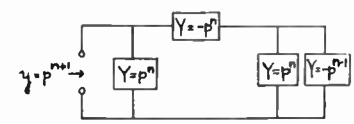

Fig. 3.

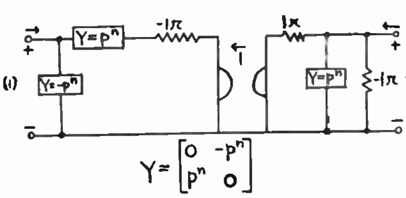

Fig. 4.

It is clear that $Z(p)$ may be synthesized by a dual process.

Suppose now that $S(p)$ is specified, and neither the $Z(p)$ nor $Y(p)$ representations corresponding to this S exists. Since S exists, the admittance matrix Y_A of an augmented network exists,[2] corresponding to the network for $S(p)$ with a unit positive resistor added in series to each port. $Y_A=\frac{1}{2}(I-S)$. $Y_A(p)$ is synthesized as described above to give the augmented network N_A. To find N corresponding to S, we "de-augment" N_A by adding -1 ohm resistors to each port of N_A. No attempt has been made to minimize the number of elements, but the synthesis given proves the general theorem:

Any $n\times n$ scattering matrix of rational real functions of p can be represented by a linear, time invariant, lumped n-port network containing only passive elements and negative resistors.

The number of resistors can be reduced by the following technique. Consider $Y(p)$ and suppose all boundary poles have been removed, so that $Y(j\omega)$ is bounded. Simple poles on $p=j\omega$ with positive residue matrices are removable as passive lossless networks, and higher-order boundary poles as well as simple boundary poles with non-positive residue matrices are synthesized by a simple modification of the technique given above in connection with Figs. 1–4. Write $Y(p)=Y_1(p)+Y_2(p)$, where, by combining appropriate terms of a partial fractions expan-

[2] H. J. Carlin, "The scattering matrix in network theory," IRE TRANS. ON CIRCUIT THEORY, vol. CT-3, pp. 88–97; June, 1956.

sion, $Y_1(p)$ has only left-half p-plane poles and $Y_2(p)$ has only right-half p-plane poles. Now $Y(p)=\hat{Y}_1(p)+\hat{Y}_2(p)$, where $\hat{Y}_1(p)=G+Y_1(p)$, $\hat{Y}_2(p)=-G+Y_2(p)$. $G=\text{diag}(g_1, g_2, \cdots, g_n)$ where the g_k are all real, non-negative, and may be chosen equal to each other, with g_k the maximum value required to make $\hat{Y}_1(p)$ and $-\hat{Y}_2(-p)$ positive real matrices. This can always be done with a real finite g_k since $Y(j\omega)$ is bounded, and $\hat{Y}_1(p)$ and $-\hat{Y}_2(-p)=G-Y_2(-p)$ are both analytic in the right half of the p plane.[1] The positive real matrix $\hat{Y}_1(p)$ may always be synthesized as a passive network containing at most n resistors all positive. By a theorem of Youla,[3] if $-\hat{Y}_2(-p)$ is PR, then $\hat{Y}_2(p)$ may be synthesized as a network containing lossless elements plus at most n resistors, all negative. Combining $\hat{Y}_1(p)$ and $\hat{Y}_2(p)$ in parallel gives $Y(p)$. Utilizing duality, we may state the following general theorem.

Any $n\times n$ immittance matrix of rational functions, which has no boundary ($p=j\omega$) poles other than those of simple order with non-negative residue matrices at these boundary poles, may be synthesized as an n-port network containing only lossless elements and at most n-positive and n-negative resistors.

A driving point impedance of the above type, for example, requires at most one positive resistor and one negative resistor.

H. J. Carlin
Microwave Res. Inst.
Polytechnic Inst. of Brooklyn
Brooklyn, N. Y.

[3] Microwave Res. Inst., Polytechnic Institute of Brooklyn, Brooklyn, N. Y., MRI Quarterly Rept. No. 16, R-452.16-59, pp. 55–56; April 15, 1959. Contract No. AF-18(600)-1505.

A Signal Flow Graph Method for Determining Ladder Network Functions*

An iterative method for determining ladder network functions was described by Kuo and Leichner,[1] with the suggestion that the signal flow method was not very convenient. For comparison, a signal flow solution is presented here.

Using the same circuit as Kuo and Leichner, a ladder with series impedances $Z_1(s)$ and $Z_3(s)$ and shunt admittances $Y_2(s)$ and $Y_4(s)$, and the same equations written in their simplest forms,

$$V_2(s) = V_2(s), \tag{1}$$

$$I_2(s) = Y_4(s)V_2(s), \tag{2}$$

$$V_a(s) = I_2(s)Z_3(s) + V_2(s), \tag{3}$$

$$I_1(s) = Y_2(s)V_a(s) + I_2(s), \tag{4}$$

$$V_1(s) = I_1(s)Z_1(s) + V_a(s), \tag{5}$$

a signal flow graph may be drawn (Fig. 1).

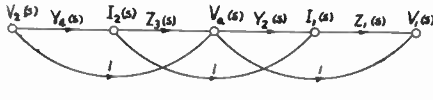

Fig. 1—A signal flow graph method for determining ladder network functions.

There are no feedback paths, so the determinant has a value of unity. The following relations may then be written by inspection[2] (if it is remembered that any node may be treated as a sink).

$$\frac{V_1(s)}{V_2(s)} = Y_4(s)Z_3(s)Y_2(s)Z_1(s) + Y_4(s)Z_3(s) + Y_4(s)Z_1(s) + Y_2(s)Z_1(s) + 1, \tag{6}$$

$$\frac{I_1(s)}{V_2(s)} = Y_4(s)Z_3(s)Y_2(s) + Y_4(s) + Y_2(s), \tag{7}$$

$$\frac{I_2(s)}{V_2(s)} = Y_4(s). \tag{8}$$

From these,

$$\begin{aligned} Z_{in}(s) &= V_1(s)/I_1(s) = \text{(6) divided by (7)};\\ I_2(s)/I_1(s) &= \text{(8) divided by (7)};\\ V_2(s)/V_1(s) &= \text{the reciprocal of (6)};\\ Z_{21}(s) &= V_2(s)/I_1(s) = \text{the reciprocal of (7)}.\end{aligned}$$

Thus, all the network functions may be obtained by inspection of one graph.

The form of the result is slightly different from that given by Kuo and Leichner, and the relative convenience or shortness of the methods may depend on the particular problem, and on the types of immittance involved.

G. H. Burchill
Nova Scotia Tech. College
Halifax, Nova Scotia

[2] S. J. Mason, "Feedback theory—further properties of signal flow graphs," Proc. IRE, vol. 44, pp. 920–926, July, 1956.

* Received by the IRE, November 2, 1959.

[1] F. F. Kuo and G. H. Leichner, "An iterative method for determining ladder network functions," Proc. IRE, vol. 47, pp. 1783–1784; October, 1959.

A Different Approach to the Approximation Problem*

The response curves that are usually desired in network theory cannot be exactly synthesized. A reasonable approximation to the desired response is therefore made and the corresponding network is synthesized. Where an infinite number of "reasonable approximations" exist, there are an infinite number of solutions to the problem.

It is possible to follow a less arbitrary approach, based upon the fact that a physically realizable response curve can be expressed as an exact function of s, where $s=j\omega$. Consider the amplitude and phase responses of curves A to D in Fig. 1, where ω_0 is a nominal cutoff frequency.

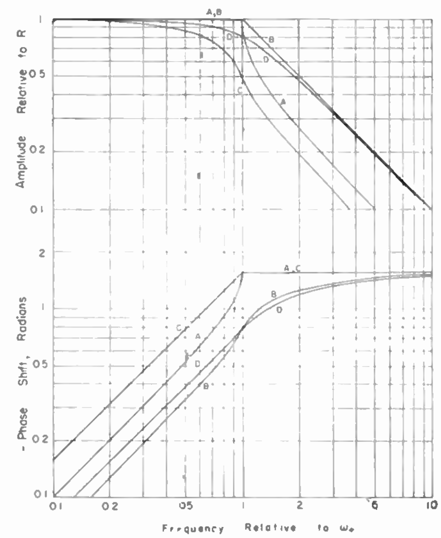

Fig. 1—Various "ideal" response curves.

For curve A, the amplitude response is flat up to ω_0 while the phase response is flat beyond ω_0. It is described by[1]

$$Z = \frac{R}{\dfrac{s}{\omega_0} + \sqrt{1 + \left(\dfrac{s}{\omega_0}\right)^2}}. \tag{1}$$

For curve B, the amplitude response is flat up to ω_0 and decreases at a 6 db/octave rate beyond ω_0. It is given by[1]

$$Z = \frac{R}{\exp\left(\dfrac{2}{\pi}\displaystyle\int_0^{s/\omega_0} \frac{\arctan x}{x}\, dx\right)}. \tag{2}$$

For curve C, the phase response is linear up to ω_0 and remains at $-\pi/2$ radians beyond ω_0. Here we have[2]

$$Z = \frac{R}{\sqrt{1+\left(\dfrac{s}{\omega_0}\right)^2}\exp\left(\dfrac{s}{\omega_0}\arctan\dfrac{\omega_0}{s}\right)}. \tag{3}$$

For curve D, the phase response is linear up to ω_0, reaching $-\pi/4$ radians, and increases to $-\pi/2$ radians beyond ω_0. Here,[2]

$$Z = \frac{R\sqrt{\epsilon}}{\sqrt{1+\left(\dfrac{s}{\omega_0}\right)^2}\exp\left[\dfrac{1}{2}\left(\dfrac{s}{\omega_0}\arctan\dfrac{\omega_0}{s}+\dfrac{\omega_0}{s}\arctan\dfrac{s}{\omega_0}\right)\right]}. \tag{4}$$

As an application of curves A and B, consider a numerical problem involving a Bode step transition.[1] The system is shown in Fig. 2. Unity transconductance amplifiers are assumed. Three of the interstage networks, Z_{RC}, consist of a 1-farad capacitor in parallel with a 1-ohm resistor. The fourth network, Z_S, is to be synthesized so as to

* Received by the IRE, October 27, 1959. This work was supported in part by the Office of Naval Research under Contract Nonr-839(05).

[1] S. Deutsch, "Synthesis of Infinite Zero-Pole Network Structures," Microwave Res. Inst., Polytechnic Inst. of Brooklyn, N. Y., R-739-59; May, 1959.

[2] S. Deutsch, "A General Class of Maximally-Flat Time Delay Response Ladders," Microwave Res. Inst., Polytechnic Inst. of Brooklyn, N. Y., R-773-59; September, 1959.

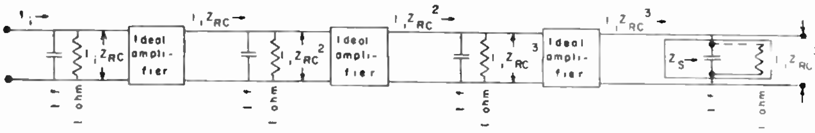

Fig. 2—The system assumed for the step transition of Fig. 3.

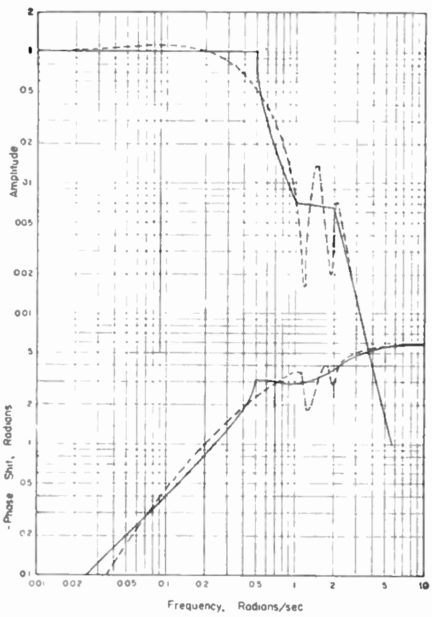

Fig. 3—Amplitude and phase responses of the step transition transfer impedance.

achieve a given system transfer impedance, Z_{TR}. The various impedances are related by $Z_{TR}=Z_{RC}{}^3Z_S$. Two restrictions are imposed on Z_S: the first shunt element must be a 1-farad capacitor, and Z_S must approach 1 ohm as s approaches zero.

The given amplitude and phase responses of Z_{TR} are shown as the solid curves in Fig. 3. From (1) and (2), we can express Z_{TR} analytically as

$$Z_{TR} = \left[\frac{s}{0.5} + \sqrt{1+\left(\frac{s}{0.5}\right)^2}\right]^{-2} \cdot \left[\exp\left(\frac{2}{\pi}\int_0^{s} \frac{\text{arc tan } x}{x}\,dx\right)\right]^2 \cdot \left[\exp\left(\frac{2}{\pi}\int_0^{\pi/2} \frac{\text{arc tan } x}{x}\,dx\right)\right]^{-4}. \quad (5)$$

Since $Z_{RC}=1/(s+1)$, the Z_S driving-point impedance is given by

$$Z_S = Z_{TR}(s+1)^3. \quad (6)$$

When (5) and (6) are combined, the following series expansion is obtained:

$$\frac{1}{Z_S} = s + 0.8197 + \frac{1.961}{s} - \frac{1.698}{s^2} + \frac{0.06414}{s^3} - \frac{1.674}{s^4} + \frac{5.706}{s^5} - \frac{3.960}{s^6} - \frac{2.820}{s^7} - \frac{3.388}{s^8} + \frac{22.93}{s^9} - \frac{10.27}{s^{10}} - \frac{40.41}{s^{11}} + \cdots. \quad (7)$$

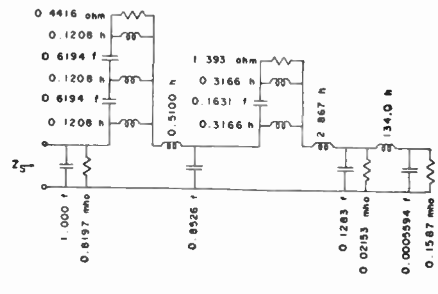

Fig. 4—The shaping network approximation for Fig. 3.

Since (7) is an infinite series, it can be realized only with an infinite number of elements. Fig. 4 shows the corresponding network approximation with 20 elements. The dotted curves in Fig. 3 show the Z_{TR} responses when the network of Fig. 4 is employed. One can approach the desired response to any degree of accuracy by carrying (7) out to additional terms and synthesizing additional elements in the network of Fig. 4.

SID DEUTSCH
Dept of Elec. Engrg.
Microwave Res. Inst.
Polytechnic Inst. of Brooklyn
Brooklyn, N. Y.

The Block Loaded Guide as a Slow Wave Structure*

Fig. 1 shows a square cross-section wave guide cut into two U-shaped parts along the center line of two opposite walls, and loaded with small copper blocks and dielectric. The blocks rest on a bed of polyfoam and lie in a line along the center of the guide. They occupy a region which, in the TE_{10} modes of the empty guide, would contain the maximum electric field. Thus, they constitute a capacitative load, which is still further increased by the strips of dielectric filling the space between them and the guide wall. Individually, the blocks are resonators with fundamental frequencies below the cutoff frequency of the guide; together they form a coupled chain, and act as a slow wave circuit.

The field configuration of the slow wave resembles that of the corresponding TE_{10} wave and is sketched in Fig. 2(b). The group velocity is controlled by the size of the gaps between blocks and side walls, by the nature of the dielectric, and by the spacing between blocks. The first two factors together constitute a loading capacity, and slow the wave in much the same manner as dielectric loading alone. The block spacing determines coupling between resonators, and can be made to give any arbitrary degree of slowing at the cost of a narrower bandwidth. A third mode of propagation, sketched in Fig. 2(d), may be compared with the TM_{11} mode of the empty guide, or with the mode of propagation along a coaxial line. In contrast with the latter, it has a low frequency cutoff, determined principally by the distance between blocks. The cutoff may be lowered by using a dielectric material to separate the blocks, or by placing smaller copper blocks between the large ones, as shown in Fig. 1(b). Both of these are methods of increasing the block to block capacity. In the notation used here, I and II are the slow wave modes analogous to the TE_{10} mode, and III is the mode analogous to the TM_{11} mode. Only one of the slow modes (I) was studied in the model. The other (II) was not provided with any dielectric loading, and was heavily damped by the cut along the guide wall. The magnetic fields of I and II have a component parallel to the length of the guide, and the field of III is mainly transverse.

The dimensions of the test structure are shown in Fig. 1 and correspond to cutoff frequencies in the empty guide of 9.5 kmc for the TE_{10} mode and 13.4 kmc for the TM_{11} mode. Three sizes of block were used—in the first two cases with a quartz dielectric, and in the last case with a stack of mica strips

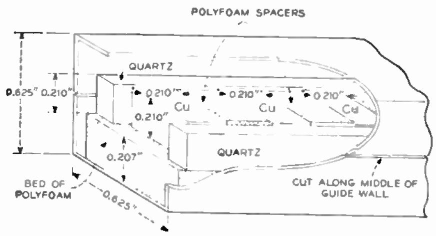

(a)

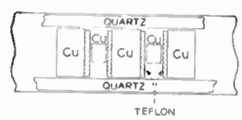

(b)

Fig. 1.

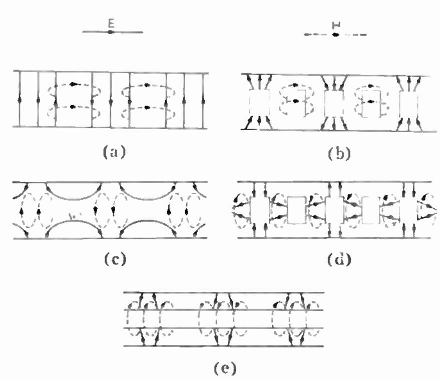

(a) (b) (c) (d) (e)

Fig. 2.

* Received by the IRE, November 25, 1959.

TABLE I

Block size	Capacity gap	Interblock spacing	Slowing factor	Mid-range frequency
0.210 inch×0.210 inch×0.360 inch	42 per cent	0.210 inch 0.420 inch 0.630 inch	4.6 7.0 14	5.5 kmc
0.210 inch×0.210 inch×0.470 inch	25 per cent	0.210 inch 0.420 inch 0.630 inch	6.3 9.5 20	4.5 kmc
0.210 inch×0.210 inch×0.560 inch	10 per cent	0.210 inch 0.420 inch	10 17	3.0 kmc

between the line of blocks and the side walls. Signals were coupled in and out by loops which could be rotated to make tests of the magnetic field direction. Loaded with n blocks, and lightly coupled to a power source and detector, the structure formed a multiply resonant system with n mode I resonances below the cutoff frequencies of the empty guide. In the ideal case, these give points on the dispersion curve of an infinite line;[1] in the model, there were unavoidable end effects, but tests performed, by adding a block at a time and repeating measurements, showed that five or six blocks gave a reasonable approximation. Slowing factors (free space velocity÷group velocity) were estimated by taking the gradient of the dispersion curve at its mid point, *i.e.*, where the blocks form $\frac{1}{4}\lambda$ sections, and where the slowing factor has a stationary minimum value. In most tests, polyfoam spacers were used between neighboring blocks, but some tests were also made with quartz spacers and with the block and teflon arrangement of Fig. 1(b). The principal effect of this change was to increase the block-to-block capacity and to bring mode III down into the mode-I range (where the two types of resonance could be distinguished by rotating the coupling loops). Mode I was hardly affected by altering the block-to-block capacity, although a small reduction in the slowing factor was noted with the Fig. 1(b) arrangement, probably because of additional electrostatic coupling between the resonating sections.

Some slowing factors for different block sizes and spacings are shown in Table I. The mid-range frequencies vary slightly with interblock spacing, and the values given are only approximate. "Capacity gap" denotes twice the distance between a block face and the side wall, expressed as a percentage of the total wall-to-wall distance. Blocks were spaced from the side walls with quartz or mica, and from one another with polyfoam.

At many of the resonances, Q-values in excess of 1000, corresponding to a loss of under $\frac{1}{2}$ db per meter at a slowing factor of 20, were obtained. This low loss is probably explained by the absence of metal-to-metal joins in the structure. It should be possible to obtain larger slowing factors by substituting strips of Al_2O_3 ceramic ($k\sim 10$) or TiO_2 ceramic ($k\sim 80$) for the quartz.

In general, the block and dielectric loaded guide is distinguished by low loss, versatility of design, and ease of construction; and it should be particularly appropriate where strong coupling with the magnetic, rather than with the electric, field is required. It may be noted that, in the test model, the region of strong electric field was filled with material, but the region of strong magnetic field (altogether $\frac{2}{3}$ of the volume) was free. As a traveling-wave maser structure it would have some special advantages. With mode I as the signal and mode III as the pump, the two H fields would be mutually perpendicular, and would overlap in the empty spaces above and below the block and dielectric strip. An external dc field applied at right angles to the length of the guide would be perpendicular to the signal field, and could have various orientations with respect to the pump. The characteristics of modes I and III can be determined with a certain amount of mutual independence, and mode III can be set beyond the mode I range, so that no fraction of the signal is coupled into the incorrect mode. Capacitative loading slows the wave, without a corresponding narrowing of the pass band. It reduces the cross section as well as the length of the structure, thus simplifying the problem of mounting in a strong magnetic field at low temperatures, and also making it possible to obtain a good filling factor, with economy in the amount of paramagnetic material and in the pumping power needed to keep it continually activated.

W. B. Mims
Bell Telephone Labs., Inc.
Murray Hill, N. J.

[1] D. A. Watkins, "Topics in Electromagnetic Theory," John Wiley and Sons, Inc., New York, N. Y., pp. 9–10; 1958.

Reduction of Sidelobe Level and Beamwidth for Receiving Antennas*

In the conventional application of the Dolph-Tchebycheff technique[1] an array of $N+1$, isotropic, in-phase radiators, spaced $\lambda/2$ apart, yields an optimized relationship between the beamwidth and sidelobe level of the antenna pattern, provided the method of combining the signals from the individual elements is the usual simple one. The weighting coefficient for each element is determined by the correspondence required between the antenna pattern $T_N(u)$ (where $u=\sin\theta$ and θ is measured from broadside), and the Tchebycheff polynomial, $T_N(x)$, of degree N.

It will be shown that if a slightly more complicated system behind the antenna is used, then an antenna pattern corresponding to T_{2N} may be obtained *on receive*. Fundamentally, the method consists of utilizing the identity:[2]

$$\frac{1}{2}T_{2N}(x) = \left(T_N(x)+\frac{1}{\sqrt{2}}\right)\left(T_N(x)-\frac{1}{\sqrt{2}}\right). \quad (1)$$

Certain features of this new technique are similar to those used in a scheme[3] for improving two-way patterns.

Fig. 1 shows a schematic drawing for the case of a nineteen-element array. The term $e_1(u, t)$ denotes the RF signal which results when signals are combined from the individual elements in the conventional Dolph-Tchebycheff manner. In addition, the center element is tapped so as to yield two equal RF signals, e_2 and e_3. The three channels are then combined as shown in Fig. 1. The complete expression for the voltage in each branch of the device is given in Table I.

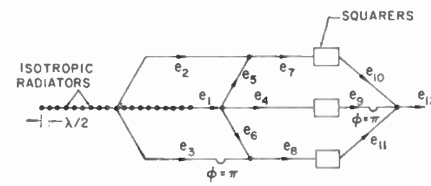

Fig. 1—Diagram illustrating new technique for reduction of sidelobe level and beamwidth for receiving antennas.

TABLE I
VOLTAGE IN EACH BRANCH OF ANTENNA SHOWN IN FIG. 1

$e_1(u,t) = \sqrt{6}\,T_{18}(u)\cos\omega t$

$e_2(u,t) = (1/\sqrt{2})\cos\omega t$

$e_3(u,t) = (1/\sqrt{2})\cos\omega t$

$e_4(u,t) = 2T_{18}(u)\cos\omega t$

$e_5(u,t) = T_{18}(u)\cos\omega t$

$e_6(u,t) = T_{18}(u)\cos\omega t$

$e_7(u,t) \equiv e_5 + e_2 = (T_{18}(u) + 1/\sqrt{2})\cos\omega t$

$e_8(u,t) \equiv e_6 - e_3 = (T_{18}(u) - 1/\sqrt{2})\cos\omega t$

$e_9(u,t) = 4T_{18}^2(u)\cos^2\omega t = 2T_{18}^2(u)(\cos 2\omega t + 1)$

$e_{10}(u,t) = (T_{18}(u) + 1/\sqrt{2})^2\cos^2\omega t = (1/2)(T_{18}^2(u) + \sqrt{2}\,T_{18}(u) + 1/2)(\cos 2\omega t + 1)$

$e_{11}(u,t) = (T_{18}(u) - 1/\sqrt{2})^2\cos^2\omega t = (1/2)(T_{18}^2(u) - \sqrt{2}\,T_{18}(u) + 1/2)(\cos 2\omega t + 1)$

$e_{12}(u,t) = e_{10} + e_{11} - e_9 = (T_{18}^2 - 1/2)(\cos 2\omega t + 1) = (1/2)T_{36}\cos 2\omega t + (1/2)T_{36}$

The output $e_{12}(u, t)$ thus corresponds to a Tchebycheff polynomial of degree 36. In principle either the time-varying or the direct current component of e_{12} may be detected.

* Received by the IRE, November 20, 1959.

[1] C. L. Dolph, "A current distribution for broadside arrays which optimizes the relationship between beam width and side lobe level," PROC. IRE, vol. 34, pp. 345–348; June, 1946.

[2] "Tables of Chebyschev Polynomials $S_n(x)$ and $C_n(x)$," NBS Appl. Math. Ser. 9, U. S. Govt. Printing Office, Washington, D. C.; December, 1952.

[3] R. L. Mattingly, Bell Telephone Labs., Private Communication; July, 1959.

Characteristics of this antenna are compared to those of several conventional arrays in Table II. Because of the lack of a unique basis for comparison of this new technique and the conventional Dolph-Tchebycheff technique, the cases below were computed. The results of the application of this new technique are listed in row one.

TABLE II
PATTERN CHARACTERISTICS

Case No.	Signal Combination Method	No. of Elements	Full Beamwidth	Sidelobe Level
1	New technique	19	10.7°	−19 db
2	Conventional	19	12.0°	−16 db
3	Conventional	19	13.3°	−19 db
4	Conventional	19	10.7°	−12.5 db

If it is required that the new and conventional techniques yield the same beamwidth, then comparison of cases 1 and 4 shows that the new technique yields sidelobes which, theoretically, are better by $6\frac{1}{2}$ db. If the sidelobe level is the primary consideration, then cases 1 and 3 show that the new technique yields a full beamwidth which is better by 2.6°. The set of weighting coefficients for cases 1 and 2 are equal except for the center element. In this last comparison the new technique yields an improvement in full beamwidth of 1.3° and the sidelobe level is improved by 3 db.

These improvements of the conventional Dolph-Tchebycheff pattern are effected at the cost of decreasing the effective one-way range by about 25 per cent. In applications where power is abundant and high discrimination is desired, this new technique could be cascaded with still further improvements in the pattern. For example, the next step in the cascade would make use of the identity:

$$\frac{1}{2}T_{4N} = 4\left[\left(T_N+\frac{1}{\sqrt{2}}\right)\left(T_N-\frac{1}{\sqrt{2}}\right)+\frac{1}{\sqrt{8}}\right]\cdot\left[\left(T_N+\frac{1}{\sqrt{2}}\right)\left(T_N-\frac{1}{\sqrt{2}}\right)-\frac{1}{\sqrt{8}}\right]. \quad (2)$$

A new technique which improves the conventional Dolph-Tchebycheff antenna pattern has been presented. It has been shown that the beamwidth and the sidelobe level may be reduced at the cost of increasing the complexity of the components behind the antenna and by allowing a decrease in the effective range.

The new technique is applicable only for receiving antennas. The nonreciprocity is due to the use of nonlinear detectors as an integral part of the scheme.

OLIVER R. PRICE
Microwave Lab.
Hughes Aircraft Co.
Culver City, Calif.

Contributors

Edward W. Allen (M'44–F'53) was born in Portsmouth, Va., on February 14, 1903. He received the E.E. degree from the University of Virginia, Charlottesville, in 1925, and the LL.B. degree from George Washington University, Washington, D. C., in 1933.

E. W. ALLEN

Joining the Federal Communications Commission in 1935, he became chief of its Technical Research Division in 1946. Since 1951, he has been Chief Engineer of the FCC; and, throughout his association with the Agency, he has been active in the development of technical standards and radio allocations. A member of the Electrical Standards Board of the American Standards Association, he has participated in electrical coordination work for many years.

Mr. Allen is also a member of the national committees of URSI and of the International Electrotechnical Union.

❖

W. L. Behrend (M'48–SM'53) was born on January 11, 1923, in Wisconsin Rapids, Wis. He received the B.S. and M.S. degrees in 1946 and 1947, respectively, both from the University of Wisconsin, Madison.

W. L. BEHREND

From 1944 to 1946, he served as an electronic technician in the U. S. Navy. In 1947, he joined the RCA Laboratories Division, Princeton, N. J., where he is now with the Systems Research Laboratory. He has been associated with the development of antennas, experimental UHF television transmitter, and color television.

Mr. Behrend is a member of Sigma Xi.

❖

Robert M. Bowie (A'34–M'37–SM'43–F'48) was born in Table Rock, Neb., on August 24, 1906. He received the B.S. degree in chemistry, and the M.S. and Ph.D. degrees in physics in 1929, 1931, and 1933, respectively from Iowa State University, Ames.

In 1933, he joined the engineering staff of Hygrade Sylvania Corporation, Emporium, Pa., to do physical research on radio tubes. In 1934, he began the establishment of a physical research laboratory, and in 1935, the laboratory was expanded with principal emphasis on television tube research. In 1939, this laboratory was split into two parts and he continued as head of the Research Department; the other part subsequently became the Picture Tube Division. In 1940, the Research Department undertook fundamental research in electronics and spectroscopy. This work was continued until 1941, when fundamental research was put aside in order that the activities of the staff might be devoted to war research. He was responsible for the establishment of the Physics Laboratory, Sylvania Electric Products Inc., Bayside, N. Y., and in 1944, became Manager of that laboratory. He has held several titles since that date, including that of Director of Engineering from 1951 to 1955, Director of Research from 1955–1958, and Vice-President of the Sylvania Research Laboratories from 1958 to 1959. In 1960, these laboratories became the General Telephone & Electronics Laboratories Incorporated, a subsidiary of General Telephone & Electronics Corporation. Dr. Bowie is Vice-President and General Manager of the Laboratories at Bayside.

R. M. BOWIE

He has made significant contributions to vacuum tube and television research, was chairman of Panel 19 of the National Television Systems Committee and is chairman of Panel 5 on Analysis and Theory of TASO. He has recently been appointed by the Governor of the State of New York to serve on the Advisory Council for the Advancement of Scientific Research and Development in New York State. He is also on the Advisory Committee of the Long Island Graduate Studies and Research Center of the Polytechnic Institute of Brooklyn, Brooklyn, N. Y.

Dr. Bowie is a Fellow of the American Physical Society and a member of Pi Mu Epsilon, Phi Lambda Upsilon, Phi Kappa Phi, Sigma Xi and Alpha Chi Sigma.

❖

Cyril M. Braum (A'30–VA'39–SM'55) was born in Sacred Heart, Minn., on March 21, 1907. He received the B.E.E. degree from the University of Minnesota, Minneapolis, in 1929.

C. M. Braum

From 1929 to 1937, he worked in broadcast and police radio station engineering, and in theater and broadcast station sound equipment installation. He worked with the Federal Communications Commission from 1937 to 1953, in various capacities: as field engineer in Chicago, Ill.; as broadcast engineer in Washington, D. C.; as chief of the FM Broadcast Division in Washington; and as chief of the Television Broadcast Division in Washington. At present, he is engineering consultant for the Joint Council on Educational Television, Washington.

Mr. Braum is a member of the AIEE and the SMPTE.

❖

Charles E. Dean (A'29–M'36–SM'43–F'60) was born in Central, S. C., on May 23, 1898. He received the A.B. degree from Harvard University, Cambridge, Mass., in 1921, and the M.A. degree in physics in 1924 from Columbia University, New York, N. Y. During this period he also worked with the Engineering Department of the Western Electric Company, the predecessor of Bell Telephone Laboratories. He studied physics at The Johns Hopkins University, Baltimore, Md., from 1924 to 1927, and received the Ph.D. degree.

C. E. Dean

He then worked for two years at the headquarters of the American Telephone and Telegraph Company, New York, N. Y. From 1929 to the present, he has been working with the staff of the Hazeltine Research Corporation, Little Neck, N. Y. His work has included various patent studies and writing or editorial activity. During World War II he was responsible for the large volume of instruction books on equipment made by Hazeltine and numerous subcontractors. This work was recognized after the war by the award of a Certificate of Commendation from the U. S. Navy. From 1952 through 1956 he played a large part in the writing and editing of the comprehensive engineering text, "Principles of Color Television," John Wiley and Sons, Inc., New York, N. Y. In 1958 and 1959 he took an active part in the Television Allocations Study Organization, acting as chairman of Panel 6 on "Levels of Picture Quality."

Dr. Dean is a Fellow of the AIEE and the Radio Club of America and a member of SMPTE.

❖

G. L. Fredendall (A'41–SM'46–F'55) was born at Kettle Falls, Wash., on December 20, 1909. He received the Ph.D. degree from the University of Wisconsin, Madison, in 1936. From 1931 to 1936, he taught electrical engineering and mathematics, and engaged in research work in mercury-arc phenomena at the University of Wisconsin.

G. L. Fredendall

Since 1936, he has been with the Radio Corporation of America, working on systems research. At present he is located at the RCA Laboratories, Princeton, N. J.

Dr. Fredendall is a member of Eta Kappa Nu, Tau Beta Pi, and Sigma Xi.

❖

Howard T. Head (A'52–SM'53) was born on December 15, 1919, in Oklahoma City, Okla. He received the B.S. degree from the University of Arkansas, Fayetteville, in 1941.

H. T. Head

Prior to World War II, he was a junior engineer with RCA Laboratories, Camden, N. J. During the war, he held various assignments as a commissioned officer with the Signal Corps Engineering Laboratories. His last assignment was that of Chief of the Technical Staff of the Director of the Signal Corps Radar Laboratory, and he was retired from active service in 1945 with the rank of Major.

Since the war, he has been with the consulting engineering firm of A. D. Ring & Associates, Washington, D. C., in which he is now a partner. He was Chairman of TASO Committee 4.1 (Measurement of Television Service Fields) and Committee 5.4 (Theoretical Studies).

Mr. Head is President of the Association of Federal Communications Consulting Engineers and a member of the AIEE, the SMPTE, the AAAS, Sigma Pi Sigma, Pi Mu Epsilon, Phi Eta Sigma, Omicron Delta Kappa, and Phi Beta Kappa.

❖

W. L. Hughes (S'48–A'50–M'55) was born in Rapid City, S. D., on December 2, 1926. He received the B.S.E.E. degree from South Dakota School of Mines and Technology, Rapid City, in 1949, and the M.S. and Ph.D. degrees in electrical engineering from Iowa State University, Ames, in 1950 and 1952, respectively.

W. L. Hughes

He worked as a transmitter engineer for the Black Hills Broadcast Company of Rapid City, and was active in the engineering development of the Iowa State University television station WOI-TV. He was an Aviation Radio Technician in the Navy during World War II. From 1952 until 1960, he taught in the Iowa State University Electrical Engineering Department and directed research in color television systems and nonlinear circuits in Iowa State's Engineering Experiment Station. In April 1960, he became Professor and Head of the School of Electrical Engineering at Oklahoma State University, Stillwater.

He was active in TASO, being a member of Panels 3 and 6 and Chairman of Committee 3.3, which did most of the field work for Panel 3. He has been a member of the Administrative Committee of the Professional Group on Broadcasting of the IRE for five years and has been Editor of the Group's Transactions for two years. His consulting work has included the subjects of community television systems, subscription television systems, and aircraft collision problems.

Dr. Hughes is a member of the AIEE, SMPTE, and ASEE.

❖

Frank G. Kear (A'24–M'31–SM'43–F'53) was born in Minersville, Pa., on October 18, 1903. He received the E.E. degree from Lehigh University, Bethlehem, Pa., in 1926, and the M.S. and D.Sc. degrees in electrical engineering in 1928 and 1933, respectively, both from the Massachusetts Institute of Technology, Cambridge.

F. G. Kear

He was associated with Dr. V. Bush in 1926–1928 in the development of the product integraph and the differential analyzer. From 1928 to 1933, he was engaged as a physicist in the Aeronautical Radio Group at the National Bureau of Standards. For the next eight years he was Chief Engineer of the Washington Institute of Technology, in charge of development of radio aids to air navigation. Since 1941, he has been a senior partner in the consulting engineering firm of Kear and Kennedy, Washington, D. C. During World War II, he was head of the Radio Section, Electronics Division, Bureau of Aeronautics, U. S. Navy.

Dr. Kear is a member of the SMPTE, the Association of Federal Communications Consulting Engineers, Eta Kappa Nu, Tau Beta Pi, Phi Beta Kappa, and Sigma Xi.

❖

Stephen W. Kershner (A'43–M'55) was born in Texas on February 8, 1918. He received the B.S.E.E. degree from the University of Texas, Austin, in 1939.

S. W. KERSHNER

He was employed for two years by the Texas Pipe Line Company at Houston, and was commissioned in the Signal Corps, U. S. Army, in 1941. During World War II, he was engaged in engineering work on radar equipment in England and later at the Signal Corps Engineering Laboratories, Fort Monmouth, N. J.

In 1945, he was released by the Army with the rank of Major, and since that time has been associated with the consulting firm of A. D. Ring & Associates, Washington, D. C. He has been a partner in the firm since January, 1953.

Mr. Kershner is a member of the American Geophysical Union, the AIEE, Eta Kappa Nu, and is a registered professional engineer of the District of Columbia.

❖

Alfred H. LaGrone (M'48–SM'51) was born in Panola County, Tex., on September 25, 1912. He received the B.S., M.S., and Ph.D. degrees, all from The University of Texas, Austin, and is a registered professional engineer.

A. H. LAGRONE

From 1938 to 1942, he was a distribution engineer with the San Antonio Public Service Co., San Antonio, Tex. From 1942 to 1946, he was on active duty with the U. S. Navy. In 1946, he accepted the position of radio engineer with the Electrical Engineering Research Laboratory at The University of Texas. In 1954, Dr. LaGrone joined the faculty of The University of Texas and is now professor of electrical engineering.

Dr. LaGrone is a member of Sigma Xi, Tau Beta Pi, and Eta Kappa Nu.

❖

Donald C. Livingston (S'51–A'52–M'52–SM'53) was born in Chicago, Ill., on August 13, 1921. He received the Ph.B. degree in physics at the University of Wisconsin, Madison, in 1943. From 1944 to 1946, he worked on the atomic bomb project at the Metallurgical Laboratory, Chicago, Ill., and at the Los Alamos Laboratory, New Mexico. He participated in the Bikini atomic bomb tests in 1946 as a member of the Los Alamos field group.

D. C. LIVINGSTON

He pursued graduate studies in physics at the Ohio State University, Columbus, from 1946 to 1952. In January, 1952, he joined the staff of the Sylvania Research Laboratories at Bayside, N. Y. For the next two years, he worked on various problems relating to the analysis of color television systems and published several papers on that subject. In 1954, he initiated a project concerned with the development of electroluminescent information display devices. He is currently concerned with computer system research.

Mr. Livingston is a member of the American Physical Society and TASO.

❖

Knox McIlwain (A'31–M'40–SM'43–F'48) was born in Philadelphia, Pa., in 1897. He received the B.S. degree from Princeton University, Princeton, N. J. in 1918 and the B.S.E.E. and E.E. degrees from the University of Pennsylvania, Philadelphia, in 1921 and 1928, respectively.

K. MCILWAIN

From 1924 to 1941 he was a professor at the Moore School of Electrical Engineering, University of Pennsylvania. He was associated with the Hazeltine Electronic Corporation, from 1941 to 1957, as Chief Consulting Engineer. He was also previously associated with the Pennsylvania Bell Telephone Company.

Since early 1956, he has been with the Burroughs Corp., Paoli, Pa. As Manager of the Special Products Division, he was responsible for, organized, and directed all engineering development and design projects in the fields of digital communications, weapons systems, air defense instrumentation, airborne control systems, telemetering, and automation. He was formerly assistant to the Vice President of Research and Engineering, where he was responsible at the staff level for all facets of the Corporation's contribution to the Air Force Intercontinental Ballistic Missile Program. He is presently manager of the Great Valley Laboratory, a major division of Burroughs Research Center, conducting the great bulk of the Corporation's military development effort.

Mr. McIlwain is a member of Eta Kappa Nu, Phi Beta Kappa, Sigma Psi, and Tau Beta Pi.

❖

Ogden Prestholdt (S'37–A'41–M'45) was born in Minneapolis, Minn., on April 5, 1917. He received the B.E.E. degree from the University of Minnesota, Minneapolis, in 1938.

O. PRESTHOLDT

For the next year and a half he taught mathematics at the University of Minnesota while continuing his studies in the fields of physics and engineering. From 1944 until the present, he has been employed in the Engineering Department of CBS, New York, N. Y. He is currently Manager, Radio-Frequency Measurements and Analyses, with responsibility for field strength surveys, radio wave propagation studies, and antenna design and performance. He has had more than twenty years of experience in the field strength survey field, including pioneer work on the UHF in 1946. He was an active member of TASO Panels 4 and 5, and made substantial contributions to TASO through work on Committees 3.3, 4.1, 5.1, 5.2, 5.3, and 5.4.

Mr. Prestholdt is a member of Eta Kappa Nu.

❖

Philip L. Rice (M'52) was born in Washington, D. C. on December 25, 1922. He attended Lawrence College, Appleton, Wis., in 1941 and received the B.S. degree from the Principia College, Elsah, Ill., in 1948.

P. L. RICE

During World War II, he was commissioned at the Yale University Air Force Communications School, and spent 18 months in Brazil setting up and operating blind-landing systems for aircraft.

In 1948 and 1949, he was employed by the firm of Raymond M. Wilmotte, Inc., in Washington, D. C. Since that time, he has been a staff member of the Central Radio Propagation Laboratory of the National Bureau of Standards. He is Chief of the Tropospheric Analysis Section of the Radio Propagation Engineering Division at Boulder, Colo.

Mr. Rice is a member of the Institute of Mathematical Statistics and the Scientific Research Society of America.

William O. Swinyard (A'37–M'39–SM'43–F'45) was born in Logan, Utah, on July 17, 1904. He received the Bachelor's degree in mathematics and physics from Utah State University, Logan, in 1927, and has done graduate work at Columbia University, New York, N. Y., and Northwestern University, Evanston, Ill.

W. O. Swinyard

In 1930, he joined the Hazeltine Corporation in Bayside, N. Y.; in 1937 he was transferred to Chicago, where he has been chief engineer of Hazeltine Research, Inc., since 1942 and vice-president and director since 1958. He has published several articles in the field of electrical engineering.

Mr. Swinyard is one of the founders of the National Electronics Conference, and served the NEC as president and chairman of the board. He is a Fellow of the Radio Club of America and the AAAS; a Professional Member of Eta Kappa Nu; and past president of the Chicago Radio Engineers Club. He is a registered professional engineer, and a member of the National Society of Professional Engineers and of the Illinois Society of Professional Engineers. He is Chairman of Panel 2 (Receiving Equipment) of TASO.

❖

Holmes W. Taylor (M'52–SM'59) was born on October 25, 1925, in New York, N. Y. After serving in the U. S. Navy in World War II, he completed his courses at the Massachusetts Institute of Technology, Cambridge, receiving the B.S.E.E. degree in 1948.

H. W. Taylor

From 1948 to 1950, he was employed in the Electronics Division of Sylvania Electric Products, Inc. In 1950, he joined Burroughs Corporation, where he has been involved in the project management of data processing systems. He is currently on a staff assignment with the Great Valley Laboratory of the Burroughs Research Center, Paoli, Pa.

Mr. Taylor is a member of RESA and the Association for Computing Machinery.

❖

Harold G. Towlson (A'39–SM'47) was born in Gouverneur, N. Y. in 1908. He received the B.Sc. degree from Clarkson College of Technology, Potsdam, N. Y. in 1929 and the M.E.E. degree from Syracuse University, Syracuse, N. Y. in 1954.

H. G. Towlson

He joined the General Electric Company, Syracuse, N. Y. in 1929 in the Student Engineering Program, and has since worked for General Electric in various engineering and managerial capacities. These include assignments as Engineer in Charge of the South Schenectady Stations of General Electric, Project Engineer on High-Power AM Transmitters, and Manager of Engineering of the Broadcast Transmitter Section. Since 1957, he has been Manager-Engineering of the Technical Products Operation of Communications Products Department of the General Electric Company.

Mr. Towlson is a member of TASO and the EIA and is a Registered Professional Engineer in New York State.

❖

George R. Town (A'37–SM'44–F'50) was born in Poultney, Vt., on May 26, 1905. He attended Rensselaer Polytechnic Institute, Troy, N. Y. where he received the E.E. degree in 1926, and the D. Eng. degree in 1929.

G. R. Town

He was an engineer in the research laboratory at Leeds and Northrup Company, Philadelphia, Pa., from 1929 until 1933. He then taught for three years at Rensselaer Polytechnic Institute. From 1936 until 1949, he was with the Stromberg-Carlson Company, Rochester, N. Y., where he was successively an engineer in the Research Laboratory, engineer in charge of the Television Laboratory, assistant director of Research, and manager of Engineering and Research. During this time he served actively on the first National Television System Committee and the Radio Technical Planning Board. In 1949, he joined the staff of Iowa State University, Ames, as associate director of the Engineering Experiment Station and professor of electrical engineering. For 20 months in 1956 and 1957, he was on leave of absence and served in Washington as executive director of the Television Allocations Study Organization. Since March 1, 1959, he has been dean of the College of Engineering at Iowa State University.

Dr. Town is a Fellow of the AIEE and a member of the National Society of Professional Engineers, the American Society for Engineering Education, Sigma Xi, Tau Beta Pi, Eta Kappa Nu, and Phi Kappa Phi.

❖

John E. Young (A'37–SM'48) was born in West Chester, Pa., in 1906. He received the B.S.E.E. degree from the Drexel Institute of Technology, Philadelphia, Pa., in 1928.

J. E. Young

On graduating, he joined the General Electric Company, Syracuse, N. Y., in their training course for radio engineers and contributed to the design of the first "Super-power Broadcast Transmitter," rated at 50 kw. He transferred to the Radio Corporation of America, Camden, N. J., in 1932 and participated in the design of the first transmitter job undertaken by the company. Since then, he has been concerned mainly with the design of broadcast transmitters and antennas, successively as a Design Engineer, Group Manager, and Section Manager.

Mr. Young is a member of TASO and the EIA.

Report of the Secretary—1959

To the Board of Directors
The Institute of Radio Engineers, Inc.

Gentlemen:

The Secretary's Report for the year 1959 is transmitted herewith and indicates, again, continued expansion of the IRE in all of its activities.

Net membership increased 11% to a total of 79,166. (See Fig. 1, and Tables I and II.) Professional Group membership increased 20% to a total of 87,027. Publications pages increased 18% and of these, TRANSACTIONS pages went up 44%. Four special issues of the PROCEEDINGS appeared during the year, making possible the publication of additional valuable papers on timely subjects. Sight must not be lost of the important accomplishments of the twenty-five Technical Committees which, assisted by 119 subcommittees and task groups, held 233 meetings and issued four new Standards, in addition to which representation of IRE on 34 committees of the American Standards Association was provided for. IRE also sponsored three committees of this body.

It should be noted that your Headquarters' facilities have been foresightedly expanded suitably to care for this growth and additional steps have been taken for meeting the expected additional activities yet to come.

Respectfully submitted,

Haraden Pratt
Secretary

January 31, 1960

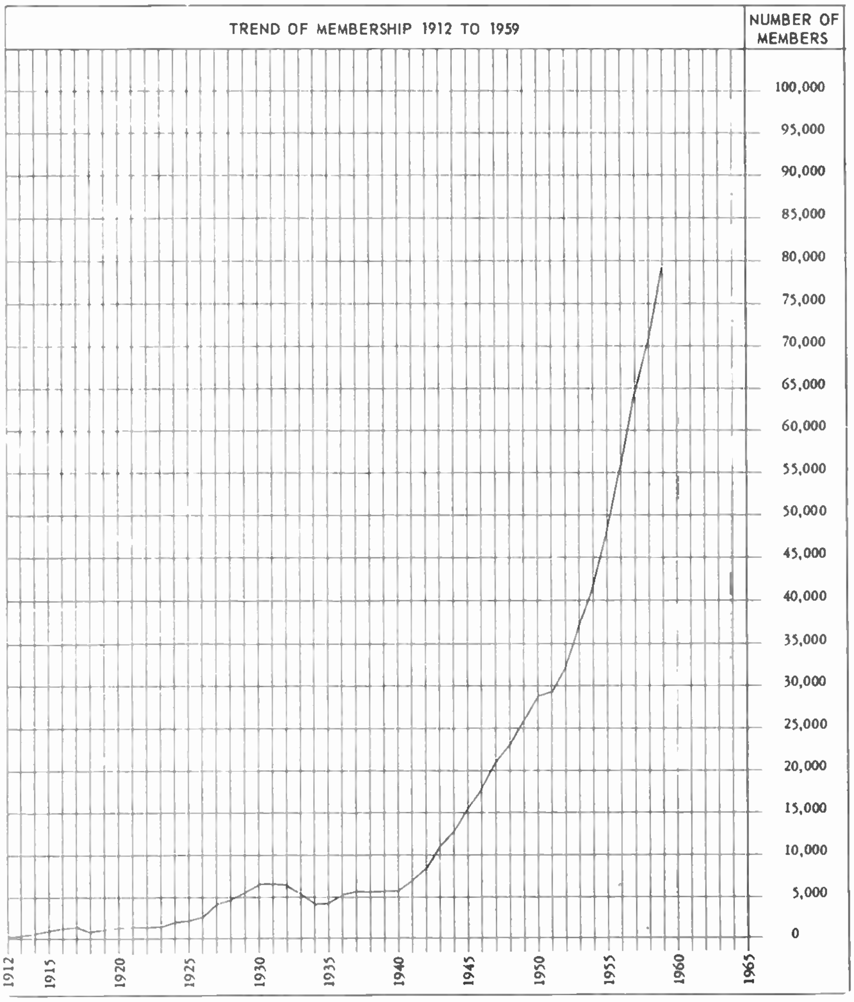

Fig. 1.

Fiscal

A condensed summary of income and expenses for 1959 is shown in Table III, and a balance sheet in Table IV (opposite).

Editorial Department

The year 1959 saw the IRE publication program continue its rapid growth. During the year the IRE published 131 issues totaling 17,968 pages, an 18% increase over 1958. The increased publication output reflected the stepped-up program of PROCEEDINGS special issues and the fact that the Professional Group TRANSACTIONS enjoyed the largest annual growth since their inception eight years ago.

PROCEEDINGS OF THE IRE

The year was highlighted by the appearance of four special issues: "The Nature of the Ionosphere—An IGY Objective" in February, "Government Research" in May, "Infrared Physics and Technology" in September, and "Bio-Medical Electronics" in

TABLE I

COMPARISON OF TOTAL MEMBERSHIP BY GRADES, 1957–1959

Grade	As of Dec. 31, 1959		As of Dec. 31, 1958		As of Dec. 31, 1957	
	Number	% of Total	Number	% of Total	Number	% of Total
Fellow	823	1	770	1.1	700	1.1
Senior Member	9,463	12	8,536	12.0	7,685	11.9
Member	38,977	49	32,373	45.4	26,115	40.3
Associate	13,165	17	14,721	20.6	16,827	25.9
Student	167,938	21	14,961	20.9	13,446	20.8
TOTALS	79,166		71,361		64,773	

TABLE II

FIVE-YEAR ANALYSIS OF MEMBERSHIP IN U. S. AND OTHER COUNTRIES

	1959	1958	1957	1956	1955
TOTAL	79,166	71,361	64,773	55,494	47,388
U. S. and Possessions	73,044	65,786	59,961	51,551	43,977
Other Countries	6,122	5,575	4,812	3,943	3,411
Per Cent Other Countries	7.7	7.8	7.4	7.1	7.2

TABLE III

SUMMARY OF INCOME AND EXPENSE, 1959

Income		
Advertising	$1,597,469	
Member Dues and Convention	1,527,984	
Subscriptions	196,644	
Sales Items, Binders, Emblems, etc.	167,176	
Investment Income	40,676	
Miscellaneous Income	1,559	
TOTAL INCOME		$3,531,508
Expense		
PROCEEDINGS Editorial Pages	$ 540,922	
Advertising Pages	838,505	
Directory	277,172	
Section Rebates	80,147	
Student Program	137,658	
Professional Group Expense	225,737	
Sales Items	71,221	
General Operations	565,805	
Convention Cost	434,266	
TOTAL EXPENSE		$3,171,433
Reserve for Future Operations—Gross		$ 360,075
Depreciation		24,285
Reserve for Future Operations—Net		$ 335,790

TABLE IV

BALANCE SHEET—DECEMBER 31, 1959

Assets		
Cash and Accounts Receivable	$ 718,317	
Inventory	26,656	
TOTAL CURRENT ASSETS		$ 744,973
Investments at Cost	1,830,927	
Buildings and Land at Cost	974,140	
Furniture and Fixtures at Cost	251,519	
Other Assets	75,041	
TOTAL		3,131,627
TOTAL ASSETS		$3,876,600
Liabilities and Surplus		
Accounts Payable	$ 96,371	
TOTAL CURRENT LIABILITIES		$ 96,371
Deferred Income	1,022,280	
Professional Group Funds on Deposit	198,955	1,221,235
TOTAL LIABILITIES		$1,317,606
Reserve for Depreciation	100,939	
Reserve for Publications	30,000	
TOTAL RESERVES		130,939
Surplus Donated	595,287	
Surplus	1,832,768	
TOTAL SURPLUS		2,428,055
TOTAL LIABILITIES AND SURPLUS		$3,876,600

November. The resulting increase in the number of PROCEEDINGS papers from 183 in 1958 to 208 in 1959 was accompanied by an expansion of the Correspondence section from 180 letters to 209 letters. Consequently, the number of editorial pages reached an all-time high of 2370 pages, as shown in Table V and Fig. 2 (next page).

The increase in special issues was largely responsible for the 25% increase in the number of papers reviewed for the PROCEEDINGS, 363 papers totaling 2965 pages. Of these, 38% were accepted, 34% were referred to the TRANSACTIONS for publication considera-tion and 28% were rejected. Three IRE Standards and one Technical Committee Report also appeared during the year.

TRANSACTIONS

The health and vigor of the Professional Groups was unmistakably evidenced by a 44% increase in TRANSACTIONS output during 1959. As shown in Fig. 2 and Table VI, total pages increased from 5388 in 1958 to 7778. The total number of papers and letters published, 1068, for the first time accounted for more than half the total IRE output (1875).

IRE CONVENTION RECORDS

The 1959 IRE NATIONAL CONVENTION RECORD, published in 10 parts, contained 223 papers and 20 abstracts totaling 2116 pages, while the 8-part IRE WESCON CONVENTION RECORD contained 107 papers and 12 abstracts totaling 1008 pages. In an important innovation, the IRE WESCON CONVENTION RECORD was published in time for distribution at WESCON.

IRE STUDENT QUARTERLY

Four issues, totaling 224 pages, were sent free to IRE Student members during the year. In addition, approximately 24,000 free copies of the September issue were distributed to all non-IRE junior and senior electrical engineering students.

IRE DIRECTORY

A new photographic method for reproducing listings from typed cards was adopted for the membership listings in the 1960 IRE DIRECTORY, resulting in a substantial savings in cost. The DIRECTORY, which was published in November, contained 1312 pages including covers, of which 570 were membership listings and information and 742 were advertisements and listings of manufacturers and products.

CONFERENCE PUBLICATIONS

The *Proceedings of the 1959 Western Joint Computer Conference*, sponsored jointly by the IRE, AIEE and Association for Computing Machinery, was published by the IRE Editorial Department. The issue contained 364 pages including covers.

NEW PUBLICATIONS

Work on two new publications was gotten under way in 1959 for issuance during 1960. The first was a five-year cumulative index to all IRE publications which came out during 1954–1958. The second was an *IRE Dictionary of Electronic Terms*, containing all definitions of terms, graphical symbols and abbreviations which have appeared in IRE Standards over the past 15 years.

Technical Activities—1959

Technical Committees

During 1959, 25 Technical Committees and their 119 subcommittees held 233 meetings, of which 222 were held at IRE Headquarters and 11 throughout the nation.

Three IRE Standards and one Technical Committee Report, having been approved by the Standards Committee and the Executive Committee, were published in the PROCEEDINGS in 1959, and reprints are now available to the public.

IRE is directly represented on 34 Committees of the American Standards Association and sponsors three: The ASA Sectional Committee on Radio and Electronic Equipment, C16; the ASA Sectional Committee on Sound Recording, Z57; and the ASA Sectional Committee on Nuclear Instrumentation, N3. Two IRE Standards received approval of the American Standards Association as American Standards in 1959, and are now available overseas through the International Standards Organization.

IRE Technical Committees participated in international standardization in 1959 by reviewing and preparing comments on documents for the United States National Committee of the International Electrotechnical Commission.

Appointed IRE Delegates on Other Bodies

The IRE appointed delegates to a number of other bodies for the one-year period—May 1, 1959, to April 30, 1960 (as listed on page 44A of the October, 1959 PROCEEDINGS).

TABLE V

VOLUME OF PROCEEDINGS PAGES

	1959	1958	1957	1956
Editorial	2370	2199	1868	1996
Advertising	2760	2169	2700	2800
TOTAL	5130	4368	4568	4796

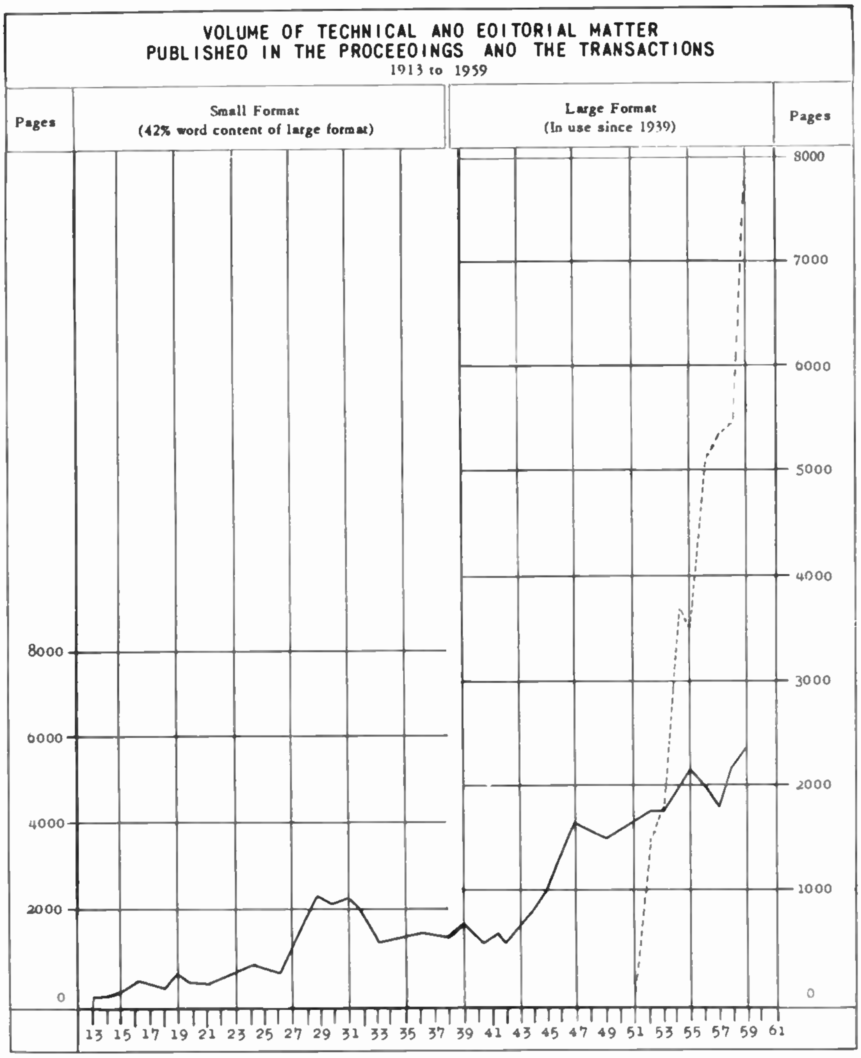

Fig. 2.

TABLE VI

VOLUME OF TRANSACTIONS PAGES

	1959	1958	1957	1956
Groups Publishing	27	26	24	23
No. of Issues	95	81	75	69
No. of Pages	7778	5388	5372	5044

The Annual Spring Meeting of the International Scientific Radio Union (URSI) was held May 5, 6, and 7, 1959, in Washington, D. C. The Fall meeting was held October 19, 20 and 21, 1959, in San Diego, Calif. The IRE Professional Groups on Antennas and Propagation, Circuit Theory, Information Theory, Instrumentation, and Microwave Theory and Techniques cosponsored these meetings. The XIIIth General Assembly of URSI will be held on September 5 through 15, 1960, at the University College of the University of London, London, England.

During 1959, the Executive Committee of the U. S. Preparatory Committee of the International Radio Consultative Committee (CCIR) held five meetings. At these meetings, the representatives of the fourteen Study Groups summarized and reported on their activities. Numerous responses to the questions under review by the Study Groups have been received in IRE during 1959. Lists of all material received from these organizations were distributed quarterly to the Chairmen of IRE Technical Committees and Professional Groups, as well as to The Joint Technical Advisory Committee.

The CCIR IXth Plenary Assembly was held at the Biltmore Hotel, Los Angeles, April 2 to 30, 1959. At this Assembly the United States' proposals were formulated for the International Telecommunication Union (ITU) conference which was held in Geneva beginning August 17, 1959, and ending December 18, 1959.

A report entitled "Radio Transmission by Ionospheric and Tropospheric Scatter," by the Joint Technical Advisory Committee, was circulated to all delegates at the Geneva conference in connection with the proposals being considered to amend the radio, telegraph and telephone regulations and to determine frequency allocations during the periods between international conferences.

The Joint Technical Advisory Committee (JTAC)

The Joint Technical Advisory Committee held a total of ten meetings for the period July 1, 1958, through June 30, 1959. The Eleventh Anniversary dinner was held in May, 1959.

Volume XVI, the cumulative Annual Report of the JTAC Proceedings was published in 1959. This included in Section I—Official Correspondence between the Federal Communications Commission and The Joint Technical Advisory Committee (IRE-EIA). Also included were items of correspondence pertinent to the activities of the JTAC. Section II of the Report contained the approved Minutes of Meetings of The Joint Technical Advisory Committee for the period July 1, 1958, through June 30, 1959.

The JTAC Subcommittee 55.1 on the Study of Forward Scatter Propagation, and its two working groups on Ionospheric Scatter Transmission, and Tropospheric Transmission rendered a report on "Radio Transmission by Ionospheric and Tropospheric Scatter." This was forwarded in preprint form to all delegates attending the CCIR Plenary conferences. This report will be published in the January, 1960, issue of the PROCEEDINGS OF THE IRE.

The International Electrotechnical Commission (IEC)

The International Electrotechnical Commission Subcommittee 12-1 on Measurements met in Ulm, Germany, from October 3 to 9, 1959. IRE secured the services of a delegate to represent the United States, and the IRE Technical Committees prepared this delegate on all items to be discussed at this meeting.

The annual meeting of the International Electrotechnical Commission was held in Madrid, Spain, June 30 to July 10, 1959. IRE did not actively participate in these meetings, since there were no meetings of IEC Technical Committee 12 on Radio Communication, or Technical Subcommittee 12-1 on Measurements scheduled at this time.

A list of all documents and material received in the Office of the IRE Technical Secretary from the IEC was distributed to the Chairmen of all Professional Groups, Technical Committees and Subcommittees.

Professional Group System

General: There are currently 28 Professional Groups operating actively within the IRE.

Approximately 65% of all IRE members have taken advantage of the Professional

Group System which now has a total membership of 87,027. Included are 5667 Student members of the IRE who have joined the Groups at the special Student member rate of $1.00 annually. Under the newly instituted Affiliate Plan, 421 scientists and medical doctors, whose major interests lie in fields other than electronics, have affiliated with a number of the Professional Groups.

All of the Groups have levied publications fees and their members are receiving the pertinent Group TRANSACTIONS regularly. In addition, a large number of company, university and public libraries have subscribed to the TRANSACTIONS of all the Groups. There is also a demand for individual Group subscriptions and individual copies of the TRANSACTIONS from outside sources.

Financial and editorial assistance were among the many services rendered by Headquarters to the Groups during 1959. The Office of the Technical Secretary provided administrative services for Group operations, the planning of meetings, advance publicity and the recording and mailing for all activities, including 838 mailings to Group members during the year.

Symposia: The procurement of papers and actual management of national symposia are entirely in the hands of the Professional Groups. Each of the Groups sponsored one or more technical meetings during this year, in addition to Technical Sessions at the IRE International Convention, the WESCON, The National Electronics Conference and other jointly sponsored meetings, for a total of 50 meetings of national import in 1959.

Publications: During the year, 27 Groups published 95 TRANSACTIONS containing 7778 pages. Since publication began in 1951, 487 issues (33,870 pages) have appeared. Full details on Group TRANSACTIONS are included in the Report of the Editorial Department.

Professional Group Chapters: 263 Professional Group Chapters have been organized by Group members in 58 IRE Sections. Chapter growth is continuing at a healthy rate. The Chapters are meeting regularly and sponsoring meetings in the fields of interest of their associated Groups in the various Sections.

Section Activities

We were glad to welcome five new Sections into the IRE during the past year. They are as follows: Benelux, Gainesville (formerly Subsection), India, Italy, and Orlando (formerly part of Central Florida Section).

The total number of Sections is now 105.

The Subsections of Sections now total 27, the following being formed in 1959: Reading (Philadelphia).

The following Subsections were dissolved in 1959: Palo Alto (San Francisco) and USAFIT (Dayton).

A growing major activity of many Sections and the larger Subsections in recent years is the publication of a local monthly Bulletin to fulfill the need for announcing to the Section members the increasing activities of the Section, including 1) Section meetings, 2) Professional Group Chapter meetings, and 3) Information on the local and national level of interest to the Section member.

Forty-eight of the Sections and Subsections are now issuing monthly publications.

Student Branches, 1959

The number of Student Branches formed during 1959 was 15. The total number of Student Branches is now 183, 118 of which operate as joint IRE-AIEE Branches and 15 as Student Associate Branches.

Following is a list of the Student Branches formed during the year: Air Force Institute of Technology, University of Alaska, University of Bridgeport, Devry Technical Institute, Duke University, University of Idaho, LaSalle College, University of Manitoba, Milwaukee School of Engineering, Mohawk Valley Technical Institute, New Bedford Institute of Technology, Northrop Institute of Technology, University of Puerto Rico, Royal Military College of Canada, San Jose State College (re-established), University of Tennessee (re-established), and West Virginia Institute of Technology.

IRE International Convention

The IRE Board of Directors, when discussing the IRE international activities in 1959, approved a change in name of the annual IRE Convention to "IRE International Convention and Radio Engineering Show." The 1959 Convention, held on March 23–26 at the Waldorf-Astoria Hotel and New York Coliseum, offered a program of 263 papers and 1200 exhibit units. A record total of 60,050 attended. This Convention continues to increase in importance each year and is internationally recognized as one of the largest conventions of its kind in the world.

It is with deep regret that this office records the death of the following members of the IRE during the year 1959.

Fellows

Goldup, Thomas E. (SM'52, F'52)
Morlock, William J. (A'43, SM'46, F'57)
Parker, Henry W. (SM'48, F'52)
Quarles, Donald A. (M'41, SM'43, F'54)
Ridenour, Louis N., Jr. (SM'52, F'55)
Van Der Pol, Balthasar (M'20, F'29, L'55)
Varian, Russell H. (A'40, SM'51, F'52)
Wheeler, Lynde P. (F'28)
Zenneck, Jonathan (F'48, L'56)

Senior Members

Allen, Donald H. (M'53, SM'54)
Beasley, William A. (A'44, SM'49)
Binns, John R. (A'26, SM'54)
Brady, John B. (A'20, M'29, SM'43)
Brown, James F. (SM'50)
Cater, John R. (S'41, A'44, M'52, SM'57)
Crossley, Alfred (A'19, M'26, SM'43, L'57)
Doane, John E. (A'41, M'44, SM'54)
Ebers, J. James (S'46, A'48, SM'53)
Friend, Halton H. (A'28, M'38, SM'43)
Given, Frederick J. (SM'49)
Guthrie, Frederick P. (A'16, M'28, SM'43, L'56)
Heiser, Edwin S. (A'28, SM'44)
Hoyler, C. N. (A'35, SM'45)
Jenssen, Matz (SM'55)
Kaulback, Harold D. (A'58, SM'59)
Kent, Roscoe (A'48, M'50, SM'50)
Kesgen, Edward W. (A'49, M'51, SM'58)
Lee, Emery H. I. (J'15, A'18, M'23, SM'43)
Lovejoy, Edwin W. (A'14, M'26, SM'43)
Maggio, John B. (M'42, SM'43)
Morse, Elwood K. (SM'58)
Nathan, Reuben (SM'54)
Peay, Lawrence W., Jr. (A'41, M'47, SM'55)
Ruth, Edward A., III (SM'52)
Sands, William F. (A'41, SM'46)
Stuckert, E. Morris (A'30, SM'47)
Tarboux, Joseph G. (SM'54)
Waldorf, S. K. (A'41, SM'45)
Waller, Bennie F. (SM'56)
Watson, Edward F. (M'45, SM'45)
Webb, James S. (A'17, SM'46, L'59)
Weedfall, W. W. (A'44, SM'58)
Wesser, C. H. (A'41, M'42, SM'43)

Members

Anders, Russell D. (A'43, M'55)
Atwood, William M. (S'58, M'59)
Barr, Ely E. (S'57, M'58)
Baruch, Sydney N. (A'44, M'55)
Baumbach, Earl J. (M'57)
Berman, Arnold D. (M'58)
Buck, Dudley A. (M'56)
Burns, John A. N. (M'58)
Canfield, Herbert H. (S'52, A'54, M'58)
Carlson, Harry A. (A'56, M'57)
Clanton, James D., Jr., (S'52, A'53, M'58)
Cox, Lemuel H. (M'47)
Croson, H. Lee (M'58)
Durham, Leland G. (S'45, A'50, M'55)
Ellsworth, John L. (S'52, M'56)
Frear, George C. (A'45, M'55)
Goldstein, William (A'52, M'58)
Gontermann, Adolf (M'56)
Green, Darrell B. (A'29, M'55)
Grimmett, Leonard J. (S'50, A'51, M'56)
Gyllstrom, Nylan D. (S'56, M'59)
Hamilton, Edwin E. (S'47, A'51, M'56)
Henderson, J. Alvin (A'50, M'58)
Hilson, Edward A. (M'57)
Hylkema, Chester G. (S'41, A'41, M'55)
Johnson, Marian S. (A'46, M'55)
Johnston, Edward L. (A'36, M'55)
Kleinberger, Robert (A'52, M'56)
Maring, Keith T. (M'54)
Marriner, Alfred W. (A'29, M'55)
Marsal, Paul A. (A'46, M'46)
Mathery, Lowell E. (S'49, A'51, M'58)
Meeker, Robert H. (M'57)
Morganstern, Richard I. (S'53, M'56)
Myers, Joseph R. (M'57)
Olson, Arthur J. (M'55)
Ossmann, Edward A. (A'45, M'55)
Poarch, M. F. (A'43, S'46, A'49, M'55)
Powers, Stephen J. (M'51)
Rappaport, Maurice B. (A'32, M'55)
Reber, John H. (S'47, A'49, M'55)
Robinson, Gordon D. (A'19, M'55, L'57)
Rothe, Mervyn E., Jr. (S'52, A'54, M'59)
Ruggi, Anthony G. (A'50, M'55)
Shortley, W. M. (A'42, M'55)
Sinclair, George W. (M'57)
Stein, Sidney (S'56, M'57)
Sutherlin, Robert F. (A'51, M'56)
Tweet, Ben O., Jr. (S'54, M'56)
Van Every, Bliss (A'46, M'58)
Walsh, Dorothy (S'51, A'52, M'57)
Welker, John J. (A'44, M'55)
Whiston, Raleigh W. (M'50)
Whittier, R. J. E. (M'54)
Wright, Robert A. (S'54, M'56)

Voting Associates

Coates, Archie L (A'35, VA'39)
Packman, M. E. (A'13, VA'39, L'51)
Ross, Kenneth B. (A'28, VA'39)

Associates

Allen, Harold A. (A'58)
Bolman, John G. (A'57)
Brown, Stanley F. (S'56, A'57)
Field, Charles (A'57)
Fitzgerald, Maurice W. (A'50)
Fogarty, Leonard L. (S'52, A'54)
Frankel, Samuel K. (A'56)
Hinrichs, Clair A. (A'54)
Kimes, Richard E. (S'49, A'51)
Nelson, Donald A. (A'44)
Phelps, Boyd (A'21)
Pierson, George E. (A'55)
Powers, Meredith L. (A'57)
Sheets, George (A'55)
Silvia, Everett R. (S'53, A'55)
Sonnenfield, Sigmund (A'57)
Spaeth, Charles A. (A'56)
Stewart, Edward A. (A'53)
Sussman, Albert B. (A'56)
Stinson, Lawrence W. (A'29)
Wetling, Thomas C., Jr., (A'58)

Students

Curti, Dino L. (S'56)
Frederickson, Albert L. (S'58)
Gardner, Jerry D. (S'58)
Morgan, Edgar W., Jr. (S'58)
Rosenbaum, Stanley H. (S'58)
Simmonds, Paul R. (S'57)
Tew, Loma O. (S'57)
Wakefield, Robert P. (S'58)

Books

Transistor Circuits, by K. W. Cattermole

Published (1959) by the Macmillan Co., 60 Fifth Ave., N. Y. 11, N. Y. 399 pages+8 index pages+9 bibliography pages+26 appendix pages+xi pages. Illus. 5¾×8¾. $14.00.

The preface states that "this book gives an introductory account of the principal functions and circuit arrangements in which transistors can be used . . . its ideal reader is primarily interested in some field of usage; he is familiar with thermionic valves and electric circuits in general, but need have no more physics and mathematics than is normally consequent on that knowledge."

The first portion of the book (Chapters 1–4) discusses, in an elementary fashion, the properties of semiconductors, the manufacture of semiconductor devices, and their electric circuit properties. Chapters 5–7 treat low-frequency amplifiers, including multistage and power amplifiers, with considerable emphasis on feedback. Chapter 8 is devoted to high-frequency parameters and amplifiers with a comparatively detailed treatment of pertinent stability aspects. Tuned and wideband amplifiers are also discussed here, as well as feedback circuits at higher frequencies. Chapter 9 treats bias supplies and stabilization.

Chapters 10–14 deal with nonlinear circuits. Chapter 10 discusses the properties of negative resistances with emphasis on point-contact transistors. Chapters 11–13 cover large-signal transistor properties, bistable circuits, sinusoidal oscillators, pulse and other waveform generation, counting and timing circuits. Chapter 14 deals with transistor nonlinearities and their use in modulators, detectors, converters, automatic gain control circuits, and also discusses the accomplishment of some of these circuit functions by switching processes.

Chapter 15 discusses the measurement of transistor properties. Chapter 16 is entitled "Fields of Application" and surveys the use of transistors and their limitations in sound reproduction, television, radio receivers, telephone and telegraph systems, computers, power supplies and measuring instruments. The various appendixes provide the reader with background in specialized topics, such as linear network analysis, transient response of transistors, saturable magnetic materials, etc.

This British book has several interesting features and certainly adds a new flavor to existing treatments on transistor circuits. The qualitative discussions are often incisive and the circuit analyses generally thorough. Several topics, *e.g.*, feedback, are treated with more emphasis than has been done in other books.

In spite of its merits, this reviewer has reservations about the book. Its principal shortcoming is the lack of tie-in between physical properties on the one hand and circuit design on the other. For example, no attempt is made quantitatively to relate the frequency and bias dependence of transistor circuit properties to physical device parameters. It is therefore not surprising that the discussions on high-frequency equivalent circuits and power amplifier properties should appear at times disjoint. Further shortcomings are: excessive emphasis on point-contact transistors, somewhat ponderous mathematics which could be avoided by appropriate use of matrix algebra, inadequate number of tables which would enable the reader to use the book as a convenient reference, occasional misleading comments, some highly questionable conclusions based on the limitations of transistors available to the author at the time when the book was written, and absence of discussion on dc amplifiers.

In conclusion, this reviewer believes that this book could well be used by the practicing transistor circuit engineer as an *additional* reference volume. Its use as an introduction to transistor circuits, by the student or by the engineer unfamiliar with the subject, appears less attractive.

ARTHUR P. STERN
General Electric Co.
Syracuse, N. Y.

Ferrites, by J. Smit and H. P. J. Wijn

Published (1959) by John Wiley and Sons, Inc., 440 W. Fourth Ave., N. Y. 16, N. Y. 347 pages+5 index pages+17 bibliography pages+xiv pages. Illus. 6×9¼. $10.00.

This is an excellent book dealing with the properties of magnetic oxides, such as ferrites and garnets. Those aspects of the theory of magnetism which are necessary for interpretation of the material properties are clearly described through the use of physical models and examples. Descriptions of numerous measurement techniques are interspersed throughout the text and tend to illustrate the significance of the properties being discussed. The organization and content of this book will make it very useful either as a text or a reference work.

JOHN H. ROWEN
Bell Telephone Labs.
Whippany, N. J.

The Birth of a New Physics, by I. Bernard Cohen

Published (1960) by Doubleday and Company, Inc., 575 Madison Ave., N. Y. 22, N. Y. 190 pages+5 index pages+5 pages guide to further reading. 34 figures. 4¼×7¼. Paperback. $.95.

This book is one of the Science Study Series, a series of paperbacks the primary purpose of which is to provide a survey of physics within the grasp of the young student or the layman.

This particular volume, written by one of America's outstanding science historians, takes the reader through one of the most important chapters in the history of science, the development of Newton's law of universal gravitation and the laws of motion. Through the lives of Copernicus, Galileo, Kepler, and Newton, can be seen the dynamic advance of science, from speculative ideas through careful observations and empirical laws, to the crowning achievement of the synthesis by Newton.

The book is interestingly written, with emphasis on the progression of ideas. It cannot help but give a greater depth of understanding of science to those young students who may not go on in science. To those of us who have become scientists, it should help to fill in a gap which most of us have in our education, namely, a too frequent lack of knowledge of the basic history of science.

C. W. CARNAHAN
Varian Associates
Palo Alto, Calif.

Crystals and Crystal Growing, by Alan Holden and Phylis Singer

Published (1960) by Doubleday and Company, Inc., 575 Madison Ave., N. Y. 22, N. Y. 275 pages+14 index pages+31 appendix pages. 137 figures. 4¼×7¼. $1.45 (paperback).

This book in the Science Study Series—generally aimed at the high school level—has more than routine interest by the originality of its writing, the wealth of illustrations, and the person of its senior author, whose intuition has contributed several piezoelectric and ferroelectric crystals to the electronic art. The book starts out on an elementary level, but develops the important concepts of both classical and X-ray crystallography soundly, including a simple explanation of piezoelectricity. The book will be read with profit by the engineer who has never been exposed to crystallography but uses single crystal materials today. It is most welcome to those who are approached by young people for help in science projects.

HANS JAFFE
Clevite Corp.
Cleveland, Ohio

Linear Circuit Analysis, by B. J. Ley, S. G. Lutz and C. F. Rehberg

Published (1959) by McGraw-Hill Book Co., Inc.' 330 W. 42 St., N. Y. 36, N. Y. 560 pages+7 index pages+xvi pages. Illus. 6¼×9¼. $12.50.

This book is designed for "upper-class or first-year graduate students" as a text for "a course in linear, lumped-constant circuit theory." Most of the book is concerned with the solution of the integro-differential equations which arise in linear circuit analysis. Fourier series and integrals are introduced, and in addition some basic concepts in linear graph theory are used to establish the proof of the number of independent Kirchhoff's equations.

The book contains nine chapters, and opens with definitions of linear circuit elements, Kirchhoff's laws and network terminology. In Chapter 2, the topological proofs of a number of independent KCL and KVL equations and the matrix formulation of node and mesh equations are presented. Apparently the authors have made an effort to present linear graph theory in as easy a way as possible and the authors' aim seems to have been largely accomplished. However, it may be desirable to change some of the definitions. For instance, according to the definition of a node (page 10) a terminal which is common to two or more multiterminal elements, such as tubes and transistors, may not be a node without implying that their equivalent circuits consist only of two-terminal elements.

Chapters 3 and 4 discuss the solutions of linear integro-differential equations with constant coefficients for steady-state and transient analysis of circuits respectively. The chapters include the superposition theorem, phasor diagrams, driving-point admittance functions in terms of the node determinant and its cofactors, the concept of poles and zeros, various numerical methods of finding zeros of polynomials, etc. Chapter 5 contains the analogy between electrical and mechanical circuits. Chapters 6 and 7 present the theory of Fourier series and integrals and their application to circuit analysis. In Chapter 8, the theory and application of the Laplace transformation are discussed. Finally, in the last chapter, the concept of equivalent circuits and the use of Thevenin's and Norton's theorems and the reciprocity theorem are illustrated.

The reviewer feels that

1. Too many subsections with headings, and a number of "theorems" may not deserve the name;
2. The illustrations are wordy and tedious, particularly in the discussion of the number of independent Kirchhoff's equations.

The author's effort to "achieve logical completeness" in the contents of the book should be praised. However, some of the excess verbiage of the book may be eliminated if some more mathematical expressions are adopted. The book may prove useful to a student for the purpose of "first having an introductory treatment of the subject matter, to be followed later by a more advanced treatment which is not just a rehash of the earlier coverage but an extension of the subject matter that probes more deeply into it."

W. H. KIM
Columbia University
New York, N. Y.

Semiconductors, by R. A. Smith

Published (1959) by Cambridge University Press, 32 E. 57 St., N. Y. 22, N. Y. 481 pages+12 index pages+1 appendix page+xvii pages. Illus. 6¼×9¼. $12.50.

This book is one of a rather large number of semiconductor treatises which have appeared within the last few years, one of which, the reader should be aware, was written by the present reviewer. The book by Smith is one of the best of these, and one of the most advanced. It deals primarily with the basic theory of solids, the conduction and other theory of semiconductors, and gives a long and critical survey of the research done all over the world on the properties of the important semiconductors. Semiconductor devices are sketchily treated, entirely in one chapter.

The author, who is in charge of the solid state work at the Great Malvern laboratory of the Royal Radar Establishment in Great Britain, has covered very much the same ground as that covered by the reviewer's book, and by similar books by Spenke, Ehrenburg, and Hannay, with emphasis on the theoretical aspects. Of the 481 pages of text, 318 are taken up by the theoretical discussions before the entrance of 115 pages of discussions of the properties of semiconductors. Devices are covered in 48 pages at the conclusion of the book.

Considering first the coverage of the book in the field of basic semiconductor physics, this reviewer considers the work the best such survey that he has seen. This judgment is from the point of view of the advanced student of the field, and of the research worker. The book is very valuable in bringing up to date (1959) the latest work on band structure, transport theory, properties of silicon and germanium, and the properties of the compound semiconductors in which the author himself has made a first-class reputation. There is a short chapter on measurement techniques.

Considered as a text, this book will serve admirably for a graduate course in semiconductors, although the extent of the mathematical treatments and the extent of the explicit use of quantum mechanical equations and relations will make it appear somewhat too sophisticated for undergraduates. Its primary value, it must be supposed, however, will be as a reference and text for research workers already familiar with the field.

Insofar as this reviewer has had the opportunity to examine the quality of the work in detail, the book is very well done. The style is clear and the text quite understandable. The discussions are heavily documented with references to the original work. This practice, while it detracts somewhat from the clarity of the work as a text, greatly aids the researcher in keeping up with the literature.

Relatively few errors have been uncovered for a work of this size. Surprisingly enough a casual reading has, however, indicated the misspelling of fifteen or more authors' names both in the text and in the index.

In any work of this size covering a wide variety of topics exceptions can be taken to the emphasis given various topics, and to the evaluation of the work of others. On the whole, however, this book is an excellent one, which should take its place as one of the best of the advanced surveys of semiconductors.

W. C. DUNLAP, JR.
Raytheon Company
Waltham 54, Mass.

RECENT BOOKS

Gaynor, Frank, *Concise Dictionary of Science*. Philosophical Library, Inc., 15 E. 40 St., N. Y. 16, N. Y. $10.00

Harris, Lawson P., *Hydromatic Channel Flows*. John Wiley and Sons, Inc., 440 Fourth Ave., N. Y. 16, N. Y. $2.75. Presents analyses for 3 flows of viscous incompressible electrically conducting fluids in high-aspect-ratio rectangular channels subjected to transverse magnetic fields.

Helvey, T. C., *Moon Base—Technical and Psychological Aspects*. John F. Rider Publisher, Inc., 116 W. 14 St., N. Y., N. Y. $1.95. Story of the technical and psychological factors surrounding the first U. S. team of human beings—two men and a woman—to be sent to the moon.

Lurch, E. Norman, *Fundamentals of Electronics*. John Wiley and Sons, Inc., 440 Fourth Ave., N. Y. 16, N. Y. $8.25. An introduction to the field written for non-engineers and technicians.

Mandl, Matthew, *Fundamentals of Electronics*. Prentice-Hall, Inc., 70 Fifth Ave., N. Y. 11, N. Y. $10.60. A comprehensive detailed coverage of elementary principles. Provides a clear, understandable approach to modern developments.

Marton, L., *Advances in Electronics and Electron Physics*, Vol. IX. Academic Press, Inc., 111 Fifth Ave., N. Y. 3, N. Y. $9.00.

Neeteson, P. A., *Vacuum Valves in Pulse Techniques*, 2nd edition. The Macmillan Co., 60 Fifth Ave., N. Y. 11, N. Y. $5.50. Several methods are developed analyzing networks containing vacuum tubes subjected to large, suddenly applied signals.

the tube being treated as a nonlinear network element.

The Radio Amateur's Handbook. The American Radio Relay League, Inc., West Hartford, Conn. $3.50. Written with the needs of the practical amateur in mind, the treatment of radio communication problems is in terms of how-to-do-it rather than abstract discussion.

Read, Oliver and Walter L. Welch, *From Tin Foil to Stereo.* Howard W. Sams and Co., Inc., the Bobbs-Merrill Co., Inc., Indianapolis 6, Inc. $9.95. An illustrated history of the phonograph.

Parker, William Vann and James Clifton Eaves, *Matrices.* The Ronald Press Co., 15 E. 26 St., N. Y. 10, N. Y. $7.50. Written for introductory college courses on the theory of matrices.

Williams, E. J., *Regression Analysis.* John Wiley and Sons, Inc., 440 Fourth Ave., N. Y. 16, N. Y. $7.50. Regression analysis is approached from both theoretical and applied viewpoints, emphasizing the practical problems of interpretation.

Wrigley, Walter and John Hovorka, *Fire Control Principles.* McGraw-Hill Book Co., Inc., 330 W. 42 St., N. Y., N. Y. $10.00. Attempts to resolve the existing multiplicity of viewpoints in the literature by separating the fire control problem from its solution, and the principles from the actual systems.

Scanning the Transactions

International. The importance of communication between engineers in different parts of the world is becoming increasingly evident. A growing number of international organizations are being formed in various technical fields to provide workers in different countries a greater opportunity for direct contact with one another. The IRE, with its recently renamed "International" Convention, its new constitutional provision for a Vice President residing elsewhere than in North America, and its Sections now operating on 5 continents, is itself an organization of rapidly growing international influence. In addition to society-type organizations like the IRE, however, there are a number of important federation-type organizations which have the very specific purpose of promoting scientific and technical progress on an international basis. One of the most recent of these is the International Federation of Automatic Control (IFAC). Founded in 1957, the IFAC is a federation of member organizations from 22 countries, each representing the technical societies interested in automatic control for the country it represents. The United States is represented in the IFAC by the American Automatic Control Council (AACC), and the IRE is represented in the AACC by the Professional Group on Automatic Control. The first major accomplishment of the IFAC is the holding of an international congress on automatic control in Moscow this year. IRE members are certain to hear more and more about the IFAC and the AACC and the important work they are doing during the coming years. (H. Chestnut, "The International Federation of Automatic Control," IRE Trans. on Automatic Control, January, 1960.)

Parametric devices and masers have pretty much hogged the pages of technical journals and books during the past few years, resulting in a great many printed words on these two subjects. The volume of articles has reached a size where a bibliography would be a very useful, if not an indispensable, guide to the literature. One such bibliography has now been published which, because it is annotated, should be doubly valuable. Although restricted to books and periodical articles, it includes no less than 379 references. The bibliography reveals some interesting indications as to the role played by IRE publications in recording, and thus contributing to, the progress of these two important fields. Approximately one-fourth of the existing literature on parametric devices is contained in the pages of the Proceedings. When the Transactions and Convention Records are taken into account, it turns out that the IRE has published 40 per cent of the articles on parametric devices and 20 per cent of the literature on masers. (E. Mount and B. Begg, "Parametric devices and masers: an annotated bibliography," IRE Trans. on Microwave Theory and Techniques, March, 1960.)

Liquid helium is closely identified with the birth of the field of cryogenics. At normal atmospheric pressure, helium liquefies only when reduced to 4.2° K. The successful liquefication of helium has made it possible to cool other materials to temperatures within a few degrees of absolute zero, revealing new phenomena such as superconductivity and resulting in important device developments such as cryotrons and solid-state masers. Although liquid helium is thus best known as a cooling agent for studying the low-temperature properties of other materials, it has some rather startling properties of its own that are worth noting. For example, it is a superfluid. It can flow through narrow channels that are impervious to any other liquid and most gases. Its viscosity is an order of magnitude smaller than that of any gas, so small that it can't be accurately measured. Liquid helium has the remarkable property of being able to creep up the side of its container in apparent defiance of gravity. This can be demonstrated by lowering an empty beaker part way into a bath of liquid helium. A thin film of helium will force its way up the outside of the beaker, over the top and down, siphoning more helium from the bath into the beaker until the level in the beaker is the same as that of the bath. Liquid helium is also the best conductor of heat known to man, conducting a pulse of heat in much the same way that the atmosphere transmits sound. In fact, the transport of heat through liquid helium is often called "second sound." (A. Juster and P. K. Shizume, "Cryogenics—a survey," IRE Trans. on Component Parts, March, 1960.)

More about polar blackouts. In recent years interest in the effects of auroral disturbances on communications has steadily increased until the Argus tests released a transient that is not likely to die out until a body of theoretical and experimental knowledge has accumulated to the point where the pertinent engineering questions have been answered. Adding to the existing data, trials of the Canadian Janet meteor-burst communication system were conducted in an auroral zone circuit during July, 1958 and from early December, 1958 until the middle of April, 1959. Tests performed in the vicinity of 40 megacycles indicated the vulnerability of the system to polar blackout and to excessive error rates with rapidly fluctuating auroral signals. Experimental data on the major blackout in July, 1959 are included. These data were obtained by the interesting technique of measuring the intensity of 30-megacycle cosmic noise emissions from the galaxy during a period when prominent solar flares were observed. The reduction in cosmic noise level which was measured after each solar flare provided data that are very useful in evaluating the increased absorption of VHF radio waves by the ionosphere during polar blackouts. (J. H. Crysdale, "Analysis of the Edmonton-Yellowknife Janet circuit," IRE TRANS. ON COMMUNICATIONS SYSTEMS, March, 1960.)

Vector Algebra. Modern weapons and space control systems operate with inputs, outputs, and disturbances which may be characterized as vector quantities. These systems include devices such as coordinate converters, fire control, and guidance computers, gyroscopic instruments, and inertial navigation systems. One of the difficulties associated with three-dimensional problems is the physical visualization of the operation. This is especially true in dynamic problems where time as well as space is involved. Intuition and simple calculations often lead to the omission of important design factors related to inobvious dynamic coupling between system variables. To reduce these errors, a systematic vector notation may be used which breaks the continuum of motion into a series of static two-dimensional problems, in much the same way that the motion picture camera reduces continuum motion to a series of still pictures. This vector notation is developed and illustrated with several practical design problems in a three-part series of tutorial articles published by the Professional Group on Automatic Control. The first part of the article was published in May, 1959, and the second section discussing vector velocities has now appeared. (A. S. Lange, "Automatic control of three-dimensional vector quantities—Part 2," IRE TRANS. ON AUTOMATIC CONTROL, January, 1960.)

Abstracts of IRE Transactions

The following issues of TRANSACTIONS have recently been published, and are now available from the Institute of Radio Engineers, Inc., 1 East 79th Street, New York 21, N. Y. at the following prices. The contents of each issue and, where available, abstracts of technical papers are given below.

Sponsoring Group	Publication	Group Members	IRE Members	Non-Members*
Antennas and Propagation	AP-8, No. 1	$2.40	$3.60	$7.20
Audio	AU-8, No. 1	.70	1.05	2.10
Automatic Computers	AC-5, No. 1	1.50	2.25	4.50
Communications Systems	CS-8, No. 1	1.85	2.80	5.55
Component Parts	CP-7. No. 1	1.20	1.80	3.60
Electronic Computers	EC-8, No. 4	1.40	2.10	4.20
Information Theory	IT-6, No. 1	1.40	2.10	4.20
Microwave Theory and Techniques	MIT-8, No. 2	2.50	3.75	7.50
Space Electronics and Telemetry	SET-6, No. 1	1.70	2.55	5.10

*** Libraries and colleges may purchase copies at IRE Member rates.**

Antennas and Propagation

VOL. AP-8, NO. 1, JANUARY, 1960

Back Scattering Cross Sections of Cylindrical Wires on Finite Conductivity—E. S. Cassedy and J. Fainberg (p. 1)

The back scattering cross sections of fine wires, taking the effect of finite conductivity into account, have been found. The variational procedure is used to find theoretical expressions for the cross section and it is concluded that the zeroth and the first-order solutions of Tai converge to one another with the addition of loss, in the region of first resonance. For fine copper, platinum and bismuth wires, experimentally determined cross sections agree with the theoretical results calculated from the zero-order solution to within 4 per cent in peak resonant values and 1.5 per cent in bandwidth.

A Multipurpose Radar Target—J. W. Carr (p. 7)

Consideration of methods of simulating a moving target by making a mechanically stationary target appear [to an MTI (Moving Target Indicator)-equipped radar] to be moving resulted in the use of crystals as switching elements in a low-voltage low-energy battery-powered device. Extending the use of these switching elements results in a target that is visible to any polarization. By applying these concepts to composite waveguide structures, a dual-band simulated target head was developed and field tested.

On Uniform and Linearly Tapered Long Yagi Antennas—Dipak L. Sengupta (p. 11)

Traveling-wave analysis of long Yagi antennas is reviewed briefly. The method of designing a Yagi antenna from this viewpoint is discussed and some experimental results are given in order to verify the analysis. A long Yagi antenna, when designed according to the Hansen and Woodyard condition, has a sidelobe ratio of 9.32 db in its radiation pattern, irrespective of the length of the antenna. It is shown that by varying the propagation constant linearly along the length of the antenna, the sidelobe ratio can be improved considerably without sactificing much of the antenna gain. This linear variation of the propagation constant may be obtained by slowly tapering the element lengths and/or element spacings along the length of the antenna. An approximate theory is developed for the linearly tapered long Yagi antenna and it is verified by actual measurements. A comparison between the radiation patterns of the uniform and the tapered long Yagi antennas clearly shows the advantage of tapering.

Design of Circular Apertures for Narrow Bandwidth and Low Sidelobes—T. T. Taylor (p. 17)

This article extends a method of antenna design described in an earlier article by the same author. A family of continuous circular aperture distributions is developed in such a way as to involve only two independent parameters, A, a quantity uniquely related to the design sidelobe level, and n, a number controlling the degree of uniformity of the sidelobes. An asymptotic approach to the condition of uniform sidelobes thus becomes possible. A companion article by Robert Hansen contains aperture distribution tables and examples.

Tables of Taylor Distributions for Circular Aperture Antennas—R. C. Hansen (p. 23)

Tables of the circular aperture distributions described in the preceding paper by Taylor are given. Steps in the design process are illustrated by examples.

High-Frequency Diffraction of Electromagnetic Waves by a Circular Aperture in an Infinite Plane Conducting Screen—S. R. Seshadri and T. T. Wu (p. 27)

The scattering of plane electromagnetic waves of wave number k by a circular aperture of radius a in an infinitely conducting plane screen of zero thickness and infinite extent is considered. In the limit of large ka and at normal incidence, the ratio of the transmission cross section to the geometrical optical value πa^2, is found up to the order $(ka)^{-5/2}$.

High-Frequency Diffraction of Plane Waves by an Infinite Slit for Grazing Incidence—S. R. Seshadri and T. T. Wu (p. 37)

The scattering of plane electromagnetic waves of wave number k by an infinite slit of width $2a$ formed by two perfectly conducting coplanar screens of zero thickness is considered. In the limit of large ka and at grazing incidence, the asymptotic series for the transmission cross section per unit length of the slit is evaluated up to the order $(ka)^{-11/2}$.

The Calculation of Reflector Antenna Polarized Radiation—Louis E. Raburn (p. 43)

A partly analytical process is described for calculating the far-zone patterns of reflector antennas which may have nonlinear polarization. Wave polarization equations are given for a focused but not necessarily symmetrical paraboloid. The process applies for any point-source feed whose radiation characteristics, including wave polarization, are known either by theory or measurements.

Calculated and measured patterns are given for a fan-beam antenna whose reflector is 120 λ high and 30 λ wide. They agree well near the axis and agree qualitatively for off-axis angles of several beamwidths. The sources of errors are discussed.

Maximum Angular Accuracy of Tracking a Radio Star by Lobe Comparison—Roger Manasse (p. 50)

A general expression is derived for the maximum angular accuracy of tracking a radio star by lobe comparison (or monopulse). This angular accuracy depends on the input signal-to-noise ratio, the wavelength, the time-bandwidth product of signal integration, and the effective length of the antenna aperture. The maximum angular accuracy can be obtained, approximately, by performing a simple correlation of odd and even components of the antenna output. Angular accuracy formulas for simple antenna dishes or for interferometers appear as special cases of the general result.

The Appendix discusses the interferometer technique in more detail, and the angular accuracy for the data processing technique used by M. Ryle is compared with that obtained from the optimum processing.

Experimental Studies of Meteor Echoes at 200 mc—J. L. Heritage, *et al.* (p. 57)

The paper describes experimental results of bistatic studies of meteor echoes at 200 mc using a high power source and highly directive antennas. The transmission paths studied ranged from 940 to 1800 km in length and included many off-great-circle paths. Diurnal burst rate curves are given for each path. Median duration of the VHF bursts is compared with theory. For certain paths, duty cycle and Doppler shift data are given. At some sites signals were received from ionization aligned with the Earth's magnetic field.

Scattering by an Infinite Array of Thin Dielectric Sheets—Robert E. Collin (p. 62)

By replacing each dielectric sheet in an infinite array of thin dielectric sheets by an infinitely thin polarization current sheet, a solution for the scattering of plane waves by such an array is obtained. The simplified periodic boundary value problem is rigorously solved by using bilateral Laplace transforms. Numerical results obtained compare favorably with those obtained by the Rayleigh-Ritz method.

Reciprocity Theorems for Electromagnetic Fields Whose Time Dependence is Arbitrary—W. J. Welch (p. 68)

Two reciprocity theorems are derived which are valid for fields whose sources may have arbitrary time dependence. The first theorem involves the electromagnetic potentials, and the second is in terms of the electric and magnetic fields directly. In both cases, it is necessary to make use of the advanced as well as the retarded solutions to Maxwell's equations. Some properties of the theorems are discussed, and, as an application, the second theorem is used to derive a variational expression for scattering of electromagnetic waves from a perfect conductor.

Frequency Scintillations of Satellite Signals Before and After the Argus Experiment—P. R. Arendt (p. 73)

Satellite signals are effected by frequency scintillations in the same manner as radio star emissions. Therefore, the Doppler shift of such signals suffers fluctuations. These alterations are a function of the variations of the electron density distribution along the radio-ray path under observation. The number and the magnitude of these scintillations are used to measure the roughness of the ionosphere (formation of a scintillation index). The paper deals with the alteration of the established scintillation index during a time interval in August and September, 1958, *i.e.*, before, during, and after the well-known Argus experiments. The observations indicate that no long-living ionospheric inhomogeneities were produced within the zones of the ionosphere which could be checked from our ground station.

Antenna Image Quality Evaluation—J. J. Myers **Part I—By an Optical Simulation Method** (p. 78)

An optical simulation method was used to study the effect of aperture illumination on image quality for a high resolution antenna. It was determined that an illumination close to uniform yields the best image, as measured by the similarity of the image to the object when similarity was judged by a group of human observers. The techniques used are described, and the results of the evaluation of a typical class of illuminations are given.

Part II—By a Medical Observer (p. 83)

A digital computer was used as a mechanical observer to evaluate antenna image quality as a function of the aperture illumination for a high resolution antenna. An illumination close to uniform was found to yield an image that was best as measured by the ease with which the mechanical observer was able to analyze the images. A description of the logical design of the observer and the results of applying it to the analysis of a typical class of illuminations are given.

Transmission-Line Missile Antennas—Ronald King, *et al.* (p. 88)

A class of protruding rocket antennas of low silhouette is analyzed in terms of an approximately equivalent circuit that consists of a shunt-driven transmission line terminated in a reactor at each end. Expressions for the currents in the several parts of the circuit are used to determine the Poynting vector and from this the radiation resistance referred to the current in the generator. The reactance is obtained from transmission-line formulas.

Radiation Pattern Synthesis with Sources Located on a Conical Surface—A. Ishimaru and G. Held (p. 91)

This paper presents various methods of synthesizing sources placed on a conical surface to produce a prescribed radiation pattern. The sources considered are a series of electric dipoles placed in free space on the surface of the cone around a set of circumferences. These circumferences are equidistant from each other, and the dipoles are oriented in the circumferential direction with no circumferential variation in intensity and phase.

A successive approximation method is employed to obtain the source function for those sources which are placed in a region where the circumferences measure approximately less than two wavelengths. For sources placed in the region where the circumference is less than approximately $(4/3)\pi$ wavelengths, an expansion formula of the product of the Bessel and exponential functions is employed. When the sources are located far from the cone tip, a method utilizing the maximum points of the Bessel function is used to compute the source function. In considering the beamwidth and the sidelobe level, the Tchebycheff pattern with the tapering effect is employed. Numerical examples are given to illustrate the effectiveness of the methods.

A Slot with Variable Coupling and Its Application to a Linear Array—Raymond Tang (p. 97)

The importance of a waveguide linear array capable of producing many different radiation patterns has led to the development of a slot radiator with variable coupling. An array of such radiators can be used as a laboratory apparatus for the evaluation of aperture distributions, or as a ground-pointing reconnaissance antenna operable at many different altitudes. The slot radiator consists of a longitudinal slot centered in the broad face of a rectangular waveguide. An adjustable iris excites the slot by introducing controlled asymmetry in the waveguide fields. The theory of operation and the characteristics of this variable coupling slot are presented. These characteristics are shown in curves usable for design purposes. A detailed discussion is given of the technique used in determining the range of conductances of this slot. The control of coupling available is demonstrated by measured radiation patterns on a 12-element array in which the conductance values are varied to obtain sidelobe ratios from 10 to 34 db. The method used in obtaining the aperture distributions for these radiation patterns is also presented.

Communication (p. 102)

Contributors (p. 123)

Announcement of IRE-URSI Joint Spring Meeting (p. 126)

Annual Index, 1959 (follows p. 126)

Audio

Vol. AU-8, No. 1,

January/February, 1960

The Editor's Corner—Marvin Camrax (p. 1)

PGA News—J. R. Macdonald (p. 2)

Calibration and Rating of Microphones—William B. Snow (p. 5)

Calibration of a microphone consists of measuring its response to some known characteristic of a sound field under specified conditions. Usually the open circuit voltage for a one-microbar sound pressure is determined. Calibrations in an anechoic chamber give plane wave response, while those in a reverberant room give the response to sound arriving from all directions—at random incidence. Techniques have been developed for measuring response with considerable efficiency. Calibrations can be made with pure tones or with wide-band signals such as noise or warbled tones. Complete calibration includes measurements of directivity and impedance as well as linearity of response. From the calibrations it is possible to calculate ratings which give quick and relatively fair comparisons between microphones. The RETMA Rating is particularly effective for the commercial types with impedance below 200,000 ohms. For small crystal and condenser microphones a statement of the noise threshold is more indicative of true performance capability. Although complete specification of microphone performance requires considerable information, the ratings dispel the main ambiguities in response figures arising from differences in impedance, circuits and test sound pressures.

Stereophonic Projection Console—B. B. Bauer and G. W. Sioles (p. 13)

A system is described for home stereophonic reproduction from a single cabinet by reflection of sound from the room boundaries. The effect is emphasized by using loudspeakers which maintain a uniform cardioid directional pattern over the useful frequency range. The directional properties are obtained with acoustic phase-shift networks.

A Transistorized Stereo Preamplifier and Tone Control Magnetic Cartridges—Alexander B. Bereskin (p. 17)

RIAA equalization with ±4 db bass control and ±8 db treble control have been achieved, along with negligible hum, noise and distortion, in a transistorized stereo preamplifier developed for use with magnetic cartridges. Simple circuit modifications adapt this preamplifier for use with most magnetic cartridges.

Bandwidth Compression by Means of Vocoders—Frank H. Slaymaker (p. 20)

Speech information may be transmitted over a bandwidth one tenth of that required for the original speech if attention is directed toward reproducing the envelope of the power density spectrum rather than the waveform itself. Pitch information can be transmitted independently of the spectrum information and the two sets of signals combined at the receiving end to resynthesize the original speech sounds. In the vocoder the power spectrum is analyzed and synthesized by means of band-pass filters. The energy for the voiced sounds is obtained from an oscillator called a buzz source, and for the fricative consonants the energy is obtained from a white noise source.

Design and Use of *RC* Parallel-*T* Networks—Gifford White (p. 26)

The *RC* parallel-*T* network with a transmission null at f_0 is described and the symmetrical lattice approach to its analysis is outlined, following a notation of Guillemin. The selection of design parameters for various principal applications, with relevant references to published work, is given.

The common applications requiring a response curve symmetrical about f_0, such as the single-frequency notch filter, the ac derivative network and the frequency discriminator are treated. In this class falls the feedback amplifier with a very narrow notch.

The use of the parallel-*T* as a low pass or a high pass is covered briefly, and it is shown how a net of more complexity can be derived to give an improvement in response. Using the symmetrical lattice equations, typical examples are worked out. The resulting networks are usually three *T* nets in parallel, or a triple-*T*. A simple feedback amplifier for obtaining a response equal to an *m*-derived *LC* filter is described as a further solution to the problem.

Typical feedback amplifier circuits giving either one-pole or two-pole response are presented. The detailed analysis of a two-pole *RC* feedback net is given, followed by practical design equations and experimental response data.

The engineering problem of component selection for network stability is discussed, since this is a major consideration in designing satisfactory circuits. Frequently, stability is the only problem not readily solved by the potential user. Temperature compensation techniques are given, together with typical experimental data on temperature errors.

Correspondence (p. 34)

Contributors (p. 35)

Automatic Control

Vol. AC-5, No. 1, January, 1960

Foundations of Control—the Editor (p. 1)

The Issue in Brief (p. 2)

The International Federation of Automatic Control—Harold Chestnut (p. 3)

The initials IFAC, standing for the International Federation of Automatic Control, are appearing more and more in the control systems literature these days. It is appropriate that readers of these Transactions be more fully aware of this organization in which they participate through the IRE's membership in the American Automatic Control Council. What are IFAC's purposes, who are its members, how does it operate, what has it accomplished? Now, after two years of existence for IFAC, these data are better known and have more significance.

Dynamic Programming and Adaptive Processes: Mathematical Foundation—R. Bellman and R. Kalaba (p 5)

In many engineering, economic, biological and statistical control processes, a decision making device is called upon to perform under various conditions of uncertainty regarding underlying physical processes. These conditions range from complete knowledge to total ignorance. As the process unfolds, additional information may become available to the controlling element, which then has the possibility of "learning" to improve its performance based upon experience; *i.e.*, the controlling element may *adapt* itself to its environment.

On a grand scale, situations of this type occur in the development of physical theories through the mutual interplay of experimentation and theory; on a smaller scale they occur in connection with the design of learning servomechanisms and adaptive filters.

The central purpose of this paper is to lay a foundation for the mathematical treatment of broad classes of such *adaptive processes*. This is accomplished through use of the concepts of dynamic programming.

Subsequent papers will be devoted to specific applications in different fields and various theoretical extensions.

The Properties and Methods for Computation of Exponentially-Mapped-Past Statistical Variables—Joseph Otterman (p. 11)

The exponentially-mapped-past (emp) statistical variables represent an approach to the statistical analysis of a process when the interest is focused on the recent behavior of the process. An exponential weighting function decreasing into the past, in the case of continuously observed processes, and a geometric ratio, in the case of discrete data, are utilized. This approach is the simplest from the point of view of ease of computation, and at the same time it possesses the advantage of some simple theoretical relationships, which are discussed. Analog computer circuits and digital computer flow diagrams which serve to compute the exponentially-mapped-past statistical variables are presented.

Generalized Weighting Function and Restricted Stability of a Linear Pulse-Modulated Error Feedback System—William A. Janos (p. 18)

A generalized weighting function is obtained for a linear feedback system with a pulse-modulated error signal. This is expressed in the form of a matrix operator acting on an input vector, the components of which are the first $R-1$ derivatives of the input, where R is the order of the unmodulated closed-loop system. In addition, since the system operator takes the form of a finite dimensional matrix, it has been possible to make and realize more stringent conditions on the transient stability; namely, a preassigned bounded output after a preassigned time.

Although the solution has been obtained generally for nonuniform pulsing, the latter stability investigation has been made only for the uniform case.

Optimization Based on a Square-Error Criterion with an Arbitrary Weighting Function—G. J. Murphy and N. T. Bold (p. 24)

Several important criteria for the performance of communication systems and control systems are reviewed, and a new criterion (the mean-weighted-square-error criterion) is then introduced. This is shown to be a special form of a very general criterion proposed earlier, but to have special significance in that it is a generalization of the familiar mean-square-error criterion.

The minimization of the mean-weighted-square error is treated in detail, and a solution for the optimum physically realizable frequency function of the system is given.

Multiple-Rate Sampled-Data Systems—Lester A. Gimpelson (p. 30)

The characterization of multiple-rate sampled-data systems by the ordinary z-transform of single-rate systems is shown. Single-rate sampling, or impulse modulation, of continuous signals is performed by an impulse modulator, M; the sampled, or "starred," function is described by the z-transform. In an analogous manner, a submultiple-rate modulator is introduced; its presence in a branch allows the passage of every nth pulse, or a train of pulses at a submultiple rate; the nomenclature of single-rate systems is continued through the performance of submultiple-rate "starring" of discrete signals and discrete filters. Table I permits starred expressions to be rewritten as functions of the z-transform in closed form. Techniques are shown for the reduction of discrete, and mixed continuous and discrete systems via flow graphs, so that, after the modulators are removed from the feedback loops, the analysis may proceed by standard methods. Representation of single- and submultiple-rate modulation in the s- and z-planes is used to demonstrate that submultiple-rate modulation of discrete signals is analogous to the impulse modulation of continuous signals.

Automatic Control of Three-Dimensional Vector Quantities—Part 2—A. S. Lange (p. 38)

In Part 1 of this paper a vector algebra was developed using a three-element column matrix to represent the vector, and a three-by-three matrix to represent a vector transformation operator. Problems in spherical trigonometry were analyzed with the use of a position vector, and the design of automatic computers to solve such problems was considered. In Part 2, the angular velocity vector is introduced for the purpose of analyzing and designing geometric stabilization systems.

Root Locus Properties and Sensitivity Relation in Control Systems—Hanoch Ur (p. 57)

The differential properties of root loci including pole sensitivity, angle of slope, and curvature at ordinary and irregular points are investigated in a unified manner. A relation between the sensitivity function and pole sensitivity is established. The sensitivity is shown to determine variations in the transfer function due to large (not only infinitesimal) variations in K. Additional properties of loci which are developed include loci of a variable pole position and the existence of asymptotes for open-loop transfer functions with no poles or zeros at infinity.

The locus is treated as a transformation of a line (the real axis) in the K plane to the s plane, and properties of analytic functions are used to simplify calculations and results. It is shown that the properties obtained can be extended to the general root locus of a noureal K.

Time Lag Systems—A Bibliography—N. H. Choksy (p. 66)

In a recent tissue of IRE Transactions on Automatic Control, Weiss has given an excellent annotated bibliography on the subject of transporation lag. He was kind enough to refer to a previous bibliography which appeared in this author's thesis (his reference number [Ch 5]). Since the latter is not generally available, the bibliography therein is given here. The items which have already appeared in Weiss' listing have been omitted; items which have appeared since the thesis was written have been included.

While most of the items here were found by library searches, acknowledgment must be made to Bellman's bibliographies as a source.

If there are items which have not been mentioned either here or in Weiss' paper, the author of the present paper would appreciate being informed about it by either a complete reference or a copy of the paper (or paper) in question.

A short introduction on the mathematical characterization of time lag systems is given before the bibliography.

Correspondence (p. 71)

Contributors (p. 73)

PGAC News (p. 75)

Communications Systems

Vol. CS-8, No. 1, March, 1960

Frontispiece and Guest Editorial—J. E. Schlaiker (p. 1)

Inverse Ionosphere—George D. Hulst (p. 3)

The distortion introduced into a long-range communication system by unpredictable multipath conditions of the ionosphere is described in this paper. A device to eliminate this particular form of distortion is then described, using a sensing technique, a logical matrix, and a signal restoration network. Since both the multipath model of the ionosphere and the restoration network are linear, the principles of superposition apply to the cascaded combination so that the described technique is generally applicable to all waveforms. Specific restoration networks are described for several typical ionosphere multipath conditions. The effects of white noise upon the correction network and the signal are noted. The inverse instrumentation can be placed in the system either as a restoration network at the receiver or as a pre-distorting network at the transmitter.

Pain-Loss Measuring Techniques and Equipment—J. Polyzou and M. Sassler (p. 9)

The planning of tropospheric scatter communication systems requires precise and reliable knowledge of the path loss. This paper describes the techniques and equipment used to evaluate proposed installations. The equipment operates in the frequency range of 875 to 940 or 1650 to 1950 mc with output powers of 10 or 100 watts. A logarithmic recording system is used which makes possible a dynamic signal recording range of 50 to 100 db. Automatic frequency control is employed to achieve a 300-cps 3-db bandwidth with moderate oscillator stabilities.

Optimum Antenna Height for Ionospheric Scatter Communication—R. G. Merrill (p. 14)

Radiation patterns of elevated antennas over spherical earth for scatter propagation in the lower ionosphere incorporating refraction, parallax, spherical divergence, tropospheric defocusing, and near-horizon diffraction have been used to compute the height gain function resulting from raising and lowering symmetric transmitting and receiving antennas for a fixed path length. This height gain function shows that a broad range of *lower* antenna heights has a gain over that antenna height computed with the same model which places the maximum of the first lobe at the path midpoint. The maximum of this function is defined as the optimum antenna height.

Results from a Three-Hop Tropsopheric Scatter Link in Norway with Parallel Operations on 900 mc and 2200 mc—H. N. Knudtzon and P. E. Gundmanson (p. 20)

A three-hop troposcatter system in Norway with simultaneous operation at 900 mc and 2200 mc is described briefly. From measurements on a 360-km hop in the period October 1957 to June 1958, it is concluded that 1) the monthly amplitude distributions are approximately Gaussian, and the 1-minute amplitude distributions are approximately of the Rayleigh type, 2) the signals are generally considerably stronger (differences up to the order of 10 db) in summer than in winter, 3) the monthly median strength of the 900-mc signals is generally 0–2 db stronger than that of the 2200-mc signals, 4) the foreground conditions may be critical, 5) the 1-minute fade duration distributions are approximately log-normal, 6) there are indications that the normalized 1-minute fade duration distributions are about equal for 900 mc and 2200 mc, 7) considerable reductions in telegraph error rate are effected by increasing orders of diversity reception, 8) the telegraph error rates are equal for 900-mc and 2200-mc signals of equal median strengths, 9) frequency-modulated telegraph multiplex equipment is slightly superior to two-tone telegraph multiplex equipment, when adjusted to equal loadings, 10) antenna radiation diagrams depend critically on local surroundings, such as woods.

Performance of a 640-Mile, 24-Channel UHF-SSB Experimental Communication System—Burt E. Nichols (p. 26)

A mock-up Communication system has been installed between Westford, Massachusetts, and Winston-Salem, North Carolina, providing a 640-mile path as a test circuit to measure performance of a 24-channel UHF-SSB system. The equipment is described, the theoretical performance of the system is given, and the performance of the system as to voice quality and signal-to-noise ratio in a telephone channel and simu ated teletype error count is shown.

Analysis of the Performance of the Edmonton-Yellowknife Janet Circuit—J. H. Crysdale (p. 33)

Trials of the Canadian Janet B system were carried out on an auroral zone circuit during July, 1958, and from early in December, 1958, until the middle of April, 1959. The July, 1958 trials, which were performed at frequencies in the vicinity of 40 mc, revealed the vulnerability of the system to polar blackout at these frequencies and to excessive error rates with rapidly fluctuating auroral signals. The objective of the trials carried out between December, 1958, and April, 1959, was the accumulation of long-term statistical data. The test message and operational procedures were designed to permit detailed analysis with an IBM 650 computer. Some preliminary results are included in this paper. Because of the basic importance of the polar blackout problem, pertinent experimental data concerning the major blackout of July, 1959, are presented and discussed.

Data Transmission Tests on Tropospheric Beyond-the-Horizon Radio System—F. E. Willson and W. A. Runge (p. 40)

This paper presents the results of data transmission tests made on both single-link and multi-link tropospheric beyond-the-horizon radio systems. Tests were made at 750 or 1300 bits per second employing both double sideband AM and FM methods of data modulation. In the single-link tests the data performance was determined for various transmission parameters such as median channel noise, peak channel noise, radio received carrier level, and order of diversity.

Data were satisfactorily transmitted on a 2400-mile circuit consisting of nine different beyond-the-horizon paths and six line-of-sight paths. The FM-type data modulation was notably superior to the AM type.

A Frequency Stepping Scheme for Overcoming the Disastrous Effects of Multipath Distortion on High Frequency FSK Communication Circuits—Arthur R. Schmidt (p. 44)

By changing frequency a small amount after transmission of each signaling element in FSK transmission, it is possible to avoid the mutual interference of the main and multipath propagated signal in a high-frequency communications system. Thus, it is practical to employ four-channel time division multiplex systems under multipath conditions that would otherwise render them useless.

This paper describes an experimental system that was produced by modifying conventional FS keyers and employing standard communications receivers in conjunction with appropriate frequency stepping means and selective filters. Operational performance data on experimental circuits will be discussed.

Transmitter Power Control in Two-Way Communications System—G. S. Axelby and E. F. Osborne (p. 48)

A typical scatter communications loop consists of two sites, each having transmitters and receivers operating simultaneously over a two-way microwave loop. In tropospheric scatter systems, disturbances in the microwave paths produce dynamic fading of RF signal levels at the receivers. To achieve high system reliability the current practice is to continuously transmit high power, adequate to maintain RF reception during the presence of severe fading. This wastes power and creates serious radio interference during favorable propagation periods.

Feedback control is applied to high reliability systems to vary the transmitted power as a function of the fading and consequently 1) to reduce operating cost by conserving transmitted power, and 2) to reduce interference to other radio networks in the area.

Other secondary advantages, including reduction of the dynamic range of received signal strength (which will ease receiver AGC and RF amplifier design), will be apparent to the reader. In order to maintain high system reliability, the automatic control at each site is simultaneous, continuous, and effective for nonreciprocal as well as for reciprocal fading. The system has been referred to as Controlled Carrier Communications.

The Sum of Log-Normal Probability Distributions in Scatter Transmission Systems—Lawrence F. Fenton (p. 57)

The long-term fluctuation of transmission loss in scatter propagation systems has been found to have a logarithmic-normal distribution. In other words, the scatter loss in decibels has Gaussian statistical distribution. Therefore, in many important communication systems (*e.g.*, FM), the noise power of a radio jump, or hop, has log-normal statistical distribution. In a multihop system, the noise power of each hop contributes to the total noise. The resulting noise of the system is therefore the statistical sum of the individual noise distributions.

In multihop scatter systems and others, such as multichannel speech-transmission systems, the sum of several log-normal distributions is needed. No exact so ution to this problem is known. The discussion presents an approximate solution which is satisfactory in most practical cases. For tactical multihop scatter systems, a further approximation is proposed, which reduces significantly the necessary computation. An example of the computation is given.

Intermodulation Distortion and Efficiency Analysis of Multicarrier Repeaters—F. Assadourian (p. 68)

Under suitable conditions a common RF repeater may be used to amplify a number of modulated carriers. The basic limitations are efficiency and intermodulation distortion introduced within the frequency band of any modulated carrier wave by the other modulated carrier waves. Any repeater contains a high-power tube for which the output-input characteristic has nonlinearities that introduce a certain amount of intermodulation distortion. Over the useful range of input levels one usually finds that high efficiency and large distortion occur at high levels and low efficiency and low distortion at low levels. The range of acceptable distortion is determined by the intended application and in turn determines an efficiency range. This paper will obtain relationships between distortion or efficiency and input power for a third-degree nonlinearity. Although similar problems have frequently been treated previously in the literature, it is felt that the present approach offers a fresh point of view.

The following assumptions will be made in the present analysis. It is assumed that the repeater has a bandwidth which accommodates the combined bandwidths of the modulated carriers but is small compared to any frequency within it. For this case the only intermodulation components in the output are of odd order. It is also assumed that the unmodulated carriers are equally spaced within the repeater pass band and have equal levels. Such a spacing should yield pessimistic distortion predictions since it is well known that they can be improved by resorting to suitable unequal spacing. For equal carrier spacing and a large number of channels it turns out that intermodulation distortion is essentially independent of carrier spacing and the exact size of the narrow repeater bandwidth. Another assumption is that the frequency transfer characteristic of the repeater is flat in amplitude and linear in phase over its pass band.

The following basic procedure in the distortion and efficiency analysis of a repeater is set up for any kind of power tube in the repeater. The repeater output-input characteristic is assumed to be known in terms of power levels at any frequency within the repeater pass band. This power characteristic is then converted into an equivalent voltage characteristic in terms of output and input peak voltages and finally into an equivalent "instantaneous" voltage characteristic which is used for multicarrier inputs. The input modulated carriers, which may be PCM-FM, for example, are replaced by two extreme cases. In one case they are replaced by unmodulated single-sideband tones of the same total power as the modulated carriers. In the second case they are replaced by flat Gaussian noise of the same total power. Distortion results for the actual case of modulated carriers should be between the corresponding results for the two extreme cases. It is apparent that the present approach does not depend on a particular type of carrier modulation.

The above type of analysis is made with either "envelope" or "instantaneous" voltage characteristics which can be approximated by odd-order cubic expressions and can be extended to cover higher odd-order approximations. Intermodulation distortion and efficiency predictions are then made in terms of the coefficients of the approximating cubic. The analysis is later applied to a klystron power amplifier. The results are plotted in the form of signal to intermodulation power and efficiency curves vs a "bunching parameter" X and against each other. These results show that, for the case of a multicarrier input, an output signal-to-distortion ratio of around 25 db corresponds to a practical efficiency of around 6 per cent.

Constant-Ratio Code and Automatic-RQ on Transoceanic HF Radio Services—John B. Moore (p. 72)

Historical development of present-day commercial teleprinter services is briefly tabulated according to dates of significant advances. The 7-unit form of basic constant-ratio code is given, and its advantages explained; indicative values of improvement are tabulated. A general description of the Automatic-RQ method and system, rather than specific designs, is given. Commercial application and growth in the international services is illustrated by that of TEX (Overseas Teleprinter Exchange) service. Improvement in error probability and reliability by use of 7-unit ARQ on such services is given in terms of character-transposition probability, net channel speed in words per minute, and practical operating experience.

Contributors (p. 76)

Component Parts

Vol. CP-7, No. 1, March, 1960

Information for Authors (p. 1)
Who's Who in PGCP (p. 2)
Thin Ferromagnetic Films—A. C. Moore (p. 3)

This article gives an account of the work at the Royal Radar Establishment (RRE), Malvern, England, on the preparation and properties of thin ferromagnetic films. The work provides the prospect of a computer store in which a million bits would occupy less than an 18-inch cube, and which would possess a switching time faster than 20 mμsec. The store would be cheap and easily constructed.

New Impregnation for Paper Capacitors—Lorant Borsody (p. 15)

The possibility was examined of improving paper capacitors by the applications of new types of impregnants. The tests proved that the paper capacitors impregnated with the various new impregnants can be improved to such an extent that they are as good as plastic film condensers in stability, heat resistance, and temperature coefficients. In addition, paper capacitors are far smaller than plastic film dielectric capacitors.

The research work undertaken showed that one way to develop the capacitors lies in research into impregnants, especially heat-resisting casting resins.

Cyrogenics—A Survey—A. Juster and P. K. Shizume (p. 26)

This paper outlines the history of man's investigations in the field of low-temperature physics. The properties and uses of liquid helium are given, and some of the phenomena which occur at temperatures near absolute zero are noted. Techniques of low-temperature experimentation are described and some of the applications of superconducting materials discussed.

Contributors (p. 34)

Electronic Computers

Vol. EC-8, No. 4, December, 1959

The Chairman's Column—Richard O. Endres (p. 431)

Transistor Pulse Circuits for 160-MC Clock Rates—W. J. Giguere, *et al.* (p. 432)

This paper consists of two parts. Parts I, by Giguere and Jamison, discusses transistor circuits capable of regenerating 6.25-mμsec, pulses at a 160-mc bit rate. Part II, by Noll, discusses techniques for multiplexing 16 digital signals with a 10-mc clock rate into a single signal with a 160-mc clock rate.

Two methods of performing the regeneration function are presented. One method consists of dc level restoration for recognition of the signal and constant current coincident circuitry for the reconstruction of the pulses. The second method consists of operating on changes in the signal for pulse recognition and the use of a bistable circuit for pulse reconstruction. Timing in the second case is obtained by a constant current coincidence gate.

Parallel-to-serial multiplexing techniques have been developed to combine sixteen parallel 10-mc clock-rate signals into a 160-mc clock-rate pulse train. The sixteen synchronous signals are applied to sixteen AND gates along with a 10-mc narrow gate pulse. The space separations of the resulting regenerated and timed AND gate output pulses is converted to time separation with only a small amount of signal loss. This is done by injecting the pulses at sixteen equally separated points on a broadband delay line. Methods have been developed to reduce spurious responses resulting from multiple reflections on the delay line.

The current mode transistor AND gates are suitable for AND/OR functions for individual 4-mμsec logic. The multiplexer may also be used as a piece of test equipment to generate repetitive 16-bit binary words with a 10-mc frame rate.

A Note on the Number of Internal Variable Assignments for Sequential Switching Circuits—E. J. McCluskey, Jr. and S. H. Unger (p. 439)

An important step in the synthesis of sequential switching circuits is the assignment of binary variable states to represent internal states of the circuit. A formula is derived here which indicates the number of different assignments which can be made for flow tables having a given number of rows. There are only three essentially different assignments possible for a four-row table, and there are 140 for a five-row table.

Synthesis of Minimal-State Machines—Seymour Ginsburg (p. 441)

A technique is presented which yields a minimal-state machine satisfying a given set of behavioral specifications. The machine is constructed in the same manner as has commonly been done in the past in synthesizing a "primitive flow table." This contribution consists, not in describing a new method of synthesizing machines, but in showing that a particular instance of an established methods yields a minimal-state machine. It is shown that the basic synthesis technique may be slightly modified so as to be applicable to obtaining a minimal-state machine which has the stability conditions desired when working with unclocked circuits.

Arithmetic Operations for Digital Computers Using a Modified Reflected Binary Code—Harold M. Lucal (p. 449)

The reflected binary or Gray code has been used chiefly in analog-to-digital conversion devices because its code sequences, representing any two consecutive integral numbers, differ in only one digit. This paper presents a method for performing the arithmetic operations of addition, subtraction, multiplication, and division using a modified reflected binary code.

The modification for integral numbers is essentially the addition of an even parity check bit to the Gray code representation. This facilitates both the arithmetic operations and the detection of errors—in the arithmetic process as well as in transmission.

An adder using this code requires circuitry which is more complex than that of a conventional binary adder by a factor of about two or three. However, the adder can be used also for subtraction with little additional circuitry and without complementation. In applications where reliability requirements justify the extra circuitry needed for arithmetic error detection, the modified reflected binary code may compare favorably with the conventional binary.

Magnetic Fields of Square-Loop Thin Films of Oblate Spheroidal Geometry—H. Chang and A. G. Milnes (p. 458)

Thin films of Ni-Fe alloy may be prepared to be anisotropic and exhibit square-loop M-H characteristics. In films that are single-domained with flux changes involving only rotation of intrinsic magnetization controlled by cross-magnetization fields, very fast switching action can be obtained for storage and logic functions.

Problems of coupling to the flux changes and interaction in an array of such films require study of the magnetic-field distribution. In the treatment given, a circular, single-domain, thin film is represented by a very flat oblate spheroid. The field distribution outside the spheroid is found by assuming that the magnetic properties are characterized by an intrinsic magnetization M, constant in magnitude, but varies in direction depending on field and energy considerations.

Calculation of the field distribution is given for a typical film with diameter to thickness ratio of 10^6. From the regions over which field changes are most significant, conclusions are drawn as to the proper size of sensing loops and spacing to avoid interaction during switching in film arrays.

Electrodeposited Twistor and Bit Wire Components—S. J. Schwartz and J. S. Sallo (p. 465)

Electrodeposition of ferromagnetic materials on wire is a suitable way of producing magnetic storage elements. One form of this element, when placed under suitable torsional strain (*i.e.*, as a twistor), has magnetic properties suitable for memory application. Through research into the electrodeposition process, a new device has been developed which requires no external stressing. This device has been designated as the "bit wire." The materials possess the desirable temperature stability usually associated with ferromagnetic metals and exhibit a high signal-to-noise ratio.

Both linear selection and coincident current memory arrays have been constructed with bit wire and plated twistors. The switching characteristics and drive requirements are similar for both materials. The significant difference lies in the fabricating technique, since the bit wire requires no stressing. Both devices are packaged, since undesired strains can change their properties. This problem has been minimized by plating the bit wire material on semirigid wire or tubing. The tubular structure offers other advantages, since additional sense, drive, or inhibit wiring may be threaded through the tube.

Nondestructive Readout of Metallic-Tape Computer Cores—L. M. Lambert (p. 470)

The subject of this investigation is nondestructive readout of metallic-tape memory cores by the application of a magnetomotive force spatially in quadrature to the direction of remanent flux. A simple method of fabrication is proposed and empirical data for the design of the nondestructive read systems is obtained.

The use of nondestructive readout is not limited to digital computer circuits and no attempt has been made to use this method in any particular application; an experimental shift register was built, however, to test the method in a practical application. The nature of the system permits high-speed low-current-level operation in either digital or analog applications.

Diode-Steered Magnetic-Core Memory—A. Melmed and R. Shevlin (p. 474)

This paper describes techniques which take advantage of word arrangement to make possible large, high-speed magnetic-core memories at moderate cost. Economy is obtained by means of a two-coordinate selection system using diffused junction rectifiers as steering diodes. By taking advantage of the relatively slow recovery time of these rectifiers, automatic rewrite selection is obtained in a similar sense to that provided by a biased switch core. The familiar "inhibit" line is eliminated, reducing the memory array to a two-wire configuration. And finally, the customary core array geometry is rearranged to facilitate winding the digit wire as a balanced twisted-pair transmission line so as to eliminate the effect of post-write disturb.

The Design of a Large Electrostatic Memory—M. Graham, *et al.* (p. 479)

A large, high-speed random-access memory for the Brookhaven "Merlin" digital computer is described. This system employs barrier grid electrostatic storage tubes in a novel configuration yielding improved reliability. Basic design considerations are presented together with a description of circuitry and performance.

Systematic Scaling for Digital Differential Analyzers—Arthur Gill (p. 486)

The usefulness of large-capacity digital differential analyzers (DDA's) is severely hampered by the complexity of the scaling process. The scales needed for programming a DDA have to be compatible with the so-called "equilibrium," "topological," and "boundary" constraints, imposed by the construction of the analyzer and the nature of the problem at hand. Simultaneous trial-and-error satisfaction of all these constraints, to achieve optimal range and accuracy of computation, is practically impossible for any problem involving more than a few integrators. The paper shows how the scaling constraints can be organized in a matrix form, and how optimal scales can be produced in a systematic manner. The proposed scheme, which can be programmed for automatic execution, is adaptable for DDA's operating in conjunction with general-purpose digital computers.

Russian Visit to U. S. Computers—E. M. Zaitzeff and M. M. Astrahan (p. 489)

In April and May, 1959 an exchange of visits by computer experts took place between the U. S. and the U.S.S.R. This article will describe the series of negotiations which led up to this exchange and will also describe the visit of the Russian delegation to America. The visit of the U. S. delegation to Russia will be reported separately in a joint article edited by Willis Ware that will appear in the March, 1960 issue of IRE TRANSACTIONS ON ELECTRONIC COMPUTERS.

Correspondence (p. 498)

Contributors (p. 500)

Abstracts of Current Computer Literature (p. 507)

1959 Index to Abstracts of Current Computer Literature (p. 521)

PGEC News and Notices (p. 533)

SENEWS (p. 533)

Annual Index 1959 (Following p. 534)

Information Theory

VOL. IT-6, NO. 1, MARCH, 1960

Frontispiece—L. A. Zadeh (p. 2)

Editorial—L. A. Zadeh (p. 3)

Optimum System Theory Using a General Bayes Criterion—V. S. Pugachev (p. 4)

An extention of the general method of obtaining an optimum system developed by the author is given to include the case of nonlinear dependence of the observed function on signal parameters. The method affords effective determining of optimum systems designed for the detection and reproduction of signals in the presence of noise using various practically adequate criteria.

Quantizing for Minimum Distortion—Joel Max (p. 7)

This paper discusses the problem of the minimization of the distortion of a signal by a quantizer when the number of output levels of the quantizer is fixed. The distortion is defined as the expected value of some function of the error between the input and the output of the quantizer. Equations are derived for the parameters of a quantizer with minimum distortion. The equations are not soluble without recourse to numerical methods, so an algorithm is developed to simplify their numerical solution. The case of an input signal with normally distributed amplitude and an expected squared error distortion measure is explicitly computed and values of the optimum quantizer parameters are tabulated. The optimization of a quantizer subject to the restriction that both input and output levels be equally spaced is also treated, and appropriate parameters are tabulated for the same case as above.

A Note on *P*-nary Adjacent-Error-Correcting Codes—Bernard Elspas (p. 13)

Binary group codes described by Abramson permit the correction of all single errors and all double errors in adjacent digits, with the use of significantly fewer check digits than codes capable of correcting all double-bit errors.

This note considers the generalization of Abramson's codes to the p-nary case, where a symbol alphabet consisting of the digits 0, 1, $\cdots$, $p-1$ is used for transmission, p being a prime number. Examples of such p-nary codes are given, as well as necessary conditions for their existence. These codes bear the same relation to the p-nary Golay codes as Abramson's codes do to the familiar Hamming codes.

Some as yet unanswered questions are raised, and suggestions for further possible generalizations are given.

Codes for the Correction of "Clustered" Errors—Siegfried H. Reiger (p. 16)

A method is described which permits the systematic construction of codes capable of error-free transmission, provided errors occur in "clusters" of limited duration. The method is valid for error clusters of any prescribed duration. The codes are relatively easy to implement and decoding operations are straightforward. Specific examples are given and applications to teletype transmission are discussed.

A Class of Codes for Signaling on a Noisy Continuous Channel—John L. Kelly, Jr. (p. 22)

A class of codes for continuous channels is described. These are block codes in which the code words can be computed from a much smaller set of generators. It is shown that codes of this type exist which will yield arbitrarily small error rates at any signaling rate below channel capacity. In fact, if the generators are chosen at random, it is shown that the expected error rate obeys a bound established by Shannon for general random codes.

A Bibliography of Information Theory (Communication Theory—Cybernetics) Third Supplement—F. Louis H. M. Stumpers (p. 25)

Correspondence (p. 51)

Contributors (p. 56)

Microwave Theory and Techniques

VOL. MTT-8, NO. 2, MARCH, 1960

Editorial—Harold M. Barlow (p. 131)

Broad-band Coaxial Choked Coupling Design—Howard M. King (p. 132)

Equations and curves are presented to predict the frequency bandwidth of coaxial choke couplings in terms of the choke parameters. Choke couplings discussed are those applicable to rotary joints and dc isolation units.

A Study of Multielement Transmission Lines—Hiroshi Kogo (p. 136)

Although many papers have been published on the subject of multielement transmission lines, the application to practical problems seems rather inconvenient. The author proposes a solution to the general equations which relate the voltage difference between the lines and the mesh current. Under particular conditions, it is shown that only a single type of propagating mode exists. In this case, the solution has been obtained by the so called "decomposition method," *i.e.*, assuming several virtual two element transmission lines in lieu of the existing multielement transmission line. The problem has been solved by means of the resolved superposed virtual lines taking into account the existing boundary condition.

Measurement of Relative Phase Shift at Microwave Frequencies—G. A. Finnila, *et al.* (p. 143)

A method is described for measuring the relative phase shift of microwave devices, such as traveling-wave tubes, which utilizes the serrodyne technique to transfer the measurements into the audio-frequency range. The method is used to measure the phase shift incidental to the variation of the dc potentials applied to the several electrodes of a 2- to 4-kmc traveling-wave tube. This method is particularly useful in coaxial systems, where accurately calibrated phase shifters (and attenuators without phase shift) are not available.

Resonant Modes in Waveguide Windows—M. P. Forrer and E. T. Jaynes (p. 147)

Analysis and experimental verification of a class of resonant fields, called ghost-modes, occurring in waveguide dielectric windows, are presented. Numerical solutions for a simple geometry are given through universal curves. Knowledge about ghost-modes has importance to designers of high-power windows. It also leads to a measuring technique for dielectric constants through a frequency measurement.

Temperature Compensation of Coaxial Cavities—J. R. Cogdell, *et al.* (p. 151)

This paper describes a technique for temperature compensation of coaxial cavities by controlling the capacitance between the end of the center conductor and an end plate across the outer conductor. A formula is derived for this capacitance which is verified experimentally. Supplemental design data are also obtained experimentally.

A Graphical Method for Measuring Dielectric Constants at Microwave Frequencies—Charles B. Sharpe (p. 155)

This paper describes a graphical method for measuring the real and imaginary parts of the dielectric constant $\epsilon/\epsilon_0 = \epsilon' - j\epsilon''$ of materials at microwave frequencies. The method is based on the network approach to dielectric measurements proposed by Oliner and Altschuler in which the dielectric sample fills a section of transmission line or waveguide. In contrast to their method, the network representing the dielectric sample is analyzed in terms of the bilinear transformation

$$\Gamma' = \frac{a\Gamma + b}{c\Gamma + s}; \quad ad - bc = 4.$$

The analysis proceeds from the geometric properties of the image circle in the Γ plane obtained by terminating the output line in a calibrated sliding short.

The technique described retains the desirable features of the network approach but avoids the necessity of measuring both scattering coefficients. As a result the procedure is more direct and, in the case of the TEM configuration, leads to an entirely graphical solution in which the complex dielectric constant can be read from a Smith chart overlay.

Wide-Band Strip-Line Magic-T—E. M. T. Jones (p. 160)

This paper presents theoretical performance calculations of a novel form of wide-band strip-line Magic-T that uses two dual strip-line band-pass filters. When all four ports are terminated in the same impedance, the VSWR at each port is less than 1.47 over a 2:1 frequency band, while the isolation between opposite ports is greater than 20 db over this frequency band.

A General Theorem on an Optimum Stepped Impedance Transformer—Henry T. Riblet (p. 169)

With the assistance of a mathematical theorem demonstrated by Eaton in a companion paper, it is shown rigorously, in the limit of small impedance transformation, that the familiar binomial impedance transformer, consisting of equal quarter-wave steps, is the shortest, monotonic, maximally-flat, stepped, transmission-line transformer having steps commensurate in length with the midband guide-wavelength, and coincident zeros at the mid-band frequency.

It is shown how this theorem places very severe limitations on any effort to improve on the performance of a quarter-wave transformer by increasing the number of its impedance steps without a corresponding increase in its length.

Minimal Positive Polynomials—James E. Eaton (p. 171)

A proof is given of a purely mathematical theorem on the polynomial of lowest degree with positive coefficients having a prescribed root of unity as a multiple root.

H. J. Riblet has conjectured the theorem below. In the preceding paper, he applies his theorem to optimum impedance transformer design.

Complementarity in the Study of Transmission Lines—G. Owyang and R. King (p. 172)

The principle of complementarity is applied to the slot transmission line. The properties of a dual circuit are investigated. The pairs of several possible duals for a given configuration are correlated and new quantities are defined for use with different types of circuits. A complete parallelism between the two-wire line and the two-slot line is established for the ideal cases and is extended by approximation to include the practical cases.

Measurements were made with a two-slot transmission line and its associated probing system. The method of testing the line for balance is discussed. The transverse distribution of the longitudinal current and the attenuation constant were measured.

The analogy between the steady-state field in a conducting medium and the electrostatic field in a dielectric is investigated. The expressions for the constants of a two-slot line are given in a form that permits a ready evaluation from experimental data obtained with the electrolytic tank. The measured results are compared with theoretical values.

High Resolution Millimeter Wave Fabry-Perot Interferometer—William Culshaw (p. 182)

The design and operation of a microwave Fabry-Perot interferometer at wavelengths around 6 mm is described. This uses reflectors which are simple, easy to make, and which are capable of scaling for operation at short wavelengths in the ultramicrowave region. With power reflection coefficients around 0.999, very sharp fringes and Q values around 100,000 were obtained on the interferometer. Effects of diffraction in the interferometer are considered, and wavelength measurements with this particular interferometer indicate that accuracies of 0.04 per cent are obtained without any diffraction correction. Advantages of such an interferometer for ultramicrowaves are that the component parts are large compared with the wavelength, the effects of diffraction decrease with the wavelength, and the problem of maintaining a high Q with a single mode of propagation and a structure of adequate size is made much easier. Such an interferometer forms the cavity resonator for ultramicrowaves. It can thus be used for such conventional purposes as wavelength measurements, wavelength spectral analysis, dielectric constant, and loss measurements, or as the cavity resonator for frequency stabilization, or as the cavity resonator for a millimeter- or submillimeter-wavelength maser.

Boundary Conditions and Ohmic Losses in Conducting Wedges—Robin M. Chisholm (p. 189)

The present work is concerned with the boundary conditions required to calculate the ohmic losses occurring in metallic wedges under the influence of electromagnetic waves which are sinusoidal in time. The validity of the surface impedance condition used in calculating waveguide wall losses is examined carefully, and a "modified" surface impedance condition, which can be applied to wedge problems in which the perfectly conducting solution is known, is developed. A simple waveguide having a circular cross section, a sector of which is occupied by a metal wedge, is used as an example. The tangential magnetic field variations along the surface of the wedge are shown graphically, demonstrating, near the tip of the wedge, a large deviation from the tangential magnetic field of the perfectly conducting solution.

On the Theory of the Ferrite Resonance Isolator—E. Schlomann (p. 199)

The attenuation constants for both directions of propagation in a rectangular waveguide loaded with a small slab of ferrite are calculated by means of perturbation theory. The maximum attainable ratio of reverse to forward attenuation is found to be inversely proportional to the square of the bandwidth, with a constant of proportionality that is dependent on the shape of the ferrite slab and the proximity of cutoff. The figure of merit is largest for the case of a thin ferrite slab magnetized perpendicular to the plane of the slab. It is shown that a significant increase in the figure of merit can be obtained by proper use of the anisotropy of grain-oriented materials or single crystals.

Analysis of Microwave Measurement Techniques by Means of Signal Flow Graphs—J. K. Hunton (p. 206)

Microwave measurement techniques can be analyzed more simply by using signal flow graphs instead of the customary scattering matrices to describe the microwave networks used in the measuring system. This is because the flow graphs of individual networks are simply joined together when the networks are cascaded and the solution for the system can be written down by inspection of the over-all flow graph by application of the nontouching loop rule. This paper reviews the method of setting up flow graphs of microwave networks and the rule for their solution. A single directional-coupler reflectometer system for measuring the reflection coefficient of a load is then analyzed by this method. The analysis shows how auxiliary tuners can be used to cancel residual error terms in the measurement of the magnitude of the reflection coefficient at a particular frequency. The analysis also shows how an additional tuner can be used to measure the phase angle of the reflection coefficient. These reflectometer techniques are particularly useful in the measurement of very small reflections.

Stepped Transformers for Partially Filled Transmission Lines—D. J. Sullivan and D. A. Parkes (p. 212)

In recent years, partially-filled transmission lines have been used to improve the characteristics of various ferrite and garnet devices. This paper presents a generalized outline for determining the approximate effective guide wavelength and characteristic impedance of two types of (dielectric-loaded) partially-filled transmission line. The results are used to determine the geometries required for the design of optimum stepped transmission line transformers. The stepped transitions are designed to yield a Tchebycheff-type response for any given bandwidth. The measured results for stepped transitions in partially filled coaxial line and partially filled double-ridge waveguide are presented. The data are found to approximate the theory closely.

Parametric Diodes in a Maser Phase-Locked Frequency Divider—M. L. Stitch, *et al.* (p. 218)

The use of an ammonia-beam maser in a portable frequency standard requires a frequency divider which can be transistorized. A divider which uses no microwave tubes and hence one that can be transistorized is described. An ammonia-maser-controlled signal generator used to tune up the divider is also described. It is found that the use of a parametric diode frequency multiplier substantially improves the lock-in performance of the divider. Some data are given for comparing the performance of the maser frequency divider with and without the parametric diode frequency multiplier.

Parametric Devices and Masers: An Anno-

Space Electronics and Telemetry

Vol. SET-6, No. 1, March, 1960

Astronomy for the Nonastronomer—Robert R. Newton (p. 1)

Kinematical observations of the solar system have attained an accuracy reached in few other areas of measurement. The adequate description of these observations requires an elaborate and accurate terminology. This paper defines and discusses most of the important terms, coordinate systems, and methods of time reckoning which are used by astronomers in describing the motion of the solar system. No previous background in astronomy on the part of the reader is required. Warning is also given concerning terms whose meanings look obvious, but which in fact do not mean what they seem to.

Energy Spectra of FM System with Low Beta, High Deviation Ratio, and MF Which Approaches Carrier Frequency—Sheldon L. Simmons (p. 17)

A technique was developed at the Naval Air Missile Test Center to determine energy spectra of an FM system which has a low Beta, a high deviation ratio, and a modulation frequency which approaches the carrier frequency. This technique may be used for analysis of any FM wave and yields theoretical results which conform closely to actual operating results.

How Environment Affects Magnetic Recording Tape—Clarence B. Stanley (p. 19)

The increasing emphasis on higher and higher operating and/or storage temperatures for data acquisition apparatus requires a critical appraisal of the behavior of available magnetic recording tapes as their rated operating limits are approached or exceeded.

Among the criteria that bear examination are the dimensional stability, strength and toughness of the substrate, and the chemical stability of the binder and the magnetic material.

Unexpected physical effects can be experienced within the generally accepted "safe" environmental limits. Critical temperatures and observed effects are described.

Threshold Improvement in an FM Subcarrier System—Benn D. Martin (p. 25)

The paper is concerned with the causes and characteristics of threshold behavior in pulse-averaging and phase-coherent ("phase-locked loop") FM subcarrier discriminators. An analytical discussion of the basic elements of each form of discriminator is first presented, leading to a comparison of the devices for input modulation indexes of one and five, in the presence of noise. For the first time in the literature, the effect of additional output filtering following the ideal phase-coherent loop is discussed. Finally, the requisite modulation characteristics for an improved threshold in a phase-locked loop discriminator are presented, followed by a brief description of the approaches which may be taken in the design of such a system.

The Astronautic Chart—Roy C. Spencer (p. 34)

The Astronautic chart is a nomograph or alignment chart so arranged that a single straight line marks off values of the velocity, mass, mean distance, period, and acceleration of any two-body orbiting system. It is illustrated with numerous examples of orbits of planets about the sun, moons about their planets, and artificial earth satellites.

All scales give correct values at the extremities of the minor diameter of the elliptical orbit. In the case of binary stars where the masses are comparable, the scales also give correct values of the *total mass, total separation, relative velocity*, and *relative acceleration*.

A Versatile PAM/PDM Decommuntation Station—J. A. Adams and W. T. Johnson (p. 38)

The growing complexity of data-handling systems and the need for less complicated and smaller decommutation devices led to the development of the PAM/PDM decommutation station shown in Fig. 1. The PAM/PDM data-handling capability of this station is 100 channels and, for the system shown, the utilized panel space is $26\frac{1}{4}$ inches.

The Navy's Portable Satellite Tracking Stations—F. M. Ashbrok and D. D. Stevenson (p. 41)

The stations described recover Doppler frequencies to an accuracy of one part in 10^9 and subcarrier oscillator frequencies to 15 kc bandwidths. Coherent phase detection and a tracking local oscillator to minimize required reception bandwidth maximizes signal sensitivity. Station portability accommodates rapid changes of location as dictated by satellite projects and the flexibility of the receiving and recording equipment due to unitized construction permits inexpensive modifications to accommodate present and future satellite programs.

Ground Antenna for Space Communication System—K. W. Linnes, *et al.* (p. 45)

The accurate tracking and telemetering of space probes requires the use of very sensitive receiving equipment and large antennas. The TRAC(E) system developed by the Jet Propulsion Laboratory utilizes an 85-foot-diameter, equatorially mounted, parabolic reflector. The antenna, similar to those used for radio astronomy, is located near Goldstone Lake near Barstow, Calif. The mechanical and electrical characteristics of the antenna and its subsystems are discussed, and its performance and the way it was used in tracking the lunar probe Pioneer IV are described. Limitations imposed on the space communication system by the ground antenna are discussed, and possible methods of improvement are listed.

Problems in Space Exploration—Robert Jastrow (p. 55)

IRIG, Inter-Range Instrumentation Group—History, Functions and Status, 1959—Beuhring W. Pike (p. 59)

The Inter-Range Instrumentation Group (IRIG) was established in 1952 by the commanders of the United States guided missile test ranges, principally for the purpose of facilitating the interchange of information on range instrumentation. Today, the IRIG consists of a Steering Committee and ten Technical Working Groups. Among other activities, the IRIG prepares and disseminates recommended standards and other documents (such as glossaries of terms and catalogs of range instruments) to advance the range instrumentation art.

Telemetry Working Group of the Inter-Range Instrumentation Group—Beuhring W. Pike (p. 61)

One of the ten Technical Working Groups of the IRIG (Inter-Range Instrumentation Group, established by the commanders of the United States guided missile test range), is the Telemetry Working Group (TWG). Among other activities, the TWG has prepared several System Standards that have been published as IRIG Recommendations.

Contributors (p. 65)

Abstracts and References

Compiled by the Radio Research Organization of the Department of Scientific and Industrial Research, London, England, and Published by Arrangement with that Department and *Electronic Technology* (incorporating *Wireless Engineer* and *Electronic and Radio Engineer*), London, England

NOTE: The Institute of Radio Engineers does not have available copies of the publications mentioned in these pages, nor does it have reprints of the articles abstracted. Correspondence regarding these articles and requests for their procurement should be addressed to the individual publications, not to the IRE.

The number in heavy type at the upper left of each Abstract is its Universal Decimal Classification number. The number in heavy type at the top right is the serial number of the Abstract. DC numbers marked with a dagger (†) must be regarded as provisional.

The Index to the Abstracts and References published in the PROC. IRE from February, 1959 through January, 1960 is published by the PROC. IRE, June, 1960, Part II. It is also published by *Electronic Technology* (incorporating *Wireless Engineer* and *Electronic and Radio Engineer*) and included in the April, 1960 issue of that Journal. Included with the Index is a selected list of journals scanned for abstracting with publishers' addresses.

UDC NUMBERS

Certain changes and extensions in UDC numbers, as published in PE Notes up to and including PE 666, will be introduced in this and subsequent issues. The main changes are:

Artificial satellites:	551.507.362.2	(PE 657)
Semiconductor devices:	621.382	(PE 657)
Velocity-control tubes, klystrons, etc.:	621.385.6	(PE 634)
Quality of received signal, propagation conditions, etc.:	621.391.8	(PE 651)
Color television:	621.397.132	(PE 650)

The "Extensions and Corrections to the UDC," Ser. 3, No. 6, August, 1959, contains details of PE Notes 598–658. This and other UDC publications, including individual PE Notes, are obtainable from The International Federation for Documentation, Willem Witsenplein 6, The Hague, Netherlands, or from The British Standards Institution, 2 Park Street, London, W.1., England.

ACOUSTICS AND AUDIO FREQUENCIES

534.23:621.396.677.3 1463

Comparison between the Performances of a Time-Averaged Product Array and an Intraclass Correlator—D. C. Fakley. (*J. Acoust. Soc. Amer.*, vol. 31, pp. 1307–1314; October, 1959.) A 'class I' array of the type discussed by Berman and Clay (336 of 1958) operating with four receiving elements, is shown to offer no advantage over an intraclass correlator in respect of detection performance and resolving power.

A list of organizations which have available English translations of Russian journals in the electronics and allied fields appears at the end of the Abstracts and References section.

534.232 1464

Mutual Radiation Impedance of Sources on a Sphere—C. H. Sherman. (*J. Acoust. Soc. Amer.*, vol. 31, pp. 947–952; July, 1959.) Expressions for the mutual radiation impedance coefficient are derived in the cases of uniformly vibrating circular and rectangular acoustic sources on a rigid spherical baffle.

534.26 1465

Diffraction of a Plane Sound Wave by a Semi-infinite Thin Elastic Plate—G. L. Lamb, Jr. (*J. Acoust. Soc. Amer.*, vol. 31, pp. 929–935; July, 1959.) The problem is formulated in terms of a) an integral equation, relating the discontinuity in pressure across the diffracting plate to its flexural displacement, and b) the usual fourth-order thin-plate differential equation governing the flexural motion of the plate when driven by the pressure discontinuity.

534.522.1 1466

The Effect of a Progressive Ultrasonic Wave on a Light Beam of Finite Width—K. L. Zankel. (*Naturwiss.*, vol. 46, pp. 105–106; February, 1959. In English.) Expressions are given for the application of refraction methods, such as that used by Breazeale *et al.* (3538 of 1959), to the measurement of the pressure of a sinusoidal ultrasonic wave and that of a distorted finite-amplitude wave.

534.522.1 1467

Effects of a Progressive Ultrasonic Wave on a Light Beam of Arbitrary Width—L. E. Hargrove, K. L. Zankel, and E. A. Hiedemann. (*J. Acoust. Soc. Amer.*, vol. 31, pp. 1366–1371; October, 1959.) Theoretical expressions (1466 above) are developed and compared with experimental results.

534.6:534.231 1468

Random Sound Field in Reverberation Chambers—C. G. Balachandran. (*J. Acoust. Soc. Amer.*, vol. 31, pp. 1319–1321; October, 1959.) Results are given of an experiment to compare the efficiency of different diffusing devices in the production of a completely random sound field. A rotating vane was found to be superior to other devices. A comparison of two test signals showed the superiority of random noise over a warble tone.

534.6:534.84 1469

Pulse Technique applied to Acoustical Testing—A. C. F. Cho and R. B. Watson. (*J. Acoust. Soc. Amer.*, vol. 31, pp. 1322–1326; October, 1959.) Brief description of a system in which pulses of variable length and repetition rate are transmitted on spot frequencies between 1 and 12 kc. The received signal may be gated and delayed to allow separation of direct and reflected sound pulses. Results of extensive tests made with the equipment in a large lecture hall are given.

534.614–14 1470

Transistorized Velocimeter for Measuring the Speed of Sound in the Sea—C. E. Tschiegg and E. E. Hays. (*J. Acoust. Soc. Amer.*, vol. 31, pp. 1038–1039; July, 1959.) See 1296 of 1958 (Greenspan and Tschiegg).

534.75 1471

Auditory Adaptation in Noise—H. N. Wright. (*J. Acoust. Soc. Amer.*, vol. 31, pp. 1004–1012; July, 1959.) The initial rate, extent and recovery from auditory adaptation were measured in both the presence and absence of noise in ten normal ears by the fixed-intensity method at 250, 1000 and 4000 cps.

534.76 1472

Some Measurements on the Effects of Interchannel Intensity and Time Differences in Two-Channel Sound Systems—D. M. Leakey. (*J. Acoust. Soc. Amer.*, vol. 31, pp. 977–986; July, 1959.) A theory is developed based on the assumption that the brain is sensitive to interaural time difference and its variation with head movement. This is in reasonable agreement with practical results.

534.78 1473

Effect of Sample Duration on the Articulation of Sounds in Normal and Clipped Speech—R. Ahmend and R. Fatehchand. (*J. Acoust. Soc. Amer.*, vol. 31, pp. 1022–1029; July, 1959.) Whether or not vowels are clipped, their segment lengths can be considerably reduced with little effect on articulation. This does not hold for consonants, with the exception of unclipped semivowels. The high articulation of interrupted speech is discussed and some results are given.

534.79 1474

On the Validity of the Loudness Scale—S. S. Stevens. (*J. Acoust. Soc. Amer.*, vol. 31, pp. 995–1003; July, 1959.) Objections to the sone scale are considered and it is shown how the form of the scale may be verified by cross-modality matchings.

534.84:061.3 1475

International Convention on Architectural and Room Acoustics—(*Hochfrequenz. und Elektroak.*, vol. 67, pp. 97–168; January, 1959.) The text is given of 15 out of 40 papers presented at a convention held in Dresden, September 5–8, 1957.

534.844 1476
Sabine Reverberation Equation and Sound Power Calculations—R. W. Young. (*J. Acoust. Soc. Amer.*, vol. 31, pp. 912–921; July, 1959.) A review of sound power and decay formulas and an assessment of their practical use. The Sabine reverberation equation, given a certain interpretation, is found to be the most suitable for general engineering purposes.

534.846 1477
Acoustoelectronic Auditorium—H. F. Olson. (*J. Acoust. Soc. Amer.*, vol. 31, pp. 872–879; July, 1959.) Description of the design of an auditorium and sound reinforcement apparatus as an integrated system.

534.88 1478
Use of Pressure-Gradient Receivers in a Correlator Receiving System—M. J. Jacobson and R. J. Talham. (*J. Acoust. Soc. Amer.*, vol. 31, pp. 1352–1362; October, 1959.) Theoretical analysis of a steerable correlator receiving system containing two directional receivers. The computer signal-to-noise ratio at the output is compared with that of a system containing two omnidirectional receivers.

534.88 1479
Hydrophone Minor Lobes produced by Volume Scattering—T. G. Bell. (*J. Acoust. Soc. Amer.*, vol. 31, pp. 1304–1307; October, 1959.) A method is given for calculating approximately the minor-lobe response of a directional hydrophone due to volume scattering.

534.88:534.232.089.6 1480
Pressure Phone for Hydrophone Calibrations—C. C. Sims and R. J. Bobber (*J. Acoust. Soc. Amer.*, vol. 31, pp. 1315–1318; October, 1959.) A small closed system for the absolute calibration of a standard hydrophone at frequencies up to 5 kc is described.

621.395.623.7.001.4:534.76 1481
Evaluation of a Stereophonic Loudspeaker by Multiple Microphone Arrays—R. W. Carlisle and A. Schwartz. (*J. Acoust. Soc. Amer.*, vol. 31, pp. 1348–1351; October, 1959.) A system is described for measuring the effective frequency response of a stereophonic loudspeaker arrangement in a live room. The method is shown to be superior to the anechoic-chamber method at low frequencies.

621.395.623.742 1482
A Method of Mechanical Damping of Dynamic Loudspeakers by Porous Materials—L. Keibs. (*Tech. Mitt. BRF, Berlin*, vol. 3, pp. 7–12; October, 1959.) Design theory regarding the damping of loudspeaker cones to eliminate self-resonances is given, and a method of measurement of damping effects is outlined.

621.395.625.3 1483
Improving the Dynamic Range of Tape Recording—L. H. Bedford. (*Wireless World*, vol. 66, pp. 104–106; March, 1960.) Compensation for manual compression of the input signal using a pilot tone outside the AF range.

621.395.625.3:538.221 1484
Particle Interaction in Magnetic Recording Tapes—Woodward and Dellatorre. (*See* 1723.)

621.395.625.3:681.846.7 1485
The Transport Mechanism of the Magnetic-Tape Recorder for Reporters—O. W. Meier. (*Tech. Mitt. BRF, Berlin*, vol. 3, pp. 12–21; October, 1959.) Details are given of a battery-operated portable tape recorder used by the East German broadcasting authorities. A comparative table is included of the mechanical specifications for nine types of portable recorder of European manufacture.

621.395.625.3:681.846.7 1486
The Transistor Amplifier of the Magnetic-Tape Recorder Type R20 for Reporting—A. Tolk. (*Tech. Mitt. BRF, Berlin*, vol. 3, pp. 21–25; October, 1959.) Circuit and performance details of a battery-operated recorder are given. See 1485 above.

621.315.212 1487
Reflection Coefficient Curves of Compensated Discontinuities on Coaxial Lines and the Determination of the Optimum Dimensions—A. Kraus. (*J. Brit. IRE*, vol. 20, pp. 137–152; February, 1960.)

621.315.687.029.6+621.372.855 1488
Microwave Terminations—G. Bostick. (*Electronics*, vol. 33, pp. 50–51; January 8, 1960.) Characteristics and relative costs of the four major classes of coaxial-cable and waveguide terminations.

621.372.2:621.372.51 1489
100:1 Bandwidth Balun Transformer—J. W. Duncan and V. P. Minerva. (PROC. IRE, vol. 48, pp. 156–164; February, 1960.) The design theory is given for a balun made by cutting away the outside wall of a coaxial cable. The input reflection coefficient gives a Tchebycheff response in the pass band. The measured voltage SWR did not exceed 1.25:1 over a 50:1 bandwidth and the dissipation loss was less than 0.1 db over most of the range.

621.372.2.012.11 1490
The Smith Chart: Part 3—Matching Transmission Lines to Aerials and Uses of Stubs—R. A. Hickson. (*Wireless World*, vol. 66, pp. 141–146; March, 1960.) Considers various matching elements with detailed examples. Parts 1 and 2: 749 of March.

621.372.8 1491
TM Waves in Submillimetric Region—C. A. Martin and A. E. Karbowiak. (PROC. IRE, vol. 48, pp. 250–251; February, 1960.) Discussion of 13 of 1959 (Karbowiak) with author's comment. The attenuation characteristics for certain modes of c rcular waveguide are shown to increase indefinitely with frequency and not to follow an $f^{-5/2}$ law as suggested earlier.

621.372.8:621.385.63 1492
A Class of Waveguide-Coupled Slow-Wave Structures—J. Feinstein and R. J. Collier. (IRE TRANS. ON ELECTRON DEVICES, vol. ED-6, pp. 9–17; January, 1959. Abstract, PROC. IRE, vol. 47, p. 611; April, 1959.)

621.372.823:621.372.852.5 1493
Round Waveguide with Double Lining—H. G. Unger. (*Bell Sys. Tech. J.*, vol. 39, pp. 161–167; January, 1960.) A mathematical analysis of the effects of thin base layers of low-loss material at bends indicates a reduction of the TE_{01} loss, and mode filtering.

621.372.825 1494
Surface Resistance of Corrugated Conductors—T. Hosono. (PROC. IRE, vol. 48, p. 247; February, 1960.) The average surface resistance is shown to be more than that of a plain surface, indicating that losses may be less in plain circular waveguide than in those made from spaced disks. This reverses an earlier conclusion [see *Proc. IEE*, Part B, vol. 106, supplement pp. 37–46 (Gent); 1959].

621.372.85 1495
Evanescent Modes in a Partially Filled Gyromagnetic Rectangular Waveguide—C. T. Tai. (*J. Appl. Phys.*, vol. 31, pp. 220–221; January, 1960.) A demonstration of the existence of these modes, based on the asymptotic form of the characteristic equation.

621.396.67:621.315.1:621.391.812.63.029.45 1496
A Very-Low-Frequency Antenna for Investigating the Ionosphere with Horizontally Polarized Radio Waves—R. S. Macmillan, W. V. T. Rusch, and R. M. Golden. (*J. Res. Nat. Bur. Stand.*, vol. 64D, pp. 27–35; January/February, 1960.) The radiation characteristics of resonant horizontal $\lambda/2$ dipoles have been verified experimentally and the effects of ground conductivity investigated. The loading of an existing power transmission line to convert a section of it into a dipole is described. See also 1672 of 1959 (Golden *et al.*).

621.396.674.095(204) 1497
Basic Experimental Studies of the Magnetic Field from Electromagnetic Sources Immersed in a Semi-infinite Conducting Medium—M. B. Kraichman. (*J. Res. Nat. Bur. Stand.*, vol. 64D, pp. 21–25; January/February, 1960.) Measurements have been made of the magnetic field in air due to different dipoles and loops energized at 296 kc and immersed in a tank containing a sodium chloride solution.

621.396.677 1498
Effect of Antenna Size on Gain, Bandwidth, and Efficiency—R. F. Harrington. (*J. Res. Nat. Bur. Stand.*, vol. 64D, pp. 1–12; January/February, 1960.) A theoretical analysis in which both near-zone and far-zone directive gains are considered. The maximum gain for a wide-band antenna is approximately that of the uniformly illuminated aperture. Higher gain can only be obtained if the antenna is a narrow-band device. For large antennas the input impedance is highly frequency-sensitive and no significant gain over a uniformly illuminated aperture is possible.

621.396.677:523.164 1499
Resolving Power of Three Antenna Patterns Derived from the Same Aperture—A. E. Covington and G. A. Harvey. (*Canad. J. Phys.*, vol. 37, pp. 1216–1229; November, 1959.) An analysis is made of the problem of deducing the spatial distribution of RF energy in an astronomical source which is smaller than the beamwidth of the antenna. The antenna pattern is represented by a series of Fourier components, and the problem is then similar to those met in the design of filters. Particular cases studied are a) a pair of equally intense point sources, and b) a uniformly bright line.

621.396.677.3:534.23 1500
Comparison between the Performances of a Time-Averaged Product Array and an Intraclass Correlator—Fakley. (*See* 1463.)

621.396.677.7:621.372.826 1501
Surface-Wave Resonance Effect in a Reactive Cylindrical Structure Excited by an Axial Line Source—A. L. Cullen. (*J. Res. Nat. Bur. Stand.*, vol. 64D, pp. 13–19; January/February, 1960.) The existence of strong resonance phenomena has been established theoretically. In a particular example, only 1.1 per cent of the power delivered to the line source is radiated in unwanted modes. The distance of the source from the cylinder does not affect the result in a first-order approximation.

621.396.677.73:621.391.812.62.029.64 1502
Over-Sea Propagation of Microwaves and Anti-reflected-Wave Antenna—Kawazu, Kato and Morita. (*See* 1754.)

AUTOMATIC COMPUTERS

681.142:061.3 1503
Computers head for 1000-MC/s Operation—T. Maguire. (*Electronics*, vol. 33, pp. 55–59; January 29, 1960.) Report of recent develop-

ments in phase-locked oscillators, tunnel diodes and cross-film cryotrons, based on papers presented at the Computer Conference, Boston, Mass. December 1–3, 1959.

681.142:537.312.62 1504
Low-Temperature Storage Elements—E. H. Rhoderick. (*J. Brit. IRE*, vol. 20, pp. 37–40; January, 1960.) Very high speeds and compactness are features of the Crowe cell in which a persistent current is set up around an aperture in a thin superconducting film.

621.142:621.374.3 1505
Pulse-Height-to-Digital Signal Converter—W. W. Grannemann, C. D. Longerot, R. D. Jones, D. Endsley, T. Summers, T. Lommasson, A. Pope, and D. Smith. (*Electronics*, vol. 33, pp. 58–60; January 8, 1960.) A transistorized analog/digital converter provides 7-digit binary outputs for an input of 0–2 volts at a maximum sampling rate of 13,000 pulses /sec.

681.142:621.374.5:534–8 1506
Supersonic Delay-Line Memory Device for Parametron Signal—S. Yamada and K. Kuri. (*Rep. Elec. Commun. Lab., Japan*, vol. 7, pp. 167–169; May, 1959.) Results obtained with an experimental 0.5-mm-diameter brass-wire delay line are given. Suitable coupling circuits are shown.

681.142:621.395.625.3 1507
Factors Influencing the Applications of Magnetic Tape Recording to Digital Computers—D. P. Franklin. (*J. Brit. IRE*, vol. 20, pp. 9–21; January, 1960.)

681.142:621.395.625.3 1508
A Magnetic-Disk, Random-Access Memory—A. C. Glover. (*J. Brit. IRE*, vol. 20, pp. 22–24; January, 1960.) 5×10^5 alphanumeric characters can be stored with average access time 0.5 second.

681.142:621.395.625.3 1509
Magnetic-Film File for Computer Storage—A. St. Johnston. (*J. Brit. IRE*, vol. 20, pp. 25–30; January, 1960.) A 35-mm oxide-coated film store is described in which the pickup head is not in contact with the oxide. The high-quality backing medium gives complete freedom from drop-outs.

681.142:621.395.625.3 1510
High-Speed Digital Storage using Cylindrical Magnetic Films—G. R. Hoffman, J. A. Turner, and T. Kilburn. (*J. Brit. IRE*, vol. 20, pp. 31–36; January, 1960.) Digital stores consisting of closed magnetic circuits deposited on long glass tubes are described.

681.142:621.395.625.3 1511
A High-Density File Drum as a Computer Store—L. Knight and M. P. Circuit. (*J. Brit. IRE*, vol. 20, pp. 41–45; January, 1960.) A packing density of 1000 bits/inch has been obtained using specially designed heads floating on an oil film which automatically maintains a head/track spacing of 0.002 inch.

CIRCUITS AND CIRCUIT ELEMENTS

621.318.4 1512
Analysis of Quality Factor of Annular-Core Inductors—V. E. Legg. (*Bell Sys. Tech. J.*, vol. 39, pp. 105–126; January, 1960.) A summary of formulas used to determine Q factor is supplemented with a discussion of optimum design procedures. In particular, eddy currents and dielectric losses, and the effects of distributed capacitance are considered.

621.318.57 1513
The Ferreed—a New Switching Device—A. Feiner, C. A. Lovell, T. N. Lowry, and P. G. Ridinger. (*Bell Sys. Tech. J.*, vol. 39, pp. 1–30; January, 1960.) Properties of a magnetic-reed switch responsive to the resonant field of a ferrite are considered. Switching times are in the microsecond range and dual winding facilitates coincident-pulse control. The application to switching arrays is discussed.

621.318.57:621.372.44 1514
Binocular-Type Parametron—K. Fukui, M. Shindo, T. Kurata, and K. Habara. (*Rep. Elec. Commun. Lab., Japan*, vol. 7, pp 152–166; May, 1959.) The method of manufacture and characteristics of a parametron with a new type of ferrite core comprising a segmented disk with two apertures are described. Power consumption is about one quarter that of the toroidal-core type [410 of February (Hanawa and Kusunoki)].

621.318.57:621.382.23 1515
Microwave Switching with Computer Diodes—M. Bloom. (*Electronics*, vol. 33, pp. 85–87; January 15, 1960.) Characteristics are given of single- and double-throw Ge junction-diode switches. Satisfactory tests have been made on a coaxial switch at 1 watt and an X-band waveguide switch at 4 watts RF power.

621.319.4:621.317.7 1516
An Oscillating Capacitor of High Stability—M. von Ardenne and E. Klar. (*Nachrichtentech. Z.*, vol. 9, pp. 26–28; January, 1959.) The precision unit described is designed for use with high-resistance dc or direct-voltage measuring equipment where high stability is required. Currents of 10^{-15}–10^{-16} ampere were detected with an input resistance of $10^{13}\Omega$.

621.372:621.3.092 1517
Certain Asymptotic Relations between Frequency and Time Functions—H. Dobesch. (*Nachrichtentech. Z.*, vol. 9, pp. 13–18; January, 1959.) The relations are considered with reference to networks to which a transient is applied, and including the effect of group delay.

621.372.5 1518
Linear Network Synthesis—O. C. Bown. (*Electronic Tech.*, vol. 37, pp. 122–126; March, 1960.) "The rational fraction approximation is obtained directly in terms of the pole-zero locations in the p-plane by a process of successive approximation. The method differs from other known successive approximation techniques in being purely graphical apart from a final numerical relaxation process. A simple step-by-step account is given of the practical procedure."

621.372.54:621.398 1519
Low-Pass Filter for Subaudio Frequencies—R. C. Onstad. (*Electronics*, vol. 33, pp. 88–90; January 15, 1960.) Details are given of a low-pass RC filter suitable for use in a missile-borne telemetry system. The filter incorporates a transistor feedback amplifier and has a flat response from dc to 0.7 cps and an attenuation slope of 15 db per octave.

621.372.6 1520
Immittance Properties of Nonreciprocal Networks—A. W. Keen. (Proc. IRE, vol. 48, pp. 248–250; February, 1960.) Certain known networks are described in terms of the unitor, a nonreciprocal circuit element. These include the Batt-Duffin immittance synthesizing cycle, impedance inversion and conversion circuits and the symmetrical lattice network. See 2871 of 1959.

621.372.632:621.375.132 1521
Negative Feedback in Frequency-Changers—D. G. Tucker. (*Electronic Tech.*, vol. 37, pp. 96–98; March, 1960.) Two different forms of negative feedback are discussed; one has only passive elements in the feedback path [2018 of 1952 (Boggs)] and the other has an active element with characteristics identical to those of the forward path (297 of 1950). Their application to frequency changers is considered with reference to gain stability.

621.373 1522
The Quality of Oscillators with Differently Located Losses—W. Herzog. (*Nachrichtentech. Z.*, vol. 12, pp. 21–28; January, 1959.) A Π-network oscillator with parallel and series losses is investigated to determine whether the Q-factor can be improved by a reduction of load impedance in conjunction with an appropriate increase in oscillator gain. The reduction of load impedance is effected by considering the loss impedance to be added in parallel with the load.

621.373.4:621.376.32 1523
A Voltage-Tuned Resistance-Capacitance Oscillator—W. D. Ryan and F. E. Hetherington. (*Electronic Engrg*, vol. 32, pp. 108–110; February, 1960.) A circuit is given for an AF oscillator whose frequency of oscillation is dependent on an applied dc potential by virtue of the variable capacitance of selenium dry-disk rectifiers with reverse bias. The characteristics of suitable rectifiers are discussed.

621.373.44:621.373.2 1524
The Generation of Short High-Power Pulses by means of Spark-Gap Switches—G. Sahner. (*Nachrichtentech. Z.*, vol. 8, pp. 36–43 and 558–566; January and December, 1959.) The characteristics of the discharge current in spark-gap circuits are calculated. Tests were made on a triggered pulse-generator circuit comprising two series-connected spark gaps; equipment used and results obtained are described.

621.373.51:621.372.44 1525
Parametric Oscillations with Point-Contact Diodes at Frequencies Higher than Pumping Frequency—L. U. Kibler. (Proc. IRE, vol. 48, pp. 239–240; February, 1960.) The signal and idler frequencies are symmetrically placed with respect to a multiple of the pumping frequency. The results are consistent with the Manley-Rowe relations (see *e.g.* 773 of March).

621.373.52.029.62 1526
Designing High-Power Transistor Oscillators—W. E. Roach. (*Electronics*, vol. 33, pp. 52–55; January 8, 1960.) A step-by-step procedure is given for the design of oscillators for operation at frequencies up to 300 mc.

621.374.32:621.385.63:621.373.43 1527
A High-Speed Binary Counter based on Frequency Script Techniques—V. Met. (Proc. IRE, vol. 48, pp. 243–244; February, 1960.) An extension of previous experimental investigations into bistable oscillators (3428 of 1957).

621.374.32:621.385.832 1528
Fast Counting Circuits using E1T Tubes—V. Radeka. (*Electronic Engrg.*, vol. 32, pp. 92–95; February, 1960.) A theoretical investigation into the use of Type E1T counter tubes [3614 of 1952 (Jonker *et al.*)] at pulse repetition frequencies up to 1 mc, together with a practical design of circuit.

621.374.4 1529
Efficient Harmonic Generation—G. F. Montgomery. (Proc. IRE, vol. 48, pp. 251–252; February, 1960.) Practical harmonic generators are reviewed briefly and the most efficient is shown to be the rectifier-amplifier type. A transistor amplifier provides best efficiency at low powers.

621.374.42 1530
A Stabilized Locked-Oscillator Frequency Divider—P. R. Scott, Jr. (Proc. IRE, vol. 48,

pp. 192–200; Feburary, 1960.) The results of an analysis of the divider are presented in a graphical form suitable for design purposes.

621.375.133:621.391.822 1531
Negative-Capacitance Amplifier Noise—M. Robinson and J. Weinmann. (*Electronic Tech.*, vol. 37, pp. 127–129; March, 1960.) "The inherent limitations of negative-capacitance feedback, due to the finite time constant and internal noise of an actual amplifier, are discussed. It is shown that the limitation, caused by noise, applies to any circuit that is designed to reduce the input RC time constant."

621.375.9:538.569.4 1532
Ferromagnetic Amplifiers—A. F. H. Thomson. (Proc. IRE, vol. 48, pp. 259; February, 1960.) Note on an absorption of microwave power observed with a magnetized Y-Fe garnet sphere in a microwave field at a frequency approximately twice that corresponding to the magnetization.

621.375.9:538.569.4 1533
Maser Behaviour: Temperature and Concentration Effects—T. H. Maiman. (*J. Appl. Phys.*, vol. 31, pp. 222–223; January, 1960.) Maser action has been achieved with ruby at temperatures up to 195°K; results are given for operation at 77°K.

621.375.9:538.569.4 1534
A Tunable X-Band Ruby Maser—P. D. Gianino and F. J. Dominick. (Proc. IRE, vol. 48, p. 260; February, 1960.) Performance figures and details of simplified tuning arrangements are given.

621.375.9:621.372.44 1535
The Parametric Amplifier—C. R. Russell. (*Brit. Commun. Electronics*, vol. 7, pp. 94–98 and 190–194; February and March, 1960.) The mode of operation of parametric devices is explained and general features of semiconductor-diode, ferrite and beam-type amplifiers are discussed.

621.375.9:621.372.44 1536
Noise Consideration of the Variable-Capacitance Parametric Amplifier—M. Uenohara. (Proc. IRE, vol. 48, pp. 169–179; February, 1960.) A simplified theory, assuming the noise source is a resistance in series with the variable capacitance, gives calculated gain and noise figures agreeing with measured values for Si, Ge, and GaAs diodes.

621.375.9:621.372.44:621.385.6 1537
Some Possible Causes of Noise in Adler Tubes—Lea-Wilson: Adler, Hrbek, and Wade. (*See* 1834.)

621.376.32:621.382 1538
Wide-Band F.M. with Capacitance Diodes—C. Arsem. (*Electronics*, vol. 32, pp. 112–113; December 4, 1959.) Two circuits are described using voltage-variable capacitors to modulate a tube oscillator.

GENERAL PHYSICS

530.145:061.3 1539
Mathematical Problems of the Quantum Theory of Particles and Fields—(*Nuovo Cim.*, vol. 14, supplement pp. 1–211; 1959.) The text is given in English of 12 papers presented at an international course held at Varenna, July 21–August 9, 1958.

537.214 1540
Approximation Formulae for the Electrostatic Energy of a Space Charge—O. Emersleben. (*Naturwiss.*, vol. 46, pp. 64–65; January, 1959.) An asymptotic approximation for the es potential is derived which does not contain terms denoting the number and magnitude of the individual charges making up a space-charge cloud.

537.214:537.226 1541
The Electromagnetic Energy Stored in a Dispersive Medium—T. Hosono and T. Ohira. (Proc. IRE, vol. 48, pp. 247–248; February, 1960.) An expression for energy is derived by treating the dielectric as a two-terminal network having a frequency-dependent admittance.

537.311.1 1542
Damping Method in the Theory of Electrical Conductivity—R. Zigenlaub. (*Fiz. Tverdogo Tela*, vol. 1, pp. 1053–1061; July, 1959.) A method is suggested for calculating the conductivity tensor similar to the "time-fluctuation" method used in quantum field theory.

537.311.33 1543
A More Precise Theory of Plasma Recombination—V. L. Bonch-Bruevich. (*Fiz. Tverdogo Tela*, vol. 1, pp. 1076–1083; July, 1959.) Recombination coefficients are derived for two models: deep traps and third- and fifth-group impurity traps in Ge and Si.

537.311.33 1544
Theory of the Method of Thermal Conductivity Measurement Proposed by A. V. Ioffe and A. F. Ioffe—M. A. Kaganov. (*Zh. tekh. Fiz.*, vol. 28, pp. 2364–2367; November, 1958.) See 1661 below.

537.525 1545
Build-Up of a Discharge in Argon—M. Menes. (*Phys. Rev.*, vol. 116, pp. 481–486; November 1, 1959.) Measurements of the rate of build-up at pressures of 5–60 cm Hg, and theoretical interpretation of results.

537.533:621.385.6 1546
Time-Dependent Electron Flow—M. C. Pease. (*J. Appl. Phys.*, vol. 31, pp. 70–76; January, 1960.) General relations are given, from which a single-vector differential equation can be deduced which determines all possible solutions in the case of a constant uniform magnetic field. The application of certain time-varient solutions of this equation to anomalous behavior in various magnetron-type devices is considered.

537.533.74 1547
Double Scattering of Electrons with a Dipole Moment—M. H. Zaidi. (*Phys. Rev.*, vol. 116, pp. 241–243; October 15, 1959.) Quantum-mechanical analysis of the case where magnetic and electric fields are present between the two targets gives the same results as are obtained by treating the electrons as classical spinning tops with magnetic moments and classical electric dipoles.

537.533.79:538.221 1548
Interaction between Electron Beam and Magnet—S. Yamaguchi. (*Nuovo Cim.*, vol. 14, pp. 248–249; October 1, 1959. In English.) The diffraction effect noted when an electron beam grazes a sharp edge of a magnet (about 2000 Å thick) is described and interpreted. See 3636 of 1959.

537.533.8 1549
The Time Constant of Secondary Emission—H. W. Streitwolf and W. Brauer. (*Z. Naturforsch.*, vol. 13a, pp. 700–701; August, 1958.) See also 1178 of April (Streitwolf).

537.56 1550
Transport Phenomena in Slightly Ionized Gases: Low Electric Fields—M. S. Sodha. (*Phys. Rev.*, vol. 116, pp. 486–488; November 1, 1959.) Calculation of transport properties, in the presence of a magnetic field. For low electric fields E the results can be expressed as linear functions of E^2.

537.56 1551
Asymmetrical Triple-Probe Method for Determining Energy Distribution of Electron in Plasma—T. Okuda and K. Yamamoto. (*J. Appl. Phys.*, vol. 31, pp. 158–162; January, 1960.) The method is an improvement on one previously given [2687 of 1956 (Yamamoto and Okuda)]. A much greater range of electron energies can be examined and it can be used in electrodeless discharges.

537.56:537.29 1552
Action of a D. C. Electric Field on a Plasma: Establishment of the Equation giving the Distribution Function—A. Brin, J. L. Delcroix, and Y. Ozias. (*Compt. rend. acad. sci., Paris*, vol. 249, pp. 1093–1095; September 28, 1959.

537.56:538.56 1553
Excitation of Oscillations in a Plasma Layer—M. Sumi. (*J. Phys. Soc. Japan*, vol. 14, pp. 1093–1097; August, 1959.) Application of theory developed earlier (1513 and 2534 of 1959) to the excitation of standing waves in a uniform plasma.

537.56:538.56 1554
Oscillations of a Cylindrical Cavity in a Completely Ionized Pasma—L. M. Kovrizhnykh. (*Zh. Eksp. Teor. Fiz.*, vol. 36, pp. 839–841; March, 1959.) Investigation of the oscillations of a cylindrical cavity in a perfectly conducting plasma with applied magnetic field. The system is shown to be stable and under certain conditions waves cannot propagate along the cavity.

537.56:551.510.5 1555
Sealed-Room Experiments on the Equilibrium of Ionization in Air—O. C. Jones, R. S. Maddever, and J. H. Sanders. (*J. Atmos. Terr. Phys.*, vol. 17, pp. 134–144; December, 1959.) An attempt to determine the correct form of the equation by making measurements of as many of the quanitities appearing in the equation as possible.

538.221:537.312.62 1556
Possible Explanation of the "Coexistence" of Ferromagnetism and Superconductivity—B. T. Matthias and H. Suhl. (*Phys. Rev. Lett.*, vol. 4, pp. 51–52; January 15, 1960.) A discussion based on the suggestion that superconducting regions extend only through the thicknesses of the ferromagnetic domain walls.

538.3 1557
Electromagnetic Energy/Momentum Tensor in the Presence of Charged Matter—S. Mavridès. (*Compt. rend. acad. sci., Paris*, vol. 249, pp. 637–639; August 3, 1959.)

538.3:512.99 1558
The Method of Combinative Numbers (Nombres Combinatifs) in the Study of Electromagnetic Fields—M. P. Zlatev. (*Onde élect.*, vol. 39, pp. 908–912; December, 1959.) Maxwell's field equations and Poynting's theorem are given in group-number form. The method is proposed for problems where the use of complex numbers would give an ambiguous result.

538.561:537.56 1559
Radiation from a Current-Carrying Ring which Moves Uniformly in a Plasma Located in a Magnetic Field—L. S. Bogdankevich. (*Zh. Eksp. Teor. Fiz.*, vol. 36, pp. 835–838; March, 1959.) Estimation of losses due to Vavilov-Cherenkov radiation for a current-carrying ring which moves uniformly in a plasma perpendicular to its plane and parallel to an external magnetic field.

538.561:539.12:523.165 1560
Radiation from High-Speed Particles—P. A. Cherenkov. (*Science*, vol. 131, pp. 136–142; January 15, 1950.) Translation of Nobel Prize lecture. See also 824 of March.

538.561:539.12:537.56 1561
General Characteristics of Vavilov-Cherenkov Radiation—I. E. Tamm. (*Science*, vol. 131, pp. 206–210; January 22, 1960.) The application of the theory of Cherenkov radiation to problems of plasma physics is considered.

538.566+534.2 1562
The Exactness of the Solution of a Radiation or Diffraction Problem—P. Poincelot. (*Compt. rend. acad. sci., Paris*, vol. 249, pp. 950–951; September 7, 1959.) Criteria of uniqueness may be applied to various problems of propagation in media satisfying linear equations. See also 3628 of 1959.

538.566:535.42 1563
Diffraction of a Plane Electromagnetic Wave by a Perfectly Conducting Paraboloid of Rotation—V. A. Fok and A. A. Fedorov. (*Zh. Tekh. Fiz.*, vol. 28, pp. 2548–2566; November, 1958.) Exact solution for arbitrary angle of incidence and polarization. Asymptotic formulas for the surface current distribution are derived for wavelengths small compared with the focal length of the paraboloid.

538.566:535.42 1564
Approximate Calculations of the Diffraction of Plane Electromagnetic Waves by some Metallic Bodies: Part 2—P. Ya. Ufimtsev. (*Zh. Tekh. Fiz.*, vol. 28, pp. 2604–2616; November, 1958.) Application of the approximate method described in Part 1 (2711 of 1958) to diffraction of a plane EM wave by a perfectly conducting disk or cylinder. Results are shown graphically and compared with experimental data.

538.566:535.43 1565
Scattering by Nonspherical Particles—J. M. Greenberg. (*J. Appl. Phys.*, vol. 31, pp. 82–84; January, 1960.) "The small-angle scattering approximation of Schiff (see 1408 of 1957) is applied to several nonspherical body shapes. Effects of orientation and elongation are discussed."

538.569.4:621.391.883.2 1566
Signal-to-Noise Ratio in Nuclear Magnetic Resonance—R. Chidambaram. (*Proc. Phys. Soc.*, vol. 75, pp. 163–164; January, 1960.) The amplifier noise is expressed in terms of an equivalent input grid resistance rather than in terms of a noise figure.

538.569.4.029.6:536.46 1567
Absorption and Dispersion of Microwaves in Flames—J. Schneider and F. W. Hofmann. (*Phys. Rev.*, vol. 116, pp. 244–249; October 15, 1959.) The dependence of the high-frequency electric conductivity and the optical constants of a weakly ionized gas on the microwave frequency, the electron-molecule collision frequency, the electron concentration and an external magnetic field are discussed.

539.2:537.311.33 1568
The Influence of Lattice Vibrations on Energy and Lifetime of the Exciton—H. Haken. (*Z. Phys.*, vol. 155, pp. 223–246; May 22, 1959.) The exciton is treated as a system of two particles with Coulomb-potential interaction which are coupled to the quantized field of lattice vibrations.

539.2:548.0 1569
New Method for Calculating Wave Functions in Crystals and Molecules—J. C. Phillips and L. Kleinman. (*Phys. Rev.*, vol. 116, pp. 287–294; October 15, 1959.) Advantage is taken of crystal symmetry to construct wave functions which are best described as the smooth part of symmetrized Bloch functions.

GEOPHYSICAL AND EXTRATERRESTRIAL PHENOMENA

523.164:621.396.677 1570
Interferometer using Two Aerials with Variable Spacing at the Nançay Radio-Astronomy Station—J. Lequeux, É. Le Roux, and M. Vinokur. (*Compt. rend. acad. sci., Paris*, vol. 249, pp. 634–636; August 3, 1959.) Radiation at 21 cm λ is received by two parabolic reflectors which can be moved along a track 1500 meters long running E–W; a second track 400 meters long runs N–S. A 53.7-mc signal from a common local oscillator is transmitted by coaxial cables to the antenna sites, multiplied and mixed with the received signals. Resulting 30-mc signals are conveyed via the same cables to a correlator/detector. Results obtained with the apparatus are shown.

523.164:621.396.677 1571
Resolving Power of Three Antenna Patterns Derived from the Same Aperture—Covington and Harvey. (*See* 1499.)

523.164.32 1572
Absorption, Refraction and Scintillation Measurements at 4700 Mc/s with a Travelling-Wave-Tube Radiometer—J. P. Castelli, J. Aarons, C. Ferioli, and J. Casey. (*Planet. Space Sci.*, vol. 1, pp. 50–56; January, 1959.) A report of measurements of solar RF radiation at sunrise during July 1957, with a note on the equipment used. This consisted of a Dicke-type radiometer, a tuned-RF receiver and a 6-foot parabola antenna on an altazimuth mount.

523.164.32:523.75 1573
The Correlation of Bursts of Solar Radio Emission in the Centimetre Range with Flares and Sudden Ionospheric Distriburbances—O. Hachenberg and A. Krüger. (*J. Atmos. Terr. Phys.*, vol. 17, pp. 20–33; December, 1959.) Statistical investigations of observations during the first six months of the I.G.Y. reveal a close correlation between bursts in the cm-λ range and S.I.D.'s. It is concluded that both the cm-λ radiation and the ionizing radiation responsible for S.I.D.'s are generated by superthermal electrons.

523.165 1574
Sudden Increase of Cosmic-Ray Intensity—H. R. Anderson. (*Phys. Rev.*, vol. 116, pp. 461–462; October 15, 1959.) Report on simultaneous observations in U.S.A. and New Zealand which are not in accord with simple solar impact-zone theory.

523.165 1575
Primary Heavy Cosmic Rays near the Geomagnetic Equator—O. B. Young and F. W. Zurheide. (*Nuovo. Cim.*, vol. 14, pp. 90–98; October 1, 1959. In English). Results are given of measurements by balloon at 100,000 feet altitude above Guam, 4°N geomagnetic latitude.

523.165:523.74 1576
The Sun as a Source of Cosmic Rays of Intermediate Energies—J. Katzman. (*Canad. J. Phys.*, vol. 37, pp. 1207–1215; November, 1959.) Cosmic-ray intensity, as measured with a narrow-angle telescope and thick absorber, shows a sunspot-cycle variation. Correlations with F_2-layer ionization and solar RF flux are shown.

523.165:523.745 1577
Primary Cosmic-Ray Intensity near Solar Maximum—F. B. McDonald .(*Phys. Rev.*, vol. 116, pp. 462–463; October 15, 1959.) Results of measurements of proton and α-particle fluxes and energy spectra are given. Comparison is made with an electric-field model.

523.165:551.593.9 1578
Cherenkov Radiation in the Atmosphere—J. V. Jelley. (*Planet. Space Sci.*, vol. 1, pp. 105–111; April, 1959.) A review of theoretical and experimental work.

523.5 1579
Ambipolar Diffusion of a Meteor Trail and its Relation with Height—E. L. Murray. (*Planet. Space Sci.*, vol. 1, pp. 125–129; April, 1959.) Regression lines have been derived for the relation between log D and height, where D is the ambipolar diffusion coefficient. See 100 of 1956 (Weiss).

523.745:551.510.535 1580
A Daily Index of Solar Activity based on E-Layer Ionization (July 1937–December 1958)—C. M. Minnis and G. H. Bazzard. (*J. Atmos. Terr. Phys.*, vol. 17, pp. 57–64; December, 1959.) "The electron density in a Chapman layer can be related to the intensity of the incident solar ionizing radiation. This relation has been adopted as the basis for computing a daily index of the radiation intensity using the critical frequency of the E layer at Slough. Precautions have been taken to minimize errors due to irregularities in the behavior of the layer and to the difficulty in identifying the E-layer cusp. The standard deviation of the residual errors in the index is estimated to be 2 per cent. The index has been tabulated for the period 1 July 1957 to 31 December 1958."

550.385 1581
Rapid Fluctuations during Magnetic Disturbance—J. Lawrie. (*J. Atmos. Terr. Phys.*, vol. 17, pp. 145–149; December, 1959.) A numerically simple ratio is defined and used to examine space relationships of rapid geomagnetic fluctuations during disturbance.

550.385:539.16 1582
Geomagnetic Effects of High-Altitude Nuclear Explosions—A. G. McNish. (*J. Geophys. Res.*, vol. 64, pp. 2253–2265; December, 1959.) The observations discussed were made after the two Johnston Island explosions in August 1958, at four stations within 2000-km radius, and at Apia near the conjugate point [see also 3709 of 1959 (Matsushita)]. Effects at the first four observatories are attributed to overhead currents caused by increased ionization by γ rays, while effects at Apia are explained as being caused by artificial auroras.

550.385:539.16 1583
Simultaneous Recordings in France, at the Equator and in the Antarctic, of Magnetic Effects caused by the "Argus Experiment"—É. Selzer. (*Compt. rend. acad. sci., Paris*, vol. 249, pp. 1133–1135; September 28, 1959.) Geomagnetic disturbances were observed at French I.G.Y. stations for all three explosions.

550.385.37:061.3 1584
Symposium on Pulsations and Rapid Variations in Geomagnetism and Earth Currents—(*J. Geomag. Geoelect.*, vol. 10, pp. 135–225; 1959.) The text is given of the following papers read at a symposium in Tokyo, Jap., April 3–4, 1959.

a) **Ionizations in the Outer Atmosphere Inferred from Whistling Atmospherics**—J. Outsu and A. Iwai (pp. 135–142).

b) **Hydromagnetics in the Earth's Outer Atmosphere**—T. Tamao (pp. 143–150).

c) **The Acceleration of Particles in the Outer Atmosphere**—T. Obayashi (pp. 151–152).

d) **Morphology of S.S.C. and S.S.C.***—S. Abe (pp. 153 163).

e) **Some Remarks on the Morphology of Geomagnetic Bays**—N. Fukushima (pp. 164–171).

f) **Some Characters of Geomagnetic Pulsation *pt* and Accompanied Oscillation *spt***—K. Yanagihara (pp. 172–176).

g) **Morphology of the Geomagnetic Pulsation**—T. Watanabe (pp. 177–184.)

h) **Particles of Aurorae and Geomagnetic Pulsations**—Y. Kato and T. Watanabe (pp. 185–194).

i) **Hydromagnetic Oscillation of the Outer Ionosphere and Geomagnetic Pulsation**—T. Watanabe (pp. 195–202).

j) **Geomagnetic Pulsation accompanying the Intense Solar Flare**—Y. Kato, T. Tamao and T. Saito (pp. 203–207).

k) **On the Frequency of Geomagnetic Pulsation *pc***—T. Yoshimatsu (pp. 208–213).

l) **Studies of the Local Character of the Geomagnetic Pulsation *pc***—S. Utashiro (pp. 214–220).

m) **Preliminary Studies on the Daily Behaviour of Rapid Pulsation**—Y. Kato and T. Saito (pp. 221–225).

550.385.37:551.594.5 1585
Micropulsations in the Earth's Magnetic Field Simultaneous with Pulsating Aurora—W. H. Campbell. (*Nature, Lond.*, vol. 185, p. 677; March 5, 1960.) Preliminary results are given.

550.385.4 1586
Hydromagnetic Theory of Geomagnetic Storms—A. J. Dressler and E. N. Parker. (*J. Geophys. Res.*, vol. 64, pp. 2239–2252; December, 1959.) The sudden commencement of a magnetic storm is attributed to the collision of solar plasma with the geomagnetic field, the disturbance being propagated to earth by a hydromagnetic wave. The initial positive phase is attributed to sustained pressure by the plasma, the main negative phase by break-up and diffusion of the plasma, which is trapped in orbits in the Van Allen belt, and the recovery by conversion of trapped protons into neutral hydrogen.

551.507.362:061.3 1587
I.G.Y. Rockets and Satellites: A Report on the Moscow Meetings, August 1958—W. W. Kellogg. (*Planet. Space Sci.*, vol. 1, pp. 71–84; January, 1959.) A report of the Technical Symposia on Rockets and Satellites which formed part of the proceedings of the Fifth Meeting of C.S.A.G.I. in Moscow, July 31–August 9, 1958.

551.507.362.2+629.19 1588
Artificial Earth Satellites and Space Travel: Part 2—Satellite and Moon-Probe Design—C. W. M. Tilenius. (*VDI Z.*, vol. 102, pp. 85–92 and 121–127; January 21, and February 1, 1960.) A comparison is made of the design of satellites and moon probes launched up to about mid-1959 and details of their instrumentation are given. Part 1: 1215 of April.

551.507.362.2 1589
Application of Hansen's Theory to the Motion of an Artificial Satellite in the Gravitational Field of the Earth—P. Musen. (*J. Geophys. Res.*, vol. 64, pp. 2271–2279; December, 1959.) A numerical theory, suitable for solution by computer, which has been applied in the Vanguard program.

551.507.362.2 1590
Re-entry of the Sputnik I Rocket—I. Harris and R. Jastrow. (*Planet. Space Sci.*, vol. 1, pp. 37–39; January, 1959.) An analysis of radar observations of satellite 1957α. The probable point of impact was latitude 45° N, longitude 106°E, in Outer Mongolia.

551.507.362.2 1591
Decay of Spin in Sputnik I—J. W. Warwick. (*Planet. Space Sci.*, vol. 1, pp. 43–49; January, 1959.) A secular change in spin-fading rate which occurred during the period October 4–24, 1957 is used to determine the atmospheric density near perigee.

551.507.362.2 1592
Magnetic Damping of Rotation of Satellite 1958 β2—R. H. Wilson, Jr. (*Science*, vol. 130, pp. 791–793; September 25, 1959.) From radio observation of Vanguard I eddy-current induction theory gives a value of 0.115 ±0.001 G for the mean magnetic field normal to the spin axis of the satellite.

551.507.362.2 1593
Geomagnetic Rotational Retardation of Satellite 1959 α1 (Vanguard II)—R. H. Wilson, Jr. (*Science*, vol. 131, pp. 223–225; January 22, 1960.) Radio observations indicated a rapid exponential retardation of satellite rotation. Analysis of EM couples acting on the conducting and magnetic parts of the satellite gives a value of 0.158 G for the mean ambient geomagnetic field and confirms the eddy-current theory applied to Vanguard I (1952 above).

551.507.362.2:523.165 1594
Study of the Cosmic-Ray Soft Component by the 3rd Soviet Earth Satellite—S. N. Vernov, A. E. Chudakov, E. V. Gorchakov, J. L. Logachev, and P. V. Vakulov. (*Planet. Space Sci.*, vol. 1, pp. 86–93; April, 1959.)

551.507.362.2:551.510.535 1595
Measurement of Solar and Diurnal Effects in the High Atmosphere by Artificial Satellites—H. A. Martin and W. Priester. (*Nature, Lond.*, vol. 185, pp. 600–601; February 27, 1960.)

551.507.362.2:551.510.535 1596
Observations of the Russian Satellites and the Structure of the Outer Terrestrial Atmosphere—H. K. Paetzold. (*Planet. Space Sci.*, vol. 1, pp. 115–124; April, 1959.) Radio and optical observations are analyzed.

551.507.362.2:551.510.535 1597
The Determination of the Electron Distribution in the Upper Ionosphere from Satellite Doppler Observations—F. H. Hibberd and J. A. Thomas. (*J. Atmos. Terr. Phys.*, vol. 17, pp. 71–81; December, 1959.) By simultaneous reception at two frequencies, one of which is an approximate multiple of the other, a monotonic electron distribution can be determined exactly. The method is illustrated for Sputnik I.

551.507.362.2:551.510.535 1598
Derivation and Analysis of Atmospheric Density from Observations of Satellite 1958 Epsilon—G. F. Schilling and C. A. Whitney. (*Planet. Space Sci.*, vol. 1, pp. 136–145; April, 1959.)

551.507.362.2:551.510.535 1599
The Density Distribution in the Upper Atmosphere—K. H. Schmidt. (*Naturwiss.*, vol. 46, p. 138; February, 1959.) The results of measurements of atmospheric density made by earth satellites are plotted as a function of altitude in comparison with curves for two model atmospheres.

551.507.362.2:551.510.535 1600
Absorption and Electron Distribution in the F_2 Layer determined from Measurements of Transmitted Radio Signals from Earth Satellites—A. N. Kazantsev. (*Planet. Space Sci.*, vol. 1, pp. 130–135; April, 1959.) A comparison is made between measured and theoretically derived values of field strength of received signals on 20 mc when the satellite is in the region of maximum electron concentration and in regions above and below this level. Field-strength curves for distances up to 16,000 km are given.

551.507.362.2:621.317.361 1601
Measurement of the Doppler-Fizeau Effect with Artificial Satellites—G. Boudouris, J. Bournazel, and E. Vassy. (*Onde élect.*, vol. 39, pp. 934–938; December, 1959.) A simple method is described for measuring the Doppler frequency within ±1 cps by comparison with the signal from a calibrated LF oscillator.

551.507.362.2:621.391.812.33 1602
The Scintillation of Radio Signals from Satellites—K. C. Yeh and G. W. Swenson, Jr. (*J. Geophys. Res.*, vol. 64, pp. 2281–2286; December, 1959.) Signals from satellites 1957 α2, and 1958 δ2, recorded during a 20-month period, are analyzed for evidence of scintillation. Night-time scintillation correlates with ionospheric "spread F" and apparently originates at heights of about 220 km at latitudes greater than 40°N. Daytime scintillation appears to originate in smaller inhomogeneous regions below 220 km more widely distributed in latitude.

551.507.362.2:621.391.812.6 1603
Observations of Ionization Induced by Artificial Earth Satellites—J. D. Kraus, R. C. Higgy, D. J. Scheer, and W. R. Crone. (*Nature, Lond.*, vol. 185, pp. 520–521; February 20, 1960.) Major enhancements of WWV 20-mc signals occur 15 minutes before and 8 minutes after the time of nearest approach of 1958 δ. Radar echoes which appear to originate at range of 1958 δ are discussed.

551.510.53 1604
Energy Sources of the Upper Atmosphere—V. I. Krassovsky. (*Planet. Space. Sci.*, vol. 1, pp. 14–19; January, 1959.) Variable heating of the upper atmosphere is considered to be caused by electric currents which are induced by magnetic fields "frozen" into the corpuscular streams.

551.510.53:551.507.362 1605
An Interim Atmosphere derived from Rocket and Satellite Data—I. Harris and R. Jastrow. (*Planet. Space Sci.*, vol. 1, pp. 20–26; January, 1959.) A model atmosphere is proposed for temperatue latitudes at altitudes up to 400 km.

551.510.535 1606
Large-Scale Movements of Ionization in the Ionosphere—D. F. Martyn. (*J. Geophys. Res.*, vol. 64, pp. 2178–2179; December, 1959.) An instability mechanism for deviations in ionization density is suggested for which the predicted temporal and spatial morphologies appear to be consistent with those of the occurrence of sporadic E, spread F and radio-star scintillations.

551.510.535 1607
Fall-Day Auroral-Zone Atmospheric Structure Measurements from 100 to 188 km.—R. Horowitz, H. E. LaGow and J. F. Giuliani. (*J. Geophys. Res.*, vol. 64, pp. 2287–2295; December, 1959.) Atmospheric density and pressure profiles are obtained using measurements made with rocket-borne ionization gauges.

551.510.535 1608
A Relationship between the Lower Ionosphere and the [OI] 5577 Nightglow Emission—J. W. McCaulley and W. S Hough. (*J. Geophys. Res.*, vol. 64, pp. 2307–2313; December, 1959.) Correlation is found between the 5577 Å emission and radio echoes obtained with a 0.1–2 mc ionosonde.

551.510.535 1609

The Electron Density Distribution in the F Region of the Ionosphere—A. J. Hirsh. (*J. Atmos. Terr. Phys.*, vol. 117, pp. 86–95; December, 1959.) A theory of electron loss in the ionosphere [414 of 1957 (Bates & Massey)], is examined in numerical detail. Under certain conditions which are well defined, the theory leads to the type of $h'(f)$ curve observed in practice for the lower F region. See also 2579 of 1959 (Yonezawa *et al.*).

551.510.535 1610

Ionization below the Night-Time F Layer—J. E. Titheridge. (*J. Atmos. Terr. Phys.*, vol. 17, pp. 126–133; December, 1959.) Using the method described in 1616 below, the low-lying ionization for Slough and Watheroo has been studied throughout summer and winter nights during periods of maximum and minimum solar activity. The decay of ionization was consistent with an effective recombination coefficient of 2×10^{-8} cm³/sec.

551.510.535 1611

Travelling Disturbances Originating in the Outer Ionosphere—K. Bibl and K. Rawer. (*J. Geophys. Res.*, vol. 64, pp. 2232–2238; December, 1959.) The vertical velocity component of traveling disturbances coming from outside and propagating through the ionosphere is determined as 115 ± 35 msec. Oscillation-like phenomena have a large range of quasi-periods between $\frac{1}{4}$ and 12 hours.

551.510.535:532.5:061.3 1612

International Symposium on Fluid Mechanics in the Ionosphere—(*J. Geophys. Res.*, vol. 62, pp. 2037–2238; December, 1959.) Review and verbatim report of the transactions of a symposium held in New York, July 9–15, 1959. Some of the papers presented are listed below, others have been abstracted separately.

a) **Constitution of the Atmosphere at Ionospheric Levels**—M. Nicolet (pp. 2092–2101).

b) **Ionizations and Drifts in the Ionosphere**—J. A. Ratcliffe (pp. 2102–2111).

c) **Measurements of Turbulence in the 80- to 100-km Region from the Radio Echo Observations of Meteors**—J. S. Greenhow and E. L. Neufeld (pp. 2129–2133).

d) **Scattering of Waves and Microstructure of Turbulence in the Atmosphere**—A. M. Oboukhov (pp. 2180–2187).

e) **Effect of a Magnetic Field on Turbulence in an Ionized Gas**—J. W. Dungey (pp. 2188–2191).

f) **Note on some Observational Characteristics of Meteor Radio Echoes**—P. M. Millman (pp. 2192–2194).

g) **On the Spectrum of Electron Density Produced by Turbulence in the Ionosphere in the Presence of a Magnetic Field**—I. D. Howells (pp. 2198–2199).

h) **Evidence of Elongated Irregularities in the Ionosphere**—B. Nichols (pp. 2200–2202).

i) **Geomorphology of Spread F and Characteristics of Equatorial Spread F**—R. W. H. Wright (pp. 2203–2207).

j) **An Interpretation of certain Ionospheric Motions in Terms of Atmsopheric Waves**—C. O. Hines (pp. 2210–2211).

k) **On the Influence of the Magnetic Field on the Character of Turbulence in the Ionosphere**—G. S. Golitsyn (pp. 2212–2214).

l) **Magnetohydrodynamics of the Small-Scale Structure of the F Region**—J. P. Dougherty (pp. 2215–2216).

m) **Electrodynamic Stability of a Vertically Drifting Ionospheric Layer**—J. A. Fejer (pp. 2217–2218).

n) **Turbulent Spectra in a Stably Stratified Atmosphere**—R. Bolgiano, Jr. (pp. 2226–2229).

o) **Relation of Turbulence Theory to Ionospheric Scatter Propagation Experiments**—A. D. Wheelon (pp. 2230–2231). Summary only.

551.510.535:550.385 1613

Geomagnetic Distortion of the F_2 Region on the Magnetic Equator: Part 2—H. Maeda. (*J. Geomag. Geoelect.*, vol. 11, pp. 1–5; 1959.) An extension of work described earlier [see 3257 of 1955 or 424 of 1956 (Hirono and Maeda)] to study the relation between diurnal variations of f_0F_2 for years of different sunspot number and the phase of geomagnetic S_q variations. F_2-region distortion is explained by vertical ionization drift due to the es field extended from the E region.

551.510.535:551.594.6 1614

Constant Ionosphere Height for Audio-Frequency Propagation—F. Hepburn. (*Nature, Lond.*, vol. 185, p. 599; February 27, 1960.) From an analysis of smooth-type waveforms (3312 of 1959) a constant height of 83 km ±2 km has been estimated for winter storms. There was no systematic variation with the onset of night-time conditions.

551.510.535:621.391.812.63 1615

The Calculation of Real and Virtual Heights of Reflection in the Ionosphere—J. E. Titheridge. (*J. Atmos. Terr. Phys.*, vol. 17, pp. 96–109; December, 1959.) A method is described by which an $N(h)$ profile can be calculated using only about 20 readings of either the ordinary or extraordinary $h'(f)$ trace. The calculation, which takes about 15 minutes, can be used in reverse to derive an $h'(f)$ curve from an $N(h)$ profile.

551.510.535:621.391.812.63 616

The Use of the Extraordinary Ray in the Analysis of Ionospheric Records—J. E. Titheridge. (*J. Atmos. Terr. Phys.*, vol. 17, pp. 110–125; December, 1959.) It is shown that, by using the ordinary and extraordinary traces, estimates may be made of the electron content and also the electron density distribution in a) the region represented by reflections at frequencies less than f_{min}; b) in the valley between the E and F layers.

551.510.535(98):523.164 1617

An Example of Heavy Absorption in the V.H.F. Band in the Arctic Ionosphere—L. Harang and J. Tröim. (*Planet. Space Sci.*, vol. 1, pp. 102–104; April, 1959.) Observations of meteor echoes and of RF noise from the Cassiopeia source, in the 40–45-mc band show very heavy absorption in the early morning of July 7, 1958.

551.594 1618

Observations of Unusual Radiofrequency Noise Emission and Absorption at 80 Mc/s—H. J. A. Chivers and H. W. Wells. (*J. Atmos. Terr. Phys.*, vol. 17, pp. 13–19; December, 1959.) The noise enhancements observed during periods of solar activity are classified as smooth or abrupt. While smooth changes occur in both day and night hours, the abrupt increases are observed only near local midnight. The smooth enhancements occur almost simultaneously with the absorption of radiation in a sector of the northern sky.

551.594.5 1619

Hydrogen Emission and Two Types of Auroral Spectra—G. I. Galperin. (*Planet. Space Sci.*, vol. 1, pp. 57–62; January, 1959.) Various characteristics of auroral activity including radio reflections have been correlated with the hydrogen emission.

551.594.5:523.164 1620

Auroral Ionization and the Absorption and Scintillation of Radio Stars—H. J. A. Chivers and J. S. Greenhow. (*J. Atmos. Terr. Phys.*, vol. 17, pp. 1–12; December, 1959.) The absorption of radiation from Cygnus, when observed at low latitudes, and radar back-scatter echoes are related to a layer associated with auroral activity.

551.594.5:539.16 1621

Artificial Auroras Resulting from the 1958 Johnston Island Nuclear Explosions—J. M. Malville. (*J. Geophys. Res.*, vol. 64, pp. 2267–2270; December, 1959.)

551.594.5:621.391.8 1622

A Daytime Maximum of Oblique Auroral Reflexions Observed in the Auroral Zone—A. Egeland, B. Hultqvist, and J. Ortner. (*Nature, Lond.*, vol. 185, p. 519; February 20, 1960.) Observations made at 92.8 mc over the period March–June 1959 show a daytime maximum between 1200–1600 MET.

551.594.5:621.391.812.6.029.63 1623

Observed Characteristics of an Ultra-High-Frequency Signal Traversing an Auroral Disturbance—James, Bird, Ingalls, Stone, Day, Lockwood, and Presnell. (*See* 1749.)

551.594.6 1624

A Comparison of Sferics as Observed in the Very-Low-Frequency and Extremely-Low-Frequency Bands—L. R. Tepley. (*J. Geophys. Res.*, vol. 64, pp. 2315–2329; December, 1959). The VLF component is almost always followed by a component of extremely low frequency (10–1000 cps), but about one-third of these ELF components are not preceded by VLF components. Positive-polarity ELF waveforms predominant during daytime and their median amplitudes always exceed those of the negative-polarity waveforms which predominate at night.

551.594.6 1625

Sweepers—N. C. Gerson and W. H. Gossard. (*J. Atmos. Terr. Phys.*, vol. 17, pp. 82–85; December, 1959.) Sweepers are atmospherics which are present in the HF band predominating between 20 and 30 mc. Many of them occur in trains where the period between successive sweepers is nearly constant. Frequency coverage for any sweeper can vary from 75 to 1500 kc and may have a duration varying between 0.1 and 18 seconds.

551.594.6:621.391.812.63 1626

The Propagation of Electromagnetic Waves in Ionized Gases (with Special Reference to "Whistlers"): Parts 1 & 2.—Northover. (*See* 1759.)

LOCATION AND AIDS TO NAVIGATION

621.396.96 1627

In Fog and Rain—Sight, IR or Radar?—M. E. Seymour. (*Electronics*, vol. 33, pp. 64–66; January 29, 1960). Tables and curves are given for the comparison of infrared and radar systems of detection under various weather conditions.

621.396.96 1628

Experimental Determination of the Radar Scatter Cross-Section of Cylindrical Metal Objects—E. Meyer, H. Kuttruff, and H. Severin. (*Z. angew. Phys.*, vol. 11, pp. 1–6; January, 1959.) Measurements of the scatter cross-section of metal cylinders with length/diameter ratio 10:1 were made using EM and acoustic waves. The cross section was measured as a function of angle of incidence and of ratio $l:\lambda$ in the range 1.8–25, and was found to increase monotonically with this ratio.

621.396.96:621.317.3 1629

Noise Temperature in a Radar System—H. H. Grimm. (Proc. IRE, vol. 48, p. 246; February, 1960.) Note of measurements made on an L-band radar system using parametric amplifying circuits.

621.396.963.325 1630

Statistical Properties, Frequency Spectrum and Suppression of Low Frequencies in Radar P.P.I. Displays—H. Groll and E. Vollrath. (*Nachrichtentech. Z.*, vol. 12, pp. 33–40; January, 1959.) The statistical distribution of targets as a function of display radius is determined and the relation of radar-signal frequency spectrum to display content is discussed. The effect of low-frequency suppression by means of signal-controlled carrier modulation is described.

MATERIALS AND SUBSIDIARY TECHNIQUES

531.788:621.385.032.94 1631

Outgassing caused by Electron Bombardment of Glass—B. J. Todd, J. L. Lineweaver, and J. T. Kerr. (*J. Appl. Phys.* vol. 31, pp. 51–55; January, 1960.) The method of measuring outgassing by bombardment with 20-kev electrons is described. Oxygen was found to be the main constituent of the gas produced by the electron bombardment.

531.788.7 1632

The Magnetron Gauge: a Cold-Cathode Vacuum Gauge—P. A. Redhead. (*Canad. J. Phys.*, vol. 37, pp. 1260–1271; November, 1959.) An ionization gauge with axial magnetic field is described. The ion-current/pressure relation is linear over the range $10^{-4}-5+10^{-10}$ mm Hg and the sensitivity about 45 times greater than that of a standard Bayard-Alpert gauge.

535.5:061.3 1633

International Symposium on Residual Gases in Electron Tubes and Similar High-Vacuum Systems—(*Nuovo Cim.*, vol. 12, supplement pp. 297–329; 1959). Summaries, some in English, are given of papers presented at a symposium held at Como, September 23–25, 1959.

535.215:539.23 1634

Formation of Caesium Antimonide: Part 1—Electrical Resistivity of the Film of Caesium-Antimony System—K. Miyake. (*J. Appl. Phys.*, vol. 31, pp. 76–81; January, 1960.) The preparation of Cs-Sb films in which the atomic ratio of Cs to Sb varied from 0.91 to 4.86 is described. Measurements of their resistivity in the range $-70°$ to $+70°$C are given, and thermal activation energies deduced.

535.215:546.48'221 1635

Contactless Electrical Excitation of Electrons in CdS Single Crystals—K. W. Böer and U. Kümmel. (*Z. Naturf.*, vol. 13a, pp. 698–699; August, 1958.) Conductivity glow curves were obtained using an experimental arrangement in which direct contact between metal electrodes and crystal surface is avoided by means of mica inserts. Results agree with those obtained by direct-contact methods.

535.215:546.48'221 1636

Application of Electro-optical Effects in the Analysis of the Electrical Conduction Process in CdS Single Crystals—K. W. Böer, H. J. Hänsch, and U. Kümmel. (*Z. Phys.*, vol. 155, pp. 170–183; May 22, 1959.) Description of electro-optical methods for rendering visible current and electric-field inhomogeneities (see also 3757 of 1959). Photographs of some of the effects obtained are reproduced and discussed.

535.215:546.482'21 1637

Inhomogeneous Field Distribution in CdS Single Crystals in the Range of High Field Strengths—K. W. Böer. (*Z. Phys.*, vol. 155, pp. 184–194; May 22, 1959.) Optical effects obtained by the method discussed in 1636 above are ascribed to internal field-strength inhomogeneities. A mechanism is proposed which may lead to a revised conception of the process of electrical breakdown.

535.215:546.48'221:548.0 1638

Dislocations in Two Types of CdS Crystals.—D. C. Reynolds and S. J. Czyzak. (*J. Appl. Phys.*, vol. 31, pp. 94–98; January, 1960.)

535.215:546.883 1639

Field Dependence of Photoelectric Emission from Tantalum—J. L. Gumnick and D. W. Juenker. (*J. Appl. Phys.*, vol. 31, pp. 102–108; January, 1960.) An accelerating electric field was used.

535.37:546.47'221 1640

Some Properties of Zinc Sulphide Crystals Grown from the Melt—A. Addamiano and M. Aven. (*J. Appl. Phys.*, vol. 31, pp. 36–39; January, 1960.) Density and stability of structure were studied for annealing temperatures in the range 700°–1150°C.

535.37:546.48'221 1641

Exciton Spectrum of Cadmium Sulphide—D. G. Thomas and J. J. Hopfield. (*Phys. Rev.*, vol. 116, pp. 573–582; November 1, 1959.) Measurements of reflectance and fluorescent spectra at 77° and 4.2°K are described. The reflectivity results lead to the idenitification of three exciton series which are discussed with reference to the band structures at $\mathbf{k}=0$.

535.37:546.48'221 1642

A.C. Impedance Measurements on Insulated CdS Crystals—H. Kallmann, B. Kramer, and G. M. Spruch. (*Phys. Rev.*, vol. 116, pp. 628–632; November 1, 1959.)

537.227 1643

Variation in Ferroelectric Characteristics of Lead Zirconate Titanate Ceramics due to Minor Chemical Modifications—R. Gerson. *J. Appl. Phys.*, vol. 31, pp. 188–194; January, 1960.) The changes in the properties of lead zirconate titanate due to niobium or lanthanum additions are attributed to a high domain-wall mobility in response to applied electric fields.

537.227 1644

Structure of Ferroelectric Domains in Triglycine Sulphate—H. Toyoda, S. Waku, and H. Hirabayashi. (*J. Phys. Soc. Japan*, vol. 14, pp. 1003–1011; August, 1959.) Domain structures are studied by etching in various alcohols.

537.227 1645

Etch Pits corresponding to Dislocations in Ferroelectric Guanidinium Aluminum Sulphate Hexahydrate—T. Nakamura. (*J. Phys. Soc. Japan*, vol. 14, pp. 1022–1029; August, 1959.)

537.227:621.318.57 1646

Model for Switching and Polarization Reversal in Colemanite—H. H. Wieder. (*J. Appl. Phys.*, vol. 31, pp. 180–187; January, 1960.) A model based on random nucleation followed by extensive sideways displacement of the 180 degrees nucleated domains is proposed for the switching mechanism. It gives good agreement with experimental characteristics.

537.228.1 1647

Piezoelectric Properties of Polycrystalline Lead Titanate Zirconate Compositions—D. A. Berlincourt, C. Cmolik, and H. Jaffe. (PROC. IRE, vol. 48, pp. 220–229; February, 1960.) Data are given for the low-signal elastoelectric properties of compositions ranging from $PbZr_{0.48}Ti_{0.52}O_3$ to $PbZr_{0.6}Ti_{0.4}O_3$.

536.228.1 1648

Reduction of Frequency-Temperature Shift of Piezoelectric Crystals by Application of Temperature-Dependent Pressure—E. A. Gerber. (PROC. IRE, vol. 48, pp. 244–245; February, 1960.) A control system is described for use where crystal ovens are not practicable. Pressure is applied to the crystal by a bimetal strip.

537.228.1:549.514.51 1649

Effect of Initial Stress in Vibrating Quartz Plates—A. D. Ballato and R. Bechmann. (PROC. IRE, vol. 48, pp. 261–262; February, 1960.) Experimental curves show the effect on the frequency of vibration of compressional stress applied to the edge.

537.311.32:546.22:539.12.04 1650

Bombardment Conductivity and Photoconductivity in Rhombic Sulphur—P. J. Dean, B. S. H. Royce, and F. C. Champion. (*Proc. Phys. Soc.*, vol. 75, pp. 119–135; January 1, 1960.)

537.311.33+537.226 1651

The Influence of Field Emission on the Distribution of Strong Fields in Solids—E. I. Adirowitsch (Adirovich). (*Z. Phys.*, vol. 155, pp. 195–205; May 22, 1959.) The kinetics of changes in inhomogeneous field distribution in solid dielectrics and semiconductors are investigated with reference to Böer's interpretation of the phenomena (1637 above).

537.311.33 1652

Shapes of Etch Hillocks and Pits and their Correlation with Measured Etch Rates—B. A. Irving. (*J. Appl. Phys.*, vol. 31, pp. 109–111; January, 1960.) Gives a condition for hillock stability additional to those of Batterman (1186 of 1958).

537.311.33 1653

Theory of Inversion Layers on Semiconductor Surfaces—E. Groschwitz and R. Ebhardt. (*Z. angew. Phys.*, vol. 11, pp. 9–19; January, 1959.) The physical properties and construction of inversion layers are investigated, without and with the application of an external field.

537.311.33 1654

On the Frequency Dependence of the Field Effect in Semiconductors: Part 2—A. E. Yunovich. (*Fiz. Tverdogo Tela*, vol. 1, pp. 1092–1101; July, 1959.) Results of an analysis for the case when current carriers of both signs are present in the bulk of the semiconductor and on its surface, show that the frequency dependence of the field effect is governed by certain time constants. Expressions are obtained for the effective mobility and conditions are given under which minority carriers can be neglected. For earlier work see 2788 of 1958 and *Zh. tekh. Fiz.*, vol. 28, pp. 698–693; April, 1958.

537.311.33 1655

The Effect of an Electric Field on the Decay of Excess Carriers in Semiconductors—B. K. Ridley. (*Proc. Phys. Soc.*, vol. 75, pp. 157–161; January 1, 1960.) "Sweep-out" effects increase the decay rate and can affect the form of the decay. Expressions are given for the decay rate when the decay curve is approximately exponential; results agree with experimental data for one sample.

537.311.33 1656

Minority-Carrier Current in a Linearly Graded Drift Field—D. P. Kennedy. (*J. Appl. Phys.*, vol. 31, pp. 218–219; January, 1960.) Equations are given, with the results of some numerical calculations.

537.311.33 1657

On a Relation between Various Theories for the Scattering of Current Carriers in Semiconductors—G. E. Pikus. (*Zh. tekh. Fiz.*, vol. 28, pp. 2390–2401, November, 1958.) Mathematical analysis based on the Bardeen-Shockley deformation-potential theory. When the energy minimum is not located in the center of the Brillouin zone the Berthe-Sommerfeld scattering theory leads to the same results as the deformation-potential method.

537.311.33 1658
Application of the Equivalent Orbital Method to the Study of Band Structure in $A^{III}B^{V}$ Compounds—A. I. Gubanov and A. A. Nran'yan. (*Fiz. Tverdogo Tela*, vol. 1, pp. 1044–1052; July 1959.)

537.311.33:535.215:538.63 1659
New Parallel Photoelectromagnetic Effect—A. Amith. (*Phys. Rev.*, vol. 116, pp. 330–333; October 15, 1959.) The effect described is the net flow of carrier pairs in a direction transverse to the applied magnetic field, due to a difference in surface recombination velocities of opposite parallel surfaces. Theory is given and experiments on an n-type Ge crystal $0.2\times 1.2\times 0.7$ cm are described.

537.311.33:535.215–15 1660
The Theory of Optical Properties of Electronic Semiconductors in the Infrared Region of the Spectrum—V. I. Cherepanov. (*Fiz. Tverdogo Tela*, vol. 1, pp. 1035–1043; July, 1959.)

537.311.33:536.21.083 1661
Measurement of Thermal Conductivity of Semiconductors near Room Temperature—A. V. Ioffe and A. F. Ioffe. (*Zh. tekh. Fiz.*, vol. 28, pp. 2357–2363; November, 1958.) Brief description of an improved apparatus and discussion of its performance.

537.311.33:537.32 1662
Method of Eliminating Heat from Semiconductor Cooling Devices—E. A. Kolenko, A. G. Shcherbina and V. G. Yur'ev (*Zh. tekh. Fiz.*, vol. 28, pp. 2543–2545; November, 1958.) Brief description of the method, and list of useful substances which have a high latent heat of fusion.

537.311.33:537.324 1663
Investigation of the Intermetallic Compound Bi_2Te_3 and the Solid Solutions $Bi_{2-x}Sb_xTe_3$ and $Bi_2Te_{3-x}Se_x$ with regard to their Suitability as Material for Semiconductor Thermoelements—U. Birkholz. (*Z. Naturforsch.*, vol. 13a, pp. 780–792; September, 1958.) Thermoelectric characteristics were determined for a number of materials. A thermoelement of p-type $Bi_{0.6}Sb_{1.4}Te_3$ with n-type Bi_2Te_3 had an experimentally determined efficiency of 2.14×10^{-3} per °C, equivalent to a maximum of Peltier-effect cooling of 80°C.

537.311.33:546.24 1664
On the Structure of the Hole Band in Tellurium—L. I. Korovin and Yu. A. Firsov. (*Zh. tekh. Fiz.*, vol. 28, pp. 2417–2427; November, 1958.) The observed close dependence of the absorption coefficient on the polarization of incident infrared radiation is used to define more accurately the hole band structure in Te. It is shown that this band has one degenerate extreme for $k=0$ or two degenerate extrema along the k_z axis.

537.311.33:546.24 1665
Hot Holes in Tellurium—Y. Kania. (*J. Phys. Soc. Japan*, vol. 14, p. 1118; August, 1959). Measurements made at 77°K indicate that the energy loss of holes in Te is due mainly to acoustic-phonon scattering.

537.311.33:[546.28+546.289 1666
Germanium and Silicon Liquidus Curves—C. D. Thurmond and M. Kowalchik. (*Bell Sys. Tech. J.*, vol. 39, pp. 169–204; January, 1960.) Supplementing existing results with new measurements, it is reported that all but 2 of 26 binary-system liquidus curves can be described by a two-constant equation. Evidence is cited indicating that the constants of the equation can be used to estimate the excess free energy of the solutions. 55 references.

537.311.33:[546.28+546.289 1667
Ion-Bombardment Etching of Silicon and Germanium—J. A. Dillon, Jr., and R. M. Oman. (*J. Appl. Phys.*, vol. 31, pp. 26–28; January, 1960.) Etch patterns greatly differing from those produced by chemical etching are obtained.

537.311.33:[546.28+546.289 1668
Mass-Spectrometer Determination of the Amount and Composition of Gases Absorbed on the Surface of Germanium and Silicon Single Crystals—V. M. Kozlovshaya. (*Fiz. Tverdogo Tela*, vol. 1, pp. 1027–1034; July, 1959.)

537.311.33:[546.28+546.289 1669
Solid Solubilities of Impurity Elements in Germanium and Silicon—F. A. Trumbore. (*Bell Sys Tech. J.*, vol. 39, pp. 205–233; January, 1960.) New results for Pb-Ge, Zn-Ge, In-Ge, Sb-Si, Ga-Si, and Al-Si systems are compared with existing data. The correlation of solid solubilities k^{o} and $k^{o\prime}$ with heats of solution and atom size of impurity elements is considered. 90 references.

537.311.33:546.28 1670
Thermal Expansion of Silicon—L. Maissel. (*J. Appl. Phys.*, vol. 31, p. 211; January, 1960.) New measurements of the expansion coefficient in the temperature range 50–850°C, for (111) and (110) crystal orientations.

537.311.33:546.28 1671
The Temperature Dependence of the Low-Level Lifetime and Conductivity Mobility of Carriers in Silicon—D. M. Evans. (*J. Electronics Control*, vol. 7, pp. 112–122; August, 1959.) "The temperature dependence of the low-level lifetime in silicon has been found to be consistent with that expected from the theory based on a low level of injection, a low density of recombination centres and a single energy level for the recombination centres. The temperature dependence of the conductivity mobility has also been determined."

537.311.33:546.28 1672
Impurity Effects upon Mobility in Silicon—R. A. Logan and A. J. Peters. (*J. Appl. Phys.*, vol. 31, pp. 122–124; January, 1960.) Measurements on sufficiently pure silicon show a mobility/temperature variation of the form $T^{-1.5}$ for n-type and T^{-2} for p-type material, at temperatures below 100°K. At higher temperatures the mobility is further reduced, presumably by optical-mode scattering.

537.311.33:546.28 1673
High-Field Effect in Boron-Doped Silicon—R. D. Larrabee. (*Phys. Rev.*, vol. 116, pp. 300–301; October 15, 1959.) A linear current/voltage relation was observed at 77°K up to fields of 10^{4} v/cm.

537.311.33:546.28:538.569.4 1674
Millimetre Cyclotron Resonance in Silicon—C. J. Rauch, J. J. Stickler, H. J. Zeiger, and G. S. Heller. (*Phys. Rev. Lett.*, vol. 4, pp. 64–66; January 15, 1960.) Measurements are reported at 2.1 mm λ on high-purity n-type Si between 1.2° and 50°K.

537.311.33:546.28:539.12.04 1675
Measurement of the Lifetime of Carriers Generated in Silicon by Electron Bombardment—A. Vapaille. (*Compt. rend. acad. sci., Paris*, pp. 648–650; vol. 249.) Measurements of lifetime down to 1 μsec have been made by a pulse deflection method. The resistance of a p-type crystal increased under the effect of bombardment at energies below 15 kev; above 20 kev the resistance decreased. An unusual variation of life-time with temperature was observed in a high-resistivity p-type crystal.

537.311.33:546.28:539.12.04 1676
Energy Levels in Neutron-Irradiated n-type Silicon—G. Kupprecht and C. A. Klein. (*Phys. Rev.*, vol. 116, pp. 342–343; October 15, 1959.)

537.311.33:546.289 1677
Procedure against Thermal Conversion in Germanium—O. Mikami. (*Rep. Elect. Commun. Lab., Japan*, vol. 7, pp. 204–206; June, 1959.) The Ge wafer is etched in a CP-4 solution, washed in distilled deionized water and annealed for four hours at 490–500°C in a quartz tube which has been washed with aqua regia and fluoric acid.

537.311.33:546.289 1678
On the Influence of Ga and Fe on the Thermal Conductivity of Germanium—G. B. Abdullaev, G. M. Aliev, and N. I. Chetverikov. (*Zh. tekh. Fiz.*, vol. 28, pp. 2368–2371; November, 1958.)

537.311.33:546.289 1679
Interaction between Arsenic and Aluminum in Germanium—J. O. McCaldin. (*J. Appl. Phys.*, vol. 31, pp. 89–94; January, 1960.) It is found that As diffusing in Ge at 800°C is attracted to regions of heavy Al doping, and these regions show an enhanced solubility for As.

537.311.33:546.289 1680
Electronic Surface States and the Cleaned Germanium Surface—P. Handler and W. M. Portnoy. (*Phys. Rev.*, vol. 116, pp. 516–526; November, 1959.) The surface conductivity and the field-induced surface conductivity are shown to be almost independent of temperature over the range 77°–300°K. A qualitative two-dimensional band model is presented which correlates most of the experimental results.

537.311.33:546.289 1681
Remarks on the Oxidation, after Heat Treatment, of Germanium Surfaces Oriented along a (111) Plane—L. Gouskor. (*Compt. rend. acad. sci., Paris*, vol. 249, pp. 671–673; August 3, 1959.)

537.311.33:546.289 1682
The Nature of Relaxation Processes in the Field Effect—V. I. Lyashenko and N. S. Chernaya. (*Fiz. Tverdogo Tela*, vol. 1, pp. 1005–1014; July, 1959.) Report of an investigation of long-term changes in the field effect in n- and p-type Ge in different atmospheres.

537.311.33:546.289:537.32:538.63 1683
The Magnetic Variation of Thermoelectric Power of Germanium at Low Temperatures—J. Erdmann. (*Z. Naturforsch.*, vol. 13a, pp. 650–662; August, 1958.) Measurements were made on Ge single crystals with various donor or acceptor concentrations in a transverse magnetic field in the temperature range 20°–90°K. Results are in qualitative agreement with Appel's theory (555 of February). See also 2794 of 1958 (Erdmann *et al.*).

537.311.33:546.289:539.23 1684
Remarks on some Electrical Properties of Very Thin Films of Germanium—C. Uny. (*Compt. rend. acad. sci., Paris*, vol. 249, pp. 645–647; August 3, 1959.) Aging effects and deviations from Ohm's law are described. Ge films show closer analogies with films of Cu than with those of Ag or Au (3350 of 1959).

537.311.33:546.431'42–31 1685
The Influence of Oxygen, Hydrogen and Water Vapour on the Electrical Conductivity of Barium Oxide and Barium-Strontium Oxide—J. Rudolph. (*Z. Naturforsch.*, vol. 13a, pp. 757–767; September, 1958.)

537.311.33:546.47–31 1686
On the Problem of Exo-electron Emission of Semi-conductors—R. Merold. (*Naturwiss.*,

vol. 46, pp. 138–139; February, 1959.) An interpretation of exo-electron emission effects in ZnO is given leading to some conclusions as to the mechanism of this process.

537.311.33:[546.681'241+546.682'241 1687
The Infrared Absorption of Gallium Telluride (Ga_2Te_3) and Indium Telluride (In_2Te_3)—G. Harbeke and G. Lautz. (*Z. Naturforsch.*, vol. 13a, pp. 775–779; September, 1958.) Evaluation and interpretation of results obtained in measurements described in 3121 of 1958, and comparison with similar investigations of other authors.

537.311.33:546.681'241 1688
The Structure Sensitivity of Gallium Telluride (Ga_2Te_3) to Very Small Additions of Cu—G. Harbeke and G. Lautz. (*Z. Naturforsch.*, vol. 13a, pp. 771–775; September, 1958.) See 3031 of 1959.

537.311.33:546.681'86 1689
Some Data on Diffusion and the Effect of Impurities on the Electrical Properties of Gallium Antimonide—B. I. Boltaks and Yu. A. Gutorov. (*Fiz. Tverdogo Tela*, vol. 1, pp. 1015–1021; July, 1959.)

537.311.33:546.682'19 1690
The Form of the Conductivity Band of Indium Arsenide—D. Geist. (*Z. Naturforsch.*, vol. 13a, pp. 699–700; August, 1958.) Results of susceptibility measurements are compared with those derived from theoretical calculations of band structure.

537.311.33:546.682'19 1691
Infrared Absorption of *n*-Type Indium Arsenide—F. Matossi. (*Z. Naturforsch.*, vol. 13a, pp. 767–770; September, 1958.) Measurements were made on InAs with donor concentration about $10^{16}cm^{-3}$ at temperatures in the range 120°–475°K. For investigations of absorption in *p*-type InAs see 3892 of 1958 (Matossi and Stern).

537.311.33:546.682'86 1692
The Formation Enthalpy of III/V Compounds—A. Schneider and K. Klotz. (*Naturwiss.*, vol. 46, p. 141; February, 1959.) The enthalpy of InSb was determined by a direct calorimetric method.

537.311.33:546.682'86 1693
Growth of InSb Crystals in the (111) Polar Direction—H. C. Gatos, P. L. Moody, and M. C. Lavine. (*J. Appl. Phys.*, vol. 31, pp. 212–213; January, 1960.) Discussion of an atomic model put forward to explain the differences observed in growth of InSb crystals depending on the polarity of the seed crystal.

537.311.33:546.682'86 1694
Behaviour of InSb Surfaces during Heat Treatment—D. Haneman. (*J. Appl. Phys.*, vol. 31, pp. 217–218; January, 1960.) Deals with the formation and movement of hillocks on the InSb surface.

537.311.33:546.682'86 1695
Thermomagnetic Effects in InSb.—V. P. Zhuze and I. M. Tsidil'kovskil. (*Zh. tekh. Fiz.*, vol. 28, pp. 2372–2381; November, 1958.) An investigation of the transverse and longitudinal Nernst-Ettingshausen effects, the thermo-EMF, the conductivity and Hall effect of seven InSb samples with differing impurity content. It is shown that for temperatures between 120° and 765°K the scattering of current carriers occurs chiefly in the acoustic mode.

537.311.33:546.682.86:538.569.4 1696
Spin Resonance of Conduction Electrons in InSb—G. Bemski. (*Phys. Rev. Lett.*, vol. 4, pp. 62–64; January 15, 1960.) A summary of spin-resonance phenomena in the concentration range 2×10^{14}–3×10^{15} electrons/cm^2.

537.311.33:[546.821–31+546.281–31 1697
Electrical Conductivity of Certain Titanium and Vanadium Oxides—S. M. Ariya and N. I. Bogdanova. (*Fiz. Tverdogo Tala*, vol. 1, pp. 1022–1026. July, 1959.)

537.311.33:621.317.3 1698
Further Consideration of Bulk Lifetime Measurement with a Microwave Electrodeless Technique—Jacobs, Ramsa, and Brand. (*See* 1729.)

537.533.8 1699
Variation of Secondary Electron Emission of Single Crystals with Angle of Incidence—A. J. Dekker. (*Phys. Rev. Lett.*, vol. 4, pp. 55–57; January 15, 1960.)

537.533.8 1700
On the Correlation of the Coefficients of Secondary Electron Emission from Nonmetals Caused [respectively] by Ion and Electron Bombardment—V. M. Lovtsov. (*Zh. tekh. Fiz.*, vol. 28, pp. 2469–2472; November, 1958.) Brief investigation of the physico-chemical properties of Mg-MgO and KCl film-type emitters. Results are shown graphically

537.533.8 1701
Electron Reflection Reflection and Secondary Electron Emission from Metallic Surfaces for Low-Energy Primary Electrons: Part 2—I. M. Bronshteln and V. V. Roshchin. (*Zh. tekh. Fiz.*, vol. 28, pp. 2476–2486; November, 1958.) Investigation on the secondary emission from Pt, Cu, Ag, Au and Al. Part 1: 234 of January.

537.533.8:539.23 1702
Temperature Dependence of the Secondary Electron Emission Coefficient of NaCl Films—M. V. Gomoyunova. (*Zh. tekh. Fiz.*, vol. 28, pp. 2473–2475; November, 1958.) It is shown that in the temperature range $-196°$ to 320°C the emission coefficient can be expressed by Dekker's formula (3194 of 1954).

537.583 1703
Variation of the Work Function of an Electron from a Metal under the Influence of an Absorbed Layer of Molecules of Barium Oxide—N. D. Morgulis. (*Fis. Tverdogo Tela*, vol. 1, pp. 1125–1132; July, 1959). Experimental investigation of the temperature dependence of the work function and the effect of BaO molecules deposited on the base layer of a metal.

538.221 1704
Spontaneous Magnetizations of some Gadolinium Alloys—S. Arajs and D. S. Miller. (*J. Appl. Phys.*, vol. 31, pp. 213–215; January, 1960.) Special attention is paid to the variation of magnetization with temperature.

538.221 1705
Internal Ferromagnetic Resonance in Small Cobalt Particles—J. C. Anderson. (*Proc. Phys. Soc.*, vol. 75, pp. 33–39; January 1, 1960.)

538.221 1706
Internal Ferromagnetic Resonance in Magnetite—J. C. Anderson and B. Donovan. (*Proc. Phys. Soc.*, vol. 75, pp. 149–151; January 1, 1960.) Results are quoted for a colloidal suspension of magnetite over the temperature range 30°–90°C.

538.221 1707
Investigation of Weak Ferromagnetism in the $MnCO_3$ Single Crystal—A. S. Borovik-Romanov. (*Zh. Eksp. Teor. Fiz.*, vol. 36, pp. 766–781; March, 1959.) Description of experiments carried out in the temperature range 1.3–300°K. A ferromagnetic moment is observed only in the base plane; along the trigonal axis the crystal is paramagnetic. In the temperature range 1.5–23°K, the ferromagnetic moment is proportional to the square of the temperature. Theoretical formalas are obtained which are qualitatively in agreement with experimental results.

538.221:537.122 1708
On the Interaction between Conduction Electrons in Ferromagnetics—A. I. Akhiezer and I. Ya. Pomeranchuk. (*Zh. Eksp. teor. Fiz.*, vol. 36, pp. 859–862; March, 1959.) Analysis showing that in a ferromagnetic material there is an additional attraction between conduction electrons which is due to spin-wave exchange.

538.221:621.318.124 1709
Cobalt-Free Ferrites with Perminvar Loop—E. Röss. (*Naturwiss.*, vol. 46, p. 65; January, 1959.) Note on polycrystalline Mn-Zn ferrites with relatively stable perminvar effect.

538.221:621.318.124:548.73 1710
X-Ray Study of Ferromagnetic Domains in Cobalt Zinc Ferrite—K. M. Merz. (*J. Appl. Phys.*, vol. 31, pp. 147–154; January, 1960.) Diffraction curves of the (400) reflection broadened when a magnetic field was applied to the crystal.

538.221:621.318.134 1711
Determination of Molecular Field Coefficients in Ferrimagnets—G. T. Rado and V. J. Folen. (*J. Appl. Phys.*, vol. 31, pp. 62–68; January, 1960.) An improved analytical method is presented for determining the three molecular field coefficients which yield the best agreement between the Néel theory and the experimental curve of saturation moment /temperature for a given ferrimagnetic material. The analysis of experimental data on samples of Li and Mg-Fe ferrites is given.

538.221:621.318.134 1712
Rectangular Hysteresis Loop Ferrites with Large Barkhausen Steps—A. P. Greifer and W. J. Croft. (*J. Appl. Phys.*, vol. 31, pp. 85–88; January, 1960.) Observations have been made at low temperatures of large discontinuities (steps) in the 60-cps hysteresis loops of polycrystalline ferrites containing copper. At the temperature for step formation, which is a function of copper content, the coercivity decreases and the loop squareness approaches unity.

538.221:621.318.134 1713
Temperature Dependence of Magnetic Crystal Anisotropy of Nickel Ferrite—G. Elbinger. (*Naturwiss.* vol. 46, p. 140; February, 1959.) The anisotropy constant was determined in the temperature range $-185°$ to $+450°$C from measurements of magnetic torque.

538.221:621.318.134 1714
The Thermomagnetic Behaviour of Pure Nickel Ferrite—L. F. Bates and H. Clow. (*Proc. Phys. Soc.*, vol. 75, pp. 17–23; January 1, 1960.) The small heat exchanges produced during the magnetization process were measured for a rod specimen at $-10°$C and $+18°$C. Some support is found for the Lilley disperse-field theory.

538.221:621.318.134 1715
Magnetization and Coercive Force of Nickel-Zinc Ferrites particularly with Added Impurities—W. Holzmüller and T. Kampf. (*Nachrichtentech. Z.*, vol. 9, pp. 44–46; January, 1959.) Measurements were made on ferrites containing impurities up to 15 per cent in volume, of BeO, ThO_2,Cr_2O_3 and WO_2, and results show that irreversible magnetization effects are due to Bloch-wall displacements.

538.221:631.318.134 1716
Concerning the Arbitrary Reversal of the Magnetic Polarity of Mn-Mg and Ni-Zn Ferrites—V. V. Kobelev and I. I. Nadashkevich. (*Fiz. Tverdogo Tela*, vol. 1, pp. 1140–1146; July, 1959.) The investigation shows that the periodic application of current pulses of alternating polarity to toroidal ferrite cores produces an individual hysteresis cycle which is shifted in the direction of the initial magnetic state.

538.221:621.318.134 1717
The Variation of Magnetization of a Single Crystal of $PbO \cdot 6Fe_2O_3$ as a Function of the Field—R. Pauthenet and G. Rimet. (*Compt. rend. acad. sci., Paris*, vol. 249, pp. 656–658; August 3, 1959.) Results of experiments on uniaxial crystals are explained in terms of domain phases. See also 3806 of 1959 (Giron and Pauthenet).

538.221:621.318.134 1718
Magnetic Properties of the Mixed Garnets $(3-x)Y_2O_3 \cdot xGd_2O_3:5Fe_2O$,—E. E. Anderson, J. R. Cunningham, Jr., and G. E. McDuffie. (*Phys. Rev.*, vol. 116, pp. 624–625; November 1, 1959.)

538.221:621.318.134 1719
Neutron Study of the Crystal and Magnetic Structures of $MnFe_{2-t}Cr_tO_4$—S. J. Pickart and R. Nathans. (*Phys. Rev.*, vol. 116, pp. 317–322; October 15, 1959.) Powder neutron-diffraction measurements at temperatures down to 4.2°K are used for an accurate determination of the nuclear-structure parameters.

538.221:621.318.134 1720
Magnetic Properties of the Manganese Chromite-Aluminates—P. L. Edwards. (*Phys. Rev.*, vol. 116, pp. 294–300; October 15, 1959.) The mixed-crystal spinel series $MnCr_{2-t}Al_tO_4$ has been studied experimentally; results are compared with theory.

538.221:621.318.134:538.569.4 1721
Some Peculiarities of Multiplet Ferromagnetic Resonance in Ferrites—V. N. Lazukin. (*Zh. Eksp. Teor. Fiz.*, vol. 36, pp. 682–689; March, 1959.) Investigation at 9200 and 14,640 mc of multiple resonances in inhomogeneously magnetized single and polycrystalline samples at room temperature and at liquid-nitrogen temperature. Results are shown for various spherical and ring-shaped samples of Mn-Zn and Mn-Mg ferrites.

538.221:621.318.134:538.569.4 1722
Theory of Ferromagnetic Resonance in Rare-Earth Garnets: Part 2—Line Widths—P. G. de Gennes, C. Kittel, and A. M. Portis. (*Phys. Rev.*, vol. 116, pp. 323–330; October 15, 1959.) Theoretical results describe the order of magnitude and the temperature dependence of observed line widths assuming that the relaxation time of the relevant rare-earth ions is $\approx 10^{-12}$ second at 400°K. Part 1: 1322 of April (Kittel).

538.221:621.395.625.3 1723
Particle Interaction in Magnetic Recording Tapes—J. G. Woodward and E. DellaTorre. (*J. Appl. Phys.*, vol. 31, pp. 56–62; January, 1960.) In two different recording tapes particle interaction was found to be appreciable and a significant factor in determining the bulk magnetic properties and the recording performance of tapes.

538.222 1724
Simultaneous Determination of Particle Size and Magnetization in the Ångstrom Region by the Measurement of the Collective Paramagnetism—A. Knappwost. (*Naturwiss.*, vol. 46, pp. 65–66; January, 1959.) The investigation of spontaneously magnetized domains of size from 10 to about 100 Å is facilitated by the method described.

538.222:539.2 1725
Threshold Energy for Lattice Displacement in α-Al_2O_3—G. W. Arnold and W. D. Compton. (*Phys. Rev. Lett.*, vol. 4, pp. 66–68; January 15, 1960.)

538.652 1726
The Saturation Magnetostriction of Polycrystals—R. R. Birss. (*Proc. Phys. Soc.*, vol. 75, pp. 8–16; January 1, 1960.) Relations between the single-crystal and polycrystalline saturation magnetostriction constants are derived for cubic materials.

MATHEMATICS

512.99:538.3 1727
The Method of Combinative Numbers (Nombres Combinatifs) in the Study of Electromagnetic Fields—Zlatev. (*See* 1558.)

MEASUREMENTS AND TEST GEAR

621.3.018.41(083.74) 1728
Frequency Measurement of Standard-Frequency Transmissions against Caesium-Beam Resonator Standard—S. N. Kalra. (*Canad. J. Phys.*, vol. 37, pp. 1328–1329; November, 1959.) A table shows the frequency deviations of the 60-kc MSF, 16-kc GBR and 60-kc KK2XE1 transmissions as measured daily in Ottawa during August 1959, and the mid-monthly mean frequency of WWV. Figures are to be published monthly, *ibid.*

621.317.3:537.311.33 1729
Further Consideration of Bulk Lifetime Measurement with a Microwave Electrodeless Technique—H. Jacobs, A. P. Ramsa, and F. A. Brand. (Proc. IRE, vol. 48, pp. 229–233; February, 1960.) Describes a method of measurement of the lifetime of excess carriers in semiconductors using a steady light source, which does not involve electrode attachments and also reduces the effects of surface recombination.

621.317.31:537.312.62 1730
Measuring Critical Current in Cryogenic Circuits—J. I. Pankove and R. Drake. (*Electronics*, vol. 33, pp. 52–53; January 22, 1960.) Details are given of test equipment which automatically traces the characteristic curve of a cryogenic device, supplying a current of up to 2A to the contact for periods <100 μsec.

621.317.335:621.315.212 1731
Continuous Measurement of Capacitance of Coaxial Cables during Manufacture—D. Wolff. (*Nachrichtentech. Z.*, vol. 12, pp. 29–32; January, 1959.)

621.317.6:621.391.883.2 1732
A Simple Technique for Measuring the Signal-to-Noise Ratio at the Output of a Pulsed Sinusoid Matched Filter—H. E. White. (Proc. IRE, vol. 48, pp. 241–242; February, 1960.)

621.317.7:621.319.4 1733
An Oscillating Capacitor of High Stability—von Ardenne and Klar. (*See* 1516.)

621.317.723:621.375.4 1734
A Multirange Electrometer Amplifier Using Variable Feedback—J. H. Leck and W. E. Austin. (*Electronic Engrg.*, vol. 32, pp. 106–107; February, 1960.) A description of a stable electrometer amplifier using transistors and a miniature electrometer tube, which has proved satisfactory for measuring currents down to 10^{-15}A.

621.317.726 1735
A Peak Voltmeter intended for the Measurement of Isolated High-Voltage Pulses—G. Giralt and E. Krouk. (*Compt. rend. acad. sci., Paris*, vol. 249, pp. 1042–1044; September 21, 1959.) Details are given of the blocking method described earlier [920 of 1959 (Giralt)]. The duration of the pulse may be from 0.1 μs to 10 ms. The use of a special air capacitor enables measurements to be made of voltages up to 400 kv.

621.317.733 1736
Measurement of Impedance in the Audio-Frequency Range—D. Karo. [*Engineer* (*London*), vol. 208, pp. 687–690; November 27, 1959.] A bridge circuit is described in which the number of resistance standards is reduced to the minimum and the effect of the remaining residuals eliminated by two consecutive balancing procedures. Results obtained with the new circuit are compared with those given by conventional bridges.

621.317.75:621.374 1737
Transistorized Slicer Analyses Signal Amplitude—T. A. Bickart. (*Electronics*, vol. 33, pp. 70, 72; January 29, 1960.) A circuit for the measurement of amplitude probability density functions is described, comprising inverter, diode AND gate, Schmitt trigger and integrator. See 1976 of 1959.

621.317.79.029.6:551.510.62 1738
Limit of Spatial Resolution of Refractometer Cavities—W. J. Hartman. (*J. Res. Nat. Bur. Stand.*, vol. 64D, pp. 65–72; January /February, 1960.) Filter factors are derived which determine an upper limit for the wave numbers for which refractometer measurements can be used to calculate the spectrum of refractivity.

OTHER APPLICATIONS OF RADIO AND ELECTRONICS

537.376:681.61 1739
Electroluminescent Alphanumeric Display—T. Hamburger. (*Electronics*, vol. 33, pp. 49–51; January 22, 1960.) Information from a conventional typewriter keyboard is displayed sequentially on five alphanumeric indicators. The five characters can be selectively or totally erased. The indicators are in effect lossy capacitors and require a 230-volt 400-cps excitation to give the rated brightness.

621.36+621.56]:537.322 1740
Figure of Merit for Thermionic Energy Conversion—N. S. Rasor. (*J. Appl. Phys.*, vol. 31, pp. 163–167; January, 1960.) The optimum performance for emission-limited thermionic energy conversion is derived. Methods of reducing fundamental performance limitations are briefly discussed and a figure of merit is given which applies to both thermionic and thermoelectric conversion.

621.36+621.56]:537.322 1741
Calculation of Efficiency of Thermoelectric Devices—B. Sherman, R. R. Heikes, and R. W. Ure, Jr. (*J. Appl. Phys.*, vol. 31, pp. 1–16; January, 1960.) A procedure has been developed for the exact calculation of the efficiency of thermoelectric generators and cooling devices in which the parameters of the materials have arbitrary temperature dependence. Approximate and exact methods are employed and compared in the numerical evaluation of the results.

621.384.612.11 1742
Zero-Gradient Synchrotron at the Argonne National Laboratory—[*Engineer* (*London*), vol. 208, pp. 492–495; October 23, 1959.] Description of the 12.5-Bev proton synchrotron under construction at Lemont, Illinois.

621.384.7 1743
The Splitting of a Beam of Particles into Two Beams by means of an Electrostatic Bi-

prism—A. Septier. (*Compt. rend. acad. sci., Paris*, vol. 249, pp. 662–664; August 3, 1959.) Calculations show that the two emergent beams are not deformed.

621.385.833 1744

Factors affecting Contrast and Resolution in the Scanning Electron Microscope—T. E. Everhart, O. C. Wells, and C. W. Oatley. (*J. Electronics Control*, vol. 7, pp. 97–111; August, 1959.)

621.387.462:621.382.2 1745

Tiny Semiconductor is Fast, Linear Detector—S. S. Friedland, J. W. Mayer, and J. S. Wiggins. (*Nucleonics*, vol. 18, pp. 54–56, 59; February, 1960.) A shallow diffused Si *p-n* junction operated with reverse bias forms a space-charge region which acts as an ionization chamber capable of giving a high-resolution response proportional to incident particle energy.

621.398:551.507.362.2 1746

Data Conversion Circuits for Earth-Satellite Telemetry—D. N. Carson and S. K. Dhawan. (*Electronics*, vol. 33, pp. 82–84; January 15, 1960.) Details are given of two pulse-height analyzer circuits suitable for use in artificial satellites.

621.398:629.19 1747

Solid-State Guidance for Able-Series Rockets—R. E. King and H. Low. (*Electronics*, vol. 33, pp. 60–63; January 29, 1960.) Circuits used in the second-stage rocket for pitch, yaw and roll control are described.

PROPAGATION OF WAVES

621.391.81+621.396]:(98):061.3 1748

Conference on Arctic Communication—Kirby and Little. (*See* 1776.)

621.391.812.6.029.63:551.594.5 1749

Observed Characteristics of an Ultra-High-Frequency Signal Traversing an Auroral Disturbance—J. C. James, L. E. Bird, R. P. Ingalls, M. L. Stone, J. W. B. Day, G. E. K. Lockwood, and R. I. Presnell. [*Nature* (*London*), vol. 185, pp. 510 512; February 20, 1960.] Signals transmitted on a frequency of 440 mc from a station in the auroral zone were observed at two mid-latitude stations after reflection from the moon. Results show a rapid fluctuation of the polarization of the signal received and an increase in the rate of fading, but no measurable absorption.

621.391.812.62 1750

An Extract Earth-Flattening Procedure in Propagation around a Sphere—L. Y. C. Koo and M. Katzin. (*J. Res. Nat. Bur. Stand.*, vol. 64D, pp. 61–64; January/February, 1960.) Exact differential equations for the spherical geometry are obtained in terms of equations of the plane-earth type, and solutions of these hold for arbitrarily large heights and distances.

621.391.812.62.029.55 1751

Measurements of Coastal Deviation of High-Frequency Radio Waves—C. W. McLeish. (*J. Res. Nat. Bur. Stand.*, vol. 64D, pp. 57–59; January/February, 1960.) "The angular deviation of the phase front of a wave propagated across a fresh water shoreline has been measured over the frequency range from 3 to 20 Mcs. The deviation is found to be roughly half that which theoretically would be obtained if the same sites were adjacent to infinitely conducting surfaces."

621.391.812.62.029.63 1752

A Note regarding the Mechanism of U.H.F. Propagation Beyond the Horizon—A. D. Watt, E. F. Florman, and R. W. Plush. (PROC. IRE, vol. 48, p. 252; February, 1960.) Results are given which provide some evidence for the existence of a "scatter volume."

621.391.812.62.029.63 1753

Investigations of Propagation over Radio-Link Paths Within and Beyond Optical Range at 1.1 to 1.3 Gc/s—U. Kühn. (*Tech. Mitt. BRF, Berlin*, vol. 3, pp. 32–41; October, 1959.) Statistical analysis of results of long-term measurements made on five different paths in East Germany. For path lengths beyond optical range night-time field-strength increases >40db over daytime values were frequently observed. For earlier results see 3095 of 1959.

621.391.812.62.029.64+621.396.677.73 1754

Over-Sea Propagation of Microwaves and Anti-reflected-Wave Antenna—S. Kawazu, S. Kato, and K. Morita. (*Rep. Elect. Commun. Lab., Japan*, vol. 7, pp. 171–191; June, 1959.) An experimental three-element stacked array for suppressing the reflected wave is described. Measured field strengths are compared with those obtained using a single horn and with calculated values.

621.391.812.624 1755

Tropospheric Scatter Propagation and Atmospheric Circulations—W. F. Moler, and D. B. Holden. (*J. Res. Nat. Bur. Stand.*, vol. 64D, pp. 81–93; January/February, 1960.) Scattering angle and intensity of dielectric fluctuations at high wave numbers are found to be dependent on the refractive layering and thermal stability of the air mass which are known to be functions of the vertical velocity in the atmosphere. It is shown that the direction and magnitude of the vertical velocity can be inferred from the upper tropospheric wind velocity divergence, and received scattered signals are well correlated with this quantity.

621.391.812.624 1756

Frontal Perturbation of a Tropospheric Scatter Path—D. R. Hay and G. E. Poaps. (*Canad. J. Phys.*, vol. 37, pp. 1272–1282; November, 1959.) The fading rate of 500-mc transmissions over an 85-mile path is found to rise when the path is disturbed by a weather front situated so that any part of the frontal zone lies between the surface and 3000 feet at the path mid-point.

621.391.812.63 1757

On the Mode of Propagation in the E Layer—W. R. Piggott and J. Bhattacharyya. (*J. Atmos. Terr. Phys.*, vol. 17, pp. 150 157; December, 1959.) Examination of f_0E data shows that the mode of propagation near the maximum of the *E* layer is quasi-transverse for all values of dip from 0 degrees to approximately 89 degrees. It is confirmed that the traces extending about $f_H/2$ above f_0E are due to sporadic-E and not to magneto-ionic effects.

621.391.812.63 1758

Radio Scattering in the Lower Ionosphere—H. G. Booker. (*J. Geophys. Res.*, vol. 64, pp. 2164–2177; December, 1959.) Radio scattering phenomena observed in the frequency range 30–100 mc indicate the presence of irregularities of electron density with corrugation wavelengths from 120 to 360 meters. The irregularities are approximately isotropic.

621.391.812.63:551.594.6 1759

The Propagation of Electromagnetic Waves in Ionized Gases (with Special Reference to "Whistlers"): Parts 1 and 2—F. H. Northover. (*J. Atmos. Terr. Phys.*, vol. 17, pp. 158–178; December, 1959.) An investigation of the propagation of waves along more or less complete columns of ionization which follow approximately the lines of force of the earth's magnetic field. In Part 1 a general theory of wave propagation in conducting gases is developed. In Part 2 the propagation of the plane-wave mode along stationary columns is examined.

621.391.812.63:621.391.826.2 1760

Around-the-World Echoes Observed on a Transpolar Transmission Path—J. Ortner. (*J. Geophys. Res.*, vol. 64, pp. 2464–2467; December, 1959.) Investigation of the College, Alaska—Kiruna path during winter 1958/1959, using an 18-mc back-scatter sounder and a Yagi pointing northward, showed a long delay signal attributable to an around-the-world path. The signal strength sometimes equalled that of the short-path pulses, indicating tilted reflection paths above the *D* region.

621.391.812.63.029.45 1761

Transmission Loss Curves for Propagation at Very Low Radio Frequencies—J. R. Wait. (IRE TRANS. ON COMMUNICATIONS SYSTEMS, vol. CS-6, pp. 58–61; December, 1958. Abstract, PROC. IRE, vol. 47, p. 494; March, 1959.)

621.391.812.63.029.45:621.396.67:621.315.1 1762

A Very-Low-Frequency Antenna for Investigating the Ionosphere with Horizontally Polarized Radio Waves—Macmillan, Rusch, and Golden. (*See* 1496.)

621.391.812.8:551.510.535 1763

The Calculation of the M.U.F. Factor for a Nonparabolic Ionospheric Layer—M. D. Vickers. (*J. Atmos. Terr. Phys.*, vol. 17, pp. 34–45; December, 1959.) "A method is described for calculating the ray path of a radio wave through the ionosphere as represented by an *N*(*h*) profile based on experimental data. A few such paths are calculated and from these m.u.f. factors are obtained. These factors are compared with those which would have been obtained had the existing methods of calculation been used. In most cases the differences are less than 4 per cent."

621.391.814.2 1764

Layered-Earth Propagation in the Vicinity of Point Barrow, Alaska—G. M. Stanley. (*J. Res. Nat. Bur. Stand.*, vol. 64D, pp. 95–97; January/February, 1960.) "The relative field strength of a vertically polarized low-frequency radio signal was measured as a function of distance over several radial paths in the vicinity of Point Barrow, Alaska. The attenuation of the recorded signal was very much less than predicted by the theory of propagation of a ground wave signal over a plane, homogeneous, infinitely conducting earth. The analysis of these data in terms of a plane, layered, finitely conducting earth appears to resolve the anomaly."

RECEPTION

621.376.23 1765

Detecting Signals by Polarity Coincidence—B. M. Rosenheck. (*Electronics*, vol. 33, pp. 67–69; January 29, 1960.) Details are given of a type of dual-input phasemeter for the detection of weak signals in the frequency range 1–500 cps in a high noise background.

621.391.821 1766

Determination of the Amplitude Probability Distribution of Atmospheric Radio Noise from Statistical Moments—W. G. Crichlow, C. J. Roubique, A. D. Spaulding, and W. M. Beery. (*J. Res. Nat. Bur. Stand.*, vol. 64D, pp. 49–56; January/February, 1960.) An empirically derived graphical method is presented and possible errors are discussed.

621.391.821 1767

Measured Frequency Spectra of Very-Low-Frequency Atmospherics—T. Obayashi. (*J. Res. Nat. Bur. Stand.*, vol. 64D, pp. 41–48; January/February, 1960.) New continuously recording spectroscopes have been developed for the frequency ranges 1–10 kc and 5–70 kc. Observations with the equipment provide further experimental proof of the mode theory of VLF propagation.

621.391.821:539.16 1768
Effects of High-Altitude Nuclear Explosions on Radio Noise—C. A. Samson. (*J. Res. Nat. Bur. Stand.*, vol. 64D, pp. 37–40; January/February, 1960.) Atmospheric noise recorded at Kekaha, Hawaii, on frequencies between 13 kc and 20 mc fell by up to 32 db during the hour following the first explosion.

621.396.62:621.397.62 1769
The Combined Television/Radio Receiver and its Problems—R. S. Hildersley. (*J. Brit. IRE*, vol. 20, pp. 155–166; February, 1960.) Circuit details of a combined receiver are described. The sound IF circuits incorporate a double superheterodyne system and the frequency of the RF oscillator is stabilized in band II using a point-contact Ge diode as a variable-reactance device.

621.396.621 1770
Transformerless Circuits for Broadcast Receivers—R. C. V. Macario and N. E. Broadberry. (*Wireless World*, vol. 66, pp. 110–113; March, 1960.) Various circuits are simplified by taking advantage of the greater versatility of resistors, capacitors and transistors, to permit the omission of transformers and other wire-wound components.

621.396.662:621.372.632 1771
One-Tube Oscillator Mixers for TV and F.M. Tuners—E. H. Hugenholtz. (*Electronics*, vol. 33, pp. 76–79; January 15, 1960.) The circuits described use either a single triode tube as oscillator mixer or a semi-conductor diode as mixer with a triode or pentode oscillator tube. Spurious coupling is limited by balanced bridge networks and the isolating action of the diode. Results are better than those obtained with conventional circuits.

621.396.665:621–526 1772
The Application of Linear Servo Theory to the Design of A.G.C. Loops—W. K. Victor and M. H. Brockman. (Proc. IRE, vol. 48, pp. 234–238; February, 1960.) Expressions are derived specifying the performance of an agc system with respect to step and ramp changes in signal level, frequency response, receiver gain error as a function of receiver noise, etc. Close agreement with measured values is achieved.

621.396.666 1773
Evaluation of I.F. and Base-Band Diversity Combining Receivers—R. T. Adams and B. M. Mindes. (IRE Trans. on Communications Systems, vol. CS-6, pp. 8–13; June, 1958. Abstract, Proc. IRE, vol. 46, pp. 1665–1666; September, 1958.)

STATIONS AND COMMUNICATION SYSTEMS

621.376.53 1774
A S/N Improvement Factor on P.A.M.-F.M. whose Received Pulse is Cosine-Squared—A. Watanabe. (Proc. IRE, vol. 48, pp. 257–258; February, 1960.) Formulas are derived for the signal/noise improvement factor when low-pass filters and integrated demodulation circuits are used. Figures are given for typical cases.

621.396:681.84.087.7 1775
New Stereophonic Broadcasting System—G. D. Browne. (*Brit. Commun. Electronics*, vol. 7, pp. 204–205; March, 1960.) General features of a fully compatible time-multiplex system are described.

621.396+621.391.81](98):061.3 1776
Conference on Arctic Communication—R. C. Kirby and C. G. Little (*J. Res. Nat. Bur. Stand.*, vol. 64D, pp. 73–80; January/February, 1960.) Brief report of the conference held at Boulder, Colo., March 3–6, 1959, with abstracts of the twenty-two papers presented.

621.396.2:621.391.812.624 1777
Dependence of the Maximum Range of Tropospheric Scatter Communications on Antenna and Receiver Noise Temperatures—A. H. Hausman. (IRE Trans. on Communications Systems, vol. CS-6, pp. 35–38; December, 1958. Abstract, Proc. IRE, vol. 47, p. 494; March, 1959.)

621.396.65:621.395.665.1 1778
Compandor Loading and Noise Improvement in Frequency Division Multiplex Radio-Relay Systems—E. M. Rizzoni. (Proc. IRE, vol. 48, pp. 208–220; February, 1960.) "Graphical and numerical means are developed to compute the additional effective loading caused by the use of syllable compandors on the input of a multichannel radio-relay system, and to evaluate the noise improvement yielded by the compandor in a telephone channel."

621.396.932 1779
Mobile Maritime Service. Routes: Spain–South America, Spain–Persian Gulf—R. Gea Sacasa. (*Rev. Telecommunicación, Madrid*, vol. 14, pp. 7–20; September, 1959.) Signal-strength assessments of ships' transmissions received at Cadiz are related to forecasts by the Gea method. See also 3859 of 1959.

SUBSIDIARY APPARATUS

621.3.087.4:621.395.625.3 1780
More Bandwidth for Magnetic Recorders—D. R. Steele. (*Electronics*, vol 33, pp. 44–47; January 8, 1960.) Details are given of the design of recorder circuits having a bandwidth 250 cps–250 kc to take advantage of recent increase in recording-head response.

621.314.63:621.382.2 1781
Some Performance Parameters of Silicon Junction Power Rectifiers—D. R. Coleman. (*Electronic Engrg*, vol. 32, pp. 98–102; February, 1960.) The temperature dependence of the characteristics of Si rectifiers, and temperature control in terms of thermal resistance are discussed. A method is given for the calculation of power dissipation and ratings.

621.316.721/.722:621.382.3 1782
Compensation of the Effect of Temperature on the Reference Voltage of Transistor Stabilized Power Supplies—É. Cassignol, P Chauson, G. Giralt, and J. C. Polisset. (*Compt. rend. acad. sci., Paris*, vol. 249, pp. 59–661; August 3, 1959.) The voltage/temperature characteristic of the reference source (Zener diode or primary cell) is compensated by that of the base-emitter region of the transistor error amplifier. See 3642 of 1958 (Cassignol and Giralt).

621.316.722:621.318.435.3 1783
A Transductor Regulator for Stabilized Power Supplies—A. N. Heightman. (*J. Brit. IRE*, vol. 20, pp. 105–123; February, 1960.) A description is given of a single-core full-wave transductor circuit and its mode of operation. A tube-type regulator to deal with rapid disturbances is also described. Both regulators are incorporated in a stabilized 250-volt, 1-ampere power supply.

621.316.722.078.3 1784
Economy in the Series Stabilizer—D. J. Coflins, and J. R. Pearce. (*Electronic Engrg.*, vol 32, pp. 95–97; February, 1960.) Consideration of the efficiency of series stabilizer circuits under almost constant load conditions. A resistive shunt to the series element can improve efficiency.

TELEVISION AND PHOTOTELEGRAPHY

621.397:621.317(083.74) 1785
I.R.E. Standards on Television: Measurement of Differential Gain and Differential Phase, 1960—(Proc. IRE, vol. 48, pp. 201–208; February, 1960.) Standard 60 I.R.E. 23. S1.

621.397:621.391 1786
Video Information Theory—P. Neidhardt. (*NachrTech.*, vol. 9, pp. 18–23; January, 1959.) The application of the concepts and results of communication theory to the transmission of television signals is considered with the intention of formulating a specific video information theory.

621.397:621.391.837 1787
Investigations on the Replacement of the Subjective Assessment of Picture Quality by a Physical Criterion—W. Kroebel and G. Moll. (*Z. angew. Phys.*, vol. 11, pp. 27–35; January, 1959.) See also 4222 of 1959 (Kroebel).

621.397:621.391.837 1788
The Visibility of Picture Details of Moving Objects in Television—I. Bornemann. (*Nachrichtentech. Z.*, vol. 9, pp. 8–12; January, 1959.) The causes of the losses in detail entropy in the reproduction of moving objects are analyzed.

621.397.13:535–1/3 1789
A High-Grade Industrial Television Channel with reference to Infrared Operation—J. H. Taylor. (*J. Brit. IRE*, vol. 20, pp. 77–85; January, 1960.) Details are given of the system design including vidicon camera head, amplifier, control unit and monitor with reference to normal requirements. Infrared operation is discussed.

621.397.132 1790
A Review of Colour Television in the U. K.—R. D. A. Maurice. (*Electronic Engrg.*, vol. 32, pp. 68–73; February, 1960.)

621.397.132 1791
Monochrome Reproduction of Colour TV Signal—R. D. A. Maurice. (*Electronic Tech.*, vol. 37, pp. 116–119; March, 1960.) In a color-television system using the standard NTSC method of gamma correction the deterioration in orthochromatism of the monochrome compatible picture can be reduced by the presence of the dot pattern due to the chrominance subcarrier. A "notch" or subcarrier-elimination filter is thus undesirable in monochrome receivers.

621.397.132 1792
The Change in Skin-Colour Tints caused by Phase Errors in Colour Television—P. Neidhardt. (*Nachrichtentech. Z.*, pp 4–7; January, 1959.) From a consideration of the color changes which can be tolerated and their relation to phase errors originating in the receiver it is concluded that phase errors of ±10 degrees are not objectionable.

621.397.332.12 1793
Reduction of Television Bandwidth by Frequency-Interlace—E. A. Howson and D. A. Bell. (*J. Brit. IRE*, vol. 20, pp. 127–136; February, 1960.) A method analogous to the NTSC color television system is used to obtain a bandwidth reduction of a monochrome signal by a factor of 2:1. Various interference effects are discussed.

621.397.335 1794
Timebase Synchronization and Associated Problems—P. L. Mothersole. (*J. Brit IRE*, vol. 20, pp. 57–72; January, 1960.) The requirements of timebase oscillator and synchronization circuits are discussed with reference to both positive and negative modulation systems. Examples of these and noise-limiting circuits together with the effects of noise on synchronization are given.

621.397.612:621.318.57 1795
A Television Master Switcher—B. Mars-

den. (*J. Brit. IRE*, vol. 20, pp. 47–53; January, 1960. Discussion.) Switching methods are reviewed. The use of crystal diodes enables a low-consumption, reliable and compact switching system to be built with a response substantially flat to 6 mc. Reference is made to development work in which transistor pulse generators are used to achieve vision switching between successive frames of the television waveform.

621.397.62:621.396.62 1796
The Combined Television/Radio Receiver and its Problems—Hildersley. (*See* 1769.)

621.397.743 1797
The Technical Limits to Full Television Coverage of Germany by Wireless Transmission—W. Scholz. (*Elektrotech. Z.*, vol. 80, pp. 548–550; August 11, 1959.) 30 per cent of the area of the German Federal Republic cannot be covered by wireless transmission in the dm range because of multipath propagation due to the nature of the terrain. Distribution of received programs by cable offers a solution to the problem.

621.397.743 1798
Television Relay Links in the Č.S.R.—A. Ditl. (*Nachrichtentech. Z.*, vol. 9, pp. 23–25; January, 1959.) Description of radio-link equipment in use in Czechoslovakia.

621.397.743.029.64 1799
Microwave Television Mobile Relay for Outside Broadcasting—J. Polonsky. (*J. Brit. IRE*, vol. 20, pp. 91–102; February, 1960.) Principal causes of distortion and problems of cross-talk in microwave systems are discussed and a brief description is given of equipment operating in the range 6400–6900 mcs.

TUBES AND THERMIONICS

621.382.22 1800
Dipole Mode of Minority Carrier Diffusion with Reference to Point-Contact Rectification—B. R. Gossick. (*J. Appl. Phys.*, vol. 31, pp. 29–35; January, 1960.) An analysis of diffusion from a point source is used to investigate the importance of the dominant higher (dipole) mode relative to the fundamental (unipole) mode. The dipole mode is found to offer superior HF performance, which is partially offset by an inferior dc characteristic.

621.382.22 1801
The Germanium Microwave Crystal Rectifier—A. C. MacPherson. (IRE TRANS. ON ELECTRON. DEVICES, vol. ED-6, pp. 83–90; January, 1959. Abstract, PROC. IRE, vol. 47, p. 612; April, 1959.)

621.382.23 1802
Conductance and Voltage Transfer Coefficient of a Semiconductor Diode in the Transient State—E. I. Adirovich. (*Fiz. Tverdogo Tela*, vol. 1, pp. 1115–1124; July, 1959.) Frequency, phase and transient characteristics of a circuit with a *p-n* junction and a series ohmic resistance are calculated. Characteristic time constants and critical frequencies are derived and a method of determining diode parameters, in particular for measurement of low values of lifetime, is described.

621.382.23 1803
Gallium Arsenide Tunnel Diodes—K. G. Hambleton, J. J. Low, and R. J. Sherwell. [*Nature* (*London*), vol. 185, pp. 676–677; March 5, 1960.] Characteristics of experimental Zn-doped GaAs diodes are noted.

621.382.23 1804
Pressure Dependence of the Current/Voltage Characteristics of Esaki Diodes—S. L. Miller, M. I. Nathan, and A. C. Smith. (*Phys. Rev. Lett.*, vol. 4, pp. 60–62; January 15, 1960.) Measurements on narrow-junction diodes at room temperature and at pressures up to 30,000 kg/cm² are reported and results are compared with theory. See 1784 of 1958 (Esaki).

621.382.23:546.289:535.34–15 1805
Investigation of Induced Absorption of Infrared Radiation in a Germanium Diode—Yu. I. Ukhanov. (*Zh. tekh. Fiz.*, vol. 28, pp. 2410–2416; November, 1958.) Quantitative investigation of the variation of infrared absorption in a Ge junction diode due to injected holes. The cross-section and effective mass of absorption centers are calculated.

621.382.23:621.316.722 1806
The Characteristics and Applications of Zener (Voltage-Reference) Diodes—J. A. Chandler. (*Electronic Engrg.*, vol. 32, pp. 78–86; February, 1960.)

621.382.23:621.318.57 1807
Electrical Properties of Gold-Doped Diffused Silicon Computer Diodes—A. E. Bakanowski and J. H. Forster. (*Bell Sys. Tech. J.*, vol. 39, pp. 87–104; January, 1960.) Theoretical investigations show that, to a first approximation, reverse recovery time is inversely proportional to gold atom concentration. This is supported by experimental evidence for gold concentrations in the range 8×10^{16} cm^{-3} to 1.2×10^{15} cm^{-3} (recovery times 0.7–35 mμsec). Accompanying changes in reverse and forward currents are also considered.

621.382.23:621.372.44 1808
***P-N-P* Variables-Capacitance Diodes**—J. F. Gibbons and G. L. Pearson (PROC. IRE, vol. 48, pp. 253–255; February, 1960.) A simplified circuit model is used to derive the properties of the device and the design and fabrication are described.

621.382.3:621.317.7 1809
Automatic Measurement of Transistor Beta—E. P. Hojak. (*Electronics*, vol. 32, pp. 114–115; December 4, 1959.) The base current is automatically varied until a predetermined collector current is obtained. The final base current is a direct measure of beta.

621.382.3.01 1810
On the Use of Physical rather than Four-Pole Parameters in a Standard Transistor Specification—D. F. Page. (PROC. IRE, vol. 48, p. 261; February, 1960.) Comment on 1008 of 1959 (Armstrong).

621.382.333 1811
On Calculating the Current Gain of Junction Transistors with Arbitarry Doping Distributions—H. L. Armstrong. (IRE TRANS. ON ELECTRON DEVICES, vol. ED-6, pp. 1–5; January, 1959. Abstract, PROC. IRE, vol. 47, p. 611; April, 1959.)

621.382.333 1812
Transient Analysis of Junction Transistors—W. F. Gariano. (IRE TRANS. ON ELECTRON DEVICES, vol. ED-6, pp. 90–100; January, 1959. Abstract, PROC. IRE, vol. 47, p. 612; April, 1959.)

621.382.333 1813
Effect of Transient Voltages on Transistors—H. C. Lin and W. F. Jordan, Jr. (IRE TRANS. ON ELECTRON DEVICES, vol. ED-6, pp. 79–83; January, 1959. Abstract PROC. IRE, vol. 47, p. 612; April, 1959.)

621.382.333 1814
Influence of the Surface and Volume Recombination on α and the Collector Reverse Current in Alloy Junction Transistors—B. Ya. Moĭzhes. (*Zh. tekh. Fiz.*, vol. 25, pp. 2402–2409; November, 1958.) Formulas are derived for the current gain α and collector reverse current in symmetrical and nonsymmetrical transistors, in presence of surface and volume recombination.

621.382.333 1815
A Modification of the Theory of the Variation of Junction-Transistor Current Gain with Operating Point and Frequency—A. W. Matz. (*J. Electronics Control*, vol. 7, pp. 133–152; August. 1959.). A modified solution of the continuity equation for minority-carrier flow is presented, with an extension to ac conditions. The observed maximum in the variation of common-base cutoff frequency with emitter current is explained. Experimental results are presented which show that transistor base widths may be smaller than is normally supposed.

621.382.333 1816
The Voltage Dependence of Reverse Currents in Alloy Transistors—A. Götzberger. (*Z. angew. Phys.*, vol. 11, pp. 6–9; January, 1959.) Investigations of transistor characteristics in relation to the punch-through effect.

621.382.333:621.318.57 1817
Transistor Bias Method Raises Breakdown Point—H. Somlyody. (*Electronics*, vol. 33, pp. 48–49; January 8, 1960.) The application of reverse-biasing technique to permit switching at voltages higher than the rated values.

621.382.333:621.318.57 1818
Germanium *p-n-p-n* Switches—I. A. Lesk. (IRE TRANS. ON ELECTRON DEVICES, vol. ED-6, pp. 28–35; January, 1959. Abstract, PROC. IRE, vol. 47, p. 611; April, 1959.)

621.382.333.3 1819
On the Frequency Dependence of the Magnitude of Common-Emitter Current Gain of Graded-Base Transistors—M. B. Das and A. R. Boothroyd. (PROC. IRE, vol. 48, pp. 240–241; February, 1960.) The current gain is investigated theoretically and it is shown that it should fall by 6 db per octave increase in frequency, provided the effect of the emitter junction capacitance is small.

621.382.333.32 1820
A Double-Base Diode with Hook Mechanism—T. Tominaga, S. Kanai, and A. Sato. (*Rep. Elect. Commun. Lab., Japan*, vol. 7, pp. 133–137; May, 1959.) The device described has a thin layer of *p*-type Ge in the conductivity-modulated region of the original double-base diode. With this form of construction, the base-current power dissipation may be reduced to about 1/100th of its original value.

621.382.333.33 1821
Influence of Technology and of Diffusion on the Characteristics of a Drift-Type Transistor—J. Mercier. (*Onde élect.*, vol. 39, pp. 869–875 and pp. 897–907; November and December, 1959.) Characteristics of drift-type transistors are studied theoretically and an equivalent circuit is proposed. Parameters for the determination of performance are derived and used in the synthesis of a transistor element.

621.383.5:546.289:621.391.822 1822
Noise Phenomena in Photovoltaic Germanium Cells—M. Teboul. (*Compt. rend. acad. sci., Paris*, vol. 249, pp. 651–653; August 3, 1959.) The total noise at Ge photovoltaic junctions has been measured as a function of polarization and illumination and compared with calculated shot noise.

621.385.3.029.6 1823
Large-Signal Theory of U.H.F. Power Triodes—A. D. Sutherland. (IRE TRANS. ON ELECTRON DEVICES, vol. ED-6, pp. 35–47; January, 1959. Abstract, PROC. IRE, vol. 47, pp. 611–612; April, 1959.)

621.385.6 1824

Independent Space Variables for Small-Signal Electron-Beam Analyses—D. L. Bobroff. (IRE Trans. on Electron Devices, vol. ED-6, pp. 68–78; January, 1959. Abstract, Proc. IRE, vol. 47, p. 612; April, 1959.)

621.385.6 1825

Electron-Beam Flow in Superimposed Periodic and Uniform Magnetic Fields—J. R. Anderson. (IRE Trans. on Electron Devices. vol. ED-6, pp. 101–105; January, 1959. Abstract, Proc. IRE, vol. 47, p. 612; April, 1959.)

621.385.6 1826

Theory of the Focusing of Sheet Beams in Periodic Fields—P. A. Sturrock. (*J. Electronics Control*, vol. 7, pp. 153–161; August, 1959.) Equations are given taking account of space charge, and stability and perveance are discussed. Any such focusing system is convergent if space charge is neglected. See 1827 below.

621.385.6 1827

Magnetic Deflection Focusing—P. A. Sturrock. (*J. Electronics Control*, vol. 7, pp. 162–168; August, 1959.) A scheme for focusing sheet beams by means of a periodic configuration of magnetic fields directed transverse to the beam is presented. Coupling between the beam and fast EM waves is possible.

621.385.6:537.533.1.08 1828

A Microwave Electron-Velocity Spectrograph—P. B. Wilson and E. L. Ginzton. (IRE Trans. on Electron Devices, vol. ED-6, pp. 64–68; January, 1959. Abstract, Proc. IRE, vol. 47, p. 612; April, 1959.)

621.385.623.5:621.396.62 1829

Reflex Klystrons as Receiver Amplifiers—K. Ishii. (*Electronics*, vol. 33, pp. 56–57; January 8, 1960.) An investigation of the performance of a Type-2K25 reflex klystron as an *X*-band amplifier is described.

621.385.624.2 1830

The Effect of Space Charge on Bunching in a Two-Cavity Klystron—T. G. Mihran. (IRE Trans. on Electron Devices, vol. ED-6, pp. 54–64; January, 1959. Abstract, Proc. IRE. vol. 47, p. 612; April, 1959.)

621.385.63 1831

Travelling-Wave-Tube Efficiency Degradation due to Power Absorbed in an Attenuator—C. K. Birdsall and C. C. Johnson. (IRE Trans. on Electron Devices, vol. ED-6, pp. 6–9; January, 1959. Abstract, Proc. IRE, vol. 47, p. 611; April, 1959.)

621.385.63:621.317.74 1832

Measurement of Internal Reflections in Travelling-Wave Tubes using a Millimicrosecond Pulse Radar—D. O. Melroy and H. T. Closson. (Proc. IRE, vol. 48, pp. 165–168; February, 1960.) A stroboscopic gating system produces a slowed-down facsimile of the recurrent pulses for display on a low-frequency CRO. Reflections with return losses of 40 db are easily observed.

621.385.63:621.375.9:621.372.44 1833

Waves on a Filamentary Electron Beam in a Transverse-Field Slow-Wave Circuit—A. E. Siegman. (*J. Appl. Phys.*, vol. 31, pp. 17–26; January, 1960.) The waves on a filamentary electron beam in a longitudinal dc magnetic field, and their interaction with a transverse-field slow-wave circuit, are studied in detail. The beam is found to carry four waves. This type of interaction may prove to be of practical importance, for instance in an electron-beam parametric amplifier.

621.385.63:621.375.9:621.372.44 1834

Some Possible Causes of Noise in Adler Tubes—C. P. Lea-Wilson, R. Adler, G. Hrbek, and G. Wade. (Proc. IRE, vol. 48, pp. 255–257; February, 1960.) Discussion of 321 of 1959 (Adler, Hrbek, and Wade) with reference to partition noise and noise caused by non-uniform electric field, by spread of axial velocities and by collisions between electrons and ions.

621.385.63.032.269 1835

A Gun and Focusing System for Crossed-Field Travelling-Wave Tubes—O. L. Hoch and D. A. Watkins. (IRE Trans. on Electron Devices, vol. ED-6, pp. 18–27; January, 1959. Abstract, Proc. IRE, vol. 47, p. 611; April, 1959.)

621.385.632 1836

The Design and Characteristics of a Megawatt Space Harmonic Travelling-Wave Tube—M. Chodorow, E. J. Nalos, S. P. Otsuka, and R. H. Pantell. (IRE Trans. on Electron Devices, vol. ED-6, pp. 48–53; January, 1959. Abstract, Proc. IRE, vol. 47, p. 612; April, 1959.)

621.385.632.12 1837

Strapped Bifilar Helices for High-Peak-Power Travelling-Wave Tubes—D. A. Watkins and D. G. Dow. (IRE Trans. on Electron Devices, vol. ED-6, pp. 106–114; January, 1959. Abstract, Proc. IRE, vol. 47, p. 612; April, 1959.)

621.385.64.032.213.13 1838

Dispenser-Cathode Magnetrons—G. A. Espersen. (IRE Trans. on Electron Devices, vol. ED-6, pp. 115–118; January, 1959. Abstract, Proc. IRE, vol. 47, p. 612; April, 1959.)

MISCELLANEOUS

621.38.004.6 1839

Reliability Analysis Techniques—C. A. Krohn. (Proc. IRE, vol. 48, pp. 179–192; February, 1960.) Recently evolved analytical techniques are effective in reducing failures and increasing reliability in electronic equipment.

ERRATUM

Abstract 1453 in the previous issue should read as follows—

Tuning and the Equivalent Circuit of Multi-resonator Magnetrons—T. S. Chen. (*J. Electronics Control*, vol. 7, pp. 33–51; July, 1959.) An equivalent circuit is synthesized from the input-admittance function determined from the properties of the waveguide used to tune the magnetron. This circuit is used to calculate wide-band tuning characteristics, which agree with measurements for waveguide tuning systems with and without iris coupling.

Translations of Russian Technical Literature

Listed below is information on Russian technical literature in electronics and allied fields which is available in the U. S. in the English language. Further inquiries should be directed to the sources listed. In addition, general information on translation programs in the U. S. may be obtained from the Office of Science Information Service, National Science Foundation, Washington 25, D. C., and from the Office of Technical Services, U. S. Department of Commerce, Washington 25, D. C.

PUBLICATION	FREQUENCY	DESCRIPTION	SPONSOR	ORDER FROM:
Acoustics Journal (Akusticheskii Zhurnal)	Quarterly	Complete journal	National Science Foundation—AIP	American Institute of Physics 335 E. 45 St., New York 17, N. Y.
Automation and Remote Control (Avtomatika i Telemekhanika)	Monthly	Complete journal	National Science Foundation—MIT	Instrument Society of America 313 Sixth Ave., Pittsburgh 22, Pa.
	Monthly	Abstracts only		Office of Technical Services U. S. Dept. of Commerce Washington 25, D. C.
Journal of Abstracts, Electrical Engineering (Reseratiynyy Zhurnal: Electronika)	Monthly	Abstracts of Russian and non-Russian literature		Office of Technical Services U. S. Dept. of Commerce Washington 25, D. C.
Journal of Experimental and Theoretical Physics (Zhurnal Eksperimentalnoi i Teoreticheskoi Fiziki)	Monthly	Complete journal	National Science Foundation—AIP	American Institute of Physics 335 E. 45 St., New York 17, N. Y.
Journal of Technical Physics (Zhurnal Tekhnicheskoi Fiziki)	Monthly	Complete journal	National Science Foundation—AIP	American Institute of Physics 335 E. 45 St., New York 17, N. Y.
Proceedings of the USSR Academy of Sciences: Applied Physics Section (Doklady Akademii Nauk SSSR: Otdel Prikladnoi Fiziki)	Bimonthly	Complete journal		Consultants Bureau, Inc. 227 W. 17 St., New York 22, N. Y.
Radio Engineering (Radiotekhnika)	Monthly	Complete journal	National Science Foundation—MIT	Pergamon Institute 122 E. 55 St., New York 22, N. Y.
	Monthly	Abstracts only		Office of Technical Services U. S. Dept. of Commerce Washington 25, D. C.
Radio Engineering and Electronics (Radiotekhnika i Elektronika)	Monthly	Complete journal	National Science Foundation—MIT	Pergamon Institute 122 E. 55 St., New York 22, N. Y.
	Monthly	Abstracts only		Office of Technical Services U. S. Dept. of Commerce Washington 25, D. C.
Solid State Physics (Fizika Tverdogo Tela)	Monthly	Complete journal	National Science Foundation—AIP	American Institute of Physics 335 E. 45 St., New York 17, N. Y.
Telecommunications (Elekprosviaz')	Monthly	Complete journal	National Science Foundation—MIT	Pergamon Institute 122 E. 55 St., New York 22, N. Y.
	Monthly	Abstracts only		Office of Technical Services U. S. Dept. of Commerce Washington 25, D. C.
Automation Express	10/year	A digest: abstracts, summaries, annotations of various journals		International Physical Index, Inc. 1909 Park Ave., New York 35, N. Y.
Electronics Express	10/year	A digest: abstracts, summaries, annotations of various journals		International Physical Index, Inc. 1909 Park Ave., New York 35, N. Y.
Physics Express	10/year	A digest: abstracts, summaries, annotations of various journals		International Physical Index, Inc. 1909 Park Ave., New York 35, N. Y.
Express Contents of Soviet Journals Currently being Translated into English	Monthly	Advance tables of contents of translated journals		Consultants Bureau, Inc. 227 W. 17 St., New York 22, N. Y.
Technical Translations	Twice a month	Central directory in the U. S. of translations available from all major sources in the U. S.	OTS and Special Libraries Assoc.	Superintendent of Documents U. S. Gov't Printing Office Washington 25, D. C.